UNIVERSIDADE DE LISBOA

FACULDADE DE CIÊNCIAS

Phylogenetic analysis, paleoenvironmental and paleobiogeographic interpretation of theropod dinosaurs from the Upper Jurassic of the Lusitanian Basin

Doutoramento em Geologia

Especialidade Paleontologia e Estratigrafia

Elisabete Fernandes de Almeida Malafaia

Tese orientada por:

Mário Albino Pio Cachão

e

Francisco Javier Ortega Coloma

Documento especialmente elaborado para a obtenção do grau de doutor

2017

UNIVERSIDADE DE LISBOA

FACULDADE DE CIÊNCIAS

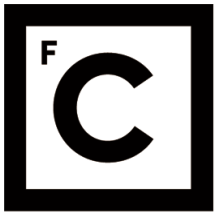

Ciências
ULisboa

Phylogenetic analysis, paleoenvironmental and paleobiogeographic interpretation of theropod dinosaurs from the Upper Jurassic of the Lusitanian Basin

Doutoramento em Geologia
Especialidade Paleontologia e Estratigrafia

Elisabete Fernandes de Almeida Malafaia

Tese orientada por:
Mário Albino Pio Cachão
e
Francisco Javier Ortega Coloma

Júri:
Presidente:

- Maria da Conceição Pombo de Freitas, Professora Catedrática da Faculdade de Ciências da Universidade de Lisboa

Vogais:

- Francisco Javier Ortega Coloma, Professor Titular da Facultad de Ciencias da Universidad Nacional de Educación a Distancia
- Rafael Royo-Torres, Investigador da Fundación Conjunto Paleontológico de Teruel-Dinopolis
- Rui Alexandre Ferreira Castanhinha, Professor Auxiliar Convidado do Departamento de Biologia da Universidade de Aveiro
- Vanda Faria dos Santos, Investigadora Auxiliar do Museu Nacional de História Natural e da Ciência da Universidade de Lisboa

Documento especialmente elaborado para a obtenção do grau de doutor

Investigação Financiada pela Fundação para a Ciência e Tecnologia no âmbito da bolsa de doutoramento SFRH / BD / 84746 / 2012

2017

"Ver um Mundo num grão de areia

E um Paraíso numa flor selvagem

Ter o Infinito na palma da mão

E a Eternidade numa hora"

Blake 1972 in Auguries of Innocence

CONTENTS

SECOND PART

THIRD PART

ABSTRACT

ABSTRACT

The currently known record of Upper Jurassic theropod dinosaurs from the Lusitanian Basin is relatively abundant and diverse. It includes mainly medium to large-sized forms belonging to primitive theropod clades, such as Ceratosauria, or Tetanurae, including Megalosauridae and Allosauroidea. Small-sized and more derived theropods have also been identified based mainly on isolated elements. This study provides new information about the Portuguese Upper Jurassic record of theropod dinosaurs. The main objective of this research is to improve the knowledge about the evolutionary history of these dinosaur faunas. Several unpublished specimens collected in different sites of the Consolação, Turcifal and Bombarral-Alcobaça sub-basins indicate the presence of previously unidentified clades, including non-megalosaurid megalosauroids and a form of derived allosauroid closely related with Carcharodontosauria. These new specimens suggest a greater diversity among the Late Jurassic theropod faunas from the Lusitanian Basin than previously known.

The Late Jurassic theropod fauna of the Lusitanian Basin have been traditionally interpreted as being closely related to those of correlative sedimentary sequences from the North American Morrison Formation and from the African Tendaguru Formation. Most of the genera currently known in the Portuguese record have a closely related taxon at the North American record and most of them were previously interpreted as belonging to species shared by both landmasses. However, more recently the Portuguese forms have been reinterpreted as separate species exclusive for the Lusitanian Basin. This faunal composition seems to indicate an incipient vicariant evolution of the dinosaur faunas from the Late Jurassic of the Lusitanian Basin suggesting that the seaway(s) between North America and Iberia represented barriers to the dispersion of these faunas. However, these barriers may have had different effects on different species, which would explain the stronger affinities of the fauna of theropods between the Lusitanian Basin and Morrison Formation than those of other dinosaur faunas such as the sauropods. Despite this similarity, it has been identified in the Portuguese record some dinosaur groups that apparently are absent in correlative North American strata and that are more closely related with Gondwanan faunas. These differences may indicate differential patterns of regional extinction and ecological constraints such as environmental preferences.

Keywords: Upper Jurassic, Lusitanian Basin, Theropoda, Phylogeny, Paleobiogeography.

RESUMO

RESUMO

O registo de dinossáurios terópodes do Jurássico Superior da Bacia Lusitânica é relativamente abundante e diverso. Este registo inclui sobretudo formas de médio ou grande porte que pertencem a clados de terópodes primitivos, como por exemplo Ceratosauria ou Tetanurae (incluindo Megalosauroidea e Allosauroidea). Pequenos terópodes mais derivados são também conhecidos mas, até ao momento, estão representados principalmente por escassos restos isolados. Este estudo acrescenta nova informação sobre o registo de terópodes do Jurássico Superior português e propõe uma actualização da interpretação filogenética dos taxa representados. O objectivo principal deste trabalho é avaliar as relações de parentesco entre os terópodes conhecidos no Jurássico Superior português e os taxa representados em outras faunas correlativas do contexto peri-Norte Atlântico.

O registo português de ceratossáurios é relativamente escasso, incluindo um conjunto de material atribuído a *Ceratosaurus* e alguns dentes isolados identificados, preliminarmente, como pertencendo a abelissaurídeos. *Ceratosaurus* está representado por elementos apendiculares, de um único individuo, recolhidos em Valmitão (Lourinhã), em níveis da Formação Praia da Amoreira-Porto Novo (Kimmeridgiano superior). Estes exemplares partilham com *Ceratosaurus*, um género de terópodes descrito na Formação de Morrison (América do Norte), uma combinação única de características que inclui: (i) trocânter menor do fémur baixo, relativamente à margem dorsal da cabeça femoral; (ii) crista tibiofibularis orientada obliquamente em relação ao áxis da diáfise femoral; (iii) presença de uma crista infrapopliteal na superfície posterior da parte distal do fémur; (iv) crista cnemial da tíbia bem desenvolvida; (v) côndilo medial da tíbia contínuo com a superfície proximal. Na descrição original de parte do exemplar de Valmitão (ML352) foram notadas algumas diferenças relativamente à espécie *Ceratosaurus nasicornis*, descrita na Formação de Morrison. Contudo, algumas dessas diferenças são compatíveis com variações individuais relacionadas, por exemplo, com ontogenia ou dimorfismo sexual. Os exemplares de Valmitão são, neste momento, indistinguíveis das formas norte-americanas, sendo atribuídos a *Ceratosaurus* aff. *nasicornis*.

O registo de Tetanurae do Jurássico Superior da Bacia Lusitânica é abundante e diversificado, incluindo exemplares interpretados como pertencendo a Megalosauroidea, Allosauroidea e Coelurosauria. Os megalossauroides estão representados por um conjunto de elementos do esqueleto craniano e pós-craniano recolhidos em diferentes locais, sobretudo na faixa costeira entre Torres Vedras e Caldas da Rainha. Alguns destes exemplares foram originalmente atribuídos à espécie *Torvosaurus tanneri* descrita na Formação de Morrison mas são, actualmente, interpretados como representando uma nova espécie exclusiva da Bacia Lusitânica: *Torvosaurus gurneyi*. Elementos do esqueleto axial atribuídos a megalossauroides, descritos neste trabalho, mostram diversas diferenças relativamente a *T. tanneri* mas não é possível verificar, neste momento, se correspondem a características de *T. gurneyi* ou se representam um táxon distinto, ainda não identificado no registo da Bacia Lusitânica. Por outro lado, alguns dentes isolados apresentam características compatíveis com megalossauroides não-megalossaurídeos e são interpretados, de forma preliminar, como pertencendo a um piatnitzkyssaurídeo estreitamente relacionado com *Marshosaurus*. Este conjunto de materiais indica uma maior diversidade de terópodes megalossauroides no Jurássico Superior da Bacia Lusitânica do que a conhecida com base em exemplares mais completos.

O registo de allossauroides do Jurássico Superior da Bacia Lusitânica inclui *Lourinhanosaurus*, *Allosaurus* e um conjunto de materiais inéditos com características compatíveis com o clado Carcharodontosauria. *Allosaurus* é, até ao momento, o táxon mais bem representado no Jurássico Superior da Bacia Lusitânica. Este táxon inclui um conjunto de elementos cranianos e pós-cranianos

descobertos em Praia de Vale Frades (Lourinhã), Andrés (Pombal) e Guimarota (Leiria). Um exemplar recolhido em Andrés foi originalmente atribuído à espécie *Allosaurus fragilis*, descrita na Formação de Morrison. Este exemplar foi proposto como a primeira evidência robusta da presença de *Allosaurus* fora da América do Norte e de uma espécie de dinossáurios representada no registo de dois continentes. Esta descoberta promoveu um intenso debate sobre as relações paleobiogeográficas das faunas de dinossáurios do Jurássico Superior de Portugal e da América do Norte. Posteriormente, a parte de um crânio recolhido em Praia de Vale Frades foi interpretado como pertencendo a uma espécie exclusiva da Bacia Lusitânica, *Allosaurus europaeus*. Os exemplares originalmente atribuídos a *A. fragilis* recolhidos em Andrés, juntamente com outros materiais inéditos do esqueleto craniano e pós-craniano, descobertos no mesmo local, são dificilmente distinguíveis desta espécie típica do registo norte-americano. Algumas diferenças observadas nestes exemplares relativamente a *A. fragilis* incluem: (i) ramo jugal do escamoso estende-se para a parte posterior ultrapassando o nível do processo pterigóide; (ii) concavidade bem desenvolvida na superfície posterolateral do supraoccipital, adjacente ao contacto com os processos paroccipitais; (iii) presença de dois forâmenes distintos para os ramos do nervo hipoglosso no interior da cavidade paracondilar para o XII nervo craniano; (iv) presença de processo naso-maxilar na superfície lateral do nasal; (v) comprimento do ramo anterior do lacrimal maior do que 65% da altura do ramo ventral. A análise filogenética do conjunto de material recolhido em Andrés posiciona estes exemplares como o grupo irmão das formas norte-americanas, *A. fragilis* e *A. "jimmadseni"*. Duas autapomorfias são indicadas nesta análise para os exemplares portugueses: (i) presença de processo naso-maxilar na superfície lateral do nasal e (ii) comprimento do ramo anterior do lacrimal maior do que 65% da altura do ramo ventral.

Allosaurus europaeus é considerada uma espécie válida mas uma revisão da diagnose é proposta com base no estudo do holótipo. A nova diagnose inclui as seguintes autapomorfias: (i) ausência de contacto entre o lacrimal e a maxila; (ii) extremidade ventral do postorbital estende-se até à margem inferior da órbita; (iii) margem posterior da maxila alta dorsoventralmente e bifurcada. Os exemplares de Andrés apresentam algumas diferenças relativamente ao holótipo de *A. europaeus*, nomeadamente em duas características interpretadas como autapomorfias para esta espécie: (i) lacrimal contacta a maxila e (ii) margem posterior da maxila afilada para a parte posterior. Contudo, com base no contexto paleobiogeográfico, optamos por identificar os exemplares de Andrés como pertencendo a *Allosaurus* cf. *europaeus* aguardando a descoberta de material mais completo que permita um melhor conhecimento desta espécie portuguesa.

Lourinhanosaurus antunesi é um táxon com posição filogenética instável. Originalmente descrito como um allossauroide, tem sido interpretado como pertencendo a diferentes clados, incluindo Megalosauridae, Metriacanthosauridae e Coelurosauria. A análise filogenética aqui apresentada identifica *Lourinhanosaurus* como um allossauroide mas com uma posição instável, sendo algumas vezes posicionado num grupo juntamente com *Allosaurus* e Carcharodontosauridae (representando o grupo irmão de Metriacanthosauridae) e outras vezes na base de Allosauroidea, numa politomia com os metriacanthossaurídeos. Com base nesta análise, *Lourinhanosaurus antunesi* é considerada uma espécie válida, caracterizada por duas autapomorfias: (i) comprimento dos centros das vértebras cervicais médias aproximadamente o dobro do diâmetro da faceta articular anterior e (ii) presença de forâmen obturador do púbis completamente fechado.

A descrição de dois exemplares inéditos (SHN.036 e SHN.019) recolhidos em sedimentos das formações de Praia da Amoreira-Porto Novo e de Freixial (Valmitão e Cambelas, respectivamente) indica a presença no Jurássico Superior português de um grupo de allossauroides mais derivados, estreitamente relacionados com o clado Carcharodontosauria. A seguinte combinação de características indica uma relação de parentesco de SHN.036 com Carcharodontosauria: (i) ausência de quilha ventral

nas vértebras dorsais anteriores; (ii) presença de lâmina lateral bem desenvolvida na base do arco neural das vértebras da secção media e posterior da cauda; (iii) presença de lâmina espinoprezigapofiseal nas vértebras caudais médias que se estende desde a superfície medial da base da pré-zigapófise; (iv) presença de uma lâmina centrodiapofiseal baixa mas bem definida, associada a uma fossa centroprezigapofiseal superficial nas vértebras caudais médias; (v) presença de uma crista ventral bem desenvolvida nos centros caudais anteriores; (vi) comprimento anteroposterior da expansão distal do púbis maior do que 60% do comprimento da diáfise; (vii) superfície articular ilíaca do ísquio côncava; (viii) pedúnculo para o púbis orientado ventralmente.

Este estudo permitiu identificar representantes de clados previamente não reconhecidos, incluindo megalossauroides não-megalossaurídeos e possíveis carcharodontossáurios. Estes novos exemplares indicam uma maior diversidade na fauna de terópodes do Jurássico Superior da Bacia Lusitânica que a conhecida anteriormente. Geograficamente, o registo de terópodes ceratossaurianos está restrito à Sub-bacia da Consolação. Exemplares identificados como pertencendo a estes terópodes primitivos foram recolhidos em depósitos formados em sistemas meândricos distais da Formação de Praia da Amoreira-Porto Novo (Kimmeridgiano superior). Contudo, alguns dentes isolados atribuídos a *Ceratosaurus* indicam uma distribuição geográfica e estratigráfica mais ampla deste táxon, entre o Kimmeridgiano superior e o Tithoniano. Os megalossauroides estão representados nas sub-bacias de Consolação e de Bombarral-Alcobaça. Exemplares atribuídos a *Torvosaurus* são provenientes, maioritariamente, de depósitos fluviais da Formação de Praia da Amoreira-Porto Novo. Contudo, escassos dentes isolados foram também encontrados em depósitos de transição da Formação de Alcobaça (Kimmeridgiano-Tithoniano inferior). Os allossauroides são os terópodes com distribuição geográfica e estratigráfica mais ampla na Bacia Lusitânica. Este clado está representado nas sub-bacias de Consolação, Bombarral-Alcobaça e Turcifal. Exemplares atribuídos a allossauroides são provenientes das formações de Alcobaça, Praia da Amoreira-Porto Novo, Sobral, Freixial e Bombarral, representando um intervalo de tempo entre o Kimmeridgiano e o final do Tithoniano. Jazidas com elementos atribuídos a este clado correspondem a depósitos de paleoambientes fluviais, marinhos superficiais e salobros. Finalmente, o único táxon conhecido actualmente de terópodes coelurossáurios está restrito à Sub-bacia de Bombarral-Alcobaça e estratigraficamente, a níveis do Kimmeridgiano–Tithoniano inferior da Formação de Alcobaça. Contudo, dentes isolados atribuídos a este clado indicam uma maior diversidade e mais ampla distribuição geográfica e estratigráfica destes terópodes.

A fauna de terópodes do Jurássico Superior da Bacia Lusitânica é semelhante às conhecidas em níveis correlativos da Formação de Morrison, sendo maioritariamente composta por taxa partilhados com o registo norte-americano. Contudo, apesar desta semelhança, os terópodes da Bacia Lusitânica e da Formação de Morrison representam formas distintas, o que indica evolução vicariante destas faunas. Estes processos de vicariância poderão ter-se manifestado de diferentes formas nas distintas espécies, o que explicaria a maior afinidade das faunas de terópodes nestes territórios, relativamente a outros grupos de dinossáurios, como por exemplo os saurópodes, e de outros vertebrados. Por outro lado, a presença no registo português de clados que aparentemente estão ausentes na Formação de Morrison pode indicar padrões de extinções regionais e de restrições ambientais.

Palavras-chave: Jurássico Superior, Bacia Lusitânica, Theropoda, Filogenia, Paleobiogeografia.

FIRST PART

CHAPTER 1: INTRODUCTION

1.1. Definition and historical review of the Theropoda clade

1.2. The knowledge of Upper Jurassic theropods from the Lusitanian Basin

1.3. Geological framework of the Upper Jurassic fossil record of theropod dinosaurs from the Lusitanian Basin

CHAPTER 2: OBJECTIVES AND HYPOTHESES

2.1. Objectives and hypotheses

CHAPTER 3: MATERIALS AND METHODS

3.1. Materials

3.2. Methods

CHAPTER 1: INTRODUCTION

1.1. DEFINITION AND HISTORICAL REVIEW OF THE THEROPODA CLADE

Theropoda is a group of dinosaurs that were predominantly carnivorous, but also includes several omnivore and even herbivore forms. This is one of the most diverse groups of dinosaurs, including the smallest non-avian dinosaurs, such as *Compsognathus*, the largest land predators, such as *Tyrannosaurus*, *Giganotosaurus*, and *Carcharodontosaurus*, and the gracil ornithornimids or the bizarre therizinosaurs.

The first non-avian dinosaur to be validly named, *Megalosaurus*, was proposed in 1824 by William Buckland, based on some fossil remains of theropod dinosaurs, including a jaw fragment, vertebrae, ribs, an ilium, a pubis, and a femur, from the Middle Jurassic Stonesfield Slate of Oxfordshire. In 1866, Edward Cope divided the Dinosauria in three suborders: Orthopoda (armored and duck-billed dinosaurs), Goniopoda (carnivorous dinosaurs), and Symphypoda (small carnivorous dinosaurs and gigantic swamp-dwelling dinosaurs later, in 1883, separated in two different suborders: Hallopoda for the small carnivorous and Opisthocoela for the gigantic dinosaurs). On the other hand, Othniel Charles Marsh proposed, in 1878, a different classification system for Dinosauria, based on specimens collected in Como Bluff, Wyoming. Marsh defined the Sauropoda as "A well marked group of gigantic dinosaurs… [which] differ so widely from typical Dinosauria, that they belong rather in a suborder, which may be called Sauropoda, from the general character of the feet" (Marsh 1878, p. 412). Subsequently, in 1881, Marsh presented an outline classification of the dinosaurs in which he considered four suborders (beyond the genus *Hallopus* and *Coelurus*, which he placed in the two suborders of uncertain definition Hallopoda and Coeluria, respectively). Marsh separated the armored and the duck-billed dinosaurs (included in the Orthopoda of Cope), in the Stegosauria and Ornithopoda, respectively and placed the carnivorous dinosaurs (divided between the Goniopoda and Symphypoda of Cope) into a single "Suborder Theropoda (Beast foot). Carnivorous" (Marsh 1881, p. 423).

Theropoda (*sensu* Marsh 1881) included the Allosauridae, represented by the genera *Allosaurus*, *Creosaurus* and *Labrosaurus*. In subsequent papers, Marsh (1882, 1884) included the Megalosauridae (*Megalosaurus* = *Poikilopleuron*, *Allosaurus*, *Coelurosaurus*, *Creosaurus*), Ceratosauridae (*Ceratosaurus*), Labrosauridae (*Labrosaurus*), Zanclodontidae (*Zanclodon* and ?*Teratosaurus*), Amphisauridae (*Amphisaurus* = *Megadactylus*, ?*Bathygnathus*, *Clepsysaurus*, *Palaeosaurus*, *Thecodontosaurus*), Dryptosauridae (*Dryptosaurus* = *Laelaps*), Coeluridae (*Coelurus*), Compsognathidae (*Compsognathus*), and Hallopodidae (*Hallopus*). In this interpretation, Theropoda included animals that are currently interpreted as theropods, prosauropods and the genus *Hallopus*, which is considered a crocodylomorph (Walker 1970; Benton 1986; Rauhut 2003a).

H. G. Seeley recognized, in 1888, that the dinosaurs are members of two distinct orders defined on the basis of different osteological features. Seeley named these two major taxonomic categories the Saurischia and the Ornithischia based on the structure of the pelvis. With the acceptance of this division it was quite apparent that the Theropoda and the Sauropoda should be included within the Saurischia. This interpretation was generally accepted and followed in subsequent works for more than a century. Recently, it was proposed that this hypothesis of dinosaur phylogeny could be inaccurate considering Saurischia (sauropodomorphs + theropods) as a non-monophyletic group, with theropods closer to ornithischians than to sauropodomorphs (Baron et al. 2017, see Langer et al. 2017 for a different interpretation).

The phylogeny of Theropoda has been of great scientific interest, especially since the discovery of the relationships between extant birds and extinct theropod dinosaurs. This discovery changed our view about the history of life because not only did dinosaurs survive the Cretaceous-Tertiary extinction event, but a particular lineage of theropods is now the most diverse group of extant tetrapods (Rauhut 2003a).

Some of the most important phylogenetic studies of theropod dinosaurs in the first half of the twentieth century were carried out by von Huene (1914, 1926, 1928, 1932), Matthew (1915), and Matthew and Brown (1922). Huene regarded the Theropoda as an unnatural group and divided the Saurischia into two suborders: the Coelurosauria and the Pachypodosauria (Huene 1914). The Coelurosauria included mainly small and hollow-boned carnivorous dinosaurs, while the Pachypodosauria included large and heavy carnivores and sauropodomorphs (Colbert 1964). Huene in this classification abandoned the concept of Theropoda as originally proposed by Marsh, removing some of the larger theropods from a position contiguous to their small relatives and associating them to the sauropods. This interpretation was based on the erroneous association of cranial remains (teeth) of carnivorous Triassic archosaurs with prosauropod postcranial material (Galton 1985; Benton 1986; Rauhut 2003a). At the same time, Matthew and Brown (1922) based on the study of collections of the American Museum recovered the Deinodontidae proposed by Cope (1866) to include *Deinodon* (= *Gorgosaurus* and *Albertosaurus*), *Dryptosaurus*, and *Tyrannosaurus* (=*Dynamosaurus*). These authors noted that the deinodonts, "although paralleling the megalosaurs in their size, massive proportions, short neck and large head, differ from them and resemble the coelurids and ornithomimids in the construction of the pelvis and the elongate quadrate" (Matthew and Brown 1922, p. 375). Based on these observations, they proposed that this group was not derived from the megalosaurs as was generally considered at that time, but from some primitive coelurosaurian theropods.

Since the 1960 decade, abundant new discoveries and new phylogenetic techniques allowed a great progress in the knowledge of theropod relationships. Colbert (1964) noted significant similarities in the pelvis of carnosaurs and coelurosaurs and therefore rejected the classification proposed by von Huene, arguing for a monophyletic Theropoda clade characterized by "dolichoiliac forms in which locomotion was exclusively bipedal", whereas the Prosauropoda was defined as including "brachyiliac forms in which locomotion was largely bipedal, but to some extent quadrupedal" (Colbert 1964, p. 17). Within Theropoda, Colbert distinguished two infraorders: the Coelurosauria, to include small theropods, and the Carnosauria, to include the large taxa. Although this mainly size-dependent distinction seems rather arbitrary, both clades were interpreted as monophyletic by Colbert (1964) and subsequent authors (e.g. Charig et al. 1965; Romer 1966; Steel 1970). The discovery of the dromaeosaurid *Deinonychus antirrhopus* Ostrom 1969 and of the ornithomimosaurian *Deinocheirus* Osmolska and Roniewicz 1969, which does not fit within either of the two infraorders led to new interpretation of theropod systematics.

The phylogenetic relationships of the Dinosauria, in general and of the Theropoda in particular, have been substantially improved as result of cladistics studies. Thulborn (1984) was the first to publish a detailed cladistic analysis of theropod interrelationships, in an attempt to resolve the phylogenetic position of *Archaeopteryx*. His results deeply differentiated from previous hypotheses. The carnosaurians Allosauridae and Tyrannosauridae were widely separated and related with taxa that were at that time interpreted as belonging to Coelurosauria (Fig. 1.1.1A). Thulborn regarded *Archaeopteryx* not as the most basal bird, but as a more basal non-avian theropod arguing that modern birds are not more closely related to *Archaeopteryx* than they are to several theropod dinosaurs. Some years later, the pioneering phylogenetic work of Gauthier (1986) recognized a basal dichotomy within Theropoda between a group termed Ceratosauria and a group he named Tetanurae (Fig. 1.1.1B). According to this interpretation, Ceratosauria included taxa that were formerly regarded as coelurosaurs, as well as some taxa that were traditionally regarded as carnosaurs. Within Tetanurae, Gauthier found another dichotomy between carnosaurs and coelurosaurs. Carnosauria (*sensu* Gauthier 1986) included *Allosaurus* and *Acrocanthosaurus* and the Tyrannosauridae. The ornithomimids were regarded as the most basal coelurosaurs and the sister-group to a clade named Maniraptora, which included a basal polytomy of several genera and clades, including oviraptorosaurs, the Deinonychosauria (dromaeosaurids + troodontids), and its sister-group Avialae (including birds). This phylogenetic scheme became widely accepted in following years.

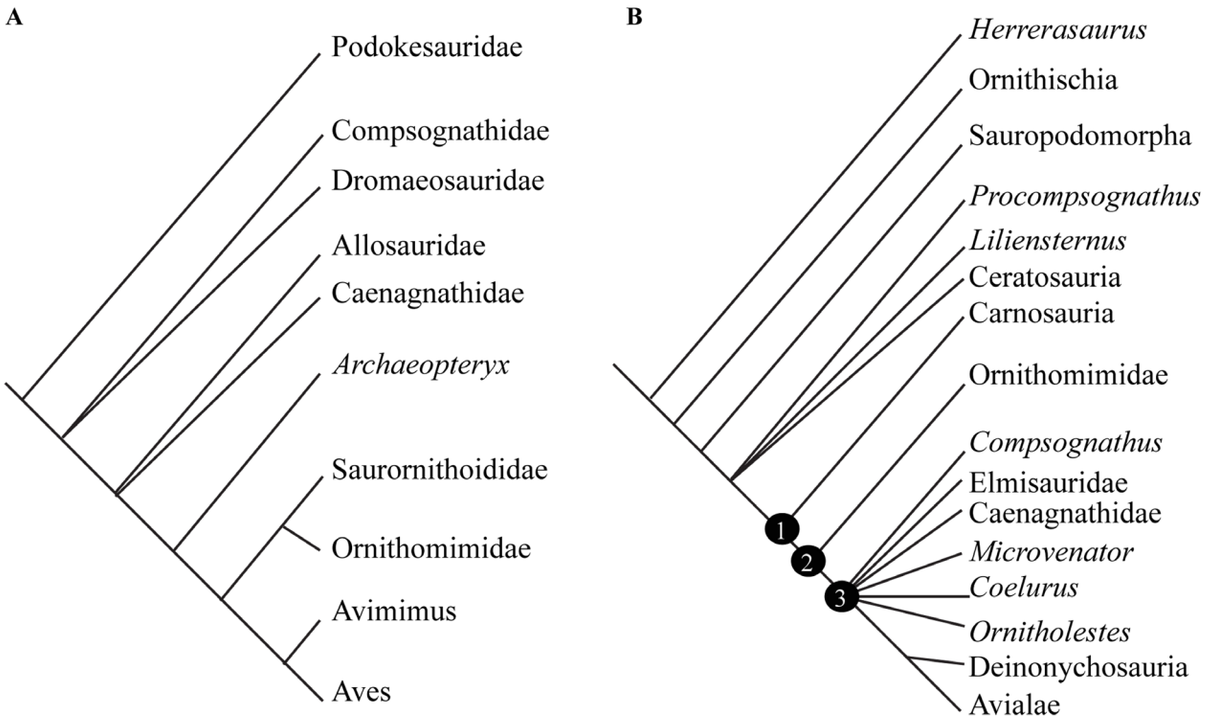

Figure 1.1.1. Early cladistic hypotheses of the phylogeny of theropod dinosaurs. (A) Thulborn (1984); (B) Gauthier (1986). Legend: 1- Tetanurae, 2- Coelurosauria, 3- Maniraptora.

In a new cladistic analysis, Novas (1992) argued for carnosaur polyphyly and included the tyrannosaurids in the Coelurosauria (Fig. 1.1.2A). Furthermore, Novas included the abelisaurids in the Ceratosauria, as the sister-group to *Ceratosaurus*. This hypothesis was followed by Pérez-Moreno et al. (1993) who, additionally, proposed a sister-group relationship between tyrannosaurids and ornithomimids. Other cladistics analysis of theropods was proposed by Holtz (1994) focusing the phylogenetic position of Tyrannosauridae. Holtz followed Novas (1992) and Pérez-Moreno et al. (1993) in the interpretation of tyrannosaurids as members of Coelurosauria and the sister-group of ornithomimosaurs and troodontids. According to this analysis, troodontids, ornithomimosaurs, tyrannosaurids, elmisaurids (=caenagnathids), and *Avimimus* share a derived condition of the metatarsus forming a monophyletic clade termed Arctometatarsalia. Within this clade, troodontids represented the sister-group to ornithomimosaurs. Oviraptorids were regarded as the sister-group to Arctometatarsalia, and a bird+dromaeosaurid clade as the sister-group to all of these coelurosaurs. Within more basal tetanuran theropods, *Torvosaurus*, *Megalosaurus*, and allosaurids were interpreted as successively more closely related outgroups to coelurosaurs.

In a more detailed analysis of basal tetanurans, Sereno et al. (1996) and Sereno (1997, 1999) proposed two monophyletic clades, the Spinosauroidea and the Allosauroidea, which formed successively closer outgroups to Coelurosauria (Fig. 1.1.2B). Spinosauroidea included the Spinosauridae, Torvosauridae and *Afrovenator*, while the Allosauroidea included *Cryolophosaurus*, *Monolophosaurus*, *Allosaurus*, Sinraptoridae and Carcharodontosauridae. These analyses also found a monophyletic Deinonychosauria clade, including troodontids and dromaeosaurids, as the sister-group to birds as was proposed by Gauthier (1986). Oviraptorosaurs and tyrannosaurids were regarded as successively closer outgroups to this clade, which was termed Paraves by Sereno (1998).

More extensive analyses of theropod phylogeny were later published by Holtz (2000) and Rauhut (2003a). In the analyses proposed by Holtz (2000), the spinosaurids, *Megalosaurus*, *Eustreptospondylus*, *Torvosaurus*, *Piatnitzkysaurus*, and *Afrovenator* were found as successively closer outgroups to Avetheropoda, including Allosauroidea and Coelurosauria (Fig. 1.1.3). The major difference of the results

recovered by Rauhut (2003a) relative to those of Holtz (2000) is in the interpretation of the relationships among basal tetanurans. The analysis of Rauhut (2003a) indicates a monophyletic Carnosauria, which includes two monophyletic clades, the Spinosauroidea and the Allosauroidea as was previously proposed by Sereno et al. (1996, 1998) and Sereno (1997, 1999).

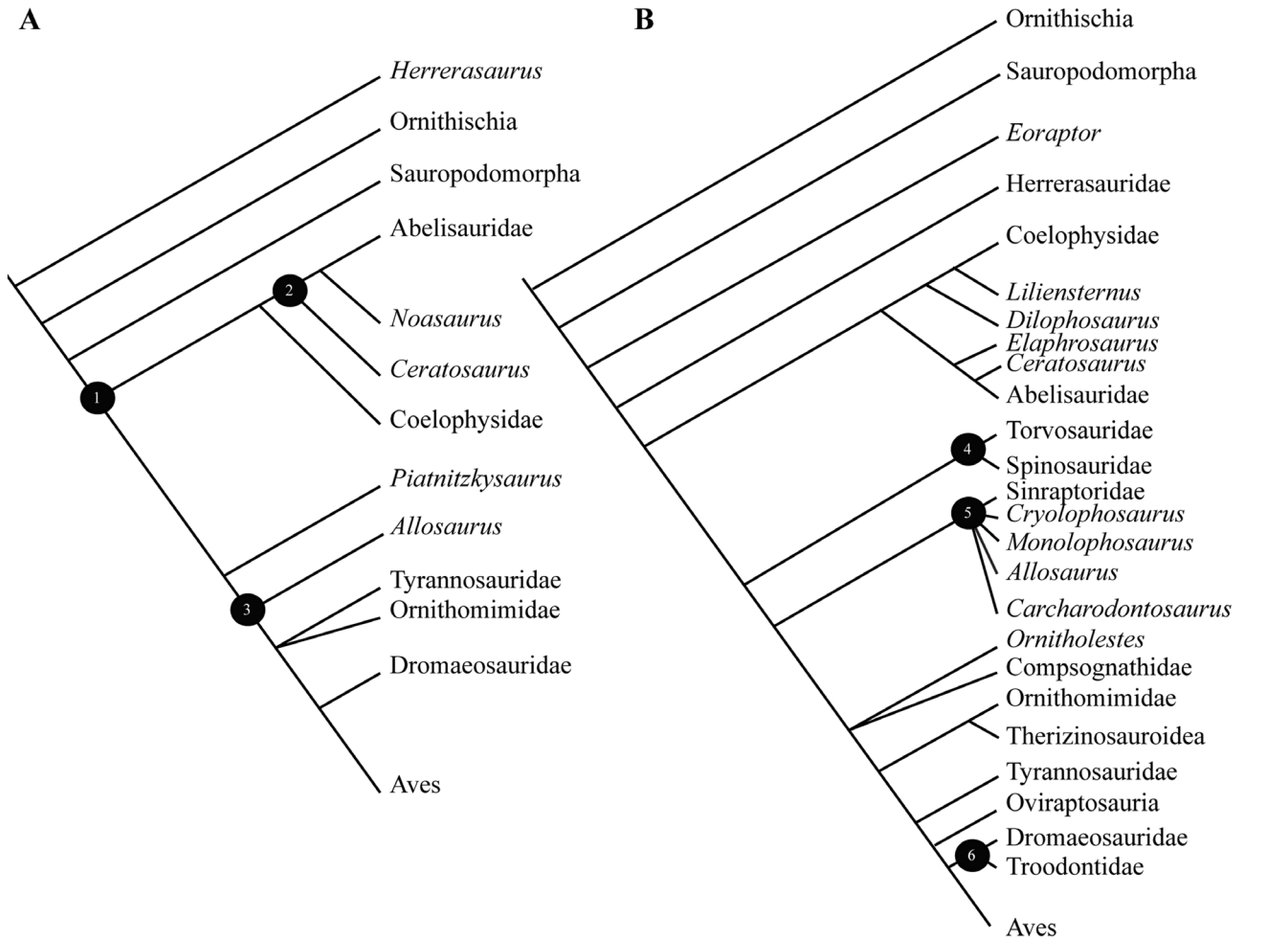

Figure 1.1.2. Cladistic hypotheses of the phylogeny of theropod dinosaurs. (A) Novas (1992); (B) Sereno (1997). Legend: 1- Theropoda, 2- Neoceratosauria, 3- Tetanurae, 4- Spinosauroidea, 5- Allosauroidea, 6- Deinonychosauria.

Some reinterpretations in the taxonomic content of some theropod clades have been proposed more recently, including the phylogenetic analysis of Ceratosauria (Carrano and Sampson 2008), Tetanurae (Carrano et al. 2012), Megalosauroidea (Benson 2010), Allosauroidea (Brusatte and Sereno 2008), Neovenatoridae (Benson et al 2010), and Coelurosauria (Senter 2007). Ceratosauria is a clade of basal theropods traditionally interpreted as the sister group of Tetanurae, including coelophysoids, Ceratosaurus, and Abelisauridae (e.g. Gauthier 1986; Bonaparte 1991; Novas 1992). More recent analyses (e.g. Rauhut 2003a; Carrano and Sampson 2008) suggested an alternative definition for Ceratosauria considering these theropods more closely related to tetanurans than to coelophysoids. Tetanurae represents the majority of theropod dinosaur diversity and the lineage leading to extant birds. The extensive analysis developed by Carrano et al. (2012) allowed a significant improvement of the phylogenetic resolution within Tetanurae. Their results position several 'stem' taxa to a succession of monophyletic clades: Megalosauroidea, Allosauroidea and Coelurosauria.

Since the description of the first remains assigned to *Megalosaurus* by William Buckland, in 1824, many incomplete or indeterminate specimens from different Mesozoic strata, have since been referred to the Megalosauridae. During several years this was a poorly understood clade that included several distinct theropod and non-theropod dinosaur specimens. The phylogenetic analysis focusing on basal

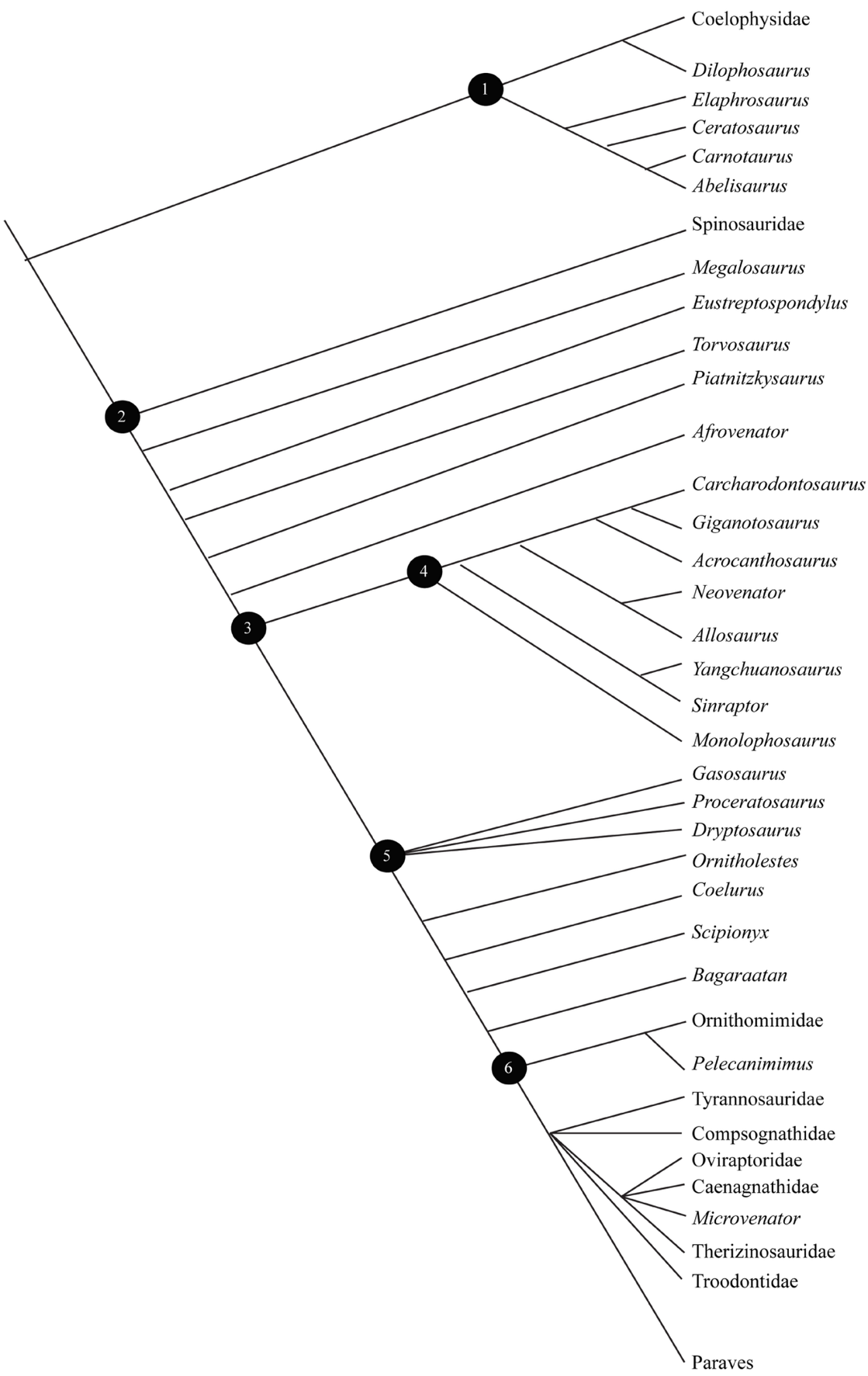

Figure 1.1.3. Cladistic hypothesis of the phylogeny of theropod dinosaurs proposed by Holtz (2000). Legend: 1- Ceratosauria, 2- Tetanurae, 3- Avetheropoda, 4- Carnosauria, 5- Coelurosauria, 6- Maniraptoriformes.

tetanuran relationships performed by Benson (2010) allowed a redefinition of *Megalosaurus* as a valid taxon and a better understand of the Megalosauroidea clade. Based on this analysis Megalosauroidea (= Spinosauroidea *sensu* Allain 2001; Sereno 1997) includes two clades basal to the traditional content of Megalosauridae + Spinosauridae, which comprise *Xuanhanosaurus* (Middle Jurassic, China, considered a metriacanthosaurid allosauroid by Carrano et al. (2012)), *Marshosaurus* (Upper Jurassic, USA), *Condorraptor* + *Piatnitzkysaurus* (Middle Jurassic, Argentina) and *Chuandongocoelurus* + *Monolophosaurus* (Middle Jurassic, China).

Allosauroidea has been the subject of extensive phylogenetic studies, but several incongruities are found in the relationships of several taxa. The phylogenetic analysis of Brusatte and Sereno (2008) argued for the placement of *Sinraptor* as a basal allosauroid, instead as more derived than *Allosaurus* as was previously proposed (e.g. Allain 2002; Currie and Carpenter 2000; Novas et al. 2005). *Neovenator* is considered as a basal member of Carcharodontosauridae and *Acrocanthosaurus* as a more derived member of Carcharodontosauridae, rather than the sister taxon of *Allosaurus* as sometimes suggested (e.g. Allain 2002; Currie and Carpenter 2000). Later, Benson et al. (2010) proposed that some allosauroid taxa, including *Aerosteon* (Upper Cretaceous Argentina), *Australovenator* (Upper Cretaceous, Australia), *Fukuiraptor* (Lower Cretaceous, Japan), and *Neovenator* (Lower Cretaceous, UK) form a diverse and globally distributed new clade named Neovenatoridae. This clade also includes other enigmatic theropods such as *Chilantaisaurus* (Upper Cretaceous, China), *Megaraptor* (Upper Cretaceous, Argentina), and *Orkoraptor* (Upper Cretaceous, Argentina) that form the Megaraptora. More recently, a different interpretation was proposed by Novas et al. (2013) for the Gondwanan megaraptorans. These authors proposed that the megaraptorans are more closely related with Coelurosauria than with Allosauroidea.

1.2. THE KNOWLEDGE OF UPPER JURASSIC THEROPODS FROM THE LUSITANIAN BASIN

The first paleontological works on Mesozoic vertebrates from Portugal were associated with the activities of the geological commission ("Comissão Geológica do Reino"). The first record of osteological dinosaur remains in these levels dates from 1863 and is attributed to the geologist Carlos Ribeiro. These remains consist of some isolated theropod teeth found among the material collected during prospection works in Upper Jurassic sediments on the littoral of Lourinhã. These teeth are labeled as coming from "Coupe du Vale do Portinheiro à Carrasqueira" (Fig. 1.2.4), near Porto Dinheiro (Lourinhã) and were described by Lapparent and Zbyszewski (1957) that assigned them as belonging to *Megalosaurus*.

Figure 1.2.4. Theropod teeth found by Carlos Ribeiro in 1863, which corresponds to the first osteological record of dinosaurs from Portugal. These specimens were described by Lapparent and Zyswewsli (1957; PL XII, Fig. 6 and 17) and assigned to (A) *Megalosaurus pombali* and (B) *Megalosaurus*. (C) original label of the specimen. Currently these specimens are housed in the collections of the MUHNAC. Scale bar (A): 50 mm; (B): 10 mm.

Later, the creation of the "Serviços Geológicos de Portugal", in 1918, which main objective was the geological mapping of the country, promotes an intense activity about the record of Mesozoic vertebrates. In these activities, later continued by the "Instituto Geológico e Mineiro", were involved mainly Swiss and French researchers, including Paul Choffat, Henri Émile Sauvage, Albert F. de Lapparent and the French-Russian geologist and paleontologist George Zbyszewski.

P. Choffat was named responsible for the study of the Mesozoic terrains of Portugal in 1883 by Nery Delgado, at that time the director of the geological works section. He established the first stratigraphic nomenclature for several Mesozoic units and in collaboration with Nery Delgado published the second Geological Chart of Portugal in 1899, which replaced the one published by Carlos Ribeiro and Nery Delgado in 1876. Choffat was also responsible for the publication of several regional charts, including those of Leiria, Arrábida, Buarcos and Montejunto. To study paleontological collections, Choffat maintained contacts with some of the most eminent European researches, such as the French zoologist and paleontologist H. É. Sauvage. Sauvage published the first study about the fossil record of vertebrates from the Mesozoic of Portugal (Sauvage 1897-98) based on a collection sent by Choffat. In this publication, Sauvage identified several osteological remains of dinosaurs (including theropods, sauropods, and iguanodontids) and other vertebrates, including fishes, anurans, chelonians, ichthyopterygians, mosasaurids, and crocodylomorphs collected in Upper Jurassic and Lower and Upper Cretaceous sediments.

Among the fossils described by Sauvage are some isolated teeth of theropod dinosaurs collected in Upper Jurassic levels, near Pombal, assigned as *Megalosaurus insignis*, in the Lower Cretaceous of Boca do Chapim identified as *Megalosaurus* aff. *superbus*, and in Upper Cretaceous strata, in the region of Coimbra, assigned to *Megalosaurus* sp. (Sauvage 1897-98). Sauvage also described a new specimen of a sauropod dinosaur named *Morosaurus marchei* based on a tooth and a caudal vertebra (Sauvage, 1897-98; pl. IV, Fig. 6–8) collected in Upper Jurassic sediments near Ourém. The caudal vertebra belongs to a theropod dinosaur as was recognized by Lapparent and Zbyszewski (1957) who assigned this specimen to *Megalosaurus insignis*. The specimens interpreted as belonging to a new species of a crocodile *Suchosaurus girardi* Sauvage 1897-98, which includes two jaw fragments with teeth (Sauvage, 1897-98; pl. IV, Fig. 4–5) and an isolated tooth (Sauvage, 1897-1898; pl. V, Fig. 6; see Fig. 5 below) collected at the locality of Boca do Chapim were later reinterpreted and assigned to the spinosaurid theropod *Baryonyx* (Buffetaut, 2007).

Figure 1.2.5. Isolated tooth described by Sauvage (1897-98) as part of the holotype of *Suchosaurus girardi* and currently attributed to the spinosaurid theropod *Baryonyx* in lateral (A) and medial (B) views; (C) original label of the specimen (MNHN/UL.I.F2.176) currently housed in the collections of the MUHNAC. Scale bar: 10 mm.

Other important contribution for the knowledge of the record of dinosaurs in Portugal was made by Jacinto Pedro Gomes. This engineer and naturalist collaborated, since 1883, with the Museu Mineralógico e Geológico (MMG) da Escola Politécnica in the study of different collections housed in the MMG. He

was also consulting engineer of the Cabo Mondego coal mine (Buarcos, Figueira da Foz) and in 1884 one of the company directors informed him about the discovery of curious marks in some sedimentary strata in the area of the mine. Gomes identified these marks as dinosaur footprints and collected them to the MMG. The notes of J.P. Gomes about these footprints were published in 1916, after his dead, in the first work on dinosaur ichnofossils from Portugal (Gomes 1916).

Since 1942, G. Zbyszewski conducted a series of systematic paleontological prospections in Upper Jurassic units on the littoral of the Lusitanian Basin, mainly between Foz do Arelho (Caldas da Rainha) and Santa Cruz (Torres Vedras). As result of these works, Zbyszewski identified a partial skeleton of a dinosaur in Pedras Muitas (Baleal, Peniche) as belonging to the stegosaur *Omosaurus* (currently synonym of *Dancentrurus*) (Zbyszewski 1946). However, it was the collaboration with A. F. de Lapparent that produced a series of works about the record of dinosaurs from the Lusitanian Basin, which were compiled in the first monograph about dinosaurs from Portugal (Lapparent and Zbyszewski 1957). Several new specimens of different dinosaur groups, including theropods, sauropods, ornithopods, and stegosaurians were described in this publication. The theropod material described by Lapparent and Zbyszewski (1957) includes mainly isolated teeth, vertebrae, some ungueal phalanges and fragments of the appendicular skeleton collected in different localities from: (i) Upper Jurassic, mostly on the littoral of the Lusitanian Basin (Caldas da Rainha and Lourinhã) and in the northern sector near Pombal and Ourém; (ii) Lower Cretaceous of Boca do Chapim; and (iii) Upper Cretaceous of Viso (Montemor o Velho). All the theropod specimens were assigned as belonging to *Megalosaurus* at that time a poorly understood taxon that included some material from the Middle Jurassic of Stonesfield (Oxfordshire, UK), but also several other fossils from different ages worldwide (Benson 2008, 2010; Carrano et al. 2012; Rauhut et al. 2016). A new theropod species *Megalosaurus pombali* Lapparent and Zbyszewski 1957 was proposed based on three isolated teeth collected in "Vale de Portinheiro" (corresponding to the specimen collected by Carlos Ribeiro), Ribamar (Lourinhã), and Pombal. These teeth were considered distinct from those of *Megalosaurus insignis* described by Sauvage (1874) and Lapparent (1943) based on the following features: (i) larger size; (ii) less lateral compression of the crown; and (iii) position of the carinae on the distal and mesial surfaces (Lapparent and Zbyszewski 1957; p. 25 and PL. XXVIII). Lapparent and Zbyszewski (1957) also assigned some isolated dorsal and caudal vertebrae collected in Porto das Barcas, Torrinhas (Batalha) and possibly Albergaria dos Doze (Pombal) to this new species. Most of these vertebrae, with the exception of the caudal vertebrae from Torrinhas, are currently interpreted as belonging to non-theropod dinosaurs, mostly to sauropods (Mateus 2005; Mocho 2016; Mocho et al. 2016) (Fig. 1.2.6).

Figure 1.2.6. Anterior caudal vertebra from Porto das Barcas described by Lapparent and Zbyszewski (1957) and assigned to the new species *Megalosaurus pombali*. This specimen is currently interpreted as belonging to a sauropod dinosaur (Mocho 2016). (A) Drawing published by Lapparent and Zbyszewski (1957); (B) anterior view of the specimen currently housed in the collections of the MUHNAC; (C) original label of the specimen. Scale bar: 50 mm.

Other specimens from the Upper Jurassic were assigned to *Megalosaurus insignis*, which is a species described by Eudes-Deslongchamps and Lennier (1870) based on an isolated tooth found near Cap de La Hève in Normandy. This species is currently considered a nomen dubium and the tooth from Normandy is attributed to an indeterminate theropod (Carrano et al. 2012). Most of the specimens from the Upper

Jurassic of the Lusitanian Basin previously assigned to *Megalosaurus insignis* are currently assigned to other dinosaur groups (Mateus 2005; Mocho 2016). This is the case of an articulated series of five anterior caudal vertebrae (Lapparent and Zbyszewski 1957: Fig. 4, p. 24; see Fig. 1.2.7 below) associated with two additional articulated caudals from Praia da Areia Branca. These specimens have been more recently tentatively related to a teleosaurian crocodyliform (Chabli 1986; Carrano et al 2012). However, the morphology of the vertebrae indicates that they probably belong to an ornithopod dinosaur (Escaso et al. 2017). Finally, a fragment of a tooth collected in the Lower Cretaceous of Boca do Chapim was assigned to *Megalosaurus superbus* and some small teeth and ungueal phalanges found in Upper Cretaceous sediments near Viso were tentatively identified as belonging to *Megalosaurus* cf. *pannoniensis*.

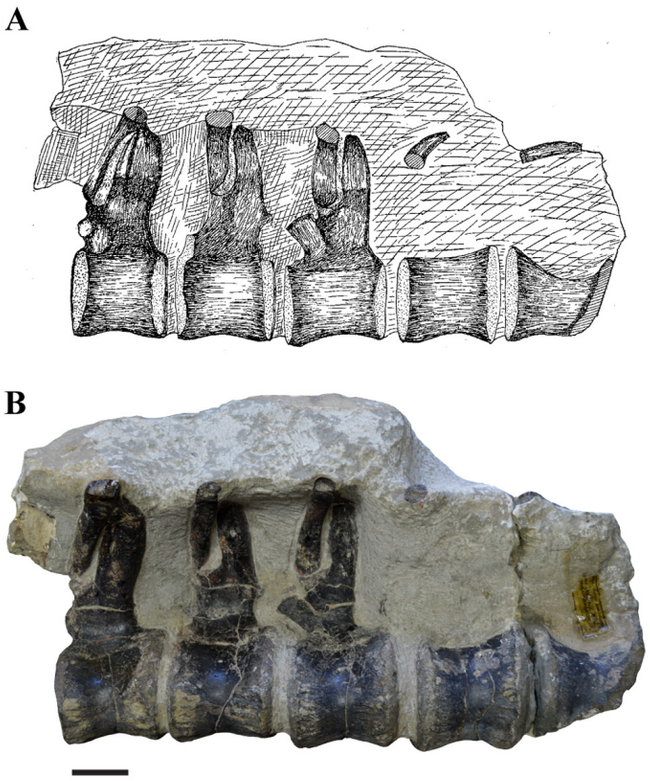

Figure 1.2.7. Articulated series of anterior caudal vertebrae from Praia da Areia Branca described by Lapparent and Zbyszewski (1957) and identified as belonging to *Megalosaurus insignis*. (A) Drawing of the specimen; (B) right lateral view of the specimen currently housed in the collections of the MUHNAC. Scale bar: 50 mm.

Since 1950, German paleontologists of the Institut für Paläontologie of the Freie Universität Berlin, including Walter Kühne and Bernard Krebs, performed paleontological researches in the Mesozoic of the Iberian Peninsula. Kühne and their students first worked in Spain and later extended the paleontological prospections to several areas in Portugal. From 1973 to 1982 they worked in the Guimarota mine exclusively for paleontological purposes, which was one of the most ambitious enterprises in the history of paleontology in Portugal. Thanks to these works a great amount of fossils of a diverse fauna of vertebrates was recovered. This fossil site is especially relevant due to the record of early mammals. It was yielded about 7000 isolated mammalian teeth, and about 800 identifiable jaws and other skull fragments of mammals belonging to docodonts, multituberculates, and holotherians (Martin 2000). In addition, among the abundant fossils collected in Guimarota also identified was a diverse fauna of dinosaurs represented mostly by isolated elements belonging to ornithischians, sauropods, and theropods (Thulborn 1973; Zinke 1998; Rauhut 2001).

The theropod record currently known from the Guimarota fossil site includes a partial pelvic girdle described as the type specimen of the basal tyrannosauroid, *Aviatyrannis jurassica* Rauhut 2003b, a small maxilla interpreted as belonging to a hatchling individual of *Allosaurus* (Rauhut and Fechner 2005), and a

geat diversity of other theropod goups represented mainly by isolated teeth. Especially abundant are teeth identified to small theropods belonging to Coelurosauria, including compsognathids, dromaeosaurines, velociraptorines, troodontids, and possibly *Richardoestesia* and *Paronychodon* (Zinke and Rauhut 1994; Zinke 1998). *Archaeopteryx* is also reported in Guimarota based on a single tooth (Weigert 1995), but this specimen was more recently considered distinct from this early avian taxon and possibly representing a yet undescribed non-avian theropod (Elzanowski 2002; Louchart and Pouech 2017). Due to the abundant fossil record and to the diversity of fauna identified, the Guimarota mine is one of the most relevant fossil sites for the study of Late Jurassic mammals and other small vertebrates.

During the second half of the twenty century an increase in the scientific interest on the fossil record of vertebrates from the Lusitanian Basin is registered by the abundant publications produced by national and international researchers. Since approximately the end of the 1970 decade, studies on the Portuguese dinosaur record have been developed mainly by research teams associated to the Universidade Nova de Lisboa and to the Museu Nacional de História Natural da Universidade de Lisboa. From these decades highlights the works of the Portuguese paleontologist Miguel Telles Antunes about the record of dinosaurs from the Upper Cretaceous of the Lusitanian Basin. Since the end of the 1970 decade, Antunes studied and collected in several fossil sites from the end of the Cretaceous, including Aveiro, Viso (Montemor o Velho), and Taveiro (Coimbra). The record of dinosaurs found in these sites consists mainly on isolated teeth, some vertebrae and phalanges (Antunes and Pais 1978; Antunes and Sigogneau-Russell 1991, 1992, 1995, 1996; Galton 1994). The theropod dinosaurs are represented by few specimens assigned mostly to small coelurosaurians, including indeterminate coelurosaurians, troodontids and dromaeosaurids. Based on some isolated teeth collected in Taveiro, Antunes and Sigogneau-Russell (1991) proposed the new species *Euronychodon portucalensis*, currently interpreted as a junior synonym of *Paronychodon* (Rauhut 2002).

This intense scientific activity and the media impact of the new discoveries promoted the creation of some local institutions such as the Grupo de Etnologia e Arqueologia da Lourinhã - Museu da Lourinhã and the Sociedade de História Natural (Torres Vedras), which have had an important role both in the research activities and in the diffusion of the results. Among the abundant discoveries of theropod dinosaurs made in the last decade of the 20th and beginning of the 21st centuries are noteworthy the eggshells associated with embryos from Paimogo, tentatively assigned to *Lourinhanosaurus* (Mateus 1997; Mateus et al. 2001) and from Porto das Barcas identified as belonging to *Torvosaurus* (Araújo et al. 2013).

1.3. GEOLOGICAL FRAMEWORK OF THE UPPER JURASSIC FOSSIL RECORD OF THEROPOD DINOSAURS FROM OF THE LUSITANIAN BASIN

1.3.1. ORIGIN AND EVOLUTION OF THE LUSITANIAN BASIN

The Lusitanian Basin is a marginal Mesozoic sedimentary basin located in the occidental margin of Iberia. It is a tectonostratigraphic structure with a maximum extension of approximately 200 km in length and 100 km in wide, of which near two thirds crop out onshore and the remaining one third is on the offshore (Kullberg et al. 2013). The Lusitanian Basin *sensu stricto* is defined as the area between Aveiro and the coast to the South of the Arrábida chain (Rasmussen et al. 1998). It is limited to the Este by the system of faults separating the sedimentary sequences that constitute the filling of the basin from the Hercynian basement, which develop along the Porto-Tomar, Arrife-Vale Inferior do Tejo and Setúbal-Pinhal Novo faults (Fig. 1.3.8). The West limit of the basin is the system of horsts of basement cropping out in the Berlenga and Farilhões islands and the North and South limits are define by the Porto Basin and by the system of faults of Arrábida, respectively (Azerêdo et al. 2003; Kullberg et al. 2006; Andrade 2006).

The Lusitanian Basin is one of a set of Atlantic margin rift-basins formed as a response to Mesozoic extension and subsequent opening of the North Atlantic Ocean (Wilson 1975; Leinfelder 1987; Rasmussen et al. 1998; Alves et al. 2002; Azerêdo et al. 2003; Kullberg et al. 2006). The Mesozoic sedimentary filling

spans from the Middle Triassic (? Ladinian-Carnian) to the Late Cretaceous (Turonian) (Rocha et al. 1996; Rey 1999; Kullberg et al. 2013) and form a NNE-SSW oriented and inverted structure with Cenozoic cover (Stapel et al. 1996). Structurally, the Lusitanian Basin is subdivided in two distinct areas, called the North and the South Lusitanian Basin (*sensu* Stapel et al. 1996) or Beira Litoral and Estremadura sub-basins (*sensu* Carvalho et al. 2005), which are separated by the Nazaré fault. This separation occurred during the middle Oxfordian due to reactivation of tardi-variscan faults, related with rifting processes, in the Central Atlantic Ocean (Pena dos Reis et al. 2011). These two tectonic fossae show distinct behavior in the subsidence curves (with the North Sector less subsident), possibly as result of differences in pre-rift crustal composition or thickness (Stapel et al. 1996). Other authors consider three sectors (North, Central and South) bounded by faults that formed major transfer zones during Mesozoic rifting phases (e.g. Alves et al. 2002; Kullberg et al. 2006). The Central Sector is limited by the Nazaré fault to the North, by the Tagus Estuary Fault to the South and by the Arrife Fault to the East (Fig. 1.3.8).

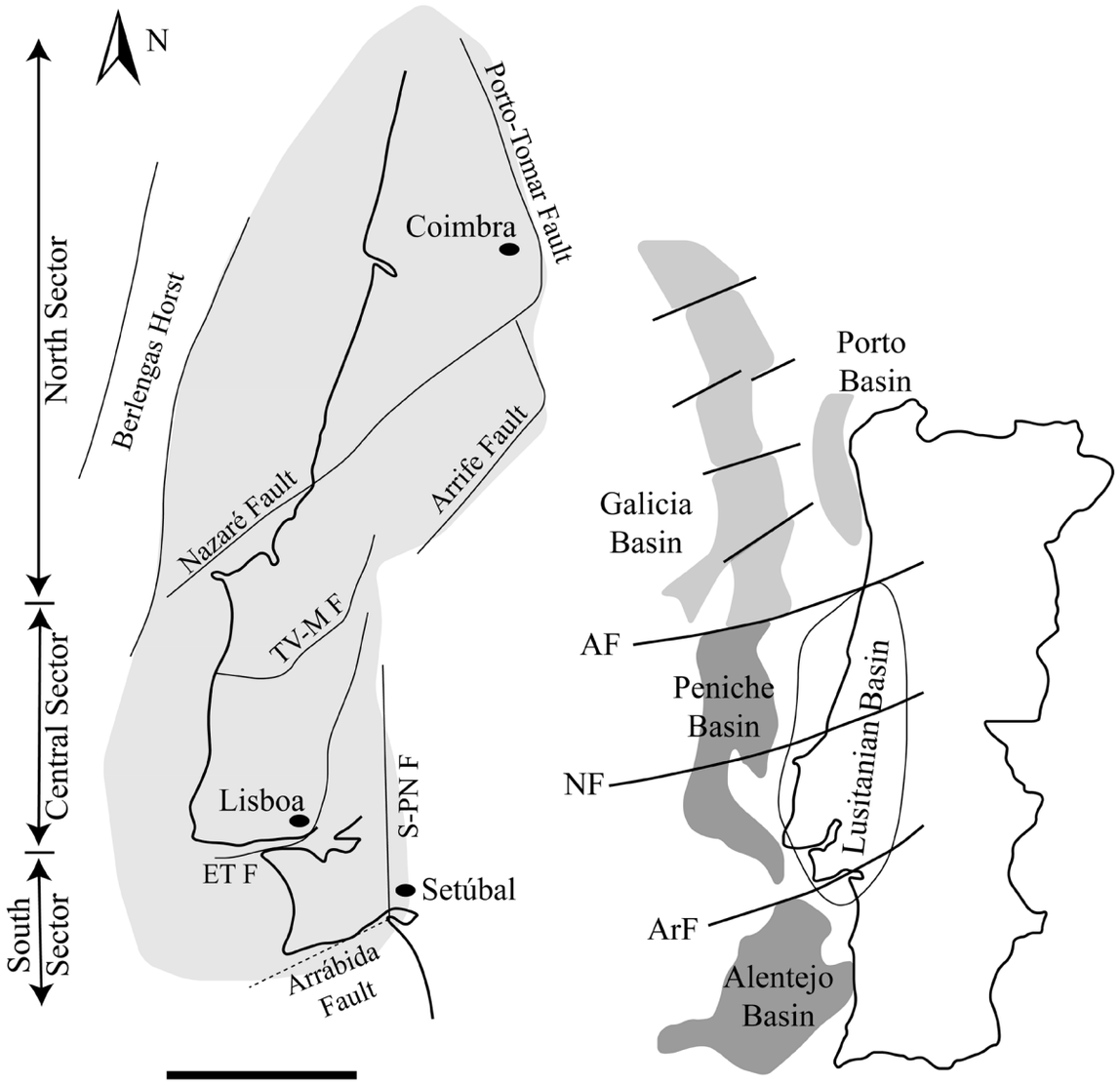

Figure 1.3.8. Structural and tectonic context of the Lusitanian Basin. Definition of the sectors *sensu* Ribeiro et al. (1996). Legend: AF, Aveiro Fault; ArF, Arrábida Fault; ET F, Estuário do Tejo Fault; NF, Nazaré Fault; S-PN F, Setúbal-Pinhal Novo Fault; TV-M F, Torres Vedras-Montejunto Fault. Scale bar: 50 km. Modified from Kullberg et al. (2013).

The Lusitanian Basin developed as an asymmetric graben basin along reactivated late Hercynian faults, which evolution is associated with the Mesozoic rifting phases, mainly in an extensional tectonic context, followed by Cenozoic inversion (Wilson 1975; Leinfelder 1987; Rasmussen et al. 1998; Kullberg et al. 2006). Periodically, regional tectonic movements related with the different phases of this geodynamic

process resulted in widespread discontinuities in the sedimentary deposition or erosion associated with uplift on a regional scale (Rasmussen et al. 1998; Azerêdo et al. 2003). Four rift phases (Fig. 1.3.9), or three with diverse rifting pulses (Carvalho et al. 2005), have been generally recorded during the Mesozoic evolution of the Lusitanian Basin (Rasmussen et al. 1998; Kullberg 2000; Alves et al. 2002; Kullberg et al. 2006). The first rifting phase occurred during the Late Triassic (Carnian–Rhaetian), the second in the Early Jurassic (between the Sinemurian and the Pliensbachian), the third during the Late Jurassic (late Oxfordian–early Kimmeridgian), and the fourth during the Early Cretaceous (late Berriasian–early Aptian) (Rasmussen et al. 1998; Alves et al. 2002, 2003; Kullberg et al. 2006).

The first rifting phase recorded in the Lusitanian Basin originated an irregular and dynamic topography of blocks delimited by normal faults, which were related with reactivation of faults in the basement (Alves et al. 2002; Azerêdo et al. 2003). Sedimentary deposition during this phase occurred within half-grabens as is indicated by the variations in thickness and depositional facies recorded on seismic and well data (Rasmussen et al., 1998; Alves et al. 2002). These sediments correspond mainly to alluvia-fluvial deposits, predominantly red conglomerates, sandstones and mudstones, which are the main constituents of the unit called "Grés de Silves" (Choffat 1880; Soares et al. 1985; Rocha et al. 1990; Stapel et al. 1996). These terrigenous deposits grades laterally and to the top to pelitic-carbonated and evaporite sediments known as "Margas da Dagorda" (Alves et al. 2002; Azerêdo et al. 2003). The accumulation of thick levels of gypsum, salgema and other evaporites indicate deposition in littoral environments (lagoon and tidal floodplain) in a warm and dry climate (Azerêdo et al. 2003). These evaporitic facies are mainly concentrated in a central zone paralleling the axis of the basin and presently expressed as salt-ridges (Rasmussen et al. 1998). This first rifting phase aborted without formation of oceanic crust and the definitive oceanic aperture would take place to the West of the limit of the Lusitanian Basin (Azerêdo et al. 2003).

The second rifting phase is associated with the first marine sedimentary event in the Lusitanian Basin and was marked by a strong and generalized subsidence in the basin (Stapel et al. 1996; Alves et al. 2002; Azerêdo et al. 2003; Pena dos Reis et al. 2011). The sedimentation in this stage comprises mainly sequences of centimeter layers of limestones and dolomites cropping out only in the East area of the North Sector of the basin (Azerêdo et al. 2003; Carvalho et al. 2005). A NW-dipping carbonate ramp developed and during the Toarcian–late Callovian a thick limestone series was deposited as result of opening of the carbonate ramp to truly marine environments, associated with post-rift regional thermal subsidence (Azerêdo 1998; Azerêdo et al. 2003; Rasmussen et al. 1998; Alves et al. 2002).

A regional hiatus, often associated with karst surfaces, range from the late Callovian to the early Oxfordian and preceding the deposition of the Upper Jurassic units (Mouterde et al. 1971, Leinfelder 1987; Montenat et al. 1998; Rasmussen et al. 1998). This hiatus, which is also recorded northern of Spain and western of France, has been interpreted as caused by regional uplift due to a new rifting phase related with an ocean-spreading episode in the Tagus Abyssal Plain and the consequent separation of the southern part of Iberia from North America (Leinfelder 1987; Mauffret et al. 1989; Wilson et al. 1989; Srivastava 1992; Rasmussen et al. 1998; Alves et al. 2002; Carvalho et al. 2005). These rifting processes induced the reactivation of Variscan fractures with emplacement of basic dikes at the basin borders (Fig. 1.3.10) and lead to differentiation of the Lusitanian Basin due to the development of complex fault- and diapir-bound sub-basins (Leinfelder and Wilson 1998; Kullberg 2000; Alves et al. 2002; Carvalho et al. 2005; Taylor et al. 2014). These sub-basins show different subsidence and filling characteristics and include the Bombarral-Alcobaça, Arruda and Turcifal sub-basins (Leinfelder and Wilson 1998; Kullberg 2000; Alves et al. 2003), and the recently proposed Consolação Sub-basin (Martinius and Gowland 2011; Taylor et al. 2014).

The Upper Jurassic rift-related units represent two different depositional stages; the first from the early to late Oxfordian and the second from the Kimmeridgian to the end of the Tithonian. The Oxfordian deposits are much variable, including lignitic freshwater marls, algal carbonates, and coral-bearing limestones (Cabaços, Cabo Mondego and Montejunto formations), corresponding to a period of widespread carbonate deposition in lacustrine to deep marine environments with strong variations of salinity (Leinfelder and Wilson 1998; Pena dos Reis et al. 2000; Alves et al. 2002; Azerêdo et al. 2002;

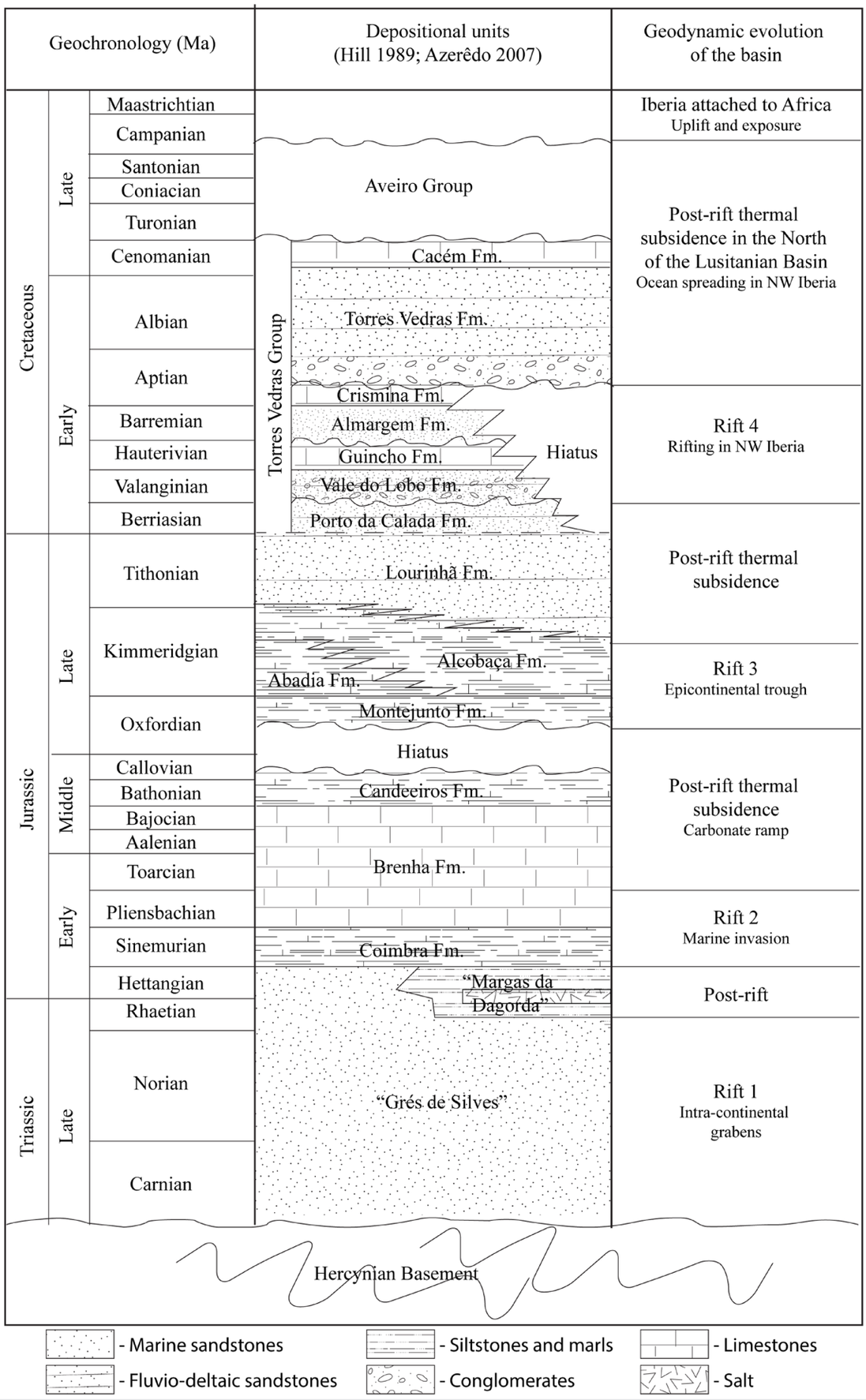

Figure 1.3.9. Simplified lithostratigraphy and tectonic evolution of the Lusitanian Basin showing the different rifting processes recorded during the Mesozoic. Modified from Alves et al. (2002) and Kullberg et al. (2006).

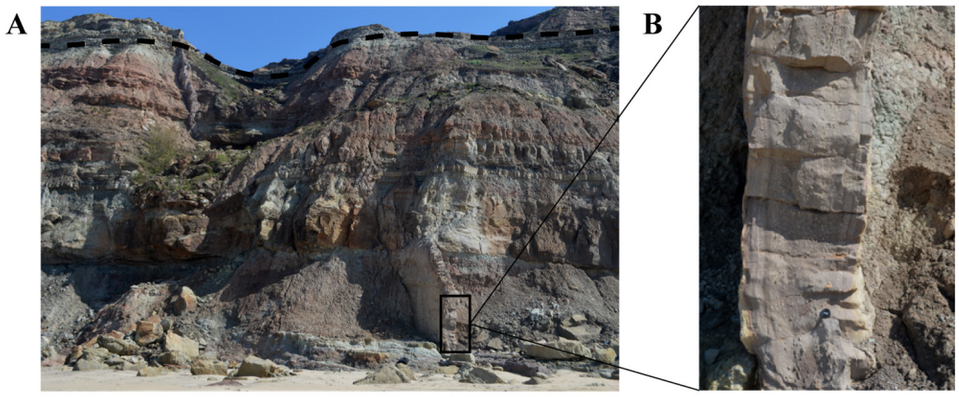

Figure 1.3.10. Basic dike in the Cambelas beach (Torres Vedras), which origin is related with the third rifting phase recorded in the Lusitanian Basin. This structure cuts the entire Upper Jurassic sequence, but not the carbonate level at the top of the sequence (represented by the dashed line in the image (A)), which is interpreted as marking the transition for the Lower Cretaceous; (B) detail of the aspect of the dike filling.

Carvalho et al. 2005; Pena dos Reis et al. 2011). These facies indicate a marked decrease in depth relative to the depositional environments of the Middle Jurassic (Leinfelder 1987; Wilson 1988). In the early Kimmeridgian, maximum subsidence occurred (Reis et al. 1997) and the basin was invaded by terrigenous, prograding sedimentation that progressively filled the basin (Hill 1988; Wilson 1988; Rey 1992; Manuppella et al. 1999; Alves et al. 2002; Carvalho et al. 2005; Kullberg et al. 2006). This second sedimentological stage is represented by shallow marine to fluvial deposits, including the Abadia and Alcobaça formations and by the predominantly fluvio-deltaic Lourinhã Formation (Leinfelder and Wilson 1989; Leinfelder 1993). The Upper Jurassic siliciclastic sequences are interrupted by transgressive episodes (e.g. Sobral Formation), which in the basin depocentres are represented by deposition of marine carbonates (Carvalho et al. 2005). The sedimentation of the end of the Jurassic reflects the progradation of siliciclastic deposits from the eastern and western margins to the central axis of the basin as result of the decrease in the tectonic subsidence (Pena dos Reis et al. 2011).

The last Mesozoic extensional event documented in the Lusitanian Basin is associated with rifting processes in the Iberia Abyssal Plain (Wilson et al. 2001; Alves et al. 2002). This rifting phase is recorded in the Central Sector of the basin by a second phase of siliciclastic influx represented by the Torres Vedras Formation (Wilson et al. 1989; Alves et al. 2002). Lower Cretaceous deposits are absent in the North Sector indicating uplift and exposure of this area of the basin (Pena dos Reis et al. 2011). At the Lower–Upper Cretaceous boundary the clastic deposition was interrupted as result of a major transgression, wich is recorded in the deposition of marine carbonates (Cacém Formation) overlapping the fluvial sediments of the Torres Vedras Formation (Rasmussen et al. 1998). During the early Late Cretaceous the evolution of the Lusitanian Basin is marked by a global transgressive event related with the breakup from the Canadian Grand Banks (Haq et al. 1988; Alves et al. 2006; Pena dos Reis et al. 2011). During the Turonian occurred a general emersion of several areas in the South and Central sectors of the basin and the sedimentation definitively ceased, recording a depositional hiatus up to the Paleogene (Pena dos Reis et al. 2011). From the Late Cretaceous onwards compressive episodes related with rotation of the African Plate, which induced the development of an extensive collision zone with Iberia, led to the abandonment and ultimately inversion of the basin with predominant uplift and exposure of most of the Mesozoic sequence (Ribeiro et al. 1990; Rasmussen et al. 1998; Alves et al. 2002).

1.3.2. LITHOSTRATIGRAPHY FOR THE UPPER JURASSIC OF THE LUSITANIAN BASIN

The Mesozoic sedimentary sequences of the Lusitanian Basin were deposited from the Middle Triassic (? Ladinian–Carnian) to the Late Cretaceous (Turonian) (Rocha et al. 1996; Rey 1999; Kullberg et al. 2013). The lithostratigraphy framework for these sequences is complex mainly due to the synsedimentary

tectonic activity and the lack of biostratigraphical marker for most sedimentary strata (Wilson 1988; Reis et al. 1996, 2000; Leinfelder and Wilson 1998; Alves et al. 2003; Leinfelder et al. 2004; Kullberg et al. 2013). The Upper Jurassic sequences of the Lusitanian Basin comprise mostly marginal-marine deposits formed in low-salinity environments and therefore classical biostratigraphic indicators, such as the ammonites, are scarce or absent in these sediments (Schneider et al. 2009). Besides, during the Mesozoic the basin occupied an intermediate position between the Boreal and Tethyan faunal provinces, which resulted in a largely endemic marine fauna (e.g. Leinfelder et al. 2004; Schneider et al. 2009). Other problems that contributed for the complex lithostratigraphic interpretation of these sequences are the rapid lateral facies changes, the development of distinct sub-basins during the Late Jurassic, and the diachronous nature of most lithological units due to the general progradation of the coastline to the South (Rasmussen et al. 1998; Alves et al. 2002, 2006; Schneider et al. 2009). This complex context justifies the multiple litostratigraphic interpretations that have been proposed for the Mesozoic sequences of the Lusitanian Basin since the XIX century (e.g. Wilson 1979; Hill 1989; Leinfelder 1987, 1993; Manuppella et al. 1999; Kullberg et al. 2006; Schneider et al. 2009; Martinius and Gowland 2011; Taylor et al. 2014).

The first lithostratigraphic studies on Jurassic sequences of the Lusitanian Basin date back from the mid-nineteen century (Sharpe, 1850). However, it was Paul Choffat who presented the first stratigraphic chart (Choffat, 1901) for these sedimentary sequences. As ammonites are scarce or absent in most of the strata, other macrofossils, such as bivalves and gastropods or microfossils, including algae and ostracods, together with lithological characteristics were used for design a lithostratigraphic scheme of the Lusitanian Basin sedimentary filling (Ramalho 1971; Fürsich 1981; Leinfelder 1987). Choffat (1901) identified three main units in the onshore deposits of the southern part of the Lusitanian Basin: Lower Lusitanian (including the Cabaços and Montejunto beds), Upper Lusitanian (corresponding to the Abadia Beds), and Neojurassic (including the Lima pseudoalternicosta Beds, Pterocerian and Freixialian).

<table>
<tr><th colspan="2" rowspan="2">English stages</th><th>French stages</th><th>Current nomen.</th><th>Choffat 1901</th><th colspan="2">Torres Vedras
Choffat 1901
(units dated after Ramalho 1971; Mouterde et al. 1973; Ruguet-Perrot 1961 Zbyszewski and Ferreira 1966; Zbyszewski and Almeida 1955)</th><th>Alcobaça and Serra dos Candeeiros
Ruget-Perrot 1961; Fança and Zbyszewski 1963</th><th>Leiria
(units dated after Teixeira and Zbyszewski 1968)</th></tr>
<tr><td>Portland.</td><td>Portlandian</td><td>Tithonian</td><td rowspan="3">Neojurassic</td><td colspan="2">Freixialian</td><td rowspan="2">Upper Sandstones with plant and dinosaur fossils</td><td rowspan="2">Portlandian and Pterocerian</td></tr>
<tr><td rowspan="3">Kimmeridgian</td><td rowspan="2">Kimmeridgian</td><td rowspan="2">Kimmeridgian</td><td colspan="2">Pterocerian</td></tr>
<tr><td>Lima pseudoal-ternicosta Beds</td><td>Amaral Coral Limestones</td><td rowspan="2">Alcobaça Beds</td><td rowspan="2">Vale de Lagares complex (including lignite beds at the base)</td></tr>
<tr><td rowspan="3">Oxfor.</td><td rowspan="3">Oxfor.</td><td rowspan="3">Oxfor.</td><td rowspan="3">Lusitanian</td><td rowspan="2">Abadia Beds</td><td>Abadia Fm.</td></tr>
<tr><td>Cabrito Fm.</td><td rowspan="2">Vale Verde Beds</td><td rowspan="2">Limestones with lamellibranchs</td></tr>
<tr><td colspan="2">Tojeira Fm.
Montejunto Beds</td></tr>
</table>

Figure 1.3.11. Correlation of the early published lithostratigraphic nomenclatures for Upper Jurassic sequences in different areas of the Lusitanian Basin. Modified from Wilson (1979).

For several years, the nomenclature proposed by Choffat was predominantly followed in works concerning the Mesozoic sedimentary levels of the Lusitanian Basin. This nomenclature was modified and adapted by geologists working in the "Companhia Portuguesa de Petróleo" during the late 1950 and 1960 decades, adding a Germanic influence to the lithostratigraphic terminology (Wilson 1979). Later, studies led by members of the "Serviços Geológicos de Portugal" (e.g. Ramalho 1971, 1981) and French researchers (e.g. Ruget-Perrot 1961; Mouterde et al. 1972) have generally used the scheme proposed by

Choffat (Fig. 1.3.11). The development of micropalaeontological (Ramalho and Rey 1969, 1975; Helmdach 1971; Ramalho 1971; 1981) and seismic studies (Rasmussen et al. 1998; Alves et al. 2002, 2006; Carvalho et al. 2005) allowed an increase in the knowledge of the origin and evolution of the Lusitanian Basin and a better understand of the sedimentary infilling. These studies suggest that foraminifera, dasycladaceans and ostracods may provide certain stratigraphic information on some of the Upper Jurassic strata (e.g. Ramalho and Rey 1969). However, as these organisms were facies-controlled, the resulting schemes are not applicable for the entire basin (Schneider et al. 2009).

Some detailed lithostratigraphic schemes for the Upper Jurassic of the Lusitanian Basin, have been proposed. Hill (1988, 1989) performed a comprehensive study on the sedimentary sequences cropping out along the littoral of the Central Sector of the Lusitanian Basin, between Ericeira (Mafra) and Consolação (Peniche). This author informally proposed the term "Lourinhã Formation" to include several sedimentary sequences span from the late Kimmeridgain to the end of the Tithonian (Fig. 1.3.12). These sequences were deposited in much variable environments, comprising mostly sandstone and mudstone facies from braided to meandriform fluvial systems, distal alluvial fans, and upper deltas, which are punctuated by episodes of estuarine and lagoon sedimentation (Hill 1989). During the late Kimmeridgian, banks of limestone (e.g. Ota Limestone in the northeastern side of the Arruda Sub-basin) developed near the margins of the basin (Wilson 1979). The Lourinhã Formation (*sensu* Hill 1989) is the most extensive lithostratigraphic unit cropping out in the Central Sector of the Lusitanian Basin, mainly in the Consolação Sub-basin, and includes from lower to upper: Praia da Amoreira, Porto Novo, Praia Azul, Assenta, and Santa Rita members. The lower levels of the Lourinhã Formation overlap a thick sequence composed mainly by marls and sandy marls corresponding to the Abadia Formation. This sequence is interpreted as deposits of submarine fans and has an association of fossil fauna composed by bivalves, foraminifers and algae (Kullberg et al. 2006; Pena dos Reis et al. 2011).

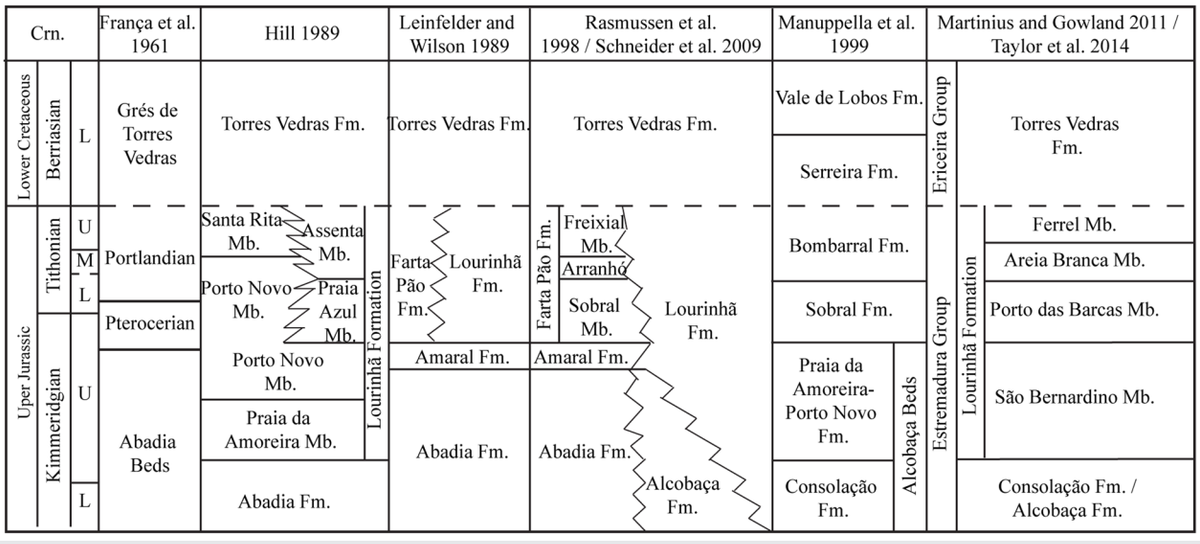

Figure 1.3.12. Lithostratigraphic schemes proposed by different authors for the Upper Jurassic sequences of the Lusitanian Basin.

The Praia da Amoreira Member includes decimeter interbedded sandstones and mudstones, massive sandstone and mudstone facies (Fig. 1.3.13A). These sediments are interpreted as deposits of distal alluvial fans with both sheet-flood and channelized flows (Hill 1989) or of meandering river systems (Taylor et al. 2014). The overlaying Porto Novo Member is composed by thick sandstone channel bodies, often with lateral accretion surfaces and cross-bedded lamination (Fig. 1.3.13B). These sandstone channels are usually isolated within thick floodplain mudstone packages often with well-developed levels of calcrete paleosoils (Fig. 1.3.13C). Intercalated with the mudstones are also flat lenses of finer sandstone of probable crevasse-splay origin (Fig. 1.3.14B). These sediments have been interpreted as distal deposits of fluvial meander systems grading laterally to upper deltaic deposits (Mateus et al. 2013). To the South,

in the littoral area of the Central Sector of the Lusitanian Basin, and to the East, in the Arruda region, the Porto Novo Member is intercalated with tongues of marine/deltaic facies corresponding to the Praia Azul Member (Wilson 1979; Leinfelder 1987; Hill 1989). The Praia Azul Member is mainly composed by marls and mudstones with tabular geometry and rare intercalations of sandstone channel bodies frequently with intense bioturbation (Hill 1989). This unit is delimited by two well-developed and laterally extensive carbonate levels, predominantly composed by an association of brackish bivalves preserved in situ and represented by complete shells, frequently with the two valves attached (Fig. 1.3.13D) (Werner 1986; Fürsich et al. 2009; Taylor et al. 2014). Finally, the upper part of the Lourinhã Formation is fully continental to the North of Santa Cruz (Torres Vedras), represented by the Santa Rita Member (Fig. 1.3.14C), but to the South it includes transitional to shallow marine intercalations of the Assenta Member. This scheme with some modifications, mainly different sets of members for the Lourinhã Formation, was followed by some recent authors (e.g. Martinius and Gowland 2011; Mateus et al. 2013; Taylor et al. 2014).

The Lourinhã Formation has been interpreted as spanning from the latest Kimmeridgian to the end of the Tithonian (Leinfelder 1993). However, some studies suggest a broader time interval for these sedimentary sequences ranging from the late Oxfordian to the early Berriasian (Alves et al. 2002).

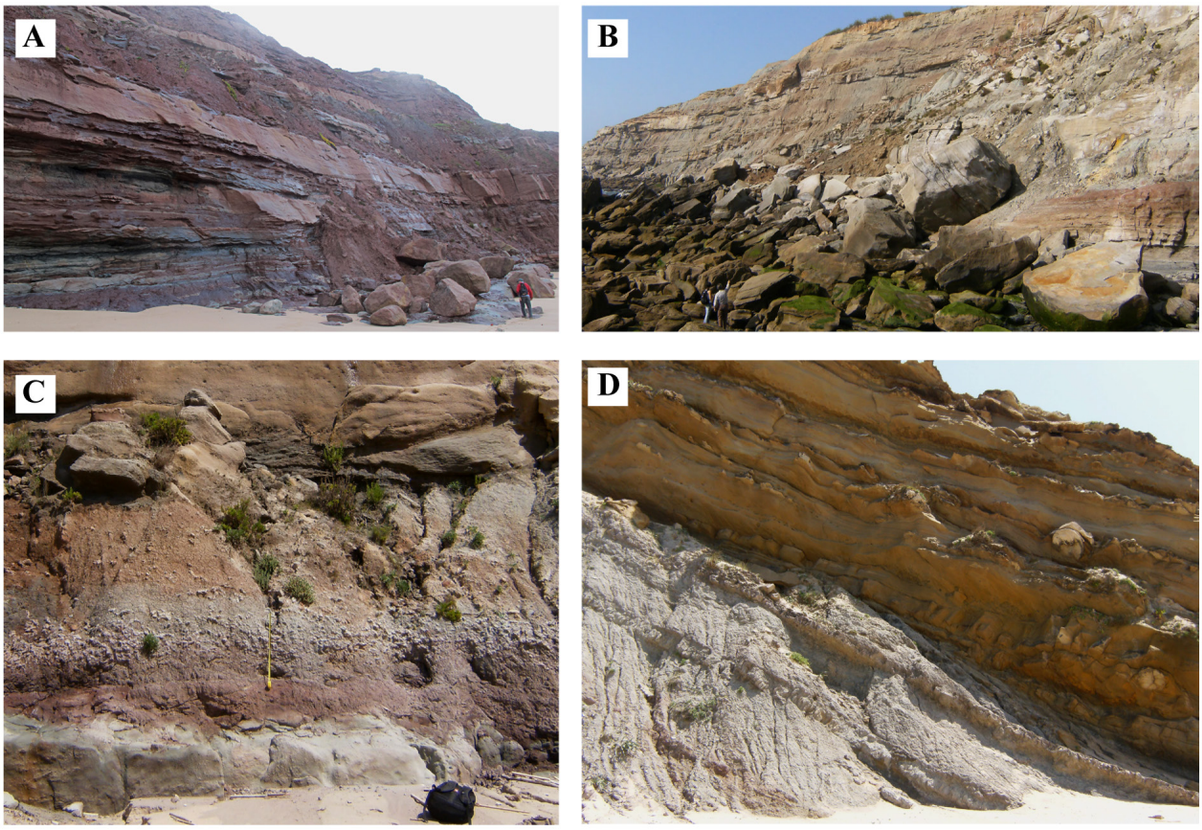

Figure 1.3.13. Some aspects of the sedimentary levels of the Lourinhã Formation (*sensu* Hill 1989) in the littoral area of the Consolação Sub-basin. (A) Sedimentary sequence of the Praia da Amoreira Member in Praia da Corva (Torres Vedras); (B) sedimentary sequence of the Porto Novo Member in the Valmitão beach (Lourinhã); (C) level of calcrete paleosoils in a sedimentary sequence of the Porto Novo Member in the Valmitão beach; (D) contact between the Praia Azul and the Santa Rita members marked by a level composed by a fossil association of bivalves, represented mostly by shells of Isognomon, in the Santa Rita beach (Torres Vedras).

Leinfelder and Wilson (1989) and Leinfelder (1993) studied mainly the sedimentary sequences of the Arruda Sub-basin and proposed a distinct lithostratigraphic scheme for the Upper Jurassic units in this area of the Lusitanian Basin. In the Arruda Sub-basin, upper Kimmeridgian deposits (equivalent to the lower levels of the Lourinhã Formation; the Praia da Amoreira and Porto Novo members *sensu* Hill 1989) are included in the Abadia Formation. Based on this scheme the Abadia Formation has a coarse

basal sequence ("Cabrito sandstones and conglomerates") grading to a marl-sandstone and turbiditic succession ("Abadia marls"), which is overlayed by the "Amaral beds". The "Amaral beds" consist almost exclusively of cross-bedded sandstones in the Torres Vedras-Montejunto area, but in the area of Arruda is characterized by medium to high-energy, biostromal coral limestones with a highly diverse biota of corals, stromatoporoids, molluscs, echinoids, and serpulids (Leinfelder and Wilson 1989; Leinfelder 1993). Leinfelder (1993) considered the "Sobral beds" (equivalent to the Praia Azul Member *sensu* Hill 1989) overlapping the "Amaral beds" as late Kimmeridgian–early Tithonian in age. Based on this interpretation, the Lourinhã Formation grades to the South, in the Arruda Sub-basin, to the Farta Pão Formation, including the Sobral, Arranhó, and Freixial members (*sensu* Leinfelder 1993). The Farta Pão Formation consists mostly of lagoon, nodular limestones and marls with development of coral biostrome in the mid part, whereas the upper levels are characterized by fluvial sandstone intercalations (Leinfelder and Wilson 1989).

Rasmussen et al. (1998) follow a scheme similar to those proposed by Leinfelder and Wilson (1989) and Leinfelder (1993), but got back to the terminology of Choffat (1901) and considered the upper Kimmeridgian–Tithonian fluvio-deltaic deposits equivalent to the Lourinhã and Farta Pão formations (*sensu* Leinfelder and Wilson 1989 and Leinfelder 1993) as the "Grés Superiores" and "Pteroceriano" (*sensu* Wilson et al. 1990). Manuppella et al. (1999) proposed a scheme similar to that of Hill (1989), but with some reinterpretations (Fig. 1.3.12). In this nomenclature, the Porto Novo and Praia da Amoreira members of the Lourinhã Formation (*sensu* Hill 1989) were mapped together in the Praia da Amoreira-Porto Novo Formation, which is included together with the Consolação Formation (equivalent to the Abadia Formation of Hill 1989) in the Alcobaça Beds. The Praia da Amoreira-Porto Novo Formation is overlying by the Sobral Formation (equivalent to the Praia Azul Member of the Lourinhã Formation *sensu* Hill 1989). The upper levels of the Lourinhã Formation, including the Assenta and Santa Rita Members of Hill (1989), are interpreted as belonging to the Bombarral Formation in the scheme of Manuppella et al. (1999).

Leinfelder (1987) poin out that the correlation between the many lithostratigraphic proposals for the upper Kimmeridgian and Tithonian of the Lusitanian Basin may be anchored in an important transgression event represented by a set of extensive carbonate levels. In the coastal area of the Consolação Sub-basin these levels correspond to the base of the "Pteroceriano" (*sensu* França et al. 1961 and Leinfelder 1986), to the Praia Azul Member (*sensu* Hill 1989), to the Sobral Member (*sensu* Manuppella et al. 1999), to the Arranhó I Member (*sensu* Fürsich et al. 2009 and Schneider et al. 2009), and to the Porto das Barcas Member (*sensu* Martinius and Gowland 2011 and Taylor et al. 2014).

The interpretation of the Alcobaça lithostratigraphic unit (Alcobaça Formation *sensu* Rasmussen et al. 1998 or Alcobaça Beds *sensu* Manuppella et al. 1999) has been diverse since the original reference by Choffat (1880). This unit is mostly a sequence of sandy mudstones and detritic limestones with rich fossiliferous associations that comprise corals, ammonoids, bivalves, echinoderms, and brachiopods (Manuppella et al. 1994). This sequence corresponds to shallow marine to transitional (deltaic and estuarine) deposits with frequent siliciclastic input (Kullberg et al. 2013). This is the most extensive Kimmeridgian unit in the Bombarral-Alcobaça Sub-basin, interfingering with the Abadia Formation and the lower levels of the Lourinhã Formation of the Turcifal, Arruda and Consolação sub-basins (Mannupella et al. 1999; Schneider et al. 2009). To the northern end of the Bombarral-Alcobaça Sub-basin, in the region of Caldas da Rainha, Alcobaça, Leiria and Pombal, the Alcobaça Formation is overlayed by a carbonated unit with abundant fossils of fishes, equinoids, ostreids, bivalves, corals and some ammonites corresponding to the Abiúl Formation (Rocha et al. 1996). In this region, the Abiúl Formation is interpreted as late Kimmeridgian–early Tithonian in age and the presence, in some levels, of bird-eyes and black pebbles suggest a lagoon sedimentary environment (Kullberg et al. 2013). In this area, the Bombarral Formation (*sensu* Manuppella et al. 1999, which is equivalent to the upper levels of the Lourinhã Formation *sensu* Hill 1989 and Leinfelder and Wilson 1989) has more marked continental facies relative to those of the southern end of the Bombarral-Alcobaça Sub-basin or of the Consolação Sub-basin. The Bombarral

Formation in the region of Caldas da Rainha, Alcobaça, Leiria and Pombal includes mostly micaceous sandstones, deposited in meandering fluvial systems and scarce levels of marine marls with carbonated concretions (Rocha et al. 1996; Kullberg et al. 2013).

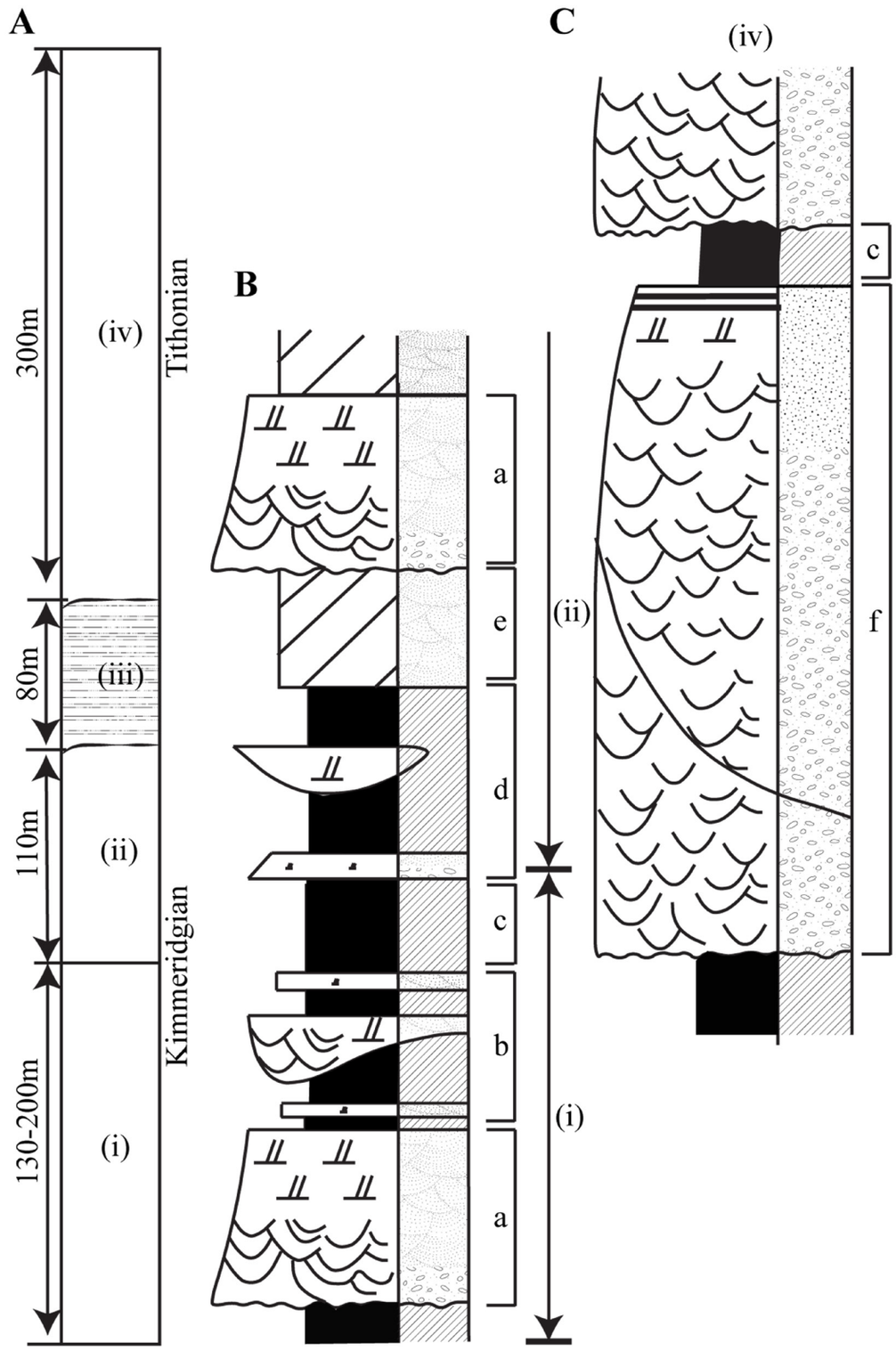

Figure 1.3.14. Facies variation of the Kimmeridgian–Tithonian sedimentary sequences in the littoral of Porto Novo (Torres Vedras). (A) Stratigraphic column with the approximate thickness of the different units cropping out in Porto Novo; (B) and (C) lithological logs of the facies (i), (ii), and (iv). These sequences correspond to units of the Lourinhã Formation (*sensu* Hill 1989), including the (i) Praia da Amoreira, (ii) Porto Novo, (iii) Praia Azul, and (iv) Santa Rita members. Legend: a, active channel; b, abandoned channel; c, floodplain; d, floodplain and crevasse; e, abandoned channel filled by lateral accretion; f, active channel with unidirectional though cross bedding (often cut by other channels). Modified from Wilson (1979).

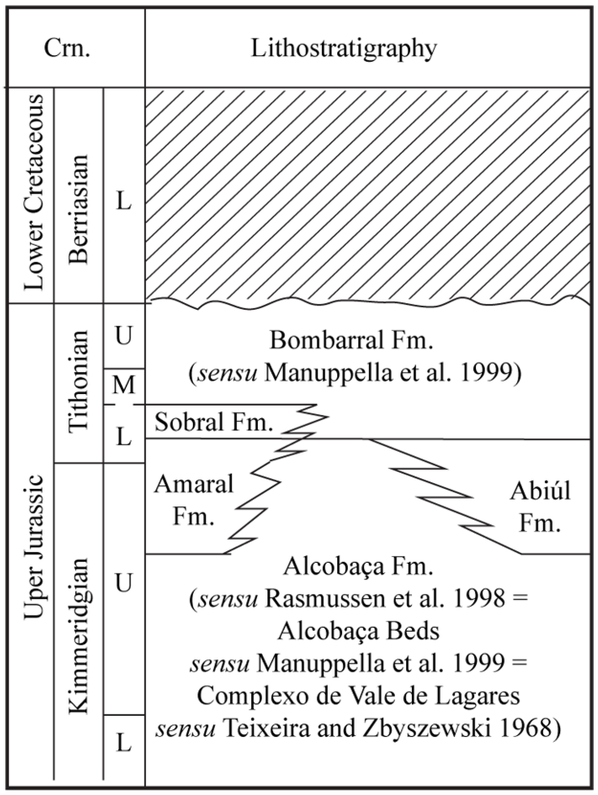

Figure 1.3.15. Lithostratigraphic nomenclature for the Upper Jurassic sequences of the Lusitanian Basin in the North part of the Bombarral-Alcobaça Sub-basin. Modified from Kullberg et al. (2013).

1.3.3. PALEOGEOGRAPHY OF THE LUSITANIAN BASIN DURING THE MESOZOIC

The origin and evolution of the Lusitanian Basin is closely related with the paleogeographic setting of Western Europe in the global context of the Mesozoic and Cenozoic breakup of Pangea. During the Late Triassic–Early Jurassic Africa began to separate from Iberia due to the opening of the Alpine Tethys and from North America, in sequence of the opening of the Central Atlantic (Pena dos Reis et al. 2011). Seafloor spreading offshore Iberian Peninsula was generally characterized by the successive opening of three segments propagating from South to North: (i) Tagus Abyssal Plain; (ii) Iberian Abyssal Plain; and (iii) Galicia Bank segment (Rasmussen et al. 1998). If this northward propagation of seafloor spreading occurred continuously (i.e. 'zipper' opening) or by a series of abrupt events with the onset of seafloor spreading jumped across transfer zones from one segment to the next is not consensual. The abrupt change in the late Barremian to late Aptian extensional deformation across the Egret transfer zone recorded in the Jeanne d'Arc Basin suggests that the northward progradation of seafloor in this region occurred by an abrupt jump from the southern to the northern Newfoundland Basin (Driscoll et al. 1995).

It is generally accept that the Late Jurassic paleogeographic evolution of the Lusitanian Basin was determined by the ongoing opening of the Central Atlantic, whereas during the Cretaceous, since the late Aptian to the early Albian, it was influenced by the opening of the North Atlantic. During the Late Jurassic, the region currently corresponding to the Western Europe consisted of a number of small islands separated by shallow continental shelves that may have been emerged during lowstands (Upchurch et al. 2002). In contrast to many other regions bordering the North Atlantic where the Late Jurassic is a period of maximum extent of seafloor spreading, the western and northern margins of Iberia recorded a period of uplift (Wilson 1975). The beginning of the North Atlantic oceanization was during the Early Cretaceous progressing from Iberia towards Greenland (Driscoll et al. 1995; Pena dos Reis et al. 2011). The temporal framework of the different evolutionary phases related with the North Atlantic opening is

not consensual. It has been proposed that seafloor spreading between Grand Banks and Iberia (in the area of Tagus Abyssal Plain) began during the late Hauterivian (Keen and De Voogd 1988), the Berriasian–Barremian (Ziegler 1988) or the early Aptian (Driscoll et al. 1995). Some studies based on magnetic, seismic reflection, and refraction data (Driscoll et al. 1995) suggest that onset of seafloor spreading to the North of the Nazaré Fault occurred after the early Aptian (Fig. 1.3.16). Wilson (1975) suggested that the structural and stratigraphic continuity between Iberian and North American basins indicates that these two areas were adjacent until the end of Jurassic.

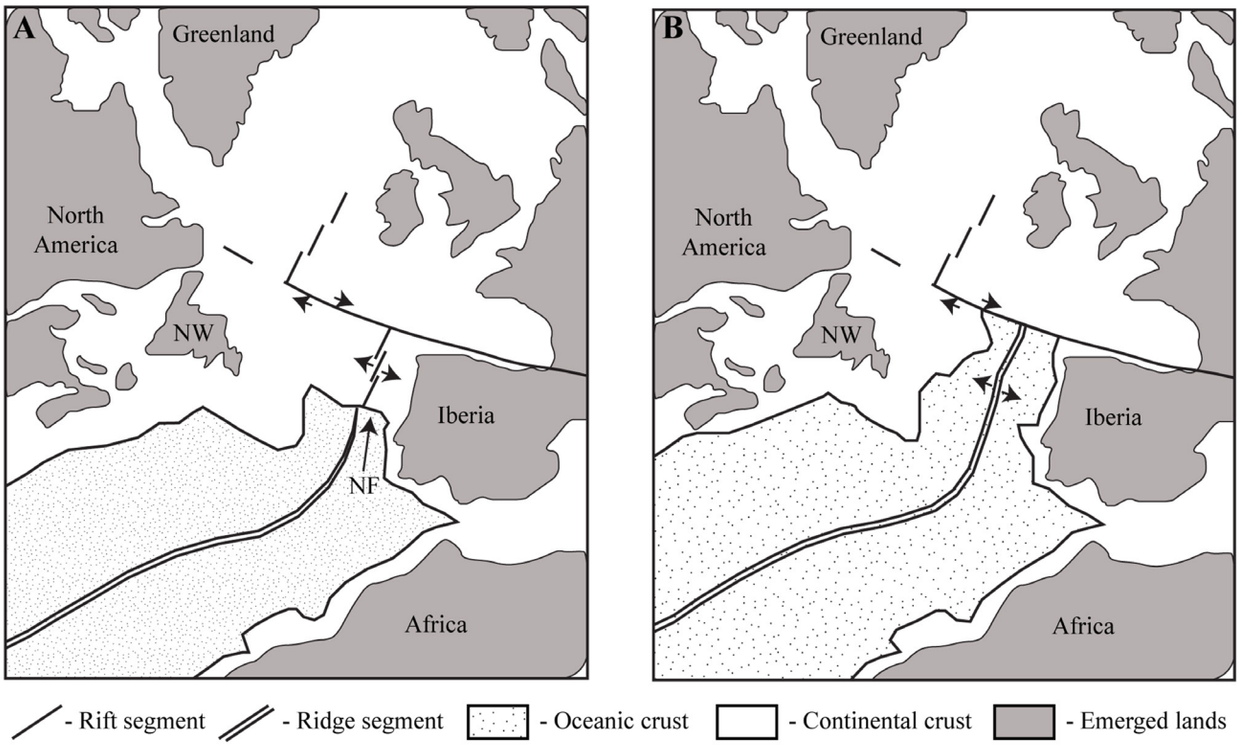

Figure 1.3.16. Interpretation of the evolution of the North Atlantic opening during the (A) late Barremian–early Aptian; and (D) late Aptian–early Albian, showing the boundary between continental and oceanic crust based on Driscoll et al. (1995). Legend: NF, Nazaré Fault.

Over approximately 150 million years, the Lusitanian Basin went through different paleogeographic scenarios from latitude around 12º N during the Late Triassic (Turell and Pares 1996) to latitude near 30º N during the Late Cretaceous (Smith et al. 1994; Golonka et al. 1996; Ziegler 1988) with the consequent passage through different climatic ranges (Pena dos Reis et al. 2011). Geochemical analyses and palaeosol morphologies in the Lourinhã Formation indicate warm and wet palaeoclimatic conditions with strongly seasonal precipitation patterns during the Late Jurassic (Myers et al. 2012). Soil temperature estimates from isotopic analysis of clay minerals in the Lourinhã Formation indicate maximum surface temperatures between 27ºC and 34ºC, which are similar to summer temperature estimates for Late Jurassic Iberia (Myers et al. 2012). The abundance of calcisols and vertisols in several sedimentary levels of the Lourinhã Formation suggests that local conditions were characterized by a highly seasonal rainfall distribution rather than overall arid conditions (Hill 1989; Myers et al. 2012).

REFERENCES

Allain R. 2002. Discovery of megalosaur (Dinosauria, Theropoda) in the middle Bathonian of Normandy (France) and its implications for the phylogeny of basal Tetanurae. Journal of Vertebrate Paleontology 22(3):548–563.

Alves TM, Gawthorpe RL, Hunt DW, Monteiro JH. 2002. Jurassic tectono-sedimentary evolution of the Northern Lusitanian Basin (offshore Portugal). Marine and Petroleum Geology 19:727–754.

Alves MT, Manuppella G, Gawthorpe RL, Hunt DW, Monteiro JH. 2003. The depositional evolution of diapir-and fault-bounded rift basins: examples from the Lusitanian Basin of West Iberia. Sedimentary Geology 162(3):273–303.

Alves TM, Moita C, Sandnes F, Cunha T, Monteiro JH, Pinheiro LM. 2006. Mesozoic–Cenozoic evolution of North Atlantic continental-slope basins: The Peniche basin, western Iberian margin. AAPG Bulletin 90(1):31–60.

Andrade B. 2006. Los braquiópodos del tránsito Jurásico Inferior-Jurásico Medio de la Cuenca Lusitánica (Portugal). Colóquios de Paleontología 56:5–194.

Antunes MT, Mateus O. 2003. Dinosaurs of Portugal. Comptes Rendus Palevol 2:77–95.

Antunes MT, Pais J. 1978. Notas sobre depósitos de Taveiro. Estratigrafia, paleontologia, idade, paleoecologia. Ciencia Terra 4:109–128.

Antunes MT, Sigogneau-Russell D. 1992. La faune de petits dinosaures du Crétacé terminal portugais. Comunicações dos Serviços Geológicos de Portugal 78(1):49–62.

Antunes MT, Sigogneau-Russell D. 1991. Nouvelles données sur les Dinosaures du Crétacé supérieur du Portugal. Comptes Rendus de l'Académie de Sciences, Paris (II) 313:113–119.

Antunes MT, Sigogneau-Russell D. 1995. O Cretácico tenninal português e o seu contributo para o esclarecimento da extinção dos dinossauros. Memórias da Academia de Ciências de Lisboa 35:131–144.

Antunes MT, Sigogneau-Russell D. 1996. Le Crétacé terminal portugais et son apport au probléme de l'extinction des dinosaures. Bulletin du Muséum National d'Histoire Naturelle de Paris 48 sér. 18 (sec.C no4):595–606.

Araújo R, Castanhinha R, Martins RMS, Mateus O, Hendrickx C, Beckmann F, Schell N, Alves LC. 2013. Filling the gaps of dinosaur eggshell phylogeny: Late Jurassic Theropod clutch with embryos from Portugal. Scientific Reports 3:1924 doi: 10.1038/srep01924.

Azerêdo AC. 1998. Calcareous debris-flow as evidence for a distally steepened carbonate ramp in West-central Portugal. Comumunicações dos Serviços Geológicos de Portugal 74:56–67.

Azerêdo AC. 2007. Formalização da litostratigrafia do Jurássico Inferior e Médio do Maciço Calcário Estremenho (Bacia Lusitânica). Comunicações Geológicas 94:29–51.

Azerêdo AC, Duarte L V, Henriques MH, Manuppella, G. 2003. Da dinâmica continental no Triássico aos mares do Jurássico Inferior e Médio. Cadernos de Geologia de Portugal, Instituto Geológico e Mineiro, Lisboa. 1–43.

Azerêdo AC, Wright PV, Ramalho MM. 2002. The Middle–Late Jurassic forced regression and disconformity in central Portugal: eustatic, tectonic and climatic effects on a carbonate ramp system. Sedimentology 49:1339–1370.

Baron MG, Norman DB, Barrett PM. 2017. A new hypothesis of dinosaur relationships and early dinosaur evolution. Nature doi:10.1038/nature21700

Benson RBJ. 2008. A redescription of '*Megalosaurus*' *hesperis* (Dinosauria, Theropoda) from the Inferior Oolite (Bajocian, Middle Jurassic) of Dorset, United Kingdom. Zootaxa 1931:57–67.

Benson RBJ. 2010. A description of *Megalosaurus bucklandii* (Dinosauria: Theropoda) from the Bathonian of the UK and the relationships of Middle Jurassic theropods. Zoological Journal of the Linnean Society 158:882–935.

Benson RBJ, Carrano MT, Brusatte SL. 2010. A new clade of archaic large-bodied predatory dinosaurs (Theropoda: Allosauroidea) that survived to the latest Mesozoic. Naturwissenschaften 97:71–78.

Benton MJ. 1986. The Late Triassic reptile *Teratosaurus* - a rauisuchian, not a dinosaur. Palaeontology 29:293–301.

Brusatte SL, Sereno PC. 2008. Phylogeny of Allosauroidea (Dinosauria: Theropoda): comparative analysis and resolution. Journal of Systematic Palaeontology 6(2):155–182.

Buckland W. 1824. Notice on the *Megalosaurus* or great Fossil Lizard of Stonesjield. Transactions of the Geological Society of London (Ser. 2)1:390–396.

Buffetaut E. 2007. The spinosaurid dinosaur *Baryonyx* (Saurischia, Theropoda) in the Early Cretaceous of Portugal. Geological magazine 144 (6):1021–1025.

Carrano MT, Sampson SD. 2008. The Phylogeny of Ceratosauria (Dinosauria: Theropoda). Journal of Systematic Palaeontology 6(2):183–236.

Carrano MT, Benson RBJ, Sampson SD. 2012. The phylogeny of Tetanurae (Dinosauria: Theropoda). Journal of Systematic Palaeontology 10(2):211–300.

Carvalho J, Matias H, Torres L, Manuppella G, Pereira R, Mendes-Victor L. 2005. The structural and sedimentary evolution of the Arruda and Lower Tagus sub-basins, Portugal. Marine and Petroleum Geology 22(3):427–453.

Chabli S. 1986. Données nouvelles sur un "Dinosaurien" Jurassique moyen du Maroc: *Megalosaurus mersensis* Lapparent 1955, et sur les Megalosaurides en général. Colloque International de Paléontologie, Toulouse:65–72.

Charig AJ, Attridge J, Crompton AW. 1965. On the origin of the sauropods and the classification of the Saurischia. Proceedings of the Linnean Society of London 176:197–221.

Choffat P. 1880. Etude stratigraphique et paléontologique des terrains Jurassiques du Portugal. Premiére Livraison. Le Lias et le Dogger au Nord du Tage. Memórias da Secção dos Trabalhos Geológicos de Portugal XIII: 1–72.

Choffat P. 1887. Reserches sur les terrains secondaires au Sud du Sado. Comunicações da Comissão dos Trabalhos Geológicos de Portugal I:222–312.

Choffat P. 1901. Notice préliminaire sur la limite entre le Jurassique et le Crétacique en Portugal. Bulletin de la Société Belge de Géologié, de Paléontologie et d'Hydrologie 15:111–140.

Colbert EH. 1964. Relationships of the Saurischian Dinosaurs. American Museum Novitates 2181:1–24.

Cope ED. 1866. Discovery of a gigantic dinosaur in the Cretaceous of New Jersey. Proceedings of the Academy of Natural Sciences of Philadelphia 18:275–279.

Currie PJ, Carpenter K. 2000. A new specimen of *Acrocanthosaurus atokensis* (Theropoda, Dinosauria) from the Lower Cretaceous Antlers Formation (Lower Cretaceous, Aptian) of Oklahoma, USA. Geodiversitas 22:207–246.

Driscoll NW, Hogg JR, Christie-Blick N, Karner GD. 1995. Extensional tectonics in the Jeanne d'Arc Basin, offshore Newfoundland: Implications for the timing of the break-up between Grand Banks and Iberia. In: Scrutton RA, Stoker MA, Shimmield GB, Tudhope AW. (Eds). Geological Society London Special Publication 90:1–28.

Elzanowski A. 2002. Archaeopterygidae (Upper Jurassic of Germany). In: Chiappe LM, Witmer LM (Eds). Mesozoic Birds: Above the Heads of Dinosaurs. University of California Press, Berkeley. 129–159.

Escaso F, Malafaia E, Mocho P, Narváez I, Ortega F. 2017. '*Megalosaurus insignis*' from Praia de Areia Branca (Lourinhã, Portugal): is it Theropoda or Ornithopoda? XXII Bienal da Real Sociedad Española de Historia Natural.

França JC, Zbyszewski G. 1963. Notícia explicativa da Folha 26-B, Alcobaca. Serviços Geológicos de Portugal.

França JC, Zbyszewski G, Almeida FM. 1961. Notícia explicativa da Folha 30-A Lourinhã. Serviços Geológicos de Portugal.

Fürsich FT. 1981. Salinity-controlled benthic associations from the Upper Jurassic of Portugal. Lethaia 14:203–223.

Fürsich FT, Werner W, Schneider S. 2009. Autochthonous to parautochthonous bivalve concentrations within transgressive marginal marine strata of the Upper Jurassic of Portugal. Palaeobiodiversity and Palaeoenvironments 89(3-4):161–190.

Galton PM. 1985. The poposaurid thecodontian *Teratosaurus suevicus* v. Meyer, plus referred specimens mostly based on prosauropod dinosaurs, from the Middle Stubensandstein (Upper Triassic) of Nordwiirttemberg. Stuttgarter Beiträge zur Naturkunde B 116:1–29.

Galton PM. 1994. Notes on Dinosauria and Pterodactylia from the Cretaceous of Portugal. Neues Jahrbuch für Geologie und Paläontologie-Abhadlungen 194(2/3):253–267.

Gauthier J. 1986. Saurischian monophyly and the origin of birds. Memoirs of the California Academy of Sciences 8:1–55.

Golonka J, Edrich ME, Ford DW, Pauken RB, Bocharova NY, Scotese CR. 1996. Jurassic Paleogeographic maps of the World. In: Morales M. Editor. The Continental Jurassic Museum of Northern Arizona, Bulletin 60:1–5.

Gomes JP. 1916. Descoberta de rastos de sáurios gigantescos no Jurássico do Cabo Mondego. Comunicações da Comissão dos Serviços Geológicos de Portugal 11:132–134.

Haq BV, Hardenbol J, Vail PR. 1988. Mesozoic and Cenozoic chronostratigraphy and cycles of sea-level change. In: Wilgus CK, Hastings BS, Posamentier H, Van Wagoner Y, Ross CA, Kendall CG. (Eds). Sea-Level Changes: an Integrated Approach. SEPM Special Publication 42:71–108.

Helmdach F-F. 1971. Stratigraphy and ostracod-fauna from the coalmine Guimarota (Upper Jurassic). Contribuição para o conhecimento da Fauna do Kimeridgiano da mina de Lignito Guimarota (Leiria, Portugal), part II. Memórias dos Serviços Geológicos de Portugal 17:41–98.

Hill G. 1988. The sedimentology and lithostratigraphy of the Upper Jurassic Lourinha formation, Lusitanian Basin, Portugal. [Ph.D. dissertation] Open University, London.

Hill G. 1989. Distal alluvial fan sediments from the Upper Jurassic of Portugal: controls on their cyclicity and channel formation. Journal of the Geological Society of London 146:539–555.

Holtz TR Jr. 1994. The phylogenetic position of the Tyrannosauride: implications for theropod systematics. Journal of Paleontology 68:1100–1117.

Holtz TR Jr. 2000. A new phylogeny of the carnivorous dinosaurs. Gaia 15:5–61.

Huene F von. 1914. Das natürliche system der Saurischia. Zentralblatt für Mineralogie, Geologie und Palaeontologie B 1914:154–158.

Huene F von. 1926. The carnivorous Saurischia in the Jura and Cretaceous formations, principally in Europe. Revista del Museo de La Plata 29:35–167.

Huene F von. 1928. Kurze Ubersicht uber die Saurischia und ihre naturlichen Zusammenhange. Palaeontologiche Zeitschrift 11:269–273.

Huene F von. 1932. Die fossile Reptil-Ordnung Saurischia, ihre Entwicklung und Geschichte. Monographien zur Geologie und Palaeontologie Serie 1(4):1–361.

Kullberg JC. 2000. Evolução tectónica mesozóica da Bacia Lusitaniana. [Ph.D. dissertation] Universidade Nova de Lisboa, Lisboa.

Kullberg JC, Rocha RB, Soares AF, Rey J, Terrinha P, Callapez P, Martins L. 2006. A Bacia Lusitaniana: Estratigrafia, Paleogeografia e Tectónica. In: Dias R, Araújo A, Terrinha P, Kullberg JC. (Eds). Geologia de Portugal no Contexto da Ibéria. Univiversidade de Évora. 317–368.

Kullberg JC, Rocha RB, Soares AF, Rey J, Terrinha P, Azerêdo AC, Callapez P, Duarte LV, Kullberg M C, Martins L, Miranda JR, Alves C, Mata J, Madeira J, Mateus O, Moreira M, Nogueira CR. 2013. A Bacia Lusitaniana: Estratigrafia, Paleogeografia e Tectónica. In: Dias R, Araújo A, Terrinha P, Kullberg JC. (Eds). Geologia de Portugal no Contexto da Ibéria. Escolar Editora, Lisboa. 195-347.

Langer MC, Ezcurra MD, Rauhut, OWM, Benton MJ, Knoll F, McPhee BW, Novas FE, Pol D, Brusatte SL. 2017. Untangling the dinosaur family tree. Nature 551 doi:10.1038/nature24011.

Lapparent AF. 1943. Les Dinosauriens jurassiques de Damparis (Jura). Mémoires de la Société Géologique de France. Nouvelle Série 47.

Lapparent AF, Zbyszewski G. 1957. Les dinosauriens du Portugal. Memórias dos Serviços Geológicos de Portugal 2:1–63,36 pls.

Leinfelder RR. 1986. Facies, Stratigraphy, and Paleogeographic Analysis of Upper? Kimmeridgian to Upper Portlandian Sediments in the Environs of Arruda Dos Vinhos, Estremadura, Portugal. München. Münchner Geowissenschaftliche Abhandlungen 7:1– 215.

Leinfelder RR. 1987. Multifactorial control of sedimentation patterns in an ocean marginal basin: the Lusitanian Basin (Portugal) during the Kimmeridgian and Tithonian. Geologische Rundschau 76:599–631.

Leinfelder RR. 1993. A sequence stratigraphic approach to the Upper Jurassic mixed carbonate - siliciclastic succession of the central Lusitanian Basin, Portugal. Profil 5:119–140.

Leinfelder RR, Wilson RCL. 1989. Seismic and sedimentologic features of the Oxfordian–Kimmeridgian syn-rift sediments on the eastern margin of the Lusitanian Basin. Geologische Rundschau 78:81–104.

Leinfelder RR, Wilson RCL. 1998. Third order sequences in an Upper Jurassic rift-related second order sequence, Central Lusitanian Basin, Portugal. In: de Graciansky P-C, Hardenbol J, Jacquin T, Vail P. (Eds). Mesozoic and Cenozoic Sequence Stratigraphy of European Basins. SEPM Special Publication 60:507–525.

Leinfelder RR, Nose M, Schmid DU, Werner W. 2004. Reefs and Carbonate Platforms in a mixed carbonate-siliciclastic setting. Examples from the Upper Jurassic (Kimmeridgian to Tithonian) of West-Central Portugal. In: Duarte LV, Henriques MH. (Eds). Carboniferous and Jurassic Carbonate Platforms of Iberia. 23rd IAS Meeting of Sedimentology, Coimbra, Field Trip Guidebook Volume 1:95–123.

Louchart A, Pouech J. 2017. A tooth of Archaeopterygidae (Aves) from the Lower Cretaceous of France extends the spatial and temporal occurrence of the earliest birds. Cretaceous Research doi: 10.1016/j.cretres.2017.01.004.

Manatschal G, Bernoulli D. 1998. Rifting and early evolution of ancient ocean basins: the record of the Mesozoic Tethys and of the Galicia-Newfoundland margins. Marine Geophysical Researches 20:371–381.

Manuppella G, Pais J, Legoinha P, Rey J, Ramalho MM, Leinfelder R, Antunes MT, Dias RP, Baptista R, Cardoso JL, Ferreira OV. 1994. Carta Geológica de Portugal na escala de 1/50000. Folha 38-B, Setúbal. Instituto Geológico e Mineiro de Lisboa.

Manuppella G, Antunes MT, Pais J, Ramalho MM, Rey J. 1999. Notícia explicativa da Folha 30-A, Lourinhã. Instituto Geológico e Mineiro de Lisboa.

Marsh OC. 1878. Principal characters of American Jurassic Dinosaurs. Part I. American Journal of Science (Series 3) 16:411–416.

Marsh OC. 1881. Principal characters of American Jurassic dinosaurs. Part V. American Journal of Science (Series 3) 125:417–23.

Marsh OC. 1882. Classification of the Dinosauria. American Journal of Science (Series 3) 133:81 –86.

Marsh OC. 1884. Principal characters of American Jurassic dinosaurs. Part VIII. The order Theropoda. American Journal of Science (Series 3) 27:329–340.

Martin T. 2000. The dryolestids and the primitive 'peramurid' from the Guimarota mine. In: Martin T, Krebs B. (Eds). Guimarota. A Jurassic Ecosystem. Verlag Dr. Friedrich Pfeil, München, Germany. 109–120.

Martinius AW, Gowland S. 2011. Tide influenced fluvial bedforms and tidal bore deposits (Late Jurassic Lourinhã Formation, Lusitanian Basin, Western Portugal). Sedimentology 58(1):285–324.

Mateus I, Mateus H, Antunes MT, Mateus O, Taquet P, Ribeiro V, Manuppella G. 1997. Couvée, oeufs et embryons d'un Dinosaure Théropode du Jurassique supérieur de Lourinhã (Portugal). Comptes Rendus de l'Académie des Sciences Paris. Sciences de la terre et des planètes 325:71–78.

Mateus O, Antunes MT, Taquet P. 2001. Dinosaur ontogeny: the case of *Lourinhanosaurus* (Late Jurassic, Portugal). Journal of Vertebrate Paleontology 21(3, Supplement):78A.

Mateus O. 2005. Dinossauros do Jurássico Superior de Portugal com destaque para os saurísquios. [Ph.D. dissertation] Universidade Nova de Lisboa, Lisboa.

Mateus O, Dinis J, Cunha PP. 2013. Upper Jurassic to Lowermost Cretaceous of the Lusitanian Basin, Portugal - landscapes where dinosaurs walked. Ciências da Terra. Special Number VIII.

Matthew WD, Brown B. 1922. The family Deinodontidae, with notice of a new genus from the Cretaceous of Alberta. Bulletin of the American Museum of Natural History 46:367–385.

Mauffret A, Mougenot D, Miles PR, Malot JA. 1989. Cenozoic deformation and Mesozoic abandoned spreading center in the Tagus Abyssal Plain (West Portugal): results of a multichannel seismic survey. Canadian Journal of Earth Sciences 26(6):1101–1123.

Myers TS, Tabor NJ, Jacobs LJ, Mateus O. 2012. Palaeoclimate of the Late Jurassic of Portugal: comparison with the Western United States. Sedimentology 59:1695–1717.

Mocho P. 2016. Evolutionary history of Upper Jurassic sauropods from the Lusitanian Basin (Portugal). [Ph.D. dissertation] Universidade Autónoma de Madrid, Madrid.

Mocho P, Royo-Torres R, Malafaia E, Escaso F, Ortega F. 2016. Systematic review of Late Jurassic sauropods from the Museu Geológico collections (Lisboa, Portugal). Journal of Iberian Geology 42(2):227–250.

Mocho P, Royo-Torres R, Malafaia E, Escaso F, Ortega F. 2017. First occurrences of non-neosauropod eusauropod procoelous caudal vertebrae in the Portuguese Upper Jurassic record. GeoBios 50:23–36.

Montenat C, Guery F, Jamet M, Berthou P-Y. 1988. Mesozoic evolution of the Lusitanian Basin: Comparisons with the adjacent margin. Proceedings of the Ocean Drilling Program, Scientific Results, Washington (Volume 103):757–775.

Mouterde R, Rocha RB, Ruget C. 1971. Le Lias moyen et supérieur de la región de Tomar. Comunicações dos Serviços Geológicos de Portugal LV:55–86.

Mouterde R, Ramalho M, Rocha RB, Ruget C, Tintant H. 1972. Le Jurassique du Portugal. Esquisse stratigraphique et zonale. Boletim da Sociedade Geológica de Portugal 18(1):75–104.

Mouterde R, Ruget C, Tintant H. 1973. Le passage Oxfordien-Kimméridgien au Portugal (régions de Torres Vedras et du Montejunto). Comptes Rendus de l'Académie des Sciences Paris Séries D 277:2645–2648.

Novas FE. 1992. La evolución de los dinosaurios carnivores. In: Sanz JL, Melendez B, Novas FE, Powell JE, Moratalla JJ, Lockley MG, Buscalioni AD, Morales J, Diéguez C. editors. Los Dinosaurios y su entorno biótico. Instituto Juan de Valdes, Cuenca:126–163.

Novas FE, de Valais S, Vickers-Rich P, Rich T. 2005. A large Cretaceous theropod from Patagonia, Argentina, and the evolution of carcharodontosaurids. Naturwissenschaften 92:226–230.

Novas FE, Agnolín FL, Ezcurra MD, Porfiri J, Canale JI. 2013. Evolution of the carnivorous dinosaurs during the Cretaceous: The evidence from Patagonia. Cretaceous Research 45:174–215.

Ortega F, Escaso F, Gasulla JM, Dantas P, Sanz JL. 2006. Dinosaurios de la Península Ibérica. Estududios Geologicos, Madrid 62(1):219–240.

Osmolska H, Roniewicz E. 1969. Deinocheiridae, a new family of theropod dinosaurs. Palaeontologica Polonica 21:5–19.

Ostrom JH. 1969. Osteology of *Deinonychus antirrhopus*, an unusual theropod from the Lower Cretaceous of Montana. Bulletin of the Peabody Museum of Natural History 30:1–165.

Pena dos Reis RPB, Proença Cunha P, Dinis JL, Trincao PR. 2000. Geological evolution of the Lusitanian Basin (Portugal) during the Late Jurassic. GeoResearch Forum 6:345–356.

Pena dos Reis RPB, Pimentel NL, Garcia AJV. 2011. A Bacia Lusitânica (Portugal): análise estratigráfica e evolução geodinâmica. Buletim das Geociências, Petrobras 9(1/2):23–52.

Pérez-Moreno BP, Sudre J, Sige B. 1993. A theropod dinosaur from the Lower Cretaceous of southern France. Revue de Paléobiologie, Volume Spécial 7:173–188.

Ramalho MM. 1971. Contribution à l'étude micropaléontologique et stratigraphique du Jurassique supérieur et du Crétacé inférieur des environs de Lisbonne (Portugal). Memórias dos Serviços Geológicos de Portugal N.S. 19:1–212.

Ramalho MM. 1981. Note préliminaire sur les microfaciès du Jurassique supérieur portugais. Comunicações dos Serviços Geológicos de Portugal 67:41–45.

Ramalho MM, Rey J. 1969. Correlations stratigraphiques dans les couches de passage du jurassique au cretace Portugal. Buletim da Sociedade Geológica de Portugal 17:31–36.

Ramalho MM, Rey J. 1975. Etat des connaissances actuelles sur le Jurassique terminal et le Crétacé basal du Portugal. Mémoires du BRGM 86:265–273.

Rasmussen ES, Lomholt S, Andersen C, Vejbæk OV. 1998. Aspects of the structural evolution of the Lusitanian Basin in Portugal and the shelf and slope area offshore Portugal. Tectonophysics 300:199–225.

Rauhut OWM. 2001. Herbivorous dinosaurs from the Late Jurassic (Kimmeridgian) of Guimarota, Portugal. Proceedings of the Geological Association 112:275–283.

Rauhut OWM. 2002. Dinosaur teeth from the Barremian of Uña, Province of Cuenca, Spain. Cretaceous Research 23:255–263.

Rauhut OWM. 2003a. The interrelationships and evolution of basal theropod dinosaurs. Special Papers in Palaeontology 69:1–213.

Rauhut OWM. 2003b. A tyrannosauroid dinosaur from the Upper Jurassic of Portugal. Palaeontology 46(5):903–910.

Rauhut OWM, Fechner R. 2005. Early development of the facial region in a non-avian theropod dinosaur. Proceedings of the Royal Society B 272:1179–1183.

Rauhut OWM, Hübner TR, Lansen K-P. 2016. A new megalosaurid theropod dinosaur from the late Middle Jurassic (Callovian) of north-western Germany: Implications for theropod evolution and faunal turnover in the Jurassic. Palaeontologia Electronica 19.2.26A:1–65.

Reis RP, Dinis JL, Cunha PP, Trincão P. 1996. Upper Jurassic sedimentary infill and tectonics of the Lusitanian Basin (Western Portugal). GeoResearch Forum, Volumes 1-2:377–386.

Reis RP, Cunha PP, Dinis JL. 1997. Hipersubsient depositional event associated with a rift climax in late Jurassic of Lusitanian Basin (W Portugal). IV Congreso Jurásico de España. Alcaniz:101–103.

Reis RP, Cunha PP, Dinis JL, Trincão PR. 2000. Geologic evolution of the Lusitanian Basin (Portugal) during the Late Jurassic. Proceedings 5th International Symposium on the Jurassic system. GeoResearch Forum 6:345–356.

Rey J. 1992. Les unités lithostratigraphiques du Crétace inférieur de la région de Lisbonne. Comunicações dos Serviços Geológicos de Portugal 78(2):103–124.

Rey J. 1999. Lower Cretaceous Depositional Sequences in the Cascais Area. European Palaeontological Association Workshop. Lisboa. Field trip A: 57.

Ribeiro A, Kullberg M.C, Kullberg JC, Manuppella G, Phipps S. 1990. A review of Alpine tectonics in Portugal: Foreland detachment in basement and cover rocks. Tectonophysics 184:357–366.

Ribeiro A, Cabral J, Baptista R, Matias L. 1996. Stress pattern in Portugal mainland and the adjacent Atlantic region, West Iberia. Tectonics 15(2):641–659.

Rocha RB, Marques J, Soares AF. 1990. Les unités lithostratigraphiques du Bassin Lusitanien au Nord de l'accident de Nazaré (Trias-Aalénien). Cahiers de l'Université Catholique de Lyon, Série Scientifique 4:121–126.

Rocha RB, Marques BL, Kullberg JC, Caetano PC, Lopes C, Soares AF, Duarte LV, Marques JF, Gomes CR. 1996. The 1st and 2nd rifting phases of the Lusitanian Basin: stratigraphy, sequence analysis and sedimentary evolution. Final Report C.E.C. Project MILUPOBAS 4 vol. Lisboa.

Romer AS. 1966. Vertebrate paleontology. Third edition. University of Chicago Press, Chicago.

Ruget-Perrot C. 1961. Études stratigraphiques sur le Dogger et le Malm inférieur du Portugal au Nord du Tage. Bajocien. Bathonien, Callovien et Lusitanien. Memórias dos Serviços Geológicos de Portugal N. S. 7:1 –197.

Sauvage H-É. 1874. Mémoire sur les Dinosauriens et Crocodiliens des terrains jurassiques de Boulogne-sue-Mer. Mémoires de la Société Géologique de France 2 X.

Sauvage H-É. 1897-98. Vértebrés fossiles du Portugal. Contribution á l'étude des poissons et des reptiles du Jurassique et du Crétacé. Mémoires de la Direction des Travaux Géologiques du Portugal.

Schneider S, Fursich FT, Werner W. 2009. Sr-isotope stratigraphy of the Upper Jurassic of central Portugal (Lusitanian Basin) based on oyster shells. International Journal of Earth Sciences (Geologische Rundschau) 98:1949–1970.

Seeley H.G. On the Classification of the Fossil Animals commonly named Dinosauria. Proceedings of the Royal Society of London 43:165–171.

Senter P. 2007. A new look at the Phylogeny of Coelurosauria (Dinosauria: Theropoda). Journal of Systematic Palaeontology 5(4):429–463.

Sereno PC. 1997. The origin and evolution of dinosaurs. Annual Review of Earth and Planetary Sciences 25:435–489.

Sereno PC. 1998. A rationale for phylogenetic definitions, with application to the higher-level taxonomy of Dinosauria. Neues Jahrbuch für Geologie und Paläontologie-Abhandlungen 210:41–83.

Sereno PC. 1999. The evolution of dinosaurs. Science 284:2137–2147.

Sereno PC, Duthell DB, Iarochene M, Larsson HCE, Lyon GH, Magwene PM, Sidor CA, Varricchio DJ, Wilson JA. 1996. Predatory dinosaurs from the Sahara and Late Cretaceous faunal differentiation. Science 272:986–991.

Sereno PC, Beck AL, Dutheil DB, Gado B, Larsson HCE, Lyon GH, Marcot JD, Rauhut OWM, Sadleir RW, Sidor CA, Varricchio DD, Wilson GP, Wilson JA. 1998. A long-snouted predatory dinosaur from Africa and the evolution of spinosaurids. Science 282:1298–1302.

Sharpe D. 1850. On the Secondary district of Portugal which lies on the North of the Tagus. Quarterly Journal of the Geological Society of London 6:135–201.

Smith AG, Smith DG, Funnell BM. 1994. Atlas of Mesozoic and Cenozoic Coastlines. Cambridge University Press, Cambridge.

Soares AF, Marques JF, Rocha RB. 1985. Contribuição para o conhecimento geológico de Coimbra. Memórias e Notícias. Publicações do Museu e Laboratório Geológico da Universidade de Coimbra 100:41–71.

Srivastava SP, Verhoef J. 1992. Evolution of Mesozoic sedimentary basins around the North Central Atlantic: a preliminary plate kinematic solution. In: Parnell J. (Eds). Basins on the Atlantic Seaboard: Petroleum Geology, Sedimentology and Basin Evolution. Geological Society, Special Publication 62:397–420.

Stapel G, Cloetingh S, Pronk B. 1996. Quantitative subsidence analysis of the Mesozoic evolution of the Lusitanian basin (western Iberian margin). Tectonophysics 266(1):493–507.

Steel R. 1970. Part 14. Saurischia. Handbuch der Paläoherpetologie [Encyclopedia of Paleoherpetology]. Gustav Fischer, Stuttgart: 1–87.

Taylor AM, Gowland S, Leary S, Keogh KJ, Martinius AW. 2014. Stratigraphical correlation of the Lourinhã Formation in the Consolação Sub-basin (Lusitanian Basin), Portugal. Geological Journal 49(2):143–162.

Teixeira C, Zbyszewski G. 1968. Notícia explicativa da folha 23-C, Leiria. Serviços Geológicos de Portugal.

Thulborn RA. 1973. Teeth of ornithischian dinosaurs from the Upper Jurassic of Portugal. Memórias dos Serviços Geológicos de Portugal N.S. 22:89–134.

Thulborn RA. 1984. The avian relationships of *Archaeopteryx*, and the origin of birds. Zoological Journal of the Linnean Society 82:119–158.

Turell JD, Pares JM. 1996. El Triasico de la Peninsula Ibérica, nuevos datos paleomagnéticos. Cuadernos de Geologia Iberica 20:367–384.

Upchurch P, Hunn CA, Norman DB. 2002. An analysis of dinosaurian biogeography: evidence for the existence of vicariance and dispersal patterns caused by geological events. Proceedings of the Royal Society of London B 269:613–621.

Walker AD. 1970. A Revision of the Jurassic Reptile *Hallopus victor* (Marsh), with Remarks on the Classification of Crocodiles. Philosophical Transactions of the Royal Society of London. Series B, Biological Sciences 257(816):323–372.

Weigert A. 1995. Isolierte Zähne von cf. *Archaeopteryx* sp. aus dem Oberen Jura der Kohlengrube Guimarota (Portugal). Neues Jahrbuch für Geologie und Paläontologie 9:562–576.

Werner W. 1986. Palökologische und biofazielle Analyse des Kimmeridge (Oberjura) von Consolacao, Mittelportugal. Zitteliana 13:3–109.

Wilson RCL. 1975. Atlantic opening and Mesozoic margin basins of Iberia. Earth and Planetary Science Letters 25(1):33–43.

Wilson RCL. 1979. A reconnaissance study of Upper Jurassic sediments of the Lusitanian Basin. Ciências da Terra (UNL) 5:53–84.

Wilson RCL. 1988. Mesozoic development of the Lusitanian basin, Portugal. Revista de la Sociedad Geológica de España 1(3-4):393–407.

Wilson RCL, Hiscott RN, Willis MG, Gradstein FM. 1989. The Lusitanian Basin of west-central Portugal: Mesozoic and Tertiary tectonic, stratigraphic, and subsidence history. In: Tankard AJ, Balkwill HR. (Eds). Extensional Tectonics and Stratigraphy of the North Atlantic Margins. AAPG Memory 46: 341–361.

Wilson RCL, Manatschal G, Wise S. 2001. Rifting along nonvolcanic passive margins: Stratigraphic and seismic evidence from the Mesozoic of the Alps and Western Iberia. In: Wilson RCL, Withmarsh RB, Taylor B, Froitzheim N. (Eds). Non-volcabic Rifting and Continantal Margins: Evidence from Land and Sea. Geological Society of London, Special Publication 187:429–452.

Zbyszewski G. 1946. Les ossements d'*Omosaurus* découverts près de Baleal, Peniche. Comununicações dos Serviços Geológicos de Portugal 135–144.

Zbyszewski G, Almeida FM. 1955. Notícia explicativa da Folha 3D-C, Torres Yedras. Serviços Geológicos de Portugal.

Zbyszewski G, Ferreira O. 1966. Notícia explicativa da Folha 3D-B, Bombarral. Serviços Geológicos de Portugal.

Zinke J. 1998. Small theropod teeth from the Upper Jurassic coal mine of Guimarota (Portugal). Paläontologische Zeitschrift 72:179–189.

Zinke J, Rauhut OWM. 1994. Small theropods (Dinosauria, Saurischia) from the Upper Jurassic and Lower Cretaceous of the Iberian Peninsula. Berliner Geowissenshaftliche Abhandlungen E13:163–177.

CHAPTER 2: OBJECTIVES AND HYPOTHESES

2.1. OBJECTIVES AND HYPOTHESES

The objective of this project is to develop a phylogenetic analysis of the record of theropod dinosaurs from the Upper Jurassic of the Lusitanian Basin. The main objective of this study is to test two generic hypotheses about the Upper Jurassic record of theropod dinosaurs of the Lusitanian Basin: (i) this record is composed by forms closely related with taxa described in correlative sedimentary levels from the Morrison Formation, indicating the existence of dispersal events among these landmasses during the Late Jurassic; or whether (ii) it is composed mainly by exclusive forms, at generic or specific levels, implying that processes of incipient vicariance were already evident in these theropod faunas.

These hypotheses were tested based on ascertain of several more specific hypotheses and objectives about the theropod fauna from the Late Jurassic o the Lusitanian Basin, which are synthesized below.

Objective 1.1. Establish if the specimens attributed to *Ceratosaurus* from the Upper Jurassic of the Lusitanian Basin may be distinguished from those known in correlative levels of the Morrison Formation.

Hypothesis 1.1. The specimens attributed to *Ceratosaurus* from the Valmitão fossil site may be assigned to a new species exclusive for the Upper Jurassic record of the Lusitanian Basin.

Objective 1.2. Test the presence of the megalosaurid *Torvosaurus tanneri* in the Upper Jurassic record of the Lusitanian Basin.

Hypothesis 1.2. The specimens attributed to *Torvosaurus* from the Praia da Vermelha (upper Kimmeridgian, Peniche) and Praia da Corva (upper Kimmeridgian, Torres Vedras) fossil sites may be assigned to the species *T. tanneri* described in the Morrison Formation.

Objective 1.3. Test the validity of the species *Torvosaurus gurneyi* and verify if all specimens attributed to megalosauroid theropods from the Upper Jurassic of the Lusitanian Basin may be assigned to this species exclusive for the Portuguese record.

Hypothesis 1.3. The diagnosis of the species *T. gurneyi* is based on features that may be related with intraspecific variability of *T. tanneri* representing a junior synonym of this North American species.

Objective 1.4. Test the presence of the allosaurid *Allosaurus fragilis* in the Upper Jurassic record of the Lusitanian Basin.

Hypothesis 1.4. The specimens attributed to *Allosaurus* from the Andrés (upper Kimmeridgian–Tithonian, Pombal) fossil site may be assigned to the species *A. fragilis* described in the Morrison Formation.

Objective 1.5. Test the validity of *Allosaurus europaeus* and verify if all specimens attributed to *Allosaurus* from the Upper Jurassic of the Lusitanian Basin from the Andrés, Guimarota (upper Kimmeridgian–lower Tithonian, Leiria), and Praia de Vale Frades (upper Kimmeridgian–lower Tithonian, Lourinhã) fossil sites may be assigned to this species exclusive for the Portuguese record.

Hypothesis 1.5. The diagnosis of the species *A. europaeus* is based on features that may be related with intraspecific variability of *A. fragilis* representing a junior synonym of this North American species.

Objective 1.6. Establish if the specimen SHN.036 from the Valmitão fossil site corresponds to a new taxon.

Hypothesis 1.6. A set of unpublished remains found in the Praia de Amoreira-Porto Novo Formation (upper Kimmeridgian) of Valmitão corresponds to a juvenile allosauroid that is distinct from both allosauroid taxa known in the Upper Jurassic of the Lusitanian Basin (i.e. *Allosaurus* and *Lourinhanosaurus*).

Objective 1.7. Establish if the specimen SHN.019 from the Cambelas fossil site corresponds to a new taxon.

Hypothesis 1.7. A set of unpublished remains found in the Freixial Formation (upper Tithonian) of Cambelas belongs to the same taxon as SHN.036 representing an allosauroid form distinct from both allosauroid taxa known in the Upper Jurassic of the Lusitanian Basin (i.e. *Allosaurus* and *Lourinhanosaurus*).

Objective 1.8. Test the validity of the species *Lourinhanosaurus antunesi* from upper Kimmeridgian–lower Tithonian of Peralta (Lourinhã) and establish a phylogenetic approach for this taxon.

Hypothesis 1.8. *L. antunesi* corresponds to a theropod form that may be assigned to other allosauroid taxon known in the Upper Jurassic of the Lusitanian Basin.

Objective 2. Establish if the phylogenetic relationships between the Portuguese and North American theropods support the previously proposed existence of Late Jurassic interchanges of these faunas.

Hypothesis 2. The composition of the theropod fauna from the Upper Jurassic of the Lusitanian Basin are composed by taxa shared with the record known in correlative sedimentary levels of the Morrison Formation.

Objective 3. Establish the theropod paleobiodiversity for the Upper Jurassic of the Lusitanian Basin.

Hypothesis 3. The theropod paleobiodiversity for the Upper Jurassic of the Lusitanian Basin includes Ceratosauria, Megalosauroidea, Allosauroidea, and Coelurosauria.

Objective 4. Establish the geographic and stratigraphic distribution of the different theropod clades represented in the Upper Jurassic record of the Lusitanian Basin.

Hypothesis 4. The theropod clades from the Upper Jurassic of the Lusitanian Basin (Ceratosauria, Megalosauroidea, Allosauroidea, and Coelurosauria) have homogeneous stratigraphic and geographical distribution.

Objective 5. Establish the relationships between the theropod taxa from the Upper Jurassic of the Lusitanian Basin and those known in correlative levels of other European sites.

Hypothesis 5. The theropod fauna represented in the Upper Jurassic record of the Lusitanian Basin show some regional endemism, as there are no taxa shared with correlative levels of other European sites.

CHAPTER 3: MATERIALS AND METHODS

3.1. MATERIALS

A systematic study of the Upper Jurassic record of theropod somatofossils from the Lusitanian Basin was performed. Several paleontological collections with Upper Jurassic theropod specimens from Portugal were accessed, including the classical material referred by Sauvage (1897-98), Zbyszewski (1946) and Lapparent and Zbyszewski (1957), which are housed in the Museu Geológico (Lisboa, Portugal) and Museu Nacional de História Natural e da Ciência (Lisboa, Portugal). Also studied were several previously described specimens, including the type material of the Portuguese taxa: *Lourinhanosaurus antunesi* Mateus 1998, *Torvosaurus gurneyi* Hendrickx and Mateus 2014, *Allosaurus europaeus* Mateus et al. 2006, and *Aviatyrannis jurassica* Rauhut 2003a, housed in the Museu da Lourinhã and in the Museu Geológico. Besides, several unpublished specimens found in the last decades and deposited in the Museu Nacional de História Natural e da Ciência (Lisboa, Portugal) and Sociedade de História Natural (Torres Vedras, Portugal) were described.

Several published and unpublished specimens from other European sites and correlative levels from North America and Africa were analysed in order to incorporate information for the phylogenetic analyses of the theropod record from the Lusitanian Basin. The accessed material is deposited in the Fundación Conjunto Paleontológico de Teruel-Dinópolis/Museo Aragonés de Paleontología (Teruel, Spain), Museo Paleontológico de Galve (Galve, Spain) and Museo de las Ciencias de Castilla la Mancha (Cuenca, Spain), Muséum national d'Histoire naturelle (Paris, France), Humboldt Museum für Naturkunde (Berlin, Germany), Natural History Museum (London, UK), Oxford University Natural History Museum (Oxford, UK), Natural History Museum of Los Angeles County (Los Angeles, Califórnia, USA), Utah Museum of Natural History (Salt Lake City, Utah, USA), Museum of Paleontology of the Brigham Young University (Provo, Utah, USA), Dinosaur National Monument (Vernal, Utah, USA), Denver Museum of Natural History and Science (Denver, Colorado, USA).

3.2. METHODS

This thesis is composed by a set of manuscripts focusing on the study of several unpublished theropod specimen collected in different Upper Jurassic fossil sites from the Lusitanian Basin. The terminology used in the anatomical description of the vertebrae laminae and fossae follows Wilson (1999) and Wilson et al. (2011), respectively. Anterior and posterior (romerian nomenclatures: Romer 1956) instead cranial and caudal therms (Baumel and Witmer 1993) were used for the description of bone orientation. Also the term caudal rib instead transverse process was used for description of the lateral projections of caudal vertebrae (following Persons and Currie 2011). Additional comments on nomenclature for the different specimens described are included on each corresponding section along the respective manuscript.

The phylogenetic analysis of the Upper Jurassic theropod record from the Lusitanian Basin was based on data matrices published by different authors, including Holtz (2000), Sereno (1999), Rauhut (2003b), Carrano and Sampson (2008), Brusatte and Sereno (2008), Benson (2010), Eddy and Clarke (2011), and Carrano et al. (2012). The data matrices were analyzed using TNT 1.1 (Goloboff et al. 2003) to find the most parsimonious trees (MPTs). The specific procedure for each analysis is explained in the corresponding section along the respective manuscript.

Multivariate statistical analyses were developed for study of a set of isolated theropod teeth. Discriminant Function Analysis (DFA), using the software IBM SPSS Statistics 17.0 program (SPSS Inc., Chicago, Illinois) and Principal Components Analysis (PCA), using PAST3 software package (Hammer et al. 2001) were performed in order to assign each morphotype to a certain taxon. These analyses were based on the datasets published by Smith et al. (2005), Hendrickx et al. (2015), and Gerke and Wings (2016). The specific procedure for these analyses is explained in the corresponding section along the respective manuscript.

REFERENCES

Baumel JJ, Witmer LM. 1993. Osteologia. In: Baumel JJ. (Eds). Handbook of Avian Anatomy: Nomina Anatomica Avium. Second Edition. Nuttall Ornithological Club, Cambridge. Massachusetts. 45–132.

Benson RBJ. 2010. A description of *Megalosaurus bucklandii* (Dinosauria: Theropoda) from the Bathonian of the UK and the relationships of Middle Jurassic theropods. Zoological Journal of the Linnean Society 158:882–935.

Brusatte SL, Sereno PC. 2008. Phylogeny of Allosauroidea (Dinosauria: Theropoda): comparative analysis and resolution. Journal of Systematic Palaeontology 6:155–182.

Carrano MT, Sampson SD. 2008. The Phylogeny of Ceratosauria (Dinosauria: Theropoda). Journal of Systematic Palaeontology 6 (2):183–236.

Carrano MT, Benson RBJ, Sampson SD. 2012. The phylogeny of Tetanurae (Dinosauria: Theropoda). Journal of Systematic Palaeontology 10:211–300.

Eddy DR, Clarke JA. 2011. New information on the cranial anatomy of *Acrocanthosaurus atokensis* and its implications for the phylogeny of Allosauroidea (Dinosauria: Theropoda). PLoS One 6:e17932.

Gerke O, Wings O. 2016. Multivariate and cladistic analyses of isolated teeth reveal sympatry of theropod dinosaurs in the Late Jurassic of northern Germany. PLoS ONE 11(7):e0158334.

Goloboff P, Farris J, Nixon K. 2003. T.N.T.: tree analysis using new technology. Program and documentation. http://www.zmuc.dk/public/phylogeny/tnt.

Hammer Ø, Harper DAT, Ryan PD. 2001. Past: Paleontological Statistics Software Package for education and data analysis. Palaeontologia Electronica 4(1):1–9.

Hendrickx C, Mateus O. 2014. *Torvosaurus gurneyi* n. sp., the largest terrestrial predator from Europe, and a proposed terminology of the maxilla anatomy in nonavian theropods. PLoS One. 9:e88905.

Hendrickx C, Mateus O, Araújo R. 2015. The dentition of megalosaurid theropods. Acta Palaeontologica Polonica, 60(3):627–642.

Holtz, TR Jr. 2000. A new phylogeny of the carnivorous dinosaurs. GAIA 15:5–61.

Lapparent AF, Zbyszewski G. 1957. Les dinosauriens du Portugal [The dinosaurs of Portugal]. Memórias Serviços Geológicos de Portugal 2:1–63.

Mateus O. 1998. *Lourinhanosaurus antunesi*, a new upper Jurassic allosauroid (Dinosauria: Theropoda) from Lourinhã, Portugal. Memórias da Academia de Ciências de Lisboa 37:111–124.

Mateus O, Walen A, Antunes MT. 2006. The large theropod fauna of the Lourinhã Formation (Portugal) and its similarity to the Morrison Formation, with a description of a new species of *Allosaurus*. In: Foster JR, Lucas SG. (Eds). Paleontology and geology of the Upper Jurassic Morrison Formation. Vol. 36. New Mexico Museum of Natural History and Science, Bulletin. 123–129.

Persons SW, Currie PJ. 2011. Dinosaur speed demon: the caudal musculature of *Carnotaurus sastrei* and implications for the evolution of South American abelisaurids. PLos ONE. 6:e25763.

Rauhut OWM. 2003a. A tyrannosauroid dinosaur from the Upper Jurassic of Portugal. Palaeontology. 46:903–910.

Rauhut OWM. 2003b. The interrelationships and evolution of basal theropod dinosaurs. Special Papers in Palaeontology 69:1–213.

Romer AS. 1956. Osteology of the Reptiles. University of Chicago Press, Chicago.

Sauvage HE. 1897-98. Vértebrés fossiles du Portugal. Contribution á l'étude des poissons et des reptiles du Jurassique et du Crétacé. Mémoires de la Direction des Travaux Géologiques du Portugal: 1–46.

Sereno PC. 1999. The evolution of dinosaurs. Science 284:2137–2147.

Smith JB, Vann DR, Dodson P. 2005. Dental morphology and variation in theropod dinosaurs: implications for the taxonomic identification of isolated teeth. The Anatomical Record Part A 285A:699–736.

Wilson JA. 1999. A nomenclature for vertebral laminae in sauropods and other saurischian dinosaurs. Journal of Vertebrate Paleontology 19 (4):639–653.

Wilson JA, D'Emic MD, Ikejiri T, Moacdieh EM, Whitlock JA. 2011. A Nomenclature for vertebral fossae in sauropods and other saurischian dinosaurs. PLoS ONE 6(2):e17114.

Zbyszewski G. 1946. Les ossements d' découverts près de Baleal (Peniche). Comunicações dos Serviços Geológicos de Portugal 28:135–144.

SECOND PART

CHAPTER 4: CERATOSAURIA

4.1. Introduction

4.2. New evidence of *Ceratosaurus* (Dinosauria: Theropoda) from the Late Jurassic of the Lusitanian Basin, Portugal

CHAPTER 5: MEGALOSAUROIDEA

5.1. Introduction

5.2. New data on the anatomy of *Torvosaurus* and other remains of megalosauroid (Dinosauria, Theropoda) from the Upper Jurassic of Portugal

CHAPTER 6: ALLOSAUROIDEA

6.1. Introduction

6.2. Vertebrate fauna at the *Allosaurus* fossil site of Andrés (Upper Jurassic), Pombal, Portugal

6.3. Analysis of the anatomy of *Allosaurus* (Tetanurae, Avetheropoda) from the Lusitanian Basin based on new specimens of the Portuguese Upper Jurassic

6.4. A juvenile allosauroid theropod (Dinosauria, Saurischia) from the Upper Jurassic of Portugal

6.5. A new allosauroid theropod specimen from Cambelas (Tithonian. Torres Vedras, Portugal)

CHAPTER 7: COELUROSAURIA

7.1. Coelurosaurian theropods from the Upper Jurassic of the Lusitanian Basin

CHAPTER 4: CERATOSAURIA

4.1. INTRODUCTION

Ceratosauria was established by Othniel Charles Marsh (1884) based on a specimen collected in the Upper Jurassic Morrison Formation in Colorado, which was described as a new species: *Ceratosaurus nasicornis*. Marsh noted a set of features unique for *Ceratosaurus* that includes: (1) fused pelvic elements; (2) coossified metatarsus; (3) midline dorsal osteoderms; and (4) median nasal horn. Based on this combination of characters Marsh considered that *Ceratosaurus* occupied a distinct position among theropods, setting it in its own clade, Ceratosauria (Marsh 1884). Few taxa were later referred to Ceratosauria (*sensu* Marsh 1884), including some fragmentary specimens from the Tendaguru Formation in Tanzania described as *Ceratosaurus* (?) *roechlingi* (Janensch 1925) and *Chienkosaurus ceratosauroides* from the Kyangyuan Series in China (Young 1942). Over time, 'Ceratosauria' fell into disuse and *Ceratosaurus* was generally considered to be an aberrant, primitive carnosaur (Carrano et al. 2012). A significant change came with the proposal of Gauthier (1986) in which he separated most theropods in two clades: Tetanurae, which included most 'carnosaurs', 'coelurosaurs' and birds, and its sister taxon Ceratosauria. Based on this proposal, Ceratosauria includes *Ceratosaurus* and some more primitive 'coelurosaurs' such as *Coelophysis* (Late Triassic, USA), *Segisaurus* (Early Jurassic, USA), *Dilophosaurus* (Early Jurassic, USA), and *Syntarsus* (Early Jurassic, Africa).

Later, Bonaparte and Novas (1985) following the description of *Abelisaurus comahuensis* (Late Cretaceous, Argentina), found several similarities between this taxon, *Ceratosaurus* and the Indian taxa *Indosaurus matleyi* and *Indosuchus raptorius*. Based on this finding, Ceratosauria was interpreted as comprising *Ceratosaurus*, coelophysoids and abelisauroids. Since then, also several taxa from Europe (*Tarascosaurus salluvicus*, *Betasuchus bredai*: Le Loeuff and Buffetaut 1991), South America (*Ilokelesia aguadagrandensis*: Coria and Salgado 2000), Africa (*Elaphrosaurus bambergi*: Holtz 1994, 2000) and Madagascar (*Majungatholus atopus*, *Masiakasaurus knopfleri*: Sampson et al. 1998, 2001) were referred to abelisauroids.

Recent studies (e.g. Carrano and Sampson 1999; Forster 1999; Rauhut 2000, 2003; Sampson et al. 2001; Carrano et al. 2002; Wilson et al. 2003; Sereno et al. 2004) suggested an alternative definition for Ceratosauria excluding Coelophysoidea and considering ceratosaurs (*Ceratosaurus* + Abelisauroidea) more closely related to tetanurans than to coelophysoids. An extensive phylogenetic analysis of Ceratosauria performed by Carrano and Sampson (2008) proposed that *Elaphrosaurus*, *Deltadromeus*, and *Spinostropheus* are the most primitive ceratosaurs, followed by *Ceratosaurus* and Abelisauroidea (Noasauridae + Abelisauridae). However, a redescription of the holotypic material of *Elaphrosaurus* from the Upper Jurassic of the Tendaguru Formation found that this taxon shares several derived characters with noasaurids and placed it in a subclade, Elaphrosaurinae, which also includes taxa from eastern Asia, within a dichotomous Noasauridae (Rauhut and Carrano 2016).

The record of ceratosaurian theropods from the Upper Jurassic of the Lusitanian Basin is relatively scarce. This record includes few specimens assigned to *Ceratosaurus* (Mateus and Antunes 2000; Mateus et al. 2006; Malafaia et al. 2015; Malafaia et al. in press) and some isolated teeth tentatively attributed to abelisaurids (Hendrickx and Mateus 2014). *Ceratosaurus* is represented by some appendicular elements of a single individual collected in sediments of the upper Kimmeridgian Praia da Amoreira-Porto Novo Formation (Mateus and Antunes 2000; Mateus et al. 2006; Malafaia et al. 2015). This set of osteological remains was found on the cliffs of the Valmitão beach (Ribamar, Lourinhã) as result of coastal erosion and collected at different times by two institutions, the Museu da Lourinhã (ML352, a right femur and a left tibia) and the Sociedade de História Natural (SHN(JJS)-65, a left femur, a right tibia, and a fragment of a left fibula). These specimens were interpreted as belonging to the same individual because they were

collected in the same site and in the same sedimentary horizon, the skeletal elements of both specimens (i.e. the femora and tibiae) have compatible size and morphology, and there are not duplicated elements (Malafaia et al. 2015).

The original descripcion of part of the specimen collected in Valmitão, (ML352) identified minor differences relative to *C. nasicornis*, including: (1) more developed fibular crest; (2) more developed notch in the distal femoral head; (3) relative position of the epiphysial expansions; (4) presence of a posterior intercondylar bridge on the femur (Mateus et al. 2006). Based on these putative differences, ML352 was interpreted as belonging to a *Ceratosaurus* sp. closer to *Ceratosaurus dentisulcatus* than to *C. nasicornis* or *Ceratosaurus magnicornis*. However, the species *C. dentisulcatus* and *C. magnicornis* proposed by Madsen and Welles (2000) are diagnosed based mainly on morphometric differences and some authors (e.g. Rauhut 2003; Carrano and Sampson 2008) interpreted both species as junior synonyms of *C. nasicornis.*

The objective of this study is to test if the specimens attributed to *Ceratosaurus* known in the Upper Jurassic record of the Lusitanian Basin may be distinguished from the North American species *C. nasicornis*. This study, based on the description of the specimen SHN(JJS)-65 and review of ML352, allowed identify a combination of features shared with the North American forms of *Ceratosaurus*, including: (1) lesser trochanter positioned low on the femur; (2) crista tibiofibularis obliquely oriented with respect to the axis of the femoral shaft; (3) infrapopliteal ridge present posteriorly on the femur; (4) large cnemial crest; and (5) medial condyle of the tibia continuous with the proximal end (Malafaia et al. 2015). Some differences noted relative to *C. nasicorsis*, such as lack of fusion of the tibia and astragalus and absence of a nutrient foramen in the proximal tibia may be related with ontogeny, sexual dimorphism and/or individual variation (Malafaia et al. 2015).

A collection of isolated teeth coming from different sites in the littoral of the Central Sector of the Lusitanian Basin, between Peniche and Torres Vedras, was also interpreted as belonging to *Ceratosaurus* (Malafaia et al. in press). These specimens were mostly collected in sediments of the Praia da Amoreira-Porto Novo Formation, but few teeth came from the Freixial and Sobral formations, spanning from the later most Kimmeridgian to late Tithonian in age. These isolated teeth are grouped in two morphotypes corresponding to different position on the tooth row.

The *Ceratosaurus* specimens from the Lusitanian Basin constitute one of the scarce evidence of basal ceratosaurian theropods known in the Upper Jurassic of Europe extending the geographical distribution of this taxon to the Iberian Peninsula. Ceratosauria was a relatively abundant and diverse clade during the Late Cretaceous, but its early evolutionary history remains poorly understood. Thus, the Portuguese specimens add significant information for the knowledge of the paleobiogeographic evolution of this clade during the Late Jurassic.

Some isolated theropod teeth collected on the cliffs of Lourinhã (ML327 and ML966) were tentatively attributed to abelisaurid ceratosaurians based on the following combination of features: (1) large crown (CH > 30 mm); (2) almost straight distal profile of the tooth; (3) transversal and short marginal undulations on the crown; (4) denticles with strongly developed interdenticular sulci; (5) DSDI close to one; (6) irregular enamel texture; and (7) presence of apically pointed denticles on the distal carina in ML 327 (Hendrickx and Mateus 2014). However, this combination of features may be also found in other theropod teeth such as *Allosaurus* (Hendrickx et al. 2015; Gerke and Wings 2016). Besides, since the presence of abelisaurids in the Upper Jurassic of Laurasia is ambiguous (Rauhut 2012; Gerke and Wings 2016) the identification of these isolated teeth needs to be confirmed based on more complete material.

REFERENCES

Bonaparte JF, Novas FE. 1985. *Abelisaurus comahuensis*, n. g., n. sp., Carnosauria del Crétacico Tardio de Patagonia. Ameghiniana 21: 259–265.

Carrano MT, Sampson SD. 1999. Evidence for a paraphyletic Ceratosauria and its implications for theropod dinosaur evolution. Journal of Vertebrate Paleontology 19 (3, suppl.): 36A.

Carrano MT, Sampson SD. 2008. The Phylogeny of Ceratosauria (Dinosauria: Theropoda). Journal of Systematic Palaeontology 6(2): 183–236. doi:10.1017/S1477201907002246

Carrano MT, Sampson SD, Forster CA. 2002. The osteology of *Masiakasaurus knopfleri*, a small abelisauroid (Dinosauria: Theropoda) from the Late Cretaceous of Madagascar. Journal of Vertebrate Paleontology 22(3): 510–534.

Coria RA, Salgado L. 2000. A basal Abelisauria Novas 1992 (Theropoda–Ceratosauria) from the Cretaceous of Patagonia, Argentina. GAIA 15: 89–102.

Forster CA. 1999. Gondwanan dinosaur evolution and biogeographic analysis. Journal of African Earth Sciences 28(1): 169–185.

Gauthier JA. 1986. Saurischian monophyly and the origin of birds. In: K. Padian (Eds.) The Origin of Birds and the Evolution of Flight. Memoirs of the California Academy of Sciences: San Francisco. 47pp.

Gerke O, Wings O. 2016. Multivariate and cladistic analyses of isolated teeth reveal sympatry of theropod dinosaurs in the Late Jurassic of northern Germany. PLoS ONE 11(7): e0158334. doi:10.1371/journal.pone.0158334.

Hendrickx C, Mateus O. 2014. Abelisauridae (Dinosauria: Theropoda) from the Late Jurassic of Portugal and dentition-based phylogeny as a contribution for the identification of isolated theropod teeth. Zootaxa 3759(1): 1–74. doi:10.11646/zootaxa.3759.1.1

Hendrickx C, Mateus O, Araújo R. 2015. The dentition of megalosaurid theropods. Acta Palaeontologica Polonica 60 (3): 627–642. doi:10.4202/app.00056.2013

Holtz TRJr. 1994. The phylogenetic position of the Tyrannosauridae: implications for theropod systematics. Journal of Paleontology 68: 1100–1117.

Holtz TRJr. 2000. A new phylogeny of the carnivorous dinosaurs. GAIA 15:5–61.

Janensch W. 1925. Die Coelurosaurier und Theropoden der Tendaguru-Schichten Deutsch-Ostafrikas. Palaeontographica 7 (Suppl. I): 1–99.

Le Loeuff J, Buffetaut E. 1991. *Tarascosaurus salluvicus* nov. gen., nov. sp., dinosaure théropode du Crétacé Supérieur du sud de la France. Géobios 24: 585–594.

Madsen JH, Welles SP. 2000. *Ceratosaurus* (Dinosauria, Theropoda) a revised osteology. Utah Geological Survey, Miscellaneous Publication 2: 1–80.

Malafaia E, Escaso F, Mocho P, Serrano-Martínez A, Torices A, Cachão M, Ortega F. (in press). Analysis of diversity, stratigraphic and geographical distribution of isolated theropod teeth from the Upper Jurassic of the Lusitanian Basin, Portugal. Journal of Iberian Geology.

Malafaia E, Ortega F, Escaso F, Silva B. 2015. New evidence of *Ceratosaurus* (Dinosauria: Theropoda) from the Late Jurassic of the Lusitanian Basin, Portugal. Historical Biology. 27(7): 938–946. doi:10.1080/08912963.2014.915820.

Marsh OC. 1884. Principal characters of American Jurassic dinosaurs. Part VIII. The order Theropoda. American Journal of Science (Series 3) 27: 329–340.

Mateus O, Antunes MT. 2000. *Ceratosaurus* sp. (Dinosauria: Theropoda) in the Late Jurassic of Portugal. Paper presented at 31st International Geological Congress, Abstracts Volume. Rio de Janeiro, Brazil.

Mateus O, Walen A, Antunes MT. 2006. The large theropod fauna of the Lourinhã Formation (Portugal) and its similarity to the Morrison Formation, with a description of a new species of *Allosaurus*. New Mex Mus Nat Hist Sci Bull. 36:123–129.

Rauhut OWM. 2003. The interrelationships and evolution of basal theropod dinosaurs. Special Papers in Palaeontology 69:1–213.

Rauhut OWM. 2012. A reappraisal of a putative record of abelisauroid theropod dinosaur from the Middle Jurassic of England. Proceedings of the Geologists' Association 123: 779–786. doi:10.1016/j.pgeola.2012.05.008.

Rauhut OWM, Carrano MT. 2016. The theropod dinosaur *Elaphrosaurus bambergi* Janensch, 1920, from the Late Jurassic of Tendaguru, Tanzania. Zoological Journal of the Linnean Society.

Sampson SD, Witmer LM, Forster CA, Krause DW, O'Connor PM, Dodson P, Ravoavy F. 1998. Predatory dinosaur remains from Madagascar: implications for the Cretaceous biogeography of Gondwana. Science 280:1048–1051.

Sampson SD, Carrano MT, Forster CA. 2001. A bizarre predatory dinosaur from the Late Cretaceous of Madagascar. Nature 409:504–506.

Sereno PC, Wilson JA, Conrad JL. 2004. New dinosaurs link southern landmasses in the mid-Cretaceous. Proceedings of the Royal Society of London, Series B 271:1325–1330.

Wilson JA, Sereno PC, Srivastava S, Bhatt DK, Khosla A, Sahni A. 2003. A new abelisaurid (Dinosauria, Theropoda) from the Lameta Formation (Cretaceous, Maastrichtian) of India. Contributions from the Museum of Paleontology, University of Michigan 31:1–42.

Young C-C. 1942. Fossil vertebrates from Kuangyuan, N. Szechuan, China. Bulletin of the Geological Society of China 22:293–309.

4.2. NEW EVIDENCE OF *CERATOSAURUS* (DINOSAURIA: THEROPODA) FROM THE LATE JURASSIC OF THE LUSITANIAN BASIN, PORTUGAL

Reference: Malafaia E, Ortega F, Escaso F, Silva B. 2015. New evidence of *Ceratosaurus* (Dinosauria: Theropoda) from the Late Jurassic of the Lusitanian Basin, Portugal. Historical Biology 27(7):938–946. http://dx.doi.org/10.1080/08912963.2014.915820

RESUMO

O género de dinossáurios terópodes *Ceratosaurus* foi, anteriormente, identificado no Jurássico Superior da Bacia Lusitânica, com base em escassos elementos atribuídos a um único indivíduo. Neste trabalho é descrito um conjunto de novos restos osteológicos atribuídos a *Ceratosaurus*, que são interpretados como parte do mesmo indivíduo descrito previamente. Estes elementos suportam a hipótese de que a distribuição deste táxon se estende do território que actualmente corresponde à América do Norte para a Europa. Anteriormente foram notadas algumas diferenças entre os exemplares portugueses e as formas Norte-americanas de *Ceratosaurus*. O estudo do conjunto de materiais aqui descrito sugere que essas diferenças podem estar relacionadas com variabilidade individual e/ou ontogenia. Os exemplares portugueses partilham com *Ceratosaurus* uma combinação única de característica, incluindo: (i) trocânter menor do fémur baixo, relativamente à margem dorsal da cabeça femoral; (ii) crista tibiofibularis orientada obliquamente em relação ao áxis da diáfise femoral; (iii) presença de uma crista infrapopliteal na superfície posterior da parte distal do fémur; (iv) crista cnemial da tíbia bem desenvolvida; e (v) côndilo medial da tíbia contínuo com a superfície proximal. Estes exemplares da Bacia Lusitânica constituem uma das escassas evidências de terópodes ceratossáurios no Jurássico Superior da Europa. Apesar da abundância, diversidade e ampla distribuição geográfica de ceratossáurios durante o Cretácico Superior, as primeiras fases da sua história evolutiva permanecem ainda mal compreendidas. Por este motivo, os exemplares portugueses constituem uma importante evidência para o conhecimento da evolução paleobiogeográfica deste clado durante o Jurássico Superior.

Palavras-chave: Ceratosauria; Bacia Lusitânica; Jurássico Superior; paleobiogeografia

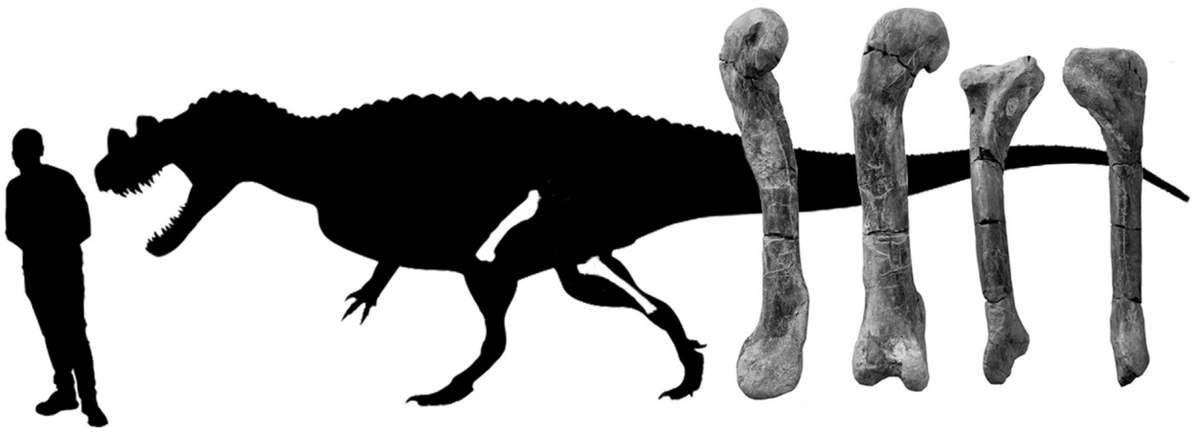

Figure 4.2.1. SHN(JJS)-65, left femur and right tibia attributed to *Ceratosaurus* from the upper Kimmeridgian of Valmitão (Lourinhã).

Historical Biology, 2015
Vol. 27, No. 7, 938–946, http://dx.doi.org/10.1080/08912963.2014.915820

Taylor & Francis
Taylor & Francis Group

New evidence of *Ceratosaurus* (Dinosauria: Theropoda) from the Late Jurassic of the Lusitanian Basin, Portugal

Elisabete Malafaia[a,b]*, Francisco Ortega[b,c1], Fernando Escaso[c,b2] and Bruno Silva[b3]

[a]*Centro de Geologia, Faculdade de Ciências da Universidade de Lisboa (FCUL), Edificio C6, Campo Grande 1749-016, Lisbon, Portugal;* [b]*Laboratório de Paleontologia e Paleoecologia, Sociedade de História Natural, Apartado 25, 2564-909 Torres Vedras, Portugal;* [c]*Grupo de Biología Evolutiva, Facultad de Ciencias, UNED, c/Senda del Rey, 9, 28040 Madrid, Spain*

(*Received 1 November 2013; accepted 14 April 2014; first published online 7 May 2014*)

A theropod assigned to *Ceratosaurus* was previously reported from the Portuguese Lusitanian Basin based on a limited number of elements of a single individual. Here, we describe newly discovered elements that likely pertain to same, earlier described, specimen. The new elements provide additional evidence that the range of *Ceratosaurus* spanned from what is now North America into Europe. Previously, some differences were noted between the Portuguese specimens and the North American *Ceratosaurus*. We consider these differences to be trivial and attribute them to individual variation and/or ontogeny. The following set of features (lesser trochanter positioned low on the femur; *crista tibiofibularis* obliquely oriented with respect to the axis of the femoral shaft; infrapopliteal ridge present posteriorly on the femur; large cnemial crest; and medial condyle of the tibia continuous with proximal end) indicate that the Portuguese specimen is assignable to *Ceratosaurus*. This record constitutes one of the scarce evidence of basal ceratosaurian theropods in the Late Jurassic of Europe. Despite the abundance, diversity and wide geographical distribution of ceratosaurs during the Late Cretaceous, its early evolutionary history remains poorly understood. The Portuguese specimens constitute an important evidence for the knowledge of the paleobiogeographic evolution of the clade during the Late Jurassic.

Keywords: Ceratosauria; Lusitanian Basin; Late Jurassic; paleobiogeography

Introduction

Ceratosauria is a clade of basal theropods traditionally interpreted as the sister group of Tetanurae, including *Ceratosaurus* and coelophysoids. Bonaparte (1991) formally included Abelisauridae in this clade but more recent analyses (e.g. Rauhut 2003; Carrano and Sampson 2008) suggested an alternative definition for Ceratosauria excluding Coelophysoidea and considering ceratosaurs more closely related to tetanurans than to coelophysoids. This phylogenetic interpretation proposes that some African taxa (e.g. *Elaphrosaurus* from the Late Jurassic of Tanzania and *Spinostropheus* from the Early Cretaceous of Niger) are basal ceratosaurians, and consider *Ceratosaurus* as the sister group of Abelisauroidea, which includes Noasauridae and Abelisauridae.

The description of *Berberosaurus liassicus* from the Early Jurassic of Morocco, interpreted as the oldest known abelisauroid (Allain et al. 2007), is used as evidence supporting the 'traditional' definition of Ceratosauria (including coelophysoids). This hypothesis suggests that the origin and early evolution of the clade are still poorly understood. Presently, this taxon is considered a basal ceratosaur outside of Abelisauroidea (Carrano and Sampson 2008).

The Middle Jurassic record of the clade is sparse, including a distal end of tibia (MB.R.2351) from Oxfordshire (England), previously described as a small basal tetanuran (Galton and Molnar 2005) but more recently reinterpreted as an early member of Abelisauroidea (Ezcurra and Agnolín 2012), some specimens from the Mahajanga Basin in Madagascar (Maganuco et al. 2005) and an almost complete skeleton from Patagonia described as a new species of abelisaurid *Eoabelisaurus mefi* Pol and Rauhut, 2012. The clade is well documented in the Late Jurassic of North America (*Ceratosaurus*), Africa (*Elaphrosaurus* and other specimens identified as indeterminate Abelisauroidea) and Asia (*Limusaurus*). Late Jurassic ceratosaurs have also been reported in several European (Portugal, Spain and Switzerland) and South-American (Uruguay) sites based on fragmentary material, mostly isolated teeth (Zinke 1998; Rauhut 2000; Canudo and Ruiz-Omeñaca 2003; Meyer and Thüring 2003; Mateus et al. 2006; Soto and Perea 2008). Some of these specimens were tentatively assigned to *Ceratosaurus* due to the presence of distinct vertical striations on the lingual surface of the teeth, a character that has been considered diagnostic of the pre-maxillary and anterior dentary teeth of *Ceratosaurus* (Madsen and Welles 2000; Soto and Perea 2008). The ceratosaurian record of Europe

*Corresponding author. Email: emalafaia@gmail.com

also includes specimens from the Early and Late Cretaceous of Spain, France and the Netherlands. The Spanish record includes the recently described putative ceratosaur species *Camarillasaurus cirugedae* Sánchez-Hernández and Benton, 2012 from the Early Cretaceous, and few fragmentary specimens from the Late Cretaceous (Pereda-Suberbiola et al. 2000). The French record includes the noasaurid *Genusaurus sisteronis* from the Early Cretaceous (Accarie et al. 1995) plus the Late Cretaceous *Tarascosaurus*, the recently described abelisaurid species *Acrovenator escotae* Tortosa, Buffetaut, Vialle, Dutour, Turini and Cheylan, 2014 and some isolated bones (Buffetaut et al. 1988; Le Loeuff and Buffetaut 1991; Allain and Pereda-Suberbiola 2003). Finally, the European record includes a proximal femur from the Late Cretaceous of Netherlands (Carrano and Sampson 2008; Pol and Rauhut 2012) identified as *Betasuchus bredai*.

Ceratosaurus has been tentatively recognised on several continents (Madsen and Welles 2000; Mateus et al. 2006; Soto and Perea 2008). Most occurrences of the genus, however, are in North America, restricted to the Brushy Basin Member of the Morrison Formation, Tithonian in age (Kowallis et al. 1998; Steiner 1998). Madsen and Welles (2000) erected two species, *Ceratosaurus magnicornis* and *Ceratosaurus dentisulcatus*, but they based their diagnoses mainly on morphometric differences. Some authors (e.-g. Rauhut 2003; Carrano and Sampson 2008) place both species junior synonyms of *Ceratosaurus nasicornis*. The only non-North American specimens currently assigned to the genus are some scarce remains from time-correlative levels of the Lusitanian Basin in Portugal that were only briefly described. These specimens include isolated teeth and some appendicular elements considered as *Ceratosaurus* sp. (Mateus and Antunes 2000; Mateus et al. 2006; Carrano and Sampson 2008).

Herein, we describe new remains from the Late Jurassic of the Lusitanian Basin that present a set of characters compatible with *Ceratosaurus*. We provide descriptions of the new elements, SHN(JJS)-65, along with the elements first reported by Mateus and Antunes (2000). Together, these elements provide the strongest evidence that the range of *Ceratosaurus* extended beyond what is now North America into Europe.

Institutional abbreviations

BYU, Brigham Young University, Utah, USA; SHN, Sociedade de História Natural, Torres Vedras, Portugal; MB, Museum für Naturkunde, Berlin, Germany; ML, Museu da Lourinhã, Lourinhã, Portugal; UMNH, Utah Museum of Natural History, Utah, USA.

Systematic paleontology

Dinosauria (Owen 1842); Theropoda (Marsh 1881); Ceratosauria (Marsh 1884).

Horizon and locality

The specimen, SHN(JJS)-65, was collected at the cliffs of the Valmitão beach between the municipalities of Torres Vedras and Lourinhã, Portugal. This locality is about 70 km north of Lisbon, in the centre of the Lusitanian Basin (Figure 1(a)).

The fossils were collected from a horizon of micaceous, fine-grained sandstones, yellow or brown in colour. The sedimentary sequence in the area of the quarry consists of thick, tabular, fluvial-channel fills of coarse- to fine-grained sandstones, intercalated with siltstones and clays, representing floodplain deposits. Plant debris is abundant, mainly in the floodplain deposits, but also fossil wood, sometimes a few metres in length, occur, primarily at the base of sandstone bodies. These sediments correspond to the lower levels of the Porto Novo Member (below the Praia Azul Member: see Hill 1988) of the Lourinhã Formation (Figure 1(c)). The Praia Azul Member (equivalent to the Sobral Formation, *sensu* Yagüe et al. 2006 and to the Sobral Member of the Farta Pão Formation, *sensu* Schneider et al. 2009) is well bounded due to the occurrence of the giant species of *Protocardia*. This member is dated, based on Sr isotopes to the latest late Kimmeridgian to middle early Tithonian (Schneider et al. 2009). Thus, the underlying Porto Novo Member is interpreted as late Kimmeridgian in age.

Material and preservation

The new specimen, SHN(JJS)-65, consists of a left femur, a right tibia and a fragment of the shaft of a left fibula. The femur and tibia are well preserved and almost complete. These fossils are curated in the vertebrate paleontology collection of the Laboratório de Paleontologia e Paleoecologia of the Sociedade de História Natural in Torres Vedras, Portugal.

The remains were part of a private collection that was recently donated to the Sociedade de História Natural. We verified that the new specimen, SHN(JJS)-65, came from the same area of the cliff as ML 352, the specimen previously identified to *Ceratosaurus* sp. (Mateus and Antunes 2000). The extraction of fossils in this area is usually dependent on cliff face erosion. Many specimens are collected in stages that can be widely separated in time, and sometimes conducted by various institutions. Although it is uncommon, this has resulted in a single individual ending up in several collections.

The original Portuguese specimen, ML 352, assigned to *Ceratosaurus* consists of an associated right femur and a

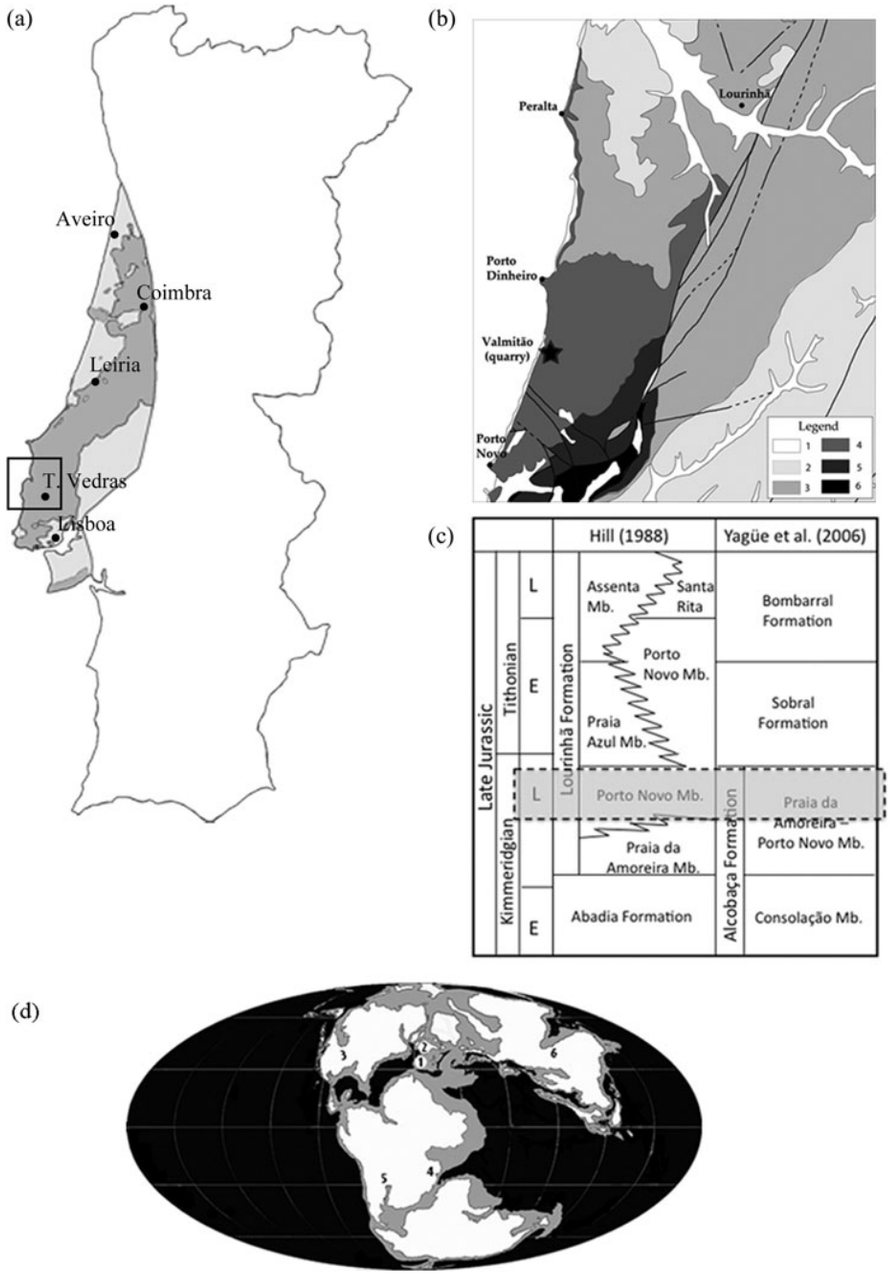

Figure 1. Geologic and geographic setting of the Valmitão quarry. (a) Portugal showing location of the Lusitanian Basin. Dark-grey areas represent Mesozoic strata. (b) Geological map quarry. Star indicates bone locality. Legend: 1, Cenozoic; 2, late Tithonian (Bombarral Formation); 3, latest Kimmeridgian–early Tithonian (Sobral Formation); 4 and 5, Kimmeridgian (Alcobaça Formation, 4 – Praia da Amoreira–Porto Novo Member, 5 – Consolação Member); 6, Lower Jurassic. Modified from Manupella et al. (1996). (c) Stratigraphy of the Valmitão section. (d) Late Jurassic ceratosaurian sites on paleogeographic map. Legend: 1, Iberian Peninsula; 2, other European sites (Switzerland); 3, USA (Morrison Formation); 4, Tanzania (Tendaguru Formation); 5, Uruguay (Tacuarembó Formation); 6, China (Shishugou Formation). Modified from Ron Blakey (2012).

left tibia. Both elements, SHN(JJS)-65 and ML 352, were found on the same sedimentary horizon and were collected from an area $<3\,m^2$. ML 352 and the specimen we describe, SHN(JJS)-65, likely pertain to the same individual because they are from the same site, the bones of both specimens (i.e. the femora and tibiae) are of the same size and morphology, and there are no duplicated bones from the same side of the body.

Description

Femur (SHN(JJS)-65/1)

The shaft is straight in anterior and posterior views and slightly arched in lateral and medial views. The femoral head projects anteromedially relative to the long axis of the shaft and horizontally relative to the dorsal level of the greater trochanter. The femoral head also presents a ventral component projecting to a level below the dorsal margin of the greater trochanter. The caput has a dorsoventrally elongated outline in medial view. On the posterior surface of the femoral head, a deep oblique groove (Figure 2(d)–(h)), interpreted as the reception for the *ligamentum capitis femoris* (Sadleir et al. 2008), forms the lateral boundary of a well-developed ridge, which extends dorsoventrally and is slightly mediolaterally orientated. The greater trochanter is anteroposteriorly compressed and becomes narrower laterally, where it merges with the posterior surface of the femoral shaft throughout a smooth curvature. On the contrary, the junction of this trochanter with the anterior surface of the femoral shaft presents a well-marked vertical ridge (Figure 2(c)). Just medial to the greater trochanter, a shallow, finger-like depression is present on the anterior surface of the proximal end of the femur (Figure 2(e)). The proximal femur is gently convex and lacks the groove or depression in the dorsal surface that is present in *Berberosaurus* (Allain et al. 2007) and *Masiakasaurus* (Carrano et al. 2002). The lesser trochanter is a robust ridge, with a triangular outline in lateral view that projects dorsally from the anterior surface of the femoral proximal end. The dorsoventral extension of the lesser trochanter is short, with the dorsal-most point below the level of the ventral border of the femoral head. There is no accessory trochanter adjacent to the lesser trochanter. The fourth trochanter is positioned on the proximal part of the shaft and extends dorsoventrally on the posterior surface, towards the medial margin. This trochanter is a wide, longitudinally short and rough crest underlain posteriorly by a vertical ridge. On the lateral surface of the femur, a well-developed crest projects horizontally from the distal end of the lesser trochanter to the lateroposterior surface of the shaft (Figure 2(d)–(f)). The morphology and position of this crest correspond to the trochanteric shelf described in other ceratosaurs (Madsen and Welles 2000; Pol and Rauhut 2012). The distal end of the femur terminates in two well-developed condyles separated distally by a deep groove. In distal view, the medial condyle is rather rectangular in outline with a rounded anterior margin. The lateral condyle is shorter and more rounded. The condyles are separated by a broad, deep and 'U'-shaped intercondylar fossa (flexor groove) posteriorly, whereas the anterior surface of the distal femur is almost flat (extensor groove absent). Inside the flexor groove, a well-developed transverse bridge of bone projects between the condyles (Figure 2(d)–(l)). This crest corresponds to the infrapopliteal ridge of Benson (2009) and is interpreted as the insertion area for the ligament of cruciate muscles (Tykoski and Rowe 2004). The *crista tibiofibularis* on the posterior surface of distal femur is incomplete but is possible to confirm that this crest is broad and slightly obliquely oriented with respect to the long axis of the femoral shaft. On the anteromedial surface of distal femur, the medial distal crest is a robust ridge although dorsoventrally short.

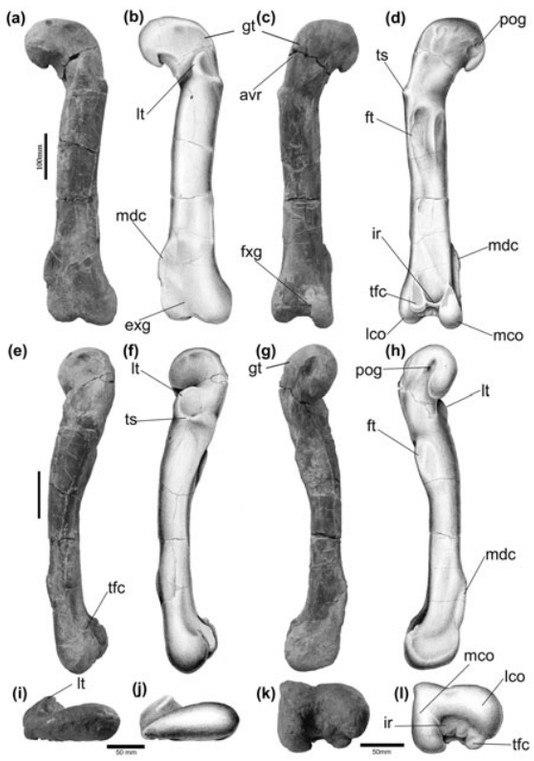

Figure 2. Left femur (SHN(JJS)-65/1) in anterior (a, b), posterior (c, d), lateral (e, f), medial (g, h), proximal (i, j) and distal (k, l) views. avr, anterior vertical ridge; ft, fourth trochanter; fxg, flexor groove; gt, greater trochanter; ir, infrapopliteal ridge; lco, lateral condyle; lt, lesser trochanter; mco, medial condyle; mdc, medial distal crest; pog, posterior groove of caput; tfc, tibiofibularis crest; ts, trochanteric shelf.

Tibia (SHN(JJS)-65/2)

In proximal view, the tibia has a rounded outline with a transversely narrow, but anteroposteriorly elongate cnemial crest that projects strongly anterolaterally. The distal end of the crest is broken off, but it is evident that it projected dorsally well above the lateral and medial condyles. Ventrally, the crest extends along the anterior surface of the tibia for c. 20% of tibia total length. The fibular crest is robust although not very elongate and is continuous with the tibial proximal margin. Proximally,

the fibular crest bifurcates and a well-marked ridge (Figure 3(f)) projects along the lateral border of the cnemial crest (= cranial ramus of the fibular crest of Smith et al. 2010). Between this ridge and the proximal expansion of the fibular crest (= caudal ramus of the fibular crest of Smith et al. 2010), a shallow and narrow fossa is interpreted as equivalent to the proximolateral fossa (Figure 3(f)). Distally, the fibular crest is straight and parallel to the shaft axis. The cranial ramus of the fibular crest forms the posterodorsal edge of the broad and deep lateral fossa. This fossa is bounded posteriorly by the fibular crest and anteriorly by the lateral projection of the cnemial crest. The lateral condyle is not separated from the main body of the tibia in proximal and lateral views, but in anterior view a deep and wide groove is present between the lateral and medial condyles. On the posterolateral surface, below the medial condyle, a well-defined oval roughness area for muscle insertion extends ventrally along the shaft (Figure 3(f)). This roughness is similar to that found in a tibia from the Early Cretaceous of Libya interpreted as for the insertion of the muscle flexor *tibialis internus* 2–4 (Smith et al. 2010). The distal end of the tibia

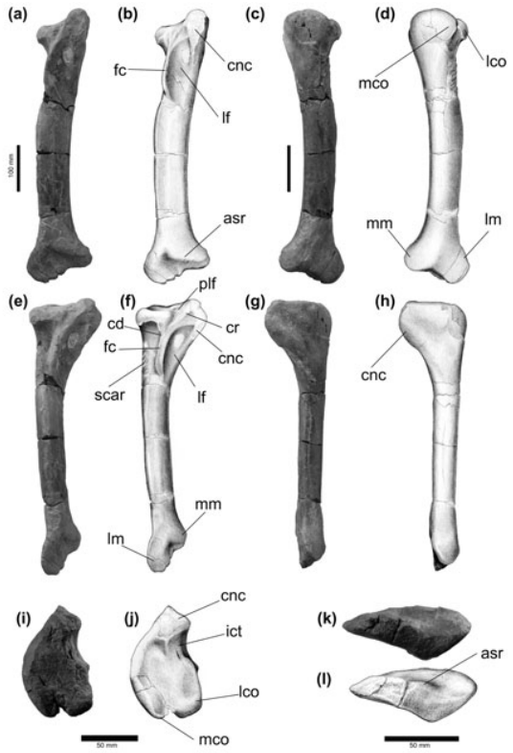

Figure 3. Right tibia (SHN(JJS)-65/2) in anterior (a, b), posterior (c, d), lateral (e, f), medial (g, h), proximal (i, j) and distal (k, l) views. asr, astragalar ridge; cd, caudal ramus of fibular crest; cnc, cnemial crest; cr, cranial ramus of fibular crest; fc, fibular crest; ict, incisura tibialis; lco, lateral condyle; lf, lateral fossa; lm, lateral malleolus; mco, medial condyle; mm, medial malleolus; plf, proximolateral fossa.

is much expanded anteroposteriorly, with a triangular outline in anterior view. The medial margin of distal tibia projects medially and slightly ventrally, whereas the lateral margin projects strongly ventrally and slightly laterally, resulting that the lateral malleolus is somewhat displaced ventrally with respect to the medial malleolus. On the distal end of the tibia, a deep groove separates the lateral and medial malleolus. The surface for the accommodation of the ascending process of the astragalus is dorsoventrally short, indicating a short ascendant process of the astragalus. This articular surface is bordered dorsomedially by an obliquely oriented crest, the supraastragalar buttress (Benson 2009).

Fibula (SHN(JJS)-65/3)

The fibula is represented by a small fragment (20.5 cm long) of the shaft (Figure 4). The shaft is rounded in cross section with a slightly anteroposterior expansion of the proximal end. The medial surface preserves the tibial flange as an oblique, rough, raised crest along the anterior surface of the shaft. Medially to the crest, a smooth concavity corresponds to the medial fossa of the fibula.

Comparison of SHN(JJS)-65 and ML 352

Bones of the new specimen, SHN(JJS)-65, and other ceratosaurian elements previously reported from the same locality (ML 352) are morphologically compatible. The preservation of the tibia separated from the proximal tarsals in both specimens is a character unusual among *Ceratosaurus*. This condition, however, is also present in a tibia (BYU 5132: Britt 1991; Elisabete Malafaia, pers. obs.) from the Dry Mesa Quarry. These elements are also separate in MB R 3625 from Tendaguru (Rauhut 2011), in the noasaurid *Velocisaurus* from the Late Cretaceous of Argentina (Carrano and Sampson 2008) and in *Berberosaurus* (Allain et al. 2007). Presently, it is not possible to know whether the apparent open articulation in the Portuguese specimens could be related with ontogeny. Another character shared by the Portuguese elements and distinct of some *Ceratosaurus* specimens from North America is the absence of a nutrient foramen at the distal end of the fibular crest. This foramen is present on UMNH VP 5278 (Elisabete Malafaia, pers. obs.) but not on BYU 5132 (Elisabete Malafaia, pers. obs.) suggesting that this is an intraspecific or sexual variation. The proximal end of the tibia in SHN(JJS)-65 seems more rounded in outline with respect to that of *Ceratosaurus*, specially because the lack of a constriction at the base of the cnemial crest as is typical in the North American forms. Although in ML 352 the morphology of the proximal end of the tibia is similar to that of other *Ceratosaurus* specimens, the apparent distinct outline in the new specimen is due to fracture of the distal end of the crest. Both specimens, SHN(JJS)-65 and ML 352, share

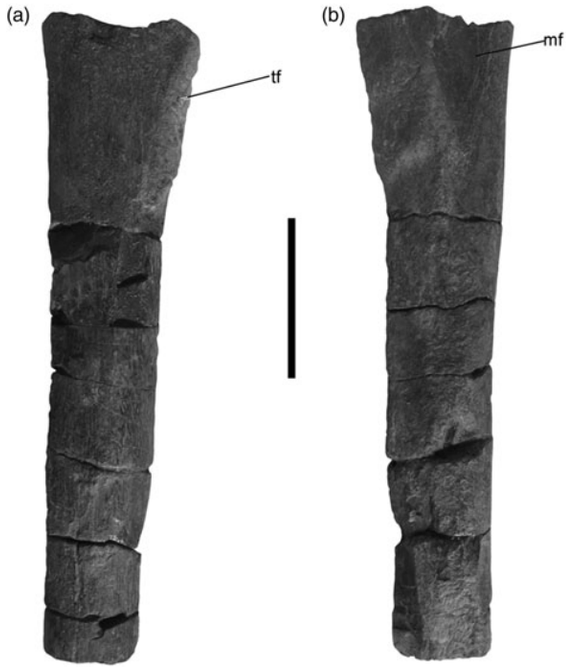

Figure 4. Left fibula (SHN(JJS)-65/3) in lateral (a) and medial (b) views. mf, medial fossa; tf, tibial flange. Scale bar: 50 mm.

the same characters and similar dimensions (see Table 1). We could not find any significant differences between them. The similarity of the available material and the provenance of both specimens from the same sedimentary horizon and likely from the same site support the hypothesis that they pertain to the same individual, collected at different times and curated in different collections.

Phylogenetic discussion

The specimen is morphologically similar to other Jurassic basal ceratosaurs, particularly *Ceratosaurus*. The following combination of characters found in the Portuguese specimens is considered diagnostic of *Ceratosaurus*: dimorphism in the morphology of the proximal femoral trochanters (character 131 of Carrano and Sampson 2008), the pronounced and sharp ridge medial epicondyle of the femur with associated striations along the medial edge (character 133 of Carrano and Sampson 2008), the presence of an infrapopliteal ridge on the posterior distal end of the femur (character 197 of Benson 2009) and the broad and obliquely oriented *crista tibiofibularis* on distal femur (character 134 of Carrano and Sampson 2008). It also shares with other non-tetanuran theropods a low lesser trochanter on the femur, placed directly below the femoral head (Rauhut 2003; Carrano et al. 2012) and the fibular crest continuous with the proximal end of the tibia (Rauhut 2003). Other characters shared with Ceratosauria are enumerated here: (1) femoral head orientation – 45° anteromedial (character 130 of Carrano et al. 2002); (2) femoral head directed ventrally (character 132 of Carrano et al. 2002); (3) well-marked sulcus along *crista tibiofibularis* of distal femur (character 136 of Carrano et al. 2002); (4) femur extensor groove absent, anterior surface of distal femur flat (character 193 of Benson 2009); (5) cnemial crest of the tibia projects considerably above the articular surface and with a marked ventral projection (character 135 of Carrano and Sampson 2008) and (6) tibia medial condyle extends distally as a ridge that merges with posterior surface of head (character 201 of Benson 2009).

The specimen described here presents a set of primitive characters for Ceratosauria shared with other Late Jurassic forms, such as the reduced longitudinal length of the medial distal crest on distal femur. The length of this crest is less than one-fourth of the total length of the shaft comparable with the condition of *Ceratosaurus* (UMNH VP 5278: Elisabete Malafaia, pers. obs.). A well-developed crest is present in the specimen MB R 3621 from the Tendaguru Formation, *Elaphrosaurus*, *Masiakasaurus* and tetanurans (Madsen 1976; Carrano et al. 2002; Rauhut 2011). The presence of an infrapopliteal ridge in

Table 1. Proportions of the femur and tibia in a range of *Ceratosaurus* specimens.

		l	mpw	dfh	mdw	mds	lti/lfe	*l*/mds	*l*/mpw	mpw/mdw
SHN(JJS)-65	Femur	650	140	65	130	54	0.88	12.04	4.64	1.08
	Tibia	570	140	–	133	46		12.39	4.07	1.05
ML352	Femur	647	135	67	140	64	0.90	10.11	3.87	1.16
	Tibia	570	170	–	130[a]	51		11.43	3.31	1.35
Ceratosaurus nasicornis USNM 4735	Femur	620	?	150	135	52	0.89	11.92	?	?
	Tibia	555	180	–	140	46		12.07	3.08	1.29
Ceratosaurus dentisulcatus	Femur UUVP 56	759	180	?	?	60	0.78	12.65	4.22	?
	Tibia UUVP 5681	594	180	–	165	90		6.6	3.3	1.09
Ceratosaurus magnicornis MWC1	Femur	630	120	?	?	65	0.82	9.69	5.25	?
	Tibia	520	190	–	132	48		10.83	2.74	1.44

Notes: All measurements are in millimetres. l, maximal length; mpw, maximal proximal width; dfh, diameter of the femoral head; mdw, maximal distal width; mds, maximal diameter of the shaft; lfe/lti, ratio between the femoral and tibial length.
[a] Estimated value.

the flexor groove of distal femur is only described in coelophysoids and *Ceratosaurus* among currently known basal theropods. The lateral fossa on the proximal end of the tibia faces laterally and slightly anteriorly as in *Ceratosaurus* (UMNH VP 5278: Elisabete Malafaia, pers. obs.), while in more derived forms, including some abelisauroids, e.g. *Majungasaurus*, this fossa is more ventrally orientated (Carrano 2007). The morphology of the astragalar ascending process, low and triangular, and of the astragalar facet, obliquely oriented with respect to the transverse axis of the distal end of the tibia, is similar to the condition described in some coelophysoids (e.g. *Gogirasaurus* Carpenter, 1997) and *Ceratosaurus* (Madsen and Welles 2000). In abelisauroids, the astragalar facet has an almost vertical orientation and the ascending process is a rectangular and laminar flange while it is laminar, triangular and highest in tetanurans (Carrano and Sampson 2008).

Portuguese specimens are more similar to *Ceratosaurus* from North America than to any other taxon. Some minor differences observed between these specimens and the North American specimens, such as lack of fusion of the tibia and astragalus and the absence of a nutrient foramen in the proximal tibia, may be a function of ontogeny, sexual dimorphism and/or individual variation.

Relative to the possible abelisaurid (MB R 3621, 3625 and 3626) described from the Tendaguru Formation (Rauhut 2011), the specimens from the Lusitanian Basin share a similar general morphology and features, such as the femoral head anteromedially directed, the presence of a well-marked trochanteric shelf on the proximal femur and the fibular crest placed proximally and continuous with the proximal end of the tibia. Differences between the Tendaguru abelisaurid and the Portuguese specimens include the femoral head more ventrally turned and the cnemial crest less dorsally expanded in the Portuguese specimens. The femur from Tendaguru lacks the infrapopliteal ridge that is present in the Portuguese specimens and in other basal ceratosaurs. SHN(JJS)-65 differs from other African taxa, including the basal ceratosaur *Berberosaurus liassicus* and the indeterminate abelisauroid from Libya (Allain et al. 2007; Smith et al. 2010) on several respects including the absence of a nutrient foramen in the tibia, the narrowest (relative to *Berberosaurus*) groove on the posterior surface of the femoral head and the narrowest (relative to the Libyan abelisauroid) proximolateral fossa.

Relative to *Genusaurus sisteronis*, a taxon considered as a basal ceratosaur but that more recently has been allied with noasaurids (Carrano and Sampson 2008), both specimens share a set of characters generally present in ceratosaurs, for example the presence of a well-developed sulcus along the distal *crista tibiofibularis* of the femur and the strongly developed cnemial crest of the tibia. However, in the specimens from the Lusitanian Basin, the cnemial crest is thinner and less dorsally expanded.

The Portuguese specimens differ from *Betasuchus bredai* on the presence of a well-developed trochanteric shelf and from *Tarascosaurus salluvicus* on the absence of a foramen at the proximal end of the lesser trochanter (Carrano and Sampson 2008).

Relative to *Camarillasaurus cirugedae*, the only comparable element is the proximal end of the tibia, which is very fragmented in the Spanish specimen. The expansion of the cnemial crest is similar in both specimens presenting an intermediate condition between the dorsally short crest of most tetanurans and the strongly expanded process of more derived ceratosaurs. In *Camarillasaurus*, the fibular crest of the tibia presents a proximal bifurcation with a segment projecting into the lateral condyle and the other in the lateral surface of the cnemial process (Sánchez-Hernández and Benton 2012). Despite the fact that this morphology of the fibular crest is quite similar to that observed in the Portuguese specimens, it is not continuous with the projection on the lateral surface of the cnemial process (figure 11 in Sánchez-Hernández and Benton 2012) contrary to the condition present in SHN (JJS)-65. In this respect, the Portuguese specimen is more similar to the Libyan specimen. A bifurcated fibular crest is a unique character shared by *Ceratosaurus*, the Iberian specimens and the abelisauroid from Libya (Tykoski and Rowe 2004; Smith et al. 2010). The Portuguese specimens differ from the Spanish and Libyan forms on the absence of a nutrient foramen at the distal end of the lateral fossa.

Conclusion

This study demonstrates that specimens SHN(JJS)-65 and ML 352 represent the same individual. This set can be assigned to *Ceratosaurus* aff. *Ceratosaurus nasicornis*, the only valid species recognised for the genus. The consideration of the Portuguese form as a member of this species, or as a new species, depends on finding new material. This identification is significant because this individual constitutes the most complete record of basal ceratosaurs in the Iberian Peninsula and one of the few records of Ceratosauria in the Late Jurassic of Europe. Our proposal reinforces the previous identification of ML 352 as *Ceratosaurus*. The Portuguese *Ceratosaurus* constitutes the strongest evidence of basal ceratosaurs from the European Late Jurassic thus reinforcing the knowledge of the early paleobiogeographic evolution of the taxa affected with the opening of the North Atlantic.

Recently, the close similarity of some dinosaurian taxa between Morrison Formation of western North America and Portugal has been recognised. This similarity is evident for stegosaurs and ornithopods but specially for theropods (e.g. *Ceratosaurus*, *Torvosaurus* and *Allosaurus*) and has

been interpreted as evidence of faunal exchanges across the proto-North Atlantic during the Late Jurassic. However, there are other groups that clearly exhibit a vicariant pattern, mainly among sauropod dinosaurs but also with crocodiles and turtles. These data compose a complex paleobiogeographic signal that probably indicates an incipient vicariance scenario manifested in different ways among distinct tetrapod groups.

Acknowledgements

This research was conducted in Laboratório de Paleontologia e Paleoecologia, Sociedade de História Natural, Apartado 25, 2564–909 Torres Vedras, Portugal. We acknowledge J. Joaquim for field assistance; I. Gromicho for the illustrations of the bones; and L. Chiappe, L. Ivy, K. Carpenter, R. Scheetz, B. Britt, M. Getty, M. Loewen, R. Irmis, D. Chure, S. Chapman, P. Jeffery and R. Castanhinha for providing specimens during their institution's collections. We appreciate the comments of the two referees that have greatly improved the manuscript.

Funding

This work was supported by the Fundação para a Ciência e Tecnologia [grant number PTDC/CTE GEX/67723/2006], Jurassic Foundation, Fundação Luso-Americana para o Desenvolvimento [grant number L07-V-22/2010] and Synthesys [grant number GB-TAF-2160]; Câmara Municipal de Torres Vedras.

Notes

1. Email: fortega@ccia.uned.es
2. Email: fescaso@ccia.uned.es
3. Email: laboratorio@alt-shn.org

References

Accarie M, Beaudoin B, Dejax J, Fries G, Michard DG, Taquet P. 1995. Découverte d'un Dinosaure Théropode nouveau (*Genusaurus sisteronis* n.g.n. sp.) dans l'Albienmarin de Sisteron (Alpes de Houte-Provence, France) et extension au Crétacéinférieur de la line cératosaurienne. C R Acad Sci Paris Sér 2. 320:327–334.

Allain R, Pereda-Suberbiola X. 2003. Dinosaurs of France. C R Palevol. 2:27–44.

Allain R, Tykoski R, Aquesbi N, Jalil N-E, Monbaron M, Russell D, Taquet P. 2007. An abelisauroid (Dinosauria: Theropoda) from the Early Jurassic of the High Atlas Mountains, Morocco, and the radiation of ceratosaurs. J Vertebr Paleontol. 27(3):610–624.

Benson RBJ. 2009. A description of *Megalosaurus bucklandii* (Dinosauria: Theropoda) from the Bathonian of the UK and the relationships of Middle Jurassic theropods. Zool J Linn Soc. 158:882–935.

Bonaparte JF. 1991. The Gondwanian theropod families Abelisauridae and Noasauridae. Hist Biol. 5:1–25.

Britt BB. 1991. Theropods of Dry Mesa Quary (Morrison Formation, Late Jurassic), Colorado, with emphasis on the osteology of *Torvosaurus tanneri*. Brigham Young Univ Geol Stud. 37:1–72.

Buffetaut E, Mechin P, Mechin-Salessy A. 1988. Un dinosaure théropode d'affinités gondwaniennes dans le Crétacé supérieur de Provence. C R Acad Sci Paris Sér 2. 306:153–158.

Canudo JI, Ruiz-Omeñaca JI. 2003. Los restos directos de dinossáurios terópodes (excluyendo Aves) en España. In: Pérez-Lorent F, editor. Dinosaurios y otros reptiles mesozoicos en España. Fundación Patrimonio Paleontológico de la Rioja. Logroño, La Rioja, Spain: Instituto de Estudios Riojanos. Universidad de la Rioja; p. 347–374.

Carpenter K. 1997. A giant coelophysoid (Ceratosauria) theropod from the Upper Triassic of New Mexico, USA. N Jb Geol Paläont Abh. 205:189–208.

Carrano MT. 2007. The appendicular skeleton of *Majungasaurus crenatissimus* (Theropoda: Abelisauridae) from the Late Cretaceous of Madagascar. J Vertebr Paleontol. 27(Suppl. 2):163–179.

Carrano MT, Benson RJ, Sampson SD. 2012. The phylogeny of Tetanurae (Dinosauria: Theropoda). J Syst Palaeontol. 10(2):211–300.

Carrano MT, Sampson SD. 2008. The phylogeny of Ceratosauria (Dinosauria: Theropoda). J Syst Palaeontol. 6(2):183–236.

Carrano MT, Sampson SD, Forster CA. 2002. The osteology of *Masiakasaurus knopfleri*, a small abelisauroid (Dinosauria: Theropoda) from the Late Cretaceous of Madagascar. J Vertebr Paleontol. 22(3):510–534.

Ezcurra MD, Agnolín FL. 2012. An abelisauroid dinosaur from the Middle Jurassic of Laurasia and its implication on theropod palaeobiogeography and evolution. Proc Geol Assoc. 123 (3):500–507.

Galton PM, Molnar RE. 2005. Tibiae of small theropod dinosaurs from Southern England. In: Carpenter K, editor. The carnivorous dinosaurs. Bloomington, IN: Indiana University Press; p. 3–22.

Hill G. 1988. The sedimentology and lithostratigraphy of the Upper Jurassic Lourinhã Formation, Lusitanian Basin, Portugal [Ph.D. dissertation]. Milton Keynes: The Open University.

Kowallis BJ, Christiansen EH, Deino AL, Peterson F, Turner CE, Kunk MJ, Obradovich JD. 1998. The age of the Morrison Formation. In: Carpenter K, Chure DJ, Kirkland JI, editors. The Upper Jurassic Morrison Formation: an interdisciplinary study. Part 1. Modern Geol 22. p. 235–260.

Le Loeuff J, Buffetaut E. 1991. *Tarascosaurus salluvicus* nov. gen., nov. sp., dinosaure théropode du Crétacé Supérieur du sud de la France. Geobios. 24:585–594.

Madsen JH, Jr. 1976. *Allosaurus fragilis*: a revised osteology. Utah Geol Min Surv Bull. 109:3–163.

Madsen JH, Jr, Welles SP. 2000. *Ceratosaurus* (Dinosauria, Theropoda) a revised osteology. Utah Geol Surv Mis Publ. 00-2:1–80.

Maganuco S, Cau A, Pasini G. 2005. First description of theropod remains from the Middle Jurassic (Bathonian) of Madagascar. Atti Soc It Sci Nat Museo Civ Stor Nat Milano. 146:165–202.

Manuppella G, Antunes MT, Pais J, Ramalho M, Rey J. 1996. Carta geológica de Portugal, 1/50.000. Folha 30-A, Lourinhã. Lisboa: Publicações do Instituto Geológico e Mineiro.

Mateus O, Antunes MT. 2000. *Ceratosaurus* sp. (Dinosauria: Theropoda) in the Late Jurassic of Portugal. Paper presented at 31st International Geological Congress, Abstracts Volume. Rio de Janeiro, Brazil.

Mateus O, Walen A, Antunes MT. 2006. The large theropod fauna of the Lourinhã Formation (Portugal) and its similarity to the Morrison Formation, with a description of a new species of *Allosaurus*. New Mex Mus Nat Hist Sci Bull. 36:123–129.

Meyer CA, Thüring B. 2003. Dinosaurs of Switzerland. C R Paleovol. 2:103–117.

Pereda-Suberbiola X, Astibia H, Murelaga X, Elorza JJ, Gómez-Alday JJ. 2000. Taphonomy of the Late Cretaceous dinosaur-bearing beds of the Laño Quarry (Iberian Peninsula). Palaeogeogr Palaeoclimatol Palaeoecol. 157:247–275.

Pol D, Rauhut OWM. 2012. A Middle Jurassic abelisaurid from Patagonia and the early diversification of theropod dinosaurs. Proc R Soc Lond B. 279:3170–3175.

Rauhut OWM. 2000. The dinosaur fauna from the Guimarota mine. In: Martin T, Krebs B, editors. Guimarota: a jurassic ecosystem. Munich: Verlag Dr. Friedrich Pfield; p. 75–82.

Rauhut OWM. 2003. The interrelationships and evolution of basal theropod dinosaurs. Spec Pap Palaeontol. 69:1–213.

Rauhut OWM. 2011. Theropod dinosaurs from the Late Jurassic of Tendaguru (Tanzania). Spec Pap Palaeontol. 86:195–239.

Ron Blakey. 2012. Global paleogeography maps, library of paleogeography. Arizona, USA: Colorado Plateau Geosystems Inc. Available from: http:// cpgeosystems.com/paleomaps.html [cited 21st October 2013].

Sadleir R, Barret PM, Powell HP. 2008. The anatomy and systematics of *Eustreptospondylus oxoniensis*, the theropod dinosaur from the Middle Jurassic of Oxfordshire, England. Palaeontogr Soc Monogr Palaeontograph. 160:1–82.

Sánchez-Hernández B, Benton MJ. 2012. Filling the ceratosaur gap: a new ceratosaurian theropod from the Early Cretaceous of Spain. Acta Palaeontol Pol. doi:http://dx.doi.org/10.4202/app.2011.0144

Schneider S, Fürsich FT, Werner W. 2009. Sr-isotope stratigraphy of the Upper Jurassic of central Portugal (Lusitanian Basin) based on oyster shells. Int J Earth Sci (Geol Rundsch). 98:1949–1970.

Smith JB, Lamanna MC, Askar AS, Bergig KA, Tshakneer SO, Abuganes MM, Rasmussen DT. 2010. A large abelisauroid theropod dinosaur from the Early Cretaceous of Libya. J Paleontol. 84(5):927–934.

Soto M, Perea D. 2008. A ceratosaurid (Dinosauria, Theropoda) from the Late Jurassic–Early Cretaceous of Uruguay. J Vertebr Paleontol. 28(2):439–444.

Steiner MB. 1998. Age, correlation, and tectonic implications of Morrison Formation paleomagnetic data, including rotation of the Colorado Plateau. In: Carpenter K, Chure DJ, Kirkland JI, editors. The Upper Jurassic Morrison Formation: an interdisciplinary study. Part 1. Modern Geol 22. p. 261–281.

Tortosa T, Buffetaut E, Vialle N, Dutour Y, Turini E, Cheylan G. 2014. A new abelisaurid dinosaur from the Late Cretaceous of southern France: Palaeobiogeographical implications. Ann Paléontol. 100(1):63–86.

Tykoski RS, Rowe T. 2004. Ceratosauria. In: Weishampel DB, Dodson P, Osmólska H, editors. The Dinosauria. 2nd ed. Berkeley, CA: University of California Press; p. 47–70.

Yagüe P, Dantas P, Ortega F, Cachão M, Santos FAM, Gonçalves R, Lopes S. 2006. New sauropod material from the Upper Jurassic of Areia Branca (Lourinhã, Portugal). N Jb Geol Paläont Abh. 240(3):313–342.

Zinke J. 1998. Small theropod teeth from the Upper Jurassic coal mine of Guimarota (Portugal). Paläontol Zeitschrifte. 72:179–189.

CHAPTER 5: MEGALOSAUROIDEA

5.1. INTRODUCTION

Tetanuran theropods represent the majority of Mesozoic carnivorous dinosaur diversity and include the lineage leading to extant Aves. This clade includes primarily carnivore theropods, but also possibly omnivorous and even herbivore forms, such as the therizinosaurs, ornithomimosaurs, and oviraptorosaurs (Benson 2010a). The term Tetanurae was proposed by Gauthier (1986) and this clade includes the earliest named dinosaur, *Megalosaurus* Buckland 1824 and a wide array of forms span nearly the entire temporal and geographic range of Dinosauria (Carrano et al. 2012).

Recent phylogenetic analyses generally agree on a monophyletic Tetanurae. However, the interrelationships of individual tetanuran taxa have been problematic. Earliest cladistic studies of tetanuran theropods (Paul 1984; Holtz 1994, 2000; Charig and Milner 1997) largely supported a primitive group of 'megalosaurs', including *Eustreptospondylus*, *Megalosaurus*, and *Torvosaurus* that were placed as successive outgroups to a clade of allosaurs comprising *Allosaurus* and *Acrocanthosaurus*, followed by the Coelurosauria. Based on this hypothesis, 'megalosaurs' represented basal tetanuran theropods more derived than 'ceratosaurs,' but with most taxa lacking synapomorphies that might support the monophyly of the group (Carrano et al. 2012). Subsequently, many of these basal tetanurans were recognized as forming a monophyletic clade, termed Megalosauroidea (Olshevsky 1995; Sereno et al. 1994, 1996; Benson 2010b; Rauhut 2003a; Holtz et al. 2004). However, if this clade is basal to the Allosauroidea + Coelurosauria group (usually called Avetheropoda or Neotetanurae; Paul 1988; Sereno et al. 1994, 1996, 1998; Holtz 2000; Holtz et al. 2004), or instead is the sister taxon to Allosauroidea within a reconstituted Carnosauria, comprising Allosauroidea and Megalosauroidea (Currie 1995; Rauhut 2003) is not consensual.

Tetanurans probably originated during the Early Jurassic and subsequently radiated into two main clades, Megalosauroidea and Avetheropoda (Carrano et al. 2012). The earliest megalosauroids are known from the Bajocian of England (*Duriavenator* and *Magnosaurus*), implying the presence also of basal avetheropods at this time (Benson 2008, 2010a). After the Callovian, tetanurans strongly diversified and dispersed as is indicated by their fossil record, which shows a widespread presence of multiple clades of both megalosauroids and avetheropods (Carrano et al. 2012).

Megalosauroidea (*sensu* Benson 2010b = Spinosauroidea *sensu* Sereno et al., 1996) includes three clades, Piatnitzkysauridae (*Xuanhanosaurus*, *Marshosaurus* and *Condorraptor* + *Piatnitzkysaurus*), Megalosauridae (*Duriavenator*, *Megalosaurus* and *Wiehenvenator* + *Torvosaurus* and a set of basal forms closely related with *Eustreptospondylus*), and Spinosauridae (includes a set of Cretaceous forms such as *Baryonyx*, *Spinosaurus*, *Suchomimus* and *Irritator*). The majority of the theropod taxa currently known from the Middle Jurassic of Europe are referred to Megalosauroidea and they show some regional endemism (Benson 2010b; Rauhut et al. 2016). A faunal turnover between the Middle and Late Jurassic is indicated by the less diverse and abundant record of megalosaurids during the Late Jurassic, when most theropods are avetheropods and allosauroids dominate the large-bodied predator niche (Benson 2010b).

The record of tetanuran theropods from the Upper Jurassic of the Lusitanian Basin is abundant and diverse. This record includes specimens belonging to the three major tetanuran clades, Megalosauroidea, Allosauroidea and Coelurosauria. Megalosauroids are represented by a set of cranial and postcranial elements collected in different Upper Jurassic sites of the Lusitanian Basin, mainly in the littoral region between Torres Vedras and Caldas da Rainha (Mateus and Antunes 2000; Malafaia et al. 2008; Hendrickx and Mateus 2014a; Malafaia et al. 2017). Some of these specimens were traditionally interpreted as closely related to the North American species *Torvosaurus tanneri*, but more recently reinterpreted as a new species exclusive of the Lusitanian Basin: *Torvosaurus gurneyi* (Hendrickx and Mateus 2014a). The study herein presented aims to verify if there are evidences for the presence of the species *T. tanneri* in the Upper

Jurassic of the Lusitanian Basin or if instead all specimens attributed to *Torvosaurus* from the Upper Jurassic of the Lusitanian Basin may be assigned to *T. gurneyi*. This analysis is based on the systematic review of the specimens assigned to *Torvosaurus* previously described in the Portuguese record and on the description of unpublished cranial and postcranial specimens collected in upper Kimmeridgian sedimentary levels of the Praia da Vermelha (Peniche) and Praia da Corva (Torres Vedras) fossil sites.

Some of the described specimens show a combination of features exclusively shared with *T. gurneyi*. In particular, a set of unpublished cranial material including an almost complete maxilla, SHN.400, is interpreted as belonging to the same individual as the holotype of *T. gurneyi*, ML1100. On the other hand, the described postcranial elements represent the most complete collection assignable to megalosauroid theropods currently known in the Portuguese Upper Jurassic. Some of these elements show certain differences relative to *T. tanneri*, but we cannot verify, at the moment, if these differences may be features of *T. gurneyi* or if they represent another megalosauroid taxon not yet identified in the record of the Lusitanian Basin.

REFERENCES

Benson RBJ. 2008. A redescription of '*Megalosaurus*' *hesperis* (Dinosauria, Theropoda) from the Inferior Oolite (Bajocian, Middle Jurassic) of Dorset, United Kingdom. Zootaxa 1931: 57–67.

Benson RBJ. 2010a. The osteology of *Magnosaurus nethercombensis* (Dinosauria, Theropoda) from the Bajocian (Middle Jurassic) of the United Kingdom and a reexamination of the oldest records of tetanurans. Journal of Systematic Palaeontology 8: 131–146.

Benson RBJ. 2010b. A description of *Megalosaurus bucklandii* (Dinosauria: Theropoda) from the Bathonian of the United Kingdom and the relationships of Middle Jurassic theropods. Zoological Journal of the Linnean Society 158: 882–935.

Carrano MT, Benson RBJ, Sampson SD. 2012. The phylogeny of Tetanurae (Dinosauria: Theropoda). Journal of Systematic Palaeontology 10: 211–300.

Charig AJ, Milner AC. 1997. *Baryonyx walkeri*, a fisheating dinosaur from the Wealden of Surrey. Bulletin of the Natural History Museum, Geology Series 53: 11–70.

Currie PJ. 1995. Phylogeny and systematics of theropods (Dinosauria). Journal of Vertebrate Paleontology 15(3 supplement): 25A.

Hendrickx C, Mateus O. 2014. *Torvosaurus gurneyi* n. sp., the largest terrestrial predator from Europe, and a proposed terminology of the maxilla anatomy in nonavian theropods. PLoS ONE 9(3):e88905. doi:10.1371/journal.pone.0088905.

Holtz TR Jr. 1994a. The phylogenetic position of the Tyrannosauridae: implications for theropod systematics. Journal of Paleontology 68: 1100–1117.

Holtz TR Jr. 2000. A new phylogeny of the carnivorous dinosaurs. GAIA 15: 5–61.

Holtz TR Jr, Molnar RE, Currie PJ. 2004. Basal Tetanurae. In: Weishampel DB, Dodson P, Osmólska H. (Eds) The Dinosauria. Second edition. University of California Press, Berkeley. 71–110.

Malafaia E, Ortega F, Silva B, Escaso F. 2008. Fragmento de un maxilar de terópodo de Praia da Corva (Jurásico Superior. Torres Vedras, Portugal). Palaeontologica Nova SEPAZ 8: 273–279.

Malafaia E, Mocho P, Escaso F, Ortega F. 2017. New data on the anatomy of *Torvosaurus* and other remains of megalosauroid (Dinosauria, Theropoda) from the Upper Jurassic of Portugal. Journal of Iberian Geology 43: 33–59.

Mateus O, Antunes MT. 2000. *Torvosaurus* sp. (Dinosauria: Theropoda) in the Late Jurassic of Portugal. Abstracts Book I Congresso Ibérico de Paleontología-XVI Jornadas de la Sociedad Española de Paleontología 15: 115–117.

Olshevsky G. 1995. African dinosaur discoveries. Science 267: 1750–1752.

Paul GS. 1984. The archosaurs: a phylogenetic study. In: Reif W-E, Westphal F. (Eds) Third Symposium on Mesozoic Terrestrial Ecosystems, Short Papers. Attempto Verlag, Tübingen. 175–180.

Paul GS. 1988. Predatory Dinosaurs of the World. Simon & Schuster, New York.

Rauhut OWM. 2003. The interrelationships and evolution of basal theropod dinosaurs. Special Papers in Palaeontology 69: 1–213.

Rauhut OWM, Hübner TR, Lanser K-P. 2016. A new megalosaurid theropod dinosaur from the late Middle Jurassic (Callovian) of north-western Germany: Implications for theropod evolution and faunal turnover in the Jurassic. Palaeontologia Electronica 19: 1–65.

Sereno PC, Forster CA, Larsson HCE, Dutheil DB, Sues H-D. 1994. Early Cretaceous dinosaurs from the Sahara. Science 266: 267–271.

Sereno PC, Dutheil DB, Iarochene M, Larsson HCE, Lyon GH, Magwene PM, Sidor CA, Varricchio DJ, Wilson JA. 1996. Predatory dinosaurs from the Sahara and Late Cretaceous faunal differentiation. Science 272: 986–991.

Sereno PC, Beck AL, Dutheil DB, Gado B, Larsson HCE, Rauhut OWM, Sadleir RW, Sidor CA, Varricchio DJ, Wilson GP, Wilson JA. 1998. A long-snouted predatory dinosaur from Africa and the evolution of spinosaurids. Science 282: 1298–1302.

5.2. NEW DATA ON THE ANATOMY OF *TORVOSAURUS* AND OTHER REMAINS OF MEGALOSAUROID (DINOSAURIA, THEROPODA) FROM THE UPPER JURASSIC OF PORTUGAL

Reference: Malafaia E, Mocho P, Escaso F, Ortega F. 2017. New data on the anatomy of *Torvosaurus* and other remains of megalosauroid (Dinosauria, Theropoda) from the Upper Jurassic of Portugal. Journal of Iberian Geology 43:33–59. doi: 10.1007/s41513-017-0003-9

RESUMO

Neste trabalho são descritos diversos elementos, do esqueleto craniano e pós-craniano de dinossáurios terópodes, incluindo duas maxilas, dentes isolados, vértebras e elementos apendiculares, provenientes de diferentes localidades do Jurássico Superior da Bacia Lusitânica. Estes elementos apresentam características compatíveis com tetanuros megalossauroides, em particular com a espécie descrita recentemente em níveis sedimentares sincrónicos da Bacia Lusitânica, *Torvosaurus gurneyi*. A distribuição geográfica e estratigráfica dos exemplares atribuídos a megalossauroides conhecidos actualmente no registo português, sugere que este clado era relativamente abundante durante o Kimmeridgiano superior e o Tithoniano inferior da Bacia Lusitânica, estando sobretudo bem representado na Sub-basia de Consolação. O estudo dos diferentes exemplares descritos permitiu testar algumas hipóteses sobre a distribuição e variabilidade de determinadas características morfológicas nas formas portuguesas relacionadas a *Torvosaurus*.

Palabras-chave: Dinosauria, Theropoda, Megalosauroidea, *Torvosaurus*, Kimmeridgiano–Tithoniano, Bacia Lusitânica

Figure 5.2.1. SHN.400, right maxilla of *Torvosaurus gurneyi* from the upper Kimmeridgian-lowermost Tithonian of Praia da Vermelha (Peniche).

J Iber Geol (2017) 43:33–59
DOI 10.1007/s41513-017-0003-9

RESEARCH ARTICLE

New data on the anatomy of *Torvosaurus* and other remains of megalosauroid (Dinosauria, Theropoda) from the Upper Jurassic of Portugal

E. Malafaia[1,2] · P. Mocho[2,3,4,] · F. Escaso[2,4] · F. Ortega[2,4]

Received: 29 June 2016 / Accepted: 4 February 2017 / Published online: 23 March 2017

Abstract A set of cranial and postcranial specimens, including two partial maxillae, several isolated teeth, vertebrae and appendicular elements of theropod dinosaurs is described. These specimens were collected in different Upper Jurassic sites from the Lusitanian Basin (Portugal) and show several characters that allow its identification as belonging to megalosauroid tetanurans. Some of these elements have a combination of features exclusively shared with other megalosaurids known in the Portuguese record, in particular with the recently described species *Torvosaurus gurneyi* from synchronic sedimentary levels. The geographic and stratigraphic distribution of the specimens of megalosauroids currently known in the Portuguese record indicates that members of this clade were relatively abundant from the upper Kimmeridgian to the lowermost Tithonian of the Lusitanian Basin, especially in the Consolação Subbasin. The analysis of the different specimens described allows testing hypotheses about the distribution and variability of some characters among the Portuguese forms related to *Torvosaurus*.

Keywords Dinosauria · Theropoda · Megalosauroidea · *Torvosaurus* · Kimmeridgian–Tithonian · Lusitanian Basin

Resumen Se describen varios elementos craneales y postcraneales, incluyendo dos fragmentos maxilares, varios dientes aislados, vértebras y elementos apendiculares de dinosaurios terópodos provenientes de diferentes localidades del Jurásico Superior de la cuenca lusitánica. Este conjunto de evidencias osteológicas presenta una combinación de caracteres que permite identificarlos como pertenecientes a tetanuros megalosauroideos. Algunos de estos elementos presentan características compartidas con *Torvosaurus gurneyi*, especie recientemente descrita en niveles sedimentarios sincrónicos. La distribución geográfica y estratigráfica de los ejemplares de megalosauroideos conocidos en la actualidad en el registro portugués sugiere que este clado era relativamente abundante en el Kimmeridgiense superior y Tithoniense inferior de la cuenca lusitánica, sobre todo en la subcuenca de Consolação. El análisis de los diferentes ejemplares descritos ha permitido comprobar algunas hipótesis sobre la distribución y variabilidad de algunos caracteres en las formas portuguesas afines a *Torvosaurus*.

Electronic supplementary material The online version of this article (doi:10.1007/s41513-017-0003-9) contains supplementary material, which is available to authorized users.

✉ E. Malafaia
emalafaia@gmail.com

P. Mocho
p.mochopaleo@gmail.com

F. Escaso
fescaso@ccia.uned.es

F. Ortega
fortega@ccia.uned.es

[1] Faculdade de Ciências, Instituto Dom Luiz and Museu Nacional de História Natural e da Ciência, Universidade de Lisboa, Bloco C6, 3° Piso, sala 6.3.57, Campo Grande, 1749-016 Lisbon, Portugal

[2] Laboratório de Paleontologia e Paleoecologia, Sociedade de História Natural, Apartado 25, 2564-909 Torres Vedras, Portugal

[3] The Dinosaur Institute, Natural History Museum of Los Angeles County, 900 Exposition Blvd, Los Angeles, CA 90007, USA

[4] Grupo de Biología Evolutiva, Facultad de Ciencias, Universidad Nacional de Educación a Distancia, Calle Senda del Rey, 9, 28040 Madrid, Spain

Palabras clave Dinosauria · Theropoda · Megalosauroidea · *Torvosaurus* · Kimmeridgiese–Tithoniense · Cuenca lusitánica

1 Introduction

Megalosauroidea is a relatively diverse and widespread group of basal tetanuran theropods known from Middle Jurassic to Upper Cretaceous strata worldwide. The clade is well represented in the Middle Jurassic of Europe (France: e.g. Allain 2002; England: e.g. Benson 2010a, b; and Germany: Rauhut et al. 2016), and South America (Argentina: Rauhut 2005), as well as from the late Middle Jurassic to early Upper Jurassic of Africa (Niger: Rauhut and Lopez-Arbarello 2009; Serrano-Martínez et al. 2015), and Asia (China: Li et al. 2009). The Upper Jurassic record of megalosauroids is more restricted and so far are only known in North America (Madsen 1976a; Britt 1991; Bakker et al. 1992; Hanson and Makovicky 2014) and Europe, such as Portugal (Mateus and Antunes 2000; Malafaia et al. 2008; Hendrickx and Mateus 2014), Spain (Gascó et al. 2012; Cobos et al. 2014), Germany (Rauhut et al. 2012), and possibly France (Vullo et al. 2014) beside some putative evidences of spinosaurids from Africa (Buffetaut 2011). The megalosauroid clade Spinosauridae is especially well represented in Cretaceous levels of Gondwanan landmasses, such as Africa (Smith et al. 2006), South America (Sues et al. 2002), and putatively in Australia (Barrett et al. 2011; see Novas et al. 2013 for discussion of this specimen), but is also known in several sites from the northern hemisphere, mainly in Asia, including in Thailand (Buffetaut and Ingavat 1986) and Laos (Allain et al. 2012). Spinosaurids are also well-represented in Europe, such as in England (Charig and Milner 1997), Spain (Canudo et al. 2008; Alonso and Canudo 2016), and Portugal (Buffetaut 2007; Mateus et al. 2011).

The European Middle Jurassic record of megalosauroids includes *Dubreuillosaurus*, *Piveteausaurus*, *Poekilopleuron* and *Streptospondylus* from France, *Duriavenator*, *Eustreptospondylus*, *Magnosaurus* and *Megalosaurus* from England, and *Wiehenvenator* from Germany, beside some specimens with uncertain systematic position but tentatively assigned to this clade (Taquet and Welles 1977; Buffetaut and Enos 1992; Allain 2001, 2002; Allain and Chure 2002; Sadleir et al. 2008; Benson 2008; 2010a; 2010b; Rauhut et al. 2016).

Late Jurassic megalosauroids are represented by three taxa, *Torvosaurus* from North America and Portugal, *Marshosaurus* from North America, and *Sciurumimus* from Germany (Madsen 1976a; Britt 1991; Chure et al. 1993; Carrano et al. 2012; Rauhut et al. 2012; Hanson and Makovicky 2014). *Edmarka rex*, a specimen from Como Bluff, in Wyoming (USA), was first described as a new species of torvosaurine (Bakker et al. 1992), but more recently has been considered a junior synonym of *Torvosaurus tanneri* (Carrano et al. 2012). Portuguese Late Jurassic megalosauroids include a set of cranial and postcranial elements traditionally interpreted as closely related to the North American species *Torvosaurus tanneri*, but more recently reinterpreted as a new species exclusive of the Lusitanian Basin: *T. gurneyi* (see Hendrickx and Mateus, 2014 for a complete list of specimens assigned to this taxon).

The species *Lourinhanosaurus antunesi*, first described as an allosauroid (Mateus 1998), was later interpreted as a megalosaurid (Mateus et al. 2006). Nevertheless, a recent analysis considered this taxon as a basal allosauroid related with Metriacanthosauridae (Benson 2010a; Hendrickx and Mateus 2012).

Herein, a set of unpublished megalosauroid cranial and postcranial remains is described. These remains include two partial maxillae, several isolated teeth and a set of vertebrae and appendicular elements collected in different sites from the Upper Jurassic of the Lusitanian Basin, mainly in the littoral region between Torres Vedras and Caldas da Rainha. Review of other previously described specimens related with this clade was performed in order to evaluate the variability of the megalosauroids from the Late Jurassic of the Lusitanian Basin.

Institutional abbreviations ALTSHN, Associação Leonel Trindade, Sociedade de História Natural, Torres Vedras, Portugal; BYU-VP, Brigham Young University, Vertebrate Paleontology Collection, Provo, Utah, USA; FCPDT, Fundación Conjunto Paleontológico de Dinópolis, Teruel, Spain; MB, Museum für Naturkunde, Berlin, Germany; ML, Museu da Lourinhã, Lourinhã, Portugal; SHN, Sociedade de História Natural, Torres Vedras, Portugal; SHN SIGAP, Sistema de Informação Geográfica Aplicado à Paleontologia of the SHN; UUVP, Utah University, Vertebrate Paleontology collection, Salt Lake City, Utah, USA; DMNH, Denver Museum of Nature and Science, Denver, Colorado, USA.

Morphometric abbreviations AL, apical length; CBL, crown base length; CBR, crown base ratio; CBW, crown base width; CDA, crown distal angle; CH, crown height; CHR, crown height ratio; CMA, crown mesial angle; DC, distocentral denticle density; MC, mesiocentral denticle density; DSDI, denticle size density index.

Morphological abbreviations acdl, anterior centrodiapophyseal lamina; adg, dorsal groove of anteromedial process; adr, dorsal ridge of anteromedial process; af, anterior foramina; al, additional lamina; alc, anterior lateral crest; af, anterior foramen; alf, alveolar foramina; alv, alveoli; amc, anterior medial crest; amp, anteromedial

process; aof, antorbital fossa; aofn, antorbital fenestra; aor, antorbital ridge; ap, ascending process; avg, ventral groove of anteromedial process; avr, ventral ridge of anteromedial process; cdf, centrodiapophyseal fossa; cpof, centropostzygapophyseal fossa; cpol, centropostzygapophyseal lamina; cprf, centroprezygapophyseal fossa; cprl, centroprezygapophyseal lamina; cr, caudal rib; d, depression; f, foramen; ic, internal cavity; idp, interdental plates; lac, surface for contact with lacrimal; mf, maxillary fossa; nac, surface for contact with nasal; nc, neural canal; hy, hyposphene; nf, nutrient foramina; nvo, neurovascular opening; pa, pathological area; pcdl, posterior centrodiapophyseal lamina; pdg, paradental groove; pl, pleurocoel; pld, pleurocentral depression; pm, surface for contact with premaxilla; podl, postzygodiapophyseal lamina; por, posterior ridge; pr, prezygapophysis; prcdf, prezygapophyseal centrodiapophyseal fossa; prdl, prezygodiapophyseal lamina; sab, supraastragalar buttress; snf, subnarial foramen; sprf, spinoprezygapohyseal fossa; tp, transverse process; tif, tubercle for the insertion of the iliofibularis muscle; vg, ventral groove; wfa, wear facet.

2 Materials and methods

2.1 Material

The specimens herein described include a fragment of a left maxilla (SHN.467), an almost complete right maxilla (SHN.400), twenty two isolated teeth, a set of postcranial elements, including dorsal and caudal vertebrae, an almost complete left fibula, a fragment interpreted as belonging to the diaphysis of a tibia (SHN.388 and SHN.469), and a fragment of the distal end of a left tibia (SHN.468). See Table 1 for a complete list of the unpublished specimens herein described.

The specimens are housed in the collections of the Sociedade de História Natural in Torres Vedras.

2.2 Anatomical nomenclature

The anatomical terminology used to describe the isolated teeth follows Smith and Dodson (2003) and Hendrickx et al. (2015a). The nomenclature used in the description of laminae and fossae pattern for the axial elements follows those proposed by Wilson (1999) and Wilson et al. (2011).

2.3 Morphometric analysis

Multivariate statistical analyses were performed in order to identify a set of isolated teeth collected in different Upper Jurassic sites from the Lusitanian Basin. It was developed a stepwise Discriminant Function Analysis (DFA) using the SPSS Statistics 17.0 program (SPSS Inc., Chicago, IL) and a Canonical Variate Analysis (CVA) using PAST3 (Hammer et al. 2001). It was followed the methodology developed by Smith (2005) and Smith et al. (2005) for quantitative analysis of isolated theropod teeth. All values were log-transformed to better reflect a normally distributed multivariate dataset. The analysis was based on the dataset of Hendrickx et al. (2015b) from which we selected twenty taxa of large-sized theropods including ceratosaurs (*Genyodectes*, *Ceratosaurus*, *Abelisaurus*, *Indosuchus*, *Majungasaurus*, *Carnotaurus* and an indeterminate abelisaurid), megalosaurids (*Duriavenator*, *Megalosaurus*, *Dubreuillosaurus* and *Torvosaurus*), allosauroids (*Allosaurus*, *Australovenator*, *Acrocanthosaurus*, *Carcharodontosaurus*, *Giganotosaurus* and *Mapusaurus*) and tyrannosauroids (*Gorgosaurus*, *Daspletosaurus* and *Tyrannosaurus*). Taxa with less than four specimens were not considered in the present analysis because its inclusion strongly reduces the percentage of original grouped cases correctly classified. We also opted not to include other taxa of basal tetanurans such as the spinosaurids, which are represented in the record of the Lusitanian Basin, because when included in the analysis the percentage of cases correctly identified reduces and because the teeth of these taxa have typical morphologies that are easily distinguished from those of megalosauroids.

The teeth were measured using a digital caliper. The variables used include CBL, CBW, CH, AL, CBR (=CBW/CBL) and CHR (=CH/CBL). Both crown mesial (CMA) and crown distal (CDA) angles were also used and were calculated using the formula resulting from the law of the cosines: CMA = arc cos ((CBL2 + AL2−CH2)/2*CBL*AL) and CDA = arc cos ((CBL2 + CH2−AL2)/2*CBL*CH). The number of mesial (MC) and distal (DC) denticles at the crown mid-height over 5 mm was also used in the analysis.

3 Geological setting

The specimens herein described were collected in different sites along the littoral area of Portugal, between the municipalities of Torres Vedras and Peniche (Fig. 1). This area corresponds to the Central Sector of the Lusitanian Basin, more specifically to the Consolação Sub-basin (sensu Taylor et al. 2014). This geological area is delimited to the south by the Santa Cruz diaper in the Torres Vedras municipality and to the north by the Caldas da Rainha diaper.

Several axial (SHN.469, SHN.388/1–12), appendicular (SHN.388/13), and cranial specimens, including two partial maxillae (SHN.467, ALTSHN.116) and four isolated teeth

(SHN.266, 364, 374, 467) were collected in the in the cliffs of Praia da Corva, in the north of the Torres Vedras municipality (Fig. 1). SHN.469 was collected in situ at the base of a fluvial-channel filling of coarse grained sandstones. The other specimens were collected in the cliffs surface as result of coastal erosion in the same area, but over a relatively long time, and generally show evidences of long weather exposure. The cliffs of Praia da Corva consist on a sequence of thick levels of massive red siltstones and claystones, intercalated with thin tabular, fluvial-channel fills of fine- to coarse grained sandstones.

Fig. 1 Geologic and stratigraphic settings of the fossil sites referred in the present work; **a** simplified geological map of the Lusitanian Basin (modified from Oliveira et al. 1992) showing the location of the different Sub-basins (sensu Taylor et al. 2014) and the localities where some of the specimens described were collected; **b** geological map of the area between Torres Vedras and Peniche (modified from Manuppella et al. 1996) showing the fossil sites were the specimens described were collected; **c** cronostratigraphic table for the Upper Jurassic of the Lusitanian Basin showing the correlation between the nomenclatures proposed by different authors (Hill 1988; Manuppella et al. 1999) for the coastal region between Santa Cruz and Salir do Porto and the cronostratigraphy for the region of Alcobaça and Caldas da Rainha

Table 1 List of unpublished megalosaurid specimens described and its geographic and stratigraphic provenance

Inventory number	Element	Geographic provenance	Formation
SHN.467	Partial left maxilla	Praia da Corva, Torres Vedras	Praia da Amoreira-Porto Novo
SHN.400	Right maxilla	Praia da Vermelha, Peniche	Praia da Amoreira-Porto Novo
SHN.067	Tooth	Almagreira, Peniche	Praia da Amoreira-Porto Novo
SHN.215	Tooth	Santa Rita, Torres Vedras	? Praia da Amoreira-Porto Novo
SHN.221	Tooth	Peralta, Lourinhã	? Sobral
SHN.257	Tooth	? Almagreira, Peniche	? Praia da Amoreira-Porto Novo
SHN.266, 364, 374	Teeth	Praia da Corva, Torres Vedras	Praia da Amoreira-Porto Novo
SHN.268	Tooth	Porto Dinheiro, Lourinhã	Praia da Amoreira-Porto Novo
SHN.294, 304, 319, 320, 381, 440, 442	Tooth	Valmitão, Lourinhã	Praia da Amoreira-Porto Novo
SHN.303, 362	Tooth	Salir do Porto, Caldas da Rainha	Alcobaça
SHN.359a	Tooth	Porto Novo, Torres Vedras	Praia da Amoreira-Porto Novo
SHN.401, 470	Tooth	Porto Dinheiro, Lourinhã	Praia da Amoreira-Porto Novo
SNH.441	Tooth	Praia dos Frades, Peniche	Praia da Amoreira-Porto Novo
SHN.388/1, 2	Centra of posterior dorsal vertebra	Praia da Corva, Torres Vedras	Praia da Amoreira-Porto Novo
SHN.388/3	Fragment of posterior dorsal vertebra		
SHN.388/4	Fragment of neural arch of dorsal vertebra		
SHN.388/5, 6	Centra of anterior caudal vertebra		
SHN.388/7, 8	Centra of caudal vertebra		
SHN.388/9	Partial mid caudal vertebra		
SHN.388/10-12	Centra of caudal vertebra		
SHN.388/13	Left fibula		
SHN.388/14	Fragment of the diaphysis of a tibia		
SHN.469	Two fused dorsal vertebrae	Praia da Corva, Torres Vedras	Praia da Amoreira-Porto Novo
SHN.468	Fragment of the distal end of a left tibia	S. Bernardino, Peniche	Praia da Amoreira-Porto Novo

Question marks indicate unknown or uncertain provenance

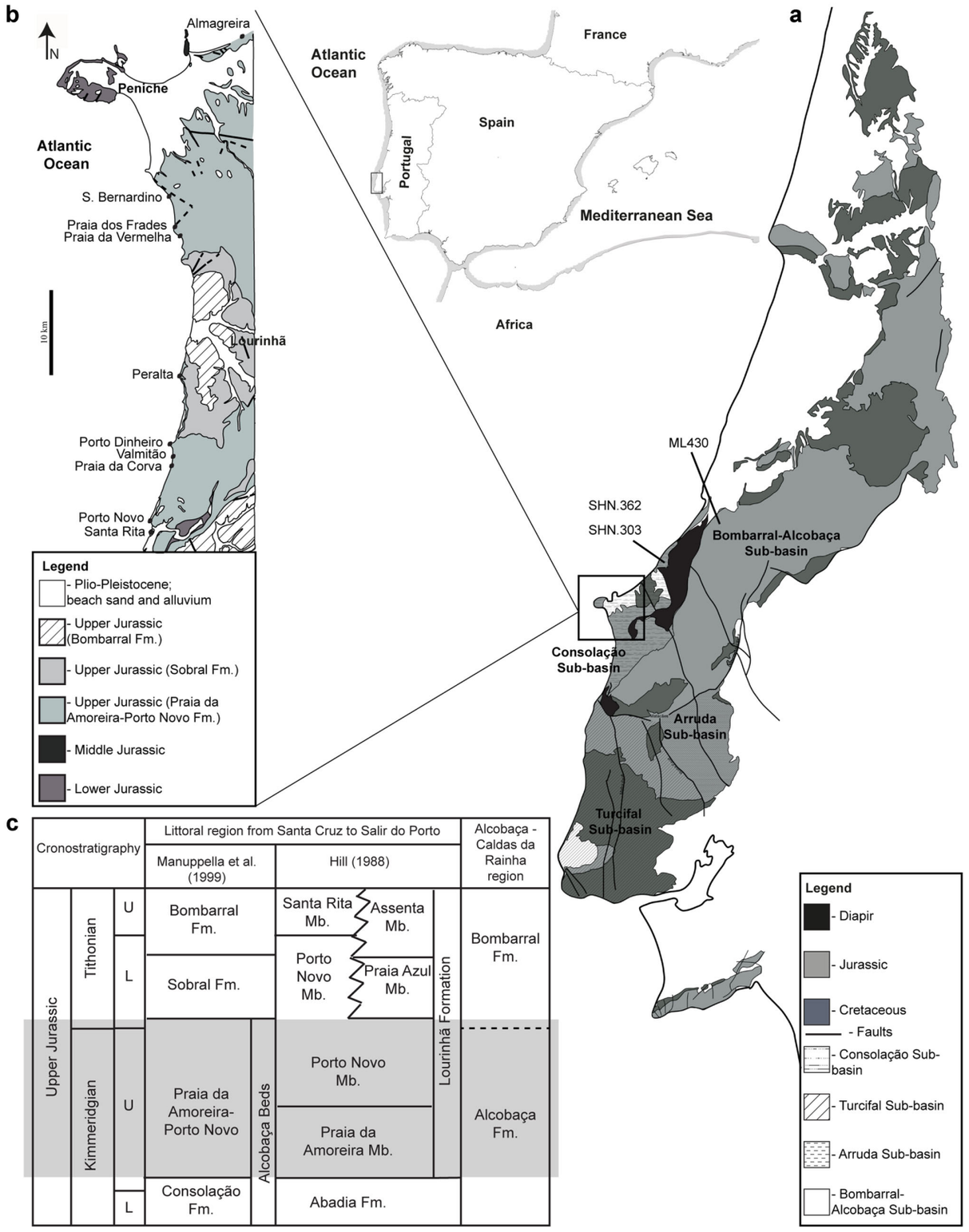
b
Almagreira
N
Peniche
Atlantic Ocean
S. Bernardino
Praia dos Frades
Praia da Vermelha
10 km
Lourinhã
Peralta
Porto Dinheiro
Valmitão
Praia da Corva
Porto Novo
Santa Rita
Legend
- Plio-Pleistocene; beach sand and alluvium
- Upper Jurassic (Bombarral Fm.)
- Upper Jurassic (Sobral Fm.)
- Upper Jurassic (Praia da Amoreira-Porto Novo Fm.)
- Middle Jurassic
- Lower Jurassic
Atlantic Ocean
France
Spain
Portugal
Mediterranean Sea
Africa
a
ML430
SHN.362
SHN.303
Bombarral-Alcobaça Sub-basin
Consolação Sub-basin
Arruda Sub-basin
Turcifal Sub-basin
Legend
- Diapir
- Jurassic
- Cretaceous
- Faults
- Consolação Sub-basin
- Turcifal Sub-basin
- Arruda Sub-basin
- Bombarral-Alcobaça Sub-basin
c
Cronostratigraphy
Littoral region from Santa Cruz to Salir do Porto
Manuppella et al. (1999)
Hill (1988)
Alcobaça - Caldas da Rainha region
Upper Jurassic
Tithonian
Kimmeridgian
U
L
U
L
Bombarral Fm.
Sobral Fm.
Praia da Amoreira-Porto Novo
Consolação Fm.
Alcobaça Beds
Santa Rita Mb.
Assenta Mb.
Porto Novo Mb.
Praia Azul Mb.
Porto Novo Mb.
Praia da Amoreira Mb.
Abadia Fm.
Lourinhã Formation
Bombarral Fm.
Alcobaça Fm.

These sediments correspond to the lower levels of the Praia da Amoreira-Porto Novo Formation (sensu Manuppella et al. 1999), which are equivalent to the Praia da Amoreira Member of the Lourinhã Fm. (sensu Hill 1988). The Praia da Amoreira-Porto Novo Fm. is the most extensive litostratigraphic unit in the Consolação Sub-basin, cropping out along most of the littoral area between Torres Vedras and Peniche (Fig. 1). The lower levels of the Praia da Amoreira-Porto Novo Fm. in the area of Praia da Corva are interpreted as upper Kimmeridgian in age (Manuppella et al. 1999; Schneider et al. 2009).

A fragment of the distal end of a tibia (SHN.468) and an almost complete maxilla (SHN.400) were collected in the cliffs of the S. Bernardino beach and at Praia da Vermelha respectively, in the Peniche municipality. These localities are placed about 15–17 km north from Praia da Corva (coordinates in SHN SIGAP database). SHN.400 was on a level of coarse sandstones, sometimes with large argillaceous clasts. The bone surface is covered in some points by a thin layer of pyrite. In the littoral area of Peniche crops out the upper levels of the Praia da Amoreira-Porto Novo Fm. This lithostratigraphic unit shows a general trend to become progressively younger to the north. Therefore, the sedimentary levels in the coastal region of Peniche correspond to the upper levels of this unit, which corresponds to the Porto Novo Member of the Lourinhã Fm. (sensu Hill 1988). These sedimentary levels are interpreted as late Kimmeridgian-lowermost Tithonian in age (Manuppella et al. 1999; Schneider et al. 2009).

Few isolated teeth from Salir do Porto in the Caldas da Rainha municipality were collected in sedimentary levels interpreted as belonging to the Alcobaça Formation (Kullberg et al. 2006; Schneider et al. 2009; Azerêdo et al. 2010). This stratigraphic unit was traditionally considered to span the entire or at least most of the Kimmeridgian to the base of the Tithonian (Rasmussen et al. 1998; Alves et al. 2002; Kullberg et al. 2006). However, more recent analysis based on Sr isotope values proposed a slightly older age for the Alcobaça Fm., from the uppermost Oxfordian to the upper Kimmeridgian (Schneider et al. 2009).

4 Systematic palaeontology

Dinosauria Owen 1842
Theropoda Marsh 1881
Megalosauroidea Fitzinger 1843
Megalosauroidea indet.

Material Two partial fused posterior dorsal vertebrae (SHN.469) (Fig. 2).

Locality and horizon Praia da Corva (Torres Vedras), Praia da Amoreira-Porto Novo Formation (upper Kimmeridgian).

Description SHN.469 corresponds to a very large and robust specimen (see supplementary material Table 1S). These vertebrae are co-ossified along the intervertebral space as well as in the base of the neural arches at least on the left side (Fig. 2). Similar vertebral fusions have been usually attributed to neoplasic ankylosis (i.e., fusion by new, abnormal bone formation) and are relatively common in large-sized theropod specimens (Petersen et al. 1972; Hanna 2002).

The centra are concave both in lateral and ventral views, with the articular facets slightly offset from the vertebral body. The anterior articular facet is circular and slightly concave, whereas the posterior one is more flat. The ventral surface of the most anterior centrum is transversely concave with a wide and shallow longitudinal groove extending along the entire length of the centrum. On the contrary, the other centrum has the ventral surface transversely convex without any groove. It is possible that the presence of a ventral groove on the former centrum may be due to distortion. There are broad and relatively deep fossae bellow the neurocentral suture corresponding to the pleurocentral depression (sensu O'Connor 2006) in other tetanurans, such as *Megalosaurus* (Benson 2010a), *Torvosaurus* (Britt 1991) or *Allosaurus* (Madsen 1976b). Small foramina are present inside the pleurocentral depression and in the lateral surface of the centra, especially near the ventral margin.

The neural arches of both vertebrae are incomplete, but preserve fragments of the prezygapophyses and of the transverse processes. A left prezygapophysis is visible on the most anterior vertebra and both prezygapophyses are partially visible in dorsal view on the other vertebra. The prezygapophyses are short, project anteriorly extending only slightly in front of the anterior articular facet. They are robust and have a well-developed centroprezygapophyseal lamina (cprl) extending from the dorsolateral margin of the centrum up to the ventral surface of the prezygapophysis. The ventral surface of the prezygapophysis is slightly concave. The transverse processes only preserve a fragment of the base. In left lateral view, the most posterior vertebra preserves the base of the transverse process projecting from the mid-length of the centrum and with well-developed anterior and posterior centrodiapophyseal lamina (acdl and pcdl). Another well-developed lamina projects from the dorsolateral margin of the prezygapophysis and connects with the dorsal surface of the transverse process. This lamina is interpreted as the prezygodiapophyseal lamina (prdl) and delimits a deep fossa, corresponding to the prezygapophyseal centrodiapophyseal fossa (prcdf). In right lateral view, the prcdf of

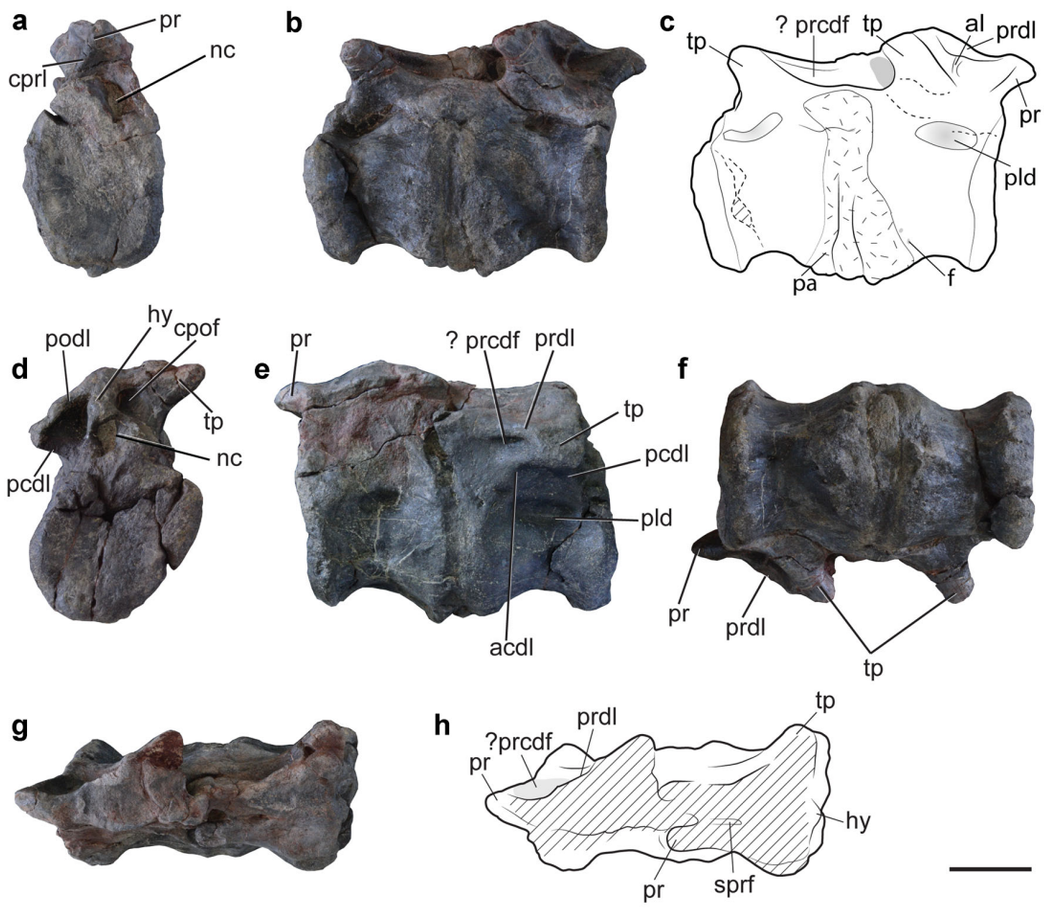

Fig. 2 Megalosauroidea indet., pathological dorsal vertebrae from Praia da Corva (SHN.469) in anterior (**a**), right lateral (**b**, **c**), posterior (**d**), left lateral (**e**), ventral (**f**), and dorsal (**g**, **h**) views. *Scale bar* 50 mm

the most anterior vertebra has a thin vertical additional lamina that subdivides this fossa (Fig. 2b, c).

In posterior view, a pair of small, but deep centropostzygapophyseal fossae (cpof) is present dorsally to the neural canal. These fossae are delimited by two laminae, the posterior centrodiapophyseal lamina (pcdl) and the postzygodiapophyseal lamina (podl). Dorsally to the neural canal, a well-developed, robust and triangular protuberance is interpreted as the hyposphene articulation.

Discussion SHN.469 is interpreted as posterior dorsal vertebrae due the lateral orientation of the transverse processes, which are supported ventrally by well-developed acdl and pcdl, the absence of parapophyses in the centra and the presence of hyposphene articulation. This specimen shares with most basal tetanurans (e.g., *Sinraptor*: Currie and Zhao, 1993; *Megalosaurus* (Benson, 2010a), and *Torvosaurus*: Britt, 1991) and basal ceratosaurs (e.g. *Ceratosaurus*: Madsen and Welles, 2000) the presence of a triangular hyposphene articulation, which is distinct from the narrow and sheet-like hyposphene of derived allosauroids and abelisaurids (Brusatte et al. 2008; Benson 2010a). These vertebrae have shallow depressions immediately ventral to the neurocentral sutures but not pleurocoels. Pleurocoels are restricted to anterior dorsal vertebrae in most basal theropods, but are present in all dorsal vertebrae of abelisaurids (e.g. *Carnotaurus*: Bonaparte et al., 1990), *Torvosaurus* (Britt, 1991), and most carcharodontosaurids (e.g., Brusatte et al. 2008; Eddy and Clarke 2011). The centra of SHN.469 are relatively short with articular facets circular in outline and almost flat. This morphology is similar to some megalosauroids such as *Megalosaurus* (Benson 2010a) and *Torvosaurus* (Britt 1991) and distinct from most other tetanurans (e.g., Madsen 1976b; Currie and Zhao 1993), which have strongly concave articular facets on dorsal vertebrae. Also the presence of deep cpof laterally to the hyposphene is a character shared with some megalosauroids (e.g., *Torvosaurus*: Britt, 1991). The vertebrae of SHN.469 are

incomplete and distorted making difficult to obtain a more accurate systematic approach, but the combination of characters described above suggests that they may be identify as belonging to an indeterminate megalosauroid.

Material A large left fibula (SHN.388/13) (Fig. 3).

Locality and horizon Praia da Corva (Torres Vedras), Praia da Amoreira-Porto Novo Formation (upper Kimmeridgian).

Description The fibula, SHN.388/13, is almost complete missing a section of the shaft close to the distal end (Fig. 3). It corresponds to a very large and robust specimen (see supplementary material Table 1S). The proximal end is more posteriorly than anteriorly expanded and the proximal articular facet is slightly convex. The proximal end strongly tapers posteriorly in a thin, blade-shaped margin. The diaphysis is robust and has a slightly broad, rough and low crest in the lateral surface approximately 255 mm below the proximal end. This crest corresponds to the tubercle for insertion of the muscle iliofibularis (Rauhut 2011). This tubercle extends anterolaterally from the anterior margin to the lateral surface for about 106 mm of the diaphysis length. The posterior surface of the fibula has a deep longitudinal concavity near the proximal end that is bounded anteriorly by a well-developed ridge. The medial surface is slightly concave proximally, just below the proximal end and almost flat distally along most of the length of the diaphysis. The distal end of the fibula is slightly expanded anteroposteriorly and rounded in distal view with slightly concave lateral and convex medial surfaces.

Discussion SHN.388/13 corresponds to a very large and robust fibula, which is significantly more robust than those of any other known theropod from the Lusitanian Basin and is only comparable with some specimens of *Torvosaurus* from the Morrison Formation (Britt 1991), to a fibula (MB R 3627) from the Tendaguru Formation assigned to an indeterminate megalosauroid (Rauhut 2011) and to the fibula of the megalosaurid *Wiehenvenator* (Rauhut et al. 2016) from the Ornatenton Formation in Germany.

SHN.388/13 has a shallow medial concavity in the proximal part contrasting with most theropods that are characterized by deep depressions, which can be narrow or wide, covering most of the medial side of the bone (Rauhut 2003; Carrano and Sampson 2008; Rauhut 2011). Such a depression is absent in MB R 3627 (Rauhut 2011) and in most other megalosauroids (Benson 2010a), including *Torvosaurus* (Britt 1991) and *Wiehenvenator* (Rauhut et al. 2016) as well as in some basal theropods (e.g. *Liliensternus*: Rauhut, 2011) and derived coelurosaurs (Rauhut 2003).

The fibula from Praia da Corva has a robust proximal end, strongly expanded anteroposteriorly and transversely wide. The morphology of the fibular proximal end is similar to those of MB R 3627 (Rauhut 2011). In at least some specimens of *Torvosaurus* (Britt 1991), the proximal end of the fibula is significantly narrowest mediolaterally. The Portuguese specimen also has a strongly developed tubercle in the lateral surface of the shaft for insertion of the iliofibularis muscle similar to that found in MB R 3627 (Rauhut 2011) and much more robust than those in some fibulae of *Torvosaurus* (e.g., BYUVP 9620). Based on this combination of characters, SHN 388/13 is here interpreted as belonging to an indeterminate megalosauroid.

Material A fragment of the distal end of a left tibia (SHN.468) (Fig. 4).

Locality and horizon S. Bernardino (Peniche), upper levels of the Praia da Amoreira-Porto Novo Formation (late Kimmeridgian-lowermost Tithonian).

Description SHN.468 corresponds to the distal end of a large left tibia. The distal end is strongly expanded transversely and slightly distally with the lateral malleolus strongly offset laterally and extending more distally relative to the medial malleolus. A robust ridge, originated in the anteromedial corner of the anterior surface, marks the dorsomedial contact of the astragalus. This ridge corresponds to the supraastragalar buttress (sensu Benson 2010a), which slopes medially making an angle of approximately 45° with the diaphysis long axis. The supraastragalar buttress delimits a well-marked, rough groove, which corresponds to the facet for reception of the ascending process of the astragalus. The supraastragalar buttress is short proximodistally (the astragalar facet is about 110 mm high) suggesting a short ascending process of the astragalus. The medial half of the anterior surface of the tibia is occupied by the triangular astragalar facet, which extends into the anterior surface of the medial malleolus. A small circular depression and three small openings are visible in the dorsal end of the astragalar facet and ventrally to the supraastragalar crest. The facet for the fibula occupies the lateral half of the anterior surface of the lateral malleolus and is marked by a series of thin striations. The lateral malleolus is strongly compressed anteroposteriorly and crest-shaped in lateral view. The medial malleolus is rounded in ventral and medial views. In distal view, the tibia has a wedge-shaped outline with the apex of the wedge, corresponding to the lateral malleolus, strongly offset laterally. The ventral surface has a deep concavity with an oval outline between the medial and lateral malleolus.

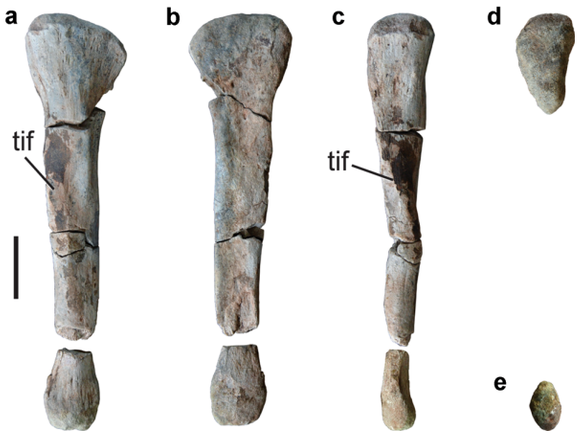

Fig. 3 Megalosauroidea indet., left fibula collected in Praia da Corva (SHN.388/13) in lateral (**a**), medial (**b**), anterior (**c**), proximal (**d**), and distal (**e**) views. *Scale bar*: 100 mm

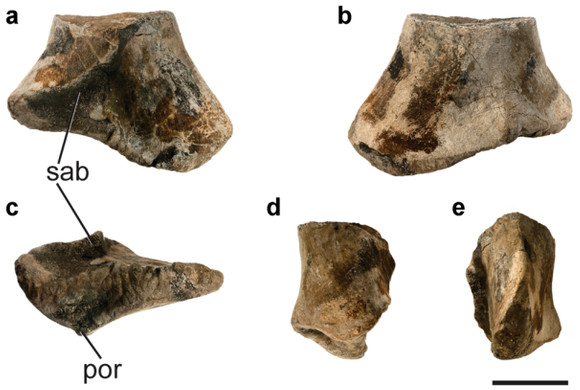

Fig. 4 Megalosauroidea indet., fragment of the distal end of a left tibia collected in S. Bernardino (SHN.468) in anterior (**a**), posterior (**b**), distal (**c**), medial (**d**), and lateral (**e**) views. *Scale bar* 50 mm

Discussion This fragment of the distal end of a large tibia has a general morphology similar to that of some specimens of *Torvosaurus* known in other sites from the Lusitanian Basin (Mateus and Antunes 2000) and in correlative levels of North America (Britt 1991). The mediolateral length of the distal end of this specimen is slightly lower than that of a tibia described in Casal do Bicho (Alcobaça) assigned to *Torvosaurus* (ML430: Mateus and Antunes 2000) and slightly larger than those of some specimens from the Morrison Formation (BYU 2016: Britt 1991). The ratio of the transverse width to the length of the distal end is comparable with those of other tetanurans, but much higher than the ratio in non-tetanuran theropods (Benson 2010a). SHN.468 shares with *Torvosaurus* (Britt 1991; Mateus and Antunes 2000) the dorsoventrally short facet for reception of the ascending process of the astragalus and the orientation of the supraastragalar butress. The angle of the same crest in *Torvosaurus* and *Ceratosaurus* is approximately 45°, but in *Allosaurus* is approximately 55° (Britt 1991). The morphology of the lateral malleolus in SHN.468 is also similar to that of *Torvosaurus* (Britt 1991; Mateus and Antunes 2000), whereas it is more rounded in more derived tetanurans (e.g., Madsen 1976b). On the other hand, the greater distal expansion of the lateral malleolus relative to the medial malleolus (lateral malleolus extending beyond the medial malleolus 7% or more of the length of the tibia) was proposed to be a derived states shared by some carcharodontosaurids (Brusatte and Sereno 2008). *Torvosaurus* (Britt 1991) seems to have an intermediate condition with the lateral malleolus extending distally beyond the medial malleolus more than in some basal allosauroids (e.g., Madsen 1976b), but less than in carcharodontosaurids (Brusatte and Sereno 2008). SHN.468 is much incomplete and the informative characters are limited, but in general the combination of characters is compatible with *Torvosaurus* and other megalosauroids being here tentatively assigned to this clade.

Megalosauridae Fitzinger 1843
Megalosauridae indeterminate

Material A set of axial elements including several vertebrae interpreted as belonging to the dorsal and caudal series (SHN.388/1–12) (Figs. 5, 6, 7 and 8).

Locality and horizon Praia da Corva (Torres Vedras), Praia da Amoreira-Porto Novo Formation (upper Kimmeridgian).

These specimens were discovered at the cliff surface as result of coastal erosion in the same place, but over a relatively long time. Therefore, and despite the compatible relative dimensions and morphology of the elements, there is no evidence that they belong to the same individual.

Description These specimens include three dorsal centra (SHN.388/1-3), a fragment of a dorsal neural arch (SHN.388/4), and eight partial caudal vertebrae (SHN.388/5-12). The dorsal centra are interpreted as belonging to the posterior part of the series. These centra are quite complete but strongly eroded. The articular facets of the dorsal centra are well expanded being about 1.4 times transversely wider than the transverse diameter of the centra (see supplementary material Table 1S). The articular facets are mostly incomplete, but the anterior facets are circular, whereas the posterior ones are more sub-oval, being significantly transversely wider than high. The centra are saddle-shaped with the ventral surface strongly concave in lateral view. The ventral surfaces of the centra are transversely wide and almost flat. All dorsal centra are broken at the level of the

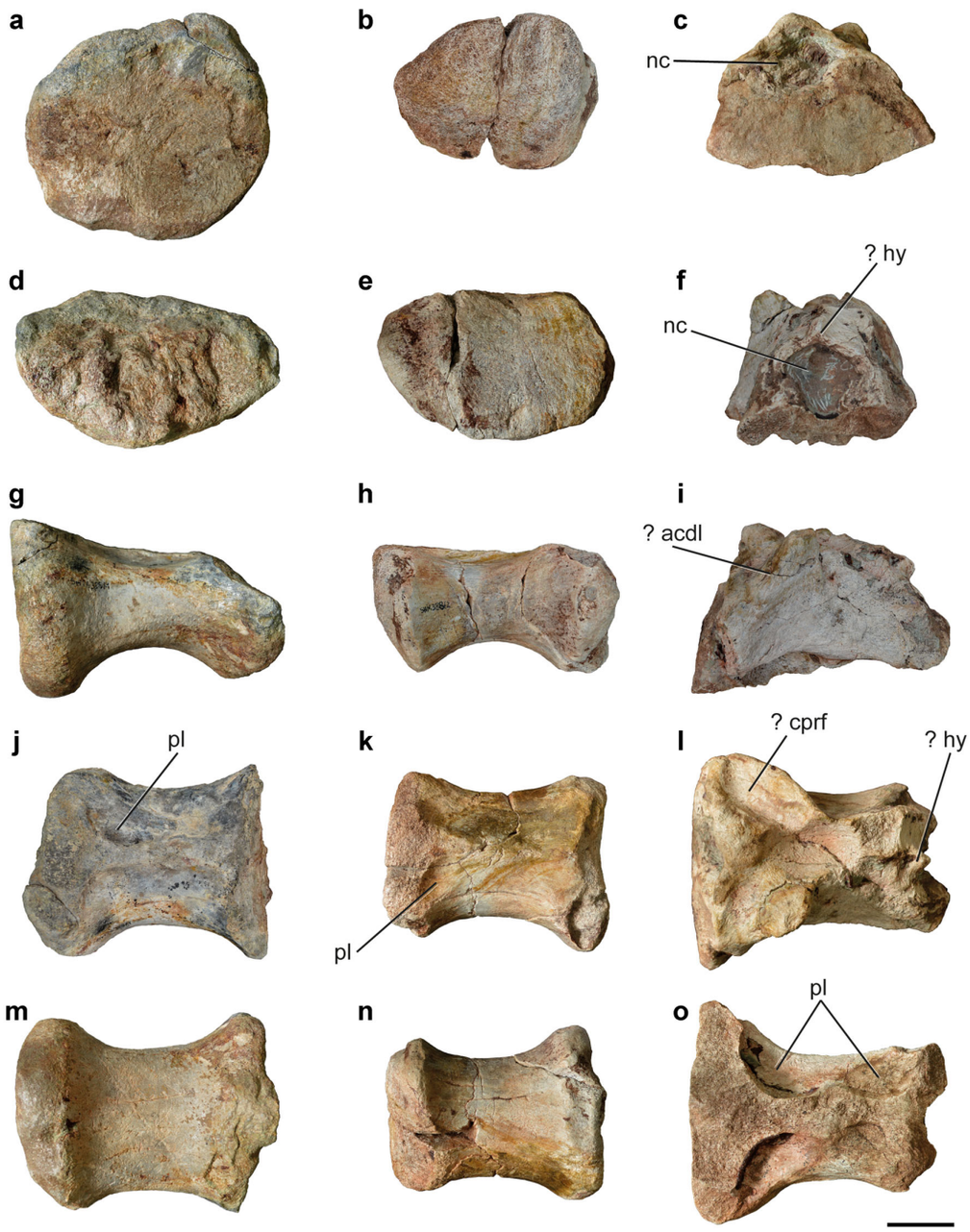

Fig. 5 Megalosauridae indet., dorsal vertebrae from Praia da Corva; from *left* to the *right*: centrum (SHN.388/1), centrum (SHN.388/2), and fragment of neural arch (SHN.388/4) in anterior (**a–c**), posterior (**d–f**), left lateral (**g–i**), dorsal (**j–l**), and ventral (**m–o**) views. *Scale bar* 50 mm

base of the neural arch. Deep pleurocoels are visible at the base of the neural arch. These pleurocoels are medially deep and the right and left pleurocoels are separated by a thin sagittal lamina with about 20 mm thick. Pleurocoels are present in all preserved dorsal vertebrae and inside them there are small concavities adjacent to the articular facets.

The only preserved fragment of a neural arch, SHN.388/4 (Fig. 5c, f, i, l, o), is posteriorly broken near the ventral margin of the neural canal, but it preserves part of the anterior articular facet. The neural canal is broad and has a circular contour. In lateral view, there is a pair of robust crests that project dorsally from the anterior margin of the

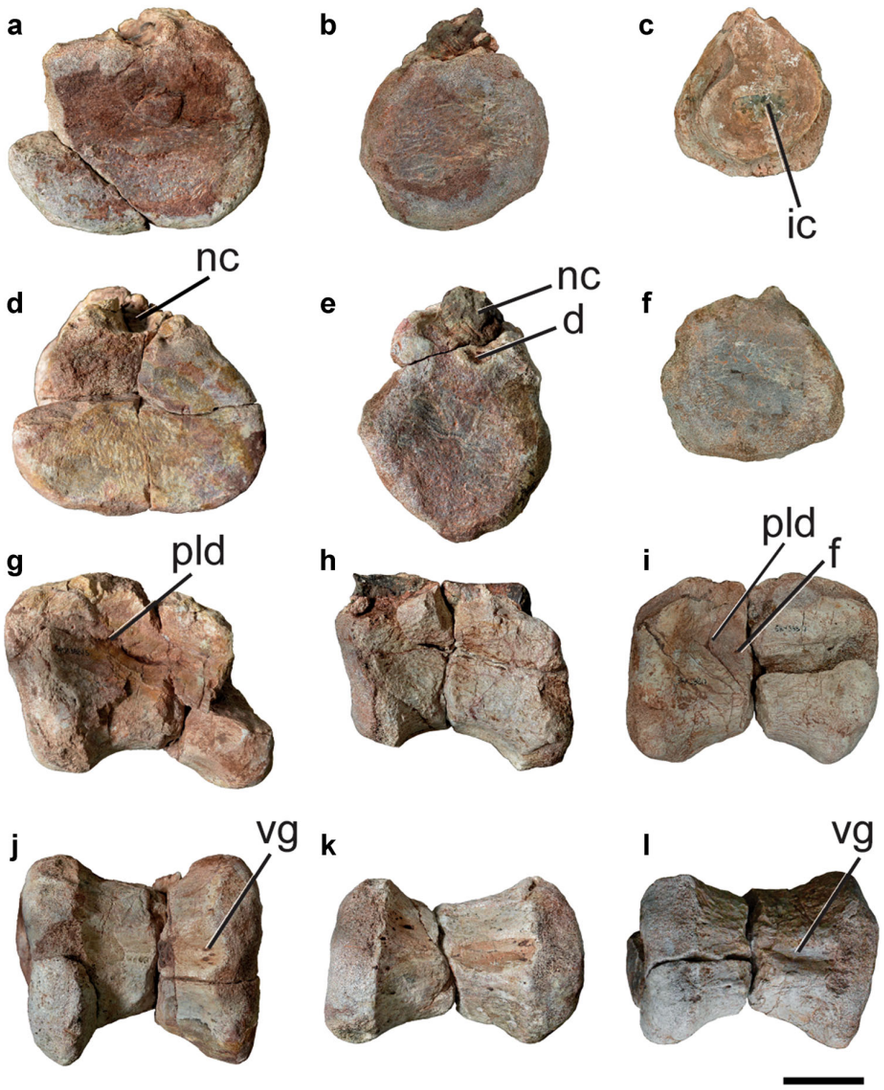

Fig. 6 Megalosauridae indet., anterior caudal vertebrae from Praia da Corva; from *left* to *right*: centrum (SHN.388/5), centrum (SHN.388/6), and centrum (SHN.388/7) in anterior (**a, b**), posterior (**d–f**), left lateral (**g–i**), and ventral (**j, k**) views; in cross-section at mid-length (**c**). *Scale bar* 50 mm

anterior articular facet, which are interpreted as the anterior centrodiapophyseal laminae (acdl). A deep fossa opens adjacent to the anterior articular facet and dorsally to the acdl. This fossa pierces the neural arch with a mediposterior orientation and is interpreted as corresponding to the centroprezygapophyseal fossa (cprf). The cprf extends deeply into the neural arch and connects with another broad fossa that is placed near the mid-length of the arch in a position that would correspond to the anterior end of the base of the neural spine. In posterior view, the neural arch has a small crest above the neural canal projecting posteriorly. This crest may correspond to the base of the hyposphene.

The caudal vertebrae are mostly represented by the centra and only two vertebrae preserve fragments of the neural arch. The exact position of these elements in the caudal series is difficult to establish due its fragmentary condition. However, based on the general morphology, SHN.388/5-7 (Fig. 6) are interpreted as belonging to the anterior part of the caudal series and the remaining elements are considered as vertebrae from the mid and posterior parts of the tail (Figs. 7 and 8). The most anterior caudal centrum, SHN.388/5 (Fig. 6a, d, g, j), is much robust than the other preserved caudal centra and even than those of the dorsal vertebrae previously described (see supplementary material Table 1S). The centrum is slightly longer than deep (length: height ratio = 1.70). This ratio is similar in most preserved caudal vertebrae, but is slightly higher in SHN.388/9-12, which may correspond to a more posterior position in the caudal series. SHN.388/5 is broken

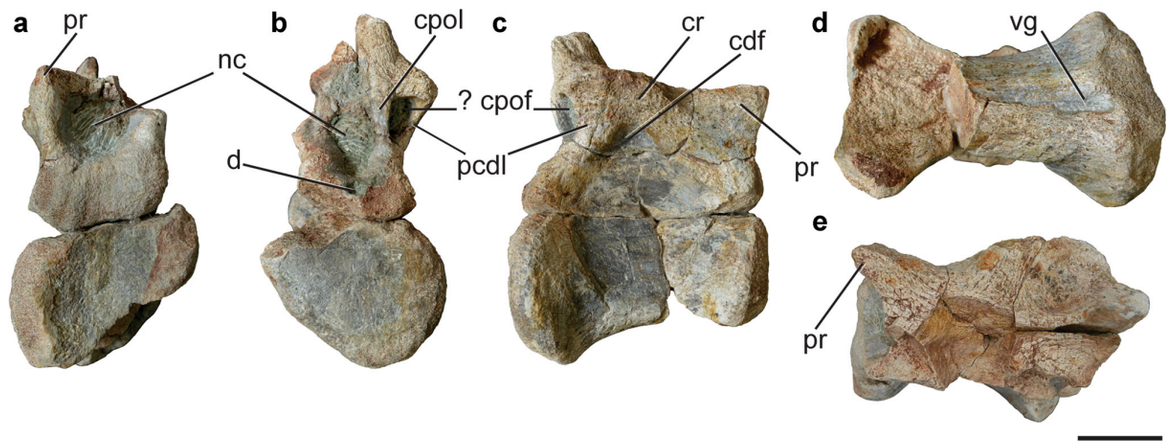

Fig. 7 Megalosauridae indet., mid caudal vertebra collected in Praia da Corva (SHN.388/8) in anterior (**a**), posterior (**b**), right lateral (**c**), ventral (**d**), and dorsal (**e**) views. *Scale bar* 50 mm

at the level of the neural canal, but the centrum is fairly well preserved. This centrum has a deep pleurocentral depression (sensu O'Connor 2006) at the base of the neural arch, which is slightly deeper in the posterior part of the centrum. A well-marked pleurocentral depression probably is present in all caudal centra, despite not visible in some specimens due to distortion. This depression is even present in the vertebra SHN.388/12 (Fig. 8d, e, l, p, t), which corresponds to the most distal caudal vertebra preserved. The articular facets have oval outlines, slightly wider than high, especially the posterior ones. The anterior facet is slightly concave, whereas the posterior one is almost flat. In lateral view, the centrum is slightly concave, with the ventral surface of the articular facet only faintly offset from the vertebral body. The posterior articular facet is in a slightly ventral position relative to the level of the anterior facet. The ventral surface of the centrum has a well-marked and broad longitudinal groove extending almost the entire length of the centrum. This ventral groove is present in all preserved caudal vertebrae and is bounded by lateral crests and deeper in most anterior centra, but still well marked in the most posterior elements. The surfaces for articulation with the chevrons are not visible probably due to the poor preservation of the facets.

In SHN.388/6, such as in SHN.388/5, the posterior articular facet is slightly displaced ventrally relative to the ventral level of the anterior one. In most posterior elements, both articular facets are at the same level ventrally.

An almost complete vertebra, SHN.388/8 (Fig. 7), preserves part of the neural arch fused with the centrum. The neural arch preserves a small fragment of the right caudal rib, the base of the neural spine, and an incomplete right prezygapophysis. In lateral view, the vertebral body is much deep, but this is in part due to lateral compression. The neural canal is broad and circular anteriorly, but has a small ventral constriction in posterior view. In posterior view, a small, rounded concavity is present ventrally to the neural canal. This concavity is also present in the vertebrae SHN.388/5, 6, 9 and 12 (Fig. 8). The caudal rib projects from the posterior part of the centrum. A small concavity is present bellow the caudal rib. A pair of deep fossae in the posterior surface of the neural arch is placed dorsolaterally to the neural canal, which are interpreted as corresponding to the cpof. These rounded fossae are delimited medially by a pair of blades, which would connect with the ventral margin of the postzygapophysis, and laterally by the posterior margin of the caudal rib. Similar fossae are also present, despite significantly shallower, in one posterior caudal vertebra (SHN.388/11).

Discussion The dorsal vertebrae (SHN.388/1-4) are interpreted as corresponding to the posterior part of the dorsal series based on the morphology of the ventral surfaces, which are flat and without any keel, and in the absence of parapophyses in the centra. Well-developed ventral keels are present in anterior dorsal vertebrae of most basal tetanurans, including *Condorraptor* (Rauhut 2005), *Torvosaurus* (Britt 1991), and *Megalosaurus* (Benson 2010a). These structures disappear to the distal part of the dorsal series in most of these taxa and the posterior centra have more flat ventral surfaces. The morphology of the dorsal centra from Praia da Corva is similar to that of posterior dorsal vertebrae of *Megalosaurus* in the flat and transversely broad ventral surface (Benson 2010a). Unfortunately, any complete dorsal series is known for *Torvosaurus*, but prominent ventral keels persist on most of the preserved dorsal centra, except in one vertebra interpreted as corresponding to the fourteen dorsal (Britt 1991),

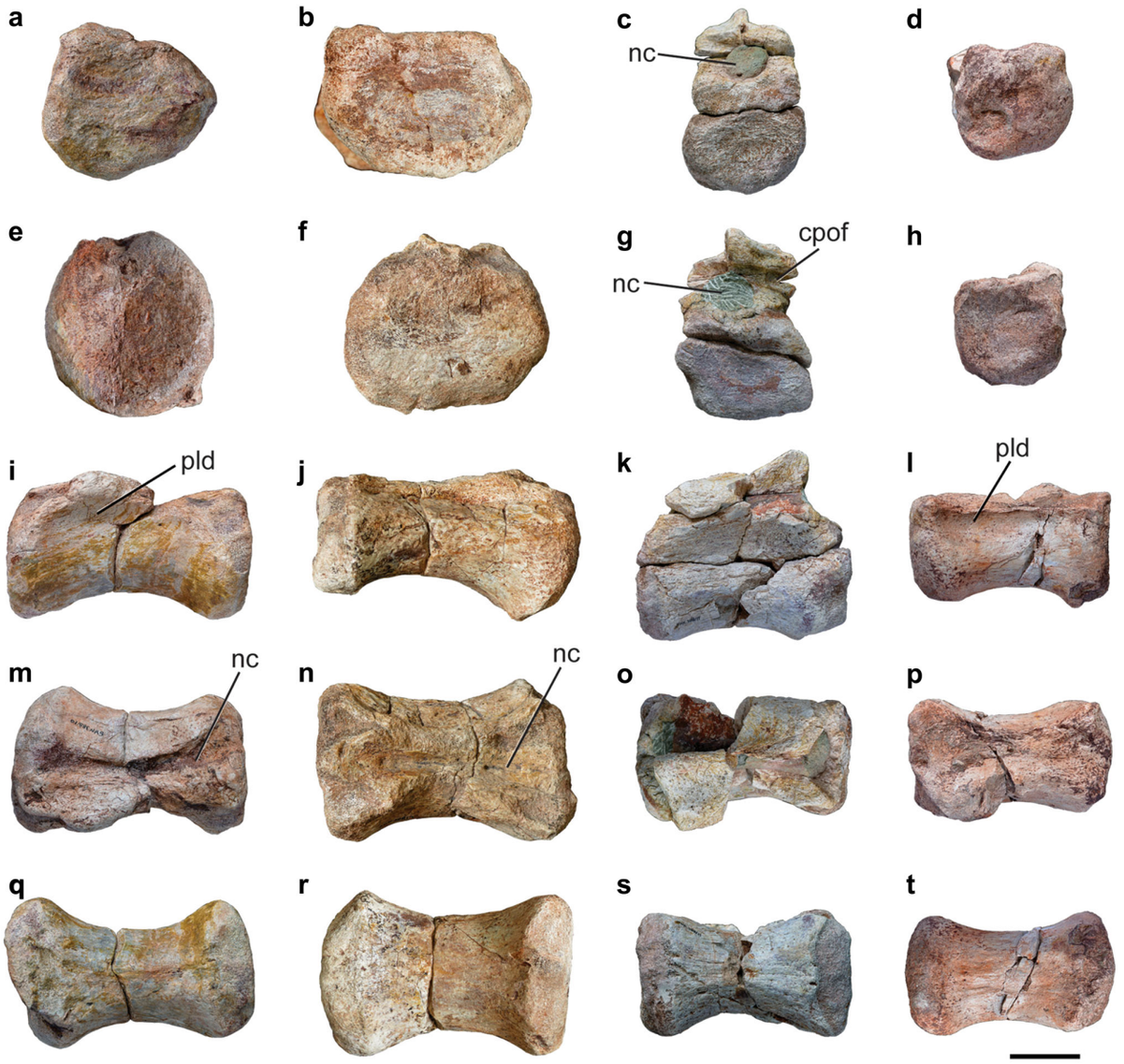

Fig. 8 Megalosauridae indet., posterior caudal vertebrae from Praia da Corva; from *left* to the *right*: centrum (SHN.388/10), centrum (SHN.388/9), partial vertebra (SHN.388/11), and centrum (SHN.388/12). *Views:* anterior (**a**–**d**), posterior (**e**–**h**), left lateral (**i**–**l**), dorsal (**m**–**p**), and ventral (**q**–**t**). *Scale bar* 50 mm

which has a flat ventral surface similar to those of *Megalosaurus* and the Portuguese specimens. Ventral keels are absent in *Eustreptospondylus* (Sadleir et al. 2008) and *Streptospondylus* (Allain 2001), but instead these taxa have a distinct double ventral ridge at least on the anterior dorsal vertebrae. The great development of the pleurocoels in these dorsal vertebrae, which occupy almost the entire length of the lateral surface and that deeply pierce the dorsal part of the centra, is an unusual character among basal theropods. Well-developed dorsal pleurocoels are common in anterior dorsal vertebrae of several megalosauroids (e.g., *Streptospondylus*: Allain, 2001, *Megalosaurus*: Benson, 2010a, *Torvosaurus*: Britt, 1991) and allosauroids (e.g., *Allosaurus*: Madsen, 1976b). Nevertheless, usually these pleurocoels become shallower or absent in most posterior dorsal centra (Madsen 1976b; Allain 2005; Benson 2010a). This trend is reversed in *Torvosaurus*, in which dorsal pleurocoels increase in size posteriorly in the dorsal series (Britt 1991).

The dorsal vertebrae from Praia da Corva show a general morphology similar to other megalosaurids and share with *Torvosaurus* the great development of the pleurocoels,

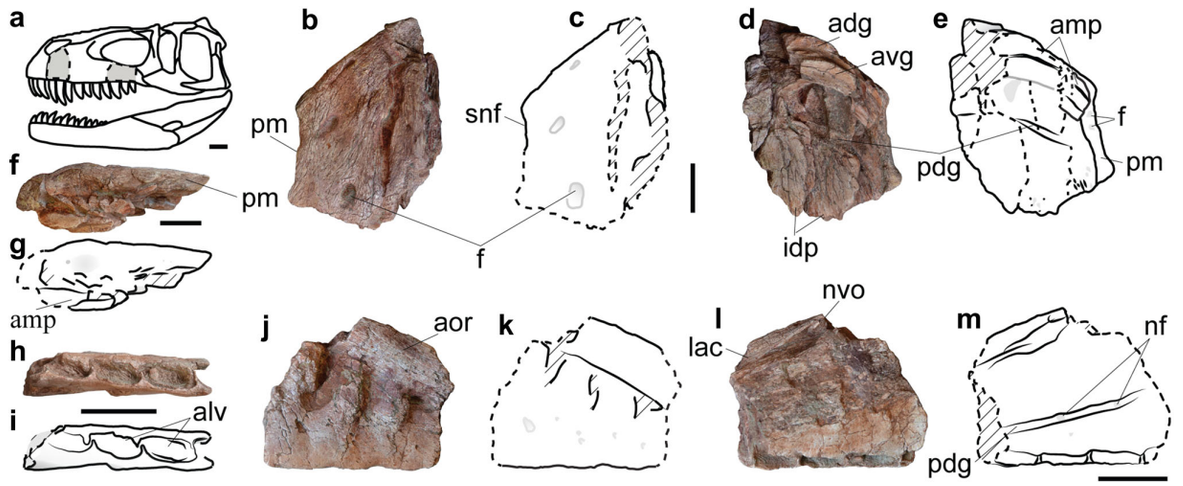

Fig. 9 *Torvosaurus* sp. fragments of a left maxilla (SHN.467); **a** illustration of a skull of *Torvosaurus* in lateral view showing the position of the specimen (copyright Scott Hartman 2013); fragment of the anterior part of the maxilla and respective interpretative line drawing in lateral (**b**, **c**), medial (**d**, **e**), and dorsal (**f**, **g**) views; fragment of the posterior part of the maxilla and respective interpretative line drawing in ventral (**h**, **i**), lateral (**j**, **k**), and medial (**l**, **m**) views. The *broken lines* represent broken areas on the specimen. *Scale bars* (**a**): 100 mm; (**b**–**m**): 50 mm

which is a feature only reported in this taxon (Britt 1991). However, these vertebrae do not have the ventral keel characteristic of most dorsal centra known for *Torvosaurus* (Britt 1991) and instead the flat ventral surface is more similar to that of *Megalosaurus* (Benson 2010a).

The caudal vertebrae have deep longitudinal grooves on the ventral surface, a character that has been considered an autapomorphy of *Ceratosaurus* (Madsen and Welles 2000) or a ceratosaurian synapomorphy (Rowe and Gauthier 1990). However, the presence of ventral grooves on caudal vertebrae has a much wider distribution among theropods and is present in most basal tetanurans (e.g., *Acrocanthosaurus*, *Allosaurus*, *Condorraptor*, *Dubreuillosaurus*, *Monolophosaurus* and *Torvosaurus*), as well as in coelophysoids (Rauhut 2003; Zhao et al. 2010). Nevertheless, the ventral groove in the caudal vertebrae of *Ceratosaurus* is broad, deep and is bounded by pronounced, ridge-like lateral margins, which contrasts with the condition of most other theropods (Tykoski 2005; Rauhut 2011). The caudal vertebrae from Praia da Corva have well-developed ventral grooves, which are deeper posteriorly and much weak or absent anteriorly in the centra, but this morphology is distinct from the broad groove in the caudal vertebrae of some basal ceratosaurs, including *Ceratosaurus* (Madsen and Welles 2000) and *Ceratosaurus* (?) *roechlingi* (Rauhut 2011).

The anterior caudal centra (SHN 388/5) is robust and has articular facets that are significantly wider than high, a character shared with *Torvosaurus* (Britt 1991), but distinct from the condition of most allosauroids (e.g., Madsen 1976b; Currie and Zhao 1993; Brusatte et al. 2008), in which the articular facets of the anterior caudal centra are higher than wide or sub-circular. The caudal vertebrae from Praia da Corva have pleurocentral depressions (subneurocentral suture fossae sensu Britt 1991) at the base of the neural arches. These fossae are especially deep and well-marked on the anterior caudal centra, but persist in the posterior elements. The presence of these depressions in caudal vertebrae is considered a feature that distinguished *Torvosaurus* from all other known Morrison theropods (Britt 1991). Similar lateral depressions are also present in *Megalosaurus* and *Wiehenvenator* (Benson 2010a; Rauhut et al. 2016).

The two caudal vertebrae that preserve part of the neural arch (SHN 388/8 and 388/11) have a pair of deep cpof dorsolaterally located to the posterior end of the neural canal bellow the postzygapophyses. The presence of these fossae on the caudal vertebrae, especially on posterior elements, is an unusual character for primitive theropods. Similar, but shallower fossae also are present in an anterior caudal vertebra (MB R 1940) from the Tendaguru Formation (Rauhut 2011; E.M. pers. obs, 2016). MB R 1940 was tentatively related to the carcharodontosaurid *Veterupristisaurus* due the presence of a high neural spine, an anteroposterior constriction at the base of the neural spine and the absence of ventral keel or groove (Rauhut 2011).

In summary, the caudal vertebrae collected in Praia da Corva are tentatively assigned to Megalosauridae due the general morphology of the anterior centra, with articular

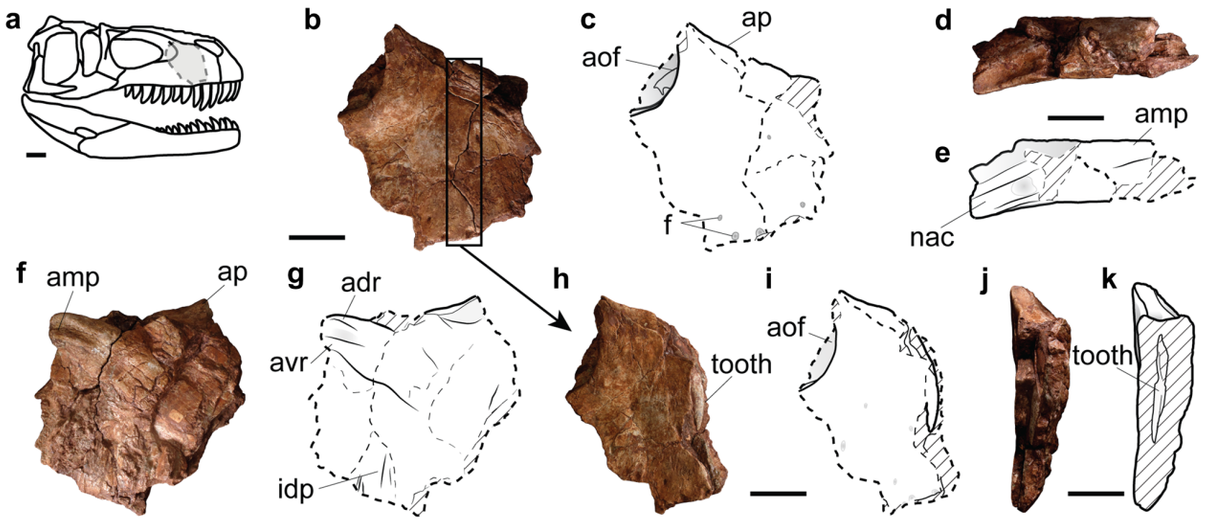

Fig. 10 *Torvosaurus* sp. fragment of a right maxilla (ALTSHN.116); **a** illustration of a skull of *Torvosaurus* in lateral view showing the position of the specimen; ALTSHN.116 and respective interpretative line drawings in lateral (**b**, **c**), dorsal (**d**, **e**), and medial (**f**, **g**) views; detail of an unerupted tooth visible throughout a fracture in anterolateral (**h**, **i**), and anterior (**j**, **k**) views. The *broken lines* represent broken areas of the specimen. *Scale bars* (**a**): 100 mm; (**b**–**k**): 50 mm

facets strongly wider than high, and the presence of well-marked pleurocentral depressions in all preserved centra. These features have been considered exclusive for *Torvosaurus* (Britt 1991; Brusatte et al. 2008). However, due the presence of some unusual characters such as the broad and deep cpof in the mid and posterior neural arches they are here identified as belonging to indeterminate megalosaurids.

Torvosaurus Galton and Jensen, 1979

Torvosaurus sp.

Material Fragments of a left maxilla associated with several indeterminate cranial fragments (SHN.467) and a fragment of the anterior end of a right maxilla (ALTSHN.116) (Figs. 9 and 10).

Locality and horizon Praia da Corva (Torres Vedras), Praia da Amoreira-Porto Novo Formation (upper Kimmeridgian).

Description SHN.467 comprises two fragments of a left maxilla, one of them corresponding to the anterior tip, and the other one to the rear part, lacking the mid-section of the element (Fig. 9). The anterior fragment is broken at the level of the third alveolus. It preserves the surface for articulation with the premaxilla and the ventral portion of the suture for the nasal. Anteriorly, the maxilla is 105 mm deep along the preserved surface for articulation with the premaxilla (see supplementary material Table 2S). This articular surface is incomplete ventrally but is nearly vertical and slightly concave in lateral view. In medial view, the premaxillary articulation is a broad and flat surface with two small foramina in the dorsal end. The opening for the subnarial foramen is a shallow and poorly defined concavity in the dorsal end of the maxillary anterior edge, which is delimited dorsally by a small, rounded protuberance.

The dorsal margin of the anterior ramus is transversely thick, with a broad but shallow concavity near its anteroposterior mid-length. The anteromedial process is found medially to the maxillary dorsal edge. This process is a robust crest anteroventrally projected in an angle of approximately 30° relative to the ventral border of the maxilla (Fig. 9). The anteromedial process is broken anteriorly and lacks most of the medial surface. Nevertheless, it is possible to verify its anterior extension, which does not exceed significantly beyond the anterior margin of the maxilla. Posteriorly, this process has two broad grooves separated by a prominent crest projected along the dorsoventral mid-height. The ventral groove is interpreted as the articular surface for the vomer and the dorsal one corresponds to the articulation with the opposite maxilla (following Allain 2002).

The anterior interdental plates are broken and collapsed mediolaterally. These plates are deeper dorsoventrally than long anteroposteriorly. The maxillary lateral surface is slightly incomplete ventrally, and so it is not possible to ascertain its extension with respect to the dorsoventral depth of the interdental plates. The most anterior

interdental plates bear a series of thin vertical crests near the ventral border, resulting on a distinct rugose ornamentation. The alveoli are strongly collapsed, but apparently, they have an oval shape. The interdental plates are delimited dorsally by a shallow paradental groove, which projects anteroventrally, so the first two interdental plates are dorsoventrally shorter than the third one.

The fragment of the posterior part of the maxilla preserves fourth alveoli (the anterior one is not complete). These alveoli are oval and slightly smaller, both mesiodistally and labiolingually, than the most mesial ones. The interdental plates are slightly shorter ventrally than the maxillary lateral wall. The paradental groove extends posteroventrally reducing the dorsoventral depth of the most posterior interdental plates. Inside this groove are visible two small foramina placed at approximately the anteroposterior mid-length of each alveolus.

The dorsal surface of the jugal ramus has a broad and deep groove bounded laterally by a high lamina, which corresponds to the anterior end of the suture for the lacrimal (Fig. 9l). In medial view, there is a deep slot on the anterior end of the preserved fragment of the jugal ramus interpreted as the posterior end of a neurovascular opening similar to that described in other specimens as the opening for the maxillary branch of the trigeminal nerve (Hendrickx and Mateus 2014). The lateral surface of the posterior part of the maxilla has a series of vertical depressions probably corresponding to the collapse of the alveoli. Dorsally to these depressions, a well-defined but low ridge extends along the dorsal end of the maxillary lateral wall. The lateral surface of the maxilla has a series of small foramina, but without any recognizable pattern. Ventrally, the lateral surface of the maxilla forms shallow waves along the alveolar margin.

Discussion SHN.467 is incomplete, but shows a set of diagnostic characters that allows an accurate systematic approach. The medial position of the anteromedial process in a relative to the dorsal surface of the maxillary anterior ramus is similar to the condition of most theropods except *Ceratosaurus*, *Dilophosaurus*, *Marshosaurus* and *Sinraptor* (Carrano et al. 2012). This specimen shares with most megalosauroids the anteroventrally inclined anterior end of junction between the medial wall of the maxilla and interdental plates (Britt 1991; Allain 2002; Sadleir et al. 2008; Benson 2008, 2010a; Carrano et al. 2012). This feature also is present in some derived allosauroids, including *Neovenator* (Brusatte et al. 2008), *Acrocanthosaurus* (Eddy and Clarke 2011), and *Carcharodontosaurus* (Brusatte and Sereno 2007). The fused interdental plates, which have a depth nearly twice the length and ventrally shorter than the lateral wall of the maxilla are exclusive characters of *Torvosaurus* among the currently known theropods (Carrano et al. 2012). The presence of a neurovascular opening piercing the jugal ramus with an anteroposterior orientation is a character shared with the holotype of *Torvosaurus gurneyi* (ML 1100), and this character was considered as a synapomorphy for *Torvosaurus* by Hendrickx and Mateus (2014).

This combination of characters allows considering SHN.467 as a member of the genus *Torvosaurus*. A preliminary description of this specimen considered some putative differences with this taxon, including the morphology of the anterior end of the anteromedial process, and the absence of a large foramen within the premaxillary suture (Malafaia et al. 2014). Nevertheless, the distinct morphology of the anterior end of the anteromedial process may be due to distortion and breakage of the medial surface of the process, and the unusual blade-shape probably corresponds to its partial preservation. Similarly, the absence of a large foramen in the premaxillary suture may be also an artifact of preservation. The anterior end of the anteromedial process is displaced laterally and is probably covering the foramen.

ALTSHN.116 is another specimen collected in Praia da Corva that corresponds to a fragment of the anterior end of a right maxilla with an unerupting tooth (probably the third) visible along a fracture (Fig. 10). Comparing the proportions of ALTSHN.116 and SHN.467, the former might correspond to a slightly larger individual (see supplementary material Table 2S). ALTSHN.116 was previously assigned to *Torvosaurus* sp. (Malafaia et al. 2008) and more recently included in the species *T. gurneyi* (Hendrickx and Mateus 2014). This specimen is very incomplete and distorted, but shows some diagnostic features that allow its identification to *Torvosaurus* as was previously noted. However, the assignation to *T. gurneyi* is more debatable because any of the supposed shared characters (e.g., the ventral extension of the interdental plates relative to the lateral wall and the morphology of the ventral margin of the plates) are observed in ALTSHN.116 due the poor preservation.

Material A set of twenty one isolated teeth (SHN.067, SHN.215, SHN.221, SHN.257, SHN.266, SHN.268, SHN.294, SHN.303-304, SHN.319-320, SHN.359a, SHN.362, SHN.364, SHN.374, SHN.381, SHN.401, SHN.440, SNH.441-442, SHN.470) (Fig. 11).

Locality and horizon Praia da Corva and Santa Rita (Torres Vedras), Valmitão and Porto Dinheiro (Lourinhã), Almagreira and Praia dos Frades (Peniche), Praia da Amoreira-Porto Novo Formation (upper Kimmeridgian–lowermost Tithonian); Peralta (Lourinhã), ? Sobral Formation (upper Kimmeridgian–lower Tithonian); Salir do Porto (Caldas da Rainha), Alcobaça Formation (upper Kimmeridgian).

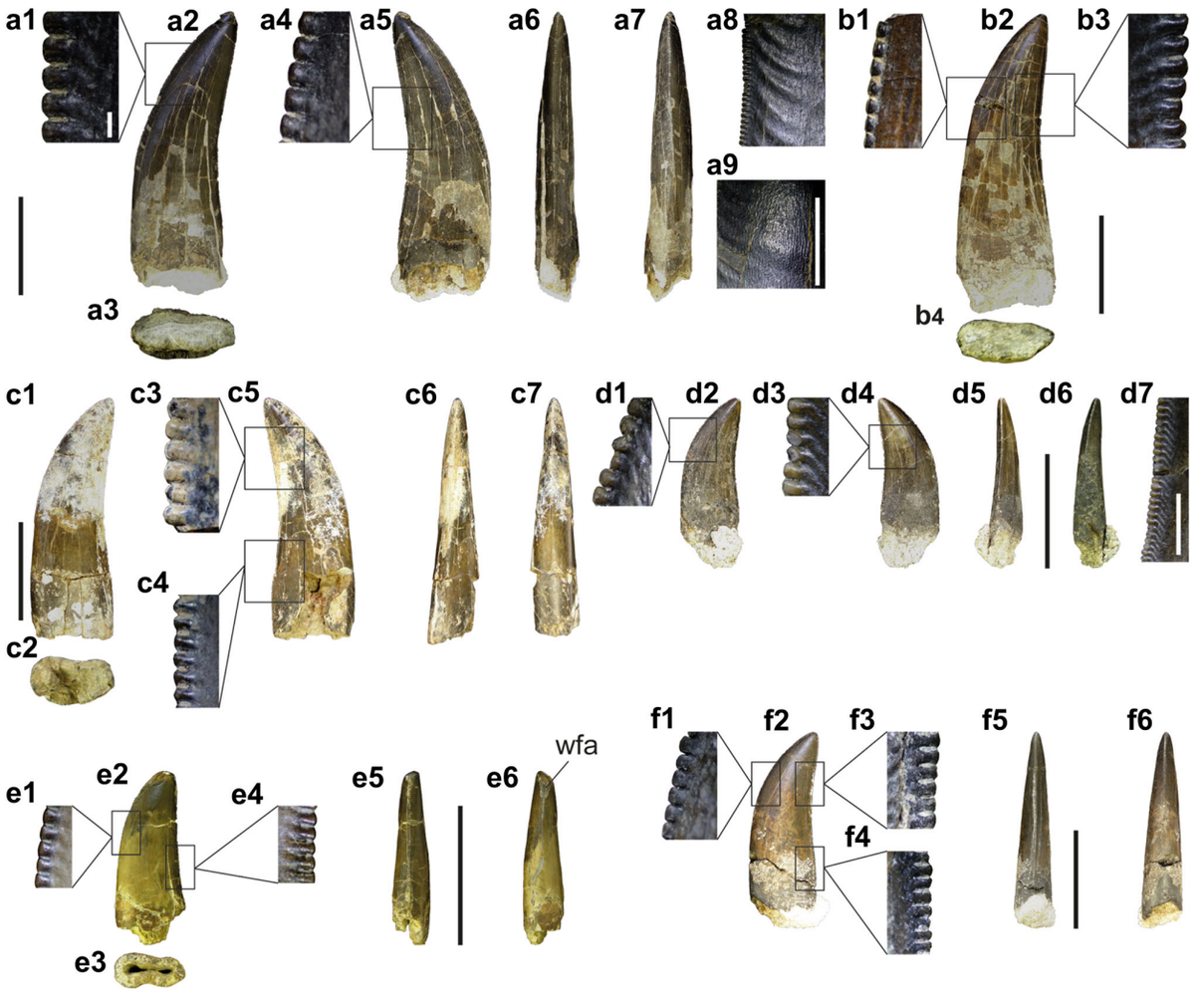

Fig. 11 *Torvosaurus* sp., selected isolated teeth from different sites in the Upper Jurassic of the Lusitanian Basin; **a** SHN.067; **b** SHN.401; **c** SHN.441; **d** SHN.266; **e** SHN.215; **f** SHN.319, in lingual (a_2, b_2, c_1, d_2, e_2, f_2), labial (a_5, c_5, d_4), distal (a_6, c_6, d_5, e_5, f_5), and mesial (a_7, c_7, d_6, e_6, f_6) views; cross-section at the crown base (a_3, b_4, c_2, e_3); mesial denticles (a_1, b_1, d_1, e_1, f_1,); distal denticles (a_4, b_3, c_3, c_4, d_3, e_4, f_3, f_4); details of the crown showing marginal undulations (a_8); ornamentation (a_9); and interdenticular sulci (d_7). *Scale bars* 50 mm for the crowns; 1 mm for the denticles; (a_8–a_9, d_7): 10 mm

Description These isolated teeth are interpreted as lateral teeth because they are moderately compressed labiolingually and have almost symmetrical mesial and distal carinae (Fig. 11). In some teeth, the mesial carinae are slightly displaced into the lingual surface of the crown base, which suggests a more mesial position in the tooth row (Hendrickx et al. 2015b). The crowns are slightly curved apically with convex mesial carina and almost straight distal one, in lateral view. Most of these teeth are very large, with crown heights (AL) ranging between 40.25 and 152.84 mm (average c. 87.05 mm), mesiodistal length of the crown base (CBL) between 6.2 and 48.38 mm (average c. 31.26 mm) and labiolingual width of the crown base (CBW) between 3.57 and 22.89 mm (average c. 16.18 mm) (see supplementary material Table 3S). The crowns are blade-shaped and moderately labiolingually compressed with crown base ratio (CBR) ranging between 0.41 and 0.72 (average c. 0.53). The crown bases are oval in cross-section, with slightly convex labial and lingual surfaces. Some crowns have shallow concavities at approximately the mid-length of both lingual and labial surfaces. Both carinae are serrated, bearing relatively large denticles along the entire height of the distal carinae, but denticles end at approximately one-half or three-quarters the height of the mesial carinae. The denticles are perpendicular to the carinae, chisel-shaped, with rounded apices and are lower mesiodistally than wide apicobasally. Between 5 and 10 denticles per 5 mm are present at the

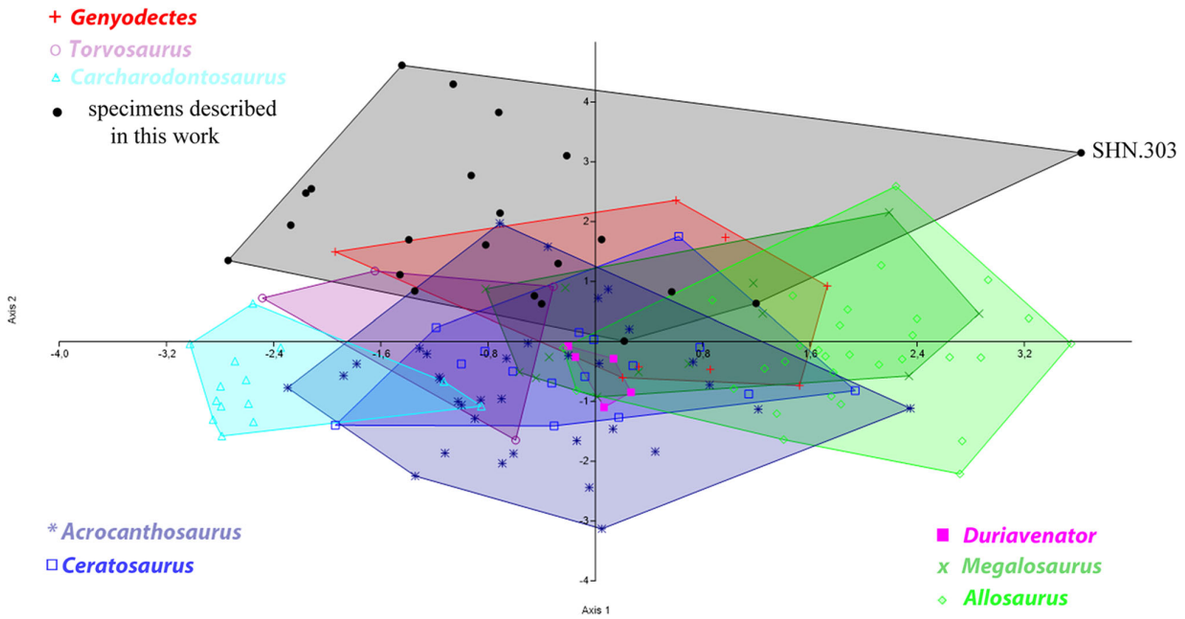

Fig. 12 Graphical results of the Canonical Variate Analysis (CVA) of 142 teeth including the 21 isolated teeth from the Lusitanian Basin and teeth of 8 theropod taxa groupings along the first two canonical axes of maximum discrimination in the dataset (Eigenvalue of Axis 1 = 1.883, which accounted for 44.21% of the variation; Eigenvalue of Axis 2 = 1.02, which accounted for 23.97% of the variation). Log-transformed values for the variables CBL, CBW, CH, AL, CBR, CHR, MC, DC, CDA, and CMA were used in the analysis

mid-height of both carinae (average c. 6.83 in the mesial carina and 7.91 in the distal carina), with an average of denticle density ratio of approximately 0.95. The denticles extend to the apices of the crowns and decrease slightly in size to the base. Some crowns show well-developed and basally projected marginal undulations and interdenticular sulci (sensu Hendrickx et al. 2015a), mostly adjacent to distal denticles. These teeth have a distinct ornamentation of the enamel produced by a series of thin, irregular crenulations. When present, wear facets extend mostly along the mesial carina (sometimes covering almost half of the crown height).

Discussion A Discriminant Function Analyses (DFA) was performed using squared Mahalanobis distance. This analysis recovered a percentage of accuracy of 79.3% when probability is calculated considering all the groups equal and eliminating the specimens with absent values of some variable, but this percentage diminish to 76.6% if missing values are replaced by the average. When probability is calculated based on different group sizes, the percentage of accuracy increases for 82.1%. The analysis used 6 canonical discriminant functions (CBL, CBW, CH, AL, CBR, and CHR) from which the first and second functions explain 83.4% of the variability. Based on this analysis ten teeth (SHN.067, 221, 268, 304, 319, 320, 401, 441, 442 and 470) where recovered as belonging to *Torvosaurus* as the most probable group, and five (SHN.215, 266, 374, 364 and 440) as the second most probable group. Two teeth (SHN.294 and 362) were identified as belonging to *Megalosaurus*, one tooth (SHN.359a) as *Allosaurus*, and one tooth (SHN.257) as *Daspletosaurus*. Two teeth (SHN.303 and 381) were excluded from the statistical analysis due absence of data.

A Canonical Variate Analysis (CVA) was also developed. The plot of the results for a reduced dataset, including *Genyodectes*, *Ceratosaurus*, *Duriavenator*, *Megalosaurus*, *Torvosaurus*, *Allosaurus*, *Acrocanthosaurus* and *Carcharodontosaurus* shows that the morphospace occupied by the described isolated teeth is clearly separated from those of *Allosaurus*, *Carcharodontosaurus* and *Duriavenator* (Fig. 12). With respect to other large-sized theropods, such as *Genyodectes*, *Ceratosaurus*, *Megalosaurus*, *Torvosaurus* and *Acrocanthosaurus*, there is some overlap of the correspondent morphospaces, reflecting a similar morphology among these taxa namely in the relative dimensions and denticles density (Hendrickx et al. 2015b).

A new analysis developed with a reduced dataset, including ceratosaurs (*Genyodectes* and *Ceratosaurus*) and megalosaurids, shows some overlap of the morphospaces occupied by the set of the studied teeth and those of *Torvosaurus* (Fig. 13).

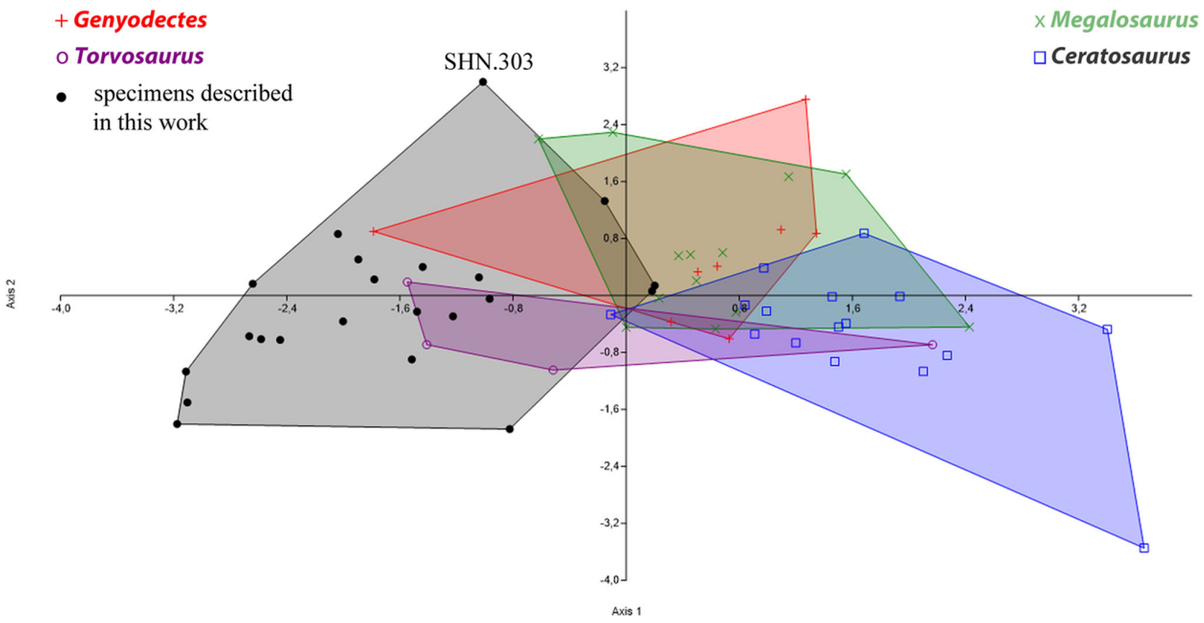

Fig. 13 Graphical results of the Canonical Variate Analysis of a reduced dataset, including the ceratosaurs *Genyodectes* and *Ceratosaurus* and the megalosaurids *Megalosaurus* and *Torvosaurus* groupings along the first two canonical axes of maximum discrimination in the dataset (Eigenvalue of Axis 1 = 1.906, which accounted for 82.98% of the variation; Eigenvalue of Axis 2 = 0.2497, which accounted for 10.87% of the variation). Log-transformed CBL, CBW, CH, AL, CBR, CHR, MC, DC, CDA and CMA were used in the analysis

The morphology of these isolated teeth from the Portuguese Upper Jurassic is similar to those of other megalosaurid specimens. The presence of shallow concavities centrally positioned on the basolingual part of the crown is a feature shared with *Torvosaurus*, *Megalosaurus*, *Duriavenator* and *Afrovenator*, whereas the basolingual surface of the lateral crowns is flat in *Dubreuillosaurus* and *Magnosaurus* (Hendrickx et al. 2015b). The morphology of the denticles (chisel-like, with rounded apices, quadrangular in outline, low mesiodistally and relatively wide apicobasally) and the denticle density in the distal and mesial carinae are also characters shared with *Torvosaurus*, *Megalosaurus* and other megalosauroids (Hendrickx et al. 2015b).

These specimens from the Upper Jurassic Portuguese record are also similar to some isolated teeth described in the Upper Jurassic of Spain, from different localities of the Villar del Arzobispo Formation in Teruel (Formicho Alto, Riodeva and Galve) and Valencia (Alpuente) Provinces (Suñer et al. 2005; Canudo et al. 2006; Royo-Torres et al. 2009; Gascó et al. 2012; Cobos et al. 2014). The Spanish teeth share with the specimens from the Lusitanian Basin the large size of the crowns, with AL between 101 and 61 mm and CBL between 33 and 45 mm, which are only comparable with teeth of carcharodontosaurids, megalosaurids and tyrannosaurids (Smith et al. 2005; Cobos et al. 2014). The denticle density is also similar (MC and DC about 9 and 8 denticles per 5 mm, respectively). Besides, some teeth from the Villar del Arzobispo Fm. (FCPT-1980 and MAP-4473) have well-developed marginal undulations and enamel ornamentations similar to those observed in the Portuguese specimens. These isolated theropod teeth from the Villar del Arzobispo Fm. and the set of teeth from the Lusitanian Basin may be related to the same morphotype suggesting the presence of *Torvosaurus* or a closely related megalosaurid taxon in the Spanish Upper Jurassic as was suggested by Cobos et al. (2014).

Torvosaurus gurneyi 2014

Material An almost complete right maxilla (SHN.400) (Figs. 14 and 15).

Locality and horizon Praia da Vermelha (Peniche), upper levels of the Praia da Amoreira-Porto Novo Formation (upper Kimmeridgian-lowermost Tithonian). This specimen was originally in a private collection, which since 2008 has been managed by the SHN. Based on descriptions of the private collector, it was possible to verify that SHN.400 was collected at the type locality of *Torvosaurus gurneyi*, a left maxilla (ML 1100) housed in the Museu da Lourinhã. In the description of the new species, the authors placed Praia da Vermelha in Lourinhã, but in fact this locality belongs to the Peniche municipality. SHN.400

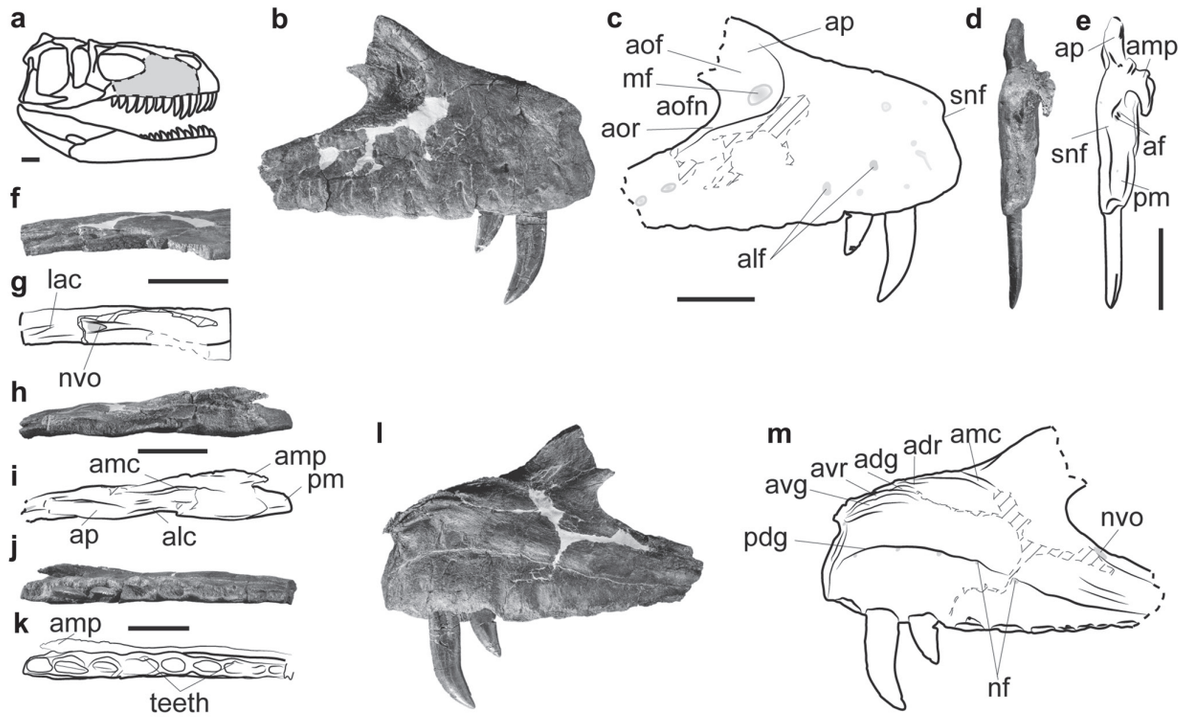

Fig. 14 - *Torvosaurus gurneyi*, right maxilla from Praia da Vermelha (SHN.400); **a** illustration of a skull of *Torvosaurus* in lateral view showing the position of the specimen; **b–m**, SHN.400 and respective interpretative line drawings in lateral (**b**, **c**), anterior (**d**, **e**), dorsal (**h**, **i**), ventral (**j**, **k**), and medial (**l**, **m**) views; detail of the jugal ramus in dorsal view (**f**, **g**). The *broken lines* represent broken areas on the specimen. *Scale bars* (**a**): 100 mm; (**b–m**): 50 mm

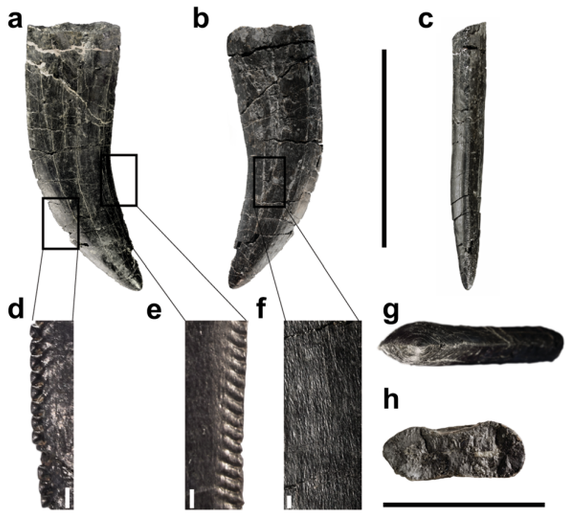

Fig. 15 *Torvosaurus gurneyi*, second maxillary tooth of SHN.400 in medial (**a**), lateral (**b**), mesial (**c**), and apical (**g**) views; cross-section of the crown base (**h**), detail of the mesial denticles (**d**), detail of the distal denticles (**e**), and detail of the texture of the enamel in the mid-section of the crown (**f**). *Scale bars* (**a–c**, **g, h**): 50 mm; (**d–f**): 1 mm

corresponds in size and morphology to the holotype of *T. gurneyi* (ML 1100), the preservation of both specimens is quite similar and both are complementary. Therefore, it is here considered that SHN.400 and ML 1100 probably belong to the same individual.

Description SHN.400 corresponds to an almost complete right maxilla (Figs. 11 and 12). The jugal ramus is broken posteriorly at the level of the tenth alveolus lacking the most posterior part, including the surface for contact with the jugal. The ascending ramus is also broken, but preserves a small fragment of the ventral part. The total length of the preserved maxillary body is 465 mm (see supplementary material Table 2S). The specimen preserves two erupted teeth corresponding to the second and third maxillary teeth. The tips of another two erupting teeth are visible medially inside the fourth and seventh alveoli.

In lateral view, the ventral edge of the maxilla is slightly upturned anteriorly, and sharply tapered to the rear. The second to the sixth alveoli are sub-equal in size and slightly largest than the first alveolus. Most posterior alveoli are smaller both in mesiodistal length and in labiolingual width.

The maxillary anterior ramus is well developed. The anterior margin of the maxilla has a slight dorsoposterior orientation and is gently concave in lateral view. In anterior view, the surface for contact with the premaxilla is transversely concave with a shallow vertical groove delimited by a well-developed and anteriorly projected crest. Two small foramina are visible in the ventral surface of this groove. The subnarial foramen is in the anterodorsal part of the premaxilla articular surface. This foramen is a shallow concavity measuring approximately 12 mm dorsoventrally. As in SHN.467, this foramen is delimited dorsally by an anteriorly projected, small, and rounded bulge. A large and deep sub-oval foramen is placed medially to this bulge.

In dorsal view, the anterior ramus of the maxilla is mediolaterally thick and has a shallow and wide oval depression for articulation with the ventral process of the nasal. Backward to this concavity, two longitudinal, parallel and well-developed crests project along the medial and lateral surfaces of the maxillary dorsal margin forming a deep concavity at the base of the ascending process. The medial crest extends from the anterior end of the articulation with the nasal ventral process along the dorsal surface of the anteromedial process. This crest has a gently concave profile, and merges posteriorly with the base of the maxillary ascending process. The lateral ridge is shorter and extends through the base of the ascending process.

The anteromedial process is relatively low dorsoventrally and sharply tapered anteriorly. This process projects anteroventrally from the dorsal end of the maxillary medial surface and bears two well-defined ridges extending along the entire length of the process and delimiting two deep and longitudinal grooves. The maxillary ascending process is relatively robust, but mediolaterally thin. The dorsal end of the process projects posteriorly in an angle of approximately 45° with the ventral margin of the antorbital fenestra. In lateral view, the ascending process has a *lamina medialis* (sensu Witmer 1997), which delimits the anteroventral corner of the antorbital fenestra, and a *lamina lateralis* delimiting the anterior end of the antorbital fossa. In posterior view, the ascending process has a small concavity filled with sediment at the base of the anterolateral surface. This concavity is concealed by the *lamina lateralis* of the ascending process and thus it is not visible in lateral view neither opens medially. The position and morphology of this opening is coincident with the promaxillary fossa (sensu Witmer 1997). Besides this opening, a shallow and poorly defined maxillary fossa is present on the lateral surface of the ascending process at approximately the mid-length.

The antorbital fossa occupies almost the entire length of the ascending process, but has a small ventral extension, with the ventral margin roughly coincident with the ventral border of the antorbital fenestra. In lateral view, the maxilla has a robust antorbital ridge projecting longitudinally across the dorsal surface (Fig. 11c). This ridge extends from near the anterior end of the antorbital fossa, but almost disappears posteriorly. The dorsal margin of the jugal ramus has a deep groove opening medially and extending along most of the preserved length. A wide opening is visible inside the anterior end of this groove, which pierces the dorsal margin of the jugal ramus with an anteroposterior orientation. This opening corresponds to a neurovascular opening (Fig. 11g, m). Posteriorly, the dorsal surface of the jugal ramus has a deep and narrow slot, marking the suture with the ventral ramus of the lacrimal.

In medial view, the interdental plates are fused to each other, and occupy almost half of the dorsoventral depth of the maxillary medial surface. These plates are delimited dorsally by a narrow, but relatively deep paradental groove, inside which there are several small foramina placed at approximately the mid-length of each alveolus. As in SHN.467, the maxilla from Praia da Vermelha has the paradental groove projecting ventrally on the anterior end, so the first interdental plate is ventrodorsally lower than the second and third ones. Posteriorly, the paradental groove is ventrally projected resulting in the shortness of the most posterior interdental plates; the ventrodorsal depth of the interdental plates at the level of the ninth alveolus is approximately one-quarter the depth of that at the second one. The lateral surface of the maxillary body is pierced by a series of large and deep foramina arranged along the ventral margin.

The second and third maxillary teeth are preserved on their respective alveoli. The second tooth is probably fully erupted, but the third one is interpreted as an erupting tooth (Fig. 12). The crowns are labiolingually compressed, slightly distally curved, and with mesial and distal serrated carinae. In the third tooth, both mesial and distal carinae extend along the entire height of the crown. This contrasts with the condition in the second tooth in which the distal carina extends along the entire height of the crown, whereas the mesial one ends at approximately one third of the crown height. Interdenticular sulci (sensu Hendrickx et al. 2015a) are visible on the second tooth at the base of the denticles, especially on the middle denticles of the distal carina (Fig. 12). The denticles are relatively large (about six denticles per 5 mm), chisel-like with rounded apices, and slightly mesiodistally higher on the distal carina. The enamel has a distinctive ornamentation produced by a series of thin, irregular crenulations (braided sensu Hendrickx et al. 2015a).

Discussion SHN.400 shares with some megalosauroids the presence of a well-developed anterior ramus of the maxilla (Carrano et al. 2012). A short maxillary anterior ramus is generally present on basal theropods, including ceratosaurs

as well as in some derived allosauroids. Among megalosauroids, a long anterior ramus of the maxilla is present in *Dubreuillosaurus* (Allain 2002) and *Afrovenator* (Sereno et al. 1994), in spinosaurids (Charig and Milner 1997), in *Wiehenvenator* (Rauhut et al. 2016), and in *Torvosaurus* (Britt 1991), but not in *Megalosaurus* (Benson 2010a). As in SHN.467 and ALTSHN.116, the anteromedial process in SHN.400 has a medial position relative to the dorsal surface of the maxillary anterior ramus. SHN.467 and SHN.400 also share the reduced dorsoventral depth of the first interdental plate relative to that of most posterior ones. This character is related with the anteroventral orientation of the paradental groove that is typical in tetanurans, except in *Allosaurus*, *Baryonyx*, *Neovenator*, *Sinraptor* and *Piatnitzkysaurus* (Carrano et al. 2012). SHN.467 is distinct from SHN.400 in the absence of a longitudinal ridge dorsally to the interdental plates. However, this is probably due crushing of SHN.467 in this area that produced an almost flat medial surface.

The moderate ventral extension of the antorbital fossa in SHN.400 is a character shared with megalosauroids (e.g., *Torvosaurus*: Britt, 1991; Hendrickx and Mateus 2014; *Wiehenvenator*: Rauhut et al., 2016; and *Eustreptospondylus*: Sadleir et al., 2008), most derived allosauroids (e.g., *Carcharodontosaurus*: Brusatte and Sereno, 2007 and *Mapusaurus*: Coria and Currie, 2006), but also with some primitive theropods such as *Majungasaurus* (Sampson and Witmer 2007). The anteroventral margin of the antorbital fossa is demarcated by a well-developed raised ridge contrasting with most theropods, in which the limit between the antorbital fossa and the lateral wall is graded or stepped (Carrano et al. 2012). SHN.400 shares this feature with *Marshosaurus bicentesimus*, *Wiehenvenator albati*, *Torvosaurus tanneri* (but scored as graded or stepped by Carrano et al. 2012), and *Torvosaurus gurneyi* (Carrano et al. 2012; Hendrickx and Mateus 2014; Rauhut et al. 2016). A similar ridge also is present in *Masiakasaurus knopfleri* (Carrano et al. 2002), *Sinraptor dongi* (Currie and Zhao 1993), and "*Yangchuanosaurus*" *hepingensis* (Carrano et al. 2012).

A shallow and poorly delimited maxillary fossa similar to that on the specimen from Praia da Vermelha is only found in *Torvosaurus* among the currently known theropods (Britt 1991; Carrano et al. 2012; Hendrickx and Mateus 2014). Most megalosaurids have large and well-developed maxillary fossae (e.g., Allain 2002; Sadleir et al. 2008; Benson 2010a). On the other hand, most allosauroids are characterized by the presence of well-developed maxillary fenestrae, which broadly opens medially (Madsen 1976b; Currie and Zhao 1993; Brusatte et al. 2008; Sereno and Brusatte 2008; Ortega et al. 2010), or by the absence of any fossa or fenestra, as in *Carcharodontosaurus*, *Giganotosaurus* and *Mapusaurus* (Carrano et al. 2012). The absence of a maxillary fossa/fenestra is also reported in most spinosaurids, including *Baryonyx*, *Irritator* and *Spinosaurus* (Charig and Milner 1997; Sues et al. 2002; Carrano et al. 2012).

The combination of characters described above allows considering SHN.400 as a member of the genus *Torvosaurus*. Other maxilla collected in Praia da Vermelha (ML 1100), probably belonging to the same individual as SHN.400, was firstly assigned to the North American species *Torvosaurus tanneri* (Mateus et al. 2006), and more recently reinterpreted as an exclusive species of the Lusitanian Basin, *T. gurneyi* (Hendrickx and Mateus 2014). The new species was diagnosed based on two autapomorphies: maxilla with fewer than eleven teeth, and interdental plates nearly coincident with the lateral wall of the maxillary body. ML 1100 preserves eight maxillary alveoli and the authors estimate a maximum number of ten teeth. The new specimen (SHN.400) has nine completely preserved alveoli and is broken across the tenth alveolus where a small fragment of the tooth is visible, and so the maxillary teeth account on this specimen is, at least, equal to that estimated for ML 1100. Although, the specimen only preserves the most anterior end of the suture for contact with the lacrimal and since the tooth row may extend behind the anterior end of this suture as in other megalosaurids (e.g., *Dubreuillosaurus*: Allain, 2002; *Megalosaurus*: Benson, 2010a; *Wiehenvenator*: Rauhut et al., 2016), it is not possible to exclude the possibility that the complete maxilla may have more than ten teeth. Furthermore, this character is even more difficult to assess once the tooth count is usually high variable both through ontogeny and within the same species or even in the same individual (e.g., Rauhut and Fechner 2005; Hendrickx and Mateus 2014; Canale et al. 2015).

The interdental plates in SHN.400 are slightly shorter dorsoventrally than the maxillary lateral wall, a condition similar to that observed in ML 1100 (Hendrickx and Mateus 2014), and also in other megalosaurids (e.g., *Megalosaurus*: Benson, 2010a). In *Torvosaurus tanneri* (Britt 1991), and *Wiehenvenator albati* (Rauhut et al. 2016) the interdental plates end well dorsal relative to the lateral wall of the maxillary body. However, this high position of the interdental plates on the North American specimen was interpreted as result in part of crushing (Britt 1991). Rauhut et al. (2016) proposed that the interdental plates placed considerably dorsal to the lateral alveolar margin as a synapomorphy of the clade containing *Megalosaurus*, *Torvosaurus*, and *Wiehenvenator*. ML 1100 and SHN.400, differ from *T. tanneri* (Britt 1991) in the morphology of the ventral end of the interdental plates, which is straight in the Portuguese specimens, whereas they end ventrally in broad, V-shaped points in the specimen from North America. *Wiehenvenator albati* (Rauhut et al. 2016) differs from

both the Portuguese and North American forms of *Torvosaurus* (Britt 1991; Hendrickx and Mateus 2014) because the interdental plates are separated in this Germany taxon.

Other differences mentioned between *T. tanneri* and the specimen ML 1100 are the morphology of the anterior part of the maxillary medial shelf and of the anteromedial process. SHN.400 is fairly complete and well preserved, and together with ML 1100, new data are obtained improving the previous description. Hendrickx and Mateus (2014) reported the presence on ML 1100 of a convexity corresponding to the posterior part of the medial shelf, but they considered that it is distinct from the ridge present in *Torvosaurus tanneri*. Herein, this convexity is considered homologous to the ridge of *T. tanneri* despite apparently slightly less developed in the Portuguese specimens. However, in the North American specimen this area is badly distorted and thus it is difficult to verify if this character is an artifact of preservation. This is also the case of other characters, such as the more prominent medial shelf of the jugal ramus in *T. tanneri* than in ML 1100. Other differences reported between ML 1100 and *T. tanneri* are related with the morphology of the anteromedial process. In SHN.400, the dorsal ridge of the anteromedial process extends further posteriorly than the ventral one as in *T. tanneri* (Britt 1991) and other megalosaurids (e.g., *Dubreuillosaurus*: Allain, 2002), and apparently contrasting with the condition described in *T. gurneyi* (Hendrickx and Mateus 2014), in which it was considered that these ridges end at the same level posteriorly. The analysis of ML 1100 allows identifying some distortion in this area, which may have led to misinterpretation of these characters once the morphology of these ridges in SHN.400 is similar to that of *T. tanneri* (see Fig. 14l, m). In both SHN.400 and ML 1100 the dorsal and ventral grooves of the anteromedial process are narrowest than those of *T. tanneri* (BYU-VP 9122).

SHN.400 has a well-developed concavity filled with sediments within the anteroventral corner of the antorbital fossa immediately anterior to the maxillary fossa. A similar concavity is reported in ML 1100 (Hendrickx and Mateus 2014) and is also present in BYU-VP 9122 (E.M. pers. obs. 2010). The position and morphology of this concavity is compatible with the promaxillary fenestra described in most theropods (Witmer 1997). Despite having been traditionally considered absent a promaxillary fenestra in *Torvosaurus* and in most other megalosauroids, some analyses reported such opening extending into the anterior ramus of the maxilla as a canal in these taxa (Witmer 1997; Brusatte and Sereno 2008; Carrano et al. 2012). A well-developed promaxillary foramen in the anterior end of the antorbital fossa piercing the base of the ascending process is also described in *Wiehenvenator* (Rauhut et al. 2016), suggesting that this feature is more widely distributed among megalosauroids.

Based on the analysis of the new and published specimens, the set of maxillae identified as belonging to *Torvosaurus* (including the *T. gurneyi* holotype) currently known from the Upper Jurassic of the Lusitanian Basin have some differences with respect to the North American forms (Britt 1991). These differences are mainly related with the morphology of the maxillary medial wall and interdental plates. However, other previously mentioned differences such as the number of maxillary teeth are uncertain and cannot be confirmed based on the available elements.

5 Conclusion

Osteological evidences identified as belonging to the basal tetanuran clade Megalosauroidea are relatively abundant in Upper Jurassic sedimentary levels of the Lusitanian Basin. Some of the fossils herein described have a combination of characters that allows assigning them to the genus *Torvosaurus*, identified in this record based on few isolated specimens. The new specimens herein described suggest that megalosauroid theropods are especially well-represented in the Consolação Sub-basin, but some specimens are also known from the Alcobaça-Bombarral Sub-basin. The megalosauroid specimens currently known in the Lusitanian Basin were collected in sediments interpreted as belonging to the Praia da Amoreira-Porto Novo, Sobral and Alcobaça formations, ranging from the upper Kimmeridgian to the lowermost Tithonian.

The described postcranial elements are incomplete and generally poorly preserved but, as a whole, they represent the most abundant collection assignable to megalosauroid theropods currently known in the Portuguese Upper Jurassic. These specimens show a combination of characters shared with other megalosauroid theropods, but most of them are too incomplete to allow a more accurate phylogenetic interpretation. However, it was identified some differences between these Portuguese specimens and the remains of *Torvosaurus* known in the Morrison Formation, especially in the elements of the axial skeleton. It is not possible to verify, at the moment, if these differences may be features of the Portuguese species *Torvosaurus gurneyi* or if they represents another megalosauroid taxon not yet identified in this record.

Some of the described elements, such as a fibula (SHN.388/13), have some similarities to an isolated fibula attributed to an indeterminate megalosauroid from the Tendaguru Formation, such as the morphology of the strongly expanded and robust proximal end. However, due the fragmentary nature of both specimens it is not possible, for the moment, a more comprehensive interpretation of their possible relationships.

A set of unpublished cranial material assigned to *Torvosaurus* was also described, including a specimen

interpreted as belonging to the same individual as the holotype of *Torvosaurus gurneyi*. The analysis of these specimens allows a better understand of the cranial morphology of this species. However, it is not possible to test some of the putative differences previously identified between the Portuguese and North American *Torvosaurus* species. In fact, a supposedly lower number of maxillary teeth in the former, which was proposed as an autapomorphy of the Portuguese form, may be an artifact of preservation once it is not possible to know at the moment the exact number of teeth in the complete maxilla.

Acknowledgements This work was supported by SFRH/BD/84746/2012 PhD scholarship, financed by the "Fundação para a Ciência e Tecnologia" (Portugal). Individual grants to E.M. visits for review collections were financed by the Jurassic Foundation, Fundação Luso-Americana para o Desenvolvimento [Grant Number L07-V-22/2010] and Synthesys [grant number GB-TAF-2160 and FR-TAF-4911]. The study was also supported by a protocol between CMTV and SHN. We thank J. Barrinha for photographs of some elements, J. J. Santos and C. Anunciação for field assistance, M. Cachão and N. Pimentel for comments to the paper, and for allow accessing specimens to B. C. Silva (SHN, Portugal), R. Castanhinha and C. Tomás (ML, Portugal), V. Santos (MUHNAC, Portugal), E. Espilez and R. Royo-Torres (Fundación Conjunto Paleontológico de Teruel-Dinópolis, Spain), E. D. Berenguer and J. I. Canudo (Museo de Ciencias Naturales, Universidad de Zaragoza, Spain), R. Allain (MNHN, France), L. Chiappe (NHMLAC, USA), L. Ivy and K. Carpenter (DMNH, USA), T. Schossleitner (HNM, Germany), R. Scheetz and B. Britt (BYU, USA), M. Getty, M. Loewen, and R. Irmis (NHMU, USA), D. Chure (DINO, USA), S. Chapman (NHMUK, UK), and P. Jeffery (OUMNH, UK). Comments made by X. P. Suberbiola, an anonymous reviewer and the editor helped improve an early version of this paper.

References

Allain, R. (2001). Redescription of *Streptospondylus altdorfensis*, Cuvier's theropod dinosaur, from the Jurassic of Normandy. *Geodiversitas, 23*(3), 349–367.

Allain, R. (2002). Discovery of megalosaur (Dinosauria, Theropoda) in the middle Bathonian of Normandy (France) and its implications for the phylogeny of basal Tetanurae. *Journal of Vertebrate Paleontology, 22*(3), 548–563. doi: 10.1671/0272-4634(2002)022[0548:DOMDTI]2.0.CO;2.

Allain, R. (2005). The postcranial anatomy of the megalosaur *Dubreuillosaurus valesdunensis* (Dinosauria Theropoda) from the Middle Jurassic of Normandy, France. *Journal of Vertebrate Paleontology, 25*(4), 850–858. doi: 10.1671/0272-4634(2005)025[0850:TPAOTM]2.0.CO;2.

Allain, R., & Chure, D. J. (2002). *Poekilopleuron bucklandii*, the theropod dinosaur from the Middle Jurassic of Normandy. *Palaeontology, 45*(6), 1107–1121. doi:10.1111/1475-4983.00277.

Allain, R., Xaisanavong, T., Richin, P., & Khentavong, B. (2012). The first definitive Asian spinosaurid (Dinosauria: Theropoda) from the early Cretaceous of Laos. *Naturwissenschaften, 99*(5), 369–377. doi:10.1007/s00114-012-0911-7.

Alonso, A., & Canudo, J. J. (2016). On the spinosaurid theropod teeth from the early Barremian (Early Cretaceous) Blesa Formation (Spain). *Historical Biology, 28*(6), 823–834. doi:10.1080/08912963.2015.1036751.

Alves, T. M., Gawthorpe, R. L., Hunt, D. W., & Monteiro, J. H. (2002). Jurassic tectono-sedimentary evolution of the northern Lusitanian Basin (offshore Portugal). *Marine and Petroleum Geology, 19,* 727–754. doi:10.1016/S0264-8172(02)00036-3.

Azerêdo, A. C., Cabral, C. M., Martins, J. M., Loureiro, I. M., & Inês, N. (2010). Estudo estratigráfico dum novo afloramento da Formação de Cabaços (Oxfordiano) na região da Serra do Bouro (Caldas da Rainha. *Comunicações Geológicas, 97,* 5–22.

Bakker, R. T., Siegwarth, J. D., Kralis, D., & Filla, J. (1992). *Edmarka rex*: A new, gigantic theropod dinosaur from the middle Morrison Formation, Late Jurassic of the Como Bluff outcrop region. *Hunteria, 2,* 1–24.

Barrett, P. M., Benson, R. B. J., Rich, T. H., & Vickers-Rich, P. (2011). First spinosaurid dinosaur from Australia and the cosmopolitanism of Cretaceous dinosaur faunas. *Biology Letters, 7,* 933–936. doi:10.1098/rsbl.2011.0466.

Benson, R. B. J. (2008). A redescription of '*Megalosaurus*' *hesperis* (Dinosauria, Theropoda) from the Inferior Oolite (Bajocian, Middle Jurassic) of Dorset, United Kingdom. *Zootaxa, 1931,* 57–67.

Benson, R. B. J. (2010a). A description of *Megalosaurus bucklandii* (Dinosauria: Theropoda) from the Bathonian of the UK and the relationships of Middle Jurassic theropods. *Zoological Journal of the Linnean Society, 158*(4), 882–935. doi:10.1111/j.1096-3642.2009.00569.x.

Benson, R. B. J. (2010b). The osteology of *Magnosaurus nethercombensis* (Dinosauria, Theropoda) from the Bajocian (Middle Jurassic) of the United Kingdom and a re-examination of the oldest records of tetanurans. *Journal of Systematic Palaeontology, 8*(1), 131–146. doi:10.1080/14772011003603515.

Bonaparte, J. F., Novas, F. E., & Coria, R. A. (1990). *Carnotaurus sastrei* Bonaparte, the horned, lightly built carnosaur from the Middle Cretaceous of Patagonia. *Contributions in Science, Natural History Museum of Los Angeles County, 416,* 1–41.

Britt, B. (1991). Theropods of Dry Mesa Quarry (Morrison Formation, Late Jurassic), Colorado, with emphasis on the osteology of *Torvosaurus tanneri*. In B. J. Kowallis & K. Seeley (Eds.), *Young University Geology Studies* (pp. 1–72). Beijing: China Ocean Press.

Brusatte, S. L., Benson, R. B. J., & Hutt, S. (2008). The osteology of *Neovenator salerii* (Dinosauria: Theropoda) from the Wealden Group (Barremian) of the Isle of Wight. *Monograph of the Palaeontographical Society, 162,* 1–75.

Brusatte, S. L., & Sereno, P. C. (2007). A new species of *Carcharodontosaurus* (Dinosauria: Theropoda) from the Cenomanian of Niger and a revision of the genus. *Journal of Vertebrate Paleontology, 27,* 902–916. doi: 10.1671/0272-4634(2007)27[902:ANSOCD]2.0.CO;2.

Brusatte, S. L., & Sereno, P. C. (2008). Phylogeny of Allosauroidea (Dinosauria: Theropoda): Comparative analysis and resolution. *Journal of Systematic Palaeontology, 6*(2), 155–182. doi:10.1017/S1477201907002404.

Buffetaut, E. (2007). The spinosaurid dinosaur *Baryonyx* (Saurischia, Theropoda) in the Early Cretaceous of Portugal. *Geological Magazine, 144*(6), 1021–1025.

Buffetaut, E. (2011). An early spinosaurid dinosaur from the Late Jurassic of Tendaguru (Tanzania) and the evolution of the spinosaurid dentition. *Oryctos, 10,* 1–8.

Buffetaut, E., & Enos, J. (1992). Un nouveau fragment crânien de dinosaure théropode du Jurassique des Vaches Noires (Normandie, France): remarques sur la diversité des théropodes jurassiques européens. *Comptes Rendus de l'Academie des Sciences Paris Série II, 314,* 217–222.

Buffetaut, E., & Ingavat, R. (1986). Unusual theropod dinosaur teeth from the Upper Jurassic of Phu Wiang, northeastern Thailand. *Revue de Paléobiollogie, 5,* 217–220.

Canale, J. I., Novas, F. E., Salgado, L., & Coria, R. A. (2015). Cranial ontogenetic variation in *Mapusaurus roseae* (Dinosauria: Theropoda) and the probable role of heterochrony in carcharodontosaurid evolution. *Paläontologische Zeitschrift, 89*(4), 983–993. doi:10.1007/s12542-014-0251-3.

Canudo, J. I., Gasulla, J. M., Gómez-Fernández, D., Ortega, F., Sanz, J. L., & Yagüe, P. (2008). Primera evidencia de dientes aislados atribuidos a Spinosauridae (Theropoda) en el Aptiano inferior (Cretácico Inferior) de Europa: Formación Arcillas de Morella (España). *Ameghiniana, Revista de la Asociación Paleontogica Argentina, 45*(4), 649–662.

Canudo, J. I., Ruiz-Omeñaca, J. I., Aurell, M., Barco, J. L., & Cuenca-Bescós, G. (2006). A megatheropod tooth from the late Tithonian-middle Berriasian (Jurassic-Cretaceous transition). *Neues Jahrbuch für Geologie und Paläontologie, 239,* 77–99.

Carrano, M. T., Benson, R. B. J., & Sampson, S. D. (2012). The phylogeny of Tetanurae (Dinosauria: Theropoda). *Journal of Systematic Palaeontology, 10,* 211–300.

Carrano, M. T., & Sampson, S. D. (2008). The phylogeny of Ceratosauria (Dinosauria: Theropoda). *Journal of Systematic Palaeontology, 6*(2), 183–236. doi:10.1017/S1477201907002246.

Carrano, M., Sampson, S. D., & Forster, C. A. (2002). The osteology of *Masiakasaurus knopfleri*, a small abelisauroid (Dinosauria: Theropoda) from the Late Cretaceous of Madagascar. *Journal of Vertebrate Paleontology, 22*(3), 510–534. doi: 10.1671/0272-4634(2002)022[0510:TOOMKA]2.0.CO;2.

Charig, A. J., & Milner, A. C. (1997). *Baryonyx walkeri*, a fish-eating dinosaur from the Wealden of Surrey. *Bulletin of the Natural History Museum of London, 53,* 11–70.

Chure, D. J., Madsen, J. H., & Britt, B. B. (1993). New data on theropod dinosaurs from the Late Jurassic Morrison FM. (MF). *Journal of Vertebrate Paleontology, 13*(3), 30A.

Cobos, A., Lockley, M. G., Gascó, F., Royo-Torres, R., & Alcalá, L. (2014). Megatheropods as apex predators in the typically Jurassic ecosystems of the Villar del Arzobispo Formation (Iberian Range, Spain). *Palaeogeography, Palaeoclimatology, Palaeoecology, 399,* 31–41.

Coria, R. A., & Currie, P. J. (2006). A new carcharodontosaurid (Dinosauria, Theropoda) from the Upper Cretaceous of Argentina. *Geodiversitas, 28,* 71–118.

Currie, P. J., & Zhao, X.-J. (1993). A new carnosaur (Dinosauria, Theropoda) from the Jurassic of Xinjiang, People's Republic of China. *Canadian Journal of Earth Sciences, 30*(10–11), 2037–2081.

Eddy, D. R., & Clarke, J. A. (2011). New information on the cranial anatomy of *Acrocanthosaurus atokensis* and its implications for the phylogeny of Allosauroidea (Dinosauria: Theropoda). *PLoS ONE*, *6,* e17932. doi:10.1371/journal.pone.0017932.

Fitzinger, L. J. (1843). *Systema reptilium* (p. 106). Wien: Braumüller et Seidel.

Gascó, F., Cobos, A., Royo-Torres, R., Alcalá, L., & Mampel, L. (2012). Theropod teeth diversity from Villar del Arzobispo Formation (Tithonian–Berriasian) at Riodeva (Teruel, Spain). *Palaeobiodiversity and Palaeoenvironments, 92*(2), 273–286.

Hammer, Ø., Harper, D. A. T., & Ryan, P. D. (2001). Past: Paleontological Statistics Software Package for education and data analysis. *Palaeontologia Electronica, 4*(1), 1–9.

Hanna, R. R. (2002). Multiple injury and infection in a sub-adult theropod dinosaur *Allosaurus fragilis* with comparisons to *Allosaurus* pathology in the Cleveland-Lloyd Dinosaur quarry collection. *Journal of Vertebrate Paleontology, 22*(1), 76–90. doi: 10.1671/0272-4634(2002)022[0076:MIAIIA]2.0.CO;2.

Hanson, M., & Makovicky, P. J. (2014). A new specimen of *Torvosaurus tanneri* originally collected by Elmer Riggs. *Historical Biology, 26*(6), 775–784. doi:10.1080/08912963.2013.853056.

Hendrickx, C., Mateus, O. (2012). Ontogenetical changes in the quadrate of basal tetanurans. In R. Royo-Torres, F. Gascó, L. Alcalá (Eds.), 10th Annual Meeting of the European Association of Vertebrate Palaeontologists. Teruel, *¡Fundamental!* (Vol. 20, pp. 1–290).

Hendrickx, C., & Mateus, O. (2014). *Torvosaurus gurneyi* n. sp., the largest terrestrial predator from Europe, and a proposed terminology of the maxilla anatomy in nonavian theropods. *PLoS ONE, 9*(3), e88905. doi:10.1371/journal.pone.0088905.

Hendrickx, C., Mateus, O., & Araújo, R. (2015a). A proposed terminology of theropod teeth (Dinosauria, Saurischia). *Journal of Vertebrate Paleontology, 35*(5), e982797. doi:10.1080/02724634.2015.982797.

Hendrickx, C., Mateus, O., & Araújo, R. (2015b). The dentition of megalosaurid theropods. *Acta Palaeontologica Polonica, 60*(3), 627–642. doi:10.4202/app.00056.2013.

Hill G. (1988). *The sedimentology and lithostratigraphy of the Upper Jurassic Lourinhã Formation, Lusitanian Basin Portugal*. (Ph.D. dissertation, Milton Keynes, The Open University). 337 pp.

Kullberg, J. C., Rocha, R. B., Soares, A. F., Rey, J., Terrinha, P., Callapez, P., et al. (2006). A bacia Lusitaniana: Estratigrafia, Paleogeografia E Tectónica. In R. Dias, A. Araújo, P. Terrinha, & J. C. Kullberg (Eds.), *Geologia de Portugal no contexto da Ibéria* (pp. 317–368). Évora: Universidade de Évora.

Li, F., Peng, G., Ye, Y., Jiang, S., & Huang, D. (2009). A new carnosaur from the Late Jurassic of Qianwei, Sichuan, China. *Acta Geologica Sinica, 83*(9), 1203–1213.

Madsen, J. H., Jr. (1976). A second new theropod dinosaur from the Late Jurassic of east central Utah. *Utah Geology, 3*(1), 51–60.

Madsen, J. H. Jr. (1976b [1993]). *Allosaurus fragilis*: A revised osteology. Utah Geological Survey Bulletin 109 (2nd edn.). Salt Lake City. *Utah Geological Survey*. 163 pp.

Madsen, J. H., Jr., & Welles, S. P. (2000). *Ceratosaurus (Dinosauria, Theropoda) a revised osteology* (pp. 1–80). Salt Lake: Utah Geological Survey. Miscellaneous Publication.

Malafaia, E., Ortega, F., Escaso, F., Silva, B. (2014). *New cranial remains assigned to Megalosauridae (Dinosauria: Theropoda) from the Late Jurassic of Lusitanian Basin (Portugal)*. Program and Abstracts Book 74th Annual Meeting of the Society of Vertebrate Paleontology p. 175.

Malafaia, E., Ortega, F., Silva, B., & Escaso, F. (2008). Fragmento de un maxilar de terópodo de Praia da Corva (Jurásico Superior. Torres Vedras, Portugal). *Palaeontologica Nova SEPAZ, 8,* 273–279.

Manuppella, G., Antunes, M. T., Pais, J., Ramalho, M., & Rey, J. (1996). *Geological Map of Portugal, scale 1/50.000. Sheet 30-A, Lourinhã* (p. 175). Lisboa: Publicações do Instituto Geológico e Mineiro.

Manuppella, G., Antunes, M. T., Pais, J., Ramalho, M. M., & Rey, J. (1999). *Noticia Explicativa da Carta Geológica 30-A, Lourinhã* (p. 83). Lisboa: Instituto Geológico e Mineiro.

Marsh, O. C. (1881). Classification of the Dinosauria. *American Journal of Science, 23,* 241–244.

Mateus, O. (1998). *Lourinhanosaurus antunesi*, A New Upper Jurassic Allosauroid (Dinosauria: Theropoda) from Lourinhã, Portugal. *Memórias da Academia de Ciências de Lisboa, 37,* 111–124.

Mateus, O., & Antunes, M. T. (2000). *Torvosaurus* sp. (Dinosauria: Theropoda) in the Late Jurassic of Portugal. *Abstracts Book I Congresso Ibérico de Paleontología-XVI Jornadas de la Sociedad Española de Paleontología., 15,* 115–117.

Mateus, O., Araújo, R., Natário, C., & Castanhinha, R. (2011). A new specimen of the theropod dinosaur *Baryonyx* from the early

Cretaceous of Portugal and taxonomic validity of *Suchosaurus*. *Zootaxa, 2827,* 54–68. doi:10.11646/%25x.

Mateus, O., Walen, A., Antunes. M.T. (2006). The large theropod fauna of the Lourinhã Formation (Portugal) and its similarity to the Morrison Formation, with a description of a new species of *Allosaurus*. In J. R. Foster, S. G. Lucas (Eds.), *Paleontology and Geology of the Upper Jurassic Morrison Formation* (Vol. 36, pp. 123–129). New Mexico Museum of Natural History and Science Bulletin.

Novas, F. E., Agnolín, F. L., Ezcurra, M. D., Porfiri, J., & Canale, J. I. (2013). Evolution of the carnivorous dinosaurs during the Cretaceous: The evidence from Patagonia. *Cretaceous Research, 45,* 174–215.

O'Connor, P. M. (2006). Postcranial pneumaticity: an evaluation of soft-tissue influences on the postcranial skeleton and the reconstruction of pulmonary anatomy in archosaurs. *Journal of Morphology, 267,* 1199–1226. doi:10.1002/jmor.10470.

Oliveira, J.T., Pereira, H., Ramalho, M., Antunes, M.T. (1992). Carta Geológica de Portugal, scale 1:500000. Serviços Geológicos de Portugal.

Ortega, F., Escaso, F., & Sanz, J. L. (2010). A bizarre, humped Carcharodontosauria (Theropoda) from the Lower Cretaceous of Spain. *Nature, 467*(7312), 203–206. doi:10.1038/nature09181.

Owen, R. (1842). Report on British fossil reptiles. Part II. *Reports of the British Association for the Advancement of Science, 1841,* 60–204.

Petersen, K., Isakson, J., & Madsen, J. H., Jr. (1972). Preliminary study of paleopathologies in the Cleveland-Lloyd dinosaur collection. *Proceedings of the Utah Academy of Sciences, 49,* 44–47. doi:10.7717/peerj.940.

Rasmussen, E. S., Lomholt, S., Andersen, C., & Vejbaek, O. V. (1998). Aspects of the structural evolution of the Lusitanian Basin in Portugal and the shelf and slope area offshore Portugal. *Tectonophysics, 300,* 199–225. doi:10.1016/S0040-1951(98)00241-8.

Rauhut, O. W. M. (2003). The interrelationships and evolution of basal theropod dinosaurs. *Special Papers in Palaeontology, 69,* 1–213.

Rauhut, O. W. M. (2005). Osteology and relationships of a new theropod dinosaur from the Middle Jurassic of Patagonia. *Palaeontology, 48*(1), 87–110.

Rauhut, O. W. M. (2011). Theropod dinosaurs from the Late Jurassic of Tendaguru (Tanzania). *Special Papers in Palaeontology, 86,* 195–239.

Rauhut, O. W. M., & Fechner, R. (2005). Early development of the facial region in a non-avian theropod dinosaur. *Proceedings of the Royal Society B, 272,* 1179–1183. doi:10.1098/rspb.2005.3071.

Rauhut, O. W. M., Foth, C., Tischlingerd, H., & Norell, M. A. (2012). Exceptionally preserved juvenile megalosauroid theropod dinosaur with filamentous integument from the Late Jurassic of Germany. *PNAS, 109*(29), 11746–11751. doi:10.1073/pnas.1203238109.

Rauhut, O. W. M., Hübner, T. R., & Lanser, K.-P. (2016). A new megalosaurid theropod dinosaur from the late Middle Jurassic (Callovian) of north-western Germany: Implications for theropod evolution and faunal turnover in the Jurassic. *Palaeontologia Electronica, 19,* 1–65.

Rauhut, O. W. M., & López-Arbarello, A. (2009). Considerations on the age of the Tiouaren Formation (Iullemmeden Basin, Niger, Africa): Implications for Gondwanan Mesozoic terrestrial vertebrate faunas. *Palaeogeography, Palaeoclimatology, Palaeoecology, 271,* 259–267.

Rowe, T., & Gauthier, J. (1990). Ceratosauria. In D. Weishample, P. Dodson, & H. Osmolska (Eds.), *The Dinosauria* (pp. 151–168). Berkeley: University of California Press.

Royo-Torres, R., Cobos, A., & Alcalá, L. (2009). Diente de un gran dinosaurio terópodo (Allosauroidea) de la Formación Villar del Arzobispo (Titónico-Berriasiense) de Riodeva (España). *Estudios Geológicos, 65*(1), 91–99.

Sadleir, R., Barrett, P. M., & Powell, H. P. (2008). The anatomy and systematics of *Eustreptospondylus oxoniensis*, a theropod dinosaur from the Middle Jurassic of Oxfordshire, England. *Monograph of the Palaeontological Society, 160*(627), 1–82.

Sampson, S. D., & Witmer, L. M. (2007). Craniofacial anatomy of *Majungasaurus crenatissimus* (Theropoda: Abelisauridae) from the Late Cretaceous of Madagascar. *Journal of Vertebrate Paleontology, 27,* 32–104. doi: 10.1671/0272-4634(2007)27[32:CAOMCT]2.0.CO;2.

Schneider, S., Fürsich, F. T., & Werner, W. (2009). Sr-isotope of the Upper Jurassic of central Portugal (Lusitanian Basin) based on oyster shells. *International Journal of Earth Sciences, Geologische Rundschau, 98,* 1949–1970.

Sereno, P. C., & Brusatte, S. L. (2008). Basal abelisaurid and carcharodontosaurid theropods from the Lower Cretaceous Elrhaz Formation of Niger. *Acta Palaeontologica Polonica, 53*(1), 15–46. doi:10.4202/app.2008.0102.

Sereno, P. C., Wilson, J. A., Larsson, H. C. E., Dutheil, D. B., & Sues, H.-D. (1994). Early Cretaceous dinosaurs from the Sahara. *Science, 266,* 267–270.

Serrano-Martínez, A., Ortega, F., Sciscio, L., Tent-Manclús, J. E., Bandera, I. F., & Knoll, F. (2015). New theropod remains from the Tiourarén Formation (?Middle Jurassic, Niger) and their bearing on the dental evolution in basal tetanurans. *Proceedings of the Geologists' Association, 126*(1), 107–118. doi:10.1016/j.pgeola.2014.10.005.

Smith, J. B. (2005). Heterodonty in *Tyrannosaurus rex*: implications for the taxonomic and systematic utility of theropod dentitions. *Journal of Vertebrate Paleontology, 25*(4), 865–887. doi: 10.1671/0272-4634(2005)025[0865:HITRIF]2.0.CO;2.

Smith, J. B., & Dodson, P. (2003). A Proposal for a standard terminology of anatomical notation and orientation in fossil vertebrate dentitions. *Journal of Vertebrate Paleontology, 23*(1), 1–12. doi: 10.1671/0272-4634(2003)23[1:APFAST]2.0.CO;2.

Smith, J. B., Lamanna, M. C., Mayr, H., & Lacovara, K. J. (2006). New information regarding the holotype of *Spinosaurus aegyptiacus* Stromer, 1915. *Journal of Paleontology, 80*(2), 400–406. doi: 10.1666/0022-3360(2006)080[0400:NIRTHO]2.0.CO;2.

Smith, J. B., Vann, D. R., & Dodson, P. (2005). Dental morphology and variation in theropod dinosaurs: implications for the taxonomic identification of isolated teeth. *The Anatomical Record Part A: Discoveries in Molecular, Cellular, and Evolutionary Biology, 285*(2), 699–736. doi:10.1002/ar.a.20206.

Sues, H.-D., Frey, E., Martill, D. M., & Scott, D. M. (2002). *Irritator challengeri*, a spinosaurid (Dinosauria: Theropoda) from the Lower Cretaceous of Brazil. *Journal of Vertebrate Paleontology, 22*(3), 535–547. doi: 10.1671/0272-4634(2002)022[0535:ICASDT]2.0.CO;2.

Suñer, M., de Santisteban, C., & Galobart, A. (2005). Nuevos restos de Theropoda del Jurásico Superior-Cretácico Inferior de la Comarca de los Serranos (Valencia). *Revista Española de Paleontología, N.E. X, 10,* 93–99.

Taquet, P., & Welles, S. P. (1977). Redescription du crâne de dinosaur théropode de Dives (Normandie). *Annales de Paléontologie (Vertébrés), 63*(2), 191–206.

Taylor, A. M., Gowland, S., Leary, S., Keogh, K. J., & Martinius, A. W. (2014). Stratigraphical correlation of the Late Jurassic Lourinhã Formation in the Consolação Sub-basin (Lusitanian Basin), Portugal. *Geological Journal, 49*(2), 143–162. doi:10.1002/gj.2505.

Tykoski, R.S. (2005). Anatomy, ontogeny, and phylogeny of coelophysoid theropods. (Ph.D. Dissertation, The University of Texas, Austin), 553 pp.

Vullo, R., Abit, D., Ballévre, M., Billon-Bruyat, J.-P., Bourgeais, R., Buffetaut, É., et al. (2014). Palaeontology of the Purbeck-type (Tithonian, Late Jurassic) bonebeds of Chassiron (Oléron Island, western France). *Comptes Rendus Palevol, 13,* 421–441. doi:10.1016/j.crpv.2014.03.003.

Wilson, J. A. (1999). A nomenclature for vertebral laminae in sauropods and other saurischian dinosaurs. *Journal of Vertebrate Paleontology, 19*(4), 639–653. doi:10.1080/02724634.1999.10011178.

Wilson, J. A., D'Emic, M. D., Ikejiri, T., Moacdieh, E. M., & Whitlock, J. A. (2011). A nomenclature for vertebral fossae in sauropods and other saurischian dinosaurs. *PLos ONE, 6*(2), e17114. doi:10.1371/journal.pone.0017114.

Witmer, L. M. (1997). The evolution of the antorbital cavity of archosaurs: A study in soft-tissue reconstruction in the fossil record with an analysis of the function of pneumaticity. *Journal of Vertebrate Paleontology, 17*(1), 1–76.

Zhao, X.-J., Benson, R. B. J., Brusatte, S. L., & Currie, P. J. (2010). The postcranial skeleton of *Monolophosaurus jiangi* (Dinosauria: Theropoda) from the Middle Jurassic of Xinjiang, China, and a review of Middle Jurassic Chinese theropods. *Geological Magazine, 147*(1), 13–27. doi:10.1017/S0016756809990240.

SUPPLEMENTARY MATERIAL

	Centrum, length	Centrum, depth	Centrum transverse width	Centrum, ratio length : depth	Anterior articular facet, width	Anterior articular facet, height	Posterior articular facet, width	Posterior articular facet, height
Dorsal vertebrae								
SHN.388/1	101,84	47,84	81,51	2,13	104,5	78,92	117,27	81,08
SHN.388/2	127,54	48,91	90,32	2,61	118,11	110,7	128,87	81,64
SHN.388/3	116,38	50,62	69,64	2,30	89,59	86,4	119,17	86,96*
SHN.469	141,2	97,82	88,6	1,44	126,66	151,47	?	?
	141,53	89,51	90,85	1,58	?	?	130,87	150,91
Caudal vertebrae								
SHN.388/5	111,5	65,74	90,66	1,70	137,57	117,31	139,09	103,53
SHN.388/6	109,41	61,89	60,36	1,77	98,42	87,92	96,09	91,1
SHN.388/7	96,96	73,87	80,79	1,31	109,55*	99,32*	107,62	96,75
SHN.388/8	127,21	109,86	51,64	1,16	85,78*	97,67*	92,7	93,59
SHN.388/9	118	45,72	64,39	2,58	90,01	60,05	87,81	69,25*
SHN.388/10	108,77	39,14	57,37	2,78	87,25	86,68*	?	?
SHN.388/11	113,78	71,52	51,45	1,59	74,36	69,69	77,28	70,33
SHN.388/12	100,21	59,19	57,35	1,69	?	?	73,02	64,49

Fibula	Diaphysis, length	Diaphysis, maximum diameter	Diaphysis, minimum diameter	Diaphysis, ratio minimum diameter : length	Proximal end, maximum length	Proximal end, maximum transverse width	Distal end, maximum length	Distal end, maximum transverse width
SHN.388/13	630	81,22	47,25	0,075	153,41	77,6	81,93	52,08
Tibia								
SHN.468	?	146,74*	116*	?	?	?	100,2	283

Table 1.- Measurements of the postcranial specimens of megalosauroids described. All measurements are in millimeters; * estimated measurement
Tabla 1.- Medidas de los ejemplares postcraneales de megalosauroideos descritos. Todas las medidas están en milímetros; * medida estimada

	SHN.467	ALTSHN.116	SHN.400	ML 1100	BYU-VP 9122
Lenght	?	?	465 [1]	612	520 [1]
Lenght of the antorbital body	?	?	306	310	347
Depth of the anterior margin along the contact with the premaxill	105*	120*	125	122	111
Depth of the anterior end of the anteromedial process	27*	31	24	?	20*
Depth of the interdental plates at the level of the third alveolus	86,45*	?	90,44	106	67
Mesiodistal lenght of the first alveolus	38,31	?	41,35	?	47
Labiolingual width of the first alveolus	22,28*	?	25,95	?	?
Mesiodistal lenght of posterior alveoli	30,33	?	32,38	?	40
Labiolingual width of posterior alveoli	14,7	?	17,87	?	?
Depth of alveolar process (= jugal ramus) at the anterior margin of the antorbital fenestra	?	?	155,59	170	149
Basoapical height of the second maxillary tooth	?	?	140	138	?
Basoapical height of the third maxillary tooth	?	104,45	77,69	165	?
Mesiodistal lenght of the second maxillary tooth	?	?	42,16	?	?
Mesiodistal lenght of the third maxillary tooth	?	?	40,59	?	?
Labiolingual width of the second maxillary tooth	?	?	18,74	?	?
Labiolingual width of the third maxillary tooth	?	13,23*	15,67	?	?

Table 2.- Measurements of several maxillae identified to *Torvosaurus* from the Upper Jurassic of the Lusitanian Basin and Morrison Formation. All measurements are in millimeters. [1] incomplete element, the measurement corresponds to the preserved fragment; * estimated measurement.
Tabla 2.- Medidas de diferentes maxilas asignadas a Torvosaurus provenientes del Jurásico Superior de la cuenca lusitánica y de la Formación Morrison. Todas las medidas están en milímetros. [1] elemento incompleto, la medida corresponde al fragmento preservado; * medida estimada.

Specimen	CBL	CBW	CH	AL	CBR	CHR	CDA	CMA	MC	DC	DSDI
SHN.067	47,99	22,89	141,52	145,07	0,48	2,95	84,70209	76,20365	5	5	1,00
SHN.215	25,35	12,62	62,29	63,64	0,50	2,46	81,57715	75,41259	7,5	7,5	1,00
SHN.221	30,65	17,55	79,79	84,91	0,57	2,60	88,94144	69,97098	7	6	1,17
SHN.257	22,68	15,15	57,21	60,15	0,67	2,52	86,44153	71,63977	8	8	1,00
SHN.266	26,31	12,02	57,2	66,55	0,46	2,17	97,62811	58,12388	8	10	0,80
SHN.268	36,27	16,93	91,72	98,86	0,47	2,53	90,36136	68,08756	5	6	0,83
SHN.294	23,23	13,75	52,25	56,71	0,59	2,25	88,83277	67,0917	8	8	1,00
SHN.303	34,04	18,48	?	?	0,54	?	?	?	7	6	1,17
SHN.304	25,11	14,17	65,5	65,99	0,56	2,61	80,16483	77,89536	?	8	?
SHN.319	33,69	20,4	93,87	97,05	0,61	2,79	85,36966	74,54901	8	8,5	0,94
SHN.320	39,71	21,6	109,51	116,79	0,54	2,76	90,43599	69,65811	7	7	1,00
SHN.359a	16,26	7,87	38,76	40,25	0,48	2,38	83,56663	73,02662	10	10	1,00
SHN.362	26,39	14,58	52,77	57,95	0,55	2,00	87,69709	65,46746	6,5	7	0,93
SHN.364	21,54	15,58	54,46	54,81	0,72	2,53	79,61276	77,71973	?	8	?
SHN.374	47,09	16,75	104,99	117,91	0,36	2,23	93,41973	62,67595	6	7	0,86
SHN.381	31,28	17,44	?	?	0,56	?	?	?	8,5	8	1,06
SHN.401	48,35	20,64	145,55	152,84	0,43	3,01	89,37019	72,22067	7	6	1,17
SHN.440	25,75	14,04	70,29	78,49	0,55	2,73	97,91932	62,23502	0	7	0,00
SHN.441	42,44	23,49	123,67	129,76	0,55	2,91	88,65897	72,32231	7,5	6,5	1,15
SHN.442	29,1	16,41	84,13	86,24	0,56	2,89	84,42817	76,09358	?	7	?
SHN.470	48,38	19,94	145,54	152,44	0,41	3,01	88,89457	72,65777	7	7,5	0,93

Table 3.- Measurements used in the morphometric analysis of the isolated teeth. All measurements are in millimeters.
Tabla 3.- Medidas usadas en el análisis morfométrico de los dientes aislados. Todas las medidas están en milímetros.

CHAPTER 6: ALLOSAUROIDEA

6.1. INTRODUCTION

Allosauroidea is a clade of large-bodied theropod dinosaurs that ranged from the early Late Jurassic to the Late Cretaceous (Brusatte and Sereno 2008). This clade includes the Late Jurassic theropod *Allosaurus*, which is among the best-studied dinosaur genera, represented by hundreds of specimens from the North American Morrison Formation (e.g. Madsen 1976; Smith 1998; Chure 2000; Carpenter 2010; Foth et al. 2015). Although Allosauroidea is confidently placed at the base of Tetanurae, the ingroup relationships of this clade remain mostly unresolved. Several enigmatic theropod taxa have been tentatively recovered as belonging to Allosauroidea, including *Monolophosaurus* (Sereno et al. 1996; Holtz 2000; Currie and Carpenter 2000; Novas et al. 2005) and *Cryolophosaurus* (Sereno et al. 1996). However, more recent phylogenetic analyses placed these taxa as basal non-allosauroid tetanurans (Smith et al. 2007; Brusatte and Sereno 2008; Brusatte et al. 2010). *Acrocanthosaurus* and *Neovenator* are alternatively recovered as either sister taxa to *Allosaurus* (Currie and Carpenter 2000; Holtz 2000; Allain 2002; Novas et al. 2005; Coria and Currie 2006) or as more closely related to *Carcharodontosaurus* (Sereno et al. 1996; Rauhut 2003). On the other hand, *Sinraptor* is positioned either as the basal-most allosauroid (Sereno et al. 1996; Harris 1998; Holtz 2000; Azuma and Currie 2000; Rauhut 2003; Holtz et al. 2004; Coria and Currie 2006) or as the sister taxon to carcharodontosaurids (Allain 2002). More recent phylogenetic analyses place *Sinraptor* as a basal allosauroid and *Acrocanthosaurus* within Carcharodontosauridae (Brusatte and Sereno 2008).

The interrelationships within Carcharodontosauridae are less confident, as several taxa are based on fragmentary material. Some authors recovered *Neovenator* and *Allosaurus* as sister taxa (Holtz 2000) whereas others suggest a position of *Neovenator* as closer to *Carcharodontosaurus* than to *Allosaurus* (Brusatte and Sereno 2008). A phylogenetic analysis performed by Benson et al. (2010) proposed that some of these enigmatic carcharodontosaurian taxa form a monophyletic clade called Neovenatoridae, which includes *Neovenator*, *Chilantaisaurus*, and a derived group, Megaraptora, comprising the South American species *Aerosteon riocoloradensis*, *Megaraptor namunhaiquii*, and *Orkoraptor burkei*, together with the Australian *Australovenator wintonensis* and the Japanese *Fukuiraptor kitadaniensis*. Currently, two hypotheses relative to the phylogenetic position of the megaraptorids among theropods have been discussed; one suggests that they are derived allosauroid neovenatorids (Benson et al. 2010; Carrano et al. 2012; Zanno and Makovicky 2013) and the other interprets them as tyrannosauroid coelurosaurs (Novas et al. 2013; Porfiri et al. 2014).

Allosauroids have been extensively used in discussions of Mesozoic palaeobiogeography because they comprise a long-lived and diverse group that evolved during the fragmentation of Pangaea (Harris 1998; Pérez-Moreno et al. 1999; Sereno 1999a, b; Upchurch et al. 2002). These studies identified a clade of allosauroids from the southern hemisphere, the derived carcharodontosaurids, including *Carcharodontosaurus* and *Giganotosaurus*, which may have radiated after the isolation of Gondwana during the Cretaceous (Sereno et al. 1996; Harris 1998; Pérez-Moreno et al. 1999; Sereno 1999b). Generally, these analyses match the most common hypothesis of the breakup sequence of Pangaea (Rabinowitz and LaBrecque 1979; Smith et al. 1994; Scotese 2004), with Asia becoming isolated first, followed successively by North America and then by South America and Africa. The position of Europe is ambiguous because it was constituted by a series of islands, which were intermittently exposed during much of Jurassic and Cretaceous (Smith et al. 1994). Also many taxa suggest the existence of at least temporary connection between Africa and Europe during the Cretaceous (Gheerbrant and Rage 2006; Canudo et al. 2009).

The record of allosauroid tetanurans from the Upper Jurassic of the Lusitanian Basin is abundant and relatively diverse. Currently, this record includes *Lourinhanosaurus* (Mateus 1998), *Allosaurus* (Pérez-Moreno et al. 1999; Mateus et al. 2006; Malafaia et al. 2010), and a set of remains that show a combination

of features suggesting affinities with the Carcharodontosauria clade. *Lourinhanosaurus antunesi* is an unstable taxon represented by a partial postcranial skeleton collected in Peralta (Lourinhã). It was originally described as an allosauroid (Mateus 1998) and latter interpreted as a more basal tetanuran closely related with eustreptospondyline megalosaurids (Allain 2005; Mateus et al. 2006). Subsequently, it was recovered as a member of the basal allosauroid clade Metriacanthosauridae by Benson (2010) and as a possible coelurosaur by Carrano et al. (2012). A recent phylogenetic analysis, which included some theropod specimens from the Upper Jurassic of the Lusitanian Basin supports the interpretation of *Lourinhanosaurus* as a member of Allosauroidea, but placed this taxon at the base of a more derived group comprising *Allosaurus* + Carcharodontosauria (Malafaia et al. 2016).

Allosaurus is the most abundant and well-represented tetanuran taxon currently known in the Upper Jurassic of the Lusitanian Basin. This taxon is represented by a set of cranial and postcranial remains found in three fossil sites, Praia de Vale Frades (Lourinhã), Andrés (Pombal), and Guimarota (Leiria), beside some isolated teeth collected in different sites mainly on the littoral area of the Central Sector of the Lusitanian Basin (Pérez-Moreno et al. 1999; Rauhut and Fechner 2005; Mateus et al. 2006; Malafaia et al. 2010; Malafaia et al. 2017). A specimen collected in the Andrés fossil site was assigned to the species *Allosaurus fragilis* described in correlative sedimentary levels of the Morrison Formation (USA) and was proposed as the first accurate evidence of *Allosaurus* outside North America. This discovery also represented the first dinosaur species shared by two continents and thus triggered an intense discussion concerning the paleobiogeographic relationships of Late Jurassic dinosaur faunas from the Portuguese Lusitanian Basin and the North American Morrison Formation. The presence of the species *A. fragilis* in both continents was interpreted as an evidence of faunal interchanges across the North Atlantic Ocean during the Late Jurassic. Later, a partial skull collected in Praia de Vale Frades was interpreted as belonging to a new *Allosaurus* species, *Allosaurus europaeus* (Mateus et al. 2006). This interpretation suggests that despite the theropod faunas from Portugal and North America is closely related, the evolutionary history during the Late Jurassic was marked by incipient vicariant processes probably related with the opening of the northern sector of the Atlantic Ocean. In 2005, the resumed of the field works in the Andrés fossil site allowed the discovery of several osteological remains attributed to *Allosaurus*, including abundant cranial and postcranial elements of at least three individuals. Among these specimens is the most complete cranial evidence of a theropod dinosaur known in the Portuguese Upper Jurassic. The study of the unpublished material of *Allosaurus* collected in Andrés allows verifying if the original identification of *A. fragilis* in this fossil site is supported or if instead they may be assigned to *A. europaeus*.

The Andrés fossil site is one of the most significant Portuguese fossil sites for the study of Late Jurassic continental faunas from the Lusitanian Basin due to the great abundance and diversity of fossils collected. The vertebrate fauna identified in Andrés includes semionotiform fishes, lepidosaurs closely related with *Opisthias*, neosuchian crocodylomophs, indeterminate pterosaurs and several groups of dinosaurs belonging to ornithopods, sauropods and theropods (Ortega et al. 2006; Malafaia et al. 2010; Mocho et al. 2017).

Two recently described specimens represented by a set of postcranial remains collected in Cambelas, SHN.036, and Valmitão, SHN.016, show an unusual combination of features indicating a closely relationship with *Allosaurus* and *Lourinhanosaurus*. However, the detailed description of these specimens allows identify also some differences relative to both taxa. The objective of this analysis is to test if these specimens may be assigned to an allosauroid taxon previously described in the Portuguese record (e.g. *Lourinhanosaurus* or *Allosaurus*) or if instead they represent a new taxon not yet identified. This analysis was based on review of the allosauroid specimens known in the Lusitanian Basin, including the proposal of a new phylogenetic hypothesis for *Lourinhanosaurus antunesi* and the development of an integrated phylogenetic analysis of the allosauroid record from the peri-North Atlantic context to which the new specimens, SHN.019 and SHN.036, were included. This analysis allowed identifying a unique combination of features for these specimens suggesting that they probably belong to a new carcharodontosaurian theropod taxon representing the first evidence for the presence of carcharodontosaurian theropods in the Lusitanian Basin and the oldest record of this clade in Laurasia.

REFERENCES

Allain R. 2002. Discovery of megalosaur (Dinosauria, Theropoda) in the Middle Bathonian of Normandy (France) and its implications for the phylogeny of basal Tetanurae. Journal of Vertebrate Paleontology 22:548–563.

Allain R. 2005. The postcranial anatomy of the megalosaur *Dubreuillosaurus valesdunensis* (Dinosauria: Theropoda) from the Middle Jurassic of Normandy, France. Journal of Vertebrate Paleontology 25:850–858.

Azuma Y, Currie PJ. 2000. A new carnosaur (Dinosauria: Theropoda) from the Lower Cretaceous of Japan. Canadian Journal of Earth Sciences 37:1735–1753.

Benson RBJ. 2010. A description of *Megalosaurus bucklandii* (Dinosauria: Theropoda) from the Bathonian of the UK and the relationships of Middle Jurassic theropods. Zoological Journal of the Linnean Society 158:882–935.

Benson RBJ, Carrano MT, Brusatte SL. 2010. A new clade of archaic largebodied predatory dinosaurs (Theropoda: Allosauroidea) that survived to the latest Mesozoic. Naturwissenschaften 97:71–78.

Brusatte SL, Sereno PC. 2008. Phylogeny of Allosauroidea (Dinosauria: Theropoda): comparative analysis and resolution. Journal of Systematic Palaeontology 6(2):155–182.

Brusatte SL, Benson RBJ, Currie PJ, Xijin Z. 2010. The skull of *Monolophosaurus jiangi* (Dinosauria: Theropoda) and its implications for early theropod phylogeny and evolution. Zoological Journal of the Linnean Society 158:573–607.

Canudo JI, Barco JL, Pereda-Suberbiola X, Ruiz-Omeñaca JI, Salgado L, Fernández-Baldor FT, Gasulla JM. 2009. What Iberian dinosaurs reveal about the bridge said to exist between Gondwana and Laurasia in the Early Cretaceous. Bulletin de la Société Géologique de France 180:5-11.

Carpenter K. 2010. Variation in a population of Theropoda (Dinosauria): *Allosaurus* from the Cleveland-Lloyd Quarry (Upper Jurassic), Utah, USA. Paleontological Research 14(4):250–259.

Carrano MT, Benson RBJ, Sampson SD. 2012. The phylogeny of Tetanurae (Dinosauria: Theropoda). Journal of Systematic Palaeontology 10:211–300.

Coria RA, Currie PJ. 2006. A new carcharodontosaurid (Dinosauria, Theropoda) from the Upper Cretaceous of Argentina. Geodiversitas 28:71–118.

Currie PJ, Carpenter K. 2000. A new specimen of *Acrocanthosaurus atokensis* (Theropoda, Dinosauria) from the Lower Cretaceous Antlers Formation (Lower Cretaceous, Aptian) of Oklahoma, USA. Geodiversitas 22:207–246.

Foth C., Evers S, Pabst B, Mateus O, Flisch A, Patthey M, Rauhut OWM. 2015. New insights into the lifestyle of *Allosaurus* (Dinosauria: Theropoda) based on another specimen with multiple pathologies. PeerJ PrePrints 3:e824v1. doi:10.7287/peerj.preprints.824v1.

Gheerbrant E, Rage J-C. 2006. Paleobiogeography of Africa: how distinct from Gondwana and Laurasia? Palaeogeography, Palaeoclimatology, Palaeoecology 241:224–246.

Harris JD. 1998. A reanalysis of *Acrocanthosaurus atokensis*, its phylogenetic status, and paleobiogeographic implications, based on a new specimen from Texas. New Mexico Museum of Natural History and Science Bulletin 13:1–75.

Holtz TR. 2000. A new phylogeny of the carnivorous dinosaurs. Gaia 15:5–61.

Holtz TR, Molnar RE, Currie PJ. 2004. Basal Tetanurae. In: Weishampel DB, Dodson P, Osmolska H. (Eds) The Dinosauria, 2nd edition. University of California Press, Berkeley, California. 71–110.

Malafaia E, Ortega F, Escaso F, Dantas P, Pimentel N, Gasulla JM, Ribeiro B, Barriga F, Sanz JL. 2010. Vertebrate fauna at the *Allosaurus* fossil-site of Andrés (Upper Jurassic), Pombal, Portugal. Journal of Iberian Geology 36(2):193–204.

Malafaia E, Mocho P, Escaso F, Ortega F. 2016. A juvenile allosauroid theropod (Dinosauria, Saurischia) from the Upper Jurassic of Portugal. Historical Biology: doi:10.1080/08912963.2016.1231183.

Malafaia E, Escaso F, Mocho P, Serrano-Martínez A, Torices A, Cachão M, Ortega F. 2017. Analysis of diversity, stratigraphic and geographical distribution of isolated theropod teeth from the Upper Jurassic of the Lusitanian Basin, Portugal. Journal of Iberian Geology 43:257–291.

Mateus O. 1998. *Lourinhanosaurus antunesi*, a new Upper Jurassic allosaurid (Dinosauria: Theropoda) from Lourinhã, Portugal. Memoirs of the Academy of Sciences, Lisbon 37:111–124.

Mateus O, Walen A, Antunes MT. 2006. The large theropod fauna of the Lourinhã Formation (Portugal) and its similarity to that of the Morrison Formation, with a description of a new species of *Allosaurus*. In: Foster JR, Lucas SG. (Eds) Paleontology and Geology of the Upper Jurassic Morrison Formation. New Mexico Museum of Natural History and Science, Bulletin 36:123–129.

Mocho P, Royo-Torres R, Malafaia E, Escaso F, Ortega F. 2017. Sauropod tooth morphotypes from the Upper Jurassic of the Lusitanian Basin (Portugal). Papers in Palaeontology 3(2):259–295.

Novas FE, de Valais S, Vickers-Rich P, Rich T. 2005. A large Cretaceous theropod from Patagonia, Argentina, and the evolution of carcharodontosaurids. Naturwissenschaften 92:226–230.

Novas FE, Agnolín FL, Ezcurra MD, Porfiri J, Canale JI. 2013. Evolution of the carnivorous dinosaurs during the Cretaceous: The evidence from Patagonia. Cretaceous Research 45:174–215.

Ortega F, Dantas P, Escaso F, Gasulla JM, Malafaia E, Ribeiro B. 2006. Primera cita de reptiles esfenodontos en el Jurásico Superior de la Península Ibérica. Resúmenes XXII Jornadas de Paleontología, León:152-153.

Pérez-Moreno BP, Chure DJ, Pires C, Marques da Sila C, dos Santos V, Dantas P, Póvoas L, Cachão M, Sanz JL, Galopim de Carvalho AM. 1999. On the presence of *Allosaurus fragilis* (Theropoda: Carnosauria) in the Upper Jurassic of Portugal: first evidence of an intercontinental dinosaur species. Journal of the Geological Society, London 156:449–452.

Porfiri JD, Novas FE, Calvo JO, Agnolín FL, Ezcurra MD, Cerda IA. 2014. Juvenile specimen of *Megaraptor* (Dinosauria, Theropoda) sheds light about tyrannosauroid radiation. Cretaceous Research 51:35–55.

Rabinowitz PD, LaBrecque J. 1979. The Mesozoic South Atlantic ocean and evolution of its continental margins. Journal of Geophysical Research 84(B11):5973–6002.

Rauhut OWM. 2003. The interrelationships and evolution of basal theropod dinosaurs. Special Papers in Palaeontology 69:1–213.

Rauhut OWM, Fechner R. 2005. Early development of the facial region in a non-avian theropod dinosaur. Proceedings of the Royal Society B: Biological Sciences 272:1179–1183.

Scotese CR. 2004. Cenozoic and Mesozoic paleogeography: changing terrestrial biogeographic pathways. In: Lomolino MV, Heaney LR. (Eds) Frontiers of Biogeography: New Directions in the Geography of Nature. Sinauer and Associates, Sunderland, MA. 9–26.

Sereno PC, Dutheil DB, Iarochene M, Larsson HCE, Lyon GH, Magwene PM, Sidor CA, Varricchio DJ, Wilson JA. 1996. Predatory dinosaurs from the Sahara and Late Cretaceous faunal differentiation. Science 272:986–991.

Sereno PC. 1999a. The evolution of dinosaurs. Science 284:2137–2147.

Sereno PC. 1999b. Dinosaurian biogeography: vicariance, dispersal and regional extinction. In: Tomida Y, Rich TH, Vickers-Rich P. (Eds) Proceedings of the Second Gondwanan Dinosaur Symposium. National Science Museum Monographs No. 15, Tokyo. 249–257.

Smith AG, Smith DG, Funnell BM. 1994. Atlas of Mesozoic and Cenozoic Coastlines. Cambridge University Press, Cambridge.

Smith DK. 1998. A morphometric analysis of *Allosaurus*. Journal of Vertebrate Paleontology 18(1):126–142.

Smith ND, Makovicky PJ, Hammer WR, Currie PJ. 2007. Osteology of *Cryolophosaurus ellioti* (Dinosauria: Theropoda) from the Early Jurassic of Antarctica and implications for early theropod evolution. Zoological Journal of the Linnean Society 151:377–421.

Upchurch P, Hunn CA, Norman DB. 2002. An analysis of dinosaurian biogeography: evidence for the existence of vicariance and dispersal patterns caused by geological events. Proceedings of the Royal Society of London, Series B 269:613–621.

Zanno LE, Makovicky PJ. 2013. Neovenatorid theropods are apex predators in the Late Cretaceous of North America. Nature Communications 4:2827. doi: 10.1038/ncomms3827.

6.2. VERTEBRATE FAUNA AT THE *ALLOSAURUS* FOSSIL SITE OF ANDRÉS (UPPER JURASSIC), POMBAL, PORTUGAL

Reference: Malafaia E, Ortega F, Escaso F, Dantas P, Pimentel N, Gasulla JM, Ribeiro B, Barriga F, Sanz JL. 2010. Vertebrate fauna at the *Allosaurus* fossil-site of Andrés (Upper Jurassic), Pombal, Portugal. Journal of Iberian Geology 36(2):193–204. doi:10.5209/rev_JIGE.2010.v36.n2.7

RESUMO

Neste trabalho é apresentada uma análise preliminar da diversidade de fauna de vertebrados, identificada na jazida de Andrés do Jurássico Superior da Bacia Lusitânica. Apesar de esta jazida ser conhecida desde a década de 90 do século passado, devido à descrição do primeiro exemplar atribuído ao género *Allosaurus* descoberto fora da América do Norte, os resultados aqui apresentados resultam, principalmente, do estudo de elementos recolhidos durante a segunda e terceira campanhas de escavação, em 2005. Até ao momento, foram identificados entre o material fóssil descoberto em Andrés, diversos taxa de vertebrados que incluem peixes, esfenodontes, crocodilomorfos, pterossáurios e, pelo menos, sete formas distintas de dinossáurios. A presença desta diversidade e abundância de restos osteológicos numa mesma jazida representa uma situação única no registo do Jurássico Superior português, apenas comparável à jazida clássica da antiga mina de carvão de Guimarota. Graças a estas características e à excelente preservação dos fósseis, a jazida de Andrés pode ser considerada uma localidade de referência para o estudo dos ecossistemas com vertebrados continentais do Jurássico Superior da Bacia Lusitânica. Restos de dinossáurios são os fósseis mais abundantes em Andrés e, entre estes, são particularmente abundantes elementos atribuídos a *Allosaurus*. Estas novas evidências proporcionam dados importantes para testar a hipótese filogenética proposta previamente, que identifica o primeiro conjunto de materiais de terópodes descoberto em Andrés à espécie *Allosaurus fragilis*, descrita em níveis sincrónicos da Formação de Morrison, na América do Norte. A semelhança entre os exemplares de *Allosaurus* descobertos em Andrés e as formas da Formação de Morrison sugere a existência de fluxos genéticos entre as faunas de vertebrados continentais de ambos lados do proto-Atlântico Norte durante o Jurássico Superior. Condições tectónicas favoráveis à existência de contactos pontuais entre os dois continentes é, actualmente, o melhor cenário para explicar esta semelhança de faunas.

Palavras-chave: Jurássico Superior, Portugal, Bacia Lusitânica, América do Norte, Formação de Morrison, Paleobiogeografia.

Figure 6.2.1. Partial skeleton of a sphenodont collected in the Andrés fossil site. Scale bar: 20 mm.

ISSN (print): 1698-6180. ISSN (online): 1886-7995
www.ucm.es/info/estratig/journal.htm

Journal of Iberian Geology 36 (2) 2010: 193-204
doi:10.5209/rev_JIGE.2010.v36.n2.7

Vertebrate fauna at the *Allosaurus* fossil-site of Andrés (Upper Jurassic), Pombal, Portugal

La fauna de vertebrados del yacimiento con *Allosaurus* de Andrés (Jurásico Superior), Pombal, Portugal

E. Malafaia[1,2,3]*, F. Ortega[4,3], F. Escaso[4,5,3], P. Dantas[1,2,3], N. Pimentel[6], J. M. Gasulla[5], B. Ribeiro[1], F. Barriga[1], J. L. Sanz[5]

[1] *Museu Nacional de História Natural (Universidade de Lisboa). Rua da Escola Politécnica, 58. 1250-102 Lisboa, Portugal.*
[2] *Laboratório de História Natural. Câmara Municipal da Batalha, Apart. 116. 2441-901, Batalha, Portugal*
[3] *ALT-Sociedade de História Natural, Torres Vedras. Apartado 25, 2564-909 Torres Vedras, Portugal.*
[4] *Grupo de Biología. Departamento de Física Matemática y de Fluidos, Facultad de Ciencias, UNED, Paseo Senda del Rey 9, 28040 Madrid, Spain*
[5] *Unidad de Paleontología, Facultad de Ciencias, Universidad Autónoma de Madrid, Cantoblanco, 28049 Madrid, Spain.*
[6] *Centro de Geologia da Universidade de Lisboa. Faculdade de Ciências, Campo Grande, Edifício C6. 1749-016 Lisboa, Portugal.*
Corresponding author: E. Malafaia, emalafaia@gmail.com

Received: 17/11/09 / Accepted: 30/06/10

Abstract

An overview of the faunistic diversity of the Andrés fossil-site from the Portuguese Upper Jurassic is presented. This work provides a preliminary approach on the vertebrate fauna known at present. Although this quarry is known since the 1990's, due to the description of the first robust evidence of a member of the neotetanuran genus *Allosaurus* outside North America, the results presented here are mainly derived from the analysis of the elements found during the second and third field seasons in 2005.

At the moment, among the material collected from Andrés it was identified remains that represent a diverse vertebrate fauna, including fishes, sphenodonts, crocodylomorphs, pterosaurs, and at least, seven distinct dinosaur forms. The recovery of this diverse and abundant osteological collection from one unique fossil-site is noteworthy for the Upper Jurassic Portuguese record, and only comparable with those from the Guimarota coalmine. Due to these two features plus the good preservation of the fossils, the Andrés quarry may be a site of reference for the analysis of vertebrate ecosystems from the Portuguese Upper Jurassic. Dinosaur elements are the most abundant fossils, and among them it is particularly common the presence of remains identified as *Allosaurus*. These new evidences allow testing the previous phylogenetical hypothesis ascribing the firsts theropod remains from Andrés to *A. fragilis,* a species described in synchronic levels of the North American Morrison Formation.

The similarity between the *Allosaurus* remains collected in Andrés and some specimens from the Morrison Formation seems to point the existence of a genetic flow between some continental vertebrates on both sides of the proto-north Atlantic during the Upper Jurassic. Favourable tectonic conditions for the occurrence of punctual contacts between the two continents is, at present, the best scenario for explain this situation.

Keywords: Upper Jurassic, Portugal, Lusitanian Basin, North America, Morrison Formation, Paleobiogeography

Resumen

Se presenta un análisis de la diversidad faunística del yacimiento de Andrés en el Jurásico Superior de la Cuenca Lusitánica. El presente trabajo pretende establecer un análisis preliminar de la fauna de vertebrados identificada en el yacimiento hasta la fecha. Aunque conocido desde la decada de 1990, debido a la descripción de la primera evidencia robusta de un neotetanuro del género *Allosaurus* fuera de Norteamérica, los resultados presentados derivan principalmente del análisis de elementos encontrados durante la segunda y tercera campañas de excavación en 2005.

Hasta el momento han sido identificados entre el material recogido en Andrés, representantes de diversos taxones de vertebrados que incluyen peces, esfenodontos, crocodilomorfos, pterosaurios y, al menos, siete formas distintas de dinosaurios. La presencia de esta diversidad y abundancia de restos osteológicos en el mismo yacimiento representa una situación única en el registro del Jurásico Superior portugués, tan sólo comparable a la del yacimiento clásico de la mina de carbón de Guimarota. Atendiendo a estas dos características y a la buena preservación de los fósiles, el yacimiento de Andrés puede ser considerado como una localidad de referencia para el estudio de los ecosistemas con vertebrados del Jurásico Superior portugués. Los restos de dinosaurios son los fósiles más abundantes y, entre ellos, son particularmente comunes los asignables a *Allosaurus*. Estas nuevas evidencias proporcionan importantes datos para probar la hipótesis filogenética propuesta previamente que asigna el primer terópodo descubierto en Andrés a *A. fragilis,* una especie descrita en niveles sincrónicos de la Formación Morrison en Norteamérica.

La similitud entre los restos de *Allosaurus* recogidos en Andrés y algunos de los ejemplares de la Formación Morrison, sugiere la existencia de un flujo genético entre algunos vertebrados continentales de ambos lados del proto-Atlántico norte durante el Jurásico Superior. La existencia de condiciones tectónicas favorables para la existencia de contactos puntuales entre los dos continentes es actualmente el mejor escenario para explicar esta situación.

Palabras clave: Jurásico Superior, Portugal, Cuenca Lusitánica, Norteamérica, Formación Morrison, Paleobiogeografia

1. Introduction

The quarry is found in the small township of Andrés (Pombal municipality, district of Leiria, Portugal) some 172km to the north from Lisbon and 35km to the north from Leiria (Fig. 1a). Stratigrafically, the site is located at the Meso-Cenozoic fringe of central-western Portugal in the northern sector of the Lusitanian Basin.

The discovery of the quarry in 1988 occurred during the construction of a tool warehouse and that year was performed a first palaeontological intervention. It was collected a block of rock containing part of the pelvic girdle and hindlimb elements of a large neotetanuran theropod. In the description of the specimen, it was proposed as the first robust evidence of a member of the species *Allosaurus fragilis* outside North America (Pérez-Moreno *et al*., 1999).

In 2005, it was reactivated the fieldworks at the Andrés quarry. On the sequence of this, it was recognized a great accumulation of a relatively diverse fauna of vertebrates. The diversity, abundance and good conditions of preservation in the quarry are not usual from the Portuguese Upper Jurassic and are, somehow, in the line with the classical Guimarota coalmine, in Leiria (Martin and Krebs, 2000).

2. Geological setting

The sedimentary deposits in which the quarry is included are interpreted as corresponding to the upper levels of the Alcobaça Formation (Complexo de Vale de Lagares) uppermost Kimmeridgian-lowermost Tithonian in age (Teixeira *et al*., 1966, 1968). However, the quarry is more favourably included in the unity designated as Bombarral Formation (="Grés Superiores"), which is partially equivalent to the Alcobaça Formation in the northern sector of the Lusitanian Basin (Fig. 1b, d). The "Grés Superiores" is a diachronic unity, at least in its lowermost part, but most probably lower to upper Tithonian in age (Marques *et al*., 1992; Manuppella *et al*., 1998, 2000). This unity is composed essentially by fine-grained mud-sandstones, sometimes micaceous, with intercalations of some levels of marls, silts and clays, sometimes with abundant calcareous or limonitic nodules (Manuppella *et al*., 1974, 1978). At the moment, attend to the previous argumentation, the sediments in the Andrés site are interpreted as ?upper Kimmeridgian – Tithonian in age.

The sedimentary deposits in the area of the quarry essentially comprehend levels of massive fine sandstones, sometimes micaceous with parallel lamination, and with abundant carbonized vegetal remains. Intercalated in the

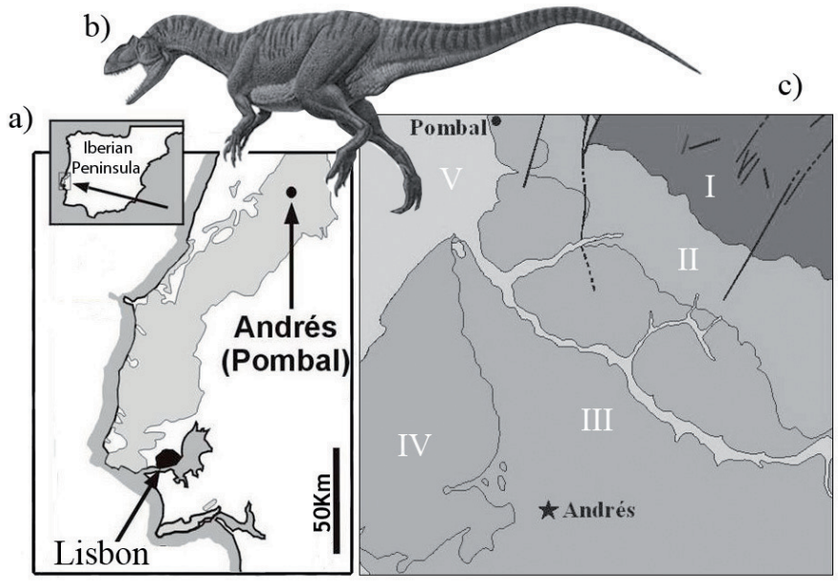

d)

Cronostratigraphy		Litostratigraphy	
UPPER JURASSIC	Tithonian	Lourinhã Group	Bombarral Fm. (= Grés Superiores)
	Kimmeridgian		Alcobaça Fm.
	Oxfordian	Montejunto Fm.	
		Cabaços Fm.	

Fig. 1.- a) Geographic localization of the Andrés fossil-site (Pombal, Upper Jurassic) on the central-western Portuguese area. The plotted area corresponds to the Lusitanian Basin. b) Simplified geological map around the Andrés locality. Legend: Upper Jurassic (I. - Oxfordian; II. - lower Kimmeridgian; III. - ? uppermost Kimmeridgian -Tithonian); IV.- Lower Cretaceous; V.- Cenozoic. c) *Allosaurus fragilis* d) Chronolitostratigraphic table. The plotted area marks the position of the Andrés quarry.

Fig. 1.- a) Localización geográfica del yacimiento de Andrés (Pombal, Jurásico Superior) en la región centro-occidental portuguesa. El área tramada corresponde a la Cuenca Lusitánica. b) Mapa geológico simplificado del entorno de la localidad de Andrés. Leyenda: Jurásico Superior (I. – Oxfordiense; II. – Kimmeridgiense inferior; III. - ? Kimmeridgiense superior – Titónico); IV. – Cretácico Inferior; V. – Cenozoico. c) *Allosaurus fragilis* d) Tabla cronolitostratigráfica. El área tramada marca la posición estratigráfica de los sedimentos en el yacimiento de Andrés.

sandstones fine levels and lens of red and grey clays occur, with abundant freshwater bivalves and some gastropods. This sequence passes laterally to levels of red massive mudstones.

The osteological remains, mainly the *Allosaurus* elements, were found in a level of fine micaceous sandstones with abundant carbonated concretions. These concretions are frequently associated with skeletal remains and in many cases with dense accumulations of them, pointing to an origin related with processes of soft tissues decomposition. In a lower sandy level with abundant carbonized remains, in some areas of the quarry, a few mainly isolated sauropod remains were found. In some clay levels and associated with clay lens, small osteological remains (fish scales, crocodile elements, dinosaur teeth, bones of sphenodonts) are very abundant.

Field analysis of the sedimentary deposits allowed the recognition of its main features and its palaeoenvironmental reconstruction. Coarse sandy lag deposits represent the erosional cut-off and initial filling of fluvial channels, whereas medium to fine sandy layers with low-angle cross-bedding and sigmoidal geometries represent channelized low-energy flows, filling-up those channels. Fine sands, with thick asymmetrical lensoidal geometries, frequently laminated and intercalated with millimetre to centimetre thick silts and clays, represent overbank crevasse-splays. Fine-grained deposits, in thick tabular geometries with massive or laminated clays and silts, mostly reddish or mottled, represent flood-plain overbank accumulations.

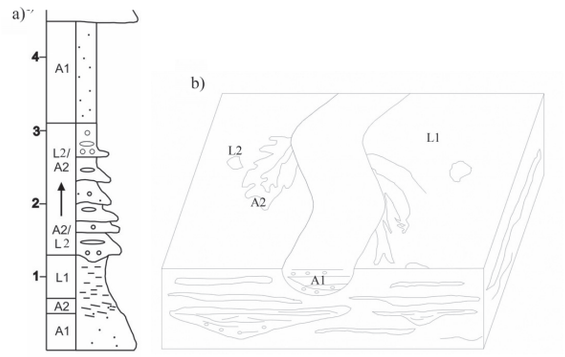

Fig. 2.- a) Lithostratigraphic log of the Andrés outcrop. Legend: A1 – Coarse sandy deposits without mica; A2 – medium to fine sandy layers with low-angle cross-bedding; L1 – massive or laminated clays and silts, mostly reddish or mottled; L2 - Fine sands, frequently laminated and intercalated with millimetre to centimetre thick silts and clays. b) Reconstruction of a fluvial-terrestrial environment that corresponds to the palaeoenvironmental interpretation in the area of the quarry.

Fig. 2.- a) Columna litoestratigráfica del afloramiento en el área del yacimiento de Andrés. Leyenda: A1 – depósitos arenosos groseros sin mica; A2 – capas de arenisca de grano medio a fino con laminación cruzada de bajo ángulo L1 – niveles de arcillas y limos compactos o laminados, por veces rojos o moteados; L2 – areniscas finas, a veces laminadas y intercaladas con niveles finos de arcillas y limos. b) Reconstrucción de un ambiente terrestre fluvial que corresponde a la interpretación paleoambiental en el área del yacimiento.

This facies association clearly indicates a medium to high-sinuosity fluvial system, with multiple channels and crevasses in a large floodplain. Seasonal climatic contrasts promoted repeated situations of immersion and emersion, testified by hidromorphic features and carbonate rhizogenic concretions developed in the floodplain clays. The sedimentological characteristics of these deposits suggest a freshwater environment located in a shallow meandering river system (Fig. 2), with low energy but still far away from the coastal influences of a deltaic system, recognized some tens of kilometres more to the west (Pimentel, 2009).

Occasionally, some very complete skeletons of tiny animals (fishes and lepidosaurs) have been found. Some partially articulated or non-dispersed skull bones and elements of the axial series of *Allosaurus* are recovered too. The orientation of the elongated bones of *Allosaurus* allows determining an almost E to W direction for the palaeodrainage at the site of the quarry. This direction is corroborated by the orientation of the channels, as perceived in outcrop, and also by the regional palaeogeographic reconstruction, with uplifted areas located to the East of the basin (Pimentel, 2009).

3. Material and methods

The set of fossils described in the present work is part of the collection of vertebrate palaeontology of the Museu Nacional de História Natural - Universidade de Lisboa (MNHN-UL). The specimens are identified with the reference MNHNUL/AND, and are deposited in this museum.

Institutional abbreviations

MNHNUL – Museu Nacional de História Natural (Universidade de Lisboa); USNM – United States National Museum

4. Vertebrate diversity

The dinosaur remains, mainly those attributed to *Allosaurus*, are at the moment the most abundant in the site. Although it has been also identified several representatives of other vertebrate taxa. It was recognized a diversity of vertebrate fauna composed by semionotiform fishes, at least one lepidosaur taxon, and representatives of three groups of archosaurs, such as crocodylomorphs, pterosaurians and dinosaurs.

4.1. Fishes

Fish remains are mainly represented by isolated rhombic scales, but occasionally more complete specimens have been recognized. It was recovered an almost complete individual of a *Lepidotes*-like semionotiform preserved in a clay lens (Fig. 3). This specimen presents a fusiform and fairly elevated body, with a maximum height situated between the posterior end of the skull and the dorsal fin, corresponding approximately to 30% of the total length. The skull is short, about one third of the total length of the body. This specimen is one of the rare occurrences of articulated semionotiform fish from the Portuguese record, highlighting the singularity of the conditions of preservation at the site.

4.2. Lepidosaurs

Cranial and postcranial bones of lepidosaurs are very common in some restricted areas of the quarry. The set of lepidosaur remains represent several individuals, probably belonging to a unique form. The most complete specimen has preserved the complete skull and the cranial part of the articulated postcranial skeleton (Fig. 4). Some other collected remains from the same area may also belong to the same individual. The sphenodontian specimens from Andrés constitute the first evidence of this group of rep-

tiles in the Iberian Peninsula. A preliminary analysis of this set of material suggests that it belongs to a close relative to the genus *Opisthias*, at the moment cited in both, the North American and European records (Ortega *et al*., 2006).

4.3. Crocodylomorphs

Crocodylomorphs are represented by cranial and postcranial elements mainly identified as indeterminate neosuchians. The cranial material includes abundant teeth (Fig. 5a) and several maxillary fragments, sometimes very complete. Concerning to the postcranial remains, at the moment it is represented only by abundant osteoderms. The teeth have conical crowns, with a relatively blunt apex. The crowns present well-developed wrinkled striae running from the base to the apex. These remains are similar to others assigned to a close relative to the genus *Goniopholis* also known from other Portuguese Upper Jurassic sites, such as the Guimarota coalmine. Some *Goniopholis* specimens from Guimarota were attributed to a particular species *G. baryglyphaeus* (Schwarz, 2002). At the moment, it was not possible to make deeper comparisons between the Andrés and Guimarota specimens, but probably both belong to close forms. The Portuguese *Goniopholis* specimens constitute the oldest evidence of this genus known at the moment in Europe and suggest also a larger area of distribution of these neosuchians than previously thought (Schwarz, 2002).

Some very small and lanceolated teeth collected in Andrés correspond to a second crocodile morphotype. These teeth have a characteristic ornamentation based on delicate ridges that are parallel at their bases but diverge toward the apex. Some of these ridges end on the mesial or distal carinae. This type of teeth is typically assigned to Atoposauridae close related to members of the genus *Theriosuchus*. As occurs with *Goniopholis,* a particular species of *Theriosuchus, T. guimarotae* has been described in Guimarota (Schwarz and Salisbury, 2005) but at present no comparison can be made with the Andrés specimens.

4.4. Pterosaurs

Pterosaurs are represented by some long and thin teeth (Fig. 5b). These teeth present straight crowns, with rounded cross-section, and strongly tapered to the apex. The surface of the crown is smooth, without ornamentation, differing from almost all the pterodactiloid ornithocheirids. Pterosaur remains are very scarcely known in the Portuguese Upper Jurassic record. The pterosaurs teeth from Andrés have a needle-like general morphology similar to some teeth described from Guimarota and tentatively assigned to *Rhamphorhynchus* (Wieckmann and Gloy, 2000).

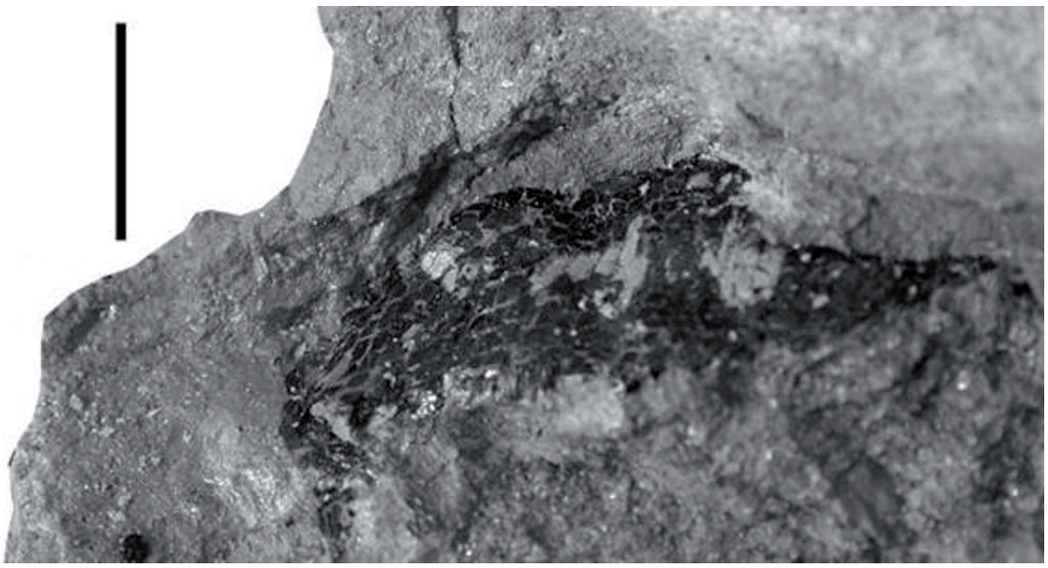

Fig. 3. - Individual of *Lepidotes*-like semionotiform preserved in a clay lens. Scale: 10mm
Fig. 3. – Individuo de semionotiforme afín a *Lepidotes* conservado en un lentejón de arcilla. Escala: 10mm.

4.5. Dinosaurs

The dinosaur elements, especially those assignable to *Allosaurus*, are at the moment the most abundant among the fossils collected in the quarry. The major diversity is verified among the sauropods. The collected sample is composed by at least seven different dinosaur forms, most of which is based in dental morphotypes that belong to theropods, sauropods, and ornithopods.

Orntithischians are represented by at least two ornithopod forms. Most of the remains identified are isolated teeth and a set of postcranial bones, the latter belonging to a small ornithopod dinosaur. The best preserved and complete tooth (Fig. 5c) is rhomb shaped, with a prominent primary ridge in the labial surface and several slight subsidiary ridges anterior to the former. These teeth presents well developed denticles on both mesial and distal carinae. Teeth with these characteristics are common in derived iguanodontians such as the camptosaurids (Norman, 2004).

Camptosaurid-like teeth from the Portuguese Upper Jurassic were previously assigned to *Draconyx* from the locality of Vale Frades, in Lourinhã (Mateus and Antunes, 2001). Since there are no diagnostic features to differentiate *Draconyx* and *Camptosaurus* teeth, there is not possible at the moment to attribute the specimens from Andrés to one of them. These specimens are thus assigned as undetermined camptosaurid ornithopod (Ortega *et al*., 2009).

A set of autopodial bones and a dorsal vertebra belonging to small ornithopods were also identified. The autopodial remains are interpreted as two phalanges I, of the digits I and III, and one pedal ungueal. The vertebra is complete and corresponds to a posterior dorsal. This vertebra presents elongated transverse processes. The total width over the maximum width of the anterior face of the centrum is 3:1, a feature shared with *Dryosaurus* (Galton, 1981). From the Portuguese Upper Jurassic record, two small dryosaurids have been briefly described, a partial skeleton referred as closely related to *Dryosaurus* (Dantas *et al.,* 2000) from Porto das Barcas (Lourinhã); and a right dentary with teeth from Zimbral (Lourinhã) assigned as aff. *Dryosaurus* (Mateus, 2007). Although small dryosaurids have been identified in the Portuguese

Fig. 4. - Sphenodont skull, in right lateral view.
Fig. 4. – Cráneo de esfenodonto en vista lateral derecha.

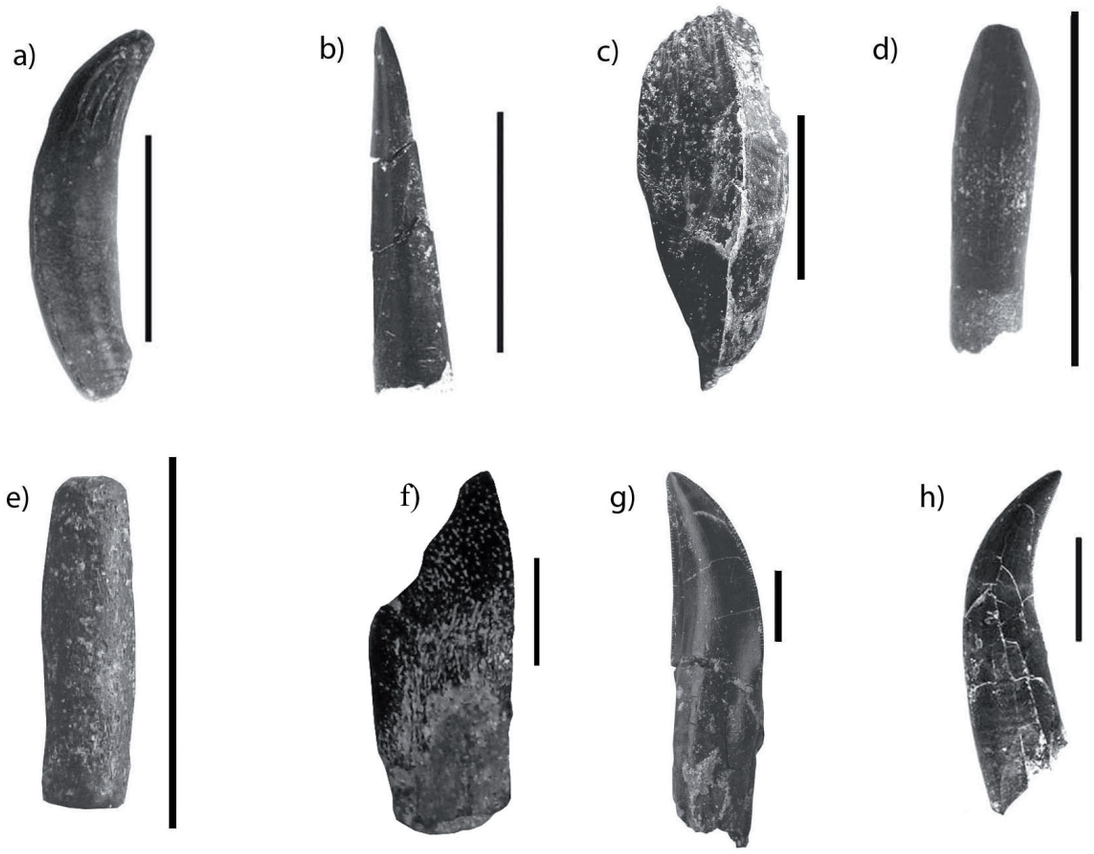

Fig. 5. - Teeth collected on the Andrés fossil-site. a) *Goniopholis* sp.; b) indeterminate pterosaur; c) camptosaurid ornithopod; d) titanosauriform sauropod; e) diplodocid sauropod; f) indeterminate neosauropod; g) *Allosaurus* sp.; h) dromaeosaurid theropod. Scale: 10 mm
Fig. 5. – Dientes recogidos en el yacimiento de Andrés. a) *Goniopholis* sp.; b) pterosaurio indeterminado; c) ornitópodo camptosaurideo; d) saurópodo titanosauriforme; e) saurópodo diplodócido; f) neosauropodo indeterminado; g) *Allosaurus* sp.; h) terópodo dromaeosaurido. Escala: 10 mm

Upper Jurassic record (Ortega *et al.,* 2009), here we prefer to refer these specimens as an undetermined form closely related to *Dryosaurus*, pending to find more diagnostic material.

Sauropods are represented by isolated teeth and some postcranial remains. The most abundant sample is composed by chisel-shape teeth with a rounded cross-section and straight crown assigned to a titanosauriform morphotype (Fig. 5d).

It was also collected some pencil-shape teeth, similar to that assigned to Diplodocoidea (Fig. 5e). Some spoon-shape, mostly incomplete, teeth (Fig. 5f) were also abundant in Andrés. These teeth have morphology similar to that described in the neosauropod *Turiasaurus* from the Tithonian - Berriasian of Spain (Royo-Torres *et al.,* 2006). Also interpreted as belonging to a juvenile neosauropod are some isolated pelvic bones and a centrum of a dorsal vertebra.

The theropods are the best represented dinosaur group due to the identification of abundant elements of at least two individuals assignable to *Allosaurus*. The recently recovered specimens increment substantially the collection of *Allosaurus* remains previously described from the site (Fig. 5g).

Theropod teeth with morphology usually attributed to dromaeosaurids were also collected in Andrés. These teeth are very laterally compressed and present a strong distal curvature of the crowns. They also present denticles

on both distal and medial carinae, which are restricted to the apices in the medial edge while distally it extends until the base of the crown (Fig. 5h).

The *Allosaurus* specimen described in 1999 and assigned to the species *A. fragilis* comprehend some cranial remains (the posterior end of a right frontal, the articular region of a right quadrate and some teeth), some vertebrae, dorsal and ventral ribs, most of the pelvic girdle and hindlimb elements and several indeterminate fragments (Pérez-Moreno *et al*., 1999; Dantas *et al*., 1999). At the moment, it was possible identify several new cranial and postcranial remains assignable to *Allosaurus*, as a right quadrate-quadratojugal (Fig. 6a), two lacrimals (Fig. 6b), a right dentary, a right frontal, the posterior end of a right mandibular ramus and a complete braincase (Fig. 6c). These cranial elements were collected at the same level, near to the remains previously described and probably correspond to the same individual. However, a complete ilium also collected from this site probably belongs to a second, larger individual.

Based on the method of Seebacker (2001) to calculate allometric length-mass relationships of dinosaurs, as well as on the comparison with other described specimens, the most complete *Allosaurus* specimen from Andrés would have about 6,5m in length and an estimated mass of 850kg. These dimensions fall on the gap of estimated size for some North American adult *Allosaurus* individuals, compare for example with the specimen USMN 4734, described by Madsen (1976), with 7,4m in length and a mass of 952 kg.

The description of *Allosaurus fragilis* in the Andrés quarry was first based mainly in the characters combination available from the pelvic girdle and hindlimb elements. These characters include: 1) large pubic peduncle of the ilium, longer than wide and much longer than the ischiatic peduncle; 2) obturator process of the ischium large, tapering and projected cranially to the level of the puboischiatic contact; 3) presence of a small notch that separates the caudodistal margin of the obturator process from the ischiatic shaft; 4) pubis with a large distal boot, which presents a well developed cranial and caudal expansion; and 5) moderately high ascending process of the astragalus (Pérez-Moreno *et al*., 1999).

The preliminary analysis of the new material, as well as the revision of the previously described specimen, support the former proposed identification of the Andrés specimens as belonging to the genus *Allosaurus*. The available material shares with some North American forms a set of autapomorphies that include: a) lacrimal with a caudal margin of the preorbital ramus concave and without a projection into the orbit; b) lacrimal with a well developed cornual process, which projects substantially above the skull table; c) squamosal with a ventral ramus that runs down the cranial margin of the quadrate and reaches at least half the height of the lateral temporal fenestra; d) squamosal with a series of striations on the lateral surface of the descending process; e) parietals with a notch in the dorsal end that separates it from the supraoccipital; f) paroccipital processes caudoventrally and laterally oriented, with the distal ends well projected below the level of the occipital condyle; g) basisphenoid separated from the basal tubera by a groove (Madsen, 1976; Chure, 2000).

The analysis of the set of material assignable as *Allosaurus* from Andrés allows identifying a combination of characters compatible with the variability previously known for the *A. fragilis* species from the North American Morrison Formation (Chure, 2000; Madsen, 1976; Malafaia *et al*., 2009a).

A new species of *Allosaurus*, *A. europaeus* was recently described on the base of a posterior part of a skull collected at the Upper Jurassic of Vale Frades, near Lourinhã (Mateus *et al*., 2006). The set of characters referred as distinctive for the proposed new species is composed by a series of states which falling into the morphological variability of *A. fragilis*, as well as by some probably misinterpreted features. The characters more definitive for the diagnose of the new species, the anterior relation of the jugal, lacrimal and maxilla, can be derivate from a misinterpretation of a fracture line in the ventral part of the lacrimal as the suture between the lacrimal and the maxilla (Malafaia *et al*., 2009a). Thus, we prefer, based on this argumentation, to consider *A. europaeus* as a *nomen dubium* until more accurate description of the type specimen.

The currently known Portuguese record of dromaeosaurids is very scarce and these theropods are only represented by some teeth described from the Guimarota coalmine, and by scarce elements collected in the Upper Cretaceous from the northern area of the Lusitanian Basin (Galton, 1996; Zinke, 1998). The collection of dromaeosaurid teeth from Guimarota includes a premaxillary tooth assigned as cf. *Dromaeosaurus* and several teeth referred to velociraptorine dromaeosaurids (Rauhut, 2000; Zinke, 1998).

The specimens from Andrés present some resemblance with the teeth assigned to *Dromaeosaurus*, as the twist of the anterior carina and the size and shape of the denticles (Currie *et al*., 1990). Based on these characters, it is considered the presence in Andrés of a representative of the dromaeosaurids that shares some conditions with *Dromaeosaurus*.

5. Palaeobiogeographical approach

The Andrés quarry constitutes one of the relatively most diverse ecosystems currently known for the continental Upper Jurassic record from Portugal. An important result from the analysis of the collected vertebrate remains consists in the identification of specimens assignable to *Allosaurus*, one of the best-known neotetanuran genera. The most recently analysed elements, mainly a set of cranial bones, also suggest a close similarity between the specimens from Andrés and some members attributed to *Allosaurus fragilis*. This hypothesis has important implications for the knowledge of the palaeobiogeographic role of the Iberian plate during the Upper Jurassic. The description of *Allosaurus fragilis* in the Andrés quarry constitutes one of the stronger evidence supporting the similarity between North American and Portuguese dinosaur faunas during the upper Kimmeridgian-Tithonian. This similarity is also supported by the presence of other taxa, as the theropods *Ceratosaurus* and *Torvosaurus* (Mateus *et al.,* 2006) or the ornithischian *Stegosaurus* (Escaso *et al.,* 2007) from others sites of the Lusitanian Basin.

Other elements compounding the collection of vertebrate fossils from the Andrés quarry, may contribute with new data for the palaeobiogeographic interpretation of these faunas. This is the case for example of the abundant and sometimes very well preserved, sphenodontian specimens whose relationship with members of the genus *Opisthias* described in North America and Europe is now in study (Ortega *et al*., 2006).

Some recent tectonic and sedimentological analysis demonstrate the occurrence of a regional regressive phase during the uppermost Kimmeridgian – lowermost Tithonian related with the opening of the northern sector of

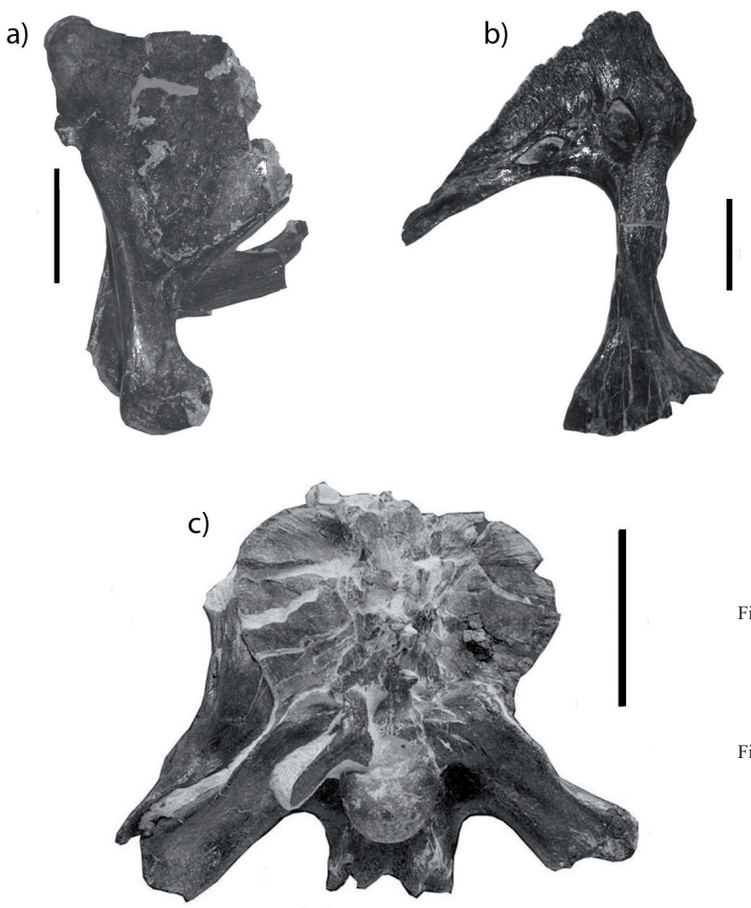

Fig. 6. - Some elements assignable as *Allosaurus* collected on the Andrés fossil-site. a) Right quadrate and quadratojugal in medial view; b) Left lacrimal in medial view; c) Braincase in occipital view. Scale a) and b): 50mm; c): 100mm.

Fig. 6. – Algunos de los elementos asignados a *Allosaurus* recogidos en el yacimiento de Andrés. a) Cuadrado y cuadradoyugal derechos en vista medial; b) Lacrimal izquierdo en vista medial; c) Basicráneo en vista occipital. Escala a) y b): 50mm; c): 100mm.

the Atlantic Ocean (Kullberg, 2006; Escaso *et al*., 2007). This regional process, opposite to the global transgression noted on this time interval, have probably favoured the increase of emerge areas between the continental masses on both sides of the incipient north-Atlantic. At the moment, it is considered, that this tectonic hypothesis suggesting favourable conditions for circulation of continental faunas between Iberia and North America during the Upper Jurassic is the best scenario for explain the known continental vertebrate distribution from the Portuguese record (Escaso *et al*., 2007).

6. Conclusions

The set of material studied from the Andrés fossil-site allows identifying the presence of at least five major vertebrate groups: fishes, lepidosaurs, crocodylomorphs, pterosaurs, and seven different forms of dinosaurs. The vertebrate remains recovered in this quarry constitute an increment of the available data for the knowledge of continental ecosystems developed during the Upper Jurassic in the Iberian Peninsula, due to its abundance and the identification of some taxa at the moment unknown on any other Iberian site, as the sphenodonts.

The identification of abundant *Allosaurus* remains suggests a distribution of this neotetanuran in Laurasia wider than it was considered during several decades. The record of *Allosaurus* from the Portuguese Upper Jurassic at the moment allows recognizing this taxon as a common theropod among vertebrate communities from the Iberian Peninsula (Mateus *et al*., 2006; Malafaia *et al*., 2009b). An important set of material, whose study is at present in progress, containing abundant and well preserved cranial bones, constitutes a strong basis for phylogenetic analysis. At the moment, all the analysed specimens present several similarities with members of *A. fragilis* (Malafaia *et al*., 2007).

The presence of *Allosaurus* specimens in the Portuguese Upper Jurassic strengthens the previously hypothesis that suggests a great similarity between vertebrate faunas developed in occidental Europe, particularly in Iberia and North America during the Upper Jurassic (Galton, 1980a,b; Galton and Powell, 1980; Pérez-Moreno *et al*., 1999; Dantas *at al*., 1999; Rauhut, 2003; Escaso *et al*., 2007). The palaeogeographic hypothesis suggesting the existence of some kind of contacts between continental vertebrate faunas from both sides of the proto north-Atlantic seems to be actually the best scenario for explain the Upper Jurassic record of some tetrapods groups from Portugal.

Acknowledgements

Acknowledgements for the participation in different aspects of the works developed in the Andrés fossil-site to António M. Galopim de Carvalho, Mauro García-Oliva, Cristina Moniz, Adán Pérez García, Liliana Póvoas, Graça Ramalheiro, Bruno Ribeiro and Jesús Santamaría. This work was developed in the context of the projects POCTI/ 1999/ PAL/ 36550- "Dinosaur Osteological and Ichnological studies of the Mesozoic of Portugal (DINOS)" and PTDC/ CTE-GEX/ 67723/ 2006 "Estudo da Fauna de Vertebrados do Jurássico Superior da Bacia Lusitânica e Implicações Paleobiogeográficas (VERT-JURA)" both financed by the "Fundação para a Ciência e a Tecnologia" (Portugal). Others institutions involved in the financing of the field activities or investigation of the authors are: a collaboration protocol of the Museu Nacional de História Natural - Universidade de Lisboa (MNHN-UL) with the Junta de Freguesia de Santiago de Litém (Pombal, Portugal) and other between the MNHN-UL and the Câmara Municipal da Batalha (Portugal). The work of the first author (EM) was also supported by a fund of the Jurassic Foundation and Fundação Luso-Americana.

References

Chure, D.J. (2000): A new species of *Allosaurus* from the Morrison Formation of Dinosaur National Monument (UT-CO) and a revision of the Theropod family Allosauridae. PhD Thesis. Columbia University: 964 p.

Currie, P.J., Rigby, Jr., J.K., Sloan, R. (1990): Theropod teeth from the Judith River Formation of southern Alberta, Canada. In: Carpenter, K., Currie, P.J. (eds.). Dinosaur Systematics: Approaches and Perspectives. Cambridge University Press, New York, 107-125.

Dantas, P., Pérez-Moreno, B.P., Chure, D.J., da Silva, C.M., dos Santos, V.F., Povoas, L., Cachão, M., Sanz, J.L., Pires, C., Bruno, G., Ramalheiro, G., Galopim de Carvalho, A.M. (1999): O dinossáurio carnívoro *Allosaurus fragilis* no Jurássico português. *Al-Madam* 8: 23-28.

Dantas, P., Yagüe, P., Hazevoet, C.J., Ortega, F., Santos, V.F., Sanz, J.L., Cachão, M., Galopim de Carvalho, A.M., Santos, J.J. (2000): Um novo Iguanodontia basal do Jurássico Superior português. *Abstracts XVI Jornadas de la Sociedad Española de Paleontologia*, Évora: 12-13.

Escaso, F., Ortega, F., Dantas, P., Malafaia, E., Pimentel, N.L., Pereda-Subelbiola, X., Sanz, J.L., Kullberg, J.C., Kullberg, M.C., Barriga, F. (2007): New evidence of shared Dinosaur Across Upper Jurassic Proto-North Atlantic: *Stegosaurus* from Portugal. *Naturwissenschaften,* 94(5): 367-374.

Galton, P.M. (1980a): *Dryosaurus* and *Camptosaurus*, intercontinental genera of Upper Jurassic ornithopod dinosaurs. *Memoirs of the Geological Society of France, NS,* 139: 103-108.

Galton, P.M. (1980b): European Jurassic ornithopod dinosaurs of the families Hypsilophodontidae and Camptosauridae *Neues Jahrbuch Für Geologie Und Paläontologie Abhandlungen*, 160: 73-95.

Galton, P.M. (1981): *Dryosaurus*, a hypsilophodontid dinosaur from the Upper Jurassic of North America and Africa: Postcranial skeleton. *Paläontologische Zeitschrift*, 55: 271-312.

Galton, P.M. (1996): Notes on Dinosauria from the Upper Cretaceous of Portugal. *Neues Jahrbuch Für Geologie Und Paläontologie Monatshefte*: 83-90.

Galton, P.M., Powell, P. (1980): The Ornithischian Dinosaur *Camptosaurus prestwichii* from the Upper Jurassic of England. *Palaeontology,* 23: 411-443.

Kullberg, J.C., Rocha, R.B., Soares, A.F., Rey, J., Terrinha, P., Callapez, P., Martins, L. (2006): A Bacia Lusitaniana: Estratigrafia, Paleogeografia e Tectónica. In: Dias, R., Araújo, A., Terrinha, P., Kullberg, J.C. (eds) Geologia de Portugal no contexto da Ibéria, Universidade Évora: 317-368.

Madsen, J.H. (1976): *Allosaurus fragilis*: a revised osteology. *Utah Geological and Mineral Survey*, 109: 163 p.

Malafaia, E., Dantas, P., Ortega, F., Escaso, F. (2007): Nuevos restos de *Allosaurus fragilis* (Theropoda: Carnosauria) del yacimiento de Andrés (Jurásico Superior; Centro-Oeste de Portugal). In: Cambra-Moo, O., Martínez-Pérez, C., Chamero, B., Escaso, F., de Esteban Trivigno, S., Marugán-Lobón, J. (eds.), *Cantera Paleontológica*: 255-271. Diputación Provincial de Cuenca, Cuenca: 398 p.

Malafaia, E., Ortega, F., Escaso, F., Dantas, P., Gasulla, J.M. (2009a): *Allosaurus fragilis* from the Portuguese Upper Jurassic. *Journal of Vertebrate Paleontology,* 29(Supplement to Number 3): 140-141A.

Malafaia, E., Ortega, F., Escaso, F., Silva, B., Ramalheiro, G., Dantas, P., Moniz, C., Barriga, F. (2009b): Análisis preliminar de un nuevo ejemplar de *Allosaurus* del Grupo Lourinhã (Jurásico Superior de Torres Vedras, Portugal). In: *Colectivo Arqueológico y Paleontológico de Salas* (ed.), *Actas de las IV Jornadas Internacionales sobre Paleontología de Dinosaurios y su Entorno*. Salas de los Infantes, Burgos: 243-251.

Manuppella, G., Barbosa, B., Machado, S., Carvalho, J., Bartolomeu, A., Azerêdo, A.C., Ramalho, M., Crosaz, R., Baptista, R., Porteiro, A., Dâmaso, B., Cunha, T.A. (1998): Carta Geológica de Portugal, folha 27-A (Vila Nova de Ourém). Escala 1: 50 000 (2ª ed.). Instituto Geológico e Mineiro, Lisboa.

Manuppella, G., Rodrigues, A., Oliveira, J., Carreira de Deus, P. (1974): Carta Geológica de Portugal, folha 23-A (Pombal). Escala 1: 50 000 (1ª ed.). Serviços Geológicos de Portugal. Lisboa.

Manuppella, G., Telles Antunes, M., Costa Almeida, C.A., Azerêdo, A.C., Barbosa, B., Cardoso, J.L., Crispim, J.A., Duarte, L.V., Henriques, M.H., Martins, L.T., Ramalho, M.M., Santos, V.F., Terrinha, P. (2000): Notícia Explicativa da Carta Geológica de Portugal, folha 27-A (Vila Nova de Ourém). Escala 1: 50 000 (2ª ed.). Instituto Geológico e Mineiro, Lisboa.

Manuppella, G., Zbyszewski, G. and da Veiga Ferreira, O. (1978): Notícia Explicativa da Carta Geológica de Portugal, da folha 23-A (Pombal). Escala 1: 50 000 (1ª ed). Serviços Geológicos de Portugal, Lisboa.

Marques, B., Olóriz, F., Caetano, P.S., Rocha, R., Kullberg, J.C. (1992): Upper Jurassic of Alcobaça Region. Stratigraphic Contributions. *Comunicações Serviços Geológicos de Portugal*, 78(1): 63-69.

Martin, T., Krebs, B. (2000): Guimarota: A Jurassic ecosystem. *Verlag Dr. Friedrich. Pfeil, Munich*: 155 p.

Mateus, O. (2007): Notes and review of the ornithischian dinosaurs of Portugal. *Journal of Vertebrate Paleontology,* 27(Supplement to Number 3): 114A.

Mateus, O., Antunes, M.T. (2001): *Draconyx loureiroi*, a new camptosauridae (Dinosauria, Ornithopoda) from the Late Jurassic of Lourinhã, Portugal. *Annales de Paléontologie*, 87(1): 61-73.

Mateus, O., Walen, A., Antunes, M.T. (2006): The large theropod fauna of the Lourinhã Formation (Portugal) and its similarity to the Morrison Formation, with a description of a new species of *Allosaurus*. *New Mexico Museum of Natural History and Science Bulletin,* 36: 123-129.

Norman, D.B. (2004): Basal Iguanodontia. In: Weishampel, D.B., Dodson, P., Osmolska, H. (eds.). *The Dinosauria 2nd Edition*: 413-437. University of California Press, Berkeley: 413-437.

Ortega, F., Dantas, P., Escaso, F., Gasulla, J.M., Malafaia, E., Ribeiro, B. (2006): Primera cita de reptiles esfenodontos en el Jurásico Superior de la Península Ibérica. *Resúmenes XXII Jornadas de Paleontología*, León: 152-153.

Ortega, F., Malafaia, E., Escaso, F., Dantas, P., Pérez García, A. (2009): Faunas de répteis do Jurássico Superior de Portugal. In: Pérez García, A., Silva, B.C., Malafaia, E., Escaso, F. *Paleolusitana* 1. Associação Leonel Trindade-Sociedade de História Natural, Torres Vedras: 43-56.

Pérez-Moreno, B.P., Chure, D.J., Pires, C., da Silva, M.C., dos Santos, V., Dantas, P., Povoas, L., Cachão, M., Sanz, J.L., de Carvalho, A.M.G. (1999): On the presence of *Allosaurus fragilis* (Theropoda, Carnosauria) in the Upper Jurassic of Portugal: first evidence of an intercontinental dinosaur species. *Journal of the Geological Society of London*, 156: 449-452.

Pimentel, N.L. (2009): Contextualização paleogeográfica das jazidas de vertebrados do Jurássico Superior da Bacia Lusitânica. In: Pérez García, A., Silva, B.C., Malafaia, E., Escaso, F. *Paleolusitana 1*. Associação Leonel Trindade-Sociedade de História Natural, Torres Vedras: 465-470.

Rauhut, O.W.M. (2000): The dinosaur fauna from the Guimarota mine. In: T. Martin, B. Krebs (eds.), *Guimarota: A Jurassic ecosystem*. Verlag Dr. Friedrich. Pfeil, Munich: 75-82.

Rauhut, O.W.M. (2003): A tyrannosauroid dinosaur from the Upper Jurassic of Portugal. *Palaeontology,* 46(5): 903-910.

Royo-Torres, R., Cobos, L., Alcalá, L. (2006): A giant European dinosaur and a new sauropod clade. *Science*, 314: 1925-1927.

Schwarz, D. (2002): A new species of *Goniopholis* from the Upper Jurassic of Portugal. *Palaeontology,* 45(I): 185-208.

Schwarz, D., Salisbury, S.W. (2005): A new species of *Theriosuchus* (Atoposauridae, Crocodylomorpha) from the Late

Jurassic (Kimmeridgian) of Guimarota, Portugal. *Geobios*, 38(6): 79-802.

Seebacker, F. (2001): A new method to calculate allometric length-mass relationships of dinosaurs. *Journal of Vertebrate Paleontology*, 21(1):51–60.

Teixeira, C., Camarate França, J., Zbyszewski, G., da Veiga Ferreira, O., de Matos, M., Oliveira, J., Rodrigues, L., Rodrigues, A., Manuppella, G. (1966): Carta Geológica de Portugal, folha 23-C (Leiria). Escala 1: 50 000 (1ª ed.). *Publicações dos Serviços Geológicos de Portugal*. Lisboa.

Teixeira, C., Zbyszewski, G., Torre de Assunção, C., Manuppella, G. (1968): Notícia Explicativa da Carta Geológica de Portugal, folha 23-C (Leiria). Escala 1: 50 000 (1ª ed.). *Publicações dos Serviços Geológicos de Portugal*, Lisboa.

Wiechmann, M.F., Gloy, U. (2000): Pterosaurs and urvogels from the Guimarota mine In: T. Martin, B. Krebs (eds.), *Guimarota: A Jurassic ecosystem*. Verlag Dr. Friedrich Pfeil, Munich: 83-86.

Zinke, J. (1998): Small theropod teeth from the Upper Jurassic coal mine of Guimarota (Portugal). *Paläontologische Zeitschriff* 72(1/2): 179-189.

6.3. ANALYSIS OF THE ANATOMY OF *ALLOSAURUS* (TETANURAE, AVETHEROPODA) FROM THE LUSITANIAN BASIN BASED ON NEW SPECIMENS OF THE PORTUGUESE UPPER JURASSIC

E. Malafaia[1,2,3]*, P. Mocho[4,5,3], F. Escaso[5,3], P. Dantas[6,3], F. Ortega[5,3]

[1] Departamento de Geologia and Instituto Dom Luiz, Faculdade de Ciências da Universidade de Lisboa, Portugal, emalafaia@gmail.com

[2] Museu Nacional de História Natural e da Ciência da Universidade de Lisboa, Portugal

[3] Laboratório de Paleontologia e Paleoecologia – Sociedade de História Natural, Torres Vedras, Portugal

[4] The Dinosaur Institute, Natural History Museum of Los Angeles County, 900 Exposition Blvd, Los Angeles, CA 90007, EUA

[5] Grupo de Biología Evolutiva, Facultad de Ciencias, UNED, c/ Senda del Rey, 9, 28040 Madrid, Spain, fescaso@ccia.uned.es; fortega@ccia.uned.es

[6] Museu da Comunidade Concelhia da Batalha

*Corresponding author

RESUMO

Neste trabalho é descrito um conjunto de elementos cranianos e pós-cranianos de dinossáurios terópodes, descobertos na jazida de Andrés (Tithonian, Bacia Lusitânica). Estes exemplares incluem a amostra mais completa de restos do esqueleto craniano de dinossáurios terópodes, conhecida actualmente no Jurássico Superior da Bacia Lusitânica. A excelente preservação dos restos permite a descrição de alguns elementos pouco conhecidos no registo fóssil de terópodes, como por exemplo o vômer, o supradentário ou o coronóide e obter uma descrição detalhada da anatomia craniana deste terópode. Os exemplares de Andrés partilham diversas sinapomorfias com os materiais de *Allosaurus* descritos na Formação de Morrison, como por exemplo a presença de um processo cornual do lacrimal bem desenvolvido, comprimido médio-lateralmente e projectado dorsalmente e de um forâmen mandibular interno ao longo da margem posteroventral do prearticular. A descrição original de alguns elementos do esqueleto pós-craniano descobertos em Andrés sugeria a presença da espécie *Allosaurus fragilis* no Jurássico Superior da Bacia Lusitânica. O estudo detalhado da colecção completa de fósseis recolhidos em Andrés permite identificar determinadas diferenças relativamente a *A. fragilis* mas também com o holótipo de *Allosaurus europaeus*. Contudo, com base no contexto paleobiogeográfico, é aqui proposta a identificação preliminar dos exemplares de Andrés como pertencendo a *Allosaurus* cf. *europaeus*, aguardando a descoberta de materiais mais completos que permitam o melhor conhecimento desta espécie portuguesa.

Palavras-chave: Theropoda, *Allosaurus europaeus*, filogenia, Jurássico Superior, Bacia Lusitânica, paleobiogeografia

ABSTRACT

A set of theropod cranial and postcranial remains found in Tithonian sediments of the Andrés fossil site is described. These specimens include the most complete cranial sample of a theropod dinosaur known in the Upper Jurassic of the Lusitanian Basin. The fine preservation allows the description of some elements that are poorly preserved in the theropod fossil record such as the vomer, supradentary and coronoid. Besides, the exceptional preservation of most elements allows obtaining a detailed description of the cranial anatomy of this theropod. The specimens from Andrés share several synapomorphies with the material of *Allosaurus* described in the Morrison Formation, such as the presence of a large, mediolaterally compressed and dorsally projecting cornual process of the lacrimal or an internal mandibular foramen along the caudoventral margin of the prearticular. The original description of some theropod postcranial elements collected in Andrés suggested for the presence of *Allosaurus fragilis* during the Late Jurassic of the Lusitanian Basin. The detailed study of the complete collection of the material from Andrés allows identify some differences relative to *Allosaurus fragilis*, but also with the holotype of *Allosaurus europaeus*. However, based on the paleobiogeographic context it is here proposed the assignation of the specimens from Andrés as *Allosaurus* cf. *europaeus* pending the discovery of more complete material that would allow a better understand of these Portuguese species.

Keywords: Theropoda, *Allosaurus europaeus*, phylogeny, Late Jurassic, Lusitanian Basin, paleobiogeography

6.3.1. INTRODUCTION

In 1999, Pérez-Moreno and collaborators described the first specimen identified to the avetheropod *Allosaurus* from the Late Jurassic of Portugal. This specimen, MNHNUL/AND.001, was found in 1988 in the Andrés fossil-site, near Pombal in the northern end of the Central Sector of the Lusitanian Basin. It comprises elements of the pelvic girdle and hind limbs (left ischium, pubes, femora, tibiae, and fibulae) collected in a single block and preserved in anatomic position, beside several isolated remains including a fragment a right quadrate, dorsal, sacral and caudal vertebrae, chevrons, dorsal ribs and gastralia (Dantas et al. 1999; Pérez-Moreno et al. 1999;). The specimen was assigned to the species *Allosaurus*

fragilis as the first evidence of *Allosaurus* outside North America. This discovery also represented the first dinosaur species shared by two continents and thus triggered an intense discussion concerning the paleobiogeographic relationships of Late Jurassic dinosaur faunas from the Lusitanian Basin and the Morrison Formation. The presence of the species *Allosaurus fragilis* in both continents was interpreted as an evidence of faunal interchanges between Iberian Peninsula and North America during the Late Jurassic. In 2006, it was described a partial skull of a theropod collected in Praia de Vale Frades (Lourinhã) in the central west of the Lusitanian Basin, which was interpreted as belonging to a new *Allosaurus* species *A. europaeus* (Mateus et al. 2006). Despite the theropod fauna from Portugal and North America are closely related, this discovery suggested the presence of incipient vicariant processes probably related with opening of the northern sector of the Atlantic Ocean.

The currently known record of *Allosaurus* from Portugal also includes a small maxilla collected in the Guimarota coal mine, near Leiria, interpreted as an *Allosaurus* hatchling (Rauhut and Fechner 2005).

In 2005, the resumed of the field-works in Andrés allowed the discovery of several osteological remains assignable to *Allosaurus*, including abundant cranial and postcranial elements of at least three individuals. The Andrés fossil site is one of the most significant Portuguese quarries for the study of Late Jurassic continental faunas from the Lusitanian Basin due the great abundance and diversity of the collected fossils. The vertebrate fauna identified in this quarry includes semionotiform fishes, lepidosaurs closely related with *Opisthias*, neosuchian crocodylomorphs, indeterminate pterosaurs and several groups of dinosaurs belonging to ornithopods, sauropods and theropods (Ortega et al. 2006; Malafaia et al. 2010).

In the present work, a detailed description for the set of cranial elements found in the Andrés fossil is presented. A phylogenetic analysis is performed in order to acess the relationship of this material within Allosauroidea, especially with *Allosaurus*. The variability on the skull morphology of *Allosaurus* is discussed.

6.3.2. TAXONOMIC AND PHYLOGENETIC HISTORY OF *ALLOSAURUS*

The first known specimen of *Allosaurus* is a posterior half of a caudal centrum, USNM 218, from northern Colorado assigned to the species *Poicilopleuron valens* (Leidy 1870). In the same work, Leidy proposed the generic name *Antrodemus* in the event of posterior discoveries of more complete material would generically distinguish this specimen from the European taxon *Poikilopleuron* (Gilmore 1920). However, *Allosaurus* and the respective genoholotypic species *A. fragilis* were described by Marsh (1877) based on an incomplete specimen, YPM 1930, from Garden Park (Colorado) in the Morrison Formation. This specimen was later considered inadequate as holotype for species or genus identification (Paul and Carpenter 2010). A specimen (UUVP 6000, currently numbered DINO 2560) from the Dinosaur National Monument Collection, consisting on a complete skull and articulated, almost complete postcranial skeleton, was specified as the neotype of *A. fragilis* by Madsen (1976). Chure (2000) noted for some problems with the approach presented by Madsen (1976) because the holotype still exists and the specimen is from younger sediments relative to YPM 1930. Latter, an associated skeleton with disarticulated skull, USNM 4734, from the type locality of *Allosaurus*, the Felch Quarry 1, was proposed as paratype by Paul (1988), topotype by Gilmore (1920) and Chure (2000) and neotype by Paul and Carpenter (2010) for *A. fragilis*. Based on comparison of the type specimen of *Antrodemus valens* with a caudal vertebra attributed to *Allosaurus fragilis*, USNM 8367, Gilmore (1920) proposed a generic identity between the two taxa. Gilmore (1920) also reviewed the validity of *Creosaurus*, considering it a junior synonym of *Antrodemus*. Attending to the law of priority, the author considered that *Antrodemus* should prevail and considered *Allosaurus* as a junior synonym of this taxon. However, most follow authors considered, as was anticipated by Gilmore (1920), that there is no justification for superseding the long-established and well-known name *Allosaurus* by the less known *Antrodemus*. Besides, Madsen (1976) noted some problems with the *Antrodemus* type, such as the lack of diagnostic characters and stratigraphic information. Following this argumentation, *Antrodemus* is generally accepted as a *nomen dubium* (Madsen 1976; Paul 1988; Glut

1997; Holtz et al. 2004; Paul and Carpenter 2010).

Currently, the *Allosaurus* genus is among the best known theropod dinosaurs. Members of this genus were the dominant theropods in the Morrison Formation, comprising 60% of the theropod fauna at the level of quarry, member and formation (Foster and Chure 1998; Chure 2000). In the Cleveland-Lloyd Dinosaur Quarry (Emery County, Utah), one of the most important dinosaur quarries in North America, a remarkable mass accumulation of at least forty-four and possibly as many as sixty individuals of *Allosaurus* provide one of the few population samples known of theropod dinosaurs (Chure 2000; Hunt et al. 2006). Despite this unusual notable record, the diversity of *Allosaurus* in the Morrison Formation has been subject of discussion. Some authors (e.g. Paul 1988) considered two distinct skull morphotypes for *Allosaurus*, a more slender form, characterized by more pointed lacrimal horns, traditionally considered as *A. fragilis*, and a larger form with lower and more rectangular skulls with smaller and less triangular lacrimal horns, tentatively assigned to "*A. atrox*" (Paul 1988). The concept of "long-faced/short-faced" *Allosaurus* species was followed by subsequent authors (Britt 1991; Bakker et al. 1992). Smith (1998) based on morphometric analysis referred *Saurophaganax maximus* to *Allosaurus*, as *A. maximus*. Although, Chure (2000) consider that *Saurophaganax* is sufficiently different from *Allosaurus* to support generic separation.

Currently, most authors consider that *A. fragilis* is the only valid species of *Allosaurus* in the Morrison Formation despite some specimens from Dinosaur National Monument in Utah (DINO 11541: Chure, 2000) and from Bighorn Basin of northern Wyoming (SMA 0005: Evers 2014), have been interpreted as representing a new species not yet formally described "*A. jimmadseni*". Other recently proposed species *Allosaurus lucasi* (Dalman 2014) is based on few and very incomplete elements collected in southwestern Colorado at McElmo Canyon from the top of the Morrison Formation. The diagnosis proposed for this species is here considered invalid because the supposed autapomorphies correspond to features that may be related with intraspecific variability.

Outside North America, several specimens were putatively identified to *Allosaurus*, including isolated remains from Switzerland (Huene 1926; Steel 1970), Russia (Riabinin 1914), Tanzania (Janensch 1925; Molnar et al. 1990), and Portugal (Pérez-Moreno et al 1999; Rauhut and Fechner 2005; Mateus et al. 2006; Malafaia et al. 2010). Excluding the Portuguese material they are considered *nomen dubium* or assigned to other theropod taxa (Chure 2000).

6.3.3. GEOLOGICAL SETTINGS

The Andrés fossil site is placed southeast of Pombal town and about 170 km to the north from Lisbon (Fig. 6.3.1). The quarry is located on levels of massive fine-grained, micaceous sandstones with parallel lamination and abundant plant debris. Thin lenticular levels of red and grey claystones with abundant freshwater bivalves and some gastropods occur frequently as intercalations in the sandstone levels. The theropod specimens were mainly found in a level of micaceous sandstones with abundant carbonated concretions, which are interpreted as filling-up of channelized low-energy flows, possibly a shallow meandering river system developed in a broad flood-plain (Malafaia et al. 2010).

These sediments are interpreted as belonging to the Bombarral Formation (*sensu* Azerêdo et al. 2010), which correspond to the "Grés Superiores" (*sensu* Choffat 1901; Marques et al. 1992). Some authors (e.g., Kullberg et al. 2013) interpreted these deposits as belonging to the Lourinhã Formation. The Bombarral Fm. is a diachronic unity, but has been interpreted as probably Tithonian in age (Marques et al. 1992; Manuppella et al. 1998, 2000).

6.3.4. INSTITUTIONAL ABBREVIATIONS

BYU-VP, Brigham Young University, Vertebrate Paleontology collection, Provo, Utah, USA; DINO/DNM, Dinosaur National Monument, Utah, USA; ML, Museu da Lourinhã, Lourinhã, Portugal; MNHNUL,

Museu Nacional de História Natural da Universidade de Lisboa, Lisbon, Portugal; MOR, Museum of the Rockies, Bozeman, USA; SMA, Sauriermuseum Aathal, Aathal, Switzerland; USNM, United States National Museum, Smithsonian Institution, Washington DC, USA; UUVP, Utah University, Vertebrate Paleontology collection; Salt Lake City, Utah, USA; YPM, Yale Peabody Museum, New Haven CT, USA.

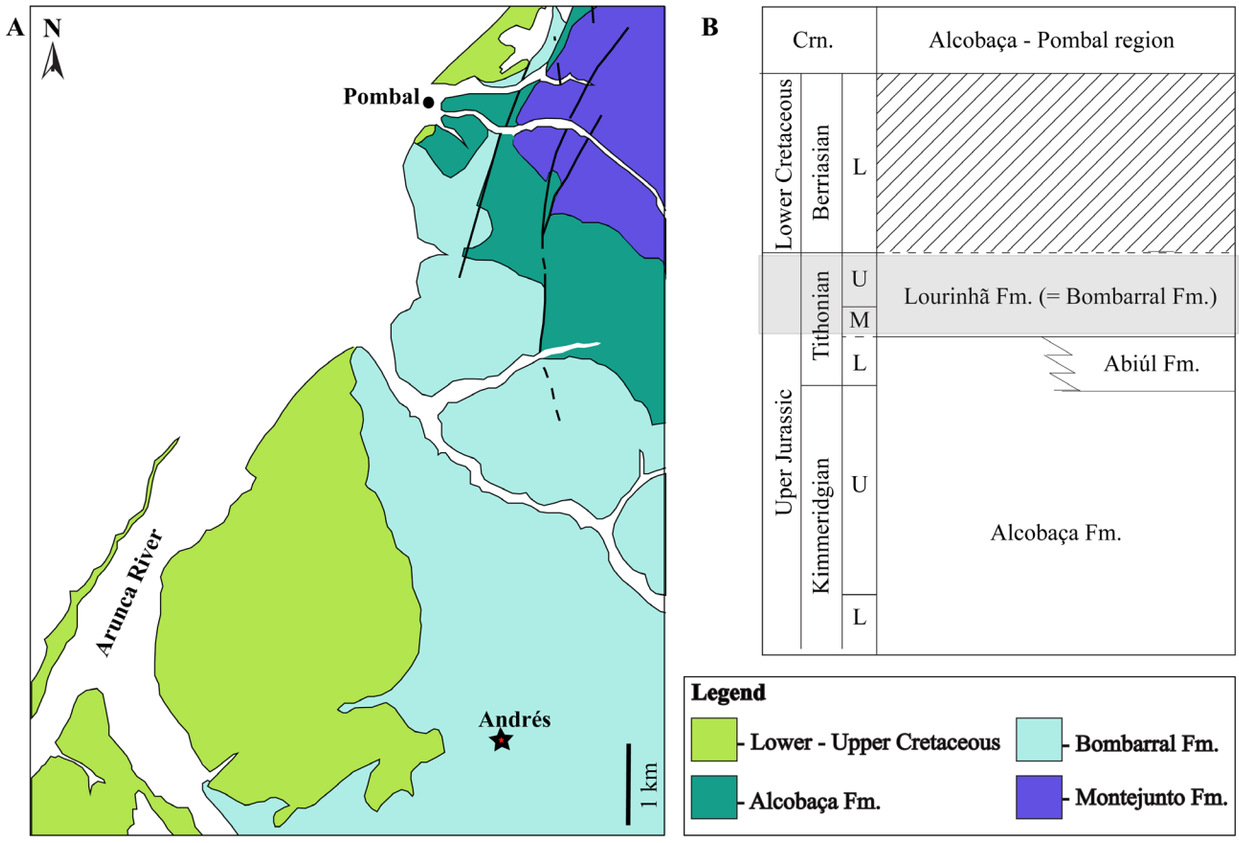

Figure 6.3.1. Geologic and stratigraphic setting of the Andrés fossil site. (A); simplified geological map of the region of Pombal (modified from Manuppella 1974) showing the location of the Andrés fossil sites; (B), cronostratigraphic table for the Upper Jurassic of the region of Pombal. The grey rectangular area marks the position of the Andrés fossil site.

6.3.5. MORPHOLOGICAL ABBREVIATIONS

Cranial skeleton

aar, antarticular process; alf, additional lateral fossa; an, surface for contact with the angular; aoc, antotic crest; aof, antorbital fenestra; ar, surface for contact with the articular; asf, anterior surangular foramen; BO, basioccipital; bpr, BS, basisphenoid; bsr, basisphenoid recess; bt, basal tubera; bv, blood vessel; ce, cervix; cm, crista metotica; CO, coronoid; co, surface for contact with the coronoid; cpr, capitate process; ct, crista tuberalis; cul, cultriform process; d, surface for contact with the dentary; df, dental foramen; dtr, dorsal tympanic recess; ec, endocranial cavity; emf, external mandibular fenestra; en, external naris; EO, exoccipital; f, foramen; fm, foramen magnum; fo, fenestra ovalis; fpca, foramen posterior condylar artery; fpct, foramen posterior chorda tympani; FR, frontal; fr, surface for contact with the frontal; glf, glenoid fossa; ids, interdenticular sulci; ifs, intrafrontal suture; inc, internal narial choana; ju, surface for articulation with the jugal; jupr, jugal process; LA, lacrimal; la, surface for articulation with the lacrimal; lc, lateral condyle; loaf, lateral antorbital fossa; lf, lateral fossa; lft, lateral temporal fenestra; LS, laterosphenoid; ls, surface for contact with the laterosphenoid; lss, lateral surangular shelf; ma, maxillary antrum; mame, muscle adductor mandibulae externus; maof, medial antorbital fossa; mc, medial condyle; mes, medial shelf; mf, metotic foramen; mhf, mylohyoid foramen; mss, medial surangular shelf; mv, medial vacuity; MX, maxilla; mx, surface for contact with the maxilla; mxf, maxillary fenestra; NA, nasal; na, surface

for contact with the nasal; nlc, nasal lateral crest; nmp; naso-maxillary process; np, neurapophisis; npf, nasal pneumatic foramen; obd, olfactory bulb depressions;oc, occipital condyle; of, orbital fenestra; ofs, orbital fossa; OP, opisthotic; or, orbital rim; orb, surface for contact with the orbitosphenoid P, parietal; p, surface for contact with the parietal; pa, surface for contact with palatine; pal, surface for contact with the palatine; papr, parietal process; par, palatine pneumatic recess; pcp, postcotyloid process; pcv, posterior canal for the middle cerebral vein; pdg, paradental groove; pdp, parietal dorsal process; PFR, prefrontal; pfr, surface for contact with the prefrontal; pm, surface for contact with the premaxilla; pmmf, posteromedial maxillary fenestra; pmpr, pendant medial process; pmr, promaxillary recess; po, surface for contact with the postorbital; popr, paroccipital process; pp, pendant process; pr, surface for contact with the prefrontal; PRE, prearticular; pre, surface for contact with the prearticular; PRO, prootic; pror, prootic recess; PS, parasphenoid; psf, posterior surangular foramen; pt, surface for contact with pterygoid; ptf, pterygopalatine fenestra; ptp, pterygoid process; ptyf, pterygoid flange; pvp, parietal ventral process; Q, quadrate; QJ, quadratojugal; qjpr, quadratojugal process; quc, quadrate cotylus; quf, quadrate foramen; retp, retroarticular process; rr, rostral ramus; sa, surface for contact with the surangular; saf, surangular adductor fossa; scr, subcondylar recess; sgr, stapedial groove; SO, supraoccipital; soc, supraoccipital crest; SPD, supradentary; SQ, squamosal; sq, surface for contact with the squamosal; sqpr, squamosal process; SUR, surangular; stf, supratemporal fossa; tf, temporal fenestra; vg, vertical groove; vo, surface for contact with vomer; vr, ventral ramus; wf, wear facet; III, IV, V, VII, XII, cranial nerves.

Postcranial skeleton

aI–IV, articulation for the first to fourth metatarsals; acdl, anterior centrodiapophyseal lamina; act, acetabulum; ast, astragalus; atr, accessory trochanter; ap, anterior process; asp, ascending process; bf, brevis fossa; bi, biceps tubercle; c, capitulum; ca, calcaneum; cdf, centrodiapophyseal fossa; cf, coracoid foramen; ch, chevron; clp, collateral lateral ligament pit; cmp, collateral medial ligament pit; cnc, cnemial crest; cpf, cupedicus fossa; cpol, centropostzygapophyseal lamina; cprl, centroprezygapophyseal lamina; cr, caudal rib; ctf, crista tibiofibularis; dg, dorsal goove; dp, diapophysis; dpr, dorsal process; ep, epipophysis; exg, extensor groove; exp, extensor pit; f, foramen; ffl, fibular flange; fh, femoral head; fi, fibula; ft, fourth trochanter; fxg, flexor groove; fxp, flexor pit; g, groove; gl, glenoid; hc, haemal canal; hcp, hooked coracoid process; hy, hypantrum; ict, incisura tibialis; IL, ilium; il, articulation for the ilium; isp, ischial peduncle; isc, ischial articulation; ivf, intervertebral foramen; lco, lateral condyle; li, interspinous ligament; lm, lateral malleolus; lr, lateral ridge; lt, lesser trochanter; mco, medial condyle; md, medial depression; mdc, mediodistal crest; mm, medial malleolus; ms, medial symphysis; nc, neural canal; ncs, neurocentral suture; nef, facet for neurapophysis; ns, neural spine; oc, facet for occipital condyle; odc, odontoid cavity; on, obturator notch; op, obturator process; pcd, pleurocentral depression; pcdl, posterior centrodiapophyseal lamina; pgr, posterior groove; pl, pleurocoel; pnr, pneumatic recess; po, postzygapophysis; pocdf, postzygapophyseal centrodiapophyseal fossa; podl, postzygodiapophyseal lamina; posdf, postzygapophyseal spinodiapophyseal fossa; pp, parapophysis; pr, prezygapophysis; prcdf, prezygapophyseal centrodiapophyseal fossa; prdl, prezygodiapophyseal lamina; pu, articulation for the pubis; pup, pubic peduncle; sab, supraastragalar buttress; sac, supraacetabular crest; sc, suture for the scapula; spol, spinopostzygapophyseal lamina; spof, spinopostzygapophyseal fossa; sprl, spinoprezygapophyseal lamina; sprf, spinoprezygapophyseal fossa; sr2–5, scar for sacral ribs; tr1-5,scar for transverse processes of sacral vertebrae; tu, tuberculum; vg, ventral groove; vp, ventral process; vk, ventral keel.

6.3.6. MATERIAL

The specimens herein described correspond to a set of cranial and postcranial remains collected in the Andrés fossil site during different fieldwork campaigns between 1988 and 2010. The specimens were mostly isolated and dispersed for about the ten square meters of the fossil site generally without association between them (Fig. 6.3.2). There are some exception such as a large concretion collected in 1988, which contained an articulated partial skeleton, including the pubes, a left isquium, femora, tibiae

and fibulae. Several duplicated elements of similar size were found among the theropod material collected in Andrés including an almost complete left ilium and a fragment of the pubic peduncle of a left ilium preserved in articulation with the pubes. Some duplicated elements of a much smaller individual were also recovered, including a fragment of a right frontal, a caudal vertebra, and several pedal phalanges. The smaller elements are approximately 44% de size of the equivalent larger specimens. This indicates a minimal number of three *Allosaurus* individuals in the Andrés fossil site.

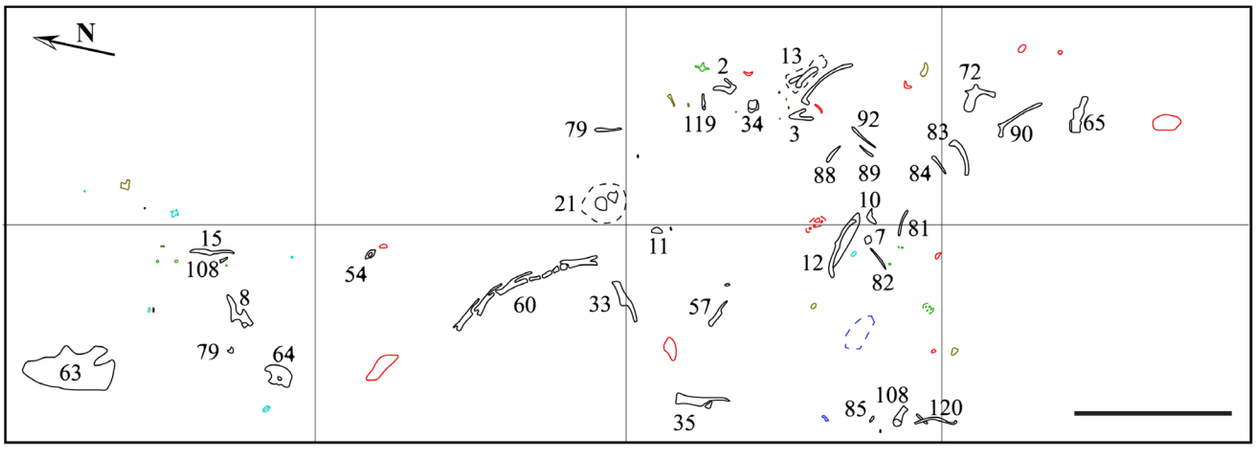

Figure 6.3.2. Quarry map of the excavation in Andrés, showing the position of the different elements found during the second fieldwork campaign (2005). Elements attributed to *Allosaurus* are marked in black and numbers refer to the number of each element (see text below). Scale bar: 100 cm.

Most of the cranial elements herein described were found in 2005 in the same sedimentary level and they have compatible size in order to belong to the same individual. These cranial elements represent the most complete theropod skull recorded in the Late Jurassic of the Lusitanian Basin (Fig. 6.3.3).

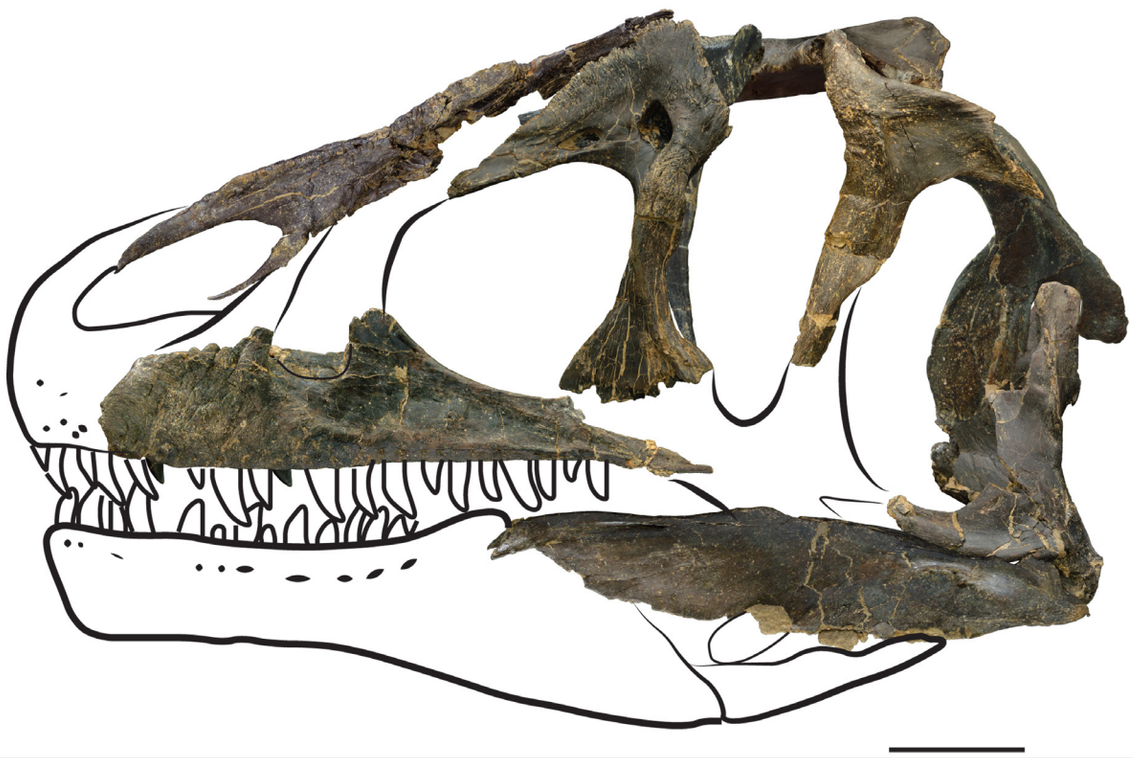

Figure 6.3.3. Cranial elements attributed to *Allosaurus* collected in Andrés. Some elements (nasal, prefrontal, squamosal, and surangular) were inverted for show the estimated reconstruction of the anatomy of the skull. Scale bar: 100 mm.

The specimens are housed in the collections of the Museu Nacional de História Natural e da Ciência da Universidade de Lisboa (Portugal). The cranial elements were compared with other *Allosaurus* and allosauroid specimens of different institutions as well as with other more basal theropods, for which cranial material is known (see Supplementary Table 6.3.1).

6.3.7. SYSTEMATIC PALAEONTOLOGY

Dinosauria Owen, 1841

Saurischia Seeley, 1887

Theropoda Marsh, 1881

Tetanurae Gauthier, 1986

Avetheropoda Paul, 1988

Allosauroidea Marsh, 1878

Allosaurus Marsh, 1877

Allosaurus europaeus Mateus, Walen and Antunes 2006

Holotype: ML415, part of the posterior end of a skull and sequence of three articulated cervical vertebrae and ribs (Mateus et al. 2006).

Horizon: Praia da Amoreira-Porto Novo Formation; upper Kimmeridgian, Late Jurassic.

Type Locality: Praia de Vale Frades, Lourinhã.

Emended diagnosis: Allosauroid theropod having the following autapomorphies: (i) no lacrimal-maxillary contact; (ii) ventral tip of the postorbital reaches the lower rim of the orbit; and (iii) dorsoventrally deep and forked posterior end of the maxilla.

Allosaurus cf. *europaeus*

Assigned material: A set of cranial and postcranial elements collected in the Andrés fossil site, including maxilla, nasal, lacrimals, prefrontal, postorbitals, frontals, palatines, quadrate, quadratojugal, squamosal, vomer, braincase, articular, surangulars, prearticular, angulars, supradentary and coronoid, isolated mesial and lateral teeth, intercentrum of the atlas, dorsal, sacral and caudal vertebrae, cervical and dorsal ribs, chevrons, coracoid, ilium, pubes, femora, tibiae, fibulae, astragalus and calcaneum, distal tarsal III, second, tird, and fourth metatarsals, and several phalanges (see text below).

6.3.8. DESCRIPTION AND COMPARISONS

6.3.8.1. Cranial skeleton

Maxilla. A well-preserved left maxilla, MNHNUL.P.AND22, was collected in the Andrés fossil. This specimen is dorsally incomplete with almost the entire ascending process broken, but preserved the articular surfaces for the premaxilla, lacrimal, and jugal (Fig. 6.3.4). The anterior maxillary body and the alveolar (= jugal ramus *sensu* Hendrickx and Mateus 2014a) are completely preserved. Also the maxillary body (*sensu* Hendrickx and Mateus 2014a) is complete and has seventeen alveoli with four erupting teeth in the second, fourth, sixth, and thirteenth alveoli. The alveoli extend to near the level of the articular surface for the lacrimal. The four anteriormost alveoli have rounded outlines, but become more oval, anteroposteriorly elongated and strongly mediolaterally compressed to the rear part of the maxilla (Fig. 6.3.4H).

The lateral surface of the maxilla is strongly ornamented by a series of thin grooves and crests and small foramina, especially along the anterior body. A row of large foramina is visible adjacent to the ventral margin of the maxilla extending from the anterior end to the level of the fifteenth alveolus. The ventral foramina are inside a groove from the level of the ninth alveolus to the posterior end, which become progressively deeper posteriorly. Other row of foramina starts near the mid-length of the anterior ramus bounding the anteroventral corner of the lateral antorbital fossa.

The maxillary anterior body is relatively short and squared-shaped in lateral view being slightly deeper than long. The surface for contact with the premaxilla is a broad and slightly concave surface in the anterior margin of the maxilla, which is bounded both laterally and medially by raised vertical crests extending anteriorly. The dorsal margin of the lateral crest probably forms the ventral border of the subnarial foramen, which would extend posterodorsally delimiting the ventral margin of the maxillary anteromedial process as in other *Allosaurus* specimens (Madsen 1976). In anterior view, a small foramen pierces the surface for articulation with the premaxilla at about the mid-height. The anterior body of the maxilla is somewhat incomplete dorsally lacking the ascending ramus and the anteromedial process. The lateral antorbital fossa occupies almost the entire lateral surface of the jugal ramus and most of the anteroposterior length of the base of the ascending ramus.

In medial view, the interdental plates are completely fused and are strongly ornamented by thin vertical crests and grooves (Fig. 6.3.4D). The individual interdental plates are nearly as deep as long and are bounded dorsally by a well-marked paradental groove (= nutrient groove *sensu* Hendrickx and Mateus 2014a), which extends along almost the entire length of the medial surface of the maxilla from the anteriormost margin to beneath the last alveolus. The paradental groove is straight and has a horizontal orientation. Small dental foramina (= nutrient foramina *sensu* Hendrickx and Mateus 2014a) are visible adjacent to the paradental groove at approximately the mid-length of each alveolus. The interdental plates have triangular ventral margins due to the presence of deep notches at its mid-length, which become more pronounced to the posterior part of the maxilla. In the last three alveoli these notches extend to the level of the paradental groove completely separating the interdental plates. The ventral margin of the interdental plates is well above the ventral margin of the maxillary lateral wall. Above the interdental plates, the medial wall of the maxilla is smooth, but shows an undulating surface (vertical interalveolar depressions *sensu* Brusatte and Sereno 2007). The medial surface of the maxilla preserves an elevated and subhorizontal dorsal ridge rising from the level of the posterior margin of the seventh alveoli. This ridge is broken anteriorly and only preserves a small fragment, but probably corresponds to the maxillary medial shelf. Posterior to the medial shelf, the maxilla preserves a fragment of the posterior lamina of the ascending process, which is slightly concave.

The jugal ramus is relatively low dorsoventrally and strongly tapers to the rear ending in a thin blunted point. The surface for contact with the palatine is a longitudinal groove extending on the mediodorsal surface of the jugal ramus from the level of the tenth alveoli to near the level of the last alveoli. This articulation is deep and bounded anteriorly by well-developed crests, becoming shallower to the rear. The posterior part of the jugal ramus has a thin blade rising from the lateral margin and projecting towards the rear to approximately the level of the last alveolus. This blade delimits a deep groove that is interpreted as the surface for articulation with the lacrimal. The dorsal surface of the jugal ramus has several small foramina, one inside the groove for the palatine and four distributed along the anteroventral margin of the medial antorbital fossa. Posterior to the last alveolus, the maxilla is mediolaterally thin with flat and slightly striated medial and lateral surfaces. The lateral surface of the jugal ramus has a deep longitudinal groove, extending slightly above the ventral margin of the maxilla, which represents the articulation for the jugal (Fig. 6.3.4B).

The ascending ramus is almost completely missing and only part of its base is preserved. Due this break, a smooth opening is visible in the dorsal surface of the maxillary anterior body at the level of the anterior lamina of the ascending ramus, which is interpreted as the promaxillary fenestra. This fenestra leads to a large fossa into the anterior end of the base of the ascending ramus. These openings correspond

to the maxillary sinus (*sensu* Madsen 1976 = maxillary antrum *sensu* Brusatte et al. 2009). Posterior to the promaxillary fenestra, a large opening corresponding to the maxillary fenestra occupies almost the entire lateral surface of the base of the ascending process. Other opening, interpreted as the posteromedial maxillary fenestra (*sensu* Hendrickx and Mateus 2014a), pierces the posterior end of the ascending ramus.

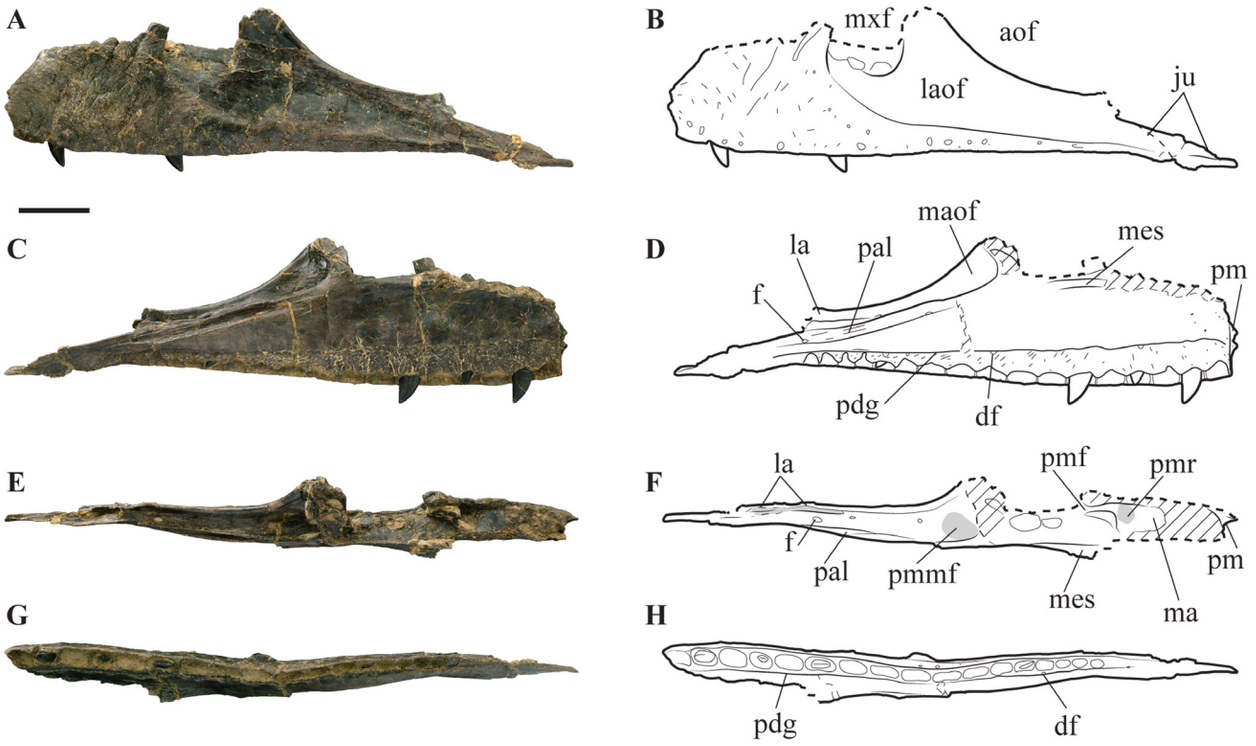

Figure 6.3.4. MNHNUL.P.AND22, left maxilla and corresponding interpretative drawing in lateral (A–B); medial (C–D); dorsal (E–F); and ventral (G–H) views. Scale bar: 50 mm.

MNHNUL.P.AND22 has a length similar to some large-sized *Allosaurus* specimens from the Morrison Formation (Gilmore 1920; Madsen 1976), but a rather lower depth (see Supplementary Table 6.3.2). This maxilla has seventeen alveoli corresponding to a number of teeth within the range known for *Allosaurus* in which the number of maxillary teeth varies from 14 to 17 with the most common situation being 16 teeth (Gilmore 1920; Madsen 1976; Chure 2000). However, Osborn (1903) mentions some specimens from the collections of the American Museum of Natural History with 18 maxillary teeth (Gilmore 1920). Madsen (1976) considered that variation in the number of maxillary teeth in *Allosaurus* would not be related with maturity or size of the specimen. Nevertheless, a small maxilla collected in the Upper Jurassic of Portugal and interpreted as belonging to a hatchling *Allosaurus* individual has thirteen teeth and based on this specimen it was proposed that the number of teeth would increase during ontogeny in this taxon (Rauhut and Fechner 2005).

The strongly tapering posterior end of the jugal ramus in MNHNUL.P.AND22 is a feature shared with most basal theropods, but distinct from *Monolophosaurus* (Brusatte et al. 2010a), *Zupaysaurus* (Arcucci and Coria 2003) and abelisaurids (e.g. Bonaparte et al. 1990) in which the maxilla maintains a relatively constant depth throughout their length.

The specimen collected in Andrés has a nearly vertical surface for contact with the premaxilla similar to *Allosaurus* (Gilmore 1920; Madsen 1976), *Neovenator* (Brusatte et al. 2008), *Monolophosaurus* (Brusatte et al. 2010a), and in at least some specimens of *Yangchuanosaurus* (Dong et al. 1983), but contrasting with the posterodorsally inclined suture of *Sinraptor* (Currie and Zhao 1993), *Acrocanthosaurus* (Harris 1998; Eddy and Clarke 2011), *Mapusaurus* (Coria and Currie 2006; Canale et al. 2014), *Eocarcharia* (Sereno

and Brusatte 2008), *Shaochilong* (Brusatte et al. 2010b), and *Carcharodontosaurus* (Brusatte and Sereno 2007). *Erectopus* shows a distinct morphology of the premaxillary suture in the maxilla being vertical ventrally, but posterodorsally oriented over the dorsal mid-height (Allain 2005a).

The presence of fused interdental plates is a feature shared with most allosauroids (Gilmore 1920; Madsen 1976; Rauhut 1995; Azuma and Currie 2000; Chure 2000; Rauhut and Fechner 2005; Coria and Currie 2006; Brusatte et al. 2008, 2010b, 2012; Canale et al. 2014). On the contrary, *Piatnitzkysaurus* (Rauhut 2007), *Monolophosaurus* (Brusatte et al. 2010a), *Erectopus* (Allain 2005a), and *Sinraptor* (Currie and Zhao 1993) have unfused maxillary interdental plates. The individual interdental plates are nearly as deep as long, as occur in *Allosaurus* and *Sinraptor* (Chure 2000). The presence of interdental plates more than twice as deep as long is a feature shared by most carcharodontosaurian allosauroids, with the exception of *Neovenator* (Carrano et al. 2012; Brusatte et al. 2009, 2012).

The antorbital fossa in MNHNUL.P.AND22 occupies most of the depth of the maxillary jugal ramus and is bounded by a low crest that separates this fossa from the rugose lateral surface of the maxilla. This is the typical condition for allosauroids (e.g. *Allosaurus*, *Eocarcharia*, *Neovenator*, and *Sinraptor*) and is quite different from the reduced fossa of some carcharodontosaurids such as *Acrocanthosaurus*, *Carcharodontosaurus*, *Giganotosaurus*, and *Mapusaurus* (Currie and Zhao 1993; Brusatte et al. 2008). Anteriorly, the antorbital fossa has a circular ventral margin delimited by a low and poorly defined ridge similar to the condition in other allosauroids (e.g. *Allosaurus* and *Sinraptor*) and *Monolophosaurus* whereas it is squared in *Neovenator*, *Eocarcharia*, *Afrovenator*, and *Dubreuillosaurus* (Brusatte et al. 2008, 2010a). The morphology and position of the ridge that marks the anteroventral margin of the antorbital fossa extending along the ventral margin of the jugal ramus and rising slightly anterodorsally to the level of the maxillary fenestra has been considered a diagnostic feature for *Allosaurus* (Britt 1991; Chure 2000).

Almost the entire ascending process of MNHNUL/P.AND22 is broken, but a preserved fragment of the posterior end suggests a relatively posterior position of the process, which would result in a short, but distinct anterior body of the maxilla similar to those of *Allosaurus* (Madsen 1976) and *Kelmayisaurus* (Brusatte et al. 2012). However, in *Allosaurus* the morphology of the maxillary anterior end is somewhat variable with some specimens (e.g. DNM 2560 and MOR 693) having slightly elongated anterior maxillary body, but in other specimens (e.g. BYU 725 5126) the anterior ramus is squared and slightly deeper than long (Rauhut 2003; Brusatte et al. 2008). In most carcharodontosaurids (e.g. *Acrocanthosaurus*: Eddy and Clarke 2011; *Eocarcharia*: Sereno and Brusatte 2008; *Carcharodontosaurus*: Rauhut 1995; Sereno et al. 1996; and *Mapusaurus*: Coria and Currie 2006; Canale et al. 2014) as well as in *Sinraptor* (Currie and Zhao 1993) and *Erectopus* (Allain 2005a), the maxillary anterior body is nearly indistinct and the anterior margin of the maxilla is almost continuous with the ascending process. On contrary, the maxillary anterior body is approximately as long as deep or even slightly longer in *Neovenator* and *Monolophosaurus* (Brusatte et al. 2008, 2010a).

In lateral view, the promaxillary fenestra in MNHNUL/P.AND22 is completely occluded by the lateral lamina of the ascending process as in *Allosaurus* and *Giganotasaurus* (Madsen 1976; Chure 2000), whereas this fenestra is broadly visible in lateral view in *Acrocanthosaurus*, *Eocarcharia*, *Yangchuanosaurus* and *Sinraptor* (Brusatte et al. 2008).

A posteromedial maxillary fenestra as is present in the specimen from Andrés is shared with *Acrocanthosaurus*, *Sinraptor*, *Carcharodontosaurus* and many non-allosauroid theropods (Eddy and Clarke 2011). This fenestra is considered absent in some specimens of *Allosaurus* and *Mapusaurus* (Eddy and Clarke 2011), but is figured in a maxilla (USNM 8335) of *Allosaurus fragilis* (Hendrickx and Mateus 2014a).

The palatal articular surface in MNHNUL/P.AND22 extends up to the level of the tenth alveolus, which is much posterior than in most other allosauroids in which this contact extends to the eight or seventh alveolous (Eddy and Clarke 2011).

The straight paradental groove in the maxilla collected in Andrés is similar to *Sinraptor* and *Allosaurus*, whereas in *Neovenator*, *Eocarcharia*, *Carcharodontosaurus*, *Shaochilong*, *Mapusaurus*, and some megalosaurids this groove is sinuous-shaped (Carrano et al. 2012; Eddy and Clarke 2011).

Nasal. An almost complete right nasal, MNHNUL.P.AND1, was collected in a block with elements of the posterior part of a left mandible. The nasal is well preserved, but was somewhat broken during fieldworks and the posterodorsal part is badly distorted especially at the level of the nasal lateral crest (Fig. 6.3.5). The bifurcating anterior part of the nasal consists of the premaxillary (dorsal) and maxillary (ventral) processes. These processes form the posterodorsal rim of the external naris, which has an oval and anteroposteriorly elongate shape. The dorsal ramus is incomplete, but it clearly shows a deep bifurcation that would receive the anterodorsal process of the premaxilla. This ramus is significantly longer and more robust than the ventral one. The ventral ramus has a shallow longitudinal groove along the ventral margin that represents the surface for the articulation with the maxilla. To the rear, this ramus has a small process projecting ventrally and separated from the ventral margin of the nasal body by a deep notch (Fig. 6.3.5G–J). This process is similar to the naso-maxillary process described in other allosauroids (Eddy and Clarke 2011).

In lateral view, a well-developed lateral crest extends along the dorsal margin of the nasal (Fig. 6.3.5B). A deep concavity divides this crest in an anterior, lower crest and a slightly higher and more ornamented posterior one. The posterior crest projects dorsomedially and corresponds to the lateral crest of the nasal typical in most theropods. To the rear, the lateral crest ends in a deep slot that is interpreted as the surface for articulation with the anterior ramus of the lacrimal. The lateral margin of the dorsal surface is ornamented by a series of well-developed ridges and grooves that continue up to the surface for articulation with the dorsal margin of the lacrimal. These ridges probably would create a continuous ornamentation similar to that of *Allosaurus* (Madsen 1976).

At approximately the anteroposterior mid-length, the nasal is broken allowing see the internal structure with several large cavities, which seems connect to each other. The lateral surface of the nasal has a series of well-developed foramina that pierce the anteroventral end and are placed in a smooth and shallow concavity corresponding to the extension of the antorbital fenestra into the nasal. In dorsal view, the nasal is an anteroposteriorly long and transversely narrow element that slightly expands anteriorly forming a low crest that arises near the base of the dorsal anterior ramus extending to the rear along about 210 mm of the dorsolateral margin of the nasal.

The medial surface of the nasal is smooth for most of the preserved anterior part and has a well-developed crest that arises from the anterior end of the dorsal ramus. This crest projects posteroventrally up to approximately the mid-length of the nasal corresponding to the medial symphysis of the nasal (Fig. 6.3.5D). Posterior to the level of the base of the ventral ramus, the medial symphysis has a flat medial margin, which is interpret as the surface for the articulation with the opposite nasal. The medial symphysis delimits a shallow and broad concavity that occupies almost the entire anterior end of the nasal medial surface. Most of the posteroventral part of the nasal is broken, but it preserves part of the anterior end and the suture for the maxilla. This suture is a shallow groove extending along the ventromedial surface of the nasal and is bounded dorsally by a low ridge subparallel to the nasal ventral margin. Ventrally, the ventral ramus has a shallow longitudinal groove that corresponds to the most anterior end of the suture for the maxilla and is separated from the nasal body by a small notch. Just dorsoposteriorly to this notch the medial surface of the nasal has a deep opening that pierces the nasal with an anterodorsal orientation (Fig. 6.3.5G).

To the rear, the nasal is a dorsoventrally thin blade that projects ventromedially and has a shallow concave dorsal surface bounded laterally by a prominent longitudinal ridge. The ventral surface has a series of thin longitudinal ridges extending along the flat posterior end of the nasal, which is interpreted as the area where the nasal would overlap the frontal (Fig. 6.3.5F). In the posterolateral end, the nasal has a process projecting posteriorly, which delimits a deep groove that would receive the anterior ramus

of the lacrimal. This process is broken, but the preserved part suggests that it would be relatively robust. Posterior to the lacrimal process, the nasal has an almost flat surface extending along the lateroventral margin, which is interpreted as the articular surface for the prefrontal (Fig. 6.3.5B).

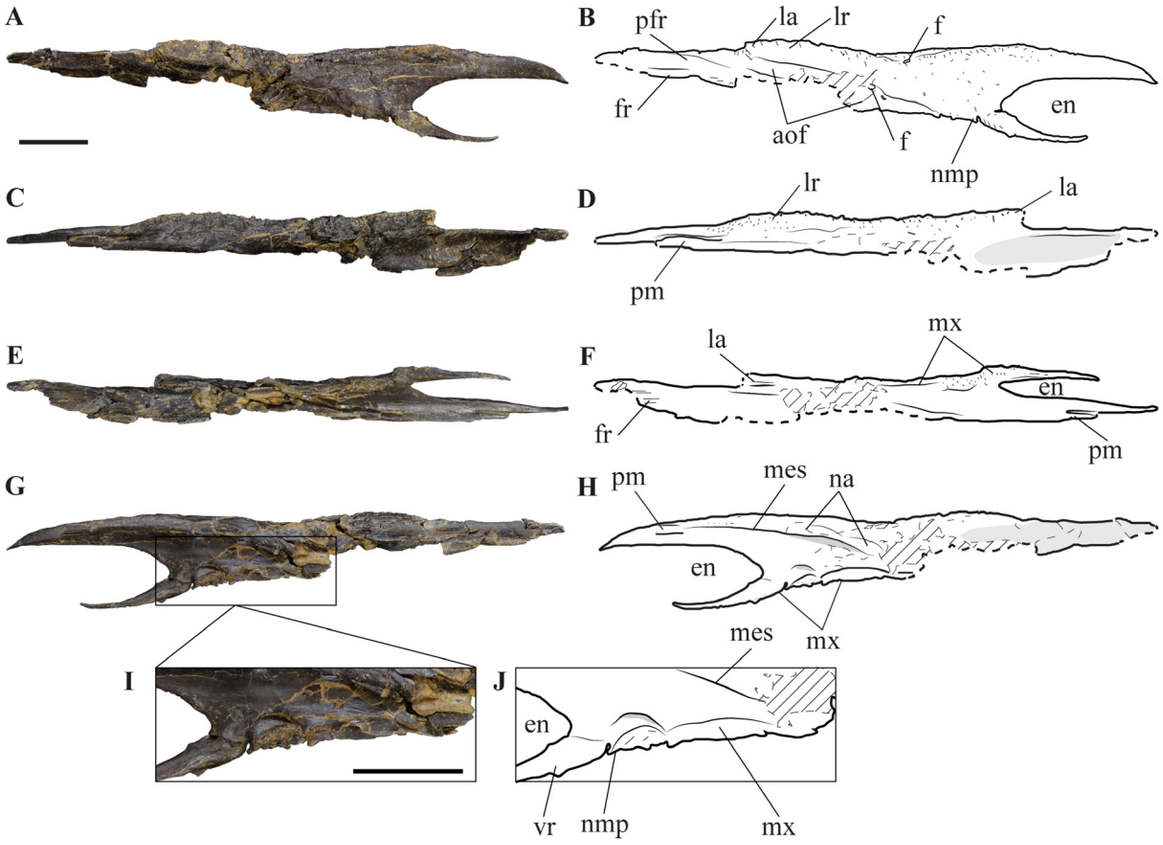

Figure 6.3.5. MNHNUL.P.AND1, right nasal and corresponding interpretative drawing in lateral (A–B); dorsal (C–D); ventral (E–F); and medial (G–H) views; I–J, detail of the ventral margin of the nasal in medial view showing the structure interpreted as the naso-maxillary process. Scale bar: 50 mm.

The Andrés specimen has unfused nasals, which is the typical condition for most allosauroids, whereas the nasals are fully or partially fused in most tyrannosaurines (Brochu 2003; Hurum and Sabath 2003) and in *Monolophosaurus* (Brusatte et al. 2010a). MNHNUL.P.AND1 has a well-developed antorbital fossa extending into the lateral surface of the nasal, a feature that has been considered as a synapomorphy for Avetheropoda (e.g. Sereno et al. 1994; Chure 2000; Brusatte and Sereno 2008). However, the participation of the nasal in the antorbital fossa is also present in *Cryolophosaurus* (Smith et al. 2007), *Dilophosaurus* (Welles 1984), and *Monolophosaurus* (Brusatte et al. 2010a), but is absent in *Acrocanthosaurus* (Brusatte et al. 2008; Eddy and Clarke 2011). In *Monolophosaurus*, *Allosaurus*, and *Sinraptor* the nasal antorbital fossa is broadly exposed in lateral view, whereas it is reduced in *Neovenator*, and restricted to the ventral surface of the nasal in *Carcharodontosaurus*, *Giganotosaurus*, and *Mapusaurus* (Brusatte et al. 2010a).

MNHNUL.P.AND1 has a low and poorly-developed lateral crest and the dorsal surface is mostly smooth. The presence of nasal crests is a character shared by several theropods, including *Dilophosaurus* (Welles 1984), *Ceratosaurus* (Gilmore 1920; Madsen and Welles 2000), *Monolophosaurus* (Brusatte et al. 2010a), *Allosaurus* (Gilmore 1920; Madsen 1976; Chure 2000), *Sinraptor* (Currie and Zhao 1993), *Acrocanthosaurus* (Currie and Carpenter 2000; Eddy and Clarke 2011), *Carcharodontosaurus* (Brusatte and Sereno 2008), *Yangchuanosaurus* (Dong et al. 1983), *Concavenator* (Ortega et al. 2010), *Neovenator* (Brusatte et al. 2008), and *Mapusaurus* (Coria and Currie 2006). However, in *Ceratosaurus* the nasal crest is restrict, developing a horn-like structure distinct from the crest of most allosauroids, which extends for most of the length of the nasal dorsal surface (Chure 2000; Madsen and Welles 2000). Most

allosauroids have strongly rough and high nasal lateral crests, but they are low and relatively smooth in *Acrocanthosaurus*, *Neovenator*, and *Sinraptor* (Dong et al., 1983; Currie and Zhao 1993; Chure 2000; Currie and Carpenter 2000; Brusatte et al. 2008, 2010; Eddy and Clarke 2011; Carrano et al. 2012). As in MNHNUL.P.AND1, most *Allosaurus* specimens have low and relatively smooth nasal crests similar to those of *Acrocanthosaurus* and *Sinraptor*. Nevertheless, this feature is somewhat variable in *Allosaurus* and some specimens have more developed crests (e.g. USNM4734: Gilmore 1920; BYU759 2028: E.M. pers. obs. 2010). This variability in the development of the nasal lateral crest has been interpreted as related with intraspecific variability, namely ontogeny and/or sexual dimorphism (Chure 2000).

The holotype of the Portuguese species *Allosaurus europaeus* (ML 415) has a much higher and rough nasal crest than MNHNUL.P.AND1. In ML 415 the lateral crest of the nasal projects dorsally well above the skull roof and also laterally, producing a prominent ridge that extends into the dorsal margin of the antorbital fossa. This feature is one of the proposed diagnostic characters for this species (Mateus et al. 2006). However, the development of the nasal lateral crest shows some variability among *Allosaurus* as was discussed above and thus probably this feature cannot be considered as part of the diagnosis. In ML 415, the nasal crest projects ventrally covering partially the anterodorsal part of the antorbital fossa, but this fossa still well visible in lateral view as occur in MNHNUL.P.AND1 as well as in *Allosaurus* (Gilmore 1920; Madsen 1976; Chure 2000) and *Sinraptor* (Currie and Zhao 1993), whereas in carcharodontosaurids (e.g. *Carcharodontosaurus*, *Giganotosaurus*, and *Mapusaurus*) the nasal crest projects ventrolaterally such that the antorbital fossa is only visible in ventral view (Sereno et al. 1996; Coria and Currie 2006; Brusatte et al. 2010a).

The lateral surface of MNHNUL.P.AND1 is slightly convex and does not have a narial fossa bounded by well-developed crests as occur in *Acrocanthosaurus* (Currie and Carpenter 2000; Eddy and Clarke 2011), *Carcharodontosaurus* (Rauhut 1995), *Concavenator* (Ortega et al. 2010; Eddy and Clarke 2011), *Mapusaurus* (Coria and Currie 2006), *Sinraptor* (Currie and Zhao 1993), and *Tyrannosaurus* (Brochu 2003). This poorly developed narial fossa is a feature shared with *Allosaurus* (Madsen 1976; Chure 2000), and *Neovenator* (Brusatte et al. 2008). The ventral margin of MNHNUL.P.AND1 has a small flange projecting anteroventrally that is interpreted as equivalent to the naso-maxillary process described in *Acrocanthosaurus* and *Carcharodontosaurus* (Eddy and Clarke 2011). This process has been considered absent in other theropods (Eddy and Clarke 2011), but its fragile nature suggests that it may be easily broken or distorted by taphonomic processes, so this feature should be seen cautiously.

The nasal collected in Andrés has the lateral and medial surfaces badly broken at the level of the nasal crest displaying a hollow internal structure, which indicates that the nasal is strongly pneumatic as in most allosauroids, including *Sinraptor* (Currie and Zhao 1993), *Allosaurus* (Gilmore 1920; Madsen 1976; Chure 2000), *Shaochilong* (Brusatte et al. 2010b), *Concavenator* (Ortega et al. 2010), *Giganotosaurus* (Carrano et al. 2012), *Mapusaurus* (Coria and Currie 2006), and *Neovenator* (Brusatte et al. 2008). Nasal pneumatic foramina are apparently absent in *Carcharodontosaurus* (Rauhut 1995) and *Acrocanthosaurus* (Eddy and Clarke 2011). The number and morphology of the nasal foramina is highly variable among allosauroids and asymmetry of pneumatic structures is not uncommon (Chure 2000). Two pneumatopores on the nasal is possibly the most common situation among allosauroids (Brusatte et al. 2010a). However, in *Neovenator* there is a single large opening (Brusatte at al. 2008, 2010a) and *Allosaurus* might have one, two or even three foramina in the nasal (Madsen 1976; Currie and Zhao 1993; Chure 2000). The holotype of *A. europaeus* has two large pneumatopores in the preserved right nasal and the presence of an "anterior foramen twice the size of the posterior" was considered a diagnostic feature for the species (Mateus et al. 2006). The authors misinterpreted the orientation of the nasal and considered the anterior foramen larger than the posterior one, whereas this is in fact the inverse situation (fig.6.3.7F). Because the number and size of nasal pneumatopores and foramina is highly variable among allosauroids some authors (e.g. Coria and Currie 2006; Chure 2000) suggest that characters related with this feature should be treated caustiosly in phylogenetic analyses. ML 415 does not seem to differentiate significantly in this feature from some North American *Allosaurus* specimens.

Lacrimal. Almost complete right, MNHNUL.P.AND2, and left, MNHNUL.P.AND3, lacrimals were found in the Andrés fossil site (Fig. 6.3.6). The right lacrimal is the most complete lacking only a small section of the ventral end of the preorbital ramus. The left lacrimal also lacks a small part of the ventral end of the preorbital ramus. In lateral view, the lacrimal has the shape of an inverted L as in most theropod dinosaurs. It consists of an almost straight ventral process (preorbital ramus) and an anteriorly tapered dorsal process (rostral ramus) projecting anteroventrally. The preorbital ramus articulates ventrally with the jugal and with the posterodorsal end of the maxilla and the rostral ramus articulates with the nasal laterally and with the ascending process of the maxilla ventrally. The rostral ramus is long, almost as long as the dorsoventral length of the preorbital ramus, but is dorsoventrally narrow and transversely thin. The anterior part of the rostral ramus projects laterally delimiting a shallow and longitudinal concavity that extends along the ventral surface representing the contact with the nasal. The dorsal margin of the anterior end of the rostral ramus has a small longitudinal notch, which is interpreted as the surface for articulation with the ascending ramus of the maxilla. Between the surfaces for the articulation with the nasal and the articulation with the maxilla, the rostral ramus of the lacrimal has a broad and longitudinal canal that pierce the dorsal surface with an anteroposterior orientation. A similar canal is described in *Sinraptor* and is interpreted as a blood vessel canal (Currie and Zhao 1993).

The preorbital ramus is almost straight and has a circular cross-section at mid-height, but sharply expands distally forming a fan-like, transversely thin, and anteroposteriorly broad blade. The ventral end of the preorbital ramus is mostly flat in lateral view. In the right lacrimal, a small notch is visible adjacent to the posteroventral margin of the ventral expansion, which is interpreted as the suture for the jugal (Fig. 6.3.6C). The dorsal extension of the suture for the jugal in the preorbital ramus is difficult to interpret, but a small vertical ridge extending dorsoanteriorly in the lateral surface is interpret as the posterior limit of this suture. The anteroventral end of the ventral expansion of the preorbital ramus has a shallow longitudinal concavity that is interpreted as the suture for the maxilla.

Dorsally, the preorbital ramus shows a strongly rough area near the base of the cornual process, which occupies almost the entire dorsal end of the lateral surface and that is bounded by low posterior and anterior crests (Fig. 6.3.6C). The anterior crest projects posteroventrally connecting with the ridge that forms the posterior margin of the suture for the jugal. The posterior crest projects to the rear and extends slightly into the orbital fenestra. The posterior surface of the preorbital ramus has a deep vertical groove, inside which two foramina are visible with the dorsal foramen slightly larger than the ventral one (Fig. 6.3.6H). This posterior groove and associated foramina correspond to the naso-lacrimal canal (*sensu* Eddy and Clarke 2011) or to the lacrimal duct (*sensu* Currie and Zhao 1993). Small foramina are also present on the anterior surfaces of the preorbital ramus (three on the right lacrimal and one on the left). On the right lacrimal these foramina are inside a shallow, but well-marked vertical groove, whereas in the left lacrimal the anterior surface of the preorbital ramus is rounded and without any visible groove (Fig. 6.3.6K–M). In medial view, the preorbital ramus has a well-marked vertical ridge projecting anterodorsally and delimiting a narrow vertical groove at approximately the mid-height of the ramus (Fig. 6.3.6D). This groove is similar to the medial vacuity described in the lacrimal of *Sinraptor* (Currie and Zhao 1993).

The dorsal surface of the lacrimal has a well-developed and strongly ornamented cornual process, which is triangular in lateral view, longer than deep and with a somewhat tapered dorsal margin. The lateral and medial surfaces of this process have several well-marked vertical crests and grooves resulting in an extremely rough appearance. These crests and grooves also extend along most of the dorsal margin of the rostral ramus. The dorsolateral surface of the lacrimal has two large pneumatic recesses; the posterior one is vertically elliptical and pierces the base of the cornual process, whereas the anterior one is horizontally elliptical and pierces the posterior end of the rostral ramus. The posterior recess on the left lacrimal is much larger than that on the right lacrimal. In the later, a vertical and relatively thin blade separates the recesses, whereas in the left lacrimal they are separated by a wider surface. The morphology of the recesses is also distinct on the right and left lacrimals. The anterior recess on the right lacrimal is

subdivided by a thin, vertical septum, which is not present in the left lacrimal. Besides, the right lacrimal has a third smaller foramen in the anterior end of the rostral ramus that is not present in the left one (Fig. 6.3.6A–C). In anterior view, two grooves separated by a thin crest at the base of the cornual process represent the articulation for the prefrontal. The medial surface of the lacrimal is mostly smooth except in the cornual process.

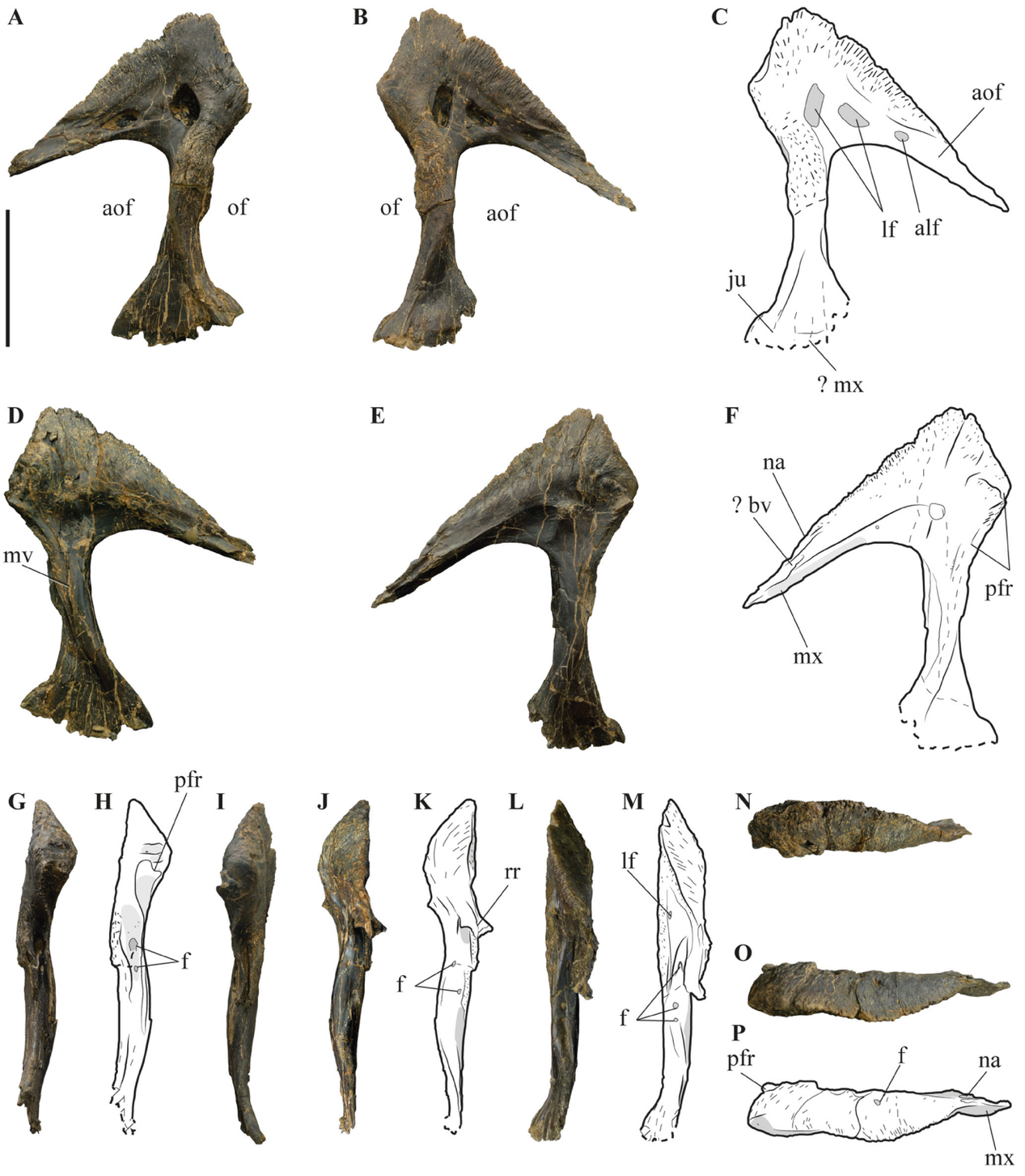

Figure 6.3.6. Lacrimals collected in Andrés and corresponding interpretative drawing. (A, D, G–H, J–K, N), left lacrimal MNHNUL.P.AND3; (B–C, E–F, I, L–M, O–P), right, MNHNUL.P.AND2, lacrimal in lateral (A–C); medial (D–F); posterior (G–I); anterior (J–M); and dorsal (N–P) views. Scale bar: 100 mm.

The lacrimals collected in Andrés have similar sizes and compatible morphology suggesting that they probably belong to the same individual. These elements are similar to other *Allosaurus* specimens described in the Morrison Formation, including in the relative proportions and orientation of the preorbital and rostral rami, and the morphology of the cornual process (Gilmore 1920; Madsen 1976; Chure 2000). A lacrimal cornual process is absent in most theropod dinosaurs and is variably developed within Allosauroidea. This process is low in *Sinraptor* (Currie and Zhao 1993), *Concavenator* (Ortega et al. 2010), *Acrocanthosaurus* (Currie and Carpenter 2000; Eddy and Clarke 2011), *Giganotosaurus* (Sereno et al. 1996; Rauhut 2003), and *Carcharodontosaurus* (Holtz 1998), but is slightly more developed in *Yangchuanosaurus* (Dong et al. 1983). A well-developed cornual process, which is longer than deep and projecting well above the skull table, has been considered as an exclusive character for *Allosaurus* among allosauroids (Chure 2000). A similarly well-developed cornual process arose independently in *Ceratosaurus* (Chure 2000; Madsen and Wells 2000), in *Monolophosaurus* (Brusatte et al. 2010a) and in *Cryolophosaurus* (Smith et al. 2007). However, the morphology of this process is somewhat variable among the *Allosaurus* specimens from the Morrison Formation. Based on different morphologies of the lacrimal cornual processes, it was suggested that some *Allosaurus* specimens from Dry Mesa Quarry, Garden Park and other localities from the Morrison Formation of similar age might belong to a distinct species from those known in slightly older localities mainly in the Cleveland-Lloyd Dinosaur Quarry and Dinosaur National Monument (Britt 1991). The specimens from Dry Mesa Quarry (BYUVP 5125: Britt 1991) and Garden Park (USNM 4734: Gilmore 1920) have lacrimal cornual processes with distinct sharply pointed apexes (Fig. 6.3.7B). In contrast, lacrimals collected in Bone Cabin Quarry (AMNH 666: Gilmore 1920) as well as in the Cleveland-Lloyd Dinosaur Quarry and in the Dinosaur National Monument (UUVP 6000: Madsen 1976; DINO 11541: Chure 2000) have blunt, rounded apexes (Fig. 6.3.7C–E). However, the presence of two distinct morphotypes of lacrimals has been also recognized among *Allosaurus* from the Cleveland-Lloyd Dinosaur Quarry and ome authors proposed that these differences would be related with intraspecific variability (Chure 2000).

The presence of large lateral pneumatic openings adjacent to the cornual process of the lacrimal is a feature common in theropod dinosaurs and has been considered a synapomorphy for Tetanurae (Sereno et al. 1994, 1996; Chure 2000). It has been suggested that these fossae in *Allosaurus* would have contained specialized lacrimal glands to keep the eye moist (Madsen 1976). However, more recently these openings have been interpreted as part of the subsidiary diverticulum of the paranasal pneumaticity (Currie and Zhao 1993; Witmer 1997). Usually, a single large pneumatic fossa is present in the lacrimal of *Allosaurus* (Madsen 1976). However, two smaller fossae are described in DINO 11541 (Chure 2000), which was considered a distinctive character of *Allosaurus* "*jimmadseni*" relative to *A. fragilis*. Nevertheless, this feature is also found in other *Allosaurus* specimens from Dry Mesa Quarry (BYUVP 5125: Britt 1991; see Fig. 6.3.7B) and Garden Park (USNM 4734: Gilmore 1920). The lacrimals collected in Andrés show two pneumatic fossae with size and position similar to these specimens from Dry Mesa Quarry and Garden Park.

The holotype of *Allosaurus europaeus* has the lacrimal cornual process slightly incomplete and distorted. In lateral view, it is lower and more rounded than in the specimens from Andrés (Fig. 6.3.7F). The narrow morphology of this process was considered a diagnostic character for this species (Mateus et al. 2006). However, the morphology of ML 415 is not significantly different from other *Allosaurus* specimens from the Morrison Formation and is compatible with the variability known for this taxon (Fig. 6.3.7). ML 415 differs from the specimens from Andrés in the presence of a single, large pneumatic fossa. However, this feature is highly variable among *Allosaurus* as was discussed above and thus this difference should be seen cautiously.

The rostral and postorbital rami of the lacrimals collected in Andrés make an angle of approximately 70° as is common in most large theropod dinosaurs with the exception of *Dubreuillosaurus* (Allain 2005b), *Torvosaurus* (Britt 1991), *Zupaysaurus* (Arcucci and Coria 2003), and coelophysids (Sues et al. 2011), which have nearly perpendicular lacrimal rami, and spinosaurids (Charig and Milner 1997; Brusatte et al. 2010b) in which the lacrimal rami form an acute angle. The rostral ramus of the lacrimals

from Andrés is almost straight in dorsal view as occur in *Allosaurus* (Gilmore 1920; Madsen 1976; Chure 2000) and *Sinraptor* (Currie and Zhao 1993). Instead, in *Acrocanthosaurus*, *Carcharodontosaurus* and *Giganotosaurus* (Chure 2000; Eddy and Clarke 2011), this ramus has a ventral lamina projecting laterally and delimiting a slightly concave surface, which corresponds to the extension of the antorbital fossa into the lacrimal in the distal end of the ramus.

In posterior view, the preorbital ramus has distinct medial and lateral layers separated by a deep sulcus, whereas the anterior margin is mostly rounded in the left lacrimal, but has a small concave surface ventrally in the right one. This morphology is distinct from most carcharodontosaurids in which a deep sulcus is present along the anterior margin of the postorbital process (Eddy and Clarke 2011). This character is somewhat variable between the right and the left lacrimals from Andrés, but the anterior groove in the right lacrimal is much restricted and less developed than that of more derived allosauroids and instead is more similar to *Sinraptor* (Currie and Zhao 1993), *Allosaurus* (Madsen 1976; Chure 2000), and *Monolophosaurus* (Brusatte et al. 2010a). The posterior lateral layer of the preorbital ramus in the specimens of Andrés is slightly projected into the orbital fenestra (Fig. 6.3.5). However, this projection is significantly less developed than in *Acrocanthosaurus*, *Giganotosaurus* or *Mapusaurus* (Coria and Currie 2006; Eddy and Clarke 2011). In contrast, the posterior margin of the lacrimal in *Monolophosaurus* (Brusatte et al. 2010a), *Concavenator* (Eddy and Clarke 2011), *Yangchuanosaurus* (Dong et al. 1983), and *Sinraptor* (Currie and Zhao 1993) is nearly straight or slightly convex. In *Allosaurus*, this feature is somewhat variable with most specimens showing a concave posterior margin of the lacrimal preorbital ramus, whereas some specimens (e.g. DINO 11541: Chure 2000 and BYU725 116169: Fig. 6.3.7A) have a short process in the posterodorsal margin of the lacrimal projecting into the orbital fenestra similar to the specimens from Andrés. The posterior margin of the preorbital ramus in both lacrimals has at least two openings. The larger of these openings probably corresponds to the naso-lacrimal canal and the other to an "orbital recess" (*sensu* Witmer 1997). The presence of similar foramina has been described in *Allosaurus* (Gilmore 1920; Madsen 1976; Chure 2000), *Sinraptor* (Currie and Zhao 1993), and *Mapusaurus* (Coria and Currie 2006). In *Acrocanthosaurus* (Eddy and Clarke 2011) a single foramen pierces the posterior margin of the preorbital ramus.

The preorbital ramus in the lacrimals collected in Andrés is ventrally incomplete, but they preserve part of the articular surfaces for the jugal and for the maxilla (Fig. 6.3.6). The lacrimal contacts the maxilla ventrally in *Allosaurus* (Madsen 1976; Chure 2000) and *Ceratosaurus* (Madsen and Welles 2000), but these elements are separated by the jugal in *Monolophosaurus* (Brusatte et al. 2010b), *Sinraptor* (Currie and Zhao 1993), *Yangchuanosaurus* (Dong et al. 1983), and *Acrocanthosaurus* (Eddy and Clarke 2011). Also, the lacrimals from Andrés does not have an articulation for the postorbital suggesting that these elements would be separated as occur in *Sinraptor* (Currie and Zhao 1993), *Allosaurus* (Madsen 1976; Chure 2000), and *Monolophosaurus* (Brusatte et al. 2010a). On contrary, in *Acrocanthosaurus*, *Giganotosaurus*, *Carcharodontosaurus*, and *Mapusaurus* the posterior margin of the cornual process of the lacrimal contacts with the postorbital (Eddy and Clarke 2011).

In the holotype of *A. europaeus* the lacrimal is interpreted as being separated from the maxilla by the jugal thus the absence of lacrimal-maxillary contact is considered as an autapomorphy for the species (Mateus et al. 2006). However, the distal end of the lacrimal is similar to those of the specimens from Andrés and to other *Allosaurus* from the Morrison Formation (Fig. 6.3.7). Based on this morphology it was previously proposed that the putative suture between the lacrimal and jugal in ML 415 is in fact a fracture and that the lacrimal in fact would articulate with the maxilla as is typical in *Allosaurus* and most allosauroids (Malafaia et al. 2007).

Prefrontal. A fairly complete right prefrontal, MNHNUL.P.AND5, was collected in Andrés (Fig. 6.3.8). This is a T-shaped element that comprises a long ventral ramus and a shorter dorsal ramus. The ventral ramus is a blade-shaped and transversely thin process that strongly tapers ventrally. The dorsal ramus is also a transversely thin and distally tapered process that projects anteroventrally making an acute angle with the

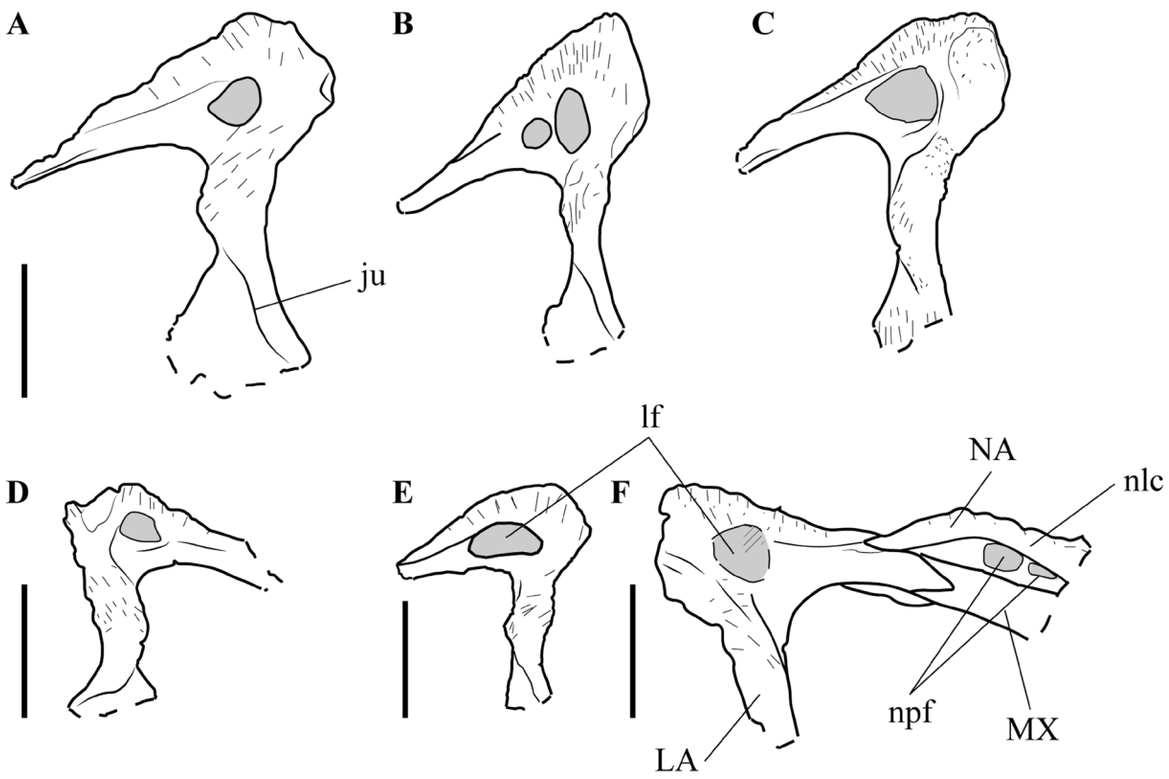

Figure 6.3.7. Interpretative drawing of lacrimals of *Allosaurus* from the Morrison Formation and Lusitanian Basin in lateral view showing the variability in the morphology of this element among this taxon. (A), left lacrimal, BYU 11619 from Dry Mesa Quarry; (B), left lacrimal, BYU 5125 from Dry Mesa Quarry showing a sharply pointed cornual process; (C), left lacrimal, UMNH VP 16664, from Cleveland Lloyd Dinosaur Quarry; (D), right lacrimal, UMNH VP 9472, from Cleveland Lloyd Dinosaur Quarry; (E), left lacrimal UNNH VP 11765 from Cleveland Lloyd Dinosaur Quarry; (F), right lacrimal articulated with part of the nasal and maxilla, ML415, from Praia de Vale Frades. Scale bar (A–D, F): 100mm; (E): 50 mm.

dorsal end of the ventral process. The prefrontal articulates with the lacrimal laterally and ventrally, with the frontal posteromedially and to the rear, and with the posterior process of the nasal to the front. In lateral view, a prominent vertical ridge projects from the dorsal end of the prefrontal and near the junction of the ventral and dorsal rami. This ridge delimits a deep and funnel-like concavity that would receive the prominent triangular process on the medial surface of the lacrimal (Fig. 6.3.8D). The prefrontal connects with the lacrimal also along most of the dorsoventral length of the ventral process (Fig. 6.3.8K–N). Medially, a shallow and broad concavity opens between the dorsal and ventral rami. Inside this concavity, there are two low crests projecting anterodorsally and a small foramen adjacent to the dorsalmost crest (Fig. 6.3.8B). Dorsally to this medial concavity, the prefrontal has a rough margin corresponding to the surface for the articulation with the frontal. The articular surface for the frontal projects from the posterodorsal end of the prefrontal up to the medial surface of the dorsal ramus. The dorsal ramus has a well-developed blade extending ventrally, which forms a deep anteroposterior slot near the junction of both rami.

In dorsal view, the dorsal ramus is smooth, slightly concave, and transversely thin, which indicate a reduced exposure of the prefrontal in the skull roof. The dorsal ramus is broken and lacks a small part of the mid-section, but a shallow longitudinal concavity is visible near the posterior end, which probably represents the surface for the articulation with the nasal. To the rear, the dorsal surface of the prefrontal has a thin, triangular, and strongly striated process projecting dorsomedially from the posteromedial end (Fig. 6.3.8B). This process would fit in a deep notch on the lateral surface of the frontal. In posterior view, the prefrontal is slightly concave with a broad dorsal end that strongly tapers ventrally. The dorsal margin of the posterior surface has a series of thin vertical ridges and grooves. A small foramen pierces the dorsal end of the prefrontal posterior surface (Fig. 6.3.8F).

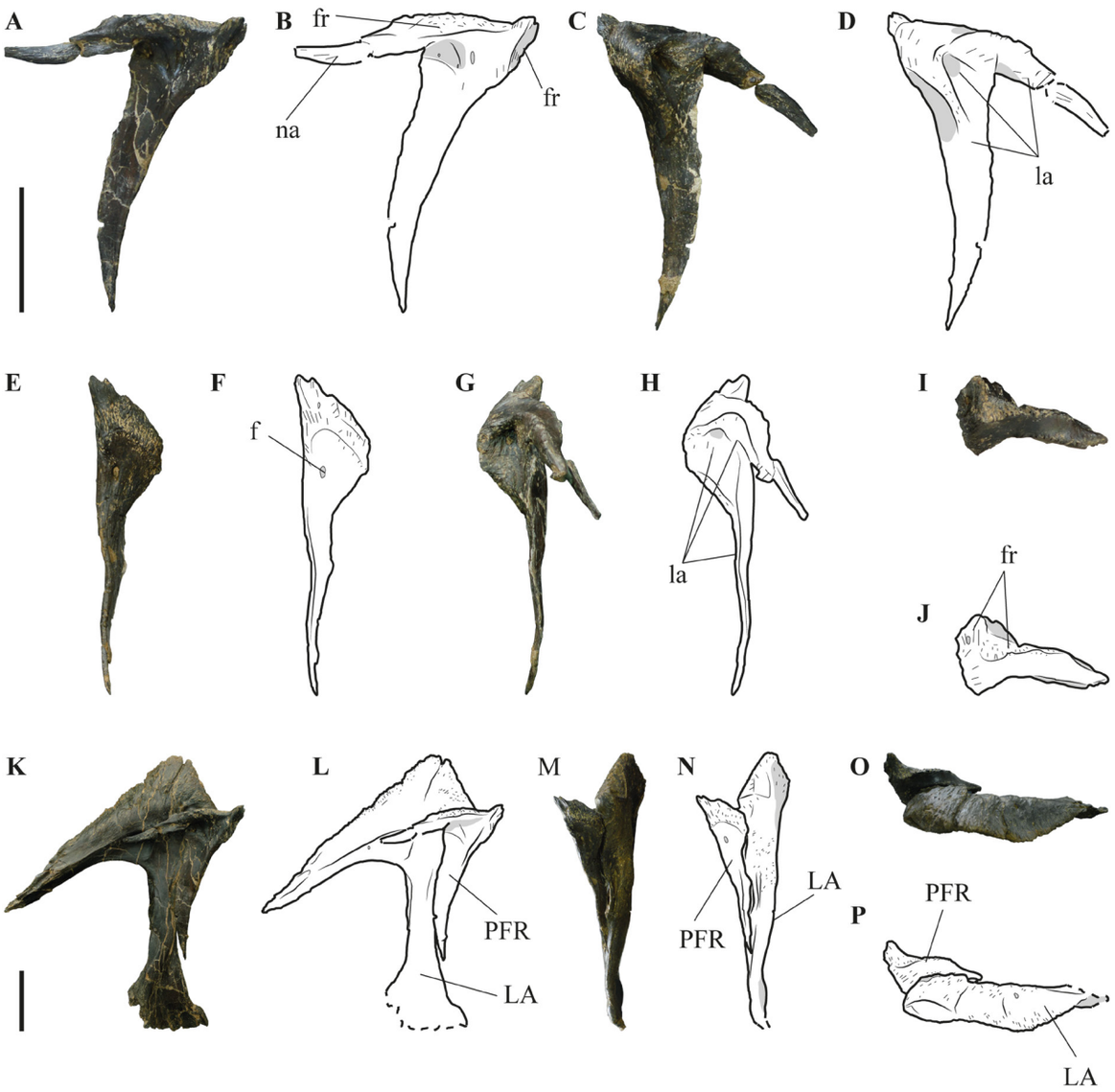

Figure 6.3.8. MNHNUL.P.AND5, right prefrontal and corresponding interpretative drawing in medial (A–B); lateral (C–D); posterior (E–F); anterior (G–H); and dorsal (I–J) views; K–P, articulated right prefrontal and lacrimal in medial (K–L); posterior (M–N); and dorsal (O–P) views. Scale bar: 50 mm.

MNHNUL.P.AND5 is separated from the lacrimal, which is the common condition for most theropod dinosaurs (e.g. *Monolophosaurus*: Brusatte et al. 2010a; *Allosaurus*: Gilmore 1920; Madsen 1976; Chure 2000; *Sinraptor*: Currie and Zhao 1993; *Yangchuanosaurus*; Dong et al. 1983; *Acrocanthosaurus*: Eddy and Clarke 2011; and *Eocarcharia*: Sereno and Brusatte 2008). These elements are fused in *Mapusaurus*, *Carcharodontosaurus*, and *Giganotosaurus* (Coria and Currie 2006; Eddy and Clarke 2011). The lateral and dorsal margins of the prefrontal are much thin suggesting that this element would have a small contribution to the dorsal orbit rim and that it would be only slightly exposed laterally as is the case in *Allosaurus* (Madsen 1976; Chure 2000). The prefrontal is broadly exposed in lateral and dorsal views in *Monolophosaurus* (Brusatte et al. 2010a) and it has an intermediate condition in *Sinraptor* (Currie and Zhao 1993).

MNHNUL.P.AND5 articulates fairly well with the lacrimal (MNHNUL.P.AND2) and with the frontal that is articulated with the braincase (MNHNUL.P.AND21) suggesting that these elements probably belong to the same individual (Fig. 6.3.8K–P). The articulation for the lacrimal is a deep funnel-like pit bounded by a robust, triangular crest similar to the condition in *Allosaurus* (Madsen 1976; Chure 2000), but distinct from the more rounded and large articular surface of *Acrocanthosaurus* (Eddy and Clarke 2011) and *Sinraptor* (Currie and Zhao 1993).

Postorbital. An almost complete left postorbital, MNHNUL.P.AND4 (Fig. 6.3.9A–J), and parts of a right postorbital, MNHNUL.P.AND20 (Fig. 6.3.9K–L), including the ventral ramus and the anteriormost portion of the squamosal process are known for the specimen from Andrés. The partial right postorbital was collected in a block containing elements of the braincase probably belonging to the same individual. The left postorbital has the ventral ramus slightly incomplete distally. This element has a T-shape in lateral view formed by an almost vertical and straight ventral ramus (jugal process), a dorsal ramus projecting posteriorly (squamosal process), and a short anterior expansion that contacts the frontal medially. The postorbital forms the anterodorsal border of the lateral temporal fenestra and the posterodorsal margin of the orbital fenestra. The jugal process is robust and anteroposteriorly broad dorsally, but strongly tapers ventrally. The ventral part of the jugal ramus has a shallow and broad concavity extending ventrally from approximately the mid-height of the process along the anterior surface, which represents the surface for articulation with the ascending process of the jugal (Fig. 6.3.9B). A broad and relatively deep concavity extends dorsally to the surface for articulation with the jugal along the medial surface of the jugal process and projects into the ventral margin of the squamosal ramus. This surface marks the extension of the lateral temporal fenestra into the postorbital and is delimited dorsally by a low, almost horizontal crest projecting along the anteroposterior mid-length of the squamosal process (Fig. 6.3.9D).

The squamosal process projects to the rear making an angle of approximately 90º with the jugal ramus. In lateral view, the squamosal process is a deep, but transversely thin blade with almost parallel dorsal and ventral margins to the front along near half of its length. Posterior to this point, a sharp step strongly reduces the depth of the process and produces a tapering posterior end. The posterior part of the squamosal process shows a well-marked dorsal concavity at approximately its mid-length and a series of thin longitudinal grooves along the dorsal and ventral surfaces representing the area for articulation with the squamosal. This process of the squamosal ramus would fit in a deep groove on the dorsolateral surface of the squamosal. In medial view, the postorbital has a deep and broad concavity, occupying the anterior end of the squamosal process, near the junction of the squamosal and jugal rami. This dorsoventrally elongated concavity is bounded by prominent crests and represents the surface for articulation with the head of the laterosphenoid (Fig. 6.3.9C–D). A series of small foramina are visible inside this concavity. Dorsal to the surface for the laterosphenoid, the postorbital has a well-marked, but shallow groove that represents the articulation for the parietal. Just anterodorsal to the articulation for the laterosphenoid, a deep groove with an anteroposterior orientation extends along the anterodorsal border of the squamosal process. This groove represents the suture for articulation with the frontal. The suture for the prefrontal is a small notch in the anterior part of the postorbital, which opens in the medial surface (Fig. 6.3.9D). In dorsal view, the squamosal process is a transversely thin ridge separated from the surface for contact with the laterosphenoid by a shallow and broad groove inside which are visible three small foramina. This groove forms the floor of the anterolateral corner of the supratemporal fossa (Fig. 6.3.9I–J).

In anterior view, the postorbital is smooth and relatively broad transversely in the dorsal part, where it forms the posterodorsal border of the orbital fenestra, but strongly tapers ventrally. The lateral surface of the postorbital has a well-developed, relatively high, and rugose crest extending along the anterodorsal margin and bounding the posterodorsal margin of the orbital fenestra.

The ventral processes of the postorbitals collected in Andrés are triangular in cross-section as occur in most non-coelurosaurian theropods, except megalosauroids (e.g. *Afrovenator*, *Torvosaurus*, *Dubreuillosaurus*) and some carcharodontosaurids (e.g. *Eocarcharia*), in which this process is U-shaped or rectangular-shaped (Rauhut 2003; Sereno and Brusatte 2008; Brusatte et al. 2010a). An anterior process extending into the orbit (intraorbital process *sensu* Sereno and Brusatte 2008) is absent in the two elements collected in Andrés. This feature would result in an unconstricted morphology of the orbit, which is interpreted as the primitive condition for theropods (Chure 2000) and is shared with *Herrerasaurus*, *Coelophysis*, *Monolophosaurus*, *Sinraptor*, *Yangchuanosaurus*, *Allosaurus* and *Aerosteon* (Gilmore 1920; Madsen 1976; Currie and Zhao 1993; Sereno et al. 2008; Brusatte et al. 2010a). On the contrary, a well-developed intraorbital process is present in abelisaurids (e.g. Coria et al. 2002) and in

some more derived tetanurans such as *Tyrannosaurus* (Brochu 2003), but also in several allosauroids, including *Concavenator* (Ortega et al. 2010), *Eocarcharia* (Sereno and Brusatte 2008), *Acrocanthosaurus* (Eddy and Clarke 2011), *Giganotosaurus* (Sereno et al. 1996) and *Carcharodontosaurus* (Brusatte et al. 2010a). On the other hand, the posterior margin of the jugal process in the specimens from Andrés has a small convexity at approximately the dorsoventral mid-height that slightly projects into the anterodorsal corner of the lateral temporal fenestra. This morphology is somewhat distinct from *Allosaurus* (Gilmore 1920; Madsen 1976) or *Monolophosaurus* (Brusatte et al. 2010a), in which the posterior margin of the ventral process of the postorbital is anteroposteriorly broad dorsally, but the posterior margin is almost straight. In this feature the postorbitals from Andrés are more similar to *Sinraptor* (Currie and Zhao 1993), *Acrochantosaurus* (Eddy and Clarke 2011), and *Mapusaurus* (Coria and Currie 2006). However, in these taxa the projection is placed more dorsally. In *A. europaeus* the posterior margin of the jugal ramus of the postorbital is slightly convex similar to the typical morphology of *Allosaurus*.

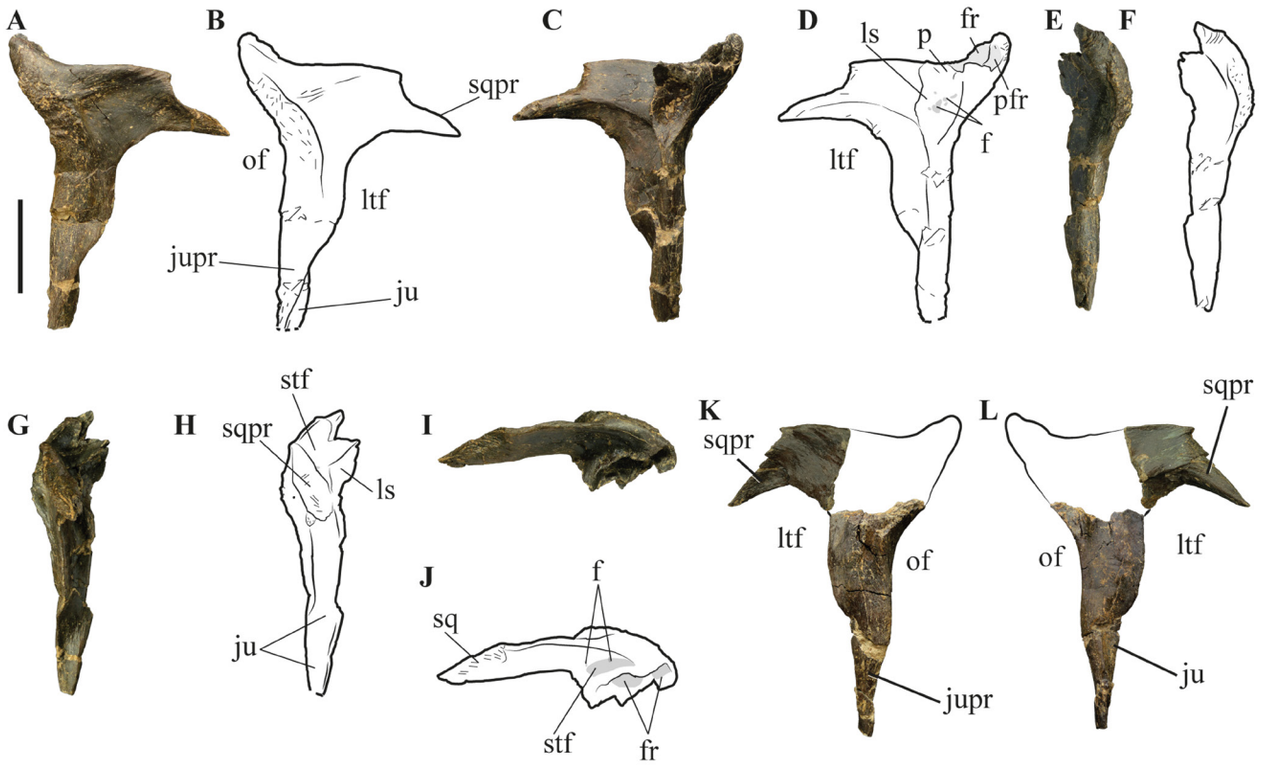

Figure 6.3.9. Postorbitals collected in Andrés and corresponding interpretative drawing. (A–J), left postorbital, MNHNUL.P.AND4; and (K–L), right postorbital, MNHNUL.P.AND20, in lateral (A–B, K); medial (C–D, L); anterior (E–F); posterior (G–H); and dorsal (I–J) views. Scale bar: 50 mm.

In MNHNUL.P.AND4 the anterior ramus is short and a surface for articulation with the lacrimal is absent suggesting that these elements would be separated. This condition is shared with *Monolophosaurus* (Brusatte et al. 2010a), *Allosaurus* (Gilmore 1920; Madsen 1976; Chure 2000) and *Sinraptor* (Currie and Zhao 1993). On contrary, in carcharodontosaurids (e.g. *Eocarcharia*: Sereno and Brusatte 2008, *Acrocanthosaurus*: Eddy and Clarke 2011), tyrannosaurids (e.g. Brochu 2003) and abelisaurids (e.g. Coria et al. 2002) the anterior ramus of the postorbital connects with the lacrimal to the front and with the frontal medially excluding the frontal from the orbital margin.

The supratemporal fenestra is represented in the dorsal surface of the postorbital by a shallow concavity that extends anteroposteriorly along almost the entire length of the posterior ramus. This condition is similar to *Aerosteon* (Sereno et al. 2008), *Saurophaganax* (Chure 2000), *Allosaurus* (Chure 2000), and *Sinraptor* (Currie and Zhao 1993), whereas in *Acrocanthosaurus* (Eddy and Clarke 2011),

Carcharodontosaurus (Eddy and Clarke 20011), *Mapusaurus* (Coria and Currie 2006), and *Eocarcharia* (Sereno and Brusatte 2008) the supretemporal fenestra is restricted to the posterior end of the dorsal surface of the postorbital. In MNHNUL.P.AND4 the surface for articulation with the laterosphenoid makes an angle of approximately 45º relative to the horizontal level as occur in *Allosaurus* and *Saurophaganax* (Gilmore 1920; Madsen 1976; Chure 2000), but distinct from *Sinraptor*, which has an almost horizontal articulation (Currie and Zhao 1993).

In lateral view, the postorbital has a vertical, strongly rugose, and low crest bounding the posterodorsal border of the orbital fenestra. The morphology of this crest is similar to *Allosaurus* (Madsen 1976; Chure 2000), *Yangchuanosaurus* (Dong et al. 1983), *Sinraptor* (Currie and Zhao 1993), *Saurophaganax* (Chure 2000), and *Aerosteon* (Sereno et al. 2008), but differs from carcharodontosaurids (e.g. *Concavenator*: Eddy and Clarke 2011; *Acrocanthosaurus*: Eddy and Clarke 2011; *Eocarcharia*: Sereno and Brusatte 2008; *Giganotosaurus*: Eddy and Clarke 2011, and *Mapusaurus*: Coria and Currie 2006), which have a strongly laterally expanded and usually vascularized postorbital boss. In *Monolophosaurus* and many other basal theropods a postorbital crest is absent (Brusatte et al. 2010a).

In the holotype of *A. europaeus* (ML 415), the ventral ramus of the postorbital is preserved in articulation with the left elements of the posterior part of the skull. In this specimen the ventral ramus of the postorbital extends approximately to the level of the ventral margin of the orbital fenestra and the ventral termination is placed well ventral to the squamosal-quadratojugal contact. The ventral ramus of the postorbital reaches approximately the level of the ventral margin of the orbital fenestra in primitive theropods (e.g. *Syntarsus*, *Coelophysis*, and *Herrerasaurus*), as well as in *Monolophosaurus* (Chure 2000; Brusatte et al. 2010a). On the contrary, the ventral margin of the postorbital is well dorsal to the ventral margin of the orbit in most allosauroids, including *Allosaurus*, *Acrocanthosaurus*, *Giganotosaurus*, and *Carcharodontosaurus* (Chure 2000). In *Sinraptor* and *Yangchuanosaurus* the ventral extention of the ramus is similar to *Allosaurus*, but the ventral margin of the ramus is well ventral to the squamosal-quadratojugal contact (Currie and Zhao 1993; Chure 2000; Eddy and Clarke 2011). Thus, a ventral ramus of the postorbital extending approximately to the level of the ventral margin of the orbital fenestra and well ventral to the squamosal-quadratojugal contact seems to be a diagnostic character for *A.europaeus* as was proposed by Mateus et al. (2006).

Frontal. A posterior part of a right frontal, MNHNUL.P.AND6, was collected during the first fieldwork (1988) in Andrés (Fig. 6.3.10). Posteriorly, in 2005, it was found an articulated braincase, which preserves fragments of the posterior part of both right and left frontals. These last elements correspond to a significantly larger individual relative to the frontal collected in 1988 (see Supplementary Table 6.3.1). Thus, indicating a minimal number of two *Allosaurus* individuals, represented with cranial elements, in the Andrés fossil site as is also suggested by the presence of other duplicate elements.

MNHNUL.P.AND6 corresponds to the posterior part of a right frontal articulated with a fragment of the parietal. The suture between the frontal and parietal is strongly interdigitated. The frontal has a rectangular outline in dorsal and ventral views, slightly narrowing to the front. The dorsal surface is mostly smooth and flat except in the posterolateral corner where a well-marked ridge extends anterolaterally from the surface for contact with the parietal. This ridge delimits a shallow concavity representing the anterodorsal border of the supratemporal fenestra (Fig. 6.3.10A–B). Laterally to this concavity, the frontal has a deep longitudinal groove that is interpreted as the surface for contact with the postorbital (Fig. 6.3.10E–F). The articulation with the prefrontal in the lateral surface of the frontal anterior part is a deep, triangular-shaped groove that would receive the tapered posterior process of the prefrontal. Between the facets for contact with the postorbital and with the prefrontal the frontal has a narrow surface representing the dorsal opening of the orbital fenestra.

The interfrontal suture is open, but the contact between the frontals should be firm due to the presence of a series of thin vertical ridges and grooves along most of its length. The ventral surface of the frontal is marked by a large, crescentric scar interpreted as the surface for articulation with the orbitosphenoid

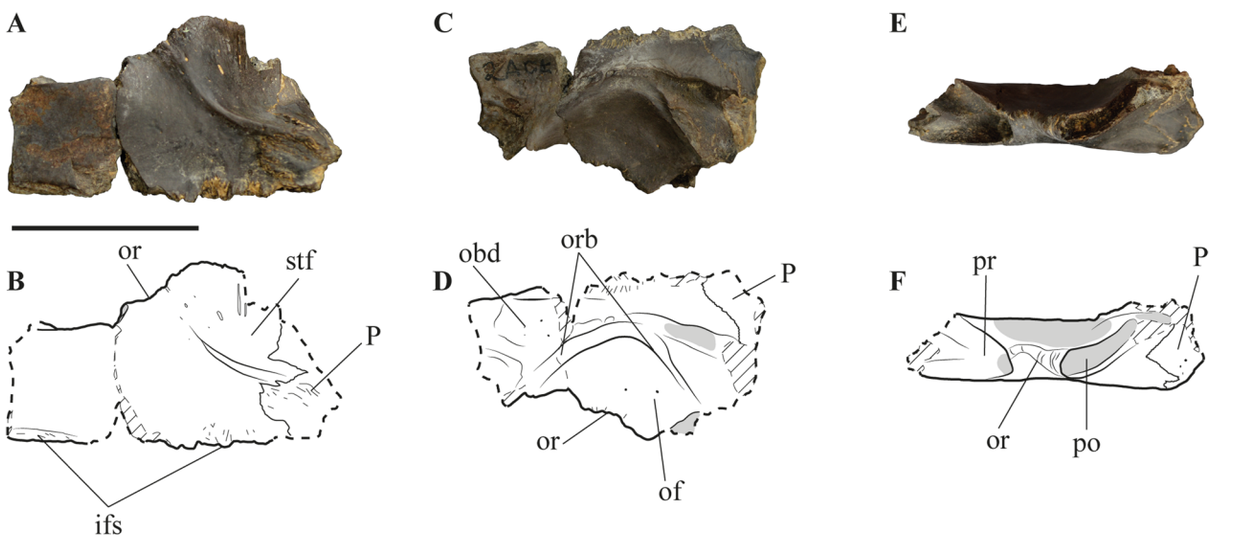

Figure 6.3.10. MNHNUL.P.AND6, right frontal and corresponding interpretative drawing in dorsal (A–B); ventral (C–D); and lateral (E–F) views. Scale bar: 50 mm.

(Fig. 6.3.10C–D). Medially to this scar and extending parasagitally along the midline of the frontal is a groove for the olfactory bulbs.

Unfused frontals are typical of most allosauroids, except for *Carcharodontosaurus*, *Acrocanthosaurus*, and *Giganotosaurus* (Chure 2000; Coria and Currie 2002; Brusatte and Sereno 2007; Eddy and Clarke 2011). These elements are also at least partially fused in *Shaochilong* and *Eocarcharia* (Brusatte et al. 2010b). Also, the suture between the frontals and the parietals is strongly interdigitated, but open as occur in *Allosaurus fragilis* (Gilmore 1920; Madsen 1976), *A.* "*jimmadseni*" (Chure 2000), *Sinraptor dongi* (Currie and Zhao 1993), and *Shidaisaurus jinae* (Wu et al. 2009). On the contrary, *Carcharodontosaurus iguidensis* (Sereno and Brusatte 2007), "*Yangchuanosaurus*" *hepingensis* (Gao 1992), and *Acrocanthosaurus atokensis* (Currie and Carpenter 2000) have fused frontoparietal sutures.

The frontals collected in Andrés show a reduced participation for the orbital rim, which has been considered the derived character for theropods and is shared with *Monolophosaurus* (Brusatte et al. 2010a), *Shidaisaurus* (Wu et al. 2009), and *Allosaurus* (Gilmore 1920; Madsen 1976; Chure 2000). In more primitive theropods, including *Cryolophosaurus* (Smith et al. 2007), and *Eustreptospondylus* (Sadleir et al. 2008) the frontal has a major contribution to this opening. On the other hand, in *Carcharodontosaurus* (Brusatte and Sereno 2007), *Giganotosaurus* (Coria and Currie 2003), *Mapusaurus* (Coria and Currie 2006), and *Acrocanthosaurus* (Currie and Carpenter 2000; Eddy and Clarke 2011) the lacrimal and the postorbital exclude the frontal from the orbital margin.

MNHNUL.P.AND.6 is approximately 60% as broad as long, which is the same ratio as for *Allosaurus* (Gilmore 1920; Madsen 1976) and most carcharodontosaurids (e.g. Eddy and Clarke 2011), whereas *Monolophosaurus* (Brusatte et al. 2010a) and *Sinraptor* (Currie and Zhao 1993) have proportionally wider and longer frontals respectively. The supratemporal fossa occupies most of the posterolateral end of the frontal (at its longest extent is near 53% of the length of the frontal) and is widely exposed in dorsal view. This condition is similar to *Monolophosaurus* (Brusatte et al. 2010a), *Allosaurus* (Madsen 1976; Chure 2000), and *Sinraptor* (Currie and Zhao 1993), wehereas carcharodontosaurids (e.g. Coria and Currie 2003) have much reduced fossae (less than 34-40% of the length of the frontal) and these are roofed over by a shelf of the frontoparietal, which strongly reduces the dorsal exposition of this opening. The supratemporal fossa extends also into the parietal as is the case in *Allosaurus* (Madsen 1976; Chure 2000), *Acrocanthosaurus* (Eddy and Clarke 2011), and *Eocarcharia* (Sereno and Brusatte 2008), but not in *Carcharodontosaurus* (Brusatte and Sereno 2007), *Giganotosaurus* (Coria and Currie 2003) or *Shaochilong* (Brusatte et al. 2010b). The opposing supratemporal fossae in *Allosaurus*, *Sinraptor*, and

Eocarcharia nearly contact medially, which is interpreted as probably representing the plesiomorphic state (Brusatte et al. 2010b). In *Shaochilong*, *Acrocanthosaurus*, *Carcharodontosaurus*, and *Giganotosaurus* these fossae are widely separated on the midline by a thick margin of the frontals (Coria and Currie 2003; Brusatte et al. 2010b; Eddy and Clarke 2011). The floor of the supratemporal fossa is smooth as in *Allosaurus* (Madsen 1976; Chure 2000) or *Sinraptor* (Currie and Zhao 1993). In *Shaochilong* (Brusatte et al. 2010a), *Carcharodontosaurus* (Brusatte and Sereno 2007), *Acrocanthosaurus* (Eddy and Clarke 2011), *Giganotosaurus* (Coria and Currie 2003), and probably *Eocarcharia* (Brusatte et al. 2010b) a sinuous crest is present inside this fossa.

Palatine. Two right palatines were collected in Andrés. The smaller element, MNHNUL.P.AND7 (Fig. 6.3.11A–H), is complete and well preserved, but the largest one, MNHNUL.P.AND8 (Fig. 6.3.11I–L), lacks the posterior part and is somewhat distorted. MNHNUL.P.AND8 is approximately twice the size of MNHNUL.P.AND7 (see Supplementary Table 6.3.1).

In medial view, the palatine is a tri-branched element formed by two anterior rami, the maxillary process and the medial symphysis (= vomeropterygoid process *sensu* Brusatte et al. 2008), and a posterior broad blade that constitutes the suture for contact with the jugal. The maxillary process is a thin and tapered ramus with a shallow longitudinal groove representing the suture with the maxilla that extends along the ventral surface for approximately the anteroposterior mid-length of the palatine. The medial symphysis is a mediolaterally thin, but dorsoventrally broad, L-shaped blade projecting anteromedially. The dorsal margin of the symphysis is nearly straight and it would articulate with the vomer in the anterior part (Fig. 6.3.11A–B). The symphysis strongly tapers to the front and has a series of thin grooves and crests along the dorsal margin corresponding to the surface for articulation with the opposite palatine. The medial symphysis and the maxillary process delimit an elongated and broad opening, which is interpreted as the fossa for the internal naris or internal narial choana.

To the rear, the palatine has two blade-like and short processes, the jugal and the pterygoid processes. The jugal process is a mediolaterally thin blade, slightly expanded dorsoventrally to the distal part and projecting back from the medial surface of the palatine. This process has a series of thin, longitudinal grooves and crests along the posteromedial surface and a deep concavity extending longitudinally along the mediodorsal margin, which represent the surface for articulation with the jugal (Fig. 6.3.11C–D). Distally, the jugal process has a deep notch between the ventral margin and the posterior part of the maxillary ramus. The pterygoid process projects posterodorsally from the lateral surface of the palatine and is slightly shorter than the jugal process. In lateral view, the pterygoid process has a well-marked groove extending anterodorsally from the posterior margin and delimiting a subcircular surface that represents the area for articulation with the pterygoid.

In lateral view, the palatine has a deep concavity between the pterygoid process and the medial symphysis corresponding to the pterygopalatine fenestra (*sensu* Eddy and Clarke 2011). In dorsal view, another deep groove extends anteroposteriorly between the jugal and the pterygoid processes (Fig. 6.3.11E–F). The lateral surface of the palatine has a deep and circular recess that pierces the posterior surface of the palatine near the base of the pterygoid process.

Both palatines have similar general morphologies, but differ in some details. MNHNUL.P.AND8 has the maxillary process slightly anteroposteriorly shorter than the medial symphysis, whereas in the smaller element these processes have approximately the same length. Other differences include the morphology of the jugal process, which is more rectangular in MNHNUL.P.AND8, and the blade connecting the medial symphysis with the pterygoid process, which projects dorsally in MNHNUL.P.AND8 and is straight in MNHNUL.P.AND7. Finally, MNHNUL.P.AND8 has a small opening in the dorsal surface in a position equivalent to the palatine recess in MNHNUL.P.AND7, but in the former this opening connects with a narrow groove in the ventral surface suggesting that it corresponds to a foramen instead a recess. Based on these differences it is not possible to exclude that MNHNUL.P.AND8 may belong to a distinct taxon, but because it is strongly distorted and incomplete a more accurate identification is not possible for the moment.

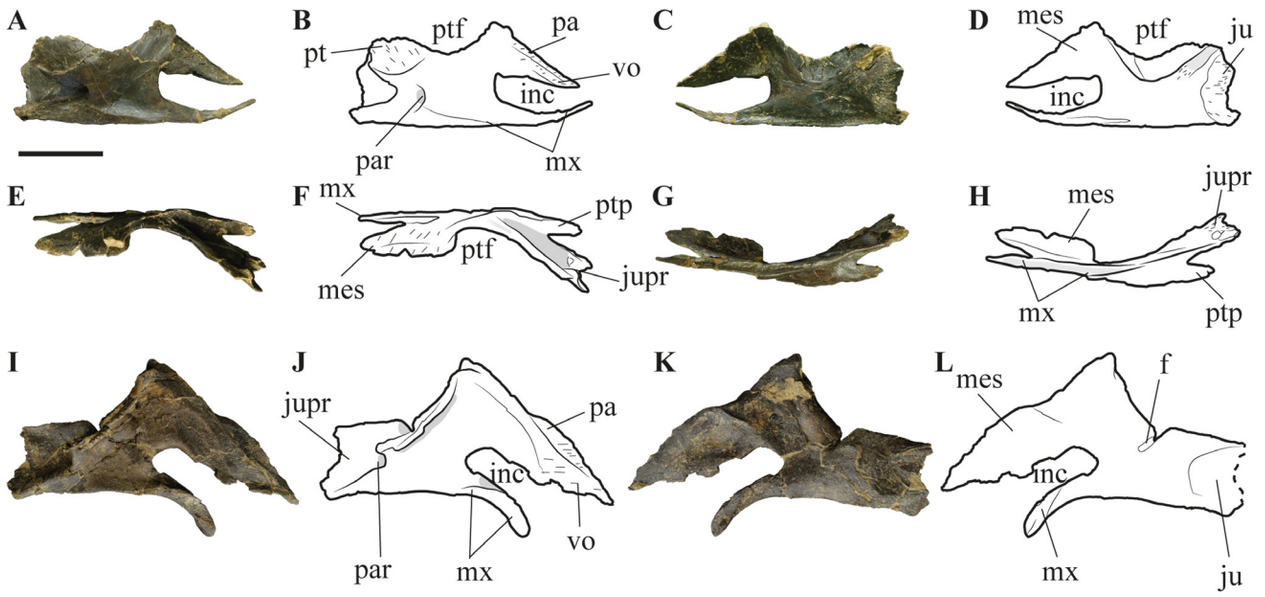

Figure 6.3.11. Right palatines collected in Andrés and corresponding interpretative drawing. (A–H), MNHNUL.P.AND7; and (I–L), MNHNUL.P.AND8 in medial (A–B, I–J); lateral (C–D, K–L); dorsal (E–F); and ventral (G–H) views. Scale bar: 50 mm.

The presence of a pneumatic palatine recess is a feature known in many theropods, including tyrannosaurids (Carr 1999), *Monolophosaurus* (Brusatte et al. 2010a), *Sinraptor* (Currie and Zhao 1993; Witmer 1997), *Neovenator* (Brusatte et al. 2008), and *Acrocanthosaurus* (Chure 2000; Eddy and Clarke 2011). In MNHNUL.P.AND7, the large recess in the lateral surface of the palatine is a noncommunicating (blind) fossae (*sensu* O'Connor 2006) indicating an apneumatic element similar to those of *Allosaurus* (e.g. Madsen 1976; Brusatte et al. 2008; Eddy and Clarke 2011). The jugal ramus extends back to the level of the pterygoid process as occur in *Sinraptor*, but not in *Allosaurus* (Madsen 1976; Currie and Zhao 1993). The vomeropterygoid process of the palatine collected in Andrés is broken and somewhat displaced ventrally, but it clearly does not extend beyond the level of the maxillary ramus. This feauture is similar to the condition in *Allosaurus* (Gilmore 1920; Madsen 1976) and distinct from *Sinraptor* (Currie and Zhao 1993). The presence of a pterygopalatine fenestra is a character shared with *Allosaurus*, *Neovenator*, and *Yangchuanosaurus*, but this fenestra is absent in *Sinraptor* (Eddy and Clarke 2011).

Quadrate and quadratojugal. The articular region of a right quadrate, MNHNUL.P.AND9, was collected during the first fieldwork campaign in 1988, and an almost complete left quadrate articulated with the quadratojugal, MNHNUL.P.AND10, was found in the second campaign in 2005 (Fig. 6.3.12). These elements have approximately the same size and similar morphology suggesting that they may belong to the same individual.

The quadrate has a nearly vertical posterior shaft connecting the articular ventral condyles with the quadrate cotylus dorsally, and a broad, thin medial blade (= pterygoid flange) that projects anteromedially. The pterygoid flange is slightly broken anterodorsally, but is fairly well-preserved. This blade is delimited ventrally by two robust crests, one projecting dorsoventrally along the medial surface of the posterior shaft and other projecting anteriorly from the anterior surface dorsally to the medial condyle. These crests form an angle of approximately 70º and delimit a transversely deep concavity (= medial fossa of the quadrate *sensu* Hendrickx and Mateus 2014b) in the ventral part of the pterygoid flange. The pterygoid flange connects dorsally with the quadrate cotylus. The quadrate cotylus represents the articular surface for the squamosal and is strongly convex in lateral view.

In lateral view, the quadrate shaft is slightly concave, projecting more to the rear dorsally relative to the level of the distal condyles. The shaft is bounded by prominent crests projecting along the medial and

lateral surfaces. These crests twist dorsally connecting with the medial surface of the quadrate cotylus and delimit a vertical groove deeper at nearly the mid-height of the shaft. In this area, the quadrate shaft is pierced by a large foramen opening near the suture with the quadratojugal, but that is entirely surrounded by the quadrate. Dorsally, the medial crest of the shaft has a deep notch that opens ventrally and is connected to the foramen by a shallow groove extending anterodorsally (Fig. 6.3.12C–D). Ventrally, the quadrate terminates in two well-developed articular condyles. The medial condyle (= entocondyle) is in a slightly more ventral position relative to the level of the lateral condyle (ectocondyle). In anterior view, the condyles project somewhat dorsally. The medial condyle is smaller than the lateral one. In ventral view, the condyles have an oval, anteroposteriorly elongated shape and are separated by a shallow transverse concavity.

The quadratojugal articulates with the posterolateral surface of the quadrate shaft along nearly its entire depth. This articular surface is somewhat sigmoid extending along the posterior surface of the quadrate shaft up to the level of the quadrate foramen and then shift dorsally to the lateral surface. The quadratojugal is an L-shaped element with a vertical ramus for articulation with the squamosal and an anterior, nearly horizontal jugal process (Fig. 6.3.12A–B). These processes are positioned in an angle of approximately 90º and form the posteroventral margin of the lateral temporal fenestra. The squamosal ramus is mediolaterally thin and relatively broad anteroposteriorly. This process is broken dorsally so the morphology of the suture with the precotyloid process of the squamosal is not possible to know. The jugal process is a robust, distally tapered ramus projecting to the front. In lateral view, the anterior part of the jugal process has a deep longitudinal groove extending along the dorsal margin, which would articulate with the quadratojugal process of the jugal. In medial view, the jugal process has a deep longitudinal concavity that extends along the ventral margin and is delimited by two crests projecting along the lateral and medial margins of the ventral surface.

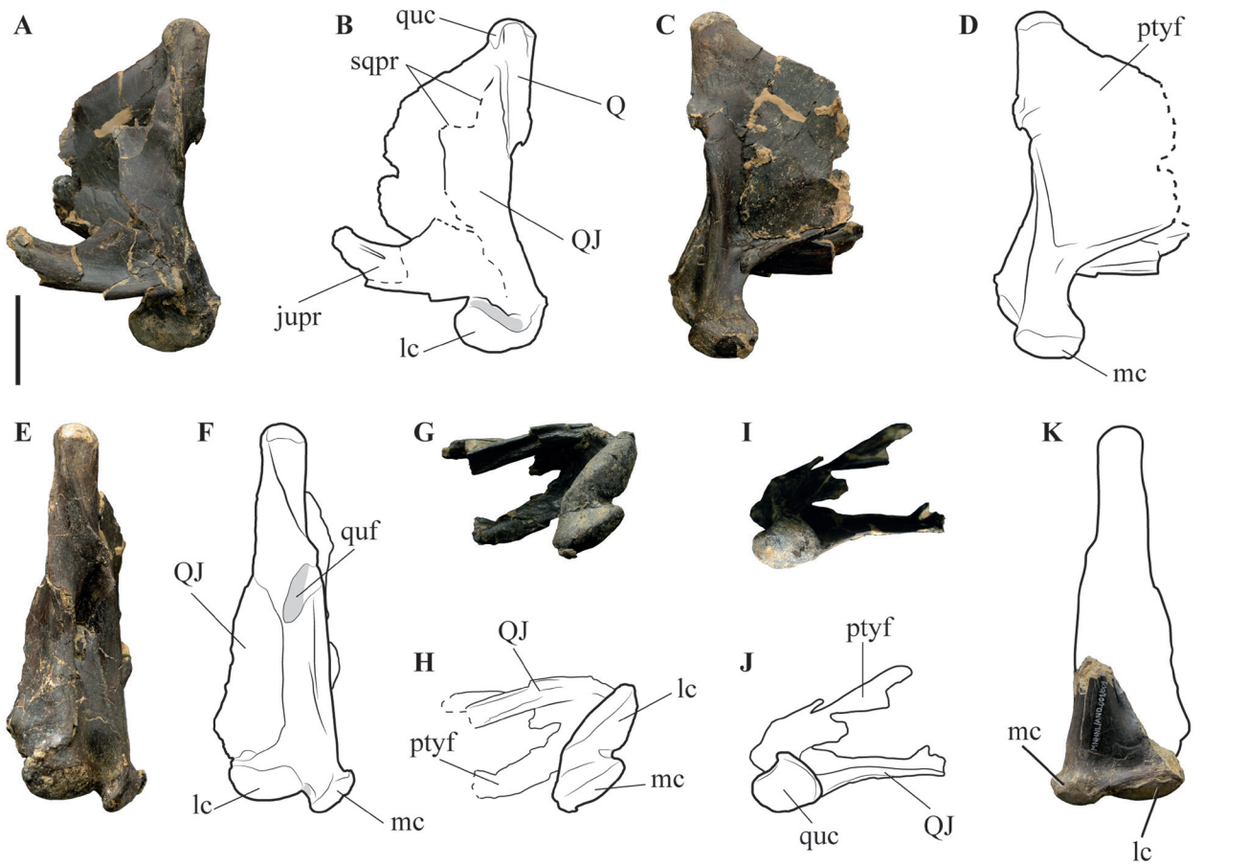

Figure 6.3.12. Quadrate and quadratojugal collected in Andrés and corresponding interpretative drawing. (A–J), left quadrate articulated with the quadratojugal, MNHNUL.P.AND10; (K), articular region of a right quadrate, MNHNUL.P.AND9; in lateral (A–B); medial (C–D); posterior (E–F, K); ventral (G–H); and dorsal (I–J) views. Scale bar: 50 mm.

MNHNUL.P.AND10 is apneumatic because it clearly does not have a medial pneumatic recess (*sensu* Eddy and Clarke 2011) at the base of the pterygoid flange. This feature is shared with most non-coelurosaurian theropods, including *Allosaurus* (Gilmore 1920; Madsen 1976), *Sinraptor* (Currie and Zhao 1993), and *Shaochilong* (Brusatte et al. 2009). In most other carcharodontosaurs such as *Acrocanthosaurus* (Currie and Carpenter 2000; Eddy and Clarke 2011), *Giganotosaurus* (Eddy and Clarke 2011), *Mapusaurus* (Coria and Currie 2006), and *Aerosteon* (Sereno et al. 2008) the quadrate is extensively pneumatized. In MNHNUL.P.AND10 the quadrate foramen is mostly enclosed by the quadrate, with a reduced contribution of the quadratojugal as occur in most allosauroids (e.g. Currie and Zhao 1993; Coria and Currie 2006; Eddy and Clarke 2011). On the contrary, in *Monolophosaurus* (Brusatte et al. 2010a) and *Tyrannosaurus*, the quadratojugal participates more extensively in the lateral rim of the quadrate foramen, whereas in *Aerosteon* (Sereno et al. 2008) the enlarged foramen is bounded entirely by the quadrate. In *Allosaurus* it is generally considered that the quadrate foramen is mostly formed by the quadrate (Madsen 1976; Eddy and Clarke 2011), but this condition seems to be somewhat variable (Brusatte et al. 2010a).

The horizontal ramus of the quadratojugal in the specimen from Andrés is incomplete, but it seems that it would taper to the front as occur in most allosauroids with the exception of *Sinraptor* and *Acrocanthosaurus*, in which it is forked (Currie and Zhao 1993; Chure 2000; Eddy and Clarke 2011). On the other hand, the dorsal ramus is anteroposteriorly thick and despite being incomplete the preserved part indicates that the suture for contact with the precotyloid process of the squamosal would be broad. This morphology is similar to *Monolophosaurus* (Brusatte et al. 2010a), *Allosaurus* (Madsen 1976; Chure 2000) and *Tyrannosaurus* (Brochu 2003), but contrasts with the anteroposteriorly narrow dorsal ramus of *Acrocanthosaurus* (Eddy and Clarke 2011), *Sinraptor* (Currie and Zhao 1993), *Yangchuanosaurus* (Dong et al. 1983), and most basal theropods (Tykoski and Rowe 2004).

In *A. europaeus* the anterior ramus of the quadratojugal projects further to the front than the level of the anterior margin of the lateral temporal fenestra (Mateus et al. 2006), as occur in *Monolophosaurus* (Brusatte et al. 2010a), *Dilophosaurus* (Welles 1984), and *Zupaysaurus* (Ezcurra 2007). However, this is unlike the condition in most other basal theropods, including *Allosaurus* (Madsen 1976), *Cryolophosaurus* (Smith et al. 2007), *Dubreuillosaurus* (Allain 2005b), *Sinraptor* (Currie and Zhao 1993), *Ceratosaurus* (Madsen and Welles 2000), *Majungasaurus* (Sampson and Witmer 2007), and coelophysids (Tykoski and Rowe 2004), in which the anterior ramus terminates ventral to the lateral temporal fenestra.

Squamosal. A complete and well-preserved right squamosal, MNHNUL.P.AND14, was collected in the Andrés fossil site (Fig. 6.3.13). In lateral view, the squamosal comprises a ventral, short and blunted ramus (postcotyloid process), an anterior, thin blade that represents the surface for articulation with the quadratojugal (quadratojugal process), and a dorsal process with a deep groove, which would receive the squamosal process of the postorbital (Fig. 6.3.13A–B). A deep, circular notch opens anteroventrally between the postcotyloid process and the quadratojugal process, which corresponds to the articulation for the quadrate cotylus. The postcotyloid process is a short ramus that projects anteroventrally and slightly constricts the opening for the quadrate cotylus ventrally. The quadratojugal process is a mediolaterally thin blade projecting anteroventrally and that slightly expands distally. The anterior margin of the quadratojugal process is convex and would project slightly into the lateral temporal fenestra, slightly constricting the posterior margin of this opening. The distal part of the quadratojugal process is broken and the morphology of the suture with the quadratojugal cannot be known. However, based on the preserved part it seems that this suture would be not straight, but most probably sigmoidal. The lateral surface of the quadratojugal process has a series of well-marked ridges and grooves. The articulation with the postorbital in the lateral surface of the dorsal ramus of the squamosal corresponds to a deep, triangular groove, which strongly broadens to the rear and divides the ramus into dorsal and ventral prongs across its entire length. Posterior to the groove for articulation with the postorbital, another shallower groove projects dorsoventrally adjacent to the dorsal margin of the articulation for the postorbital.

In posterior view, the squamosal has a fan-shape, with a thin dorsal lamina, strongly convex transversely (Fig. 6.3.13E–F). Medially to this lamina, a thin ramus (parietal process) projects anteromedially to contact with the parietal. The parietal process is a thin and relatively long ramus with a deep groove extending from the anteromedial margin of the squamosal into the dorsal surface of the parietal process. In posterior view, the postcotyloid process is strongly compressed mediolaterally forming a thin, vertical ridge. In medial view, the squamosal has a well-marked ridge surrounding the surface for articulation with the quadrate cotylus and a triangular-shaped crest that projects dorsally from the dorsal margin of the cotylus along the anterior margin of the parietal process (Fig. 6.3.13G–H). This crest delimits a deep transverse concavity representing the posterodorsal margin of the lateral temporal fenestra.

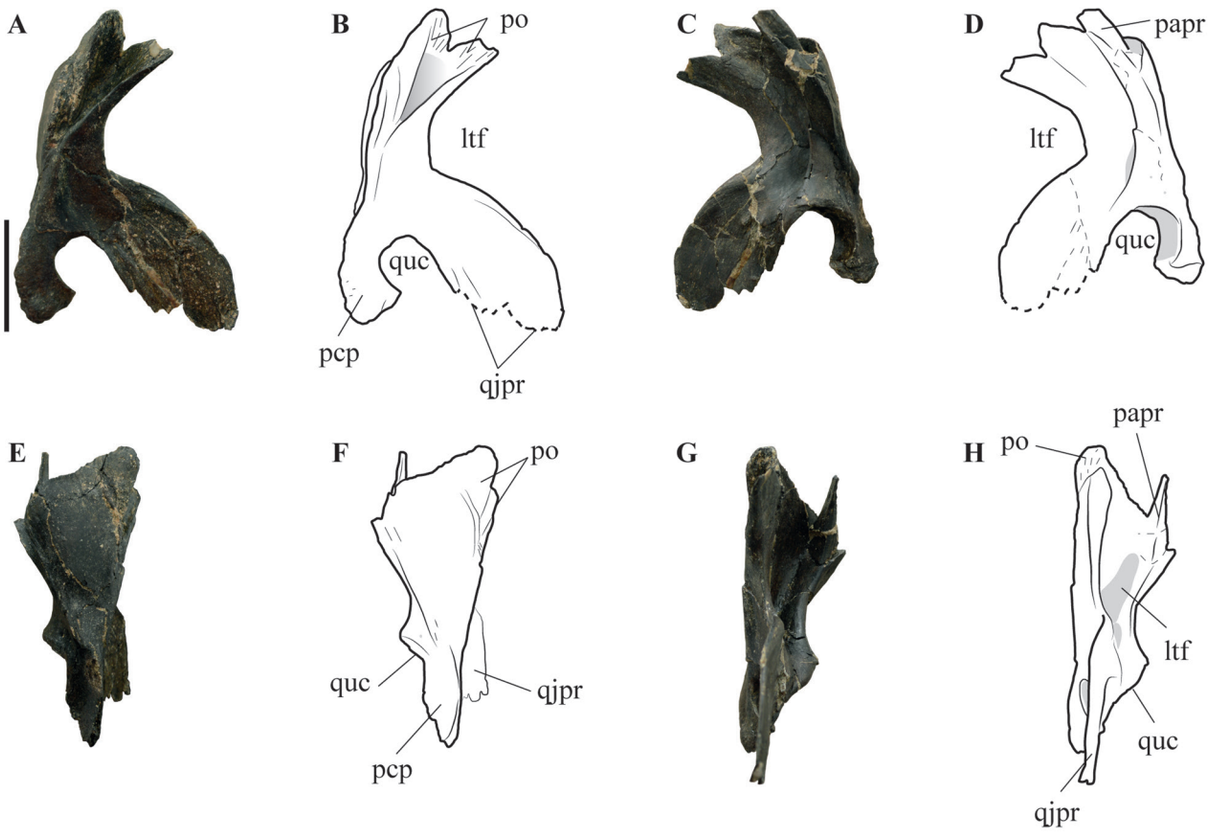

Figure 6.3.13. MNHNUL.P.AND14, right squamosal and corresponding drawing in lateral (A–B); medial (C–D); posterior (E–F); and anterior (G–H) views. Scale bar: 50 mm.

In MNHNUL.P.AND14 the anterior margin of the quadratojugal ramus projects to the front and is strongly convex, which suggests that the squamosal would slightly constrict the posterior margin of the lateral temporal fenestra as occur in *Allosaurus* (Madsen 1976; Chure 2000), *Acrocanthosaurus* (Eddy and Clarke 2011), and *Monolophosaurus* (Brusatte et al. 2010a). The specimen from Andrés shares with *A. fragilis* (Gilmore 1920; Madsen 1976), "*A. jimmadseni*" (Chure 2000), and *A. europaeus* (EM pers. obs. 2015) the presence of well-marked striations in the lateral surface of the quadratojugal ramus. This feauture has been considered a synapomorphy for *Allosaurus* (Chure 2000). The distally-tapering postcotyloid process in MNHNUL.P.AND14 is similar to *Allosaurus* (Gilmore 1920; Madsen 1976; Chure 2000), *Yangchuanosaurus* (Dong et al. 1983), and possibly *Sinraptor* (Eddy and Clarke 2011), but contrasts with the expanded process of *Monolophosaurus* (Brusatte et al. 2010a) and *Acrocanthosaurus* (Eddy and Clarke 2011). A fossa in the medial surface of the squamosal near the junction of the dorsal and quadratojugal processes (squamosal pneumatic recess *sensu* Eddy and Clarke 2011) as occur in *Acrocanthosaurus*, *Tyrannosaurus* and *Majungasaurus* (Eddy and Clarke 2011) is absent in MNHNUL.P.AND14. The specimen from Andrés shares this feature with *Allosaurus* (Madsen 1976) and *Sinraptor* (Currie and Zhao 1993).

In *A. europaeus* (Mateus et al. 2006) the quadratojugal ramus of the squamosal extends ventrally, reaching at least half the height of the lateral temporal fenestra as in other *Allosaurus* specimens (Chure 2000) and in *Monolophosaurus* (Brusatte et al. 2010a). On the contrary, in *Cryolophosaurus* (Smith et al. 2007), *Sinraptor* (Currie and Zhao 1993), and *Yangchuanosaurus* (Dong et al. 1983) this ramus is significantly shorter. In the specimen from Andrés the postcotyloid process and quadratojugal processes have similar length as occur in *Allosaurus* (Madsen 1976) and *Acrocanthosaurus* (Currie and Carpenter 2000; Eddy and Clarke 2011). This contrasts with the condition in *Monolophosaurus* (Brusatte et al. 2010a) in which the postcotyloid process is significantly shorter than the quadratojugal process.

Vomer. The vomer, MNHNUL.P.AND15, is almost complete and well preserved, but slightly compressed mediolaterally (Fig. 6.3.14). This is a long and thin element that would articulate with the premaxilla to the front, with the maxilla anterolaterally, with the palatine posterolaterally, and with the pterygoid posteromedially (Madsen 1976; Eddy and Clarke 2011). In dorsal view, the vomer bifurcates to the rear in two parallel blade-shaped and mediolaterally narrow processes. These processes are separated by a deep notch extending to near the mid-length of the vomer. This notch of the vomer has been interpreted as for receive the vomeropalatine ramus of the pterygoid in *Acrocanthosaurus* (Eddy and Clarke 2011) and *Tyrannosaurus* (Madsen 1976) or for attach inside the anterodorsal arch of the palatines in *Allosaurus* (Madsen 1976). The posterior processes or palatine blades are distally striated along the posterior part of the lateral surface where the vomer would articulate with the palatine (Eddy and Clarke 2011). To the front, the vomer is a dorsoventrally thin ramus that slightly expands mediolaterally and strongly tapers to the anterior part. The dorsal surface shows a series of thin, longitudinal crests and grooves and a well-developed longitudinal crest extending along the mediolateral mid-width. This anterior process is somewhat ventrally deflected.

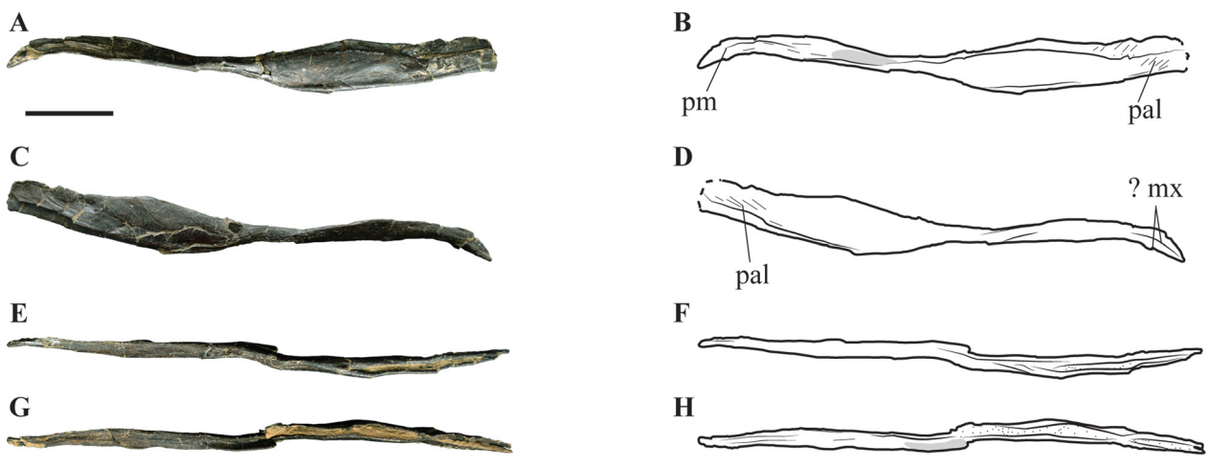

Figure 6.3.14. MNHNUL.P.AND15 vomer and corresponding interpretative drawing in left lateral (A–B); right lateral (C–D); ventral (E–F); and dorsal (G–H) views. Scale bar: 50 mm.

In *Allosaurus*, the vomer contacts the pterygoids, which has been considered the derived character for theropods (Madsen 1976). Eddy and Clarke (2011) considered that *Acrocanthosaurus*, *Sinraptor* and *Tyrannosaurus* share the plesiomorphic condition that is the vomer not contacting the pterygoids (Eddy and Clarke 2011; p. 33). However, the figuration of the palatine in the specimen of *Acrocanthosaurus* (NCSM 14345) shows the thin vomeropalatine ramus of the pterygoid fiting inside the notch between the posterior blades of the vomer (Eddy and Clarke 2011; Fig. 19 and 23). The vomer also contacts with the prerygoids in *Tyrannosaurus* (Osborn 1912; Madsen 1976; Brochu 2003).

Braincase (MNHNUL.P.AND21). An almost complete, articulated and well-preserved braincase was collected in Andrés (Fig. 6.3.15–18). This specimen includes the posterior part of the frontals, the parietals, the supraoccipital, the prootics, the exoccipital-opisthotic complex, the basioccipital, the orbitosphenoid and the laterosphenoid. A left squamosal is also preserved articulated with the braincase.

The occipital part of the braincase is constituted by the parietals, the supraoccipital, the exoccipital-opisthotic complex and the basioccipital. The foramen magnum is bounded mostly by the exoccipital-opisthotic complex laterally and by a small portion of the supraoccipital and basioccipital dorsally and ventrally respectively. The foramen is oval, slightly transversely wider than high. The occipital condyle is rounded and is formed mostly by the basioccipital and by a small portion of the exoccipital-opisthotic complex dorsally. The dorsal surface of the condyle is slightly concave representing the expansion of the foramen magnus in the condyle.

In general, the braincase is similar to those of *Allosaurus* (Gilmore 1920; Madsen 1976; Chure 2000), *Sinraptor* (Currie and Zhao 1993) and other basal allosauroids. The braincase is excavated by several pneumatic fossae and foramina indicating a highly pneumatic element, but not to the extent of carcharodontosaurids (e.g. Coria and Currie 2003; Brusatte and Sereno 2007; Brusatte et al. 2010a). MNHNUL.P.AND21 is dorsoventrally low and relatively long anteroposteriorly. Despite most of the basipterygoid processes are missing and thus the exact ventral extension of the braincase is unknown, the relative proportions are similar to those of basal allosauroids (e.g. *Allosaurus*: Madsen 1976; *Sinraptor*: Currie and Zhao 1993), as well as other basal theropods (e.g., *Piatnitzkysaurus*: Rauhut 2004; *Cryolophosaurus*: Smith et al. 2007; *Dilophosaurus*: Welles 1984). On the contrary, the braincase of carcharodontosaurids (e.g. *Giganotosaurus*: Coria and Currie 2003; *Carcharodontosaurus*: Brusatte and Sereno 2007; *Shaochilong*: Brusatte et al. 2010a), derived tyrannosaurids (e.g. *Tyrannosaurus*: Brochu 2003) and spinosaurids (e.g. *Baryonyx*: Charig and Milner 1997; *Irritator*: Sues et al. 2002) is short and much deep.

Frontals. Both frontals are broken at the level of the anterior margin of the surface for contact with the prefrontal and the anterior part is missing. The interfrontal and the frontoparietal sutures are visible along the entire preserved fragment. The frontals are almost as transversely wide (at the widest point across the level of the surface for contact with the postorbital) as are long (see Supplementary Table 6.3.1). The general morphology of these elements is similar to the isolated frontal, MNHNUL.P.AND6, described above, but this later is significantly smaller (the frontals of MNHNUL.P.AND21 are approximately 1.5 times wider than the isolated frontal). The frontals contact the parietals posterodorsally and the laterosphenoid ventrally. In dorsal view, the supratemporal fossa occupies the posterior part of the frontal and extends into the anterolateral surface of the parietal. These fossae are bounded by a pair of crescentic crests that has been interpreted as for the muscle pseudotemporalis (Chure 2000). In anteroventral view, the frontals show a deep longitudinal groove extending along the midline of the articulated frontals, which expands to the front in a broad shallow depression with lobulated shape (Fig. 6.3.16). These depressions represent the olfactory bulb cavities and are delimited by pair of low, but well-marked crests interpreted as corresponding to the sphenethmoid scars (Brusatte et al. 2010b). To the rear, the olfactory bulbs narrow and connect with the endocranial cavity through a deep groove. The shape of the olfactory bulbs is similar to those of *Carcharodontosaurus iguidensis*, *Acrocanthosaurus atokensis*, *Sinraptor dongi*, and *Allosaurus fragilis* (Rogers 1998; Paulina Carabajal and Currie 2012). In these taxa the bulbs are not divided by a septum contrasting with the condition of *Carcharodontosaurus saharicus* and *Giganotosaurus carolinii* (Paulina Carabajal and Currie 2012). The endocranial cavity is bounded by the laterosphenoids laterally, by the prootic ventrally, and by the parietal posteriorly.

Parietal. In occipital view, the parietals form the dorsal part of the braincase. These elements contact the frontals anterodorsally, the laterosphenoid anteroventrally, the supraoccipital posteromedially, the exoccipital-opisthotic complex posteroventrally, and the squamosal laterally. All these sutures are well visible despite somewhat obscured in some points due to distortion. The interparietal suture is visible dorsally and is strongly interdigitated. The frontoparietal suture is also strongly interdigitated dorsally, but becomes more sinuous ventrally. The parietals have two mediolaterally broad posterior blades expanding laterally around the supraoccipital and an anterior short process for articulation

with the frontals. The suture between the parietals and the supraoccipital is visible and has a sinusoidal contour. The parietal blades are dorsoventrally deeper than transversely wide and projecting somewhat dorsally, but do not surpass the dorsal margin of the supraoccipital (Fig. 6.3.15A–B). Ventrally, the parietal blades have a pair of thin and long processes projecting along approximately the mid-length of the dorsal margin of the paroccipital processes.

In occipital view, the conjoined parietals have a heart-shape with a shallow concavity dorsomedially at the level of the supraoccipital crest. The parietal has a tongue-like process projecting posteriorly and overlapping the supraoccipital dorsal crest (Fig. 6.3.17D–E). Together the parietal transverse crest and the supraoccipital crest form a low and poorly-developed nuchal crest. This crest is somewhat distorted, but it would probably have a rounded shape more similar to those of *Allosaurus* (Madsen 1976; Chure 2000), *Giganotosaurus* (Eddy and Clarke 2011), and *Monolophosaurus* (Eddy and Clarke 2011) than to the squared crest of *Acrocanthosaurus* (Eddy and Clarke 2011) and *Sinraptor* (Eddy and Clarke 2011). To the front, the parietals have a short process for articulation with the frontals. This anterior process is constricted to the rear by the supratemporal fossae. In dorsal view, the parietals are relatively broad and slightly concave between the supratemporal fossae.

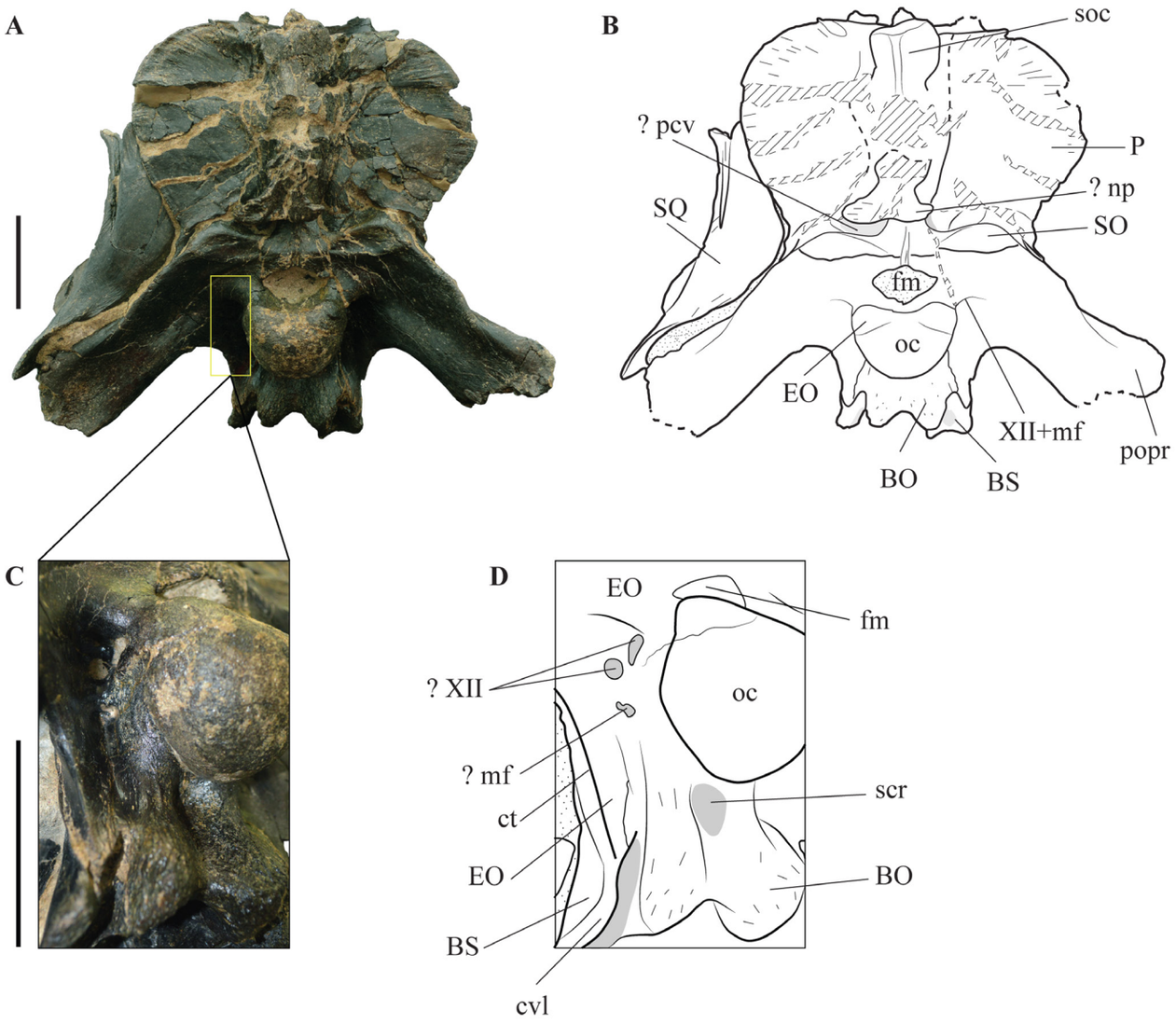

Figure 6.3.15. MNHNUL.P.AND21, braincase and corresponding interpretative drawing in occipital view (A–B); (C–D), detail of the occipital neck in ventrolateral view showing the openings for the cranial nerves. Scale bar: 50 mm.

The parietals in the specimen from Andrés are unfused as occur in *Allosaurus* (Madsen 1976; Chure 2000), whereas these elements are fused in most carcharodontosaurids as well as in several basal theropods (e.g. Brusatte and Sereno 2007; Wu et al. 2009; Brusatte et al. 2010b; Eddy and Clarke 2011; Xing et al. 2013). In occipital view, the parietal blades do not extend significantly above the skull table and it seems that they are placed slightly bellow the dorsal margin of the supraoccipital. However, the dorsal crest of the supraoccipital is strongly distorted and somewhat dorsally displaced thus the dorsal position relative to the parietal blades may be an artifact of preservation. In *Allosaurus* "*jimmadseni*" (Chure 2000) and *Yangchuanosaurus shangyuensis* (Dong et al. 1983) the transverse parietal crest is well-developed extending dorsal to the skull table and well-above the dorsal margin of the supraoccipital crest. This higher dorsal extension of the parietals is also present in other *Allosaurus* specimen (BYU 725/13679) as well as in *Carnotaurus* (Coria and Currie 2003), tyrannosaurids (Bakker et al. 1988; Coria and Currie 2003), and troodontids (Currie 1985; Coria and Currie 2003). In *A. fragilis* (Madsen 1976), *Sinraptor dongi* (Eddy and Clarke 2011), *Giganotosaurus* (Coria and Currie 2003), *Shidaisaurus* (Wu et al. 2009), *Cryolophosaurus* (Smith et al. 2007), and several other basal theropods the parietal blades extend only slightly above the supraoccipital crest. On the other hand, in *Shaochilong maortuensis* (Brusatte et al. 2010b) and *Acrocanthosaurus atokensis* (Eddy and Clarke 2011) the parietals are even with or slightly lower than the supraoccipital. In MNHNUL.P.AND21 the dorsal margin of the parietal blades is slightly concave at midline, above the supraoccipital crest. This feature is shared with *Allosaurus*, whereas in *Monolophosaurus*, *Acrocanthosaurus*, *Carcharodontosaurus*, *Sinraptor*, and *Yangchuanosaurus* the blades of the parietal meet at midline and form a continuos margin (Chure 2000; Eddy and Clarke 2011).

The anterolateral margins of the parietals, which form the medial surface of the supratemporal fenestra, are vertical thus the fossa is broadly exposed dorsally. This morphology is similar to *Allosaurus* (Madsen 1976; Chure 2000), *Sinraptor* (Currie and Zhao 1993), *Acrocanthosaurus* (Eddy and Clarke 2011), and *Eocarcharia* (Sereno and Brusatte 2008). On the contrary, the parietals project laterally and overhang the medial part of the supratemporal fossa, strongly reducing the dorsal exposition of this opening in *Carcharodontosaurus* (Coria and Currie 2003; Brusatte et al. 2010b), *Giganotosaurus* (Coria and Currie 2003), and *Shaochilong* (Brusatte et al. 2010b). Also, the medial margins of the supratemporal fenestra are almost parallel and are separated by wide, dorsally exposed parietal surfaces. This condition has been considered the derived character for Theropoda (Currie and Zhao 1993) and is shared with most allosauroids, including *Allosaurus* (Madsen 1976; Chure 2000), *Sinraptor* (Currie and Zhao 1993), and *Acrocanthosaurus* (Currie and Carpenter 2000; Eddy and Clarke 2011), but also with *Piveteausaurus* (Taquet and Welles 1977; Coria and Currie 2003). This trend is even more developed in *Giganotosaurus* (Coria and Currie 2003) and *Carcharodontosaurus* (Coria and Currie 2003; Brusatte and Sereno 2007), which have widely separated supratemporal fenestra. The plesiomorphic condition of a supratemporal fenestra separated by a narrow area of the parietals dorsal surface is present in several more basal theropods, including *Abelisaurus* (Coria and Currie 2003), *Carnotaurus* (Coria and Currie 2003), *Ceratosaurus* (Gilmore 1920), *Monolophosaurus* (Coria and Currie 2003; Brusatte et al. 2010a), *Sinosaurus* (Xing et al. 2013), and *Shidaisaurus* (Wu et al. 2009).

In occipital view, the articulated parietals of MNHNUL.P.AND21 are wider than tall as occur in *Allosaurus fragilis*, *Monolophosaurus jiangi*, and *Sinraptor dongi*, whereas they are taller than wide in *Allosaurus* "*jimmadseni*" (Chure 2000). The presence of a deep concavity ventrally to the parietal midline at the level of the suture between the supraoccipital and the parietals is a feature shared with *Allosaurus fragilis* (Madsen 1976), *A.* "*jimmadseni*" (Chure 2000), *Shaochilong maortuenis* (Brusatte et al. 2010b), *Monolophosaurus jiangi* (Brusatte et al. 2010a), and several other theropods. This concavity is filled with sediments and it is not possible to confirm, at the moment, the presence of openings for the passage for the dorsal head vein (Chure 2000; Brusatte et al. 2010a) (=caudal middle cerebral vein *sensu* e.g. Xing et al. 2014; Witmer and Ridgely 2009) within this concavity as occur in other allosauroids. Also as occur in most theropods, including *Acrocanthosaurus*, *Allosaurus*, and tyrannosaurids, the

dorsal surfaces of the frontal, the intertemporal region of the parietal and the supraoccipital are placed in the same plane in MNHNUL.P.AND21. On the contrary, in *Carcharodontosaurus* (e.g. Brusatte and Sereno 2007), *Giganotosaurus* (Coria and Currie 2003), and *Sinraptor* (Currie and Zhao 1993) an inflection at the frontoparietal suture produces upward projected parietals from the frontal plane.

Supraoccipital. The supraoccipital contacts the parietals dorsally and laterally and the exoccipital-opisthotic complex ventrally. In occipital view, the supraoccipital has the shape of an inverted T with a vertical, relatively high crest (= supraoccipital wedge *sensu* Rauhut 2003 = supraoccipital knob or tuberosity *sensu* Sampson and Witmer 2007; Brusatte et al. 2010b) extending along most of the dorsoventral height of the parietals, and two ventral processes projecting laterally. These ventral processes articulate with the dorsomedial margin of the paroccipital processes. The supraoccipital crest is complete, but strongly distorted. However, it is possible to infer the morphology, which would be massive and triangular in cross-section. This crest is slightly broader dorsally and extends somewhat above the dorsal margin of the parietal blades. However, this higher position of the supraoccipital crest relative to the parietal blades is probably an artifact of preservation, as was discussed above, and the crest would likely reached the dorsal margin of the parietal or ended slightly ventral to it. The dorsal margin of the supraoccipital is significantly narrower than the occipital condyle. The ventral processes extend laterally and form a pair of shallow concavities dorsally where they contact with the parietals (Fig. 6.3.15A–B). These concavities occupy almost the entire ventrolateral surface of the supraoccipital. The ventral processes of the supraoccipital joint medially in a narrow and shallow vertical groove that opens into the dorsal margin of the foramen magnum. This small medial extension represents the contribution of the supraoccipital to the dorsal rim of the foramen magnum.

The supraoccipital crest in MNHNUL.P.AND21 shares with *Allosaurus* (Madsen 1976; Chure 2000) several features, including: (i) similar dorsoventral extension, which is approximately the height of the supraoccipital, but that ends above the margin of the foramen magnum; (ii) wider dorsal margin relative to the ventral part; and (iii) presence of a concave dorsal surface. In *Sinraptor* (Currie and Zhao 1993) the supraoccipital crest is almost as wider dorsally as ventrally and in *Acrocanthosaurus* (Currie and Carpenter 2000; Eddy and Clarke 2011) a fold extending along the midline of the crest separates the process into two distinct knobs termed the "double boss". Some specimens of *Allosaurus* (DINO 11541: Eddy and Clarke 2011) also have a folded supraoccipital wedge. The lateromedial width of the supraoccipital crest is less than twice the width of the foramen magnum as occur in *Allosaurus* (Madsen 1976; Chure 2000), *Sinraptor* (Currie and Zhao 1993) and most other theropods (e.g. Taquet and Welles 1977; Sampson and Witmer 2007). This structure is greater than twice the width of the foramen in most carchardontosaurids, including *Shaochilong* (Brusatte et al. 2010a), *Acrocanthosaurus* (Stovall and Langston 1950), *Carcharodontosaurus* (Sereno et al. 1996), and *Giganotosaurus* (Coria and Currie 2003).

The supraoccipital participates in the dorsal margin of the foramen magnum in many basal theropods, including *Piveteausaurus* (Taquet and Welles 1977), *Monolophosaurus* (Brusatte et al. 2010a), *Baryonyx* (Charig and Milner 1997), *Dubreuillosaurus* (Allain 2005b), *Piatznitzkysaurus* (Rauhut 2004), *Cryolophosaurus* (Smith et al. 2007), *Allosaurus* (Madsen 1976; Chure 2000), *Sinraptor* (Currie and Zhao 1993), *Acrocanthosaurus* (Eddy and Clarke 2011), *Carcharodontosaurus* (Brusatte and Sereno 2007), and *Giganotosaurus* (Coria and Currie 2003). On the contrary, the supraoccipital is excluded from the foramen by the exoccipital-opisthotic complex in *Shidaisaurus* (Wu et al. 2009) and *Dilophosaurus* (Welles 1984).

Shallow concavities in the posterolateral surface of the supraoccipital, adjacent to the contact with the paroccipital processes are present in some *Allosaurus specimens* (BYU 725/13679), but are more restricted than in the specimen from Andrés and in other *Allosaurus* specimens the supraoccipital is flat in this are (Madsen 1976). Thus, these well-developed concavities seem to be a feature that distinguishes MNHNUL.P.AND21 from the *Allosaurus* specimens from the Morrison Formation.

Exoccipital-opisthotic complex (= otoccipital *sensu* Bever et al. 2013). The exoccipitals and opisthotic are completely fused without suturing, which is the typical condition in archosaurs and sauropsids in general (Currie 1997; Sampson and Witmer 2007; Bever et al. 2013). This element forms most of the ventrolateral surface of the braincase in occipital and lateral views. It contacts the supraoccipital dorsally, the parietals laterodorsally, the basioccipital posteroventrally, and the prootic to the front. The exoccipital-opisthotic complex forms the lateral margins of the basal tubera, the dorsolateral part of the occipital condyle and most of the margin of the foramen magnus. Sutures between the exoccipital-opisthotic and basioccipital are clearly visible on both sides of the condyle.

The exoccipital has two well-developed and dorsoventrally broad rami, corresponding to the paroccipital processes. These processes are broken distally, but it seems that they would slightly expand distally despite they have subparallel dorsal and ventral margins along most of its length. In anterior view, the dorsal margin of the paroccipital process is slightly concave for receive the ventral process of the parietal. In occipital view, the paroccipital processes strongly extend ventrally in an angle of approximately 45º from the horizontal. The ventralmost margin of the paroccipital processes are near at the same level as the ventral margin of the basal tubera. These processes also extend slightly to the rear with the posteriormost border slightly surpassing the posterior level of the occipital condyle. The paroccipital processes are smooth and shallowly concave in occipital view, whereas they are slightly inflated in anterior view. In anterior view, a shallow concavity is present dorsally at the base of the paroccipital processes, which is interpreted as the dorsal tympanic recess (*sensu* Witmer 1997). This recess is a simple depression and is not bounded by a ridge as occur is *A.* "*jimmadseni*" (Chure 2000) and in this aspect the specimen from Andrés is more similar to *A. fragilis*.

The exoccipital adjacent to the neck of the occipital condyle has a deep concavity delimited ventrally by a sharp horizontal ridge extending from the dorsal margin of the occipital condyle to the mid-height of the base of the paroccipital process. This concavity is sometimes called paracondylar pocket (Welles 1984) or paracondylar recess (Chure 2000). A pair of openings is visible inside this concavity, near the level of the dorsal margin of the condyle and there is another smaller opening in a slightly ventral position (Fig. 6.3.15C–D). The two larger foramina are positioned almost horizontally and are separated by a vertical septum. These foramina are interpreted as the metotic foramen for cranial nerves X and XI. The smaller ventral foramen is interpreted as the opening for the hypoglossal (XII cranial) nerve (Brusatte et al. 2010b).

In anterior view, a projection of the prootic overlaps the base of the paroccipital processes. In the anterolateral surface of the exoccipital-opisthotic, near the base of the paroccipital processes and adjacent to the suture with the prootic, opens the relatively large fenestra ovalis (Fig. 6.3.17A–C). This fenestra is bounded by the exoccipital-opisthotic to the rear and by the prootic to the front. From the fenestra ovalis projects a broad and relatively deep groove extending along the ventral margin of the paroccipital process. This groove is interpreted as the columellar or stapedial groove (Madsen 1976), which represents the pathway for the columella (stapes) to the fenestra ovalis (Smith et al. 2007). This groove may have also transmitted the internal jugular vein from the braincase (Rauhut 2004; Smith et al. 2007).

In ventral view, a staut crista metotica (metotic strut *sensu* Rauhut 2004) connects the paroccipital processes to the ventral processe of the exoccipital (Fig. 6.3.18). This crest separates the lateral and posterior surfaces of the braincase as occur in most theropods, with the exception of carcharodontosaurids (Rauhut 2004).

The exoccipital in the specimen from Andrés do not meet along the ventral margin of the foramen magnum, but are separated by a small projection of the basioccipital. Thus, the basioccipital has a small contribution for the ventral margin of the foramen, which is similar to the condition of *Allosaurus fragilis* (Madsen 1976), *Sinraptor dongi* (Currie and Zhao 1993), "*Yangchuanosaurus*" *hepingensis* (Wu et al. 2009), *Acrocanthosaurus atokensis* (Eddy and Clarke 2011), and *Shaochilong maortuensis* (Brusatte et al. 2010b). In contrast, the basioccipital is excluded from the margin of the foramen in

Allosaurus "*jimmadseni*" (Chure 2000) and apparently also in *Shidaisaurus jinae* (Wu et al. 2009) and *Carcharodontosaurus iguidensis* (Brusatte and Sereno 2007). The exoccipitals are also separated dorsomedially to the foramen magnum thus the supraoccipital has a narrow participation in the dorsal margin of the foramen magnum. This feature has been interpreted as the typical condition for most theropods (e.g. Gilmore 1920; Madsen 1976; Chure 2000; Rauhut 2004). However, this character is poorly established due to obliterating fusion or distortion in several taxa, such as most allosauroids (Currie and Carpenter 2000; Brusatte and Sereno 2007). The exoccipitals exclude the supraoccipital from the dorsal margin of the foramen magnum in several primitive theropods, including *Dilophosaurus* (Welles 1984), *Cryolophosaurus* (Smith et al. 2007), and possibly *Piveteausaurus* (Allain 2005b).

The paroccipital processes extend posteroventrally and laterally with the ventral limite of the processes positioned approximately at the same level as the basal tubera. This is the typical morphology for most theropods, including allosaurids (Gilmore 1920; Madsen 1976; Chure 2000) with the exception of *Sinraptor* (Currie and Zhao 1993), in which the paroccipital processes extend significantly more ventrally than the basal tubera as also occur in tyrannosaurids (Bakker et al. 1988) and dromaeosaurids (Colbert and Russel 1969). Paroccipital processes projecting ventrally with the distal margin located ventral to the foramen magnum has been considered by some authors as a synapomorphy for Allosauroidea (e.g. Rauhut 2003; Holtz et al. 2004). This character was used to relate *Monolophosaurus* and allosauroids (Rauhut 2003; Brusatte et al. 2010b). However, this feature is also shared with *Ceratosaurus* (Madsen and Welles 2000) and *Cryolophosaurus* (Smith et al. 2007). Nevertheless, in these taxa and in *Monolophosaurus* the distal border of the processes extends only slightly below the condyle and the proximal ventral margins are level with the mid-point of the condyle, whereas they are located entirely below the condyle in allosauroids (Madsen and Welles 2000; Brusatte et al. 2010b). Based on these observations, Brusatte et al. (2010a) proposed the ventral base of the paroccipital process, where it emerges from the metotic strut, located entirely below the occipital condyle as an exclusive condition for allosauroids. However, some carcharodontosaurids, including *Shaochilong* and possibly *Carcharodontosaurus* and *Giganotosaurus* have more dorsally positioned paraoccipital processes (Brusatte et al. 2008, 2010b).

MNHNUL.P.AND21 has three openings in the paracondylar recess as was described in *Shaochilong* (Brusatte et al. 2010b). In *Allosaurus* (Madsen 1976), *Giganotosaurus* (Brusatte et al. 2010a), *Acrocanthosaurus* (Paulina Carabajal and Currie 2012), *Baryonyx* (Charig and Milner 1997), *Ceratosaurus* (Brusatte et al. 2010b), and *Irritator* (Sues et al. 2002) it has been considered that only two openings are present. Thus, it seems that the specimen from Andrés may have two openings for the two branches of the hypoglossal (cranial XII) nerve, which would be in contrast with the condition known for most basal theropods (Brusatte et al. 2010b). Two separated foramina for the branches of the cranial nerve XII are also reported in *Sinraptor* (Currie and Zhao 1993; Paulina Carabajal and Currie 2012) and this feauture is poorly known among theropods. Thus, whether the number of hypoglossal foramina is phylogenetically informative or randomly variable is not clear at the moment (Brusatte et al. 2010b).

The exoccipital in the specimen from Andrés is flat adjacent to the foramen magnum and doest not have the pronounced dorsal rims of the foramen that are present in *Acrocanthosaurus*, *Carcharodontosaurus*, and *Giganotosaurus* (Eddy and Clarke 2011) neither the shallow depressions described in many coelurosaurs (Brusatte and Sereno 2007).

Basioccipital. The basioccipital contacts with the exoccipital-opisthotic complex posterolateraly and with the basisphenoid anteroventrally. This element forms the majority of the basal tubera and occipital condyle, but has a small contribution for the ventral margin of the foramen magnum. In occipital view, the ventral part of the basal tubera is approximately as width as the occipital condyle. The condyle is rounded and subcircular in outline, slightly wider transversely than deep dorsoventrally. In posterior view, the condyle has a kidney-shape due to the presence of a broad and shallow groove extending to the rear from the foramen magnum into the dorsal surface of the condyle. The condyle is separated

from the main body of the basioccipital by a short, but robust neck and the condyle itself is bounded by a shallow groove that separates the articular surface from the neck.

Ventrally to the occipital condyle, the basioccipital has two sharp vertical crests extending along the entire posteroventral height. These crests delimit a deep concavity, which corresponds to the subcondylar recess (*sensu* Rauhut 2004 = paracondylar recess *sensu* Chure 2000). The ventral margin of the basioccipital is slightly wider than the width below the occipital condyle and has a deep medial concavity bounded by a pair of rounded lateral processes projecting ventrally.

The ventral surface of the bacioccipital has a deep pit adjacent to the suture with the exoccipital-opisthotic complex and with the basisphenoid. This pit connects with a deep groove extending anteroposteriorly along the ventrolateral surface of the basisphenoid dorsal to the basal tubera. However, this groove does not have the large pneumatopore that has been described in most carcharodontosaurids such as *Shaochilong* (Brusatte et al. 2010b), *Carcharodontosaurus* (Brusatte and Sereno 2007), *Giganotosaurus* (Coria and Currie 200), and *Acrocanthosaurus* (Eddy and Clarke 2011). In these taxa as well as in *Piatnitzkysaurus*, small pneumatopores are also present associated with the subcondylar recess (Coria and Currie 2003; Rauhut 2004). The presence of large pneumatopores entering the posterior surface of the basioccipital ventromedial to the occipital condyle has been considered an exclusive feature of carcharodontosaurids (Brusatte and Sereno 2008; Brusatte et al. 2010b).

The basal tubera projects ventrally relative to the level of the dorsal surface of the frontals and thus it is perpendicular to a horizontal plane drawn through the occipital condyle as occur in *Allosaurus* (Madsen 1976; Chure 2000) and *Acrocanthosaurus* (Brusatte et al. 2010b). In contrast, the basal tubera is posteroventrally projected in *Shaochilong*, *Carcharodontosaurus*, *Giganotosaurus*, and *Sinraptor* (Coria and Currie 2002; Brusatte and Sereno 2007; Brusatte et al. 2010b).

The basal tubera in MNHNUL.P.AND21 is approximately as wider as the occipital condyle as occur in *Acrocanthosaurus*, *Allosaurus*, *Sinraptor*, and *Monolophosaurus* (Brusatte et al. 2010a), but contrasting with *Shaochilong*, *Carcharodontosaurus*, *Giganotosaurus*, and most other theropods in wich it is much wider transversely than the occipital condyle (Brusatte and Sereno 2007; Brusatte et al. 2010b). The lateral surfaces of the tubera are formed by descending processes of the exoccipital-opisthotic and the two elements are separated by a notch ventrally as occur in most theropods (Rauhut 2004).

The occipital condyle is nearly circular as in *Allosaurus* (Madsen, 1976; Chure, 2000) and most other theropods (Currie and Zhao 1993; Currie and Carpenter 2000; Rauhut 2004), but it is more oval in *Giganotosaurus* (Currie and Zhao 1993) and *Piveteausaurus* (Taquet and Welles 1977).

Basisphenoid-parasphenoid complex. The basisphenoid seems to be fused with the parabasisphenoid. However, the parabasisphenoid is much incomplete preserving a small fragment of the base, but almost the entire cultriform process is absent. The basisphenoid is also incomplete to the front and the basipterygoid processes are missing. In lateral view, the basisphenoid shows a deep and large concavity near the ventral end of the base of the parabasisphenoid, which is interpreted as equivalent to the pneumatic recess for a diverticulum of the anterior tympanic system (*sensu* Witmer 1997) that is present in other allosauroid specimens (Chure 2000; Brusatte et al. 2010b). This concavity is partially covered by the preotic pendant, but it is possible to verify that it is bounded by raised ventral and dorsal crests (Fig. 6.3.17A–B). The position of this recess is compatible with the prootic recess (*sensu* Witmer 1997 = lateral basisphenoidal recess *sensu* Chure and Madsen 1996), whereas the more ventral concavity corresponding to the subotic recess (*sensu* Witmer 1997) that excavates the basal tubera in several tetanurans is much shallow in the specimen from Andrés. Similar recesses are described in *Allosaurus* "*jimmadseni*" (Chure 2000), but in this specimen the ventral recess is more marked than in MNHNUL.P.AND21 and in *Allosaurus fragilis*. However, considering that pneumatic feautures are highly variable related with ontogeny (Britt 1993; Chure and Madsen 1996; Witmer 1997) or even in the same individual (Rauhut 2004), this difference possibly has not systematic significance (Chure

2000). A caudal tympanic recess opening in the anteroventral surface of the base of the paroccipital process is absent in the specimen from Andrés. This recess is tentatively identified in *Sinraptor* (Paulina Carabajal and Currie 2012). The presence of this recess is unusual for basal theropods and has been considered to be exclusive for coelurosaurs, with the exception of *Troodon* (Witmer 1997; Norell et al. 2006). Paulina Carabajal and Currie (2012) suggest that a caudal tympanic recess might be also present in *Acrocanthosaurus* and *Allosaurus*, which would indicate that this trait appeared earlier in theropod evolution. However, this recess seems to be genuinely absent in MNHNUL.P.AND21 and in some *Allosaurus* specimen (e.g. UMNH VP 16605 / UUVP 5583; UMNH VP 5472 / UUVP 3287; UMNH VP 16606 / UUVP 5961; BYU 725/13679: E.M. pers. obs. 2010) as well as in *Acrochantosaurus* (Eddy and Clarke 2011). Thus this feature may have appeared convergently in *Sinraptor* and coelurosaurian theropods (Paulina Carabajal and Currie 2012).

The metotic strut (*sensu* Witmer 1990 = crista metotica, crista tuberalis *sensu* e.g. Xing et al. 2014 or ventral buttress of other authors) is a conspicuous ridge projecting posterolaterally from the base of the paroccipital process through the lateral side of the basal tubera up to the lateral side of the basisphenoid, thus separating the lateral and posterior walls of the braincase, as in most theropods with the exception of carcharodontosaurids (Coria and Currie 2003; Smith et al. 2007).

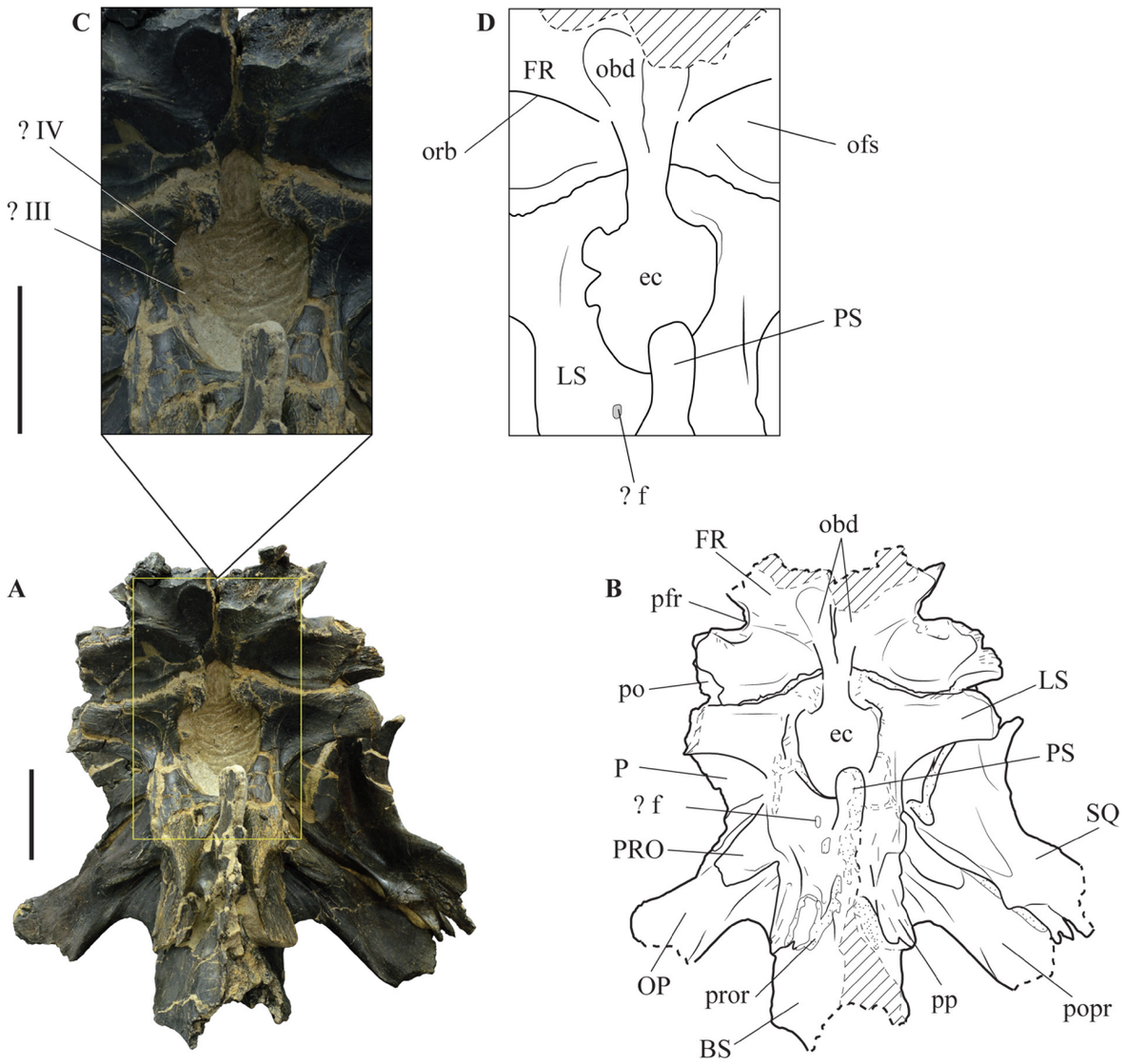

Figure 6.3.16. MNHNUL.P.AND21, braincase and corresponding interpretative drawing in anterior view (A–B); (C–D), detail of the area of the endocranial cavity showing the structure of the olfactory bulb depressions on the frontals. Scale bar: 50 mm.

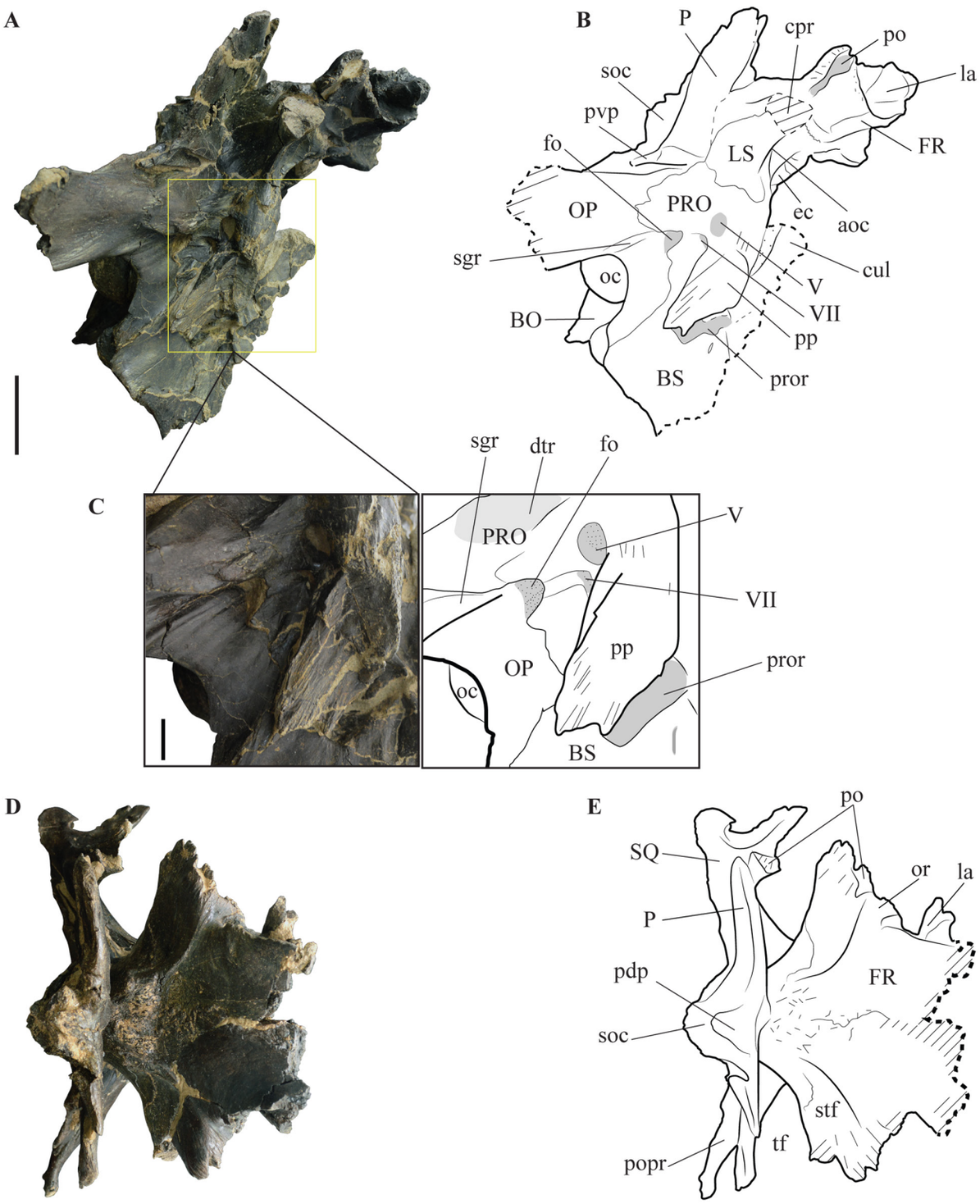

Figure 6.3.17. MNHNUL.P.AND21, Braincase and corresponding interpretative drawing in right lateral (A–B); and dorsal (D–E) views; (C), detail of the area of the lateral surface of the braincase showing the several openings for cranial nerves and pneumatic structures. Scale bar: 50 mm.

In ventral view, the basisphenoid and the basioccipital delimit a large and deep recess with a subrectangular outline ventrally and slightly tapered dorsally. This recess corresponding to the basisphenoid recess (*sensu* Witmer 1997; also sometimes called basisphenoid sinus or basicranial fontanelle *sensu* Coria and Currie 2003) is only visible in ventral view and it still partially covered by matrix thus the dorsoventral extention is not possible to know. The ventral basisphenoid recess

is partially subdivided by a thin blade projecting dorsoventrally in the mid-line of the anteroventral surface of the basioccipital (Fig. 6.3.18). This blade is probably equivalent to the septum that splits the basisphenoid recess dorsally in *Piatnitzkysaurus* (Rauhut 2004), *Acrocanthosaurus* (Eddy and Clarke 2011), and apparently also in *Carcharodontosaurus* (Brusatte and Sereno 2007). However, in *Acrocanthosaurus* (Eddy and Clarke 2011) the septum is more robust and extends from the anterior surface of the recess, wereas in MNHNUL.P.AND21 it projects from the posterior surface. In *Carcharodontosaurus* the septum is interpreted as having a mediolateral orientation thus dividing the recess into anterior and posterior chambers (Brusatte and Sereno 2007), whereas in the specimen from Andrés the septum has an anteroposterior orientation as is typical in most tetanurans (Witmer 1997; Rauhut 2004; Eddy and Clarke 2011).

Dorsally, the basisphenoid-parasphenoid complex is strongly distorted so the suture with the prootic and with the laterosphenoid it is not visible, but it seems that the parabasisphenoid makes a short contribution for the anterior floor of the endocranial cavity. The parabasisphenoid preserves only a small fragment that consists in two thin blades projecting anterodorsally from the anterior margin of the basisphenoid. These blades converge dorsally in a single, very thin blade that overlaps the pituitary fossa.

A basisphenoidal recess only visible in ventral view has been considered the primitive condition for theropods (Chure 2000) and is shared with *Allosaurus*, and *Monolophosaurus* (Gilmore 1920; Madsen 1976; Chure 2000; Zhao and Currie 1993). In *Acrocanthosaurus* (Chure and Madsen 1998; Chure 2000), *Sinraptor* (Currie and Zhao 1993), as well as in *Sinosaurus* (Xing et al. 2014) and to a lesser degree in *Piatnitzkysaurus* (Rauhut 2004) the recess is visible in posterior view.

The presence of a well-marked recess in the anterolateral surface of the basisphenoid is a feature shared with *Acrocanthosaurus* (Chure 2000), *Shaochilong* (Brusatte et al. 2010b), *Sinraptor* (Gao 1992; Currie and Zhao 1993), and *Piatnitzkysaurus* (Chure 2000). The condition in *Allosaurus* is variable as was discussed above, but a more or less-developed recess is always present is this taxon (Madsen 1976; Chure 2000).

The basisphenoid is excluded from the basal tubera by the exoccipital and it is separated from the tubera by a deep groove. This feature has been considered as an autapomorphy for *Allosaurus* (Chure 2000). Sereno et al. (1994) considered the exclusion of the basisphenoid from the basal tubera as a synapomorphy for Allosauroidea. However, the basisphenoid forms part of the basal tubera in *Acrocanthosaurus* (Chure 2000) and *Sinraptor* (Currie and Zhao 1993).

Prootic. The paired prootic contacts the laterosphenoid anterodorsally, the basisphenoid anteroventrally and the parietal posterodorsally. Sutures with these elements are mostly obscured by distortion. However, the prootic clearly overlaps the exoccipital-opisthotic to the rear extending slightly along the base of the paroccipital process and this suture is strongly sinuous (Fig. 6.3.17A–C). Laterally, the prootic contacts with the opisthotic and together they form the roof of the stapedial canal and of the fenestra ovalis.

The prootic has a pair of ventral blade-shaped processes, the preotic pendant (*sensu* Welles 1984 = ala basisphenoidalis *sensu* Taquet and Welles 1977; alar process of the laterosphenoid *sensu* Bonaparte 1986; ala basisphenoidalis *sensu* Chure and Madsen 1996; crista prootica *sensu* Currie and Zhao 1993) projecting posteroventrally as a wing-like structure that overlaps the laterodorsal surface of the basioccipital. The distinct names proposed for this process reflect the different interpreteation of various authors for the composition of this structure. Chure and Madsen (1998) proposed that the "crista prootica" is a lateral process of the basisphenoid in some, if not all, theropods. In MNHNUL.P.AND21, sutures between the prootic and basisphenoid are unclear, but it seems that the prootic overlaps the basisphenoid anteromedially and that the preotic pendant is entirely formed by the prootic. In *Shaochilong*, a raised ridge extending anterodorsally along the lateral surface of the preotic pendant is interpreted as the contact between the prootic and basisphenoid and thus the

pendant is almost evenly divided between these two elements (e.g. Brusatte et al. 2010b). The specimen from Andrés has a similar ridge but it clearly does not represent this contact, which is visible more to the rear. The preotic pendant is slightly concave in anterior view and has a series of thin vertical ridges and grooves mostly along the ventral surface.

Posterolaterally, a broad tongue-like process of the prootic, sometimes termed the caudal process, overlaps the base of the paroccipital process. At approximately the mid-height of the caudal process, the prootic has a well-marked longitudinal crest extending ventrolaterally from the base of the process. This crest extends towards the lateral process of the laterosphenoid and delimits a shallow concavity, which is interpreted as the dorsal tympanic recess (*sensu* Witmer 1997). Laterally, the prootic consists of a thin and strongly pneumatic blade between the preotic pendant and the caudal process, which is sometimes called the prootic superficial lamina (*sensu* Bever et al. 2013). Ventrally to the caudal process of the prootic and adjacent to the suture between the prootic and exoccipital, a large and funnel-shaped fenestra ovalis pierces the lateral surface of the braincase with an anteroposterior orientation. The prootic forms the dorsal margin of the fenestra ovalis as occur in *Piveteausaurus* (Taquet and Welles 1977), *Piatnitzkysaurus* (Rauhut 2004), *Allosaurus* (Chure 2000), *Carcharodontosaurus* (Brusatte and Sereno 2007), but not in other allosauroids (e.g. *Shaochilong*: Brusatte et al. 2010b) in wich the prootic terminates immediately anterodorsal to the fenestra. Dorsally to the fenestra ovalis, is another large and rounded opening, which is enclosed entirely within the prootic, which is interpreted as the trigeminal foramen (for the cranial nerve V). A smaller funnel-shaped opening interpreted as the foramen for the facial nerve (cranial nerve VII), is placed between the fenestra ovalis and the trigeminal foramen. A small groove extends posteroventrally from the trigeminal foramen to the margin of the fenestra ovalis (Fig. 6.3.17A–C). This groove is interpreted as for transmit the hyomandibular branch of the facial nerve after it emerged from the braincase (Brusatte et al. 2010a) and it does not enter the fenestra ovalis, but rather is separated from it by the raised anterior rim of the fenestra.

The pattern of foramina described above for MNHNUL.P.AND21 is similar to that described in *Allosaurus* (Chure 2000) and is not significantly different from those of other allosauroids such as *Sinraptor* (Currie and Zhao 1993), *Acrocanthosaurus* (Chure 2000) and *Shaochilong* (Brusatte et al. 2010b). The trigeminal foramen is usually bounded by the prootic posteroventrally and by the laterosphenoid anterodorsally in most theropods, including *Acrocanthosaurus* (Eddy and Clarke 2011) and *Shaochilong* (Brusatte et al. 2010b) and this seems to be also the case in MNHNUL.P.AND21. The foramen for the trigeminal nerve is filled with sediments, but it apparently consists of a single opening as in *Monolophosaurus* and possibly *Cryolophosaurus*, *Acrocanthosaurus*, *Carcharodontosaurus*, *Giganotosaurus*, and most other theropods (Coria and Currie 2003; Brusatte and Sereno 2007; Smith et al. 2007; Brusatte et al. 2010a; Eddy and Clarke 2011). In *Allosaurus* it is usually considered that the trigeminal foramen is splited into separate exits for the ophthalmic branche (V1) and the maxillary and bandibular branches (V2,3) of the trigeminal nerve (e.g. Currie and Zhao 1993; Brusatte and Sereno 2007; Brusatte et al. 2010a; Eddy and Clarke 2011; Paulina Carabajal and Currie 2012) as also occur in *Piveteausaurus* (Taquet and Welles 1977) and possibly *Sinosaurus* (Xing et al. 2014), but also in several derived tetanurans, including troodontids and tyrannosaurids (e.g. Brochu 2003). However, at least some *Allosaurus* specimens are described as having a large, circular and not divided trigeminal foramen (Chure 2000) and some specimens of *Carcharodontosaurus* and *Acrocanthosaurus* (Brusatte and Sereno 2007) have a completely divided trigeminal foramen. *Sinraptor* (Currie and Zhao 1993; Paulina Carabajal and Currie 2012) and *Dubreuillosaurus* (Allain 2005b), for example, have an intermediate condition with the trigeminal foramen dorsoventrally constricted at one point, which was interpreted as an incipient division of the foramen.

Laterosphenoid (= alisphenoid *sensu* Gilmore 1920). The laterosphenoid forms most of the lateral margins of the endocranial cavity. It overlaps the anterodorsal margin of the prootic and the anteroventral margin of the parietal within the supratemporal fenestra. The laterosphenoid contribution to the supratemporal fenestra is large, but this element is only visible within the fenestra in lateral

view. In anterior view, the conjoined laterosphenoids have a pair of robust processes, the capitate processes (*sensu* Sampson and Witmer 2007), expanding laterally around the endocranial cavity. The capitate processes have rounded distal surfaces, the distal cotylus (*sensu* Madsen 1976), which would fit in a broad oval concavity of the postorbital. Ventrolaterally, the well-developed antotic crest (*sensu* Sampson and Witmer 2007) extends from the ventrolateral surface of the laterosphenoid through the ventral margin of the capitate processe. As occur in most allosauroids (e.g. Brusatte et al. 2010b), the antotic crest is not continuous with the otosphenoidal crest in the ventral surface of the lateral process of the prootic, but instead these crests are separated by the fossa that houses the trigeminal foramen. The laterosphenoid connects laterally with the frontal and with a narrow process of the parietal. A small notch is present in the junction between the laterosphenoid, frontal and parietal and it apparently opens into the lateral temporal fenestra. The anterior surface of the capitate processes is slightly concave ventrally near the base. In cross section, these processes are triangular with strongly tapered ventral margins. Ventrally, the laterosphenoids are somewhat distorted and the suture with the prootic and with the parabasisphenoid is indiscernible.

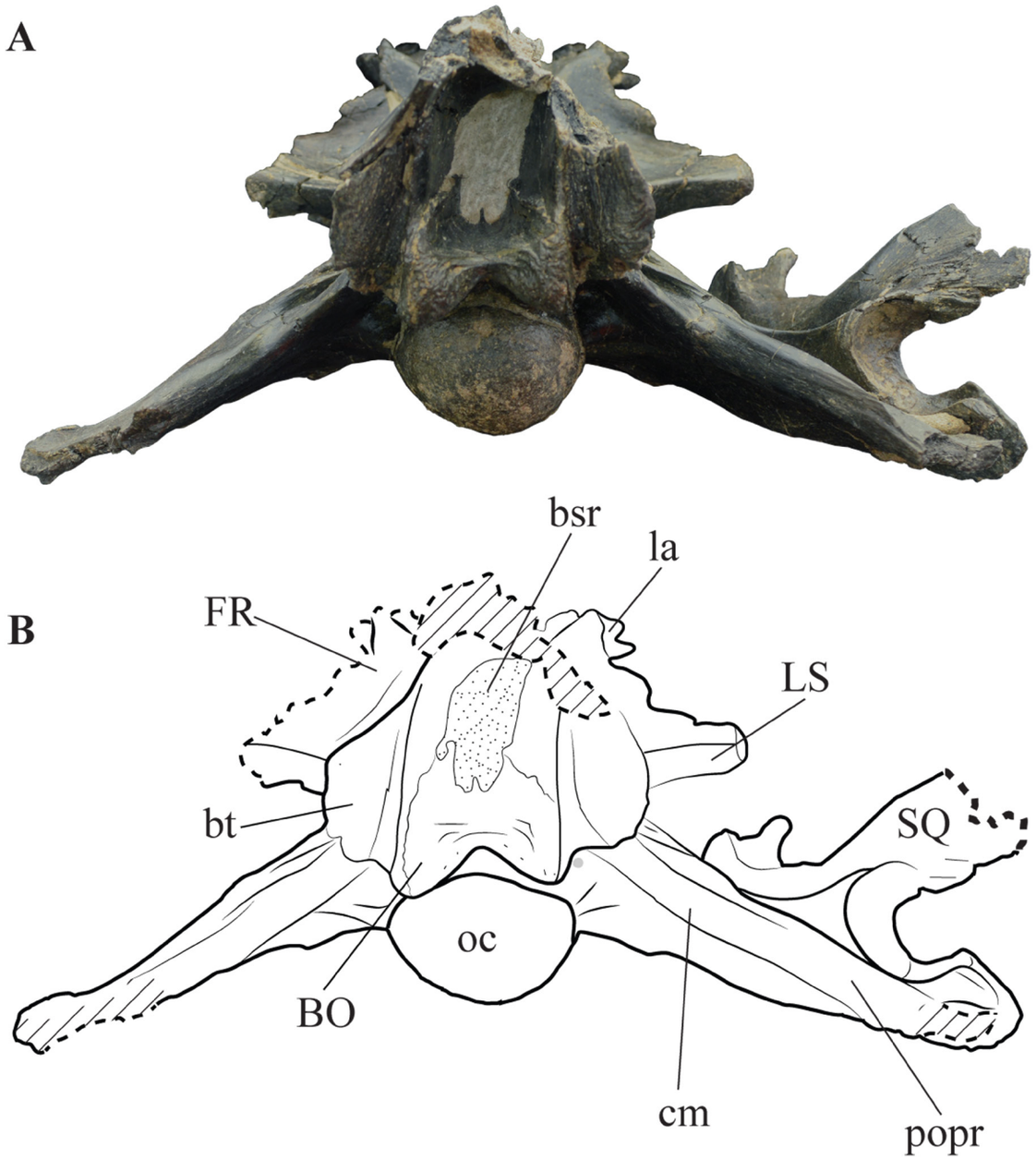

Figure 6.3.18. MNHNUL.P.AND21, braincase and corresponding interpretative drawing in ventral view. Scale bar: 50 mm.

Lower jaw

Articular. An almost complete and well-preserved right articular, MNHNUL.P.AND11, was recovered in Andrés (Fig. 6.3.19). This element lacks the blade for contact with the surangular and the dorsal end of the retroarticular process. In lateral view, the articular has a rectangular shape. The glenoid fossa, which would receive the medial condyle of the quadrate is positioned in the dorsal surface of the anterior part of the articular and is strongly concave with a semi-circular outline. In lateral view, the retroarticular process in the posterior portion of the articular is a mediolaterally thin and anteroposteriorly long blade projecting dorsomedially. This process is broken dorsally thus the precise morphology is not possible to know, but based on the preserved fragment it seems that it would be rectangular in outline.

The medial surface of the articular is broken and most of the surface for articulation with the surangular is missing except for a small fragment of the anterior part. This fragment has a series of thin ridges and grooves indicating a firm, immovable sutural contact between the articular and the surangular as occur in other *Allosaurus* specimens (Madsen 1976). A robust process interpreted as the pendant medial process extends medially from the dorsal margin of the articular between the glenoid fossa and the retroarticular process (Fig. 6.3.19A). This process forms the floor of a deep canal that extends mediolaterally corresponding to the opening for the chorda tympani. The presence of a pendant process in the articular has been considered as a synapomorphy for Allosauroidea (Sereno et al. 1996; Chure 2000). A small foramen pierces the anterior margin of the lateral surface of the articular. This foramen seems to connect with other small foramen in the floor of the openning for the chorda tympani. A similar foramen is described in *Sinraptor* and is interpreted as the passage for the posterior condylar artery (Currie and Zhao 1993). The ventral surface of the articular is a mediolaterally thin and straight blade with a shallow longitudinal groove to the front corresponding to the surface for articulation with the prearticular (Fig. 6.3.19F).

The rectangular shape of the retroarticular process in MNHNUL.P.AND11 is distinct from the semicircular process of *Acrocanthosaurus* (Eddy and Clarke 2011) and from the much more elongated process of *Sinraptor* (Currie and Zhao 1993). Beside, this process extends posteriomedially from the glenoid as occur in *Allosaurus*, whereas in most other theropods it is posterolaterally projected (Currie and Zhao 1993).

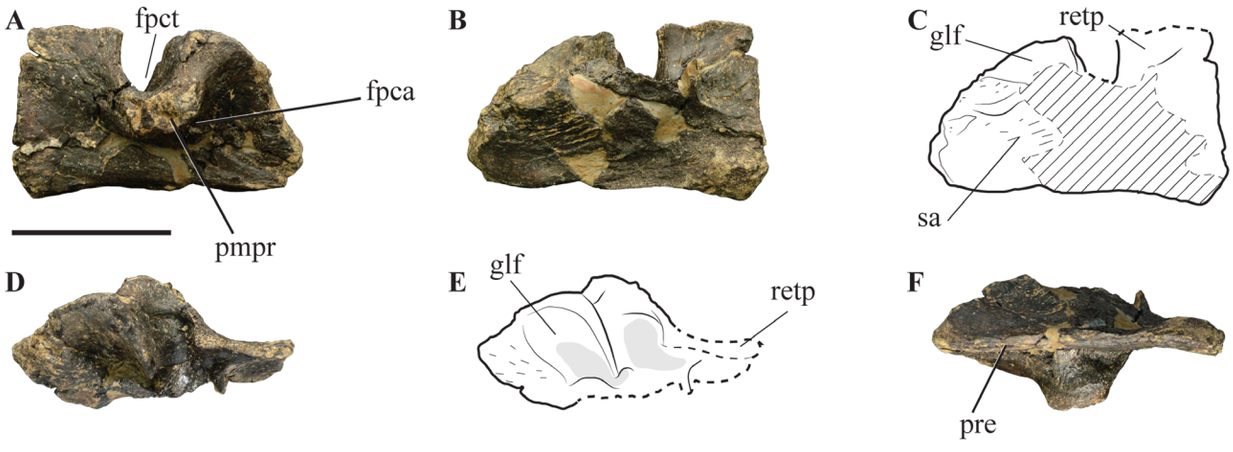

Figure 6.3.19. MNHNUL.P.AND11, right articular and corresponding interpretative drawing in medial (A); lateral (B–C); dorsal (D–E); and ventral (F) views. Scale bar: 50 mm.

Surangular. Two surangulars, one right, MNHNUL.P.AND12 (Fig. 6.3.20A–H), and one left, MNHNUL.P.AND13.3 (Fig. 6.3.20I–N), were collected in Andrés. The left surangular was in a block with the left prearticular and a fragment of the posterior part of a right nasal. The left surangular

and prearticular preserves approximately the original anatomical position, with the prearticular only slightly displaced to the rear.

The surangular is a thin, long and deep blade that strongly tapers to the front and to the rear. It articulates with the articular, antarticular and prearticular posteromedially, with the angular ventrolaterally, with the dentary to the front, and with the supradentary and coronoid anteromedially. Dorsally, the surangular has a moderately robust crest that extends anteroposteriorly. This dorsal crest extends slightly medially and laterally forming the medial and lateral surangular shelves, respectively. The lateral shelf (adductor ridge *sensu* Coria and Currie 2006) is a well-developed ridge delimiting a deep and oval concavity in the posterior part of the surangular. Three small foramina are visible inside this concavity (Fig. 6.3.20A–B). The posteriormost foramen is slightly larger than the others and is interpreted as corresponding to the posterior surangular foramen described in other allosauroids (e.g. Madsen 1976). The posterior surangular foramen pierces the posterior part of the lateral surface of the surangular with a posteroanterior orientation and it seems to connect with other foramen in the medial surface just beneath the antarticular process. Ventrally to the posterior concavity, the thin blade of the surangular shows a rough area consisting of a series of tinny oblique grooves and ridges, which is interpreted as the surface for contact with the angular. This surface starts near the posterior margin of the surangular, where a well-marked groove extends anterodorsally to near the level of the posterior surangular foramen. Anteriorly, the lateral shelf of the surangular is pierced by the anterior surangular foramen, which is located inside a deep, longitudinal groove. This foramen has been interpreted as for the branches of the inferior alveolar nerve (Currie and Zhao 1993; Brusatte et al. 2010a).

The anterior part of the surangular is a thin, tapered, and bifurcated blade that would articulate with the dentary. To the rear, the surangular also strongly tapers, developing a blunt retroarticular process that projects to the rear and somewhat dorsally. At approximately the mid-length of the ventral margin, the surangular has a deep and moderately wide notch opening anteroventrally corresponding to the external mandibular fenestra.

In medial view, the surangular has a deep concavity, delimited dorsally by the well-developed medial shelf projecting along the entire length of the dorsal surface (Fig. 6.3.20C–D). This concavity corresponds to the surangular adductor fossa. The medial shelf extends dorsally in the posterior part of the surangular, but near the mid-length becomes a mediolaterally thin blade projecting ventrally and delimiting a deep, narrow groove adjacent to the dorsal margin of the surangular. To the rear, a strongly rough, fan-shaped surface projecting dorsoventrally is interpreted as the articulation for the articular. Just anterior to the surface for the articular, a robust process corresponding to the antarticular process extends medially from the dorsomedial surface of the surangular. The medial surface of this process has a deep and vertical groove extending along most of the depth of the antarticular process. Between the surface for articulation with the angular and the antarticular process, a deep and broad glenoid fossa opens in the dorsal surface of the surangular. The anterior part of the medial surface of the surangular shows a deep and broad longitudinal groove extending from nearly the level of the anterior margin of the external mandibular fenestra. This groove corresponds to the articulation with the dentary. Posterior to the surface for articulation with the dentary, the medial shelf of the surangular has a slightly concave surface bounded dorsally by a deep longitudinal groove representing the area for articulation with the coronoid.

In dorsal view, the surangular is a relatively thick, convex element with a shallow and elliptical concavity at the mid-length, which is interpreted as the area for insertion of the muscle adductor mandibulae externus (Madsen 1976; Currie and Zhao 1993; Coria and Currie 2006; Eddy and Clarke 2011).

The presence of a retroarticular process in the posteriormost end of the lower jaw, formed by the surangular and angular, has been considered the derived condition for theropods (Chure 2000) and is shared with *Allosaurus* (Madsen 1976), *Sinraptor* (Currie and Zhao 1993), *Yangchuanosaurus* (Dong et

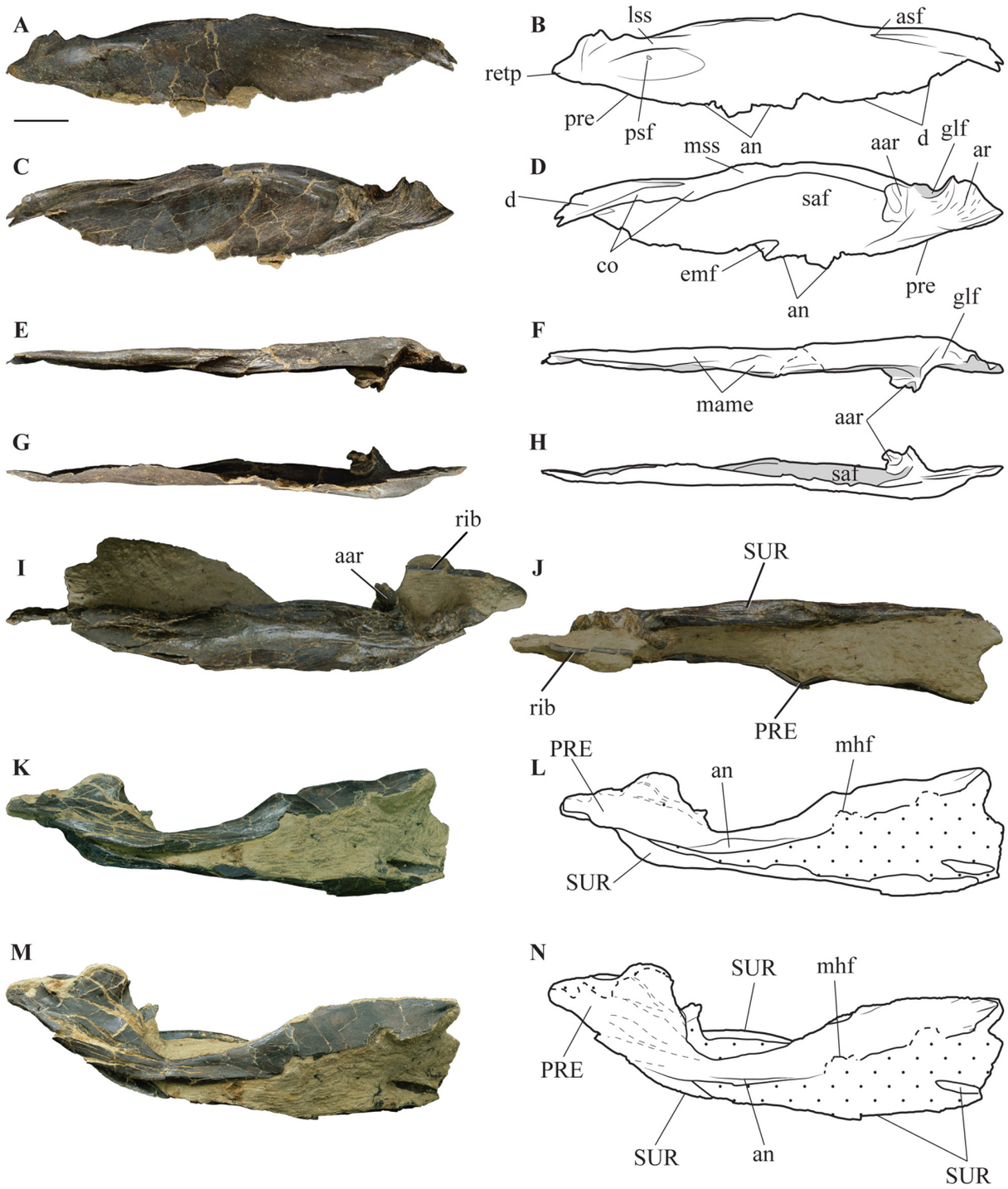

Figure 6.3.20. Surangulars and left prearticular collected in Andrés and corresponding interpretative line drawing. (A–H), right surangular, MNHNUL.P.AND12; and (I–N), left surangular articulated with the prearticular, MNHNUL.P.AND13, in lateral (A–B); medial (C–D, M–N); dorsal (E–F, J); ventral (G–H); dorsolateral (I); and ventrolateral (K–L) views. Scale bar: 50 mm.

al. 1983), and *Acrocanthosaurus*. *Cryolophosaurus* and *Monolophosaurus* lack a retroarticular process and at least in some specimens of *Sinraptor dongi*, *Yangchuanosaurus magnus* and *Acrocanthosaurus atokensis* the process is squared-shaped and more developed than those of *Allosaurus* and *Sinraptor* (Chure 2000).

The presence of a posterior surangular foramen is a feature shared with most tetanuran theropods (Madsen 1976; Dong et al. 1983; Currie and Zhao 1993; Currie and Carpenter 2000; Coria and Currie

2006; Smith et al. 2007; Eddy and Clarke 2011). In *Sinraptor dongi* (Currie and Zhao 1993), a second foramen is present ventrally to the mandibular glenoid and in most coelurosaurs the surangular foramen is generally much larger than those in more basal tetanurans (Madsen 1976). In most theropods the posterior surangular foramen is bordered dorsally by a robust shelf that may be massive and elongated as occur in *Acrocanthosaurus* (Currie and Carpenter 2000; Eddy and Clarke 2011) and *Cryolophosaurus* (Smith et al. 2007). A shorter and pendant shelf similar to that seen in the specimen from Andrés is shared with *Allosaurus* (Madsen 1976) and *Sinraptor* (Currie and Zhao 1993). On the contrary, a lateral shelf is absent in *Monolophosaurus* (Brusatte et al. 2010a). Gauthier (1986) suggested that the robust lateral surangular shelf in "carnosaurs" was associated with the insertion of enlarged pterygoideus musculature. However, no features on the shelf suggest that it served as a site of muscle insertion and Tykoski (1998) instead suggested that it represents an extensive contact for the lower infratemporal bar during adduction of the lower jaws acting to brace the posterior jaw against lateral strain (Smith et al. 2007).

The anterior surangular foramen is continuous to the front with a deep groove as occur in *Allosaurus fragilis* (Madsen 1976), *Sinraptor dongi* (Currie and Zhao 1993), *Acrocanthosaurus atokensis* (Currie and Carpenter 2000; Eddy and Clarke 2011), *Monolophosaurus jiangi* (Brusatte et al. 2010a) and many other theropods. An anterior foramen is absent in the surangular of *Allosaurus* "*jimmadseni*" (Chure 2000). Finally, a reduced external mandibular fenestra has been considered the derived condition for theropods and was proposed as a synapomorphy for Avetheropoda by Sereno et al. (1996). This condition is shared by *Monolophosaurus* (Brusatte et al. 2010a), *Allosaurus* (Gilmore 1920; Madsen 1976; Chure 2000), *Acrocanthosaurus* (Eddy and Clarke 2011), and tyrannosaurids (Brochu 2003), while the primitive condition is retained in *Sinraptor* (Currie and Zhao 1993) and *Yangchuanosaurus* (Dong et al. 1983).

Prearticular. A left prearticular, MNHNUL.P.AND13.2, was collected and is partially articulated with the surangular as was previously mentioned. As these elements still in a block only the medial surface of the prearticular is visible (Fig. 6.3.20K–N). The prearticular is a long, thin and strongly bowed element that forms the posteromedial surface of the lower jaw. This element is dorsoventrally thin at mid-length, but strongly expands to the front and back. The ventral surface of the prearticular is slightly convex and shows a longitudinal flattened surface bounded medially by a sharp ridge projecting ventrally. This surface corresponds to the articulation for the angular. The anterior part of the prearticular is a thin and tapered blade strongly projecting dorsally. The anterior blade has slightly striated dorsal and ventral surfaces corresponding to the sutures for contact with the coronoid and splenial, respectively. The ventral margin of the prearticular is somewhat distorted and incomplete, but a small notch is seen at the level of the base of the anterior expansion. This notch is interpreted as a fragment of the mylohyoid foramen (*sensu* Eddy and Clarke 2011 = internal mandibulat foramen *sensu* Madsen 1976). To the rear, the prearticular strongly widens and extends dorsally forming a moderately broad process for articulation with the antarticular and a thin posterior process for articulation with the articular.

An internal mandibular foramen in the prearticular has been considered absent in most allosauroids with the exception of *Allosaurus* (Madsen 1976; Chure 2000). The presence of this foramen has been interpreted as a synapomorphy for *Allosaurus* (Chure 2000). However, a large foramen is also present in *Acrocanthosaurus* (Eddy and Clarke 2011). The morphology of the internal mandibular foramen is somewhat variable among *Allosaurus* and it is a broadly opened notch in *A. fragilis* or a teardrop-shaped opening in *A.* "*jimmadseni*" (Chure 200).

The prearticular tapers to the rear as occur in *Allosaurus* (Madsen 1976; Chure 2000), but not in *Sinraptor* (Currie and Zhao 1993), in which the posterior part is broader and has several finger-like processes for attachment of ligaments. *Sinraptor* also lacks the neomorph antarticular that is present in *Allosaurus* (Currie and Zhao 1993). The presence of this element in MNHNUL.P.AND13.2 is inferred by the morphology of the articulation in the surangular. The prearticular in the specimen from

Andrés is slightly convex posterior to the internal mandibular foramen, suggesting a relatively straight posterior margin of the mandible as occur in *Allosaurus* (Madsen 1976; Chure 2000), *Monolophosaurus* (Brusatte et al. 2010a), and *Sinraptor* (Currie and Zhao 1993). On the contrary, this region of the mandible is deeply deflected ventrally in *Acrocanthosaurus* (Eddy and Clarke 2011).

Angular. Two almost complete and well preserved angulars, a right, MNHNUL.P.AND17, and a left, MNHNUL.P.AND16, are available for the specimen from Andrés (Fig. 6.3.21). The left angular is complete, but the right one lacks a fragment of the anterior part. These elements are long and thin blades extending anteroposteriorly and together with the prearticular form the ventral margin of the posterior mandible. The angular contacts the dentary and the splenial anterodorsally, overlaps the lateral surface of the surangular to the rear and contacts the prearticular medially.

The angular is dorsoventrally narrow along the anterior mid-length, but gradually expands to the posterior part and then tapers again ending in a narrow and strongly tapered process. In internal view, the angular forms a shallow concavity bounded to the rear by a longitudinal low crest extending along the ventral margin (Fig. 6.3.21A–B, E–F). This crest corresponds to the surface for articulation with the surangular. The angular also articulates with the surangular to the rear and this contact is represented by a striated surface that extends for most of the posterior part of the internal blade. To the rear, the angular is a dorsoventrally thin blade with a flattened area in the internal surface, which is bounded ventrally by a well-developed crest extending anteroposteriorly. This crest is interpreted as the suture for articulation with the prearticular.

The articulation with the dentary in the lateral surface of the posterior blade of the angular is marked by a shallow and longitudinal groove extending along the ventral margin (Fig. 6.3.21C–D, G –H). At aproximately the mid-length the angular has a smooth concavity corresponding to the ventral margin of the external mandibular fenestra.

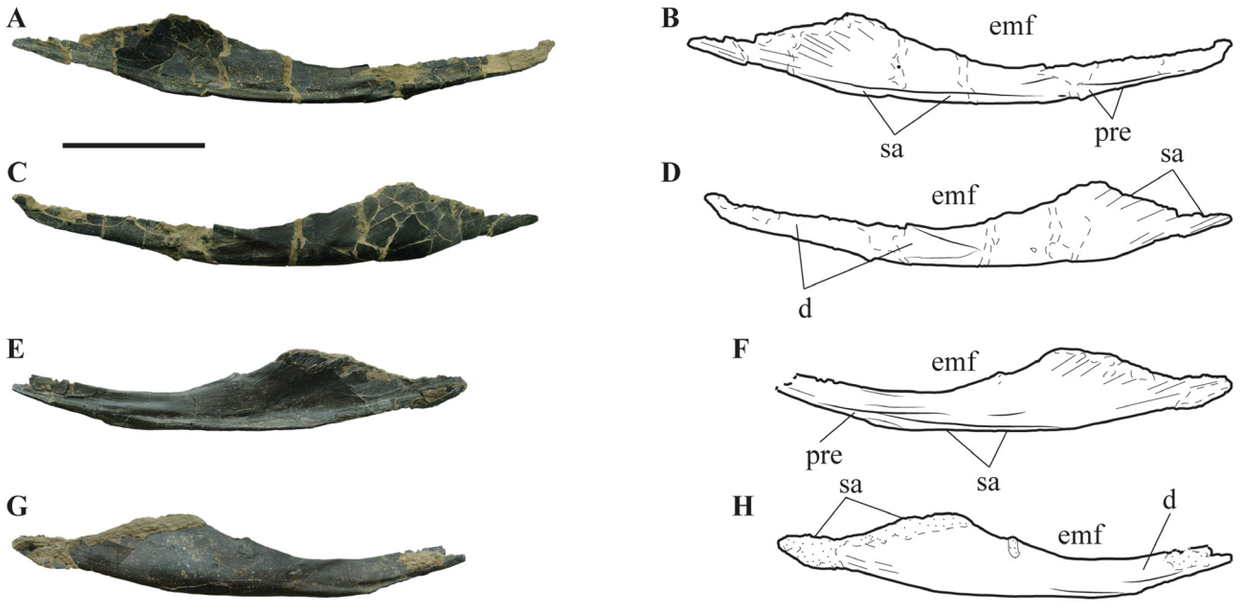

Figure 6.3.21. Angulars collected in Andrés and corresponding interpretative drawing. (A–D), left angular MNHNUL.P.AND16; and (E–H), right angular, MNHNUL.P.AND17 in medial (A–B, E–F); and lateral (C–D, G–H) views. Scale bar: 50 mm.

The angulars collected in Andrés have a general morphology similar to those of *Allosaurus* (Madsen 1976), *Sinraptor* (Currie and Zhao 1993), *Acrocanthosaurus* (Eddy and Clarke 2011), and several other theropods. They differ from *Acrocanthosaurus* in the absence of anteroposteriorly elongated fossae adjacent to the margin of the external mandibular fenestra (Eddy and Clarke 2011). Similar, but larger openings are present in the angulars of *Tyrannosaurus*, nevertheless they are absent in most other

theropods (Madsen 1976; Currie and Zhao 1993; Chure 2000; Eddy and Clarke 2011). The presence of striations on the ventral side of the ventrolateral surface of the articular suggests that the caudal prong of the angular extended to the end of the jaw articulation as occur in *A. fragilis* and *A.* "*jimmadseni*" (Chure 2000) as well as in *Cryolophosaurus* (Smith et al. 2007) and *Monolophosaurus* (Brusatte et al. 2010b). On the contrary, in *Acrocanthosaurus* (Currie and Carpenter 2000; Eddy and Clarke 2011), *Sinraptor* (Currie and Zhao 1993), *Yangchuanosaurus* (Dong et al. 1983) and many other theropods the angular terminates anterior to the posterior surangular foramen.

Supradentary and coronoid. Two thin, blade-shaped elements, MNHNUL.P.AND18, are interpreted as the left supradentary and coronoid (Fig. 6.3.22). The supradentary is broken and the posterior end is missing. This fragile element is a long and mediolaterally thin blade that expands dorsoventrally and with a pointed tip. The supradentary would probably cover the interdental plates over almost their entire length as occur in other theropods (Madsen 1976; Chure 2000; Eddy and Clarke 2011). This element has been interpreted as a protection for the vascular system and interdental plates along the lingual base of the tooth row (Madsen 1976).

In lateral view, the supradentary has a somewhat sigmoidal profile with a slightly concave dorsal margin to the front that becomes almost straight to the rear. The lateral and medial surfaces show thin longitudinal grooves extending along the entire preserved element.

The coronoid is also a mediolaterally thin blade with a triangular posterior expansion and a long anterior ramus. The posterior margin of the coronoid has a small ventral projection extending posteroventrally. This ventral process would probably have an equivalent dorsal extension, but it is broken. To the front, the coronoid strongly narrows in a dorsoventrally thin ramus with nearly parallel margins. Just anterior to the triangular posterior process, the blade of the coronoid has a well-developed crest extending ventrally. The preserved parts of the coronoid and supradentary do not connect with one another in the broken surfaces, but it seems that they belong to the same element and that the missing fragment would be very small. If this interpretation is correct it implies a supradentary-coronoid continuity as is present in *Acrocanthosaurus*, *Monolophosaurus* and some specimens of *Tyrannosaurus* (Eddy and Clarke 2011). This condition has not been reported in *Allosaurus* (Madsen 1976; Chure 2000), but as was noted by Eddy and Clarke (2011) such fusion is not commonly preserved because coronoid and supradentary elements are prone to disarticulation due to their ligamentous attachment to the mandible and therefore the supradentary-coronoid continuity may be more broadly distributed among Theropoda.

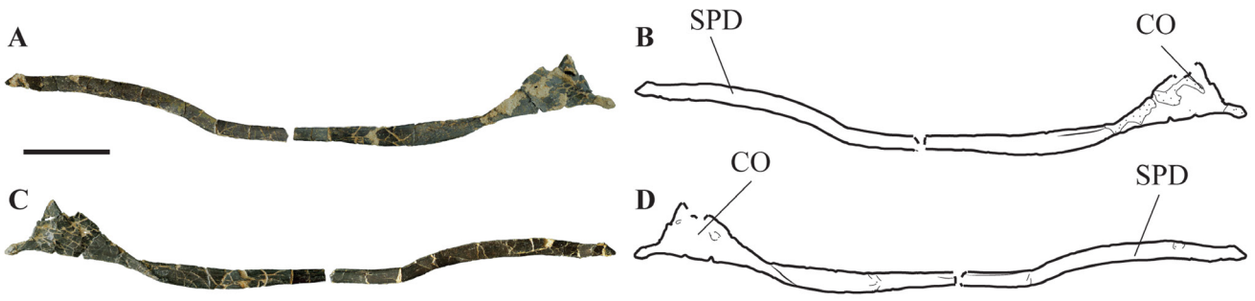

Figure 6.3.22. MNHNUL.P.AND18, left supradentary and coronoid and corresponding interpretative drawing in medial (A–B); and lateral (C–D) views. Scale bar: 50 mm.

The coronoid collected in Andrés is similar in morphology to those of *Allosaurus* (Madsen 1976), *Monolophosaurus* (Brusatte et al. 2010a), and *Tyrannosaurus* (Brochu 2003) in the triangular shape and the presence of a posterodorsal flange. In *Acrocanthosaurus*, the coronoid is sub-rectangular and the the tapering posterodorsal flange is absent (Eddy and Clarke 2011). In *Monolophosaurus* a neurovascular canal is described in the anterior part of the coronoid, which is unknown in other theropods (Chure 2000).

Isolated teeth

Several isolated teeth were collected in Andrés, including four premaxillary and seven lateral (maxillary or dentary) teeth. The premaxillary teeth are almost complete and three of them preserve fragments of the root (Fig. 6.3.23). These teeth have moderately large sized crowns (AL average 27.05 mm). The roots are larger than the crowns (at least a quarter larger) and seem somewhat tapered distally (see Supplementary Table 6.3.3). The crowns are moderately elongated (CHR average 2.25) and subcircular in cross-section with low labiolingually compression ratios (CBR average 1.01). In lateral view, the crowns are triangular with the distal carina slightly concave and the mesial carina strongly convex. The apex is centrally positioned and does not surpass the level of the distal carina.

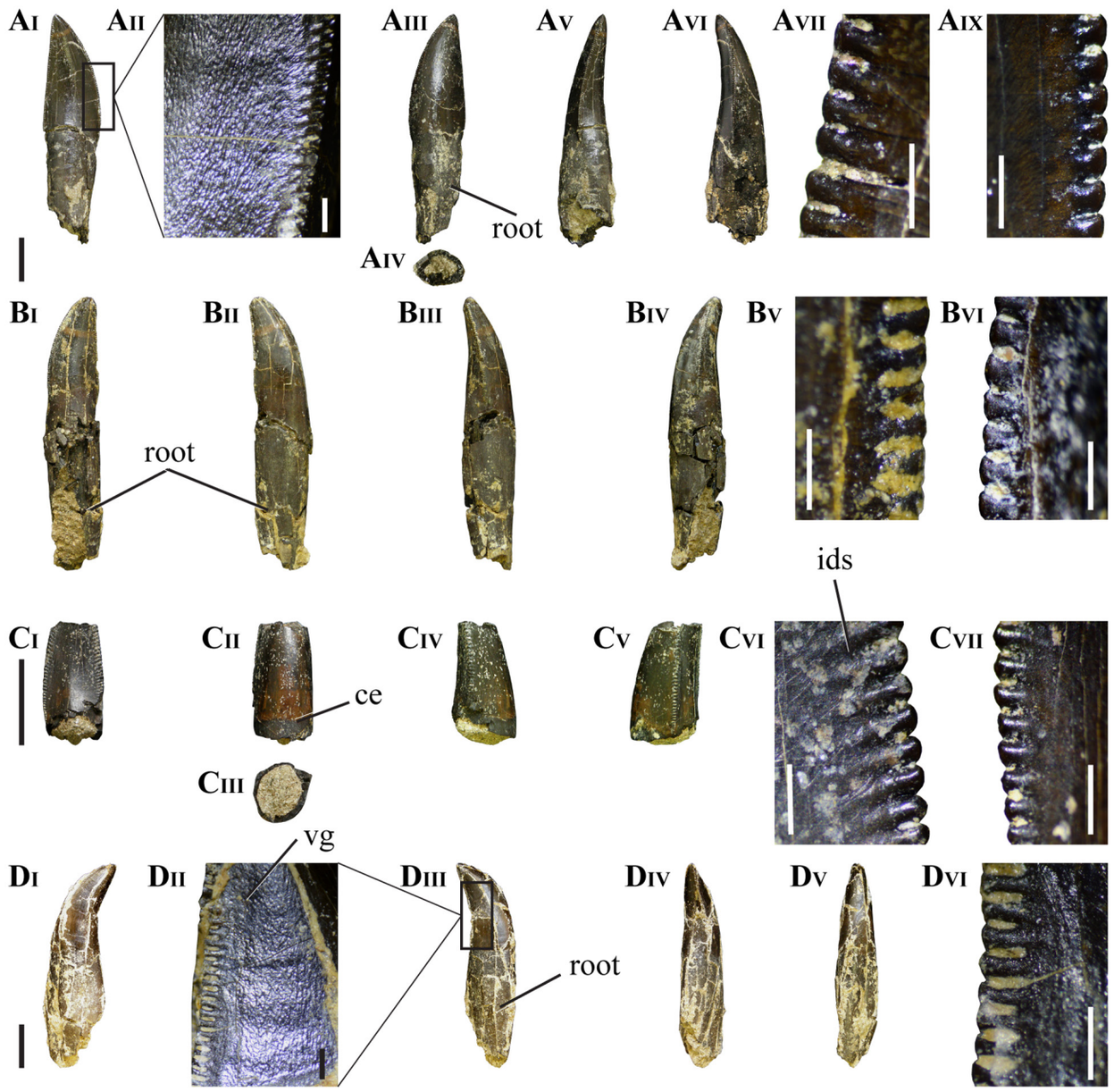

Figure 6.3.23. Isolated premaxillary teeth collected in Andrés. (A), MNHNUL.P.AND23; (B), MNHNUL.P.AND30; (C), MNHNUL.P.AND27; (D), MNHNUL.P.AND31, in lingual (A_I, B_I, C_I, D_I); labial (A_{III}, B_{II}, C_{II}, D_{III}); distal (A_V, B_{III}, C_{IV}, D_{IV}); mesial (A_{VI}, B_{IV}, C_V, D_V) views; cross-section of the root (A_{IV}) and of the crown base (C_{III}); detail of the enamel ornamentation (A_{II}, D_{II}); detail of the distal (A_{VII}, B_V, C_{VI}); and mesial (A_{IX}, B_{VI}, C_{II}, D_{VI}) denticles. Scale bar for the crowns: 10 mm; for the denticles and (A_{II}, D_{II}): 1 mm.

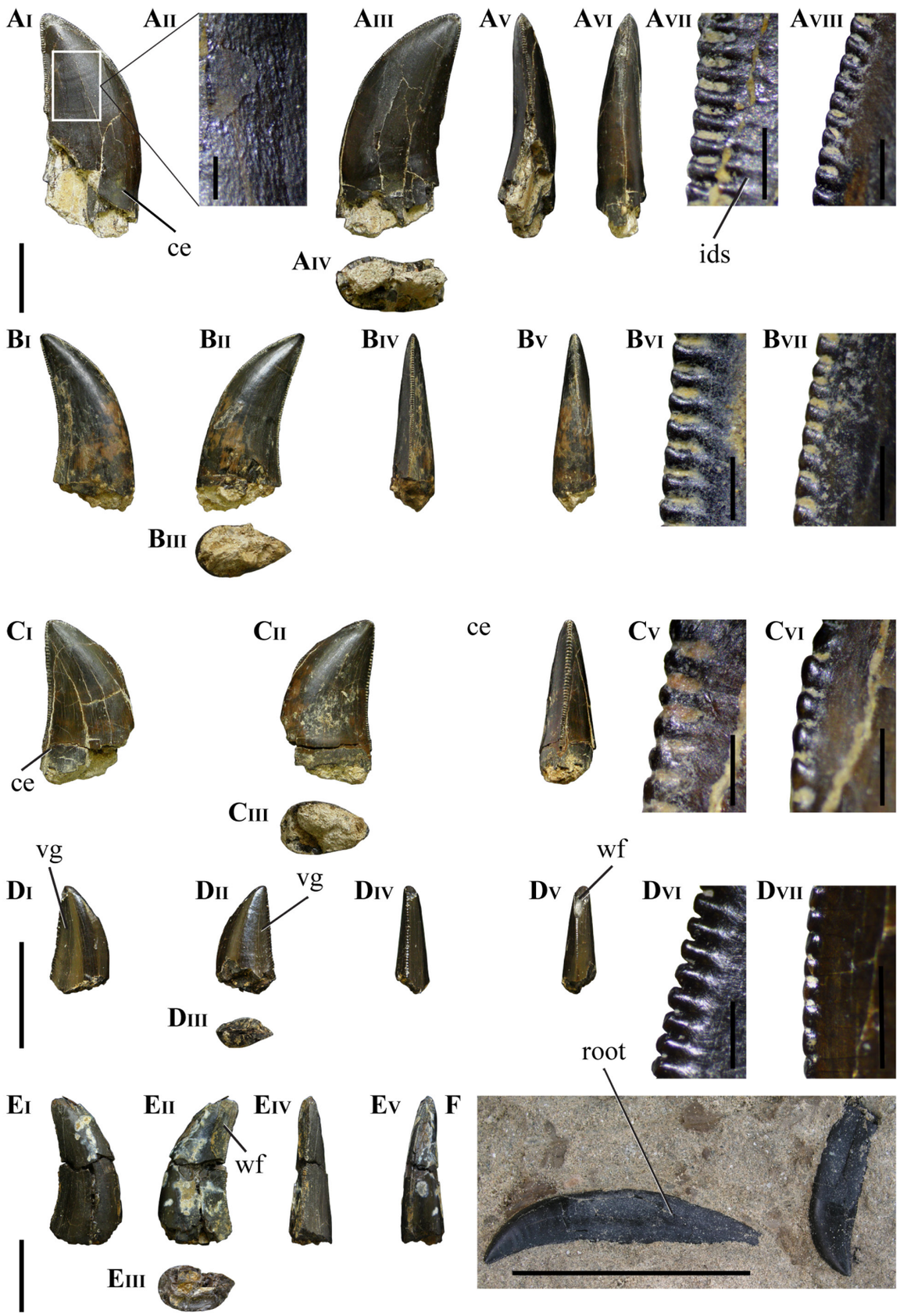

Figure 6.3.24. Isolated lateral teeth collected in Andrés. (A), MNHNUL.P.AND25; (B), MNHNUL.P.AND29; (C), MNHNUL.P.AND24; (D), MNHNUL.P.AND26; (E), MNHNUL.P.AND28; (F), MNHNUL.P.AND32, in labial (A_I, B_I, C_I, D_I, E_I); lingual (A_{III}, B_{III}, C_{II}, E_{II}, F); distal (A_V, B_{IV}, C_{IV}, D_{IV}, E_{IV}); mesial (A_{VI}, B_V, D_V, E_V); cross-section of the crown base (A_{IV}, B_{III}, C_{III}, D_{III}, E_{III}); detail of the distal (A_{VII}, B_{VI}, C_V, D_{VI}); and mesial (A_{VIII}, B_{VII}, C_{VI}, D_{VII}) denticles; detail of the enamel ornamentation (A_{II}). Scale bar for the crowns: 10 mm; for the denticles and (A_{II}): 1 mm.

Some of these specimens show fine transverse undulations and poorly-developed interdenticular sulci between distal denticles. The enamel shows thin grooves and ridges vertically oriented, wich are especially well-marked in the lingual surface (Fig. 6.3.23A_{II}, D_{II}). Mesial and distal serrated carinae are present and both extend to the cervix. Both carinae are positioned in the lingual surface.

Crowns cross-sections are subcircular and in some specimens they are salinon-shaped (*sensu* Hendrickx et al. 2016) due to the presence of vertical concavities in the lingual surface adjacent to the mesial and distal carinae (Fig. 6.3.23C_{III}). The lingual surface is slightly concave and the labial surface is strongly convex.

There is an average of 11.25 and 12 denticles per 5 mm in the mid-section of the mesial and distal carinae, respectively (see Supplementary Table 6.3.3). The mesial denticles are rounded and much short mesiodistally, whereas the distal denticles are subquadrangular with rounded apices. The denticles are separated by narrow interdenticular spaces and are perpendicularly projected to the carina.

The lateral teeth correspond mostly to crowns with some specimens preserving only small fragments of the root (Fig. 6.3.24). These are medium size teeth (AL average 24.8 mm; CBL average 12.36 mm; and CBW average 6.94 mm). The crowns are generally low (CHR average 1.85), strongly compressed labiolingually (CBR average 0.56), and slightly recurved (see Supplementary Table 6.3.3). The distal margin is slightly concave, whereas the mesial margin is strongly convex and the apex is positioned somewhat distally to the level of the distal carina.

Thin transverse undulations and poorly-developed interdenticular sulci are present in some specimens. The interdenticular sulci extend ventrally and are present only between the distal denticles. The enamel shows an ornamentation consisting in a series of thin and irregular crenulations only visible with binocular microscope (Fig. 6.3.24A_{II}). The mesial and distal carinae are serrated with the mesial carina usually extending approximately until the crown mid-height or being restricted to the apical end. The mesial carina is positioned in the mesial margin, but the distal carina has marked labial displacement. The lingual surface is usually flat or slightly convex and the labial surface is convex. In distal view, the distal margin slightly curves lingually forming a slight concavity at the base of the lingual surface. The cross-section of the crown base is elliptical or lenticular-shaped. Some specimens show a flat or slightly concave vertical surface adjacent to the distal carina on the lingual surface (Fig. 6.3.24D).

The number of denticles in the mesial and distal carinae is almost identical with an average of 15 and 12.5 denticles per 5 mm in the mid-section of the mesial and distal carinae, respectively. The interdenticular space between denticles is narrow in both carinae. The mesial denticles are usually rectangular, shorter mesiodistally than apicobasally and with rounded or flat apices, whereas the distal denticles are mesiodistally higher than basoapically wide and have slightly asymmetrical rounded apices.

6.3.8.2. Postcranial skeleton

Axial elemets. The axial skeleton is represented by the intercentrum of the atlas, fragments of postaxial cervical vertebrae, one almost complete anterior dorsal vertebra and fragments of at least five mid and posterior dorsal vertebrae, two partial sacral vertebrae, one anterior caudal vertebra, one mid caudal vertebra and at least ten almost complete posterior caudal vertebra, including an articulated sequence of five vertebrae and respective chevrons of the distal part of the tail. Axial elements include also one cervical rib, five dorsal ribs and four ventral ribs.

Intercentrum of the atlas. This is a crescent-shaped element, MNHNUL.P.AND54, with a deep concave anterior surface for the occipital condyle (Fig. 6.3.25). It is an anteroposteriorly narrow element with two lateral processes projecting anterodorsally and delimiting a transversely deep concavity for articulation with the odontoid (odontoid cavity). The anterodorsal processes would articulate with the neurapophysis distally. The articular surfaces for the neurapophysis are slightly concave, face anterolaterally and have small ventral processes extending anteriorly. The posterior surface of the

atlantal intercentrum, which would articulate with the axis, is slightly convex and bounded ventrally by a shallow groove extending along the entire width.

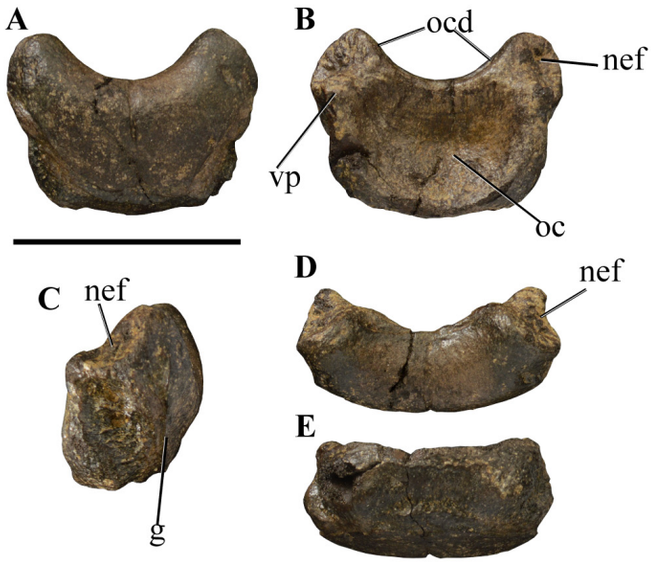

Figure 6.3.25. MNHNUL.P.AND54, intercentrum of the atlas in posterior (A); anterior (B); right lateral (C), dorsal (D); and ventral (E) views. Scale bar: 50 mm.

Postaxial cervical vertebrae. Two fragments interpreted as belonging to postaxial cervical vertebrae were collected, but they are much incomplete and distorted to allow a more detailed description.

Dorsal vertebrae. The dorsal series is represented by a complete and well preserved anterior vertebra (MNHNUL.P.AND65) and two centra of mid or posterior dorsal vertebra (MNHNUL.P.AND36 and 37). The anterior dorsal vertebra (Fig. 6.3.26) is similar to the third dorsal vertebra of *Allosaurus* (Madsen 1976) in the general morphology of the laminae and fossae, position of the papapophyses and presence of a well-developed ventral keel. It has an anteroposteriorly short centrum, nearly as high as long (see Supplementary Table 6.3.4). The articular facets are circular, with similar width and height, and the anterior articular facet is slightly convex, whereas the posterior one is concave. The anterior articular facet is bounded by a shallow groove that forms a well-marked rim around the facet. The ventral surface of the centrum has a prominent longitudinal keel extending along nearly the entire length of the centrum. This keel is triangular in ventral view more transversely expanded to the front and is separated from the ventral margin of the anterior articular facet by a notch (Fig. 6.3.26I–J). The presence of keels on the ventral surface of posterior cervical and anteriormost dorsal vertebrae is a feature shared with several tetanurans, including *Allosaurus*, *Afrovenator*, *Baryonyx*, *Torvosaurus*, *Sinraptor*, *Giganotosaurus*, and *Mapusaurus* (Gilmore 1920; Chure 2000; Carrano et al. 2012).

Relative large parapophyses are present in the lateral surface of the centrum adjacent to the anterior articular facet and immediately below the neurocentral suture. The parapophysis is dorsoventrally elongated and the articular facet is slightly concave. A small pleurocoel opens in the lateral surface of the centrum just posterior to the mid-height of the parapophysis. This pleurocoel is oval, slightly longer anteroposteriorly than high dorsoventrally. The neurocentral suture is well-visible along the entire length of the centrum and has a sinuous profile.

The neural arch is complete and well preserved despite slightly compressed anteroposteriorly. In anterior view, the prezygapophysis extend dorsally with the articular facet facing dorsomedially. The articular facet of the prezygapophysis is circular. A low, U-shaped intraprezygapophyseal lamina (tprl) connects the base of the prezygapophyses above the neural canal. From the ventrolateral surface of the prezygapophysis extends a well-developed lamina that connects with the anterolateral part of the

centrum corresponding to the centroprezygapophyseal lamina (cprl). The neural spine is relatively low being only slightly higher than the height of the anterior articular facet. The neural spine is much thin anteroposteriorly and is somewhat expanded transversely. In anterior view, the neural spine slightly expands dorsally forming a knob-shaped dorsal end. Most of the anterior surface of the neural spine is strongly rough. A shallow groove mainly marked in the dorsal part, separates the interspinous ligament from the main body of the spine.

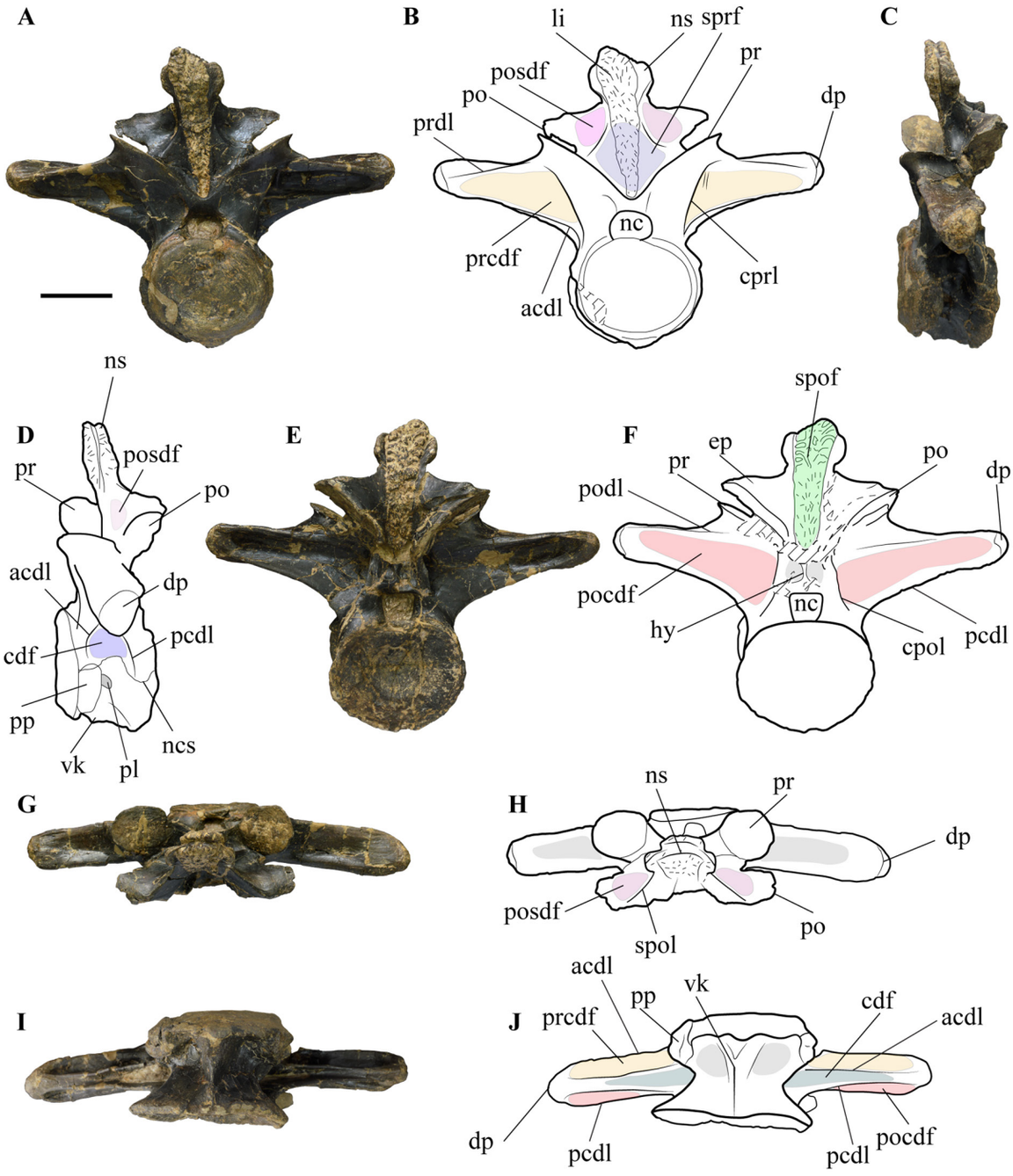

Figure 6.3.26. MNHNUL.P.AND65, anterior dorsal vertebra and corresponding interpretative drawing in anterior (A–B); left lateral (C–D); posterior (E–F); dorsal (G–H); and ventral (I–J) views. Scale bar: 50 mm.

The transverse processes are long and robust projecting horizontally relative to the centrum and are slightly tapered distally. A well-developed prezygodiapophyseal lamina (prdl) extends from the anteroventral margin of the prezygapophysis along the anterodorsal surface of the transverse process (Fig. 6.3.26A–B). The anterior centrodiapophyseal lamina (acdl) extends ventrally from the distal end

of the transverse process connecting with the anterodorsal margin of the centrum. The cprl, prdl and acdl delimit a large prezygapophyseal centrodiapophyseal fossa (prcdf) that occupies almost the entire anteroventral surface of the transverse process. The prcdf is deeper proximally and has a vertical septum separating two smaller fossae; the proximalmost fossa opens laterally and extends slightly into the prezygapophysis, whereas the distalmost one faces to the front (Fig. 6.3.26A–B). The ventral surface of the transverse processes has also a deep and narrow fossa delimited by the acdl and the posterior centrodiapophyseal lamina (pcdl) corresponding to the centrodiapophyseal fossa (cdf).

In posterior view, a well-developed, but relatively shallow postzygapophyseal centrodiapophyseal fossa (pocdf) occupies the posterior surface of the transverse process. The pocdf is delimited dorsally by a well-developed postzygodiapophyseal lamina (podl) extending from the anteroproximal margin of the postzygapophysis along the posterodorsal surface of the transverse process. The pocdf is delimited ventrally by the pcdl and medially by the centropostzygapophyseal lamina (cpol), which extends vertically from the anterodorsal part of the centrum to the posteroventral margin of the postzygapophysis. The short postzygapophysis extends posterolaterally and the articular facet face ventrolaterally and slightly to the rear. The articular facet is oval, mediolaterally elongated and mostly flat. Small epipophyses are present in the posterodorsal margin of the postzygapophyses (Fig. 6.3.26E–F). In posterior view, the neural spine is slightly concave and pointing distally. A shallow spinopostzygapophyseal fossa (spof) is delimited ventolaterally by the posterior margins of the postzygapophyses and dorsally by a pair of spinopostzygapophyseal laminae (spol) projecting from the dorsal margin of the epipophyses to the lateral margin of the neural spine. In anterior view, the spol and the spinoprezygapophyseal lamina (sprl), which extends from the base of the prezygapophysis to the lateral surface of the spine, delimit a shallow postzygapophyseal spinodiapophyseal fossa (posdf) opening at the base of the postzygapophysis and slightly extending into the lateral surface of the spine.

The neural canal is circular in anterior view and nearly quadrangular in posterior view. Above the neural canal extends a vertical sheet-shaped hyposphene similar to those of *Allosaurus*, *Neovenator* and *Acrocanthosaurus*, whereas in *Sinraptor*, *Piatnitzkysaurus* and *Torvosaurus* this structure has a triangular morphology (Currie and Zhao 1993; Brusatte et al. 2008). Laterally to the hyposphene there is a pair of small, subcircular and shallow concavities (Fig. 6.3.26E–F).

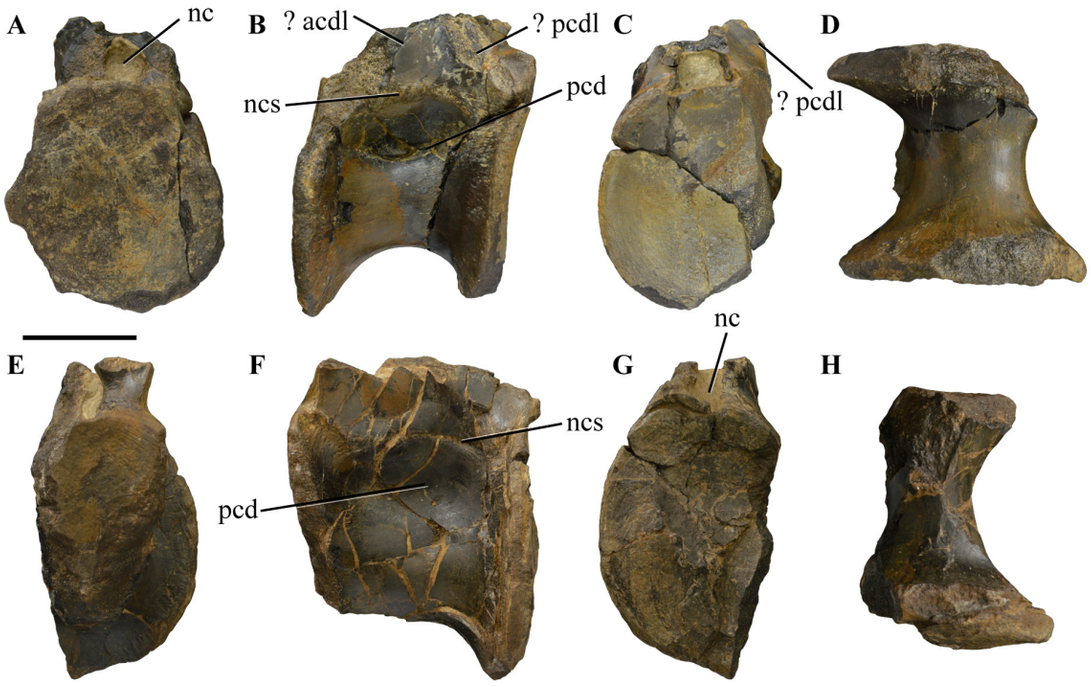

Figure 6.3.27. Mid and posterior dorsal vertebrae attributed to *Allosaurus* collected in Andrés. (A–D), MNHNUL.P.AND36; and (E–H), MNHNUL.P.AND37 in anterior (A, E); lateral (B, F); posterior (C, G); and ventral (D, H) views. Scale bar: 50 mm.

Two incomplete dorsal centra (MNHNUL.P.AND36 and 37) were collected in 1988 in Andrés (Fig. 6.3.27). The neurocentral suture is visible along the entire length of the centrum and has a sigmoidal contour. The lateral surface of the centrum has a deep pleurocentral depression that occupies almost the entire dorsal end of the centrum. The ventral surface of the centrum is rounded and slightly concave in lateral view. The ventral margin of the anterior articular facet is slightly higher relative to the level of the posterior one. A fragment of a lamina interpreted as the centroprezygapophyseal lamina is visible in the anterior end of the centrum of MNHNUL.P.AND36 (Fig. 6.3.27c).

Sacral vertebrae. The sacral series is represented by a complete centrum articulated with the anterior articular facet of a second vertebra, MNHNUL.P.AND38 (Fig. 6.3.28). This specimen is interpreted as belonging to the first and second sacral vertebrae. The articular facet is slightly concave and subcircular. The lateral surface has a shallow pleurocentral depression. The ventral surface is rounded, transversely convex and saddle-shaped in lateral view. A small foramen interpreted as the intervertebral foramen (*sensu* Benson 2010) opens laterally at the base of the neural arch adjacent to the posterior articular facet.

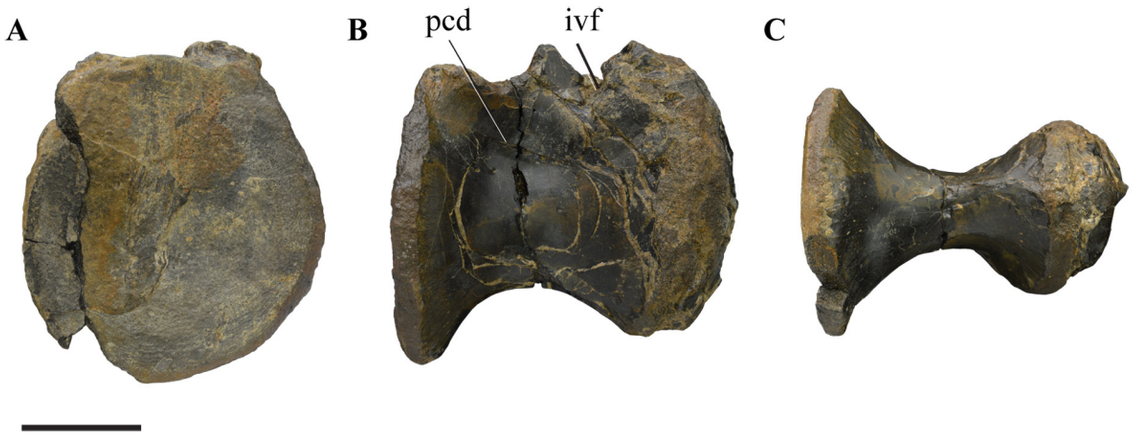

Figure 6.3.28. MNHNUL.P.AND38, sacral centrum in anterior (A); lateral (B); and ventral (C) views. Scale bar: 50 mm.

Caudal vertebrae. The caudal series is represented by one anterior, one mid and at least ten posterior vertebrae (Fig. 6.3.29–30). The anterior caudal vertebra (MNHNUL.P.AND39) has the centrum united with the neural arch, but the neurocentral suture is visible and has a sigmoidal profile (Fig. 6.3.29A–E). The centrum is compressed mediolaterally and the ventral surface has a narrow groove (Fig. 6.3.29E). The articular facets are oval, higher than wide and slightly concave. The lateral surface of the centrum has a shallow, but well-marked depression at mid-length adjacent to the base of the neural arch, which corresponds to the residual pleurocentral depression. The pre and postzygapophyses are complete and well-preserved, but the caudal ribs and neural spine are poorly preserved. The caudal ribs extend from approximately the mid-length of the centrum and are horizontal. A small depression is present in the ventral surface of the caudal rib adjacent to the posterior margin. The neural spine is blade-shaped and much thin mediolaterally. The pre and postzygapophyses are short. Deep pre and postspinal fossae are present.

The mid caudal vertebra (MNHNUL.P.AND40) preserves part of the caudal ribs and of the prezygapophyses, but not the postzygapophyses neither the neural spine (Fig. 6.3.29F–J). The ventral surface has a narrow longitudinal groove extending along approximately the mid-length of the centrum. The lateral surface of the prezygapophysis has a deep longitudinal groove delimited by two laminae; the dorsal lamina extends along the dorsal margin of the prezygapophysis and the ventral one projecting from the centrum to the lateroventral surface of the prezygapophysis.

The posterior caudal series is represented by five isolated vertebrae and a sequence of five articulated vertebrae and the respective chevrons. The posterior caudal centra are much elongated and have lost the neural spine and the caudal ribs (Fig. 6.3.29K–Y). In some of these vertebrae (e.g.

MNHNUL.P.AND41–42) the ventral surface has a broad concavity bounded by lateral and medial crests extending along most of the centrum length, but more marked at mid-length (Fig. 6.3.29O, T). The centrum is strongly concave in lateral view and the ventralmost margin of the posterior articular facet is ventrally positioned relative to the level of the anterior articular facet. The lateral surface has well-developed longitudinal crests extending along the dorsal margin of the centrum and more marked at mid-length. The articular facets are strongly concave and almost circular. Facets for chevrons are present in both articular facets, but are more marked in the posterior one. The prezygapophyses are long (approximately 80% the length of the centrum) and projecting to the front almost parallel to the dorsal margin of the centrum. The prezygapophyses slightly taper distally and have somewhat concave surfaces ventrally adjacent to the proximal end. The postzygapophyses are short and do not extend significantly beyond the level of the posterior articular facet.

In most posterior vertebrae (e.g. MNHNUL.P.AND33, 56) the articular facets are oval, wider mediolaterally than dorsoventrally deep and facets for chevrons are poorly developed or completely absent (Fig. 6.3.29P–Y). The prezygapophyses are much elongated being more than half the length of the centrum and projecting horizontally and somewhat medially making a gentle convexity laterally adjacent to the proximal part. The postzygapophyses are jointed in a thin blade with a deep dorsal groove projecting posterodorsally and are slightly more elongated relative to the previously described posterior

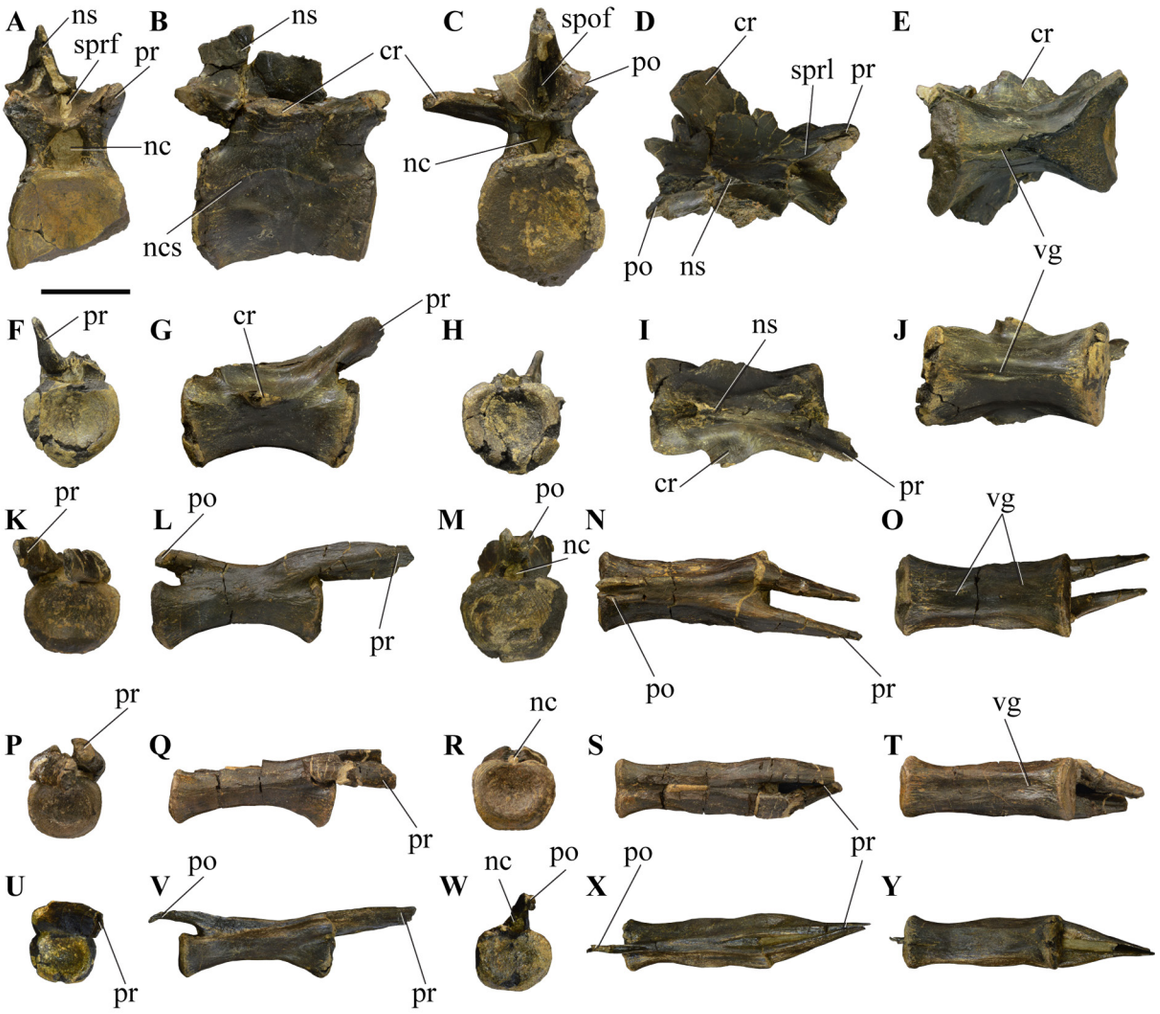

Figure 6.3.29. Caudal vertebrae attributed to *Allosaurus* collected in Andrés. (A–E), anterior caudal vertebra MNHNUL.P.AND39; (F–J), mid caudal vertebra, MNHNUL.P.AND40; (K–O), posterior caudal vertebra, MNHNUL.P.AND41; (P–T), posterior caudal vertebra, MNHNUL.P.AND42; (U–Y), posterior caudal vertebra, MNHNUL.P.AND33, in anterior (A, F, K, P, U); lateral (B, G, L, Q, V); posterior (C, H, M, R, W); dorsal (D, I, N, S, X); and ventral (E, J, O, T, Y) views. Scale bar: 50 mm.

caudal vertebrae, extending well beyond the level of the articular facet. The lateral surface of the neural arch adjacent to the postzygapophyses has a shallow concavity that extends to approximately the mid-length of the centrum. The centra are concave in lateral view and the ventral surface is mostly rounded with small concavities that are slightly more marked near the articular facets.

A sequence of 5 articulated posterior caudal vertebra with several chevrons, MNHNUL.P.AND60 (Fig. 6.3.30), was collected in Andrés during the second fieldwork campaign in 2005. The morphology of these vertebrae is similar to those of the posteriormost caudals described above. The chevrons are very small and have a pair of anterior thin processes projecting parallel to the ventral margin of the centra and a posterior blade-shaped process with a sharp ventral keel (Fig. 6.3.30E–F).

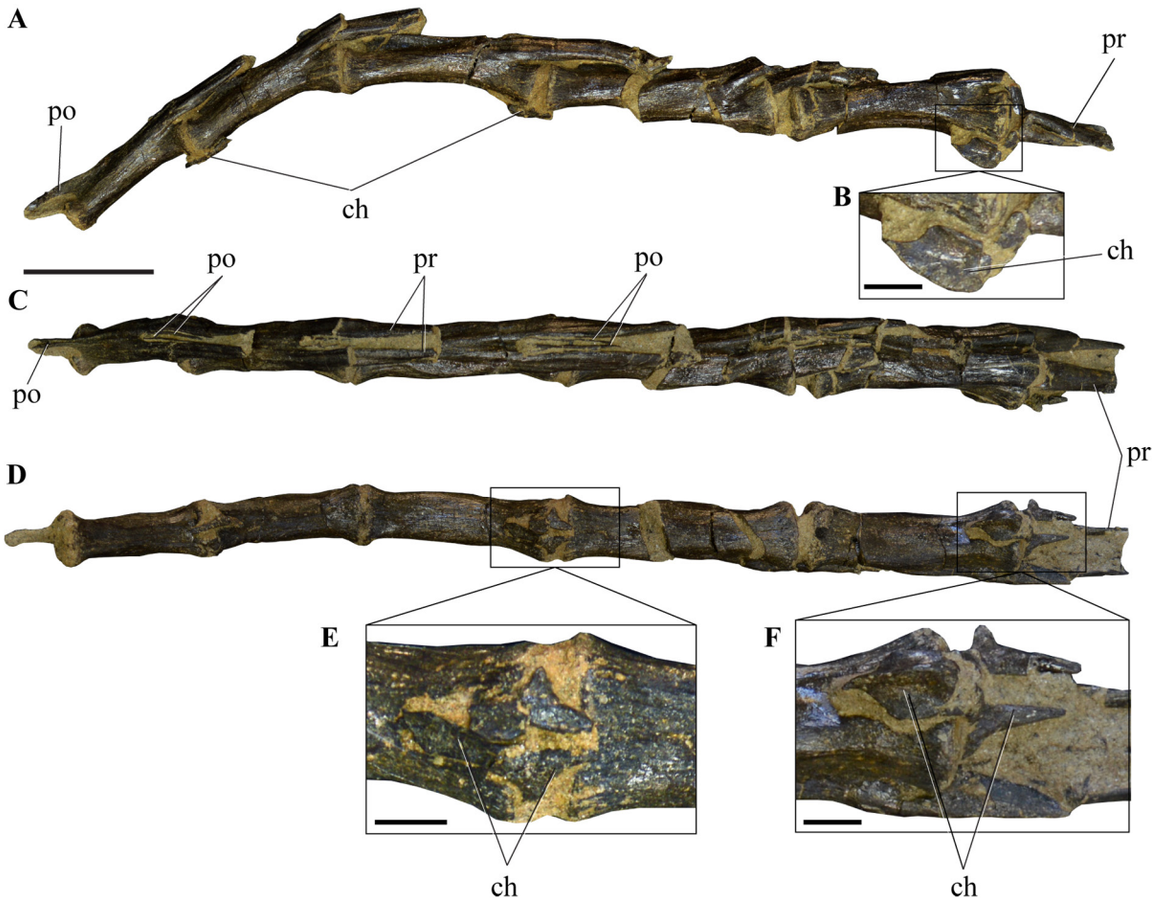

Figure 6.3.30. MNHNUL.P.AND60, sequence of five posterior caudal vertebrae in right lateral (A); dorsal (C); and ventral (D) views; (B, E–F), detail of the chevrons. Scale bar (A, C–D): 50mm; (B, E–F): 10 mm.

Cervical and dorsal ribs. One complete cervical rib, MNHNUL.P.AND55, and six dorsal ribs, MNHNUL.P.AND51–53, 76–77, and 79, are known for the specimen from Andrés. The cervical rib (Fig. 6.3.31A–B) is relatively small and has a well-developed capitulum, whereas the tuberculum is significantly smaller. The capitulum and tuberculum are close together in the proximal end of the rib and the shaft is short and tapering distally. There are two pneumatic recesses proximally between the capitulum and tuberculum; one opens in the medial surface of the capitulum and is subdivided by an approximately horizontal septum and the other pierces the dorsal surface between the blade that connects the capitulum and tuberculum. Similar pneumatic openings are reported in cervical ribs of *Allosaurus* (Madsen 1976). A high and thin process projects dorsally from the proximolateral surface of the rib.

The dorsal ribs are interpreted as belonging to the mid series because they have strongly curved shafts and are triangular proximally in anterior view (Fig. 6.3.31C–D). The capitulum is long and extends dorsomedially, whereas the tuberculum is short, proximolaterally placed, and faces dorsally.

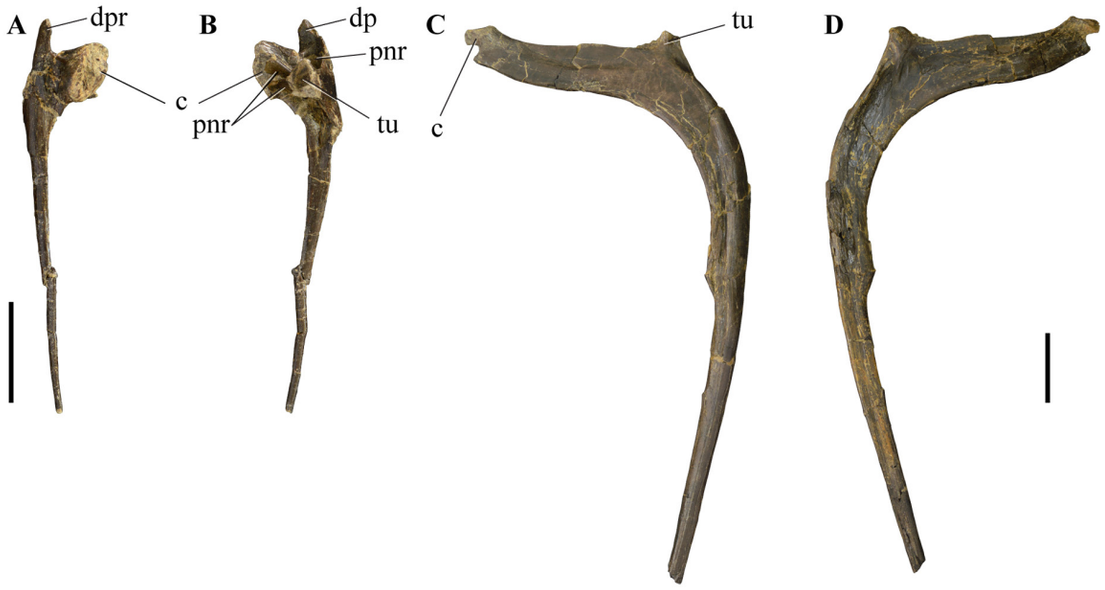

Figure 6.3.31. Ribs attributed to *Allosaurus* collected in Andrés. (A–B), cervical rib, MNHNUL.P.AND55; (C–D), dorsal rib, MNHNUL.P.AND51, in posterior (A, D); and anterior (B, C) views. Scale bar: 50 mm.

Chevrons. One almost complete isolated chevron, MNHNUL.P.AND55 (Fig. 6.3.32) was collected in Andrés. This element is interpreted as corresponding to a mid chevron based on the absence of a marked distal expansion and the slightly curved shaft. The haemal canal is large and delimited dorsally by a bridge of bone that forms part of the articulation between the chevron and the caudal vertebrae. The anterior surface of the chevron preserves a pair of well-developed anterior processes projecting anterodorsally and surrounding the haemal canal.

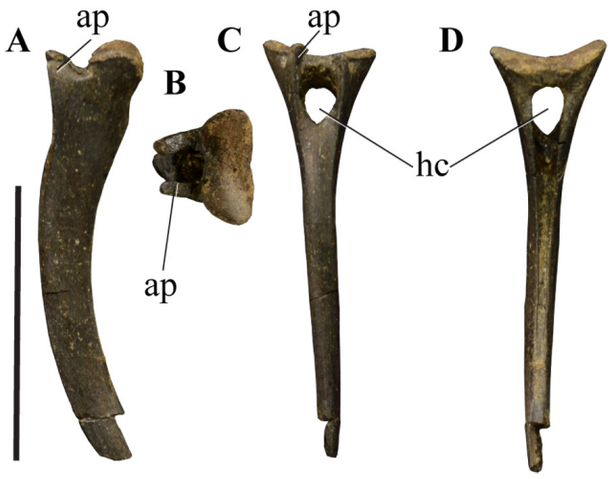

Figure 6.3.32. MNHNUL.P.AND55, anterior or mid chevron in lateral (A); proximal (B); anterior (C); and posterior (D) views. Scale bar: 50 mm.

6.3.8.2. Appendicular elements

Pectoral girdle. The pectoral girdle is represented by an almost complete and well-preserved left coracoid, MNHNUL.P.AND64 (Fig. 6.3.33).

Coracoid. It is clearly not fused with the scapula as occur in most allosauroids such as *Allosaurus* (Madsen 1976), *Neovenator* (Brusatte et al. 2008), and *Acrocanthosaurus* (Currie and Carpenter 2000). The coracoid is semicircular, deeper than long and is mostly a thin blade slightly concave laterally and convex medially. It slightly thickens proximally in the area of the glenoid fossa.

The coracoid foramen is a small opening adjacent to the dorsal margin of the coracoid, near the suture for the scapula. This foramen is circular in lateral view and in medial view it forms a slit opening anteroposteriorly. The coracoid has a well-developed hooked-shaped ventral process that is separated from the main body of the coracoid by a broad concavity. A similar long and tapering posteroventral process of the coracoid is present in spinosaurids (Charig and Milner 1997; Sereno et al. 1998) and avetheropods (Rauhut 2003). In *Megalosaurus* and in other basal theropods, such as *Ceratosaurus* (Madsen and Welles 2000), *Dilophosaurus* (Welles 1984) and *Torvosaurus* (Bakker et al. 1992) it is short and rounded.

In the lateral surface, a short biceps tubercle projecting from the ventral margin of the coracoid and bounded by a well-developed lateral ridge that connects with the ventral margin of the coracoid delimiting a shallow fossa. A coracoid tubercle is absent in *Megalosaurus* and in spinosaurids such as *Baryonyx* and *Suchomimus* (Charig and Milner 1997; Benson 2010). The angular ridge morphology of this tubercle in MNHNUL.P.AND64 is similar to those of *Allosaurus* and *Neovenator* (Brusatte et al. 2008), whereas in non-tetanuran theropods, such as *Ceratosaurus* (Madsen and Welles 2000) the tubercle forms a prominent convexity.

The articular surface for the scapula is a much mediolaterally thin and approximately straight blade. The glenoid facet is facing posteroventrally and is slightly concave.

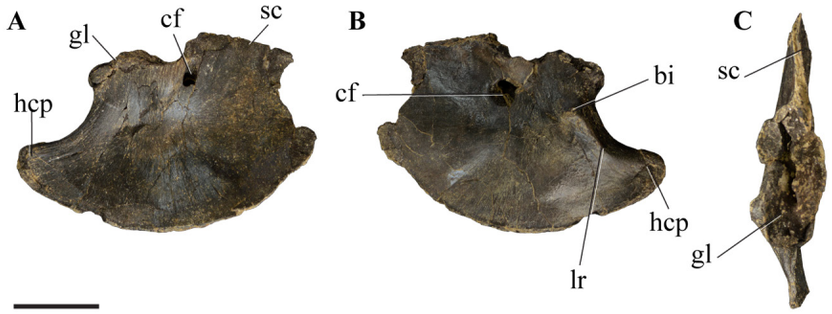

Figure 6.3.33. MNHNUL.P.AND64, left coracoid in medial (A); lateral (B); and proximal (C) views. Scale bar: 50 mm.

Pelvic girdle. The pelvis is almost complete and includes a left ilium, pubes and a left ischium. The pubes and left ischium were collected in 1988 and preserved in the original anatomic position, but the ilium was found isolated and several years latter (in 2005). Beside, the left pubis collected in 1988 is articulated with a fragment of the pubic peduncle of the ilium. Therefore, the ilium collected in 2005 belongs to a second large-sized *Allosaurus* individual.

Ilium. An almost complete and well-preserved left ilium, MNHNUL.P.AND63 (Fig. 6.3.34), is known for the specimen from Andrés. It has a low and elongated profile (iliac length:height = 3.29 see Supplementary Table 6.3.5). The anterior margin of the preacetabular process is mostly convex, but has a broad concave notch dorsally (Fig. 6.3.34A). A similar notch is present in tyrannosaurids (Rauhut 2003) and *Concavenator* (Ortega et al. 2010). This feature is variable among the *Allosaurus* specimens from the Morrison Formation. Madsen (1976) illustrated the anterodorsal margin of the preacetabular blade as convexly rounded for *A. fragilis* based on the ilium morphology of UUVP 6000 and a dorsally concave anterior margin of the ilum is not present in *A. fragilis* material from the Cleveland Lloyd Dinosaur Quarry (e.g. UMNH VP 8119) or from the Dry Mesa Quarry (BYU 725/17281) (Evers 2014). A deep and well-marked notch is present in SMA 0005 (Evers 2014) and a less distinct concavity is seen in DINO 11541 (Chure 2000), USNM 4734 (Gilmore 1920), and MOR 693 (Evers 2014).

The preacetabular process extends ventrally from the lateral surface of the ilium, forming a board notch with the anterior margin of the pubic peduncle. A shallow cupedicus fossa is present in the ventral

margin of the preacetabular process and is bounded laterally by the ventral lamina of the preacetabular process. The anteriormost margin of the preacetabular process is approximately at the level of the anterior margin of the pubic peduncle. The postacetabular process is longer than the preacetabular process. The posterior margin of the postacetabular process is nearly straight and vertical. The brevis fossa is transversely wide, deep and is bounded by robust medial and lateral blades extending along the ventral margin of the postacetabular. The lateral blade is dorsoventrally lower than the medial one and thus the brevis fossa is well visible in lateral view. The medial and lateral blades diverge distally so the brevis fossa is broader posteriorly as occur in *Allosaurus* (Madsen 1976), *Eustreptospondylus* (Sadleir et al. 2008) and *Neovenator* (Brusatte et al. 2008). On the contrary, a narrow brevis fossa with subparallel margins is present in *Lourinhanosaurus* (Mateus 1998), *Megalosaurus* (Benson 2010), *Sinraptor* (Currie and Zhao 1993) and *Torvosaurus* (Britt 1991).

The dorsal border of the iliac blade is slightly convex. The lateral surface of the iliac blade has a poorly-defined, broad and shallow concavity bounded by a series of thin radial striations (= lateral fossa of Benson 2010). A vertical swelling extending dorsally from the dorsal margin of the supraacetabular crest into the lateral fossa is not present in this specimen. Two small foramina are present on the lateral surface of the iliac blade, one near the base of the pubic peduncle inside the cupedicus fossa and another at the base of the brevis fossa. The pubic peduncle is triangular in lateral view and extends mostly ventrally and somewhat anteriorly. It is much deeper and longer than the ischial peduncle. The articular facet of the pubic peduncle is slightly concave and anteroposteriorly expanded much longer than transversely wide. The distal end of the pubic peduncle is approximately 2.12 times as long as wide (see Supplementary Table 6.3.5).

The ischial peduncle extends ventrally and slightly to the rear. It has a strongly convex articular surface and an oval cross-section that is slightly wider than long. The supraacetabular crest is relatively low and arises from the mid-height of the posterolateral surface of the pubic peduncle to the base of the ischial peduncle.

The medial surface of the iliac blade is slightly convex and has a series of well-marked radial striations, and several rough areas corresponding to the attachment scars for sacral ribs and vertebrae (Fig. 6.3.34C).

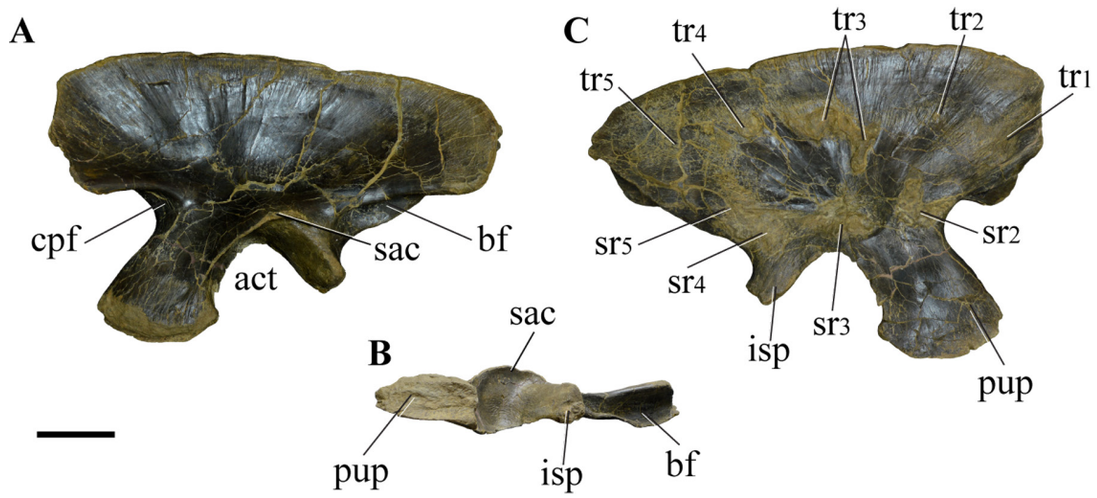

Figure 6.3.34. MNHNUL.P.AND63, left ilium in lateral (A); distal (B); and medial (C) views. Scale bar: 100 mm.

Pubes. Almost complete pubes, MNHNUL.P.AND61, is part of the first specimen collected in 1988 in Andrés in a block with the ischia and elements of the hind limbs. The left pubis is attached with a fragment of the pubic peduncle of the ilium (Fig. 6.3.35). The pubic diaphysis is straight, but its proximal end is slightly concave projecting posteriorly. The diaphysis has a teardrop shaped cross-section

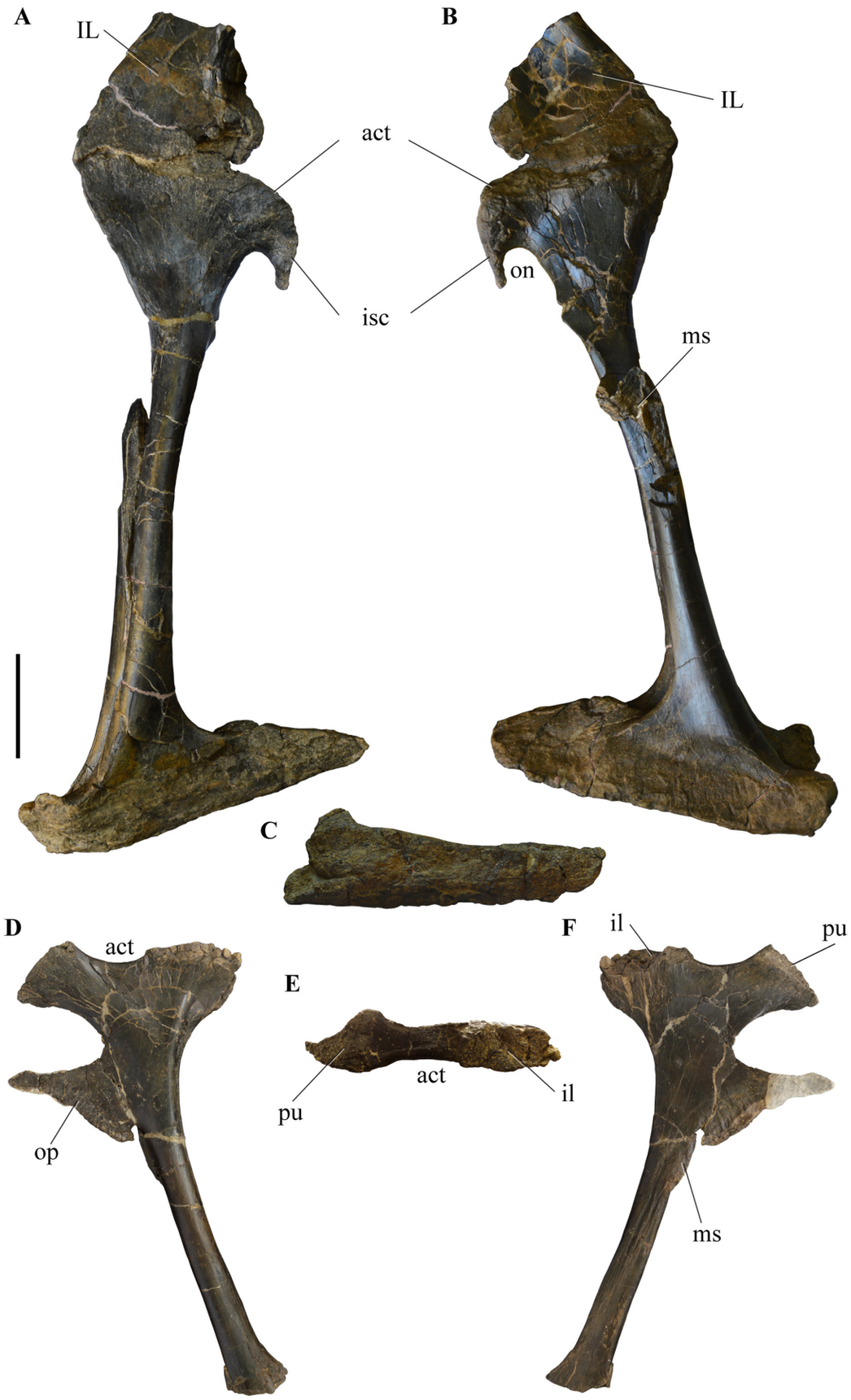

Figure 6.3.35. Pelvic elements attributed to *Allosaurus* collected in Andrés. (A–C), pubes, MNHNUL.P.AND61; (D–F), left ischium, MNHNUL.P.AND62, in left lateral (A); right lateral (B); distal (C); lateral (D); proximal (E); and medial (F) views. Scale bar: 100 mm.

as result of a circular diaphysis and a prominent medial symphysis. The medial symphysis originates proximally at the medial margin of the pubic posterior surface and extends distally along nearly the entire length of the diaphysis, ending just proximal to the distal expansion of the pubes, thus forming a small distal fenestra above the pubic boot. The proximal part of the pubis is much anteroposteriorly expanded and relatively narrow transversely. The iliac articulation is broad, with a slightly concave facet and located in the anterodorsal surface of the pubic proximal end. The ischial articulation is located on a transversely thin process projecting ventrally from the posterior surface of the pubic proximal part. This articular facet is mostly flat and faces posteromedially. The ischial process delimits a broad obturator notch that opens ventrally as in other tetanuran theropods such as *Acrocanthosaurus* (Harris 1998), *Aerosteon* (Sereno et al. 2008), *Allosaurus* (Gilmore 1920; Madsen 1976; Chure 2000), *Giganotosaurus* (Coria and Salgardo 1995), *Megaraptor* (Calvo et al. 2004) and *Neovenator* (Brusatte et al. 2008). In *Sinraptor*, the medial shelf of the pubis is dorsally extended to near the level of the ischial process and almost enclose the obturator notch (Currie and Zhao 1993). A completely closed obturator foramen is seen in the pubis of *Lourinhanosaurus* (Mateus 1998) and in *Yangchuanosaurus* (Gao 1992).

The distal parts of the pubes are fused, forming a well-developed and anteroposteriorly elongated pubic boot. The posterior expansion of the pubic boot forms an angle of approximately 70° with the diaphysis. The length of the pubic boot is approximately 65% the length of the pubic diaphysis (see Supplementary Table 6.3.5). The pubic boot is triangular in lateral and distal views, with the posterior process longer than the anterior process. The pubic boot strongly tapers to the rear forming a rounded blunt posterior margin.

Ischium. The left ischium, MNHNUL.P.AND62, is almost complete (Fig. 6.3.35D–F). The distal end is missing, but the preserved fragment shows a slight expansion. The ischial diaphysis is straight. The proximal part is strongly expanded anteroposteriorly and has two well-developed projections corresponding to the iliac and the pubic processes. The iliac process is oval in proximal view and anteroposteriorly elongated. This process is strongly concave to the rear, but less concave to the front. In posterior view, the iliac process has a crest-shape with a conspicuous tuberosity projecting ventrally along approximately one-quarter the length of the diaphysis. A shallow longitudinal concavity is present in the lateral surface of the ischium adjacent to this crest.

The pubic process is a relatively long ramus, triangular in cross-section and projecting anterodorsally. The pubic articulation is mostly flat and much rugose. In proximal view, the public process has a crescent-shape with a concave medial margin, slightly convex lateral and dorsal margins and a blade-shaped ventral surface. The acetabular margin is broad and shallow. The obturator process is a thin blade projecting to the front and is subrectangular in lateral view. This blade strongly tapers distally in a thin, blade-shaped point. The lateral and medial surfaces of the obturator process have thin longitudonal grooves and ridges, particularly in the medial surface. Ventrally, the obturator process is separated from the diaphysis by a narrow notch as occur in *Allosaurus* (Gilmore 1920; Madsen 1976; Chure 2000) and most other allosauroids (e.g. *Mapusaurus*: Coria and Currie 2006; *Sinraptor*: Currie and Zhao 1993; *Tyrannotitan*: Canale et al. 2015) except in *Neovenator* (Brusatte et al. 2008).

The large ischial incision opens anteroventrally between the pubic process and the obturator process. This opening has a rounded contour, slightly more elongated anteroposteriorly than dorsoventrally. Medially, the ischium has a low lamina extending longitudinally for approximately three-quarters of the length of the diaphysis, but an actual medial symphysis is absent.

Hindlimb. The hind limbs are almost complete including the femora, tibiae, and fibulae.

Femora. The right, MNHNUL.P.AND66, and the left, MNHNUL.P.AND67, femora are almost complete and well-preserved. The right femur is broken proximally and the greater trochanter is missing (Fig. 6.3.36A–F). The shaft is straight in anterior and posterior views and slightly arched in

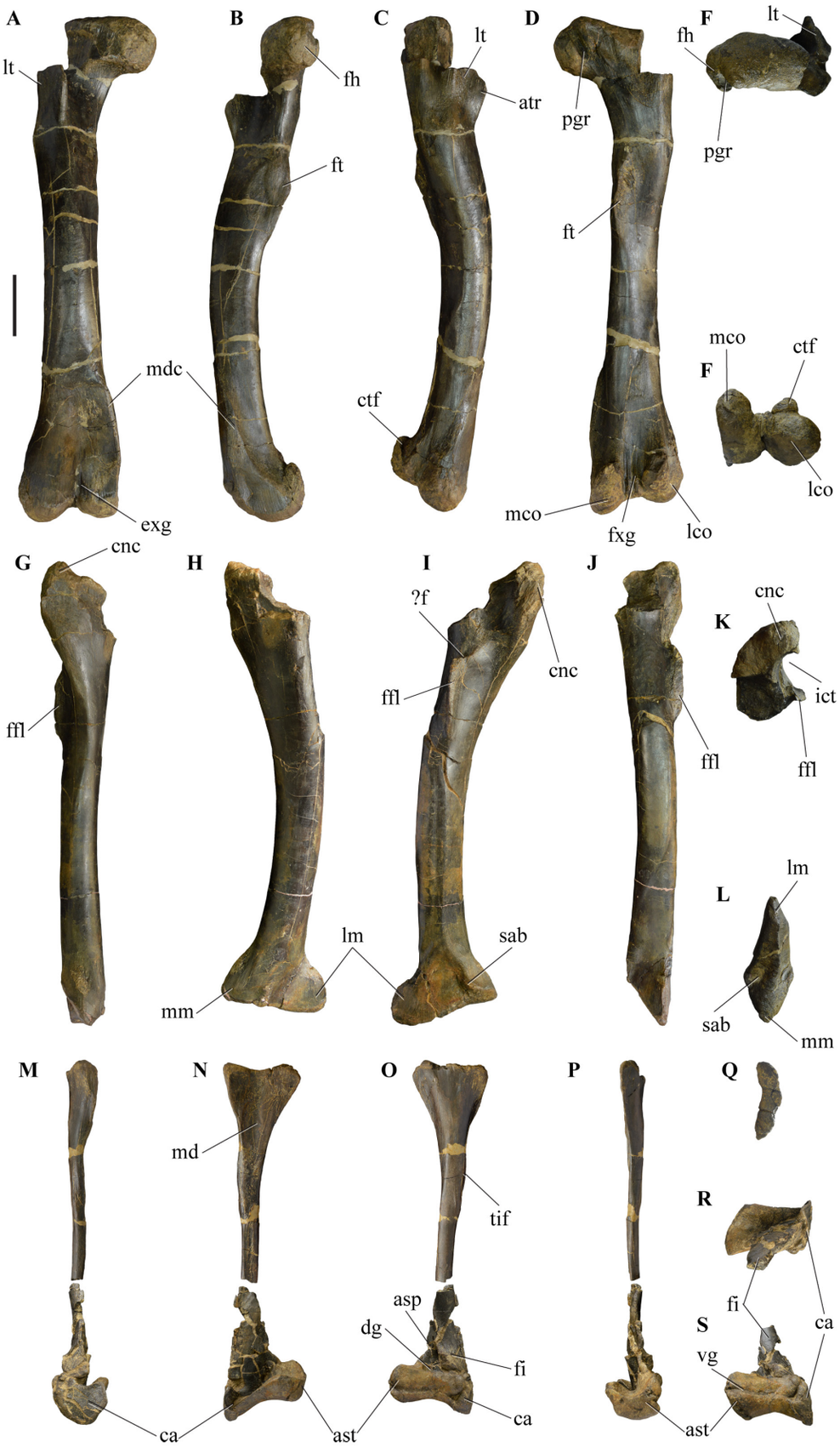

Figure 6.3.36. Hindlimb elements attributed to *Allosaurus* collected in Andrés. (A–F), right femur, MNHNUL.P.AND66; (G–L), right tibia, MNHNUL.P.AND68; (M–S), left fibula articulated with the astragalus and calcaneum, MNHNUL.P.AND71, in anterior (A, G, M); medial (B, H, N); lateral (C, I, O); posterior (D, J, P); proximal (F, K, Q, R); and distal (F, L, S) views. Scale bar: 100 mm.

lateral and medial views. The femoral head is posteromedially projected relative to the long axis of the shaft. The caput is circular in medial view and has a deep vertical groove in the posterior surface, which is bounded medially by a well-developed posterior lip of the femoral head. This groove is interpreted as the reception for the ligamentum capitis femoris (Sadleir et al. 2008). The proximal part is gently convex in proximal view. The lesser trochanter is incomplete dorsally, but is a robust blade-shaped process projecting dorsally and to the front from the lateral surface of the femur proximal part. The lateral surface has a series of thin longitudinal crests and grooves and a small rough concavity is present at the base of the lesser trochanter in the lateral surface of the diaphysis A well-developed accessory trochanter is present adjacent to the anterior surface of the lesser trochanter (Fig. 6.3.36C). A similarly developed accessory trochanter is seen in *Allosaurus* (Madsen 1976), *Neovenator* (Brusatte et al. 2008) and other avetheropods (Hutchinson 2001), but it forms a low swollen in most basal tetanurans, such as *Megalosaurus*, *Eustreptospondylus*, and *Piatnitzkysaurus* (Benson 2010).

The fourth trochanter is a robust crest positioned in the proximal part of the shaft. This trochanter extends dorsoventrally in the posteromedial surface of the femur. The lateral surface of the fourth trochanter is strongly rough with a series of deep crests and grooves extending longitudinally, especially in the dorsal part of the trochanter. The medial surface is smoother and the shaft has a shallow concave surface adjacent to the fourth trochanter. The foramen of the femur pierces the anteromedial surface of the diaphysis slightly below the level of the lesser trochanter. The distal end of the femur has two well-developed condyles. In distal view, the condyles are separated by a shallow concavity and the medial condyle is anteroposteriorly elongated, whereas the lateral one is more rounded. The condyles are separated by a deep and U-shaped flexor groove to the rear and by a shallower, but rather well-marked extensor groove to the front. Inside the flexor groove, a low transverse ridge is present. The crista tibiofibularis in the posterior surface of the distal femur is robust, rounded and projecting dorsolaterally. This crest is separated from the lateral condyle by a shallow groove.

The medial distal crest is robust projecting dorsoventrally from the anteromedial surface for approximately one-quarter the length of the diaphysis bearing a prominent anterior depression (Fig. 6.3.36A–B). A similar morphology is reported in most non-tetanuran theropods, such as '*Syntarsus*' *kayentakatae* and *Ceratosaurus* (Madsen and Welles 2000), and allosauroids, including *Allosaurus* (Madsen 1976) and *Neovenator* (Brusatte et al. 2008). On the contrary, weakly developed medial distal crest is a feature common among megalosauroids such as *Megalosaurus*, *Afrovenator*, *Baryonyx*, *Eustreptospondylus*, and *Piatnitzkysaurus* (Sadleir et al. 2008; Benson 2010).

The anterior surface of the distal femur has a shallow concave and rough surface delimited ventrally and dorsally by short crests, adjacent to the medial distal crest. A low crest extends longitudinally in the medial surface of the distal femur from the posteroventral margin of the medial condyle up to the dorsal part of the medial distal crest.

Tibiae. The right, MNHNUL.P.AND68, and left, MNHNUL.P.AND69, tibiae are almost complete and well-preserved (Fig. 6.3.36G–L). The right tibia is broken proximally and the lateral and medial condyles are missing. The diaphysis is straight in anterior and posterior view, but is strongly concave in medial view and convex in lateral view. In proximal view, the tibia has a well-developed cnemial crest, which is triangular-shaped in anterior view projecting well-above the level of the dorsal surface of the tibia proximal margin. The cnemial crest extends laterally forming a broad incisura tibialis on the anterior surface of the proximal part of the tibia. Ventrally, the cnemial crest extends as a crest-shaped process along the medial surface of the diaphysis. The anterior surface of the proximal part of the tibia has a short crest extending adjacent to the dorsal margin of the cnemial crest.

The fibular crest is robust, but transversely narrow and elongated, projecting in the anterior surface of the proximal part of the diaphysis and ends below the proximal part of the tibia. This morphology is similar to those of *Allosaurus* (Madsen 1976), *Neovenator* (Brusatte et al. 2008), and other most basal theropods such as *Ceratosaurus* (Madsen and Welles 2000), *Suchomimus* (Benson 2010), and

Torvosaurus (Britt 1991). The fibular crest is suboval in lateral view in *Megalosaurus*, *Piatnitzkysaurus* (Benson 2010) and *Sinraptor* (Currie and Zhao 1993). Besides, the crest extends to the proximal part of the tibia as a low ridge in *Ceratosaurus* (Madsen and Welles 2000; Malafaia et al. 2015) and in some basal tetanurans, such as *Piatnitzkysaurus* and *Megalosaurus* (Benson 2010). The dorsal part of the fibular crest has a deep foramen that pierces the diaphysis with a dorsoventral orientation.

The distal part of the tibia is much anteroposteriorly expanded and triangular in anterior view. The medial margin of the distal tibia extends medially and somewhat ventrally, whereas the lateral margin extends strongly ventrally and laterally thus the lateral malleolus is rather displaced ventrally relative to the medial malleolus. The medial malleolus is rounded in medial view and the lateral malleolus has a crest-shape. The distal end of the tibia is triangular in distal view and has a small concavity placed between the medial and lateral malleolus. The surface for articulation with the ascending process of the astragalus extends dorsally for approximately one-fifth the length of the tibia. This articular surface is bordered medially by a short oblique and robust supraastragalar buttress. The anterior surface of the disphysis of the tibia is flat below the level of the fibular crest. Laterally to this flat area, a shallow and longitudinal concave surface extends from the distal end of the fibular crest to the level of the dorsal margin of the lateral condyle. This concave area is bounded by a low medial crest and corresponds to the surface for contact with the fibula.

Fibulae. The right, MNHNUL.P.AND70, and left, MNHNUL.P.AND71, fibulae are complete and the left one is preserved articulated with the astragalus and carcaneum (Fig. 6.3.36M–S). The fibula is slender with a thin diaphysis and a strongly expanded proximal part. The proximal margin is boomerang-shaped in proximal view with a convex lateral surface and a strongly concave medial border. The posterior surface of the fibular proximal part forms a thin and vertical crest projecting from the articular surface ventrally into the diaphyisis. Proximally, the lateral surface of the fibula has a shallow concavity adjacent to the posterior crest. The posterior margin of the fibular proximal part extends dorsally slightly above the dorsal level of the anterior border. The proximal part strongly tapers to the rear in a thin and blade-shaped margin. The tubercle for insertion of the muscle iliofibularis is low, but has a strongly rough surface (Fig. 6.3.36O). This tubercle is placed in the anterior margin of the diaphysis near its mid-length. The medial surface of the fibula has a deep depression adjacent to the anterior surface, which is bounded to the front by a thin blade projecting medially from the anterior margin of the fibula. Dorsally, a smaller crest extends horizontally forming the dorsal margin of the medial depression. Distally, the fibula has a rounded and slightly expanded surface that articulates in a deep concavity in the dorsal surface of the calcaneum and supports the lateral surface of the ascending process of the astragalus (Fig. 6.3.36N–O).

Tarsus. The tarsus includes the left astragalus and calcaneum preserved in articulation with the fibula, one right tarsal III and the three central right metatarsals.

Astragalus and calcaneum. Left astragalus and calcaneum are preserved with the fibula as was mentioned above (Fig. 6.3.36M–S). The astragalus is a bean-shaped element in anterior view, with a strongly concave ventral surface. A deep longitudinal groove extends near the mid-height of the astragalus body along the entire length (Fig. 6.3.36S). This groove takes to a deep notch that forms part of the suture for the calcaneum. Similar groove is present in other tetanuran theropods, including *Allosaurus* (Gilmore 1920; Madsen 1976), *Acrocanthosaurus* (Evers 2014), *Australovenator* (Hocknull et al. 2009), *Mapusaurus* (Coria and Currie 2006) and *Sinraptor* (Currie and Zhao 1993).

The suture between the astragalus and calcaneum is strongly sinuous. The ascending process of the astragalus extends from the lateral mid-length of the anterodorsal surface of the astragalus. This process is much high being almost as high as the mediolateral length of the astragalus body. The ascending process is separated from the body of the astragalus by a shallow groove (Fig. 6.3.36O). In dorsal view the astragalus is strongly concave with a rounded and broad concavity medially

representing the articulation for the tibia. The calcaneum is a disk-shaped, mediolaterally thin element that becomes slightly thicker ventromedially. In lateral view, the calcaneum is crescent-shaped with a strongly concave dorsal margin for receive the distal end of the fibula.

Tarsal III. A complete and well-preserved right distal tarsal III, MNHNUL.P.AND107 (Fig 6.3.37A–C), was found among the material collected in Andrés. It is a dorsoventrally thin element with a subquadrangular shape. The dorsal surface is slightly convex and has a tapered ventral margin that narrows medially, whereas the lateral margin is concave. The ventral surface is mostly flat and has two longitudinal grooves adjacent to the lateral and medial margins. These grooves are interpreted as the surfaces for articulation with the metatarsal IV and II.

Figure 6.3.37. Elements of the tarsus attributed to *Allosaurus* collected in Andrés. (A–C), right tarsal II, MNHNUL.P.AND107; (D–E), articulated right metatarsals; (H–S), metatarsals II–IV in anterior (E, F–H); proximal (C–D, O–Q); distal (A, L–N); posterior (I–K); medial (B, R–T); and lateral (U–W) views. Scale bar: 50 mm.

Metatarsus. The metatarsus is represented by the second, MNHNUL.P.AND73, third, MNHNUL.P.AND74, and fourth, MNHNUL.P.AND75, right metatarsals (Fig. 6.3.37D–P).

Metatarsal II (Mt II). The Mt II has a thick and robust shaft that is mostly straight in anterior and medial views. The proximal part is strongly expanded anteroposterior and mediolaterally. The proximal

articular facet is semicircular in proximal view, with a flat and posteromedially facing medial surface for articulation with metatarsal III. The lateral surface of the Mt II is flat along most of its length representing a close contact with the proximal part of the metatarsal III. In medial view, the proximal part of the Mt II has a shallow longitudinal concavity in the posterior surface just below the articular facet, which would serve for articulation with the metatarsal I. Distally it has two well-developed condyles, which are separated to the rear by a deep groove. This groove extends slightly into the distal surface, but not in the anterior surface so there is a single distal condyle in anterior view. In distal view, the lateral condyle is rounded and much larger than the medial one, which has a crest-shaped. Collateral ligament pits are present on the medial and lateral sides of the distal part with the lateral pit slightly deeper than the medial one.

Metatarsal III (Mt III). The shaft of the Mt III is straight and has a subtriangular cross-section, with the posterior margin narrower than the anterior one. This morphology of the shaft of the Mt III has been considered as a synapomorphy for Tetanurae (Gauthier 1986). The proximal part is expanded, strongly elongated anteroposteriorly relative to the shaft and is subrectangular in proximal view, with a tapered posterior margin. The medial surface just below the proximal articular facet is flat representing the area for articulation with the Mt II. Unlike metatarsals II and IV, the distal condyle of Mt III is not posteriorly divided, but a shallow concavity bounded by well-developed longitudinal crests extending along the medial and lateral margins, is present in the posterior surface adjacent to the condyle. The distal condyle is slightly convex and subrectangular in distal view. The medial and lateral collateral ligament pits are approximately equal in depth.

Metatarsal IV (Mt IV). The shaft of the Mt IV is straight in lateral view and is strongly curved laterally in anterior and medial views. The shaft of metatarsal IV is also strongly curved in several basal tetanurans, such as *Allosaurus* (Madsen 1976) and *Piatnitzkysaurus* (Bonaparte 1986). The medial surface of the shaft is almost flat so it has a semioval cross-section. The proximal part has an anterioposteriorly, semioval shape in proximal view, with a slightly concave medial margin and a tapering posterior surface. This medial concavity in the proximal one-third of the shaft represents the articulation for the Mt III (Fig. 6.3.37Q). Distally it has two small condyles separated in the posterior surface by a shallow groove, but to the front there is only a single condyle. The lateral condyle has a crest-shaped and extends somewhat laterally, whereas the medial condyle is more rounded. Well-marked collateral ligament pit is present on the medial side of the distal part, but the lateral pit is much shallower and poorly defined.

Pes. The pes is represented by a right phalanx 1 of the first digit, MNHNUL.P.AND119, a right phalanx 1 of the second digit, MNHNUL.P.AND106, right, MNHNUL.P.AND109, and left, MNHNUL.P.AND108, phalanges 2 of the third digits, a right phalanx 1 of the third digit, MNHNUL.P.AND94, a right phalanx 3 of the third digit, MNHNUL.P.AND96, and an ungueal phalanx, MNHNUL.P.AND97 (Fig. 6.3.38). Besides, two much smaller phalanges 1 of the second, MNHNUL.P.AND110, and fourth, MNHNUL.P.AND118, digits were also collected in Andrés.

The phalanges are relatively slender and longer than wide. All preserved non-ungual phalanges have well-developed nearly symmetrical distal condyles except the phalanx 1-I, which has asymmetrical distal condyles with the medial condyle projecting slightly more to the rear than the lateral one. The proximal articular facets of these phalanges are slightly concave and generally circular in proximal view. Lateral and medial collateral ligament pits are well-marked in all preserved phalanges. The lateral pit is deeper than the medial one in the phalanges 1-III, 1-II, and 1-I, whereas the reverse is present in the phalanx 3-IV. In the phalanx 2-II both pits are almost equally developed. A broad concavity interpreted as for insertion of extensor muscles is present in the anterior surface above the distal condyles in the phalanges 1-III, 1-II, and 3-IV. A correspondent concavity in the posterior surface for insertion of flexor muscles is generally much shallower, but is slightly more developed in the phalanges 1-III and 1-II. The phalanges 1-II and 1-III are the most robust of all preserved phalanges and they have the proximal and distal parts strongly offset from the shaft, which gives a somewhat constricted appearance to the phalanx. The other

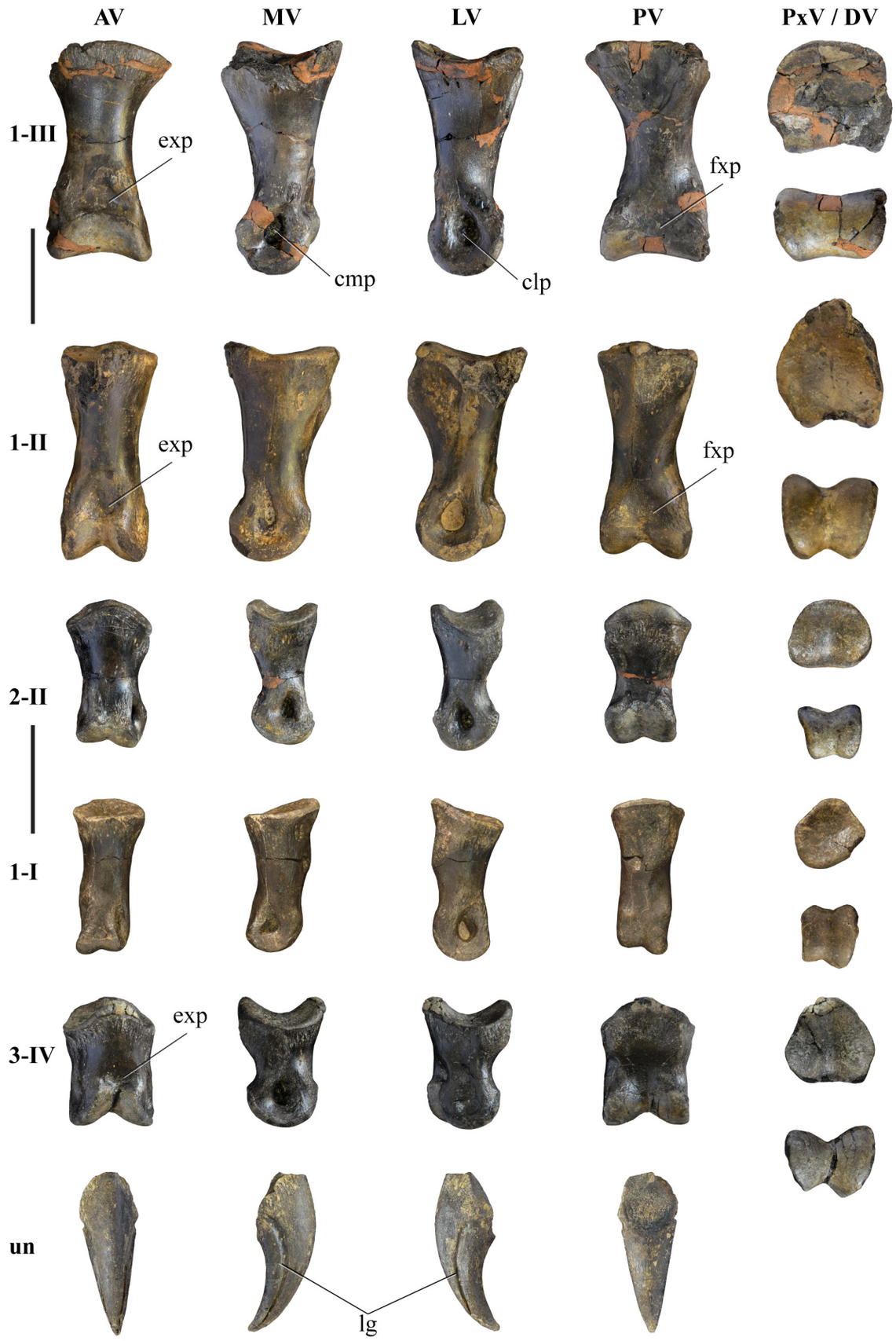

Figure 6.3.38. Pedal phalanges attributed to *Allosaurus* collected in Andrés. Top to bottom phalanx 1-III; phalanx 1-II; phalanx 2-II; phalanx 1-I; phalanx 3-IV; and ungueal phalanx. Legend: AV, anterior view; MV, medial view; LV, lateral view; PV, posterior view; PxV, proximal view; DV, distal view. Scale bar: 50 mm.

phalanges have straighter shafts. The phalanx 3-IV is subquadrangular in anterior and posterior views, with approximately parallel medial and lateral margins and nearly as transversely wide as high. The posterior surface of the phalanges 1-II and 1-III has slightly concave and rough areas adjacent to the proximal margin, which are delimited by well-developed medial and lateral ridges. The phalanges 2-II and 3-IV have almost flat posterior surface. The proximal articular facet of the phalanges 2-II and 3-IV has a low crest extending anteroposteriorly near its mid-width, which subdivides the articulation in two concavities. In the first phalanx of the digits I, II, and III this crest is absent. The ungual phalanx is broken proximally and the proximal articulation is missing. It is strongly arched in lateral view and is triangular in cross-section, with a nearlyt flat ventral surface transversely wider than the dorsal surface. A pair of longitudinal grooves extends near the mid-height of the lateral and medial surfaces of this phalanx.

6.3.9. PHYLOGENETIC ANALYSIS

6.3.9.1. Phylogeny of Allosauroidea

The term Allosauroidea was proposed by Currie and Zhao (1993) to include Allosauridae and Sinraptoridae, but not other basal tetanurans, such as 'megalosaurs' and *Monolophosaurus*. Sereno et al. (1994), proposed two clades within Carnosauria (*sensu* Gauthier 1986), the Spinosauroidea and the Allosauroidea, each progressively closer sister groups of the Coelurosauria. Subsequently, Rauhut (1995) added Carcharodontosauridae to the Allosauroidea clade. Sereno (1998) defined Allosauroidea as a stem-based clade encompassing all avetheropods closer to *Allosaurus* than to Neornithes. In turn, Padian et al. (1999) defined the Allosauroidea as a node-based taxon to include *Allosaurus*, *Sinraptor* and all descendants of their most recent common ancestor. These stem-based and node definitions may differ in content, as some basal tetanurans that fall outside the *Sinraptor* + *Allosaurus* node would be considered allosauroids in the taxonomy of Sereno (1998), but non-allosauroid carnosaurs in the system of Padian et al. (1999).

In most recent phylogenetic analysis a stem-based definition of Allosauroidea has been preferably used because the monophyly of the clade including all dinosaurs closer to *Allosaurus* than to birds has been demonstrated by nearly every large-scale study of theropod phylogeny (Brusatte and Sereno 2008; Eddy and Clarke 2011). Based on these analyses, Allosauroidea comprises Allosauridae, Sinraptoridae and Carcharodontosauria (Neovenatoridae + Carcharodontosauridae). Currently known allosaurids include *Allosaurus fragilis* (Gilmore 1920; Madsen 1976), *Allosaurus* "*jimmadseni*" (Chure 2000; Evers 2014), *Allosaurus europaeus* (Mateus et al. 2006), and *Saurophaganax maximus* (Chure 1995; Chure 2000 = *Allosaurus maximus sensu* Smith 1998). In turn, Sinraptoridae (= Metriacanthosauridae *sensu* Paul 1988) has been defined as a stem-based clade comprising *Sinraptor* and all allosaurids closer to it than to *Allosaurus* (Padian et al. 1999) or as the most inclusive clade containing *Sinraptor dongi*, but not *Allosaurus fragilis*, *Carcharodontosaurus saharicus*, or *Passer domesticus* (Sereno 2005; Brusatte and Sereno 2008). Sinraptoridae includes *Xuanhanosaurus qilixiaensis* (Dong 1984), *Yangchuanosaurus shangyouensis* (Dong et al. 1978), *Y. zigongensis* (Carrano et al. 2012) (= *Szechuanosaurus zigongensis sensu* Gao 1993), *Szechuanosaurus campi* (Young 1942) (= "*Szechuanoraptor*" *dongi sensu* Chure 2000), *Metriacanthosaurus walkeri* (Huene 1923), *Shidaisaurus jinae* (Wu et al. 2009), *Siamotyrannus isanensis* (Buffetaut et al. 1996; Carrano et al. 2012), *Sinraptor hepingensis* (Currie and Zhao 1993; Rauhut 2003; Holtz et al. 2004; Carrano et al. 2012) (= *Yangchuanosaurus hepingensis sensu* Gao 1992), *S. dongi* (Currie and Zhao 1993), and *Datalong guangxiensis* (Mo et al. 2014). Neovenatoridae comprises *Neovenator salerii* (Hutt et al. 1996; Brusatte et al. 2008), *Chilantaisaurus tashuikouensis* (Hu 1964; Benson and Xing 2008), *Siats meekerorum* (Zanno and Makovicky 2013), and the megaraptorans *Megaraptor namunhuaiquii* (Novas 1998; Calvo et al. 2004), *Aerosteon riocolonadensis* (Sereno et al. 2008), *Orkoraptor burkei* (Novas et al. 2008), *Australovenator wintonensis* (Hocknull et al. 2009), and *Fukuiraptor kitadaniensis* (Azuma and Currie 2000). Recently, a different interpretation was proposed for the phylogenetic relationships of

the megaraptorans suggesting that they are related with Coelurosauria instead of Allosauroidea (Novas et al. 2013). Finally, the Carcharodontosauridae include *Concavenator corcovatus* (Ortega et al. 2010; Cuesta et al. 2016), *Eocarcharia dinops* (Sereno and Brusatte 2008), *Shaochilong maortuensis* (Brusatte et al. 2009; 2010b), *Acrocanthosaurus atokensis* (Stovall and Langston 1950; Harris 1998; Currie and Carpenter 2000; Eddy and Clarke 2011), *Mapusaurus roseae* (Canale et al. 2014; Coria and Currie 2006), *Tyrannotitan chubutensis* (Novas et al. 2005), *Carcharodontosaurus iguidensis* (Brusatte and Sereno 2007), *Carcharodontosaurus saharicus* (Depéret and Savornin 1925), *Giganotosaurus carolinii* (Coria and Salgado 1995), *Kelmayisaurus petrolicus* (Dong 1973; Brusatte et al. 2012), and possibly *Sauroniops pachytholus* (Cau et al. 2013). Some taxa, such as *Monolophosaurus*, *Cryolophosaurus*, and *Piatnitzkysaurus* have been placed within Allosauroidea (Bonaparte 1986; Sereno et al. 1994; Chure 2000), but other authors suggested that these taxa show morphological evidence of other affinities (Zhao and Currie 1993; Rauhut 2003; Holtz et al. 2004; Smith et al. 2007; Benson 2010; Brusatte et al. 2010a; Zhao et al. 2010).

Other problematic taxa, including *Lourinhanosaurus* (Mateus 1988) from the Upper Jurassic of Portugal, *Erectopus* (Sauvage 1882; Allain 2005a) from the Lower Cretaceous of France, and *Veterupristisaurus* (Rauhut 2011) from the Upper Jurassic of Tanzania have been tentatively related with Allosauroidea, but have an unstable phylogenetic position due to the fragmentary nature of the specimens. *Lourinhanosaurus* was originally described as an allosauroid (Mateus 1998), but has been tentatively related with different clades, including Megalosauroidea (Mateus et al. 2006) and Coelurosauria (Carrano et al. 2012; Rauhut et al. 2016). *Erectopus* has been recently interpreted as a non-carcharodontosaurian allosauroid, possibly related with sinraptorids (Carrano et al. 2012) and *Veterupristisaurus* was interpreted as a carcharodontosaurid closely related with *Acrocanthosaurus* (Rauhut 2011).

6.3.9.2. Analysis

A phylogenetic analysis for the set of cranial and postcranial remains identified to *Allosaurus* collected in Andrés was performed. For this analysis it was used the data matrix proposed by Eddy and Clarke (2011), with some modifications, such as: (1) addition of *Concavenator* based on the codification proposed by Ortega et al. (2010) and firsthand review of the specimen; (2) inclusion of *Cryolophosaurus* based on the codification proposed by Smith et al. (2007); (3) integration of the specimen DINO 11541 based on descriptions of Chure (2000) and firsthand review; and (4) codification of the specimen ML 415 based of firsthand review (see Appendix 6.3.1).

Data matrices were analysed using TNT 1.1 (Goloboff et al. 2008) to find the most parsimonious trees (MPTs). A heuristic tree search was used performing 1000 replications of Wagner trees (using random addition sequences) followed by tree bisection reconnection (TBR) as swapping algorithm, saving 100 trees per replicate. Absolute and relative Bremer supports were calculated to test the robustness of the phylogenetic hypotheses.

Results

First the datamatrix proposed by Eddy and Clarke (2011) with inclusion of the specimen from Andrés was analysed. This analysis recovered 4 MPT's (TBR = 330) and the consensus tree is identical to that obtained by Eddy and Clarke (Fig. 6.3.39A). This analysis recovered two autapomorphies for the specimen from Andrés: (i) presence of a naso-maxillary process in the nasal lateral surface (# character 19) and (ii) length of the anterior ramus of the lacrimal greater than 65% the height of the ventral ramus (# character 27). The specimen shares with *Allosaurus* the following synapomorphies: (i) straight shape of the ridge across the interdental plates of the maxilla (# character 13); (ii) triangular shape of frontal articular surface in the prefrontal (# character 47); (iii) absence of a posteriorly-placed knob-like dorsal projection in the parietal (# character 55); (iv) absence of a palatine pneumatic recess (# character 84); (v) presence of a ventral notch between the obturator process and the diaphysis of the ischium (# character 153); and (vi) pubic boot 50-60% the pubic length (# character 157).

Subsequently, a new alaysis was performed in order to determining the relationships between the specimen from Andrés and other allosauroids from the Upper Jurassic of the Lusitanian Basin and from other Iberian records. In this analysis, *Cryolophosaurus* (Smith et al. 2007) and *Concavenator* (Ortega et al. 2010) as well as other allosauroid specimens from the Upper Jurassic of the Lusitanian Basin (ML370: Mateus 1998; ML415: Mateus et al. 2006; SHN.036: Malafaia et al. 2016) and Morrison Formation (DINO 11541: Chure 2000) were added to the datamatrix proposed by Eddy and Clarke (2011).

The consensus of the 1027 MPT's (TBR = 369) obtained in this analysis recovers a large politomy including most of the taxa, with the exception of the more derived carcharodontosaurs, which have a better resolution. In order to improve the resolution of this hypothesis a Prune tree and a reduced consensus was calculated excluding the taxa indicated by the Prune tree (e.g. *Tyrannotitan*, *Siamotyrannus*, and ML415). The phylogenetic hypothesis obtained after prune these taxa has a much higher resolution (Fig. 6.3.39B). This analysis recovered a unique autapomorphy for the specimen from Andrés: the presence of a pronounced groove on the astragalus separating the anterior base of ascending process from the astragalar body (# character 175). MNHNUL.P.AND is placed as the sister taxon to the North American forms of *Allosaurus* and they share several exclusive characters, including: (i) triangular shape of the frontal articular surface in the prefrontal (# character 47); (ii) absence of a knob-like posterior dorsal projection in the parietal (# character 55); (iii) basal tubera subdivided by a lateral longitudinal groove into a medial part entirely formed by the basioccipital and a lateral part entirely formed by the basisphenoid (# character 71); and (iv) absence of a palatine pneumatic recess (# character 84). Including the holoptype of *Allosaurus europaeus* in the consensus strongly reduces the resolution of the obtained phylogenetic hypothesis, mainly at the base of Allosauroidea. When included ML 415 the analysis recover a unique autapomorphy for this taxon: the ventral termination of the ventral ramus of the postorbital close to the ventral margin of the orbit and ventral to squamosal-quadratojugal contact.

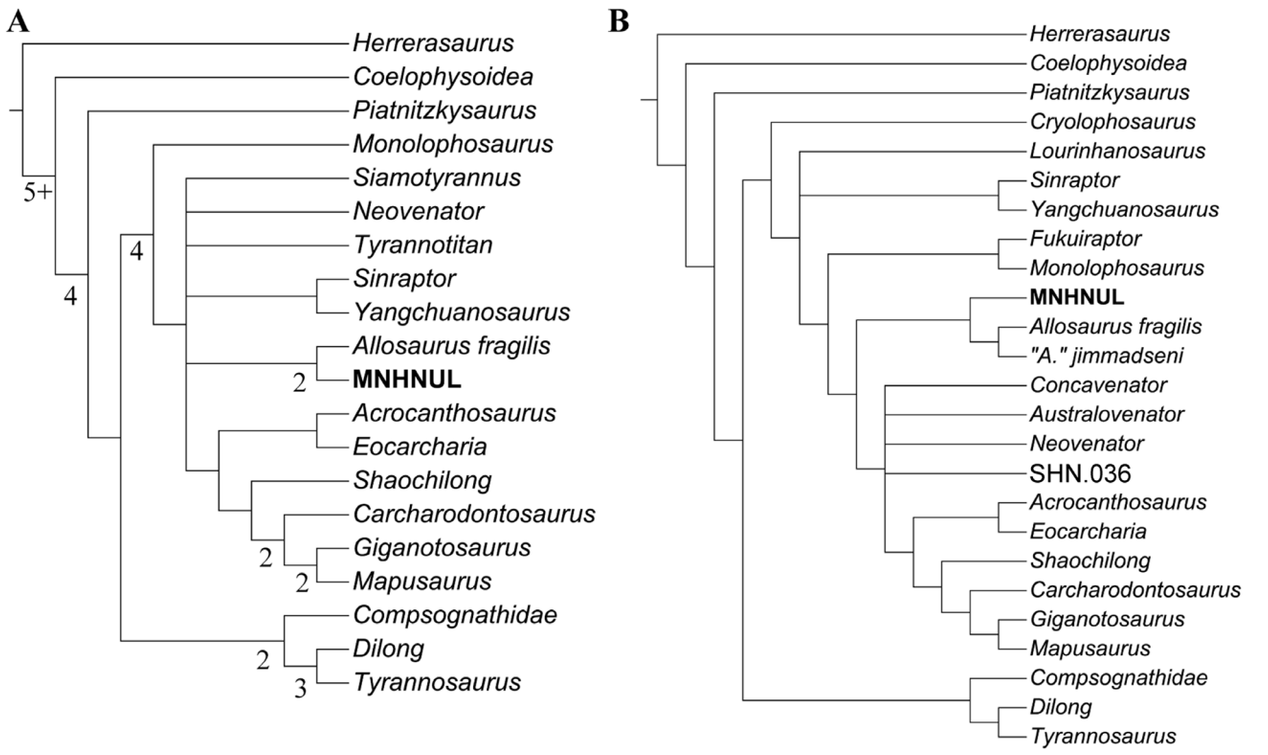

Figure 6.3.39. Phylogenetic relationships of the *Allosaurus* specimens collected in Andrés. (A) Strict consensus cladogram from 4 most parsimonious trees recovered by the analysis of the data matrix of Eddy and Clarke (2011) [Tree length = 330 steps; CI = 0.539 and RI = 0.595]; (B) strict consensus cladogram from 1027 most parsimonious trees recovered by the analysis of the modified version of the data matrix Eddy and Clarke (2011) [Tree length = 369 steps; CI = 0.510 and RI = 0.594]. Note: The numbers in the nodes represent the absolute Bremer support values.

6.3.9.3. Discussion

The set of cranial elements collected in Andrés has a combination of features compatible with *Allosaurus* sharing several features considered as synapomorphies for this taxon. Among the diagnosed features proposed for *Allosaurus* by Chure (2000) it is possible verify in the specimen from Andrés the presence of a large, mediolaterally compressed and dorsally projecting cornual process of the lacrimal and the presence of an internal mandibular foramen along the caudoventral margin of the prearticular. Based on this combination of feature the specimen from Andrés may be confidentially related with *Allosaurus* and it is hardly distinguished from the North American forms of this taxon. Some distinct features of the specimens from Andrés relative to the North American forms include: (i) jugal ramus of the squamosal extending posteriorly back to the level of the pterygoid process (shared with *Sinraptor*: Currie and Zhao 1993); (ii) well-developed concavities in the posterolateral surface of the supraoccipital, adjacent to the contact with the paroccipital processes; (iii) two separated foramina for the branches of the hypoglossal nerve within the paracondylar pocket for the cranial nerve XII (shared with *Sinraptor*: Currie and Zhao 1993; Paulina Carabajal and Currie 2012); (iv) naso-maxillary process in the nasal lateral surface (shared with *Acrocanthosaurus*: Eddy and Clarke 2011); and (v) length of the anterior ramus of the lacrimal greater than 65% of the height of the ventral ramus.

Allosaurus europaeus (Mateus et al. 2006) is diagnosed based on the following autapomorphies: (i) jugal participation in the antorbital fenestra; (ii) maxilla forked in the posterior margin; (iii) truncated ventroposterior process of the maxilla; (iv) nasal with two pneumatic foramina (the anterior foramen twice the size of the posterior); (v) posteroventral projection of the jugal more than twice the posterodorsal projection; (vi) large anterior surangular foramen; (vii) no lacrimal-maxillary contact; (viii) squamosal contacts the quadratojugal by a sigmoidal suture; (ix) squamosal extending ventrally into laterotemporal fenestra; (x) lacrimal horn narrow in lateral view; (xi) large ventral projection of the postorbital; (xii) rugose dorsal rim of the nasal; (xiii) occipital condyles placed above the squamosal-quadratojugal contact; (xiv) anterior tip of the quadratojugal is anterior to the laterotemporal fenestra; (xv) lateral lamina of the lacrimal is subtle; (xvi) palatine contacts the pterygoid dorsoposteriorlly; and (xvii) ventral tip of the postorbital reaches the lower rim of the orbit (Mateus et al. 2006). As was previously discussed, some of these features may be related with intraspecific variability such as the nasal pneumaticity, the development of the nasal lateral crest or the morphology of the lacrimal horn. Other putative differences are not significantly distinct from the morphology observed in some *Allosaurus* specimens, including: (i) development of the anterior surangular foramen; (ii) morphology of the contact between the squamosal and the quadratojugal; (iii) projection of the squamosal into the laterotemporal fenestra; (iv) anterior tip of the quadratojugal anterior to the laterotemporal fenestra (shared with DINO 11541: Chure 2000); (v) posteroventral projection of the jugal more than twice the posterodorsal projection (shared with DINO 11541: Chure 2000); (vi) position of the occipital condyles relative to the squamosal-quadratojugal contact; (vii) morphology of the lateral lamina of the lacrimal; and (viii) contact between the palatine and the pterygoid. Other characters related with the contact between the lacrimal, maxilla and jugal are expressed by two equivalent features: (i) jugal participation in the antorbital fenestra and (ii) no lacrimal-maxillary contact. The morphology of the distal part of the lacrimal is similar to those of the lacrimals collected in Andrés and to other *Allosaurus* specimens as was discussed above. Based on this similar morphology it was proposed a distinct interpretation for this suture in ML425 in which the putative contact between the lacrimal and jugal of Mateus et al. (2006) is in fact a fracture and the real suture is between the lacrimal, maxilla and jugal (Fig. 6.3.40). However, for the moment it is not possible to confirm this interpretation and thus the original interpretation of Mateus et al. (2006) is maintained. The extension of the ventral ramus of the postorbital is also expressed by two equivalent characters: (i) large ventral projection of postorbital and (ii) ventral tip of the postorbital reaches the lower rim of the orbit. This feature is dictinct from *Allosaurus* in which the ventral ramus of the postorbital ends near the orbital fenestra mid-height (Gilmore 1920; Madsen 1976; Chure 2000). Finally, the features related with the morphology of the posterior margin of the maxilla: (i) maxilla forked posteriorly and (iii) truncated

ventroposterior process of the maxilla is also apparently distict from *Allosaurus* in which the maxilla strongly tapers posteriorly as is also the case in the specimen from Andrés.

Based on this discussion it is here proposed a revised diagnosis for the Portuguese species *Allosaurus europaeus*, which includes the following autapomorphies: (i) no lacrimal-maxillary contact; (ii) ventral tip of the postorbital reaches the lower rim of the orbit; and (iii) dorsoventrally deep and forked posterior margin of the maxilla.

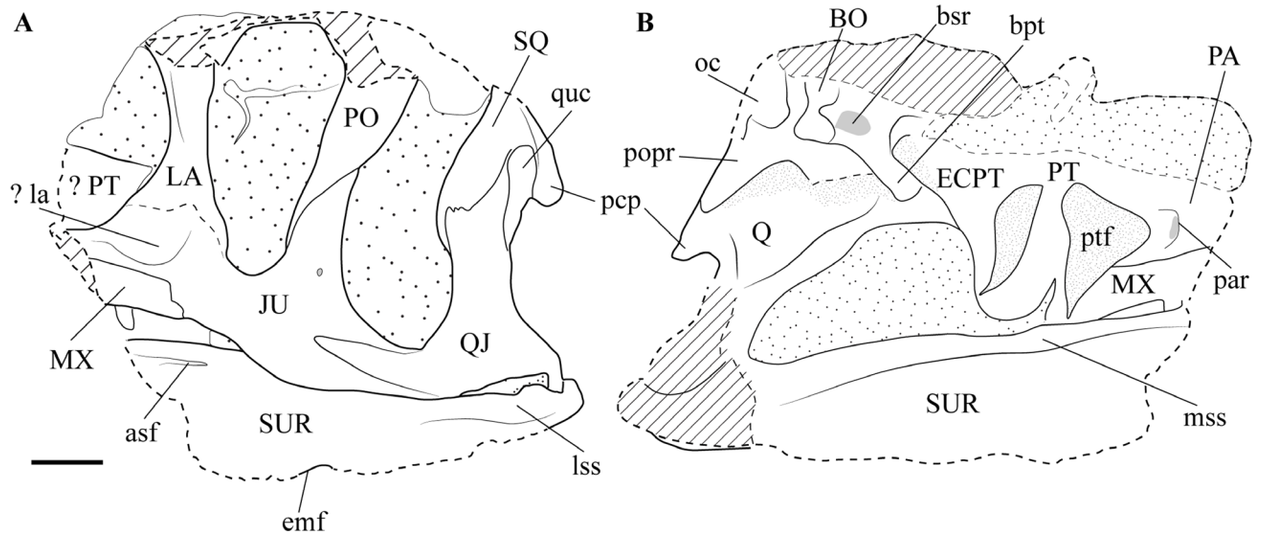

Figure 6.3.40. Interpretative drawing of the skull of the holotype of *Allosaurus europaeus* (ML415) showing our interpretation of the articulations between the lacrimal, maxilla and jugal. Scale bar: 50 mm.

6.3.9.4. Relationship between MNHNUL.P.AND and ML415

The set of cranial remains collected in Andrés has some differences relative to the *Allosaurus* specimens from the Morrison Formation as was discussed above. However, these specimens are also distinct from the holotype of *Allosaurus europaeus* in the strongly tapered posterior margin of the maxilla and in this feature MNHNUL.P.AND is more similar to the *Allosaurus* specimens from the Morrison Formation than to ML415. Also, the maxilla collected in Andrés clearly has a suture for the lacrimal as is typical for *Allosaurus* and thus this would be another difference respect to *A. europaeus*. These differences do not allow for the moment relating the specimen from Andrés with *A. europaeus* despite the identification of some differences relative to *A. fragilis*. The holotype of *A. europaeus* was collected in sediments of the Praia da Amoreira-Porto Novo Formation interpreted as upper Kimmeridgian in age (Mateus et al. 2006; Schneider et al. 2009) and the specimens from Andrés come from slightly younger sediments of the Bombarral Formation interpreted as Tithonian in age (Azerêdo et al. 2010; Kullberg et al. 2013). The differences identified between the specimens from Andrés and ML415 and the stratigraphic context may indicate that these specimens possibly belong to distinct taxa. However, for the moment, we prefer to assign the specimen from Andrés as *Allosaurus* cf. *europaeus* pending the discovery of more complete material that would allow a better interpretation of this species.

6.3.10. CONCLUSIONS

The set of remains herein described includes the most complete cranial evidence of a theropod dinosaur known in the Portuguese Upper Jurassic. The remains are generally much complete and well-preserved allowing the description of some fragile elements that are poorly known in the fossil record of theropods such as the vomer, the supradentary or the coronoid. Beside, the exceptional preservation of most elements allows a detailed description of the cranial morphology of this theropod from the

Upper Jurassic of the Lusitanian Basin. The specimens show a combination of features compatible with *Allosaurus* including several characters considered as synapomorphies for the taxon such as the presence of a large, mediolaterally compressed and dorsally projecting cornual process of the lacrimal or an internal mandibular foramen along the caudoventral margin of the prearticular. The description in 1999 of a partial postcranial skeleton collected in Andrés proposed the presence of the typical North American species *Allosaurus fragilis* in the Late Jurassic of Portugal. However, the new cranial elements herein described show some differences relative to the Morrison Formation forms, including: (i) jugal ramus of the squamosal extending posteriorly back to the level of the pterygoid process; (ii) well-developed concavities in the posterolateral surface of the supraoccipital, adjacent to the contact with the paroccipital processes; (iii) two separated foramina for the branches of the hypoglossal nerve within the paracondylar pocket for the cranial nerve XII; (iv) naso-maxillary process in the nasal lateral surface; and (v) length of the anterior ramus of the lacrimal greater than 65% of the height of the ventral ramus.

On the other hand, the Portuguese species *Allosaurus europaeus* was originally described based on several putative diagnostic features that may be mostly interpreted as related with intraspecific variability such as the nasal pneumaticity, the developedment of the nasal lateral crest and the morphology of the lacrimal horn. A revised diagnosis is proposed for this species, which may be distinguished from other *Allosaurus* forms based on the following autapomorphies: (i) no lacrimal-maxillary contact; (ii) ventral tip of the postorbital reaches the lower rim of the orbit; and (iii) dorsoventrally deep and forked posterior end of the maxilla.

The cranial elements of *Allosaurus* from Andrés differ from *A. europaeus* in two of these autapomorphies: the lacrimal contacts the maxilla and the posterior margin of the maxilla is strongly tapered. However, based on the paleobiogeographic context it is here proposed the assignation of the specimens from Andrés as *Allosaurus* cf. *europaeus* pending the discovery of more complete material that would allow a better understand of these Portuguese species.

6.3.11. ACKNOWLEDGMENTS

This work was supported by SFRH/BD/84746/2012 PhD scholarship, financed by the "Fundação para a Ciência e Tecnologia" (Portugal). Individual grants to E.M. visits for review collections were financed by the Jurassic Foundation, Fundação Luso-Americana para o Desenvolvimento [grant number L07-V-22/2010] and Synthesys [grant number GB-TAF-2160 and FR-TAF-4911]. The fieldworks were partially supported by the CMP and JFSL. We thank to Willi Henning Society for the available free TNT program, to J. Amorim and G. Gameiro for support during the fieldwork in the Andres fossil site, to M. Cachão and N. Pimentel for field assistance and comments to the paper, to G. Ramalheiro, I. Gromicho, B. Ribeiro, J. Santamaria, M. García-Oliva, J.M. Gasulla for collaboration in the fieldworks, to E. Cuesta for photographs of specimens, and for allow accessing specimens to B. C. Silva (SHN, Portugal), R. Castanhinha and C. Tomás (ML, Portugal), V. Santos, L. Póvoas and C. Lopes (MUHNAC, Portugal), R. Allain (MNHN, France), T. Schossleitner (HNM, Germany), S. Chapman (NHMUK, UK), and P. Jeffery (OUMNH, UK), L. Chiappe (NHMLAC, USA), K. Carpenter (DMNH, USA), R. Scheetz and B. Britt (BYU, USA), M. Getty, M. Loewen, and R. Irmis (NHMU, USA), D. Chure (DINO, USA).

REFERENCES

Allain R. 2005a. The enigmatic theropod dinosaur *Erectopus superbus* (Sauvage, 1882) from the Lower Albian of Louppy-le-Château (Meuse, France). In: Carpenter K. (eds.). The Carnivorous Dinosaurs. Indiana University Press:72–86.

Allain R. 2005b. The postcranial anatomy of the megalosaur *Dubreuillosaurus valesdunensis* (Dinosauria Theropoda) from the Middle Jurassic of Normandy, France. Journal of Vertebrate Paleontology 25(4):850–858.

Antunes MT, Mateus O. 2003. Dinosaurs of Portugal. Comptes Rendus Paleovol 2:77–95.

Arcucci A, Coria RA. 2003. A new Triassic dinosaur. Ameghiniana 40: 217–228.

Azerêdo AC, Cabral MC, Martins MJ, Loureiro IM, Inês N. 2010. Estudo estratigráfico dum novo afloramento da Formação de Cabaços (Oxfordiano) na região da Serra do Bouro (Caldas da Rainha). Comunicações Geológicas 97:5–22.

Azuma Y, Currie PJ. 2000. A new carnosaur (Dinosauria: Theropoda) from the Lower Cretaceous of Japan. Canadian Journal of Earth Sciences 37:1735–1753.

Bakker RT, Siegwarth J, Kralis D, Filla J. 1992. *Edmarka rex*, a new, gigantic theropod dinosaur from the middle Morrison Formation, Late Jurassic of the Como Bluff outcrop region. Hunteria 2(9):1–24.

Bakker RT, Williams MW, Currie PJ. 1998. *Nanotyrannus*, a new genus of pygmy tyrannosaur, from the latest Cretaceous of Montana. Hunteria 1(5): 30pp.

Benson RBJ. 2010. A description of *Megalosaurus bucklandii* (Dinosauria: Theropoda) from the Bathonian of the UK and the relationships of Middle Jurassic theropods. Zoological Journal of the Linnean Society of London 158:882–935.

Benson RBJ, Xing X. 2008. The anatomy and systematic position of the theropod dinosaur *Chilantaisaurus tashuikouensis* Hu, 1964 from the Early Cretaceous of Alanshan, People's Republic of China. Geological Magazine 145(6):778–789.

Bever GS, Brusatte SL, Carr TD, Xu X, Balanoff AM, Norell MA. 2013. The braincase anatomy of the Late Cretaceous dinosaur *Alioramus* (Theropoda: Tyrannosauroidea). Bulletin of the American Museum 376:1–72.

Bonaparte JF. 1986. Les Dinosaures (Carnosaures, Allosauridés, Sauropodes, Cétiosaurids) du Jurassique moyen de Cerro Cóndor (Chubut, Argentine). Annales de Paléontologie (Vert.-Invert.) Vol. 72 fasc. 3:247–289.

Bonaparte JF, Novas FE, Coria RA. 1990. *Carnotaurus sastrei* Bonaparte, the horned, lightly built carnosaur from the Middle Cretaceous of Patagonia. Contributions in Science of the Natural History Museum of Los Angeles County 416:1–42.

Brikiatis L. 2016. Late Mesozoic North Atlantic land bridges. Earth Science Reviews. doi: 10.1016/j.earscirev.2016.05.002

Britt BB. 1991. Theropods of the Dry Mesa Quarry (Morrison Formation, Late Jurassic), Colorado, with emphasis on the osteology of *Torvosaurus tanneri*. Brigham Young University Geology Studies 37:1–72.

Britt BB. 1993. Pneumatic postcranial bones in dinosaurs and other archosaurs. [Ph.D. Dissertation]. Department of Geology and Geophysics. University of Calgary. Calgary, Alberta: 383 pp.

Brochu CA. 2003. Osteology of *Tyrannosaurus rex*: insights from a nearly complete skeleton and high−resolution computed tomographic analysis of the skull. Society of Vertebrate Paleontology Memoir 7:1–138.

Brusatte SL, Sereno PC. 2007. A new species of *Carcharodontosaurus* (Dinosauria: Theropoda) from the Cenomanian of Niger and a revision of the genus. Journal of Vertebrate Paleontology 27(4):902–916.

Brusatte SL, Sereno PC. 2008. Phylogeny of Allosauroidea (Dinosauria: Theropoda): comparative analysis and resolution. Journal of Systematic Palaeontology 6:155–182.

Brusatte SL, Benson RBJ, Hutt S. 2008. The osteology of *Neovenator salerii* (Dinosauria: Theropoda) from the Wealden Group (Barremian) of the Isle of Wight. Monograph of the Palaeontographical Society 162:1–166.

Brusatte SL, Benson RBJ, Chure DJ, Xu X, Sullivan C, Hone DWE. 2009. The first definitive carcharodontosaurid (Dinosauria: Theropoda) from Asia and the delayed ascent of tyrannosaurids. Naturwissenschaften 96(9):1051–1058.

Brusatte SL, Benson RBJ, Currie PJ, Xijin Z. 2010a. The skull of *Monolophosaurus jiangi* (Dinosauria: Theropoda) and its implications for early theropod phylogeny and evolution. Zoological Journal of the Linnean Society 158:573–607.

Brusatte SL, Chure DJ, Benson RBJ, Xu X. 2010b. The osteology of *Shaochilong maortuensis*, a carcharodontosaurid (Dinosauria: Theropoda) from the Late Cretaceous of Asia. Zootaxa 2334:1–46.

Brusatte SL, Benson RBJ, Xu X. 2012. A reassessment of *Kelmayisaurus petrolicus*, a large theropod dinosaur from the Early Cretaceous of China. Acta Palaeontologica Polonica 57(1):65–72.

Buffetaut E, Suteethorn V, Tong H. 1996. The earliest known tyrannosaur from the Lower Cretaceous of Thailand. Nature 381:689–691.

Calvo JO, Porfiri JD, Veralli C, Novas FE, Poblete F. 2004. Phylogenetic status of *Megaraptor namunhuaiquii* Novas based on a new specimen from Neuquén, Patagonia, Argentina. Ameghiniana 41:565–575.

Canale JI, Novas FE, Salgado L, Coria RA. 2014. Cranial ontogenetic variation in *Mapusaurus roseae* (Dinosauria: Theropoda) and the probable role of heterochrony in carcharodontosaurid evolution. Paläontologische Gesellschaft.

Canale JI, Novas FE, Pol D. 2015. Osteology and phylogenetic relationships of *Tyrannotitan chubutensis* Novas, de Valais, Vickers-Rich and Rich, 2005 (Theropoda: Carcharodontosauridae) from the Lower Cretaceous of Patagonia, Argentina. Historical Biology 27:1–32.

Carrano MT, Benson RBJ, Sampson SD. 2012. The phylogeny of Tetanurae (Dinosauria: Theropoda). Journal of Systematic Palaeontology 10:211–300.

Cau A, Dalla Vecchia FM, Fabbri M. 2013. A thick-skulled theropod (Dinosauria, Saurischia) from the Upper Cretaceous of Morocco with implications for carcharodontosaurid cranial evolution. Cretaceous Research 40:251–260.

Charig AJ, Milner AC. 1997. *Baryonyx walkeri*, a fish-eating dinosaur from the Wealden of Surrey. Bulletin of the Natural History Museum London (Geology) 53:11–70.

Choffat P. 1901. Note preliminaire sur la limite entre le Jurassic et le Crétacique en Portugal. Bulletin de la Société Belge de Géologié, de Paléontologie et d'Hydrologie xv:111–140.

Chure DJ. 2000. A new species of *Allosaurus* from the Morrison Formation of Dinosaur National Monument (UT-CO) and a revision of the theropod family Allosauridae [PhD dissertation]. New York City: Columbia University.

Chure DJ, Madsen JH. 1996. Variation in aspects of the tympanic pneumatic system in a population of *Allosaurus fragilis* from the Morrison Formation (Upper Jurassic). Journal of Vertebrate Paleontology 16(1):63–66.

Coria RA, Salgado L. 1995. A new giant carnivorous dinosaur from the Cretaceous of Patagonia. Nature. 377(6546):224–226.

Coria RA, Currie PJ. 2003. The braincase of *Giganotosaurus carolinii* (Dinosauria: Theropoda) from the Upper Cretaceous of Argentina. Journal of Vertebrate Paleontology 22(4):802–811.

Coria RA, Currie PJ. 2006. A new carcharodontosaurid (Dinosauria, Theropoda) from the Upper Cretaceous of Argentina. Geodiversitas 28:71–118.

Coria RA, Chiappe LM, Dingus L. 2002. A new close relative of *Carnotaurus sastrei* Bonaparte 1985 (Theropoda: Abelisauridae) from the late cretaceous of Patagonia. Journal of Vertebrate Paleontology 22(2):460–465.

Cuesta E, Ortega F, Sanz JL. 2016. Phylogenetic reassessment of *Concavenator corcovatus* (Lower Cretaceous, Spain) and its implications for Carcharodontosauridae relationships. Abstract book of the 76th SVP Annual Meeting. p.122.

Currie PJ. 1985. Cranial anatomy of *Stenonychosaurus inequalis* (Saurischia, Theropoda) and its bearing on the origin of birds. Canadian Journal of Earth Sciences 22:1643–1658.

Currie PJ. 1997. Braincase anatomy. In: Currie PJ, Padian K. (Eds) The Encyclopedia of Dinosaurs. Academic Press, New York: 81–85.

Currie PJ, Zhao X–J. 1993. A new large theropod (Dinosauria, Theropoda) from the Jurassic of Xinjiang, People's Republic of China. Canadian Journal of Earth Sciences 30:2037–2081.

Currie PJ, Carpenter K. 2000. A new specimen of *Acrocanthosaurus atokensis* (Theropoda, Dinosauria) from the Lower Cretaceous Antlers Formation (Lower Cretaceous, Aptian) of Oklahoma, USA. Geodiversitas 22:207–246.

Dalman SG. 2014. Osteology of a large allosauroid theropod from the Upper Jurassic (Tithonian) Morrison Formation of Colorado, USA. Volumina Jurassica XII (2):159–180.

Dantas P, Sanz JL, Silva CM, Ortega F, Santos VF, Cachão M. 1998. *Lourinhasaurus* n. gen. Novo dinossáurio saurópode do Jurássico superior (Kimeridgiano superior-Titoniano inferior) de Portugal. V Congresso Nacional Geologia 84(1): A91–A94.

Dantas P, Pérez-Moreno BP, Chure DJ, Silva CM, Santos VF, Póvoas L, Cachão M, Sanz JL, Pires C, Bruno G, Ramalheiro G, Galopim de Carvalho AM. 1999. O dinossáurio carnívoro *Allosaurus fragilis* no Jurássico português. Al-Madam 8: 23–28.

Deparet C, Savornin J. 1925. Sur la decouverte d'une faune de vertebres albiens a Timimoun (Sahara occidental). Comptes Rendus, Academie du Sciences, Paris. 181:1108–1111.

Dong Z. 1973. Dinosaurs from Wuerho. Reports of Paleontological Expedition to Sinkiang (II): Pterosaurian Fauna from Wuerho, Sinkiang. Memoirs of the Institute of Vertebrate Paleontology and Paleoanthropology, Academia Sinica 11: 45–52.

Dong Z. 1984. A new theropod dinosaur from the Middle Jurassic of Sichuan Basin. Vertebrata PalAsiatica 22(3):213-218

Dong Z, Zhou S, Zhang Y. 1983. Dinosaurs from the Jurassic of Sichuan. Palaeontologica Sinica 162:1–136.

Eddy DR, Clarke JA. 2011. New information on the cranial anatomy of *Acrocanthosaurus atokensis* and its implications for the phylogeny of Allosauroidea (Dinosauria: Theropoda). PLoS One 6:e17932.

Escaso F, Ortega F, Dantas P, Malafaia E, Pimentel NL, Pereda-Suberbiola X, Sanz JL, Kullberg JC, Kullberg MC, Barriga F. 2007. New evidence of shared dinosaur across Upper Jurassic proto-North Atlantic: *Stegosaurus* from Portugal. Naturwissenschaften 94:367–374.

Escaso F, Silva B, Ortega F, Malafaia E, Sanz JL. 2010. A Portuguese specimen of *Camptosaurus aphanoecetes* (Ornithopoda: Camptosauridae) increases the dinosaurian similarity among the Upper Jurassic Alcobaça and Morrison Formation. Abstracts of the 70th Annual Meeting of the Society of Vertebrate Paleontology, Pittsburgh, USA. 86A pp.

Evers S. 2014. The postcranial osteology of a large specimen of *Allosaurus* "*jimmadseni*" (Dinosauria: Theropoda) from the Late Jurassic of Wyoming, U.S.A. [MsD dissertation]. Munich: Ludwig-Maximilians-University.

Ezcurra M. 2007. The cranial anatomy of the coelophysoid theropod *Zupaysaurus rougieri* from the Upper Triassic of Argentina. Historical Biology 19(2):185–202.

Foster JR, Chure DJ. 1998. Paterns of theropod diversity and distribution in the Late Jurassic Morrison Formation, western USA. Abstracts and Program of the Fifth International Symposium on the Jurassic System, International Union of Geological Sciences, Subcommission on Jurassic Stratigraphy. Vancouver, British Columbia, Canada:30–31.

Gao Y. 1992. *Yangchuanosaurus hepingensis* - a new species of carnosaur from Zigong, Sichuan. Vertebrata Palasiatica 30(4):313–324.

Gao Y. 1993. A new species of *Szechuanosaurus* from the Middle Jurassic of Dashanpu, Zigong, Sichuan. Vertebrata PalAsiatica 31(4):308–314.

Gauthier J. 1986. Saurischian monophyly and the origin of birds. In: Padian K, editor. The origin of birds and the evolution of flight. San Francisco (CA): California Academy of Science:1–55.

Gilmore CW. 1920. Osteology of the carnivorous Dinosauria in the United States National Museum, with special reference to the genera *Antrodemus* (*Allosaurus*) and *Ceratosaurus*. Bulletin of the United States National Museum 110:1–159.

Glut DF. 1997. Dinosaurs: The Encyclopedia. McFarland and Co., Inc.: xi + 1076 pp.

Goloboff PA, Farris JS, Nixon KC. 2008. TNT 1.1, a free program for phylogenetic analysis. Cladistics. 24:774–786.

Harris JD. 1998. A reanalysis of *Acrocanthosaurus atokensis*, its phylogenetic status, and paleobiogeographic implications, based on a new specimen from Texas. New Mexico Museum of Natural History and Science Bulletin 13:1–75.

Hendrickx C, Mateus O. 2014a. *Torvosaurus gurneyi* n. sp., the largest terrestrial predator from Europe, and a proposed terminology of the maxilla anatomy in nonavian theropods. PLoS One. 9:e88905.

Hendrickx C, Mateus O. 2014b. The nonavian theropod quadrate I: standardized terminology and 1 overview of the anatomy, function and ontogeny. PeerJ PrePrints 2:e379v1. doi:10.7287/peerj.preprints.379v1.

Hendrickx C, Mateus O, Araújo R. 2016. A proposed terminology of theropod Teeth (Dinosauria, Saurischia). Journal of Vertebrate Paleontology. 35(5):e982797. doi:10.1080/02724634.2015.982797

Hocknull SA, White MA, Tischler TR, Cook AG, Calleja ND, Sloan T, Elliot DA. 2009. New Mid-Cretaceous (Latest Albian) Dinosaurs from Winton, Queensland, Australia. PLoS ONE 4(7): e6190. doi:10.1371/journal.pone.0006190

Holtz TR. 1998. A new phylogeny of the carnivorous dinosaurs. Gaia 15:1–61.

Holtz TR, Molnar RE, Currie PJ. 2004. Basal Tetanurae. In: Weishampel, D.B., Dodson, P. & Osmólska, H. (Eds.), The Dinosauria, 2nd edn. University of California Press, Berkeley:71–110.

Hu S-Y. 1964. Carnosaurian remains from Alashan, Inner Mongolia. Vertebrata PalAsiatica. 8:42–63.

Huene F. 1923.Carnivorous Saurischia in Europe since the Triassic. Bulletin of the Geological Society of America. 34:449–458.

Huene F. 1926. The carnivorous Saurischia in the Jura and Cretaceous formations, principally in Europe. Revista del Museo de la Plata Tome XXIX (Tercera Serie, Tomo V): 167 pp.

Hunt AP, Lucas SG, Krainer K, Spielman J. 2006. The taphonomy of the Cleveland-Lloyd dinosaur quarry, Upper Jurassic Morrison Formation, Utah, a re-evaluation. Bulletin, New Mexico Museum of Natural History and Science 38:57–65.

Hurum JH, Sabath K. 2003. Giant theropod dinosaurs from Asia and North America: Skulls of *Tarbosaurus bataar* and *Tyrannosaurus rex* compared. Acta Palaeontologica Polonica 48(2):161–190.

Hutchinson JR. 2001. The evolution of femoral osteology and soft tissues on the line to extant birds (Neornithes). Zoological Journal of the Linnean Society 131:169–197.

Hutt S, Martill DM, Barker MJ. 1996. The first European allosauroid dinosaur (Lower Cretaceous, Wealden Group, England). Neues Jahrbuch für Geologie und Paläontologie Monatshefte 1996(10):635–644.

Janensch W. 1925. Die Coelurosaurier und Theropoden der Tendaguru-Schichten Deutsch-Ostafrikas. Palaeontographica (Suppl. 7) 1:1–99 + 10 plates.

Kullberg JC, Rocha RB, Soares AF, Rey J, Terrinha P, Azerêdo AC, Callapez P, Duarte LV, Kullberg MC, Martins L, Miranda R, Alves C, Mata J, Madeira J, Mateus O, Moreira M, Nogueira CR. 2013. A Bacia Lusitaniana: Estratigrafia, Paleogeografia e Tectónica. In: Dias R, Araújo A, Terrinha P, Kullberg JC. (Eds) Geologia de Portugal, Volume II – Geologia Meso-cenozóica de Portugal:195–347.

Lapparent AF, Zbyszewski G. 1957. Les dinosauriens du Portugal [The dinosaurs of Portugal]. Memórias Serviços Geológicos de Portugal. 2:1–63.

Leidy J. 1870. Remarks on *Poicilopleuron valens*, *Clidastes intermedius*, *Leiodon proriger*, *Baptemys wyomingensis*, and *Emys stevensonianus*. Proceedings of the Academy of Natural Sciences, Philadelphis 1870:3–5.

Madsen JH 1976. *Allosaurus fragilis*: a revised osteology. Utah Geological and Mineral Survey Bulletin 109:163pp.

Madsen JH, Welles SP. 2000. *Ceratosaurus* (Dinosauria, Theropoda) a revised osteology. Utah Geological Survey, Miscellaneous Publication 2:1–80.

Malafaia E, Ortega F, Escaso F, Silva B. 2015. New evidence of *Ceratosaurus* (Dinosauria: Theropoda) from the Late Jurassic of the Lusitanian Basin, Portugal. Historical Biology 27:938–946.

Malafaia E, Ortega F, Escaso F, Dantas P, Pimentel N, Gasulla JM, Ribeiro B, Barriga F, Sanz JL. 2010. Vertebrate fauna at the *Allosaurus* fossil-site of Andrés (Upper Jurassic), Pombal, Portugal. Journal of Ibererian Geology 36:193–204.

Manuppella G, Barbosa B, Machado S, Carvalho J, Bartolomeu A, Azerêdo AC, Ramalho M, Crosaz R, Baptista R, Porteiro A, Dâmaso B, Cunha TA. 1998. Carta Geológica de Portugal, folha 27-A (Vila Nova de Ourém). Escala 1:50000 (2ª Eds). Instituto Geológico e Mineiro, Lisboa.

Manuppella G, Antunes MT, Costa Almeida CA, Azerêdo AC, Barbosa B, Cardoso JL, Crispim JA, Duarte LV, Henriques MH, Martins LT, Ramalho MM, Santos VF, Terrinha P. 2000. Notícia Explicativa da Carta Geológica de Portugal, folha 27-A (Vila Nova de Ourém). Departamento de Geologia do Instituto Geológico e Minerio, Lisboa.

Marques B, Olóriz F, Caetano PS, Rocha R, Kullberg JC. 1992. Upper Jurassic of Alcobaça Region. Stratigraphic Contributions. Comunicações dos Serviços Geológicos de Portugal 78(1):63–69.

Marsh OC. 1877. Notice of new dinosaurian reptiles from the Jurassic Formation. American Journal of Science (series 3) 14:514–516.

Mateus O. 1998. *Lourinhanosaurus antunesi*, a new upper Jurassic allosauroid (Dinosauria: Theropoda) from Lourinhã, Portugal. Memórias da Academia de Ciências de Lisboa. 37:111–124.

Mateus O, Antunes MT. 2000a. *Ceratosaurus* sp. (Dinosauria: Theropoda) in the Late Jurassic of Portugal. Proceedings of the 31st International Geological Congress, Rio de Janeiro, Brazil.

Mateus O, Antunes MT. 2000b. *Torvosaurus* sp (Dinosauria: Theropoda) in the Late Jurassic of Portugal. I Congresso Ibérico de Paleontología/XVI Jornadas de la Sociedad Española de Paleontología; Évora, Portugal.

Mateus O, Walen A, Antunes MT. 2006. The large theropod fauna of the Lourinhã Formation (Portugal) and its similarity to the Morrison Formation, with a description of a new species of *Allosaurus*. In: Foster JR, Lucas SG. (Eds). Paleontology and geology of the Upper Jurassic Morrison Formation. Vol. 36. New Mexico Museum of Natural History and Science, Bulletin:123–129.

Mo J, Zhou F, Li G, Huang Z, Cao C. 2014. A new Carcharodontosauria (Theropoda) from the Early Cretaceous of Guangxi, Southern China. Acta Geologica Sinica. 88(4):1051–1059.

Mocho P, Royo-Torres R, Ortega F. 2014. Phylogenetic reassessment of *Lourinhasaurus alenquerensis*, a basal Macronaria (Sauropoda) from the Upper Jurassic of Portugal. Zoological Journal of the Linnean Society, 170:875–916.

Molnar RE. 1990. Problematic Theropoda: "carnosaurs". In: Weishampel DB, Dodson P, Osmolska H. (Eds). The Dinosauria. University of California Press:306–317.

Norell MA, Clark JM, Turner AH, Makovicky PJ, Barsbold R, Rowe T. 2006. A new dromaeosaurid theropod from Ukhaa Tolgod (Ömnögov, Mongolia). American Museum Novitates. 3545:1–51.

Novas FE. 1998. *Megaraptor namunhuaiquii*, gen. et sp. nov., a large-clawed, Late Cretaceous theropod from Patagonia. Journal of Vertebrate Paleontology. 18:4–9.

Novas FE, Ezcurra M, Lecuona A. 2008. *Orkoraptor burkei* nov. gen. et sp., a large theropod from the Maastrichtian Pari Aike Formation, Southern Patagonia, Argentina. Cretaceous Research 29(3):468–480.

Novas FE, de Valais S, Vickers-Rich P, Rich T. 2005. A large Cretaceous theropod from Patagonia, Argentina, and the evolution of carcharodontosaurids. Naturwissenschaften 92:226–230.

Novas FE, Agnolín FL, Ezcurra MD, Porfiri J, Canale JI. 2013. Evolution of the carnivorous dinosaurs during the Cretaceous: The evidence from Patagonia. Cretaceous Research 45:174–215.

Ortega F, Dantas P, Escaso F, Gasulla JM, Malafaia E, Ribeiro B. 2006. Primera cita de reptiles esfenodontos en el Jurásico Superior de la Península Ibérica. In: Fernández-Martínez E. (Eds). XXII Jornadas de la Sociedad Española de Paleontología:152–153.

Ortega F, Escaso F, Sanz JL. 2010. A bizarre, humped Carcharodontosauria (Theropoda) from the Lower Cretaceous of Spain. Nature 467:203–206.

Osborn H.F. 1903. The skull of *Creosaurus*. Bulletin of the American Museum of Natural History XIX (art. XXXI):697–701.

Osborn HF. 1912. Crania of *Tyrannosaurus* and *Allosaurus*. Memoirs of the American Museum of Natural History (New Series) I (part I):1–30.

Padian K, Hutchinson JR, Holtz TR Jr. 1999. Phylogenetic definitions and nomenclature of the major taxonomic categories of the carnivorous Dinosauria (Theropoda). Journal of Vertebrate Paleontology 19(1):69–80.

Paul GS. 1988. Predatory Dinosaurs of the World. Simon and Schuster, N.Y:464 pp.

Paul GS, Carpenter K. 2010. *Allosaurus* Marsh, 1877 (Dinosauria, Theropoda): proposed conservation of usage by designation of a neotype for its type species *Allosaurus fragilis* Marsh, 1877. Bulletin of Zoological Nomenclature. 67(1):53–56.

Paulina Carabajal A, Currie PJ. 2012. New information on the braincase of *Sinraptor dongi* (Theropoda: Allosauroidea): ethmoidal region, endocranial anatomy, and pneumaticity. Vertebrata PalAsiatica 50(2):85–101.

Pérez-Moreno BP, Chure DJ, Pires C, Silva CM, Santos V, Dantas P, Póvoas L, Cachão M, Sanz JL, Galopim de Carvalho AM. 1999. On the presence of *Allosaurus fragilis* (Theropoda: Carnosauria) in the Upper Jurassic of Portugal: first evidence of an intercontinental dinosaur species. Journal of the Geological Society 156:449–452.

Pimentel NL. 2009. Contextualização paleogeográfica das jazidas de vertebrados do Jurássico Superior da Bacia Lusitânica. In: Pérez García A, Silva BC, Malafaia E, Escaso F. Paleolusitana 1. Associação Leonel Trindade-Sociedade de História Natural, Torres Vedras:465–470.

Rauhut OWM. 1995. The Systematic Position of the African Theropods *Carcharodontosaurus* Stromer 1931 and *Bahariasaurus* Stromer 1934. Berliner Geowissenschaftliche Abhandlungen, E, 16.1:357–375.

Rauhut OWM. 2003. The interrelationships and evolution of basal theropod dinosaurs. Special Papers in Palaeontology 69:1–213.

Rauhut OWM. 2004. Braincase structure of the Middle Jurassic theropod dinosaur *Piatnitzysaurus*. Canadian Journal of Earth Sciences 41(9):1109–1122.

Rauhut OWM. 2007. A fragmentary theropod skull from the Middle Jurassic of Patagonia. Ameghiniana Revista de la Asociación Paleontológica Argentina 44 (2):479–483.

Rauhut OWM. 2011. Theropod dinosaurs from the Late Jurassic of Tendaguru (Tanzania). Special Papers in Palaeontology 86:195–239.

Rauhut OWM, Fechner R. 2005. Early development of the facial region in a non-avian theropod dinosaur. Proceedings of the Royal Society of London Series B, Biological Sciences 272:1179–1183.

Rauhut OWM, Hübner TR, Lanser K-P. 2016. A new megalosaurid theropod dinosaur from the late Middle Jurassic (Callovian) of north-western Germany: Implications for theropod evolution and faunal turnover in the Jurassic. Palaeontologia Electronica 19.2.26A:1–65.

Riabinin AN. 1915. A note on a dinosaur from the Trans-Baikal region. Traveaux du Museé Géologique de l'Académie des Sciences, Petrograd VIII (livr.5) 1914: 133–140.

Rogers SW. 1998. Exploring dinosaur neuropaleobiology: computed tomography scanning and analysis of an *Allosaurus fragilis* endocast. Neuron 21:673–679.

Sadlier RW, Barrett PM, Powell HP. 2008. The anatomy and systematics of *Eustreptospondylus oxoniensis*, a theropod dinosaur from the Middle Jurassic of Oxfordshire, England. Monograph of the Palaeontographical Society 627:1–82.

Sampson SD, Witmer LM. 2007. Craniofacial anatomy of *Majungasaurus crenatissimus* (Theropoda: Abelisauridae) from the Late Cretaceous of Madagascar. Journal of Vertebrate Paleontology Memoir 8:32–102.

Sauvage HE. 1882. Recherches sur les reptiles trouvés dans le Gault de l'est du bassin de Paris. Mémoires de la Société géologique de France, series 3, 2(4):1–42.

Sereno PC. 2005. Stem Archosauria – TaxonSearch. Available online at: http://www.taxonsearch.org/dev/file_home.php [version 1.0, 7 November 2005].

Sereno PC, Brusatte SL. 2008. Basal abelisaurid and carcharodontosaurid theropods from the Elrhaz Formation (Aptian-Albian) of Niger. Acta Palaeontologica Polonica 53:15–46.

Sereno PC, Wilson JA, Larsson HC, Dutheil DB, Sues H-D. 1994. Early Cretaceous dinosaurs from the Sahara. Science 266:267–272.

Sereno PC, Dutheil DB, Iarochene M, Larsson HCE, Lyon GH, Magwene PM, Sidor CA, Varricchio DJ, Wilson JA. 1996. Predatory dinosaurs from the Sahara and Late Cretaceous faunal differentiation. Science 272:986–991.

Sereno PC. 1998. A rationale for phylogenetic definitions, with application to the higher level taxonomy of Dinosauria. Neues Jahrbuch für Geologie und Paläontologie Abhandlungen 210:41–83.

Sereno PC, Beck AI, Dutheil DB, Gado B, Larsson HCE, Lyon GH, Marcot JD, Rauhut OWM, Sadleir RW, Sidor CA, Varicchio DD, Wilson GP, Wilson JA. 1998. A longsnouted predatory dinosaur from Africa and the evolution of spinosauroids. Science 282:1298–1302.

Sereno PC, Martinez RN, Wilson JA, Varricchio DJ, Alcober OA, Larsson HCE. 2008. Evidence for Avian Intrathoracic Air Sacs in a New Predatory Dinosaur from Argentina. PLoS ONE 3(9): e3303. doi:10.1371/journal.pone.0003303.

Schneider S, Fürsich FT, Werner W. 2009. Sr-isotope of the Upper Jurassic of central Portugal (Lusitanian Basin) based on oyster shells. International Journal of Earth Sciences, Geologisch Rundschau 98:1949–1970.

Smith DK. 1998. Morphometric analysis of *Allosaurus*. Journal of Vertebrate Paleontology 18(1):126–142.

Smith ND, Makovicky PJ, Hammer WR, Currie PJ. 2007. Osteology of *Cryolophosaurus ellioti* (Dinosauria: Theropoda) from the Early Jurassic of Antarctica and implications for early theropod evolution. Zoological Journal of the Linnean Society 151:377–421.

Steel R. 1970. Saurischia in: Handbuch der Paleoherpetelogy. Teil 14. Gustav Ficher Verlag:87pp.

Stoval JW, Langston W. 1950. *Acrocanthosaurus atokensis*, a new genus and species of Lower Cretaceous Theropoda from Oklahoma. American Midland Naturalist 43(3):696–728.

Sues H-D, Frey E, Martill DM, Scott DM. 2002. *Irritator challengeri*, a spinosaurid (Dinosauria: Theropoda) from the Lower Cretaceous of Brazil. Journal of Vertebrate Paleontology 22(3):535–547.

Sues H-D, Nesbitt SJ, Berman DS, Henrici AC. 2011. A late-surviving basal theropod dinosaur from the latest Triassic of North America. Proceedings of the Royal Society B 278:3459–3464.

Taquet P, Welles SP. 1977. Redescription du Crâne de dinosaur théropode de Dives (Normandie). Annales de Paléontologie (Vertébrés) T. 63 F. 2:191–206.

Tykoski RS. 1998. The osteology of *Syntarsus kayentakatae* and its implications for ceratosaurid phylogeny. [M.S. thesis] The University of Texas at Austin, Texas.

Tykoski RS, Rowe T. 2004. Ceratosauria. In: D.B. Weishampel, P. Dodson, H. Osmolska (Eds.), The Dinosauria. 2nd edition. University of California Press, Berkeley:47–70.

Welles SP. 1984. *Dilophosaurus wetherilli* (Dinosauria, Theropoda) osteology and comparisons. Palaeontographical Abteilung A Palaeozoologie-Stratigraphie 185: 85–180.

Witmer LM. 1990. The craniofacial air sac system of Mesozoic birds (Aves). Zoological Journal of the Linnean Society. 100:327–378.

Witmer LM. 1997. The evolution of the antorbital cavity of archosaurs: a study in soft-tissue reconstruction in the fossil record with analysis of the function of pneumaticity. Society of Vertebrate Paleontology Memoir 3:1–73.

Witmer L.M., Ridgely, R.C. 2009. New Insights into the brain, braincase, and ear region of tyrannosaurs (Dinosauria, Theropoda), with implications for sensory organization and behavior. The Anatomical Record 292:1266–1296.

Wu X-C, Currie PJ, Dong Z, Pan S, Wang T. 2009. A new theropod dinosaur from the Middle Jurassic of Lufeng, Yunnan, China. Acta Geologica Sinica 83(1):9–24.

Xing L, Paulina-Carabajal A, Currie PJ, Xu X, Zhang J, Wang T, Burns ME, Dong Z. 2014. Braincase anatomy of the basal theropod *Sinosaurus* from the Early Jurassic of China. Acta Geologica Sinica 8(6):1653–1664.

Young CC. 1942. Fossil vertebrates from Kuangyuan, N. Szechuan, China. Bulletin of the Geological Society of China XXII(3–4):293–309.

Zanno LE, Makovicky PJ. 2013. Neovenatorid theropods are apex predators in the Late Cretaceous of North America. Nature Communications 4:2827. doi: 10.1038/ncomms3827.

Zhao X-J, Benson RBJ, Brusatte SL, Currie PJ. 2010. The postcranial skeleton of *Monolophosaurus jiangi* (Dinosauria: Theropoda) from the Middle Jurassic of Xinjiang, China, and a review of Middle Jurassic Chinese theropods. Geological Magazine 147:13–27.33

	Premaxilla	Maxilla	Nasal	Lacrimal	Jugal	Postorbital	Quadrate	Quadratojugal	Squamosal	Parietal	Frontal	Prefrontal	Braincase	Palatine	Vomer	Pterygoid	Ectopterygoid	Epipterygoid	Articular	Antarticular	Stapes	Dentary	Splenial	Coronoid	Surangular	Angular	Prearticular	Supradentary
MNHNUL.P.AND	–	X	X	X	–	X	X	X	X	X	X	X	X	X	X	–	–	–	X	–	–	–	–	X	X	X	X	X
Allosaurus fragilis	X	X	X	X	X	X	X	X	X	X	X	X	X	X	X	X	X	X	X	X	X	X	X	X	X	X	X	X
Allosaurus "jimmadseni"	X	X	X	X	X	X	X	X	X	X	X	X	X	X	–	X	X	X	X	X	X	X	X	X	X	X	X	X
Allosaurus europaeus	–	X	X	X	X	X	X	X	X	–	–	–	X	–	?	X	X	?	–	–	–	–	–	–	X	–	–	–
Sinraptor dongi	X	X	X	X	X	X	X	X	X	X	X	X	X	X	X	X	X	X	X	?	?	X	X	?	X	X	X	X
Yangchuanosaurus shangyouensis	X	X	X	X	X	X	X	X	X	X	X	X	X	?	?	X	X	?	X	?		X	X	?	X	X	X	?
"Yangchuanosaurus" hepingensis	X	X	X	X	X	X	X	X	X	X	X	X	X	X	X	X	X	?	X	X	?	X	X	X	X	X	X	?
Neovenator salerii	X	X	X	–	–	–	–	–	–	–	–	–	–	X	–	–	–	–	–	?	?	X	–	?	–	–	–	–
Eocarcharia dinops	–	X	–	–	–	X	–	–	–	–	X	X	–	–	–	–	–	–	–	–	–	–	–	–	–	–	–	–
Tyrannotitan chubutensis	–	–	–	–	X	–	–	–	–	–	–	–	–	–	–	–	–	–	–	?	?	X	–	?	–	–	–	–
Shaochilong maortuensis	–	X	X	–	–	–	X	–	–	X	X	–	X	–	–	–	–	–	–	?	?	–	–	–	–	–	–	–
Acrocanthosaurus atokensis	X	X	X	X	X	X	X	X	X	X	X	X	X	X	X	X	X	X	X	?	?	X	X	?	X	X	X	X
Carcharodontosaurus saharicus	–	X	X	X	X	X	–	–	–	–	X	X	X	–	–	–	X	–	–	?	?	X	–	?	–	–	X	–
Carcharodontosaurus iguidensis	–	X	–	X	–	–	–	–	–	X	X	–	X	–	–	–	–	–	–	–	–	X	–	–	–	–	–	–
Mapusaurus roseae	–	X	X	X	X	X	X	–	–	–	–	X	–	–	–	–	–	–	X	?	?	X	X	?	X	–	X	–
Giganotosaurus carolinii	X	X	X	X	–	X	X	–	–	X	X	X	X	–	–	X	X	–	–	?	?	X	–	?	–	–	–	–
Concavenator corcovatus	X	X	X	X	X	X	X	–	–	?	X	?	?	?	?	?	?	?	?	?	?	X	?	?	X	?	?	?
Aerosteon riocolonadensis	–	–	–	–	–	X	X	–	–	–	–	X	–	–	–	X	–	–	–	?	?	–	–	?	–	–	X	–
Australovenator wintonensis	–	–	–	–	–	–	–	–	–	–	–	–	–	–	–	–	–	–	–	–	–	X	–	–	–	–	–	–
Erectopus superbus	–	X	–	–	–	–	–	–	–	–	–	–	–	–	–	–	–	–	–	–	–	–	–	–	–	–	–	–
Saurophaganax maximus	–	–	–	–	–	X	X	–	–	–	–	–	–	–	–	–	–	–	–	–	–	–	–	–	–	–	–	–
Shidaisaurus jinae	–	–	–	–	–	–	–	–	–	X	X	–	X	–	–	–	–	–	–	–	–	–	–	–	–	–	–	–
Fukuiraptor kitadaniensis	–	X	–	–	–	–	–	–	–	–	–	–	–	–	–	–	–	–	–	–	–	X	–	–	–	–	–	–
Kelmayisaurus petrolicus	–	X	–	–	–	–	–	–	–	–	–	–	–	–	–	–	–	–	–	–	–	X	–	–	–	–	–	–
Piveteausaurus divesensis	–	–	–	–	–	–	–	–	–	X	X	–	X	–	–	–	–	–	–	–	–	–	–	–	–	–	–	–
Monolophosaurus jiangi	X	X	X	X	X	X	X	X	X	X	X	X	X	X	?	?	?	?	X	?	?	X	X	?	X	X	X	X

Table 6.3.1. Cranial elements known for 24 allosauroid taxa.

Element			Measurements (mm)		
	Right	Left		Right	Left
Nasal, L	394*		Quadrate, D		183
Nasal, W	47,85		Quadrate, L across the distal condyles		67,73
Nasal, D	59,5		Quadrate, W		25,92
Nasal, D of the naris opening	41,57		Quadrate, L of the pterygoid wing		56,72*
Nasal, L of the naris opening	117,37		Quadratojugal, D		122,06
Maxila, L		394	Quadratojugal, L		103,77*
Maxila, D at the level of the 6th alveolus		72,46	Vomer, L	280	
Maxila, ratio D : L x 100		18,39	Coronoid and supradentary, L		344
Lacrimal, D	236	223	Articular, L	84,75	
Lacrimal, L	270	172*	Articular, D	46,99	
Lacrimal, W of the cornual process	29,28	32,3	Articular, W	35,14	
Lacrimal, L of the anterior ramus	121,27	107,07*	Surangular, L	404	390*
Lacrimal, D of the ventral ramus	130,37	129,4	Surangular, D	83,34	67,63
Prefrontal, D		130,92	Prearticular, L		375
Prefrontal, L		100,16	Prearticular, D		79,32
Postorbital, D		150,42*	Angular, L	322*	383
Postorbital, L		124,13	Angular, D	56,97	53,42
Frontal, L	65,74*		Braincase, L of the frontals	136,18*	
Frontal, W	41,37		Braincase, W dorsally across the frontals	130,15	
Frontal, D	15,1		Braincase, W of occiput across the parietals	155,5	
Palatine, L	143,16	165,7*	Braincase, D of the parientals in occipital view	91,15	
Palatine, W	65,3	58,56	Braincase, W of the basal tubera	68,04	
Squamosal, D	128,02		Braincase, W of the occipital condyle	48,32	
Squamosal, W	74,85		Braincase, D of the occipital condyle	40,05	

Abbreviations: D, maximum depth; L, maximum length; W, maximum width; * measurement estimated from broken element.

Table 6.3.2. Measurements of the cranial elements of *Allosaurus* collected in Andrés. All measurements are in millimeters.

Specimens	CBL	CBW	CH	AL	CBR	CHR	CDA	CMA	MC	DC	DSDI
MNHNUL.P.AND23	12,70	11,86	30,64	30,92	0,93	2,41	79,43	76,86	11,25	12,5	0,90
MNHNUL.P.AND27	7,21	7,38	?	?	1,02	?	?	?	12,5	12,5	1,00
MNHNUL.P.AND30	11,00	12,13	25,16	25,42	1,10	2,29	78,88	76,12	10	11	0,91
MNHNUL.P.AND31	10,25	10,19	21,00	24,80	0,99	2,05	97,80	56,70	?	12,5	?
MNHNUL.P.AND24	13,28	8,29	22,00	22,71	0,62	1,66	76,13	69,82	10,5	10,5	1,00
MNHNUL.P.AND25	13,68	6,62	26,46	28,25	0,48	1,93	83,37	68,36	15	14	1,07
MNHNUL.P.AND26	?	?	?	?	?	?	?	?	20	13,5	1,48
MNHNUL.P.AND28	10,31	6,36	20,04	21,63	0,62	1,94	84,85	67,24	?	?	?
MNHNUL.P.AND29	12,16	6,49	22,66	26,59	0,53	1,86	94,05	58,13	15	11,25	1,33

Abbreviations: CBL, crown base length; CBW, crown base width; CH, crown height; AL, apical length; CBR,crown base ratio; CHR, crown height ratio; CDA, crown distal angle; CMA, crown mesial angle; MC, mesiocentral denticle density; DC, distocentral denticle density; DSDI, denticle size density index.

Table 6.3.3. Measurements of the isolated teeth collected in Andrés. All measurements are in millimeters.

Vertebrae	AND41	AND42	AND40	AND39	AND36	AND38	AND35	AND33	AND65
Centrum, L	88,57	92,05	88,75	86,85	75,64	105,44	88,66	82,85	47,59
Centrum, D	23,33	26,81	36,89	50,8	60,95	79,78	15,79	15,71	59,6
Centrum, W	30,83	33,48	35,53	27,46	39,96	46,25	27,52	26,58	47,81
Centrum, L:W	2,87	2,75	2,50	3,16	1,89	2,28	3,22	3,12	1,00
Centrum, L:D	3,80	3,43	2,41	1,71	1,24	1,32	5,61	5,27	0,80
Anterior articular facet, W	45,53	47,46	50,7	55,16	?	102,97	31,07	28,52	80,69
Anterior articular facet, D	34,73	35,09	45,82	?	?	112,5	25,09	23,02	71,43
Anterior articular facet, D:W	0,76	0,74	0,90	?	?	1,09	0,81	0,81	0,89
Posterior articular facet, W	43,97	45,44	49,44	56,74	88,88	74,17	30,36	28,74	86,92
Posterior articular facet, D	35,17	38,06	45,83	61,3	92,46	96,57	25,53	24,69	74,12
Posterior articular facet, D:W	0,80	0,84	0,93	1,08	1,04	1,30	0,84	0,86	0,85

Abbreviations: D, maximum depth; L, maximum length; W, maximum width.

Table 6.3.4. Measurements of the vertebrae attributed to *Allosaurus* collected in Andrés. All measurements are in millimeters

Ilium	AND63	Pubes	AND61
Ilium, L	570	Shaft, L	469,8
Iliac blade, D above the acetabulum	173	Shaft, minimum diameter	45,22
Preacetabular process, L	165	Proximal end, L	207,15
Postacetabular process, L	205	Boot, L	305,68
Iliac L:D	3,29	Ratio shaft L: boot L	1,53
Pubic peduncle, L	149,45	**Ischium**	**AND62**
Pubic peduncle, W	70,34	Shaft, L	330
Pubic peduncle, D	125,43	Saft, diameter	31,53
Pubic peduncle, L:D	1,19	Proximal end, L	223
Pubic peduncle, L:W	2,12	Acetabulum, L	77,21
Ischial peduncle, L	39,06		
Ischial peduncle, W	57		
Ischial peduncle, D	74,55		
Pubic peduncle L:ischial peduncle D	0,52		

Abbreviations: D, maximum depth; L, maximum length; W, maximum width

Table 6.3.5. Measurements of pelvic elements attributed to *Allosaurus* collected in Andrés. All measurements are in millimeters.

Femur, Tibia and Fibula	AND66	AND68	AND70
Diaphysis, L	710	640	511,53
Diaphysis, maximum diameter	78,54	69,3	28,32
Diaphysis, minimum diameter	55,32	57,08	18,9
Diaphysis, ratio minimum diameter : L	0,08	0,09	0,04
Proximal end, L	67,5*	?	115,32
Proximal end, W	80,91	?	31,53
Distal end, L	153,93	106,3	?
Distal end, W	106,14	44,65	?

Abbreviations: D, maximum depth; L, maximum length; W, maximum width; * measurement estimated from broken element

Table 6.3.6. Measurements of hindlimb elements attributed to *Allosaurus* collected in Andrés. All measurements are in millimeters.

	Mt II	Mt III	Mt IV
Length	280,5	304	208
Proximal end, W	40,58	43,91	42,57
Proximal end, D	80,13	106,77	?
Distal end, W	55,22	59,1	65,56
Distal end, L	56,11	66,55	47,62
Shaft, maximum diameter	42,26	40,63	42,06

Abbreviations: D, maximum depth; L, maximum length; W, maximum width

Table 6.3.7. Measurements of the metatarsals attributed to *Allosaurus* collected in Andrés. All measurements are in millimeters.

APPENDIX 6.3.1

Data matrix

#NEXUS

begin data;

dimensions ntax=28 nchar=177;

format missing=? symbols="0~3";

matrix

Herrerasaurus 000000000001???0000?000010000000???00000?0?0?00?00000000?00??00001000000000
00??????0000000000?00?0?0000000?0000000000010?000000000000?0010100?00001?000000100
0000010000000000000

Allosaurus_fragilis 10000021021001110000012010111000000000?10000001001000000100101000
0111110000000000011101000010111101101111010012000001111?0000110001110010011001110
000311111101011111100000111011

"A. jimmadseni" 10000021021???110000012?101110?00000000?1?000??200100000?1??10100?001111
1000000000??111010000001?110110101101001200000111101000110001110?10?1100?01?000311
1110010???1110000?11011

A._europaeus ??????????????????0?12?1?1????00000????0?0?0?????????0?1??????0?????????????????
1????????1?????????1010?1201??

MNHNUL ?????021???001110010?12?10101000?????00??000000100?00?000?0?101000?00?111???????
???0111????????111110110????????????000111???0001?0???1???????1??????000311111101O?11111000
0111111

Concavenator ?????1????????0?0?10?12?1?0011????1??1??1?1?????????????1?????????????????????
??????????????01?????????????011???0??00?11??110????0?1??????0?1???1?????0???????????????

Fukuiraptor ??0?0??
0?1???????0????????????0??0??1???0?????????????????????????0?????101??11?1???????????

Australovenator ??1
010?00?????????????????????????????????????00??????10011?????????10100????1010??1????

Monolophosaurus 100021?10?1?????0??101201010000?1?01?00?000000?10010011?010?101010??000
0100?????????1110?0000111?110??00?110?00120?01001?1???00?????????????0????????001000?0?????
???1???????????

Piatnitzkysaurus ??????????????1?????????????????????????????????1??00?0????????0010??00?0100????????
??????????????????100??0?0??10?1??0?1110?0?1??????????1????0??????011?101?1????1001???????11??

Siamotyrannus ??
????????????????????????????????????011??11?????????????0??301110?????????????????

Sinraptor 00001010121?000000000121101111001001100?0000?011001000100100111110000011100
0110000?11100?0100010?100110111101001200O1?1111100011??0???10?10100?0??0?000?0111010
001111000000101011

Yangchuanosaurus ?0?01?101?1?????0??1?12?1011100???0?????0?0?????????????????????????????????
????1?10????0?2?0??0???0?0??0???1??

Acrocanthosaurus 0101101011111111111101021011111111111111111?10110111101101111010000011011000111111111101112010011?1201?0100?111102101110112??110111001101111011011111??1?11?11101011111111101????0

Carcharodontosaurus ?????1?111?111?111111020011111?111111111111??11111111?1????1110101110001??11?????1?????1?1??1????????11????01110211??????????1?1???????1?????????????????1?1?12110??1?????1???????

Eocarcharia ?????1101??1111100?????????????????????110111?????01111???0???

Giganotosaurus 0??1??21????1??111?1102?0211?111?????1??1?10?11111111011010111?1111100?1??11??1111?????1?1?01??????0?1110101100?21?10101?20??1211100?00111111?????00031111121110 1?111101011????

Mapusaurus ????????0??110?111?110??02??110?1111?111?1???10????????1??1?????????????????????????1?12??0???????11?????????????1?1???2??112??1????????101??1??????0?1???1?1110???1?11???1????

Neovenator 1001?00101?011?100?0102000???1??0?0000??????0?00?10?1?00020?10011?2??0?2110?01??0?1?0?1???????0130??101110??11?10100?1??1

Shaochilong ?????02?0???1??101?1?????????????????????????????1011110?00?0?01010??101011?????????????????????????11???0??1?????????????????????????????

Tyrannotitan ?????????????????????????????????11111???1?0?01?????????0???011??1??110101?2??00??????0??????0?1??????0?0??1?1?2?1???11????1???????

Coelophysoidea 01102000000???000?0001000?000000??00?00?100?00?00000000?0001000000000000100????0???0001000?10000?0?10?00000?000000?000020?0000?00100000??0000000000000??010000000001?0000000000000

Compsognathidae 0?0020?002????000??0000?0?0?????????0?00?1?0??0?000?000???2??1?0???????0011????????????0?0?0??01????1?01??1?1??100?00000??0?00??00?10??0000000?0??1?0?0?01?10??01??????0001?1????

Dilong 10201?200?1???1?0?000111100110?0??01?00?0?0000?10?00000?10???000?0???0??21???????????101?00???1???21?0???1?0???20?????0??????????1??????01?????10??100??021?10?????????????????

Tyrannosaurus 00201001011010 2?100010000?011001001111 0?001?10?3011010011001100010001100 0?1000000?00100101000100 1?0021?01?0110000100?0?011???0??00011001??00???0?00?01?0??021?1????1?1?????12?2100

SHN.036 ??10?????????0?0110???0000?0????0?????????????00031?111?????????????????????

Lourinhanosaurus ??101??100?0???1??01?00111??110?????????????00?2010??1000?10?0100?01?????

Cryolophosaurus ?????????????????????0112?0?1011????00?0??1??0?0?1000?000?1???00000???0??1??????????0??????????0?11????????10{01}?????00??1?????00?01????0?????????????????1??0???0?0001?0??????100?

;

end;

begin trees ;

tree tnt_1 = [&U]

(Herrerasaurus ,(Coelophysoidea ,(Piatnitzkysaurus ,((Allosaurus_fragilis ,"A."_jimmadseni ,A._europaeus ,MNHNUL ,Concavenator ,Australovenator ,Siamotyrannus ,Neovenator ,Valmitão ,Lourinhanosaurus ,Cryolophosaurus ,(Fukuiraptor ,Monolophosaurus),(Sinraptor ,Yangchuanosaurus),(Shaochilong ,Tyrannotitan ,(Acrocanthosaurus ,Eocarcharia),(Carcharodontosaurus ,(Giganotosaurus ,Mapusaurus)))),(Compsognathidae ,(Dilong ,Tyrannosaurus))))));

end ;

6.4. A JUVENILE ALLOSAUROID THEROPOD (DINOSAURIA, SAURISCHIA) FROM THE UPPER JURASSIC OF PORTUGAL

Reference: Malafaia E, Mocho P, Escaso F, Ortega F. 2016. A juvenile allosauroid theropod (Dinosauria, Saurischia) from the Upper Jurassic of Portugal. Historical Biology. DOI: 10.1080/08912963.2016.1231183

RESUMO

Neste trabalho é descrito um novo exemplar de um dinossáurio terópode descoberto em níveis sedimentares do Jurássico Superior da Bacia Lusitânica (Portugal). Este conjunto de materiais corresponde a um pequeno indivíduo juvenil, representado por elementos do esqueleto axial (vértebras cervicais, sacrais, dorsais e caudais e costelas) e da cintura pélvica. Este conjunto de restos osteológicos representa um dos exemplares mais completos de dinossáurios terópodes conhecido no Jurássico Superior de Portugal e a única evidência de um terópode juvenil identificado actualmente neste registo. A análise filogenética aqui apresentada identifica este novo exemplar como pertencendo a uma forma primitiva de Allosauroidea. Este exemplar apresenta uma combinação de características partilhadas com outros allosauroides conhecidos no Jurássico Superior da Bacia Lusitânica, *Allosaurus* e *Lourinhanosaurus* mas também diferenças relativamente a ambos taxa. Algumas destas diferenças podem estar relacionadas com a condição juvenil do exemplar mas outras características, pouco comuns, não podem ser devidamente explicadas devido a ontogenia e são interpretadas como tendo significado taxonómico. Esta combinação de características poderia justificar a descrição de um novo táxon de terópodes para o Jurássico Superior da Bacia Lusitânica. Contudo, a presença de três taxa simpátricos e praticamente sincrónicos de allossauroides primitivos estreitamente relacionados requer uma investigação mais profunda sobre a sua variabilidade intra e interespecífica.

Palabras-chave: Allosauroidea; *Allosaurus*; *Lourinhanosaurus*; Jurássico Superior; Bacia Lusitânica; análise filogenética

Table 6.4.1. Pelvic elements of SHN.036, a juvenile allosauroid specimen collected in Valmitão (upper Kimmeridgian, Lourinhã). Scale bar: 100 mm.

HISTORICAL BIOLOGY, 2017
VOL. 29, NO. 5, 654–676
http://dx.doi.org/10.1080/08912963.2016.1231183

Taylor & Francis
Taylor & Francis Group

A juvenile allosauroid theropod (Dinosauria, Saurischia) from the Upper Jurassic of Portugal

Elisabete Malafaia[a,b,c], Pedro Mocho[b,d], Fernando Escaso[b,d] and Francisco Ortega[b,d]

[a]Faculdade de Ciências and Instituto Dom Luiz, Departamento de Geologia, Universidade de Lisboa, Lisboa, Portugal; [b]Laboratório de Paleontologia e Paleoecologia, Sociedade de História Natural, Polígono Industrial do Alto do Ameal, Torres Vedras, Portugal; [c]Museu Nacional de História Natural e da Ciência, Universidade de Lisboa, Lisboa, Portugal; [d]Grupo de Biología Evolutiva, Facultad de Ciencias, Universidad Nacional de Educación a Distancia, Madrid, Spain

ABSTRACT

A new specimen of a theropod dinosaur found in Upper Jurassic sedimentary levels of the Lusitanian Basin (Portugal) is described. The specimen includes axial (cervical, dorsal, and caudal vertebrae and ribs) and pelvic elements, corresponding to a small-sized and juvenile individual. This specimen is one of the most complete theropod dinosaur from the Upper Jurassic of Portugal, and the only evidence of a post-hatchling juvenile theropod individual currently recognized in this record. The phylogenetic analysis recovered the new specimen as a basal Allosauroidea. It presents a combination of characters shared with other allosauroids already known in the Upper Jurassic of the Lusitanian Basin, *Allosaurus* and *Lourinhanosaurus*, but also some differences relative to both taxa. Some of these differences may be related to the juvenile condition of the specimen, but other unusual features cannot be properly explained by ontogeny, and are interpreted as having taxonomic significance. This combination of features might justify the description of a new theropod taxon for the Portuguese Upper Jurassic. Nevertheless, the presence of three sympatric and almost synchronic, closely related basal allosauroids requires further exploration of their intra- or interspecific variability.

ARTICLE HISTORY
Received 5 July 2016
Accepted 29 August 2016

KEYWORDS
Allosauroidea; *Allosaurus*; *Lourinhanosaurus*; Late Jurassic, Lusitanian Basin; phylogenetic analysis

Introduction

The Portuguese record of theropod dinosaurs is relatively abundant and diverse. This record includes both osteological and ichnological evidences ranging from the Middle Jurassic to the Upper Cretaceous (e.g. Lapparent & Zbyszewski 1957; Antunes & Sigogneau 1992; Galton 1996; Antunes & Mateus 2003; Ortega et al. 2006). The Upper Jurassic record from the Lusitanian Basin includes mainly medium to large-sized forms belonging to primitive theropod clades, such as Ceratosauria, or tetanurans, including Megalosauridae and Allosauroidea (e.g. Pérez-Moreno et al. 1999; Mateus et al. 2006; Malafaia et al. 2010; Hendrickx & Mateus 2014a; Malafaia et al. 2015). However, small-sized and more derived theropods have also been identified in this record, based mainly on isolated elements (Zinke 1998; Rauhut 2003; Hendrickx & Mateus 2014a; Malafaia, Ortega, & Escaso 2014). Tetanurans are the most abundant theropods so far represented in the Portuguese record. This clade is represented by several specimens identified as belonging to the megalosaurid genus *Torvosaurus* (Mateus & Antunes 2000; Mateus et al. 2006; Malafaia, Ortega, Silva, & Escaso 2008; Araújo et al. 2013; Hendrickx & Mateus 2014b; Malafaia, Ortega, Escaso, & Silva 2014). Presently, the more abundant and well-known tetanuran in this record is the allosauroid *Allosaurus* (Pérez-Moreno et al. 1999; Rauhut & Fechner 2005; Mateus et al. 2006; Malafaia et al. 2010). This taxon is represented by abundant cranial and post-cranial elements found in different sites ranging from the Kimmeridgian to the upper Tithonian. Another possible allosauroid, *Lourinhanosaurus* is represented by few postcranial remains, and possibly a nest with embryos (Mateus 1998; Mateus et al. 2001; Hendrickx & Mateus 2012). *Lourinhanosaurus* was originally described as an allosauroid (Mateus 1998), but subsequently has been interpreted as belonging to different clades, including Megalosauridae (Mateus 2005; Mateus et al. 2006), Metriacanthosauridae (Benson 2010) and Coelurosauria (Carrano et al. 2012).

The Late Jurassic theropod faunas of the Lusitanian Basin have been traditionally interpreted as being closely related to that of correlative sedimentary sequences from the North American Morrison Formation and from the African Tendaguru Formation (Pérez-Moreno et al. 1999; Antunes & Mateus 2003; Mateus et al. 2006). This hypothesis is based on the identification of several shared taxa, including *Ceratosaurus* (identified in the Lusitanian Basin and Morrison Formation and in the Tendaguru Formation), *Elaphrosaurus* (identified in the Tendaguru Formation and tentatively in the Morrison Formation), *Torvosaurus* (identified in the Morrison Formation and Lusitanian Basin), and *Allosaurus* (identified in the Lusitanian Basin and Morrison Formation and originally in the Tendaguru Formation). The specimens

CONTACT Elisabete Malafaia emalafaia@gmail.com
Supplemental data for this article can be accessed here http://dx.doi.org/10.1080/08912963.2016.1231183.

originally assigned to *Ceratosaurus* and *Allosaurus* from the Tendaguru Formation were more recently reinterpreted as indeterminate ceratosaurian and indeterminate tetanuran, respectively (Rauhut 2011). However, some isolated teeth originally described as *Labrosaurus*(?) *stechowi* were later tentatively referred to *Ceratosaurus* based on the presence of broad longitudinal grooves and ridges on the lingual side of the crown (Madsen & Welles 2000; Rauhut 2011).

A recent phylogenetic reinterpretation of *Elaphrosaurus* specimens from the Tendaguru Formation proposed that the elements from the Morrison Formation originally assigned to this taxon may be related to a distinct basal representative of the abelisauroid lineage (Rauhut & Carrano Forthcoming). Recent reviews of the theropod fauna from this African formation performed by Rauhut (2011) and Rauhut and Carrano (Forthcoming) proposed the presence of at least seven different theropod taxa, including at least four ceratosaurs (an indeterminate ceratosaur, a possible abelisaurid, a noasaurid and a small indeterminate abelisauroid) and three basal, non-coelurosaurian tetanurans (one possible megalosauroid, a carcharodontosaurid and an indeterminate basal tetanuran).

The general composition of the theropod fauna from the Tendaguru Formation apparently contrasts with that of both the North American Morrison Formation and the Lusitanian Basin because in the latter the theropod faunas were dominated by tetanurans and also abundant coelurosaurs whereas in the former ceratosaur taxa are the more abundant and diverse and coelurosaurs are unknown altogether. On the other hand, the faunal composition of theropods from the Morrison Formation and the Lusitanian Basin is very similar. Most of the genera currently known in the Portuguese record have a closely related taxon at the North American record (*Ceratosaurus*, *Torvosaurus*, *Allosaurus fragilis*, and possibly *Aviatyrannis*). This similarity has been used as evidence of faunal interchanges across the proto-North Atlantic Ocean during the Late Jurassic. However, there are also few taxa currently interpreted as endemic forms of the Portuguese record (*Lourinhanosaurus*) and some taxa that are closely related to those known in North America have more recently been reinterpreted as separate species that are exclusive to the Lusitanian Basin, including *Allosaurus europaeus* and *Torvosaurus gurneyi* (Mateus et al. 2006; Hendrickx & Mateus 2014b). This scenario suggests an incipient vicariant evolution of the Late Jurassic theropod faunas from both margins of the proto-North Atlantic Ocean.

Herein is described a new theropod specimen found in the northern end of the cliffs of Lourinhã, at the Praia de Valmitão locality (Praia da Amoreira-Porto Novo Formation, upper Kimmeridgian) in the western margin of the central sector of the Lusitanian Basin. The new specimen shows similarities with other allosauroids previously identified in the Portuguese record, *Allosaurus* and *Lourinhanosaurus*, but also some differences from both taxa. A phylogenetic discussion of the Praia de Valmitão specimen is proposed.

Institutional abbreviations

BYU, Brigham Young University, USA; DINO, Dinosaur National Monument, USA; DMNH, Denver Museum of Natural History, USA; ML, Museu da Lourinhã, Portugal; SHN, Sociedade de História Natural, Portugal; SIGAP, Sistema de Informação Geográfica Aplicado à Paleontologia; USNM, United States National Museum, USA.

Anatomical abbreviations

acdl, anterior centrodiapophyseal lamina; act, acetabulum; ail, anterior interspinous ligaments; all, additional lateral lamina; ap, anterior process; at in, atlantal intercentrum; ax, facet for axial centrum; ax c, axis centrum; ax in, axial intercentrum; bf, brevis fossa; bg, bulge; c, capitulum; cdf, centrodiapophyseal fossa; ch, facet for chevron; cpf, cupedicus fossa; cpol, centropostzygapophyseal lamina; cprl, centroprezygapophyseal lamina; cr, caudal rib; df, distal fenestra; die, distal ischial expansion; dit, distal ischial tubercle; dp, diapophysis; ep, epipophysis; fr, foramen; g, groove; hs, hyposphene; hy, hypantrum; ilc, iliac articulation; ilp, iliac peduncle; isc, ischial articulation; ist, ischial tuberosity; ivf, intervertebral foramen; lac, lateral crest; lat.spol, lateral spinopostzygapophyseal lâmina; lg, lateral groove; lr, lateral ridge; mec, medial crest; ms, medial symphysis; nc, neural canal; ncs, neurocentral suture; ne, neurapophysis; nef, facet for neurapophysis; ns, neural spine; oc, facet for occipital condyle; od, odontoid; odc, odontoid cavity; on, obturator notch; op, obturator process; pcdl, posterior centrodiapophyseal lamina; pcdf, posterior centrodiapophyseal fossa; pd, pleurocentral depression; pil, posterior interspinous ligaments; pl, pleurocoel; po, postzygapophysis; pocdf, postzygapophyseal centrodiapophyseal fossa; pop, postacetabular process; posdf, postzygapophyseal spinodiapophyseal fossa; pp, parapophysis; pr, prezygapophysis; prcdf, prezygapophyseal centrodiapophyseal fossa; prdl, prezygodiapophyseal lamina; prp, preacetabular process; prpl, prezygaparapophyseal lamina; prsdf, prezygapophyseal spinodiapophyseal fossa; puc, pulp cavity; pup, pubic peduncle; put, pubic tubercle; r, ridge; rc, recess; sac, supraacetabular crest; sdf, spinodiapophyseal fossa; spdl, spinodiapophyseal lamina; spol, spinopostzygapophyseal lamina; spof, spinopostzygapophyseal fossa; sprl, spinoprezygapophyseal lamina; sprf, spinoprezygapophyseal fossa; sr, scar for sacral rib; tpol, intrapostzygapophyseal lamina; tprl, intraprezygapophyseal lamina; tp, transverse process; tu, tuberculum.

Geological settings

The Valmitão fossil site (see SHN SIGAP database) is located in the southern end of the Lourinhã municipality, about 50 km to the northwest of Lisbon. The sedimentary sequence of the Valmitão fossil site corresponds to the upper levels of the Praia da Amoreira-Porto Novo Formation (*sensu* Manuppella et al. 1999), which corresponds to the Porto Novo Member of the Lourinhã Formation (*sensu* Hill 1988), and is interpreted as upper Kimmeridgian in age (Figure 1). These sediments correspond to deposits of a fluvial system with thick sandy channel bodies, intercalated with siltstones and claystones, corresponding to floodplain and crevasse splay deposits. The specimen herein described was collected in a lenticular, relatively thin (ca. 50 cm in thickness) layer composed mainly by argillaceous and silty sediments with dark gray color and thin planar lamination. These sediments are very rich in organic matter and preserve abundant plant debris, often with thin layers of pyrite, which suggest anoxic depositional conditions. The characteristics of these sediments

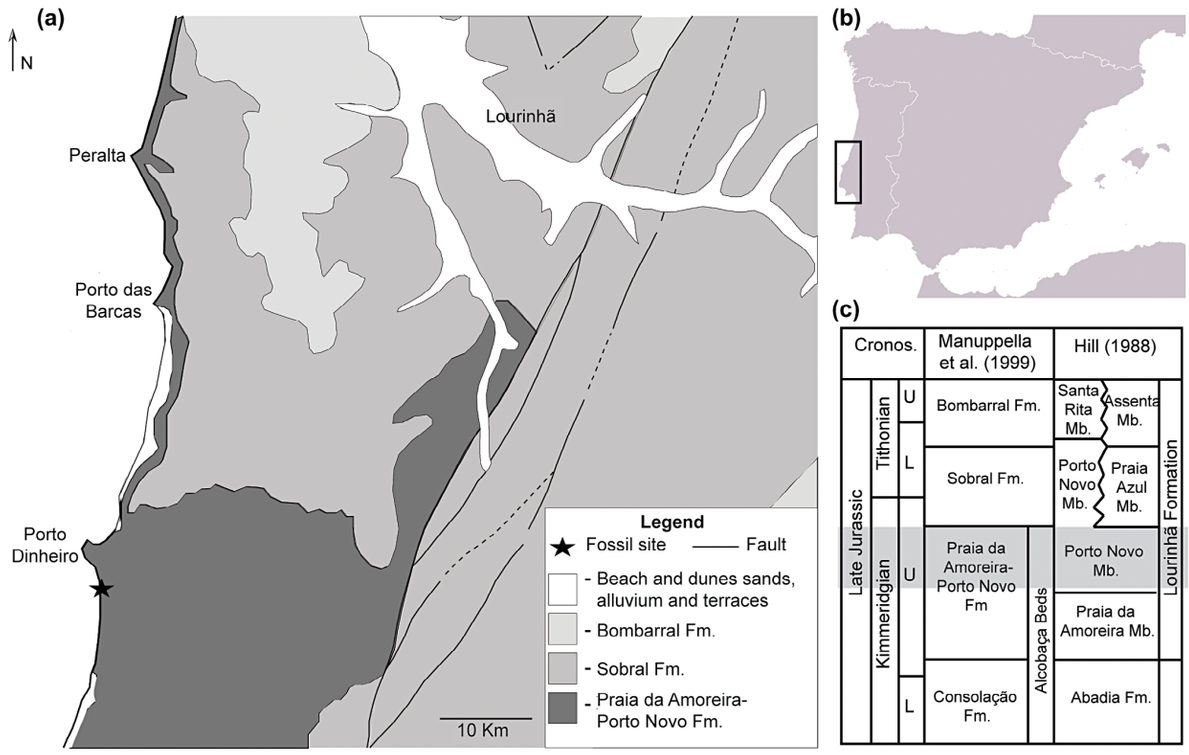

Figure 1. Geographic and geological context of the Valmitão fossil site. (a) Geological map showing the Valmitão locality (modified from Manuppella et al. 1996); (b) location of the Lusitanian Basin in the Iberian context; (c) stratigraphy for the Lusitanian Basin in the Lourinhã area based on the nomenclatures proposed by different authors (Hill 1988; Manuppella et al. 1999).

Note: The grey rectangle marks the chronostratigraphic position of the quarry.

suggest a deposition in a paleoenvironment similar to a swamp, with low energy flows and abundant vegetation developed in the floodplain of a distal meander river.

Material and methods

The specimen herein described, SHN.036, consists on a partial skeleton, including axial and pelvic elements (see Supplemental Online Material: SOM Table 1 for a complete list of the theropod elements collected in the Valmitão fossil site). The axial skeleton is represented by the atlas-axis complex, three isolated cervical neural spines, two partially preserved anterior dorsal vertebrae, ten mid and posterior centra and six isolated neural spines from the dorsal series, fragments of four sacral centra, one incomplete neural arch, fragments of one sacral neural spine, eleven caudal vertebrae, one partially preserved anterior caudal neural arch, eight incomplete chevrons, and several fragments of cervical and dorsal ribs. The axial skeleton is also represented by abundant fragments of vertebral centra and neural arches, including several isolated pre- and post-zygapophyses, fragments of caudal ribs, and fragments of neural spines. The recovered pelvic girdle elements include an almost complete right ilium, and both pubes and ischia. Three isolated teeth were collected in the same site and they have a morphology and size compatible with the postcranial elements. However, these teeth do not preserve any parts of the root, suggesting that they correspond to shed teeth. It is not possible assign these isolated teeth to the same individual as the postcranial elements and thus they are here described as part of the theropod fauna from the Valmitão fossil site.

The specimen is deposited in the collections of the Sociedade de História Natural (SHN) in Torres Vedras. It was collected by a private collector, which in 2008 donated his collection to the Torres Vedras municipality. The SHN is a public institution and the paleontological collection is managed by the Torres Vedras County. The specimen was properly collected in accordance with the Portuguese law on paleontological heritage.

All elements were found in the same sedimentary level and were collected in a small area at the same site. Besides, the consistent size of the different elements suggests that probably all belong to a single, small-sized individual.

The nomenclature used in the description of pneumaticity, laminae and fossae for the axial elements is that proposed by Wilson (1999) and Wilson et al. (2011). The lateral projections of caudal vertebrae are here referred as 'caudal ribs' in preference to the term 'transverse processes'. Although conclusive osteological evidence supporting one terminology over the other is currently lacking among theropods the accuracy of the former term has been established in developmental studies on modern sauropsids (Persons & Currie 2011).

Ontogenetic assessment of the specimen

SHN.036 presents most vertebral centra separated from the respective neural arches along their neurocentral sutures on

all preserved dorsal, sacral and anterior caudal vertebrae. Only mid and posterior caudal centra are completely fused with their neural arches. The preserved cervical vertebrae have the centra attached to their respective neural arches, but the neurocentral sutures are still visible. Also the elements that constitute the atlas-axis complex are separated. The axial intercentrum is attached to the axis, but the suture between the two elements is well visible.

The sequence of vertebral neurocentral suture closure is traditionally a criterion used to assess ontogeny for a variety of fossil archosaurs (e.g. Brochu 1996; Irmis 2007). Based on this criterion the presence of open or partially fused neurocentral sutures in most preserved cervical, dorsal and anterior caudal vertebrae of SHN.036 suggest that this specimen corresponds to a juvenile individual. However, the partially fused neurocentral sutures in some preserved cervical vertebrae does not support a posterior-anterior sequence of neurocentral suture closure, a pattern recognized in extant crocodylians or phytosaurs (Irmis 2007) and assumed for some theropod dinosaurs (Makovicky & Sues 1998; Xu et al. 2008; Parsons & Parsons 2015). Instead, this specimen presents a pattern of neurocentral suture closure that affected first the most posterior caudal vertebrae and then cervical vertebrae. This specimen suggests that the sequence of neurocentral suture closure in non-avian theropods is ambiguous and a priori application of extant crocodylian patterns to these clades is inappropriate, as was previously proposed by Irmis (2007).

Systematic palaeontology

Saurischia Seeley 1887
Theropoda Marsh 1881
Tetanurae Gauthier 1986
Avetheropoda Paul 1988
Allosauroidea Marsh 1878
Allosauroidea gen. et sp. indet.
(Figures 2–10, SOM Figures 1–4; Tables 1–2)

Description

Axial skeleton

Atlas-axis complex. The atlas-axis complex corresponds to the most anterior elements of the cervical series, and includes a paired neurapophyses, the atlantal intercentrum, the axial intercentrum, the odontoid, and the axis. In some theropod adult individuals for which this part of the skeleton is known, some elements that constitute the atlas-axis complex, mainly the axial intercentrum, odontoid and axis, are fused to each other (e.g. *Allosaurus*: Madsen 1976/1993; *Ceratosaurus*: Madsen and Welles 2000).

SHN.036 preserves the odontoid, the atlantal intercentrum, the axial intercentrum, the neurapophyses, and the axis (Figure 2). There is no fusion of the elements forming the atlas-axis complex. The axial intercentrum, the neurapophyses, and the axis are articulated, but not fused, and the suture is well visible. All the other elements were found disarticulated.

The odontoid, SHN.036/18 (Figure 2(a)–(c)), is a small element with a quadrangular outline that articulates with the atlantal intercentrum ventrally and with the axial centrum posteriorly. The ventral surface presents a shallow, transversal concavity for the occipital condyle adjacent to the distal end. The element expands slightly transversely, showing a broad and slightly concave posterior surface, which has a triangular ridge at about its transversal mid-width that corresponds to the facet for articulation with the axial intercentrum. The dorsal surface of the odontoid is slightly concave.

The atlantal intercentrum, SHN.036/19 (Figure 2(d)–(h)), is crescent-shaped with a deep anterior surface for the occipital condyle. It is anteroposteriorly narrow with two lateral processes that project anterodorsally, delimiting a transversely deep concavity for articulation with the odontoid (odontoid cavity). The anterodorsal processes would articulate with the neurapophysis distally. The posterior surface of the atlantal intercentrum, which would articulate with the axis, is almost flat and bounded ventrally by a shallow groove extending along the entire width.

The axial intercentrum is articulated with the axis and the paired neurapophyses are articulated with the neural arch of the axis, SHN.036/22 (Figure 2(k)–(p)). These elements are well preserved, but present some taphonomic deformation (mainly dorsoventral compression) and lack most of the neural arch of the axis. The right neurapophysis is completely preserved whereas the left element only preserves a small fragment of its proximal end. This element has a roughly triangular shape in lateral view, with a broad and blade-like proximal end, and a tapering distal process that projects anterolaterally. The neurapophysis articulates with the prezygapophysis of the axial neural arch and overlap slightly the dorsolateral surface of the atlantal intercentrum due distortion of the specimen. The axial intercentrum is firmly attached to the axis although these elements are not fused as is common in theropods. The axial intercentrum is anteroposteriorly narrow and has a slightly convex anterior articular facet. The ventral surface of the axial intercentrum is roughly straight and is at the same level as the ventral surface of the axis.

The axis preserves the centrum and a small fragment of the ventral part of the neural arch. The centrum is almost complete, except for the posterior articular facet that is broken. The neurocentral suture is still visible along the entire length on the right side of the centrum, and has a sinusoidal shape. Posteriorly, the pedicels project ventrally well into the lateral surface of the centrum. The posterior articular facet strongly expands laterally. The parapophyses are represented by a pair of robust processes that project laterally from the anterior end of the ventral surface of the centrum. The articular facets of the parapophyses face laterally and slightly anteriorly. In ventral view, the axial centrum has a roughly quadrangular shape, with a shallow concavity near the anterior articular facet. The posterior articular facet is oval, wider than high, and strongly concave. No pleurocoel is visible on the axial centrum, as they are present in *Allosaurus*, but we cannot exclude that this might be due to dorsoventral distortion of the specimen. The neural arch is badly damaged and only preserves the ventral end of the pedicels and the neural canal. However, on the right side, the base of the transverse process is preserved, which projects nearly up to the level of the anterior articular facet. Under the transverse process a small recess between two low ridges interpreted as the anterior and posterior centrodiapophyseal laminae (acpl and pcdl) is visible.

Postaxial cervical vertebrae. Three isolated neural spines (Figure 3) and several fragments of pre- and post-zygapophyses

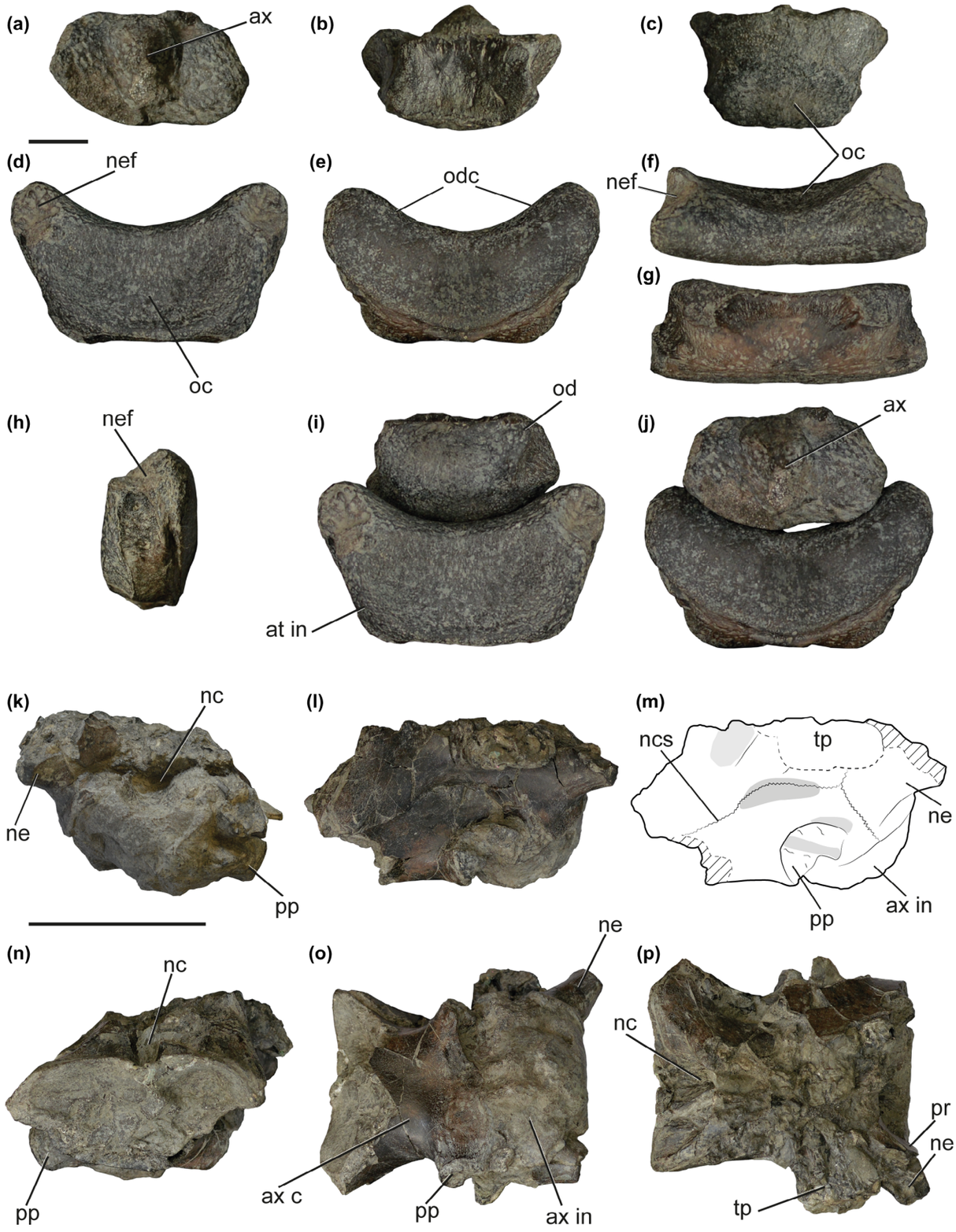

Figure 2. Atlas-axis complex of SHN.036. Odontoid, SHN.036/19, in posterior (a), dorsal (b), and ventral (c), views; atlantal intercentrum, SHN.036/18, in anterior (d), posterior (e), dorsal (f), ventral (g), and lateral (h) views; articulated odontoid and atlantal intercentrum in anterior (i), and posterior (j) views; articulated axial intercentrum, neurapophyses and axis, SHN.036/22, in anterior (k), lateral ((l), (m)), posterior (n), ventral (o), and dorsal (p) views.
Note: Scale bars ((a)–(j)) = 10 mm; ((k)–(p)) = 50 mm.

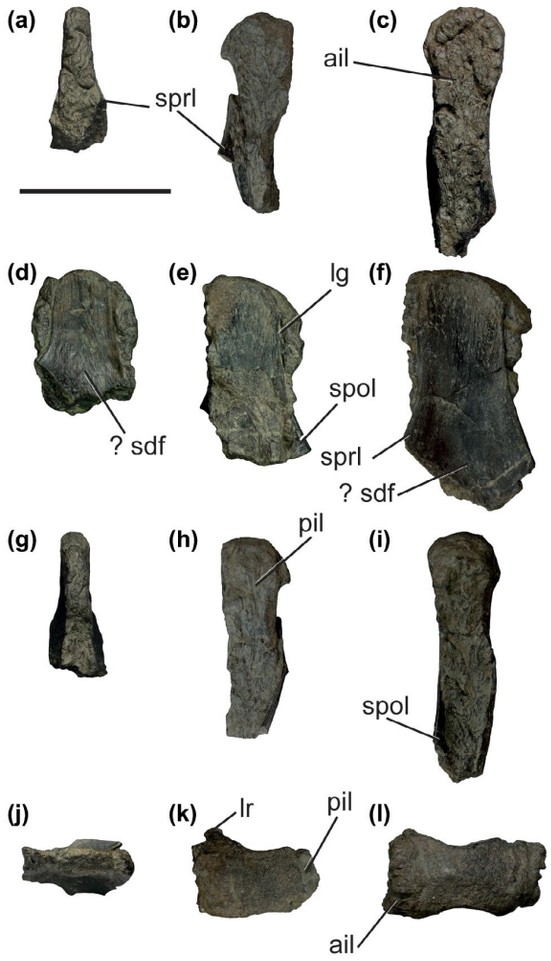

Figure 3. Cervical neural spines of SHN.036. SHN.036/16 in anterior (a), lateral (d), posterior (g), and dorsal (j) views; SHN.036/17 in anterior (b), lateral (e), posterior (h), and dorsal (k) views; SHN.036/4 in anterior (c), lateral (f), posterior (i), and dorsal (l) views.
Note: Scale bar = 50 mm.

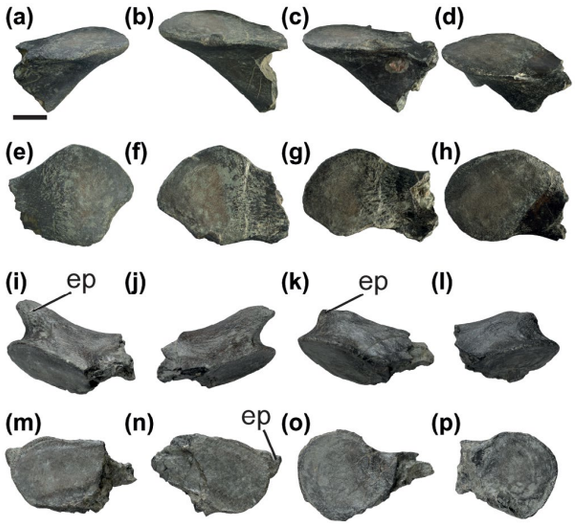

Figure 4. Fragments of cervical pre- and post-zygapophyses of SHN.036. Prezygapophyses in anterior ((a)–(d)) and dorsal ((e)–(h)) views; postzygapophyses in posterior ((i)–(l)) and ventral ((m)–(p)) views.
Note: Scale bar = 10 mm.

(Figure 4) interpreted as belonging to the cervical series were collected.

The neural spines represent cervical vertebrae because they are short dorsoventrally and anteroposteriorly, but relatively thick transversely. This morphology is similar to cervical neural spines of *Allosaurus* whereas toward the dorsal series the neural spines become dorsoventrally higher and anteroposteriorly wider (e.g. Madsen 1976/1993; Chure 2000). These neural spines present well-developed, rugose anterior and posterior scars for attachment of interspinous ligaments. The lateral surfaces of the spines present shallow and broad concavities near their bases, corresponding to the spinodiapophyseal fossa (sdf), which produces a strong constriction of the spine near the base mid-length. The dorsal surface of the spines is asymmetrically convex anteroposteriorly with the anterior end being slightly higher than the posterior one. A small lateral crest is present near the anterior margin and adjacent to the dorsal end. Towards the posterior part of the cervical series the spines become higher, anteroposteriorly wider and slightly thicker transversely.

The pre- and post-zygapophyses collected in the same site present compatible sizes and morphologies as previously described elements, suggesting that these elements are part of the same individual. The prezygapophyses have broad and flat articular facets. Some are roughly triangular in dorsal view. This morphology is compatible with prezygapophyses of anterior cervical vertebrae, whereas in most posterior cervical vertebrae these articular facets become more circular.

The postzygapophyses present well-developed epipophyses, especially in the anteriormost elements. Toward the posterior part of the cervical series the epipophyses become small bulges located on the posterodorsal surface of the postzygapophyses. The articular facets of the postzygapophyses are flat and oval in the anteriormost elements and become more circular posteriorly in the cervical series.

Cervical ribs. Several rib fragments interpreted as belonging to the cervical series were collected. Nevertheless, these elements are too incomplete to allow any informative description.

Anterior dorsal vertebrae. Two partial vertebrae corresponding to the anterior dorsal series were recovered, SHN.036/20 and 21 (Figure 5). Both vertebrae have broken neural arches and the centra are strongly distorted due lateral compression, especially marked near the anterior articular facets. The exact position of these vertebrae is difficult to ascertain. However, the morphology of these vertebrae is similar to the anteriormost dorsal vertebra of *Allosaurus* based on the dorsal position of the parapophyses relative to the more ventral position of these structures in the cervical vertebrae and in the position of the pleurocoels, which are placed posterior to the parapophyses, especially in SHN.036/20, not posterodorsal as in the cervical elements (Madsen 1976/1993). Both vertebrae are strongly opisthocoelous with very deep posterior articular

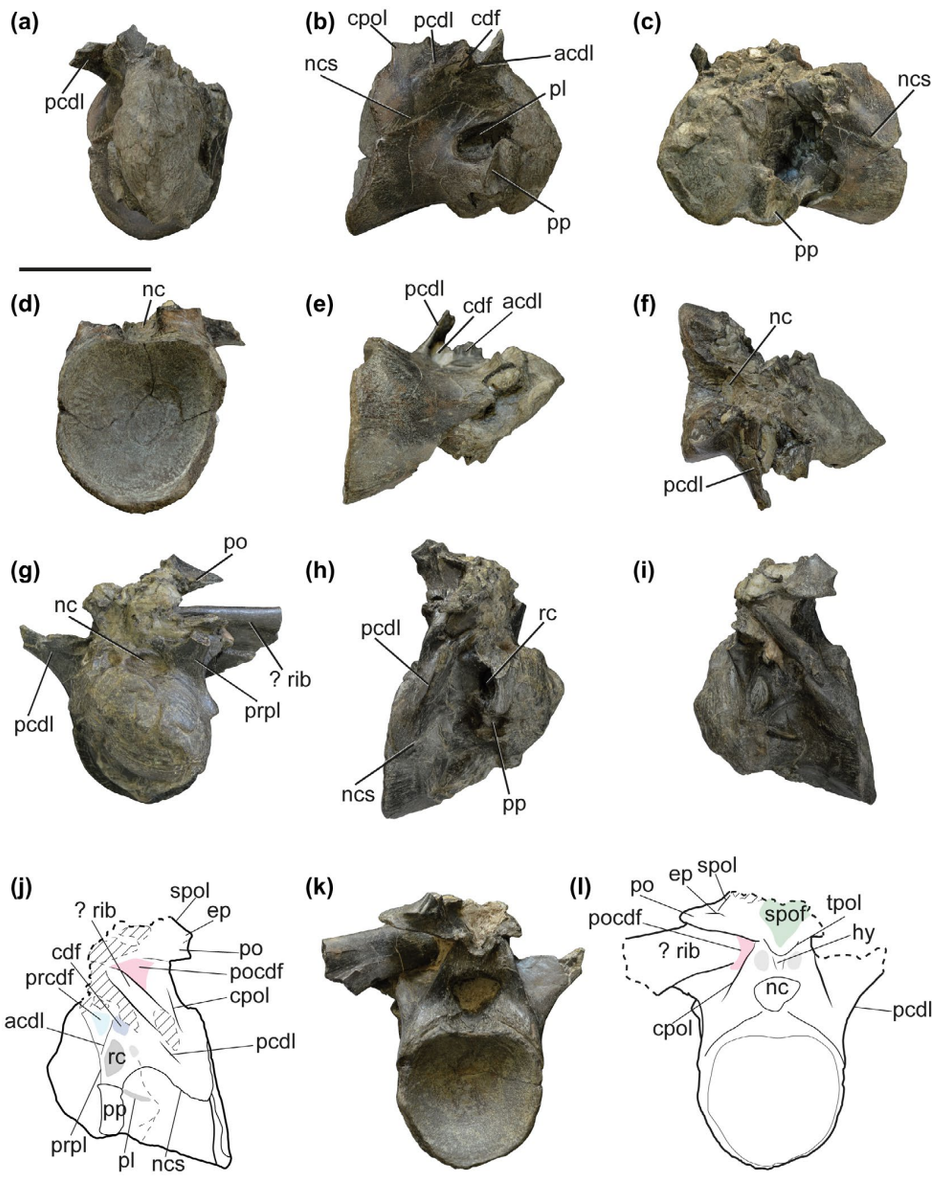

Figure 5. Anterior dorsal vertebrae of SHN.036. SHN.036/21 in anterior (a), right lateral (b), left lateral (c), posterior (d), ventral (e), and dorsal (f) views; SHN.036/20 in anterior (g), right lateral (h), left lateral (i), and posterior (k) views; interpretative line drawing ((j), (l)).
Note: Scale bar = 50 mm.

facets, which are roughly circular, slightly dorsoventrally higher than transversely wide (see SOM Table 2). The neurocentral suture is well visible along the entire length of both centra. The anterior articular facets are in a slightly dorsal position relative to the level of the posterior facets. There is a pair of large pleurocoels, one on each lateral surface of both centra. In the more anterior vertebra, SHN.036/21, the pleurocoels are in a position immediately dorsal and slightly posterior to the parapophyses, whereas in the more posterior one, SHN.036/20, they are adjacent to the posterior margin of the parapophyses. In the former vertebra, the pleurocoels are elongated, occupying almost the entire anterior half of the lateral surface of the centrum. On the right side of this element a vertical septum is visible at about the mid-length of the pleurocoel. In SHN.036/20, the pleurocoels are considerably reduced in relation to those in the more anterior vertebra.

SHN.036/21 presents a small opening bounded by the acdl and the pcdl that pierces the base of the neural arch and apparently would connect with the neural canal. A similar opening is described in the third dorsal vertebra of some *Allosaurus* specimens, and is interpreted as a branch of the pectoral ganglion or brachial plexus (Madsen 1976/1993). However, this opening seems to connect also with the centrodiapohyseal fossa (cdf) suggesting that it may be a pneumatic feature associated with

this fossa (Figure 5(e)). The oval parapophyses are dorsoventrally deep and have strongly concave articular facets. In SHN.036/21, the parapophyses are in the ventral part of the lateral surfaces of the centrum, adjacent to the anterior articular facets. However, in SHN.036/20 the parapophyses are more dorsally placed and project from the dorsal part of the centrum to the ventral end of the neural arch. The ventral surface of the centrum in SHN.036/21 presents a shallow concavity that extends along the anterior part of the centrum to about its mid-length. On the contrary, in SHN.036/20 the centrum has a low and poorly-defined longitudinal crest.

The neural arch is almost completely broken in both vertebrae. SHN.036/21 preserves a small fragment of the right pcdl, which projects anterolaterally and slightly dorsally in posterior view. In SHN.036/20 the neural arch preserves the left postzygapophysis, the ventral part of both right and left pcdl, fragments of the left acdl, and the prezygoparapophyseal lamina (prpl). The neural canal is relatively broad, circular anteriorly and slightly ventrally pointed in posterior view. The pedicels of the neural arch extend down on the lateral surface of the centrum, especially near the posterior articular facet.

The neural arch of SHN.036/20 has a pair of large and circular recesses (blind fossa *sensu* O'Connor 2006), on each lateral side, in a position immediately dorsal to the parapophyses. This recess does not penetrate deeply the centrum, which suggests that it is not a pneumatic feature. The presence of this recess is not described in any other theropod specimen and thus may be an exclusive character for SHN.036. Dorsal to this recess the well-developed centrodiapophyseal fossa (cdf) is visible, delimited by the acdl and pcdl. From the dorsal margin of the parapophysis a well-developed prpl extends dorsally along the lateral surface of the prezygapophysis. The acdl extends posterodorsally from the prpl near the level of the dorsal surface of the anterior articular facet, and both laminae delineate a relatively deep prezygapophyseal centrodiapophyseal fossa (prcdf). The pcdl arises from the level of the dorsal margin of the posterior articular facet and projects laterodorsally.

SHN.036/20 preserves the left postzygapophysis, which projects laterally, with the articular facet circular and slightly facing anteriorly. The postzygapophysis presents a small but well-defined epipophysis. From the posterior tip of the epipophysis a low lamina arises that corresponds to the spinopostzygapophyseal lamina (spol). The hyposphene articulation is a low and poorly defined vertical ridge with a roughly triangular shape. Lateral to the hyposphene there is pair of shallow concavities, which are bounded dorsally by the well-developed intrapostzygapophyseal lamina (tpol).

Mid and posterior dorsal vertebrae. The mid and posterior dorsal series is represented by at least eight partially preserved centra, several fragments of isolated prezygapophyses, five neural spines, and fragments of centra and of neural arches (Figure 6).

All preserved vertebrae of the mid and posterior dorsal series have lost the unfused neural arches. The dorsal centra are slightly longer than high, with strongly expanded articular facets. The anterior articular facets are circular and slightly concave, whereas the posterior ones are more oval (slightly higher than wide) and almost flat. In some vertebrae (e.g. SHN.036/14), the anterior articular facet is in a more dorsal position relative to the posterior one, but both articular facets are at the same level on the other preserved dorsal vertebrae. The former morphology is usually related with a more anterior position of the vertebrae in the dorsal series (Gilmore 1920; Madsen 1976/1993; Currie & Zhao 1993). The lateral surface of the centra presents deep pleurocentral depressions occupying most of the lateral surface of the centrum adjacent to the base of the neural arch. There is a small vascular foramen inside this depression in some centra. The pleurocentral depression is deeper in more anterior vertebrae as occur in other allosauroids (e.g. Gilmore 1920; Madsen 1976/1993; Chure 2000). The centra are saddle-shaped and the ventral surfaces are transversely convex to flat.

The dorsal neural spines are more robust and higher than the cervical spines. In lateral view, these elements present an almost rectangular outline and well-developed anterior and posterior scars for interspinous ligaments. The dorsal surface is slightly convex in lateral view and roughly rectangular in dorsal view. The neural spines of more posterior dorsal vertebrae are higher and transversely thicker, but shorter anteroposteriorly than those of more anterior vertebrae. The lateral surface of the neural spines presents a broad and shallow concavity, corresponding to the prezygapophyseal spinodiapophyseal fossae (prsdf) that occupies most of the base of the spine up to about its mid-height.

The prezygapophyses have flat and circular articular facets, which have ventral extensions medially corresponding to the hypantrum articulation. This articulation is delineated by well-developed and divergent surfaces, suggesting a triangular morphology of the hyposphene.

Dorsal ribs. Dorsal ribs are represented by two almost complete ribs of the mid series, a fragment of a posterior element, and several fragments of rib-shafts (Figure 7). The mid dorsal ribs have strongly curved shafts and triangular proximal ends. The capitulum is long and projects dorsomedially, whereas the tuberculum is short, proximolaterally placed, and faces dorsally. Toward the posterior end of the dorsal series the capitulum projects more dorsally, being almost vertical in SHN.036/72.

Sacral vertebrae. Two articulated partial sacral centra and two disarticulated almost complete centra are preserved (Figure 8(a)–(n)). An incomplete neural arch and a fragment of a neural spine are also interpreted as corresponding to the sacral series (Figure 8(o)–(v)).

Two vertebrae, SHN.036/11 and 12 (Figure 8(a)–(e) and (j)–(n)), are disarticulated and preserve incomplete anterior and posterior articular facets. In SHN.036/11, the anterior articular facet is circular and slightly concave. The posterior facet is broken and only a small fragment is preserved. SHN.036/11 is interpreted as the first sacral vertebra, based on the morphology of the articular facets and the presence of a small dorsal fenestra (intervertebral foramen *sensu* Benson 2010) that pierces the lateral surface of the centrum adjacent to the posterior articular facet. This fenestra is placed near the posterior articular facet and leads into the neural canal. SHN.036/12 shows a similar morphology as the aforementioned vertebra, but the centrum is slightly shorter. The posterior articular facet is circular and almost flat. This vertebra is interpreted as the last vertebra of

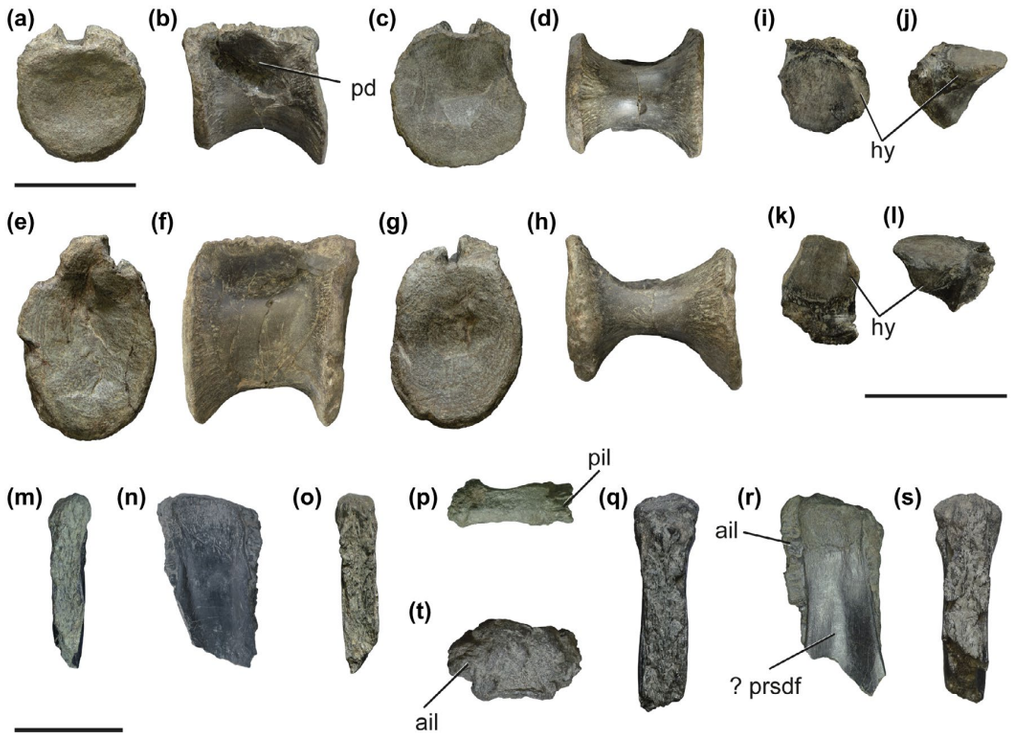

Figure 6. Elements of mid and posterior dorsal vertebrae of SHN.036. Centrum, SHN.036/14, in anterior (a), left lateral (b), posterior (c), and ventral (d) views; centrum, SHN.036/6, in anterior (e), left lateral (f), posterior (g), and ventral (h) views; prezygapophyses in dorsal ((i), (k)) and anteromedial (j), (l) views; neural spine, SHN.036/25, in anterior (m), lateral (n), posterior (o), and dorsal (p) views; neural spine, SHN.036/27, in anterior (q), lateral (r), posterior (s), and dorsal (t) views.
Note: Scale bar = 50 mm.

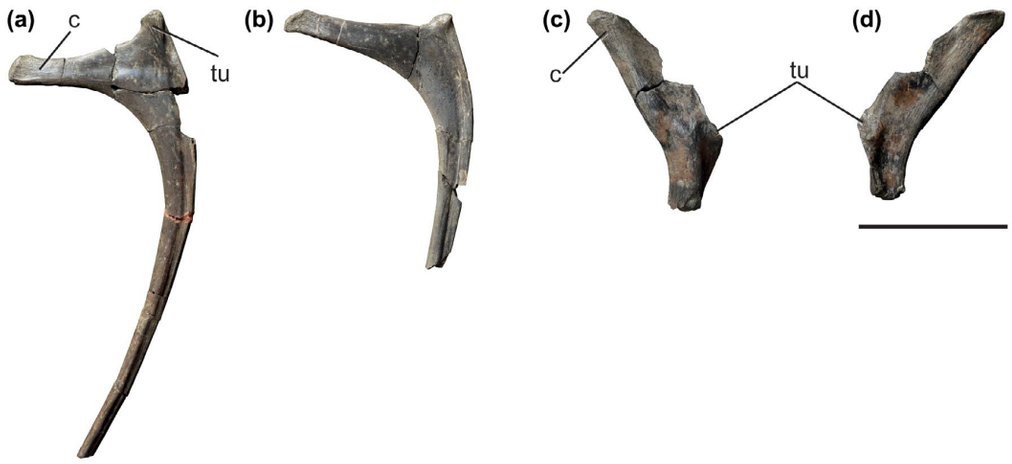

Figure 7. Dorsal ribs of SHN.036. SHN.036/70 in anterior view (a); SHN.036/71, in anterior view (b); SHN.036/72, in lateral (c) and medial (d) views.
Note: Scale bar = 50 mm.

the sacral series. Shallow pleurocentral depressions are present on the lateral surfaces of these sacral centra. Small foramina are visible inside these depressions.

The two articulated sacral vertebrae, SHN.036/40 (Figure 8(f)–(i)), are badly damaged but preserve fragments of the centra and the surface for articulation of the sacral ribs. The centra are tightly united to each other along the articular facets. As in the dorsal vertebrae, the neurocentral sutures of the sacral vertebrae are open. The ventral surfaces are transversely convex and saddle-shaped in lateral view. The scars for articulation with the sacral ribs are broad and extend to near the ventral surface of the centra. A small intervertebral foramen is visible in the most complete centrum of SHN.036/40.

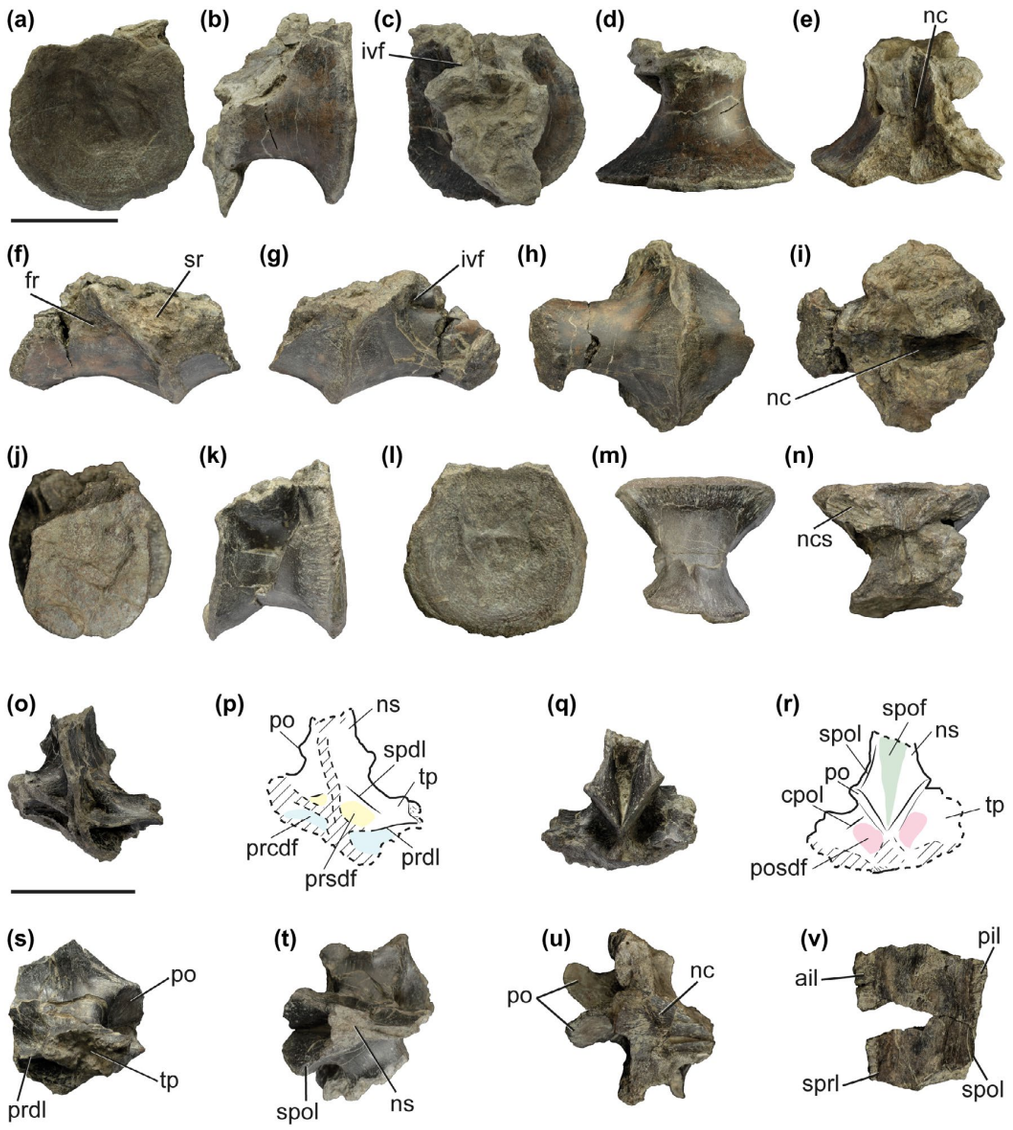

Figure 8. Elements of sacral vertebrae of SHN.036. Vertebra, SHN.36/11, in anterior (a), left lateral (b), posterior (c), ventral (d), and dorsal (e) views; vertebra, SHN.36/40, in left lateral (f), right lateral (g), ventral (h), and dorsal (i) views; vertebra, SHN.36/12, in anterior (j), left lateral (k), posterior (l), ventral (m), and dorsal (n) views; neural arch, SHN.036/5, and corresponding interpretative line drawing in anterior ((o), (p)), posterior ((q), (r)), lateral (s), dorsal (t), and ventral (u) views; neural spine, SHN.036/29, in lateral view (v).
Note: Scale bar = 50 mm.

A fragment of a neural arch, SHN.036/5 (Figure 8(o)–(u)), is interpreted as corresponding to the last sacral vertebra. It preserves the postzygapophyses, the base of the neural spine and fragments of the transverse processes. The postzygapophyses have an almost vertical and slightly lateral orientation in posterior view. In anterior view, the neural arch preserves fragments of the prdl extending from the anterolateral surface of the transverse process. Below these laminae, a pair of deep prcdf is present. From the anterodorsal surface of the transverse process arises another lamina, the spdl that projects dorsally into the base of the neural spine. Between these two laminae is the well-developed prsdf. In posterior view, the centropostzygapophyseal lamina (cpol) projects from the posterodorsal surface of the transverse process connecting with the ventral margin of the postzygapophysis. This lamina delimits a deep postzygapophyseal spinodiapophyseal fossa (posdf) that invades the base of the neural arch below the postzygapophysis. The neural spine is incomplete but it would be anteroposteriorly broad and transversely thin.

SHN.036/29 (Figure 8(v)) corresponds to a fragment of the medial section of a neural spine. It is anteroposteriorly broad and transversely thin, features that allow interpret it as a sacral spine. It presents well-developed anterior and posterior interspinous ligament scars.

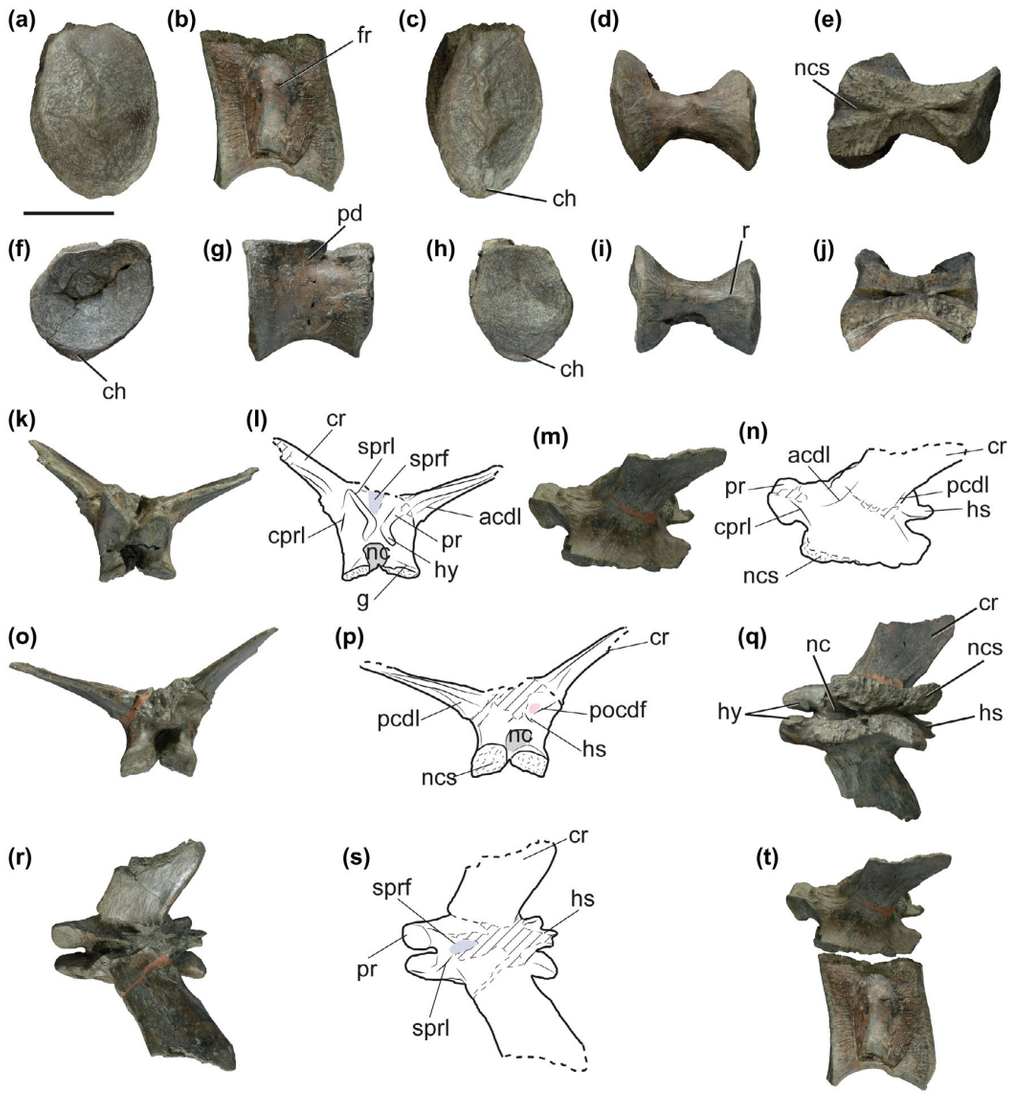

Figure 9. Anterior caudal elements of SHN.036. Centrum, SHN.036/13, in anterior (a), left lateral (b), posterior (c), ventral (d), and dorsal (e) views; centrum, SHN.036/50, in anterior (f), left lateral (g), posterior (h), ventral (i), and dorsal (j) views; neural arch, SHN.036/2, and corresponding interpretative line drawing in anterior ((k), (l)), left lateral ((m), (n)), posterior ((o), (p)), ventral (q), and dorsal ((r), (s)) views; articulated anterior caudal centrum, SHN.036/13, and neural arch, SHN.036/2, which probably belongs to the same vertebra in left lateral view (t).

Note: Scale bar = 50 mm.

Caudal vertebrae. The caudal series is represented by four anterior centra, a fragment of an anterior neural arch (Figure 9), eight partially preserved mid and posterior caudal vertebrae (Figure 10; see SOM Figure 1), an isolated fragment of neural spine, apart from several other fragments of caudal ribs and fragments of pre- and post-zygapophyses.

Based on comparisons with some *Allosaurus* specimens the anterior caudal vertebrae are here considered those that present caudal ribs in a high position in the neural arch (caudal 1–18), mid caudal vertebrae in which the caudal ribs are found in the centrum (caudal 19–25), and posterior caudal vertebrae those posterior to the so-called transition point, in which caudal ribs are absent.

The neural arch is unfused with the centrum in all preserved anterior caudal vertebrae. The most anterior centrum, SHN.036/13, fits well with SHN.036/2, an anterior neural arch (Figure 9(t)). Although they do not articulate due to distortion, we interpret that both elements probably belong to the same vertebra. This centrum is the most robust of the preserved anterior caudal centra and presents a well-developed facet for chevron articulation on the ventral margin and adjacent to the posterior articulation. An anterior facet for a chevron is absent, suggesting that this vertebra probably corresponds to the first caudal. The centrum is almost as long as high and the articular facets are only slightly offset in ventral and lateral views. The articular facets are oval, higher than wide in the first caudal vertebra (SHN.036/13),

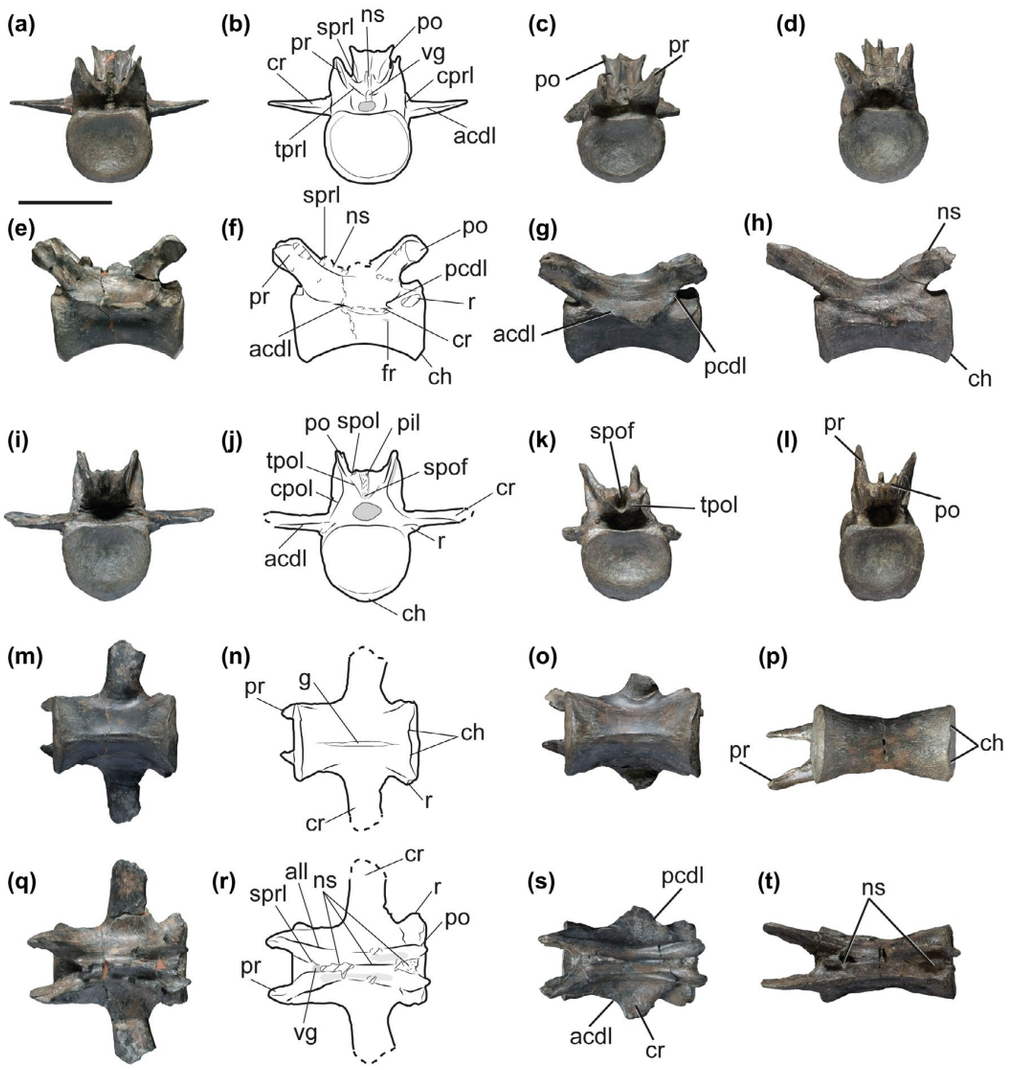

Figure 10. Mid and posterior caudal vertebrae of SHN.036. SHN.036/55 and interpretative line drawing in anterior ((a), (b)), left lateral ((e), (f)), posterior ((i), (j)), ventral ((m), (n)), and dorsal ((q), (r)) views; SHN.036/56 in anterior (c), left lateral (g), posterior (k), ventral (o), and dorsal (s) views; SHN.036/59 in anterior (d), left lateral (h), posterior (l), ventral (p), and dorsal (t) views.
Note: Scale bar = 50 mm.

but almost circular in most posterior elements. The anterior articular facet is strongly concave and the posterior one is almost flat, as is common in caudal vertebrae of most theropods (e.g. Madsen 1976/1993; Rauhut 2005). The lateral surface presents two small foramina near the base of the neural arch and within a shallow pleurocentral depression. The pleurocentral depression gradually disappears to the posterior part of the caudal series. In dorsal view, the neurocentral suture occupies almost the complete width of the dorsal surface of the centra at their mid-length. The ventral surfaces of the most anterior preserved caudal centra (e.g. SHN.036/13) are transversely convex but they present a low longitudinal ridge, more pronounced adjacent to the articular facets, in most posterior centra (e.g. SHN.036/51).

The anterior neural arch preserves the prezygapophyses and almost complete caudal ribs, but neither the postzygapophyses nor the neural spine. The prezygapophyses are short, robust and the articular facets are dorsomedially projected. Two ventral and divergent laminae project from the prezygapophyses, delimiting a broad triangular opening above the neural canal that corresponds to the hypantrum. The presence of hyposphene-hypantrum articulation in caudal vertebrae is an unusual character for allosauroids. This structure is generally absent in *Allosaurus*, but is present at least in the first two caudal vertebrae of SMA 0005 (Evers 2014). A well-marked spinoprezygapophyseal lamina (sprl) projects from the dorsolateral margin of the prezygapophyseal articulation and would connect with the ventral part of the neural spine, bounding a narrow and deep spinoprezygapophyseal fossa (sprf). The caudal ribs are robust, aliform and project posterolaterally from about the mid-length of the neural arch, with a sub-horizontal orientation. The distal tip of the caudal ribs

is slightly expanded anteroposteriorly and their bases are oval in cross-section. There are two poorly defined laminae on the ventral surface of the caudal ribs projecting along each the anterior and posterior margin, which are interpreted as corresponding to the acdl and pcdl, respectively. These laminae delimit a pair of shallow concavities on the anterior and posterior part of the ventral surface of the ribs that might correspond to the prezygapophyseal and postzygapophyseal centrodiapophyseal (prcdf and pocdf), respectively.

The other anterior caudal centra have both anterior and posterior facets for articulation with chevrons. The posterior chevron facets are much more developed than the anterior ones, as is typical in the caudal series of other allosauroids (e.g. Gilmore 1920; Madsen 1976/1993; Chure 2000). All the anterior caudal centra present small vascular foramina in the dorsal end of the lateral surfaces. These foramina are also present in some mid and posterior caudal vertebrae.

The mid and posterior caudal vertebrae preserve the centrum fused with the neural arch (Figure 10). These elements are interpreted as corresponding to a position between the twentieth and twenty-eighth caudal vertebrae. These vertebrae have elongated centra, with an elongation index between 1.95 and 2.96. One mid caudal vertebra (SHN.036/54) has oval articular facets that are slightly higher than wide, but in most posterior vertebrae the articular facets are more sub-circular. Both the anterior and posterior articular facets are slightly concave. In some mid caudal vertebrae the ventral surface has a longitudinal, shallow groove bounded by low crests. The caudal ribs are sub-horizontal, posterolaterally projected, and not distally expanded. The prezygapophyses are short in some mid caudal vertebrae, extending only slightly beyond the anterior articular facet but they progressively increase in length to the posterior part of the tail.

In the most posterior preserved caudal vertebrae the prezygapophyses extend for more than half of the centrum length. The centroprezygapophyseal lamina (cprl) arises from the anterolateral surface of the prezygapophysis and extends posteroventrally to the lateral surface of the centrum, almost connecting with the base of the caudal rib. Dorsal to the cprl the lateral surface of the prezygapophysis presents a deep concavity that occupies almost its entire length. This concavity becomes progressively restricted to the base of the prezygapophyseal process towards the posterior end of the caudal series. A lamina extends along the dorsal margin of the prezygapophyses and connects at about the mid-length of the neural arch with another lamina that extends along the dorsal surface of the postzygapophyses; this last lamina is interpreted as the lateral spol (lat. spol, *sensu* Wilson 2012). The first described lamina is interpreted as the 'additional lateral lamina' described by Rauhut (2011) in caudal vertebrae of theropods from the Tendaguru Formation (Figure 10(r)). The additional lateral lamina and the lat. spol form an almost continuous lamina, especially in the mid caudal vertebrae, delimiting a shallow longitudinal concavity lateral to the neural spine.

In some mid caudal vertebrae (e.g. SHN.036/55) there is a vertical groove between the prezygapophyses that connects the neural canal with the sprf. This groove is not present in most posterior vertebrae and instead a well-developed intraprezygapophyseal lamina (tprl) delimits the sprf ventrally. In some mid caudal vertebrae (e.g. SHN.036/54) a small sprl is visible, projecting from the medial surface of the prezygapophyseal process. The postzygapophyses are short, extending only slightly beyond the posterior articular facet of the centrum in all preserved vertebrae.

A small spinopostzygapophyseal fossa (spof), delimited ventrally by the tpol and laterally by the spol, is preserved in some mid and posterior caudal vertebrae (e.g. SHN.036/55-57). In some vertebrae, the well-developed cpol projects from the ventral surface of the postzygapophyses and connects with the posterior margin of the caudal ribs. Fragments of neural spines are present on almost all preserved vertebrae. The neural spine of the mid caudal vertebrae is low, placed posteriorly and has a small anterior process that arises between the prezygapophyses.

The lateral surface of some vertebrae presents a pair of sharp ridges at the level of the dorsal margin of the posterior articular facet. These ridges project posterolaterally almost to the level of the base of the pcdl but do not connect with this lamina, and they disappear in most posterior elements.

Chevrons. There are seven almost complete chevrons and several other fragments (Figure 11). These elements are interpreted as corresponding to anterior and mid chevrons based on the absence of a marked distal expansion and the roughly straight to slightly curved shaft. The most complete chevrons of SHN.036 are similar to those between the first and fifteenth caudal vertebrae of other allosauroids (e.g. Madsen 1976/1993; Chure 2000). The most anterior chevrons present almost straight shafts, but the elements become more curved toward the distal part of the tail. The haemal canal is very large and delimited dorsally by a bridge of bone that forms part of the articulation between the chevron and the caudal vertebrae. The anterior surface of some chevrons preserves a pair of well-developed anterior processes that project anterodorsally, surrounding the haemal canal.

Pelvic girdle

The pelvic girdle is represented by an almost complete right ilium, fragments of the left ilium (including portions of the postacetabular process and of both pubic and ischial peduncles), and both pubes and ischia.

Ilium. The right ilium, SHN.036/80 (Figure 12(a)–(c)), is almost complete, although somewhat fractured, mostly at the ends of both the pre- and post-acetabular processes. The ilium has a high and relatively short profile. The anterior margin of the preacetabular process is broken but the preserved dorsal margin is smoothly convex. The preacetabular process projects ventrally from the lateral surface of the ilium, forming a board notch with the anterior margin of the pubic peduncle. The ventral margin of the preacetabular process presents a shallow cupedicus fossa, which is bounded laterally by a ventral lamina of the preacetabular process. The most anterior margin of the preacetabular process is almost at the level of the anterior border of the pubic peduncle.

The postacetabular process has its posterior margin broken above the brevis fossa. However, it is possible to verify that this process is somewhat longer than the preacetabular process. It is also possible to infer the morphology of the brevis fossa based on a portion of the proximal end preserved in the right ilium and the distal end preserved in a fragment of the postacetabular process of the left ilium (Figure 12(d)–(f)). Robust medial and lateral

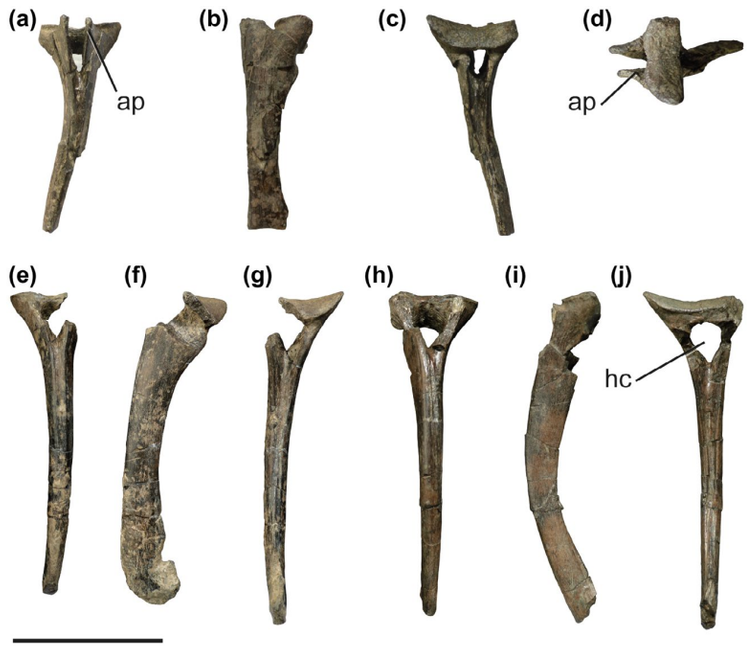

Figure 11. Chevrons of SHN.036. SHN.036/64 in anterior (a), left lateral (b), posterior (c), and dorsal (d) views; SHN.036/68 in anterior (e), left lateral (f), and posterior (g) views; SHN.036/65 in anterior (h), left lateral (i), and posterior (j) views.
Note: Scale bar = 50 mm.

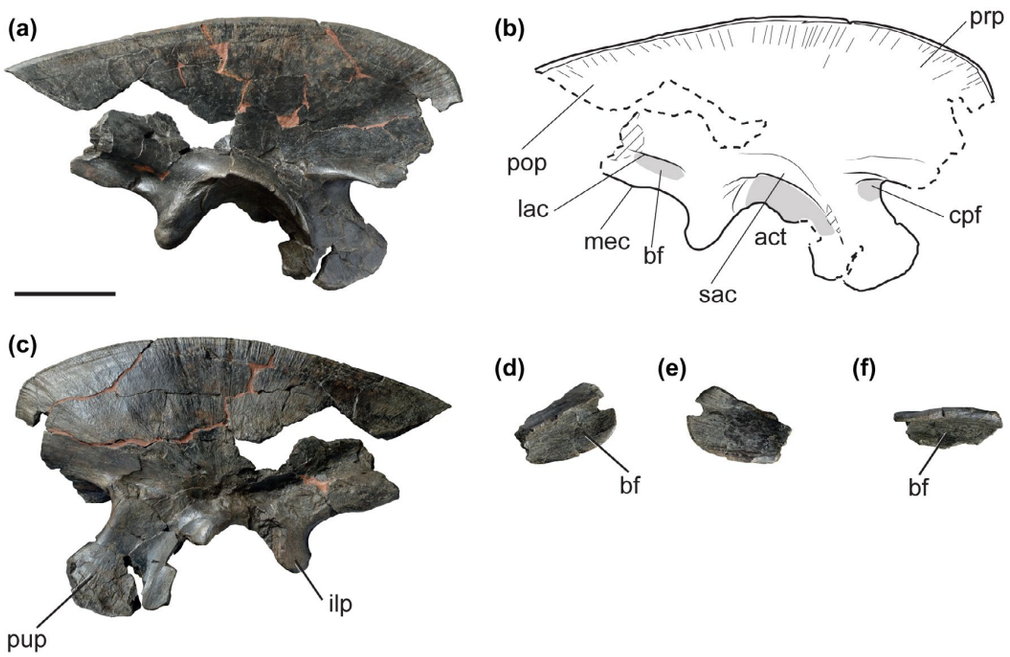

Figure 12. Ilia of SHN.036. Right ilium, SHN.036/80, and corresponding interpretative line drawing in lateral ((a), (b)) and medial (c) views; fragment of the postacetabular process of the left ilium, SHN.036/81, in lateral (d), medial (e), and ventral (f) views.
Note: Scale bar = 100 mm.

crests extending along the ventral margin of the postacetabular process bound the deep and transversely wide brevis fossa. Because the lateral crest is dorsoventrally shorter than the medial one the brevis fossa is well visible in lateral view. The medial and lateral crests project nearly parallel so the brevis fossa has almost the same transverse width along its entire length.

The dorsal border of the iliac blade is roughly straight along most of its length with a slightly ventral deflection toward the posterior part of the ilium. The lateral surface of the iliac blade bears a poorly-defined, broad and shallow concavity bounded by a series of thin, radial striations (= lateral fossa of Benson 2010). The iliac blade is poorly preserved but it is possible to observe a weak vertical swelling extending dorsally from the dorsal margin of the supraacetabular crest into the lateral fossa. Three small foramina are present on the lateral surface of the iliac blade, one near the base of the pubic peduncle dorsally to the supraacetabular crest, another adjacent to the preacetabular notch, and a third at the base of the brevis fossa.

The pubic peduncle is roughly triangular in lateral view and projects anteroventrally. It is much deeper and longer than the ischial peduncle. The articular facet of the pubic peduncle is somewhat concave and anteroposteriorly expanded. The distal end of the pubic peduncle is about 2.7 times as long as wide. The ischial peduncle projects ventrally and slightly posteriorly. It has a strongly convex articular surface and an oval cross-section that is slightly wider than long. The supraacetabular crest is very prominent and projects strongly laterally and somewhat ventrally, occluding the anterodorsal part of the acetabulum in lateral view. This crest arises from about the mid-height of the pubic peduncle to the level of the base of the ischial peduncle.

The medial surface of the iliac blade is slightly convex having a series of well-marked radial striations, and some poorly defined rough areas that correspond to the attachment scars for sacral ribs and vertebrae. However, because this lamina is strongly fractured and distorted it is not possible to know the number of attachment scars.

Pubes. Almost complete left and right pubes (SHN.036/82, Figure 13(a)–(j)) are known for the Valmitão specimen. The pubic diaphysis is straight, but its proximal end is slightly concave and projects posteriorly. The diaphysis has a teardrop-shaped cross-section as a result of a circular diaphysis and a prominent medial symphysis. The left pubis has a small but well-defined vertical bulge near the proximal part of the lateral surface of the diaphysis, which is bounded posteriorly by a deep groove and has a series of thin vertical striations on its surface. The medial symphysis originates proximally at the medial margin of the pubic posterior surface and migrates to the anterior surface distally. The symphysis forms a blade and extends for almost the entire length of the diaphysis, ending just proximal to the distal expansion of the pubis, thus forming a small distal fenestra above the pubic boot. Proximally, the medial symphysis projects dorsally and somewhat posteriorly. The proximal end of the pubis is well anteroposteriorly expanded and relatively narrow transversely. The iliac articulation is broad, with a slightly concave facet and located in the anterodorsal surface of the pubic proximal end. The ischial articulation is located on a transversely thin process that projects ventrally from the posterior surface of the pubic proximal end. This articular facet is almost flat and faces posteromedially. The ischial process delimits a broad obturator notch that opens ventrally. Ventrally to the ischial process, a dorsal projection of the medial symphysis forms the ventral margin of a large pubic fenestra opening posteriorly. Although the ischial process and the dorsal extension of the symphysis are broken, it seems very unlikely that the fenestra was closed. The proximal end of the pubis presents a low but sharp pubic tubercle extending dorsomedially from the anterolateral surface of the pubic diaphysis to the anterior margin of the iliac process.

The distal ends of both pubes are fused, forming a well-developed pubic boot. The posterior expansion of the pubic boot forms an angle of about 70° with the diaphysis. The length of the pubic boot is about 68% the length of the pubic diaphysis. The pubic boot is triangular in lateral and distal views and is strongly anteroposteriorly expanded, with the posterior process more developed than the anterior process. The anterior process of the pubic boot is wide and projects somewhat laterally with the anterior surface almost flat. Both right and left components of the pubic boot are not fully fused, being separated anteriorly by a deep sulcus, which results in a Y-shape in anterior view to this distal pubic expansion. The pubic boot strongly tapers posteriorly, forming a rounded blunt posterior end.

Ischia. Two almost complete and well preserved ischia (SHN.036/83 and 84), were collected in the Valmitão fossil site. The left ischium has the proximal end broken and only preserves a small fragment of the obturator process (Figure 13(k)–(n)). On the other hand, the right ischium is almost complete and well preserved (Figure 13(o)–(y)). The ischial diaphyses are almost straight in lateral view and their length is approximately the same as the length of the pubic diaphysis. The proximal end projects laterally, giving the ischium a strongly concave and curved appearance in posterior and anterior views. The distal end is slightly expanded and has a roughly triangular cross-section. The medial surface of the distal end is flat and rugose, suggesting that both ischia would be firmly attached in this area. The distal margin of the distal expansion is strongly convex and semicircular.

The proximal end of the ischium is anteroposteriorly expanded and supports two processes, the iliac and pubic processes. The iliac process has a crescent shape in proximal view with strongly convex lateral margin and almost straight medial surface. From the posterior border of the iliac process originates a conspicuous ischial tuberosity that projects ventrally along about 1/4 the length of the diaphysis. Adjacent to this crest and in the lateral surface of the ischium there is a shallow longitudinal concavity. The pubic process is a relatively long ramus with triangular cross-section and that projects anterodorsally. The pubic articulation is almost flat but notably rugose. The acetabular margin is strongly concave and anteroposteriorly long. Ventral to the pubic process, the right ischium preserves a small fragment of the obturator process, which forms a thin blade that is broken both dorsal and ventrally. Between the pubic process and the dorsal margin of the obturator process is a large incision that opens anteroventrally. The ventral end of the obturator process is broken in the right ischium, and just a small fragment of this process is preserved in the left one. Therefore, it is not possible to verify the presence of a notch between the obturator process and the ischial diaphysis. Medially, the ischium presents a low lamina extending longitudinally for about 3/4 the length of the diaphysis. This lamina articulates with a correspondent groove on the opposite ischium, but they do not form an actual medial symphysis. The medial surface of the ischium presents several thin grooves and ridges proximodistally oriented over most of

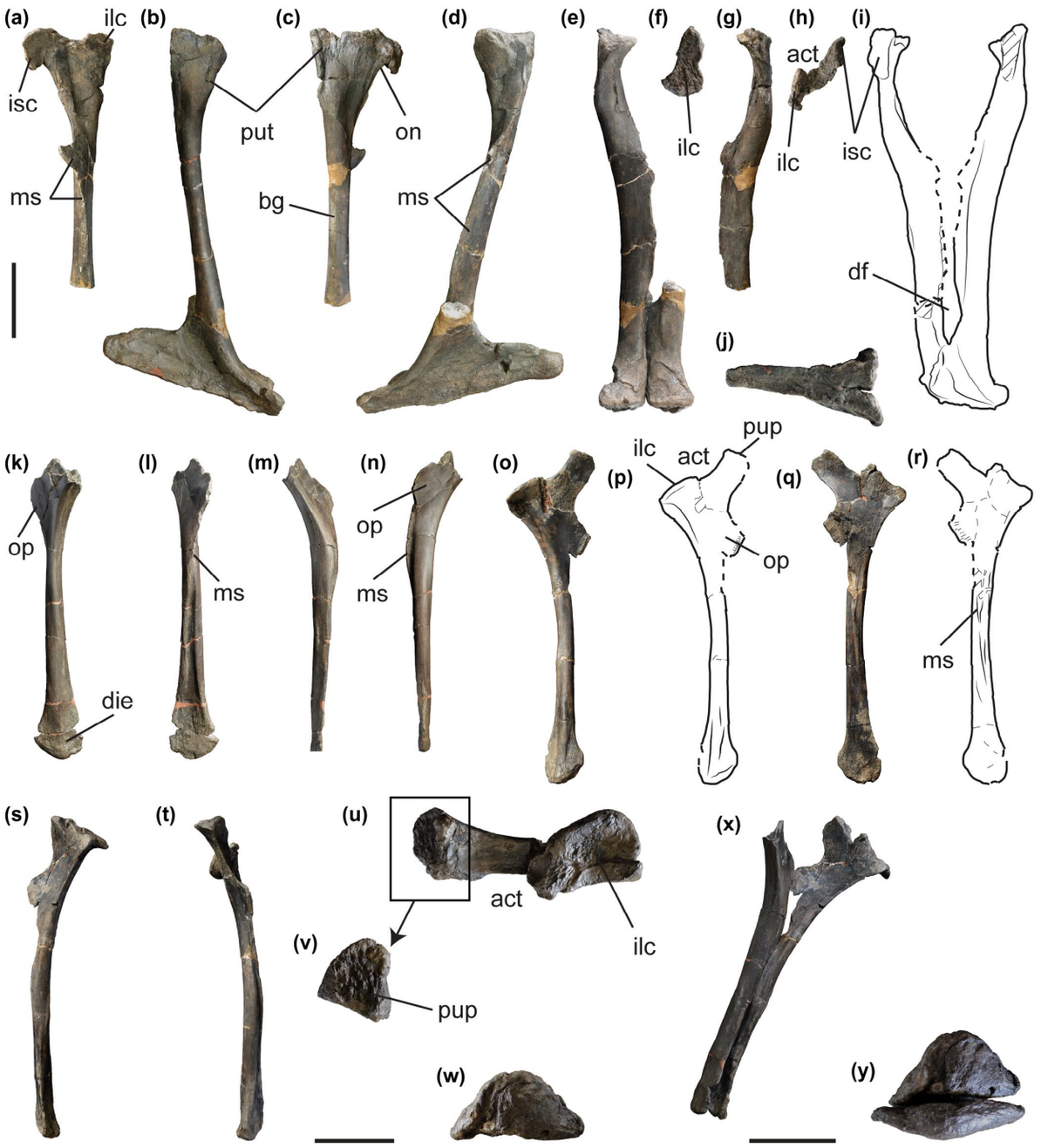

Figure 13. Pelvic elements of SHN.036. ((a)–(j)), pubes, SHN.036/82; ((k)–(y)), ischia; partial left pubis in medial (a), lateral (c), anterior (g), and proximal (h) views; right pubis articulated with a distal fragment of the left pubis in lateral (b), medial (d), anterior (e), proximal (f), and distal (j) views; interpretative line drawing of the complete pubes in posterior view (i); left ischium, SHN.036/83, in lateral (k), medial (l), posterior (m), and anterior (n) views; right ischium, SHN.036/84, and corresponding interpretative line drawing in lateral ((o), (p)), medial ((q), (r)), posterior (s), anterior (t), proximal ((u)–(v)), and distal (w) views; articulated ischia in posterolateral (x) and distal (y) views.
Notes: Scale bars ((a)–(t)) = 100 mm; ((u)–(y)) = 50 mm.

its area. These are especially evident along the proximal end of the medial lamina.

Other theropod remains from the Valmitão fossil site

Three small teeth were collected in the same site as the previously described post-cranial elements. These teeth correspond to shed teeth and are here described as part of the theropod fauna from the Valmitão fossil site.

Two of these teeth, SHN.36/30 and 31 (Figure 14(a)–(i)) present similar morphologies and compatible size, and are here tentatively related to the same specimen. The third tooth SHN.36/32 (Figure 14(j)–(r)) is smaller and presents a somewhat distinct

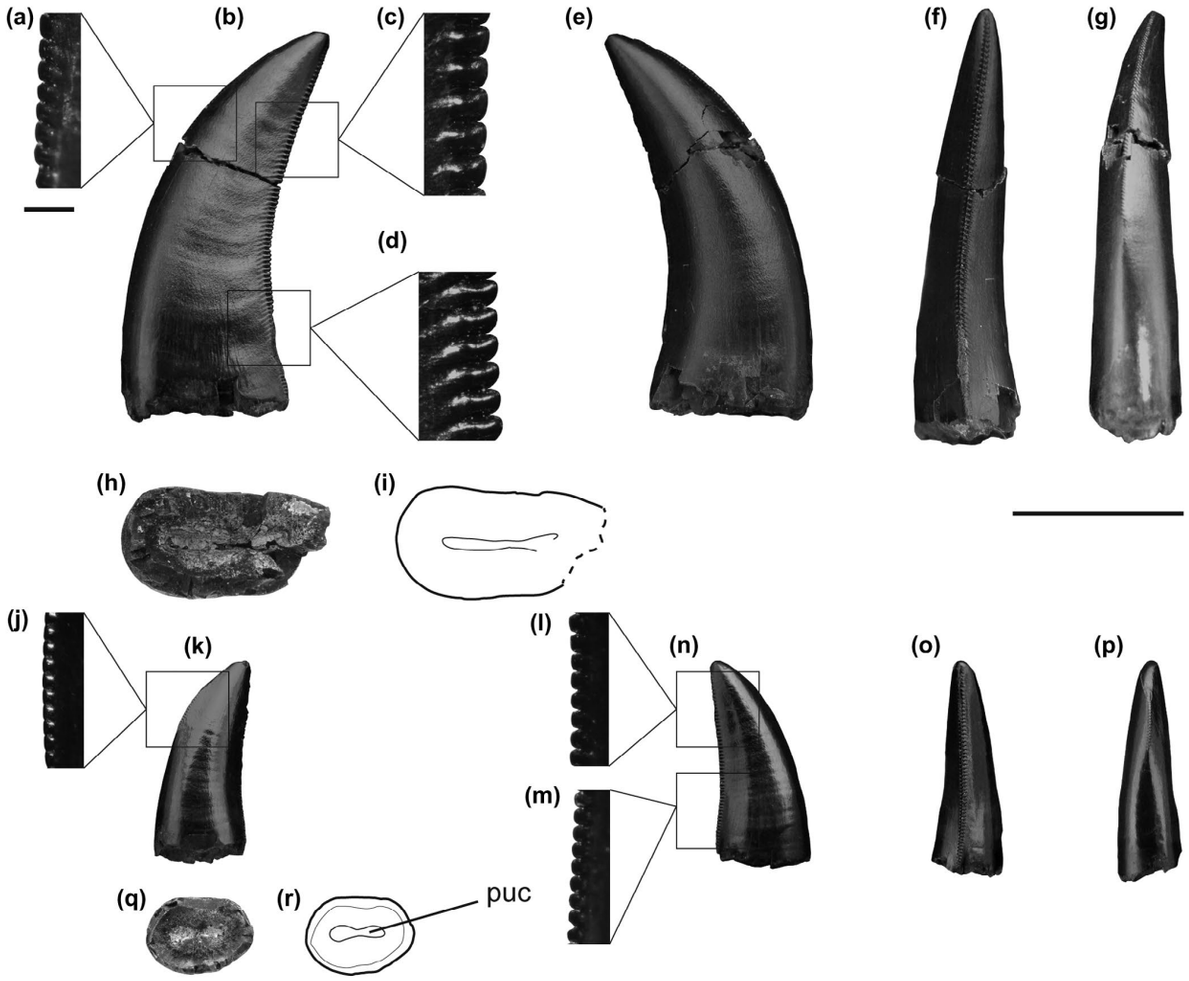

Figure 14. Theropod teeth collected in the Valmitão fossil site and possibly associated with the postcranial elements of SHH.036. Tooth, SHN.036/31, mesial denticles (a), crown in lingual view (b), distal denticles ((c), (d)), crown in labial view (e), crown in distal view (f), crown in mesial view (g), and cross section of the crown base and corresponding interpretative line drawing ((h), (i)); tooth, SHN.036/32, mesial denticles (j), crown in labial view (k), distal denticles ((l), (m)), crown in lingual view (n), crown in distal view (o), crown in mesial view (p), cross section of the crown base and corresponding interpretative line drawing ((q), (r)).
Notes: Scale bars ((b), (e)–(i), (k), (n)–(r)) = 1 mm; ((a), (c)–(d), (j), (l)–(m)) = 10 mm.

morphology, which may suggest that it belongs to a different individual, but it is also possible that these differences were related with the position in the tooth row.

The teeth present the ziphodont condition typical of lateral teeth in most theropod dinosaurs. The crowns are relatively small, with a height (CH) < 25 mm and mesiodistal length (CBL) between 5.60 and 11 mm (see SOM Table 3). SHN.036/30 and 31 have strongly labiolingually compressed and moderately elongated crowns (Crown Base Ratio, CBR = 1.90–2.48 and Crown Height Ratio, CHR = 4.52–4.07) whereas SHN.036/32 presents a more rounded cross-section at the crown base (CBR = 1.44; CHR = 3.17). Both mesial and distal carinae present small denticles. The distal carina extends to the base of the crown, but the mesial one ends at about the mid-height or 1/3 of the crown height. SHN.036/30 and 31 present an average of 22 denticles per 5 mm at the mid-height of mesial carinae and 18.5 in the distal ones. In SHN.36/32, the denticles are smaller with an estimated count of 25 denticles per 5 mm in the mesial carina and 23 in the distal one. The denticles are rectangular, with the major axis mesiodistally oriented, and slightly rounded apices. All denticles are perpendicular to the carina and present reduced interdenticular space. The distal denticles are slightly larger at the mid-height of the carina, decreasing in size towards the base and the apex of the crown. In lateral view, the mesial carinae are convex and the distal ones are concave, both positioned almost symmetrically with respect to one another, i.e. the mesial and distal carinae are situated in the mesial and distal surfaces respectively. The lingual and labial surfaces are slightly convex mesiodistally and the crowns have lanceolate cross-sections (*sensu* Hendrickx et al. Forthcoming). The enamel has slight irregular texture, but does not present wrinkles between denticles. In some teeth shallow transverse undulations are visible, extending between the carinae

on both lingual and labial surfaces. SHN.036/32, presents a small wear facet on the apical tip extending slightly on the lingual surface.

The morphology of the isolated teeth collected in the Valmitão fossil site is compatible with lateral teeth of basal tetanurans. They have a slightly higher number of denticles on the distal carina than the lateral teeth of *Allosaurus* (Hendrickx et al. 2015). However, a decreasing in the number of denticles through ontogeny is a character recognized in other allosauroids (Canale et al. 2014).

Phylogenetic analysis

A cladistic analysis was performed, using the data matrix of Carrano et al. (2012). The data matrix includes 37 taxa (*Herrerasaurus* as the outgroup) coded in 351 unordered and equally weighted characters. A total of 53 characters were coded for SHN.036, 20 corresponding to the axial skeleton and the remaining 33 to the pelvic girdle. TNT v1.1 (Goloboff et al. 2008) was used to search for most-parsimonious trees (MPTs). The resulting data matrix was analyzed under a traditional tree search, performing1000 replications of Wagner trees (using random addition sequences), followed by tree bisection reconnection as swapping algorithm and saving 100 trees per replication. A new analysis was performed using a modified version of Carrano et al. (2012) data matrix, to which 32 characters from Novas et al. (2013), 1 character from Benson (2010), 5 characters from Brusatte and Sereno (2008), and 1 character from Eddy and Clarke (2011) were added (see SOM Appendix 1 and 2).

Results

The analysis of the data matrix of Carrano et al. (2012) recovered 440 MPTs with lengths of 866 steps [Consistency Index (CI) = 0.477, Retention Index (RI) = 0.633]. The present analyses (Figure 15(a)) recovered SHN.036 as a basal Tetanurae, a poorly resolved group containing a polytomy that includes SHN.036, *Fukuiraptor*, *Lourinhanosaurus*, *Neovenator*, *Allosaurus*, megalosauroids, metriacanthosaurids, carcharodontosaurids, the Megaraptora *Megaraptor* + *Aerosteon* and the coelurosaurs *Compsognathus* + *Ornitholestes*. The analysis of the modified version of the Carrano et al. (2012) data matrix recovered 130 MPTs with lengths of 961 steps [CI = 0.465; RI = 0.606]. This hypothesis (Figure 15(b)) shows a higher resolution within Avetheropoda. SHN.036 is placed as a member of Allosauroidea within a group containing *Allosaurus*, *Lourinhanosaurus* and Carcharodontosauridae in a politomy. This group represents the sister clade to *Szechuanosaurus* plus Metriacanthosauridae (*Siamotyrannus*, *Metriacanthosaurus*, *Yangchuanosaurus* and *Sinraptor*).

SHN.036 is assigned to Tetanurae based in the presence of a much larger pubic peduncle of the ilium relative to the ischial peduncle (>130%), and a pubic peduncle length to width ratio >1. Within tetanurans this specimen shares with Allosauroidea the strong constriction of posterior dorsal central, the rounded morphology of the ischial peduncle of the ilium, the presence of a fossa cuppedicus in the ilium, and an ischium length more than 80% the pubis length. SHN.036 shares with the group containing *Lourinhanosaurus*, *Allosaurus* and Carcharodontosauridae the presence of a large medial fenestra above the pubic boot, the distal expansion of the pubis with well-developed anterior component, the length of the pubic boot being more than 30% the length of the diaphysis, and the presence of a posteriorly-directed flange on the iliac peduncle of the ischium. The cladistic analysis recovered four autapomorphies for SHN.036, the flat ventral surface of anterior caudal vertebrae (shared with *Herrerasaurus*, *Elaphrosaurus*, and *Concavenator*), the anterior and mid chevrons with unexpanded distal end (shared with *Ceratosaurus*, *Majungasaurus*, *Dubreuillosaurus*, *Lourinhanosaurus*, *Concavenator*, *Megaraptor*, and *Compsognathus*), the large supraacetabular crest of the ilium (shared with *Herrerasaurus*, most ceratosaurians, *Cryolophosaurus*, and *Fukuiraptor*), and the straight morphology of the ventral margin of the pubic boot with the anterior process placed at the same level as the posterior process.

Discussion

SHN.036 is a small-sized, juvenile specimen, which is relatively complete and well-preserved. The size of the most complete elements of SHN.036, especially those of the pelvic girdle, are less than half (about 40%) the size of the correspondent elements of adult *Allosaurus* specimens (e.g. USNM 4734 or USNM 740) and about 60% the size of DINO 11541 (Gilmore 1920; Chure 2000). Based on this comparison the size of SHN.036 is estimated in about 3–3.5 m in length.

This specimen was preliminarily assigned to *Allosaurus* although some differences with respect to *A. fragilis* were identified, which were interpreted as being related to ontogeny (Malafaia, Ortega, Silva, Escaso, & Dantas 2008). However, a more comprehensive analysis of the specimen based on the review of *Allosaurus* individuals in different ontogenetic states suggests that some of these differences fall outside the range of variability related to ontogeny known for this taxon.

The new specimen differs from *Allosaurus* in several aspects mainly related with the morphology of the axial elements. The position of the anterior surface of the axial intercentrum projecting roughly horizontal with respect to the ventral surface of the axis centrum, whereas it projects dorsally in *Allosaurus* as well as in most other allosauroids, including *Sinraptor*, *Neovenator*, *Acrocanthosaurus*, and *Giganotosaurus* (Gilmore 1920; Currie & Zhao 1993; Chure 2000; Currie & Carpenter 2000; Brusatte et al. 2008). SHN.036 shares this character with more primitive theropods such as *Ceratosaurus*, *Dilophosaurus* and *Piatnitzkysaurus* (Madsen & Welles 2000; Zhao et al. 2010). Also, the position of the parapophysis in the ventral surface of the axis contrasts with those of *Allosaurus*, *Sinraptor*, and *Neovenator*, in which the parapophyses are situated in the lateral surface of the centrum (Gilmore 1920; Currie & Zhao 1993; Brusatte et al. 2008). The centrum of the axis is shorter in the Valmitão specimen (ratio maximum anteroposterior length: minimum mediolateral width = ca. 1.31), but this element is considerably elongated (ratios between 3.4 and 2.75) in *Allosaurus* (e.g. USNM 8367 and 4734: Gilmore 1920). Finally, the ventral surface of the axis is flat in SHN.036, similar to that of *A. fragilis,* but the specimen DINO 11541 presents a ventral keel (Gilmore 1920; Chure 2000). Other distinctive characters between SHN.036 and *Allosaurus* are the absence of ventral keel on anterior dorsal vertebrae, and

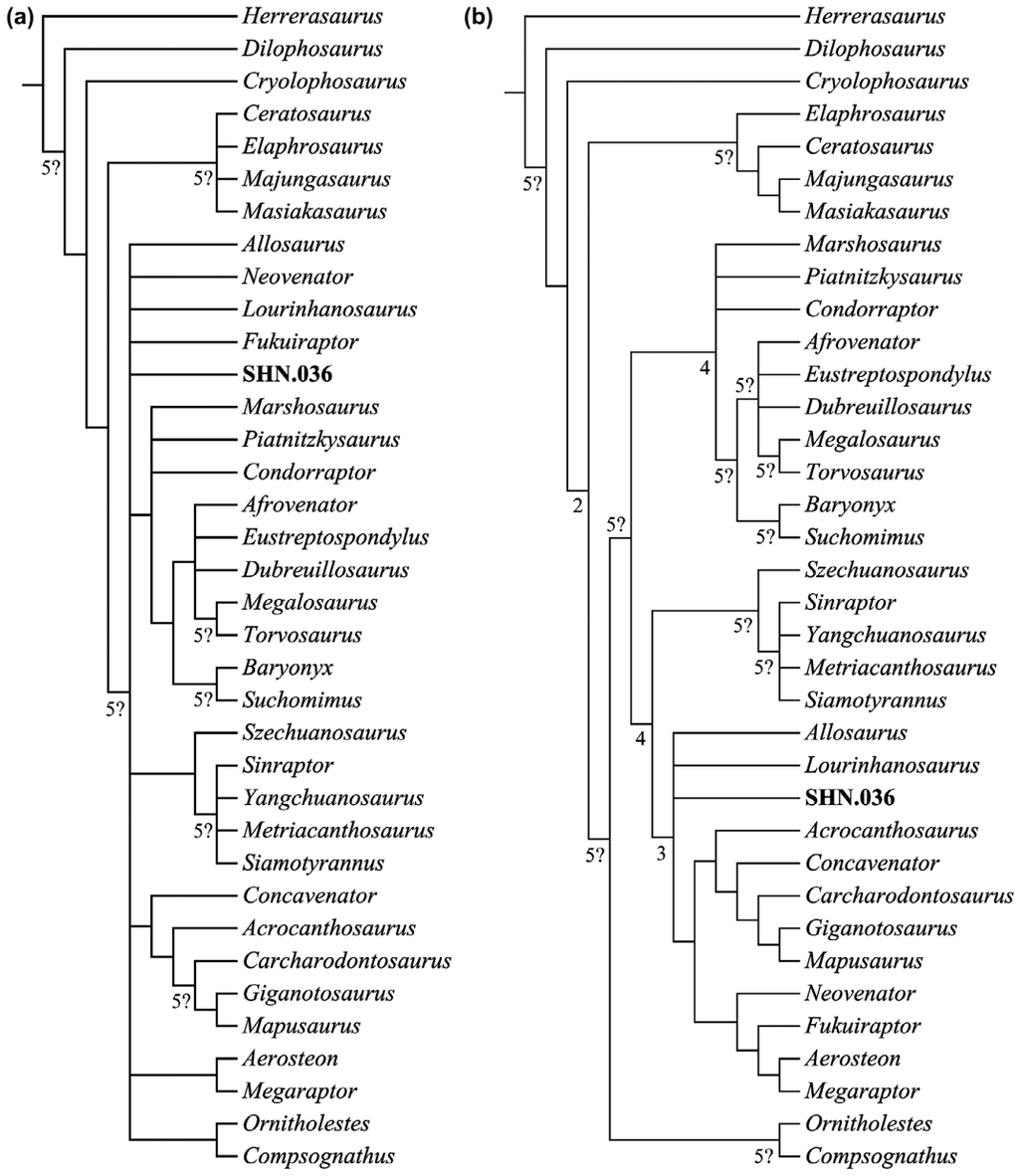

Figure 15. Phylogenetic relationships of SHN.036. (a) strict consensus cladogram from 440 most parsimonious trees recovered by the analysis of the data matrix of Carrano et al. (2012) [Tree length = 866 steps; CI = 0477 and RI = 0633]; (b) strict consensus cladogram from 130 most parsimonious trees recovered by the analysis of the modified version of the data matrix of Carrano et al. (2012) [Tree length = 961 steps; CI = 0465 and RI = 0606].
Note: The numbers in the nodes represent the absolute Bremer support values.

the triangular morphology of the hypantrum. Also, the presence of hyposphene-hypantrum articulation in at least one anterior caudal vertebra is an unusual character for *Allosaurus*, but this feature is present in the anteriormost elements of SMA 0005 (Evers 2014). In *Allosaurus*, most anterior dorsal vertebrae present well-developed ventral keels (Gilmore 1920; Chure 2000). The presence of keels on the ventral surface of posterior cervical and anterior dorsal vertebrae is also reported in several other tetanurans, including *Afrovenator*, *Baryonyx*, *Torvosaurus*, *Sinraptor*, *Giganotosaurus*, and *Mapusaurus* (Carrano et al. 2012). On the other hand, the presence of low and poorly-defined ventral keel on anterior dorsal centra is considered an autapomorphy for *Neovenator* (Brusatte et al. 2008).

The triangular morphology of the hyposphene in the dorsal vertebrae of SHN.036 contrasts with the sheet-like structure of most tetanurans (e.g. *Allosaurus*, *Neovenator*, and *Acrocanthosaurus*) and *Carnotaurus*, but is more similar to that of *Sinraptor*, *Piatnitzkysaurus* or *Torvosaurus* (Currie & Zhao 1993; Brusatte et al. 2008). Also a hyposphene–hypantrum articulation is mostly absent in the caudal series of *Allosaurus,* but this articulation persist in the tail of some specimens as is also the case in more primitive forms such as *Monolophosaurus* and

Sinraptor, and in some more derived allosauroids, including *Neovenator* (Currie & Zhao 1993; Brusatte et al. 2008; Zhao et al. 2010; Evers 2014).

SHN.036 has an unusual morphology in mid caudal centra with a pair of well-developed lateral crests projecting from the dorsal margin adjacent to the anterior articular facet. Similar crests are present in some allosauroids, including some *Allosaurus* specimens (BYU 725/13259: E.M. pers. obs. 2010; DMNH 2149: Rauhut 2011) but are usually much less developed. Similarly developed crests are present in another specimen from the Portuguese Upper Jurassic (SHN.019: Malafaia et al. 2007) and in the carcharodontosaurid *Veterupristisaurus milneri* from the Tendaguru Formation (Rauhut 2011). However, the morphology of these crests in SHN.036 is distinct from that of *Veterupristisaurus* because in the latter they are placed on the neural arch at the level of the base of the prezygapophyses and connect with the anterior margin of the caudal rib, whereas in the Portuguese specimen they project from the dorsal margin of the articular facet and do not reach the dorsal rib. The specimen from Valmitão shares with *Veterupristisaurus* the presence of sprl in the mid caudal vertebrae extending from the medial surface of the base of the prezygapophysis and being flanked laterally by an additional lateral lamina (*sensu* Rauhut 2011).

The pelvic elements of SHN.036 present morphologies similar to that of *Allosaurus* but they are distinct in several details. The ilium is roughly oval in outline with a strongly convex dorsal margin, and it is relatively short anteroposteriorly, which is somewhat distinct from the almost straight and elongated ilium of some *Allosaurus* specimens (Gilmore 1920; Madsen 1976/1993; Chure 2000). Another unusual character of the ilium of SHN.036 is the supraacetabular crest that forms a prominent ventrolaterally projecting shelf. This morphology is similar to the hypertrophied supraacetabular crest present in *Monolophosaurus* and some nontetanuran theropods such as *Ceratosaurus* and *Dilophosaurus* (Zhao et al. 2010; Carrano et al. 2012). However, in SHN.036, this crest projects only slightly ventrally whereas in *Monolophosaurus* the ventral component overlaps the anterodorsal region of the acetabulum in lateral view. Some small *Allosaurus* specimens (e.g. UUVP 10 863: E.M. pers. obs. 2010) have a more oval, shorter and higher, morphology of the ilium and with well-developed supraacetabular crest, more similar to that of SHN.036, suggesting that these features are related with intraspecific variation.

Comparison of SHN.036 with other allosauroids from the Portuguese Upper Jurassic

The currently known Portuguese Upper Jurassic record of theropod dinosaurs includes at least two allosauroid taxa: *Allosaurus* and *Lourinhanosaurus* (e.g. Mateus 1998; Mateus et al. 2006; Pérez-Moreno et al. 1999). Among these, *Allosaurus* is the most abundant and well known taxon in this territory, being represented by several fairly complete specimens, including cranial and postcranial partial skeletons. Some *Allosaurus* specimens found in the Portuguese record were assigned to the well-known, typical North American species *A. fragilis* (Pérez-Moreno et al. 1999; Malafaia et al. 2010), but other more recent findings were interpreted as belonging to a new and exclusive species, *A. europaeus* (Mateus et al. 2006). A review of the *Allosaurus* specimens from the Upper Jurassic of the Lusitanian Basin is in progress, but a comparison between SHN.036 and the currently known Portuguese *Allosaurus* specimens was performed. *A. europaeus* is represented by a partial skull and a series of cervical vertebrae collected in Praia de Vale Frades (Lourinhã). Unfortunately, there are no overlapping elements that allow its comparison with the Valmitão specimen. The species *A. fragilis* was first identified in the Portuguese Upper Jurassic based on an almost complete pelvic girdle and partial hind limbs collected in the Andrés fossil site, near Pombal (Pérez-Moreno et al. 1999). Subsequently a large collection of other osteological remains assigned to *Allosaurus* was found in the same quarry, including a fairly complete skull (Malafaia et al. 2010). Overlapping elements between SHN.036 and these *Allosaurus* specimens include the atlantal intercentrum, dorsal, sacral and caudal vertebrae, dorsal ribs, chevrons, ilium, ischium and pubis. Some differences may be verified between SHN.036 and the specimens from Andrés, including the absence of a ventral keel in anterior dorsal vertebrae and the higher and shorter morphology of the ilium in the former. Also the pubes differ in some details, such as the dorsally projected anterior component of the pubic boot in the specimen from Andrés, whereas in SHN.036 the boot is straight in distal view, and the strong dorsal projection of the medial symphysis of the pubes from Valmitão, which is not present in those from Andrés.

Lourinhanosaurus antunesi was based on a specimen (ML 370) collected in Peralta (Lourinhã) that includes cervical, dorsal, sacral and caudal vertebrae, cervical and dorsal ribs, chevrons, an almost complete pelvic girdle, and elements of the hind limbs, including partial femora, right tibia and fibula and a fragment of a metatarsal (Mateus 1998). Several elements of the specimen are preserved in anatomic connection and the set of remains was interpreted as corresponding to a single individual. It was originally described as an allosauroid (Mateus 1998) and latter interpreted as a more primitive tetanuran closely related with megalosaurid eustreptospondylins (Mateus 2005; Mateus et al. 2006). Subsequently it was recovered as a member of the basal allosauroid clade Metriacanthosauridae (Benson 2010). An isolated left femur (ML 555) collected in Porto das Barcas (Lourinhã), and a nest with embryonic osteological remains (ML565) found in Paimogo (Lourinhã), were also tentatively assigned to this taxon (Mateus 2005; Hendrickx & Mateus 2012). These specimens were found in sediments interpreted as belonging to the Sobral Formation (*sensu* Manuppella et al. 1999), which is equivalent to the Praia Azul Member of the Lourinhã Formation *sensu* Hill (1988) and is dated from the Kimmeridgian–Tithonian boundary (Fürsich 1981; Manuppella et al. 1999; Schneider et al. 2009). This sedimentary unity overlaps the Praia da Amoreira-Porto Novo Formation in which SHN.036 was collected.

Lourinhanosaurus antunesi is interpreted as an allosauroid based on the absence of an articular groove on the proximal surface of the femoral head and an aliform femoral lesser trochanter (Mateus 1998; Carrano et al. 2012). The species was originally diagnosed based on the follow autapomorphies: vertebral centra longer than tall, neural spines of anterior caudal vertebrae with well-developed spike-like anterior processes, pubic blade perforated by a large vertical ellipsoidal foramen, and femoral lesser trochanter well separated from the main body axis of the

femur in lateral view. The morphology of the lesser trochanter in ML 370 is similar to that of *Allosaurus* and other allosauroids except in the slightly short dorsal extension that may be related with incomplete preservation of the distal end of the trochanter. In addition, a femoral lesser trochanter well separated from the diaphysis in lateral view is a character present in all allosauroids, including *Allosaurus* and *Sinraptor* (Gilmore 1920; Madsen 1976/1993; Currie & Zhao 1993; Chure 2000). Mateus (2005) and Mateus et al. (2006) suggested a close relationship of *Lourinhanosaurus* with the French taxon *Streptospondylus altdorfensis*, based on the presence of bifurcated hypapophysis in the last cervical vertebra (Mateus 2005). The specimen ML 370 presents a low ventral keel that is anteriorly bifurcated in the fifth preserved vertebrae of the cervical series. However, this structure is probably not similar to the well-developed bifurcated ventral keel associated to each hypapophysis present in posterior cervical vertebrae of *Eustreptospondylus* and in the first dorsal vertebrae of *Streptospondylus* (Sadleir et al. 2008; Allain 2001; E.M. pers. obs. 2015).

More recently, the phylogenetic analysis of Benson (2010) recovered *Lourinhanosaurus* as a basal allosauroid and the sister taxon of a clade comprising *Metriacanthosaurus* + *Sinraptor*. Our analysis supports the interpretation of *Lourinhanosaurus* as a member of Allosauroidea, but it is placed at the base of a more derived group comprising SHN.036 + *Allosaurus* + Carcharodon tosauridae, which forms the sister clade of *Szechuanosaurus* + *Si amotyrannus* + *Metriacanthosaurus* + *Yangchuanosaurus* + *Sinra ptor*. *Lourinhanosaurus* shares with *Allosaurus* and most carcharodontosaurids the posterior articular facet of cervical vertebrae being strongly ventrally offset relative to the anterior ones, the presence of a posteriorly-directed flange on the iliac peduncle of the ischium, the small and lobular morphology of the lateral condyle of the tibia, and the high and oblique angle of the dorsal margin of the ascending process of the astragalus. On the other hand, the presence of a fully closed and large fenestra on the proximal end of the pubis is a character shared with *Sinraptor* and distinct from the open notch present in *Allosaurus* and many other allosauroids. However, the fragmentary nature of the specimen does not allow a robust phylogenetic approach and thus it seems more reasonable for the moment to consider *Lourinhanosaurus* as an indeterminate basal allosauroid.

Taxonomic status of SHN.036

The new specimen presents several shared features with Allosauroidea, including the morphology of dorsal centra, which are strongly constricted laterally due the presence of deep pleurocentral depressions, and the overall morphology of the slender pelvic elements. However, as was discussed above, SHN.036 presents also several differences relative to the most common morphology of *Allosaurus* individuals known from both North America and Portugal. Some of these differences may be related with intraspecific variation, including the presence of hyposphene-hypantrum articulation in the anteriormost caudal vertebrae, the short and relatively high morphology of the ilium with a strongly developed supraacetabular crest. However, other features fall outside the range of variability related with intraspecific variation known for this taxon. These features include the absence of ventral keel on anterior dorsal vertebrae, the position of the parapophysis in the ventral surface of the axis, the presence of a pair of large recesses in the neural arch of anterior dorsal vertebra, the sprl projecting from the medial surface of the prezygapophyseal process, and the almost flat ventral surface of the pubic boot with the anterior and posterior processes placed at the same level.

This combination of characters suggests that SHN.036 is closely related to but distinct from *Allosaurus*. Regarding *Lourinhanosaurus* the available elements of SHN.036 do not allow to verify two of the autapomorphies of this taxon due the fragmentary nature of the specimen: all the vertebral centra being longer than tall (this condition is reversed in the preserved anterior dorsal vertebrae of SHN.036) and the presence of well-developed spike-like anterior processes on the neural spines of anterior caudal vertebrae. In addition, the presence of a pubic blade perforated by a foramen, a third autapomorphy of *Lourinhanosaurus*, is not present in SHN.036.

SHN.036 is also distinct of other allosauroids currently known from Europe, such as the basal carcharodontosaurids *Concavenator* and *Neovenator* from the Early Cretaceous of Spain and England, respectively (Naish 1999; Brusatte et al. 2008; Ortega et al. 2010). SHN.036 differs from these taxa in the morphology of the distal end of the ischium, which does not form a boot-like expansion. The ilium of the Portuguese specimen can be distinguished from that of *Concavenator* in the absence of a hook-like ventral process of the preacetabular process. The Portuguese specimen shares some unusual characters with *Veterupristisaurus* from the Upper Jurassic of the Tendaguru Formation, including the sprl projecting from the medial surface of the prezygapophyseal process and the presence of well-developed additional lateral laminae projecting along the dorsal margin of the prezygapophyseal process. However, the general morphology of the mid caudal vertebrae collected in Valmitão is distinct from that of the African taxon in the absence of strongly laterally expanded cprl, forming a broad, funnel-shaped entrance to the neural canal, and the much shallower longitudinal groove in the ventral surface of the centra. Other fossils from the Tendaguru Formation include a right ilium assigned to an indeterminate tetanuran theropod collected in the same sedimentary level as the holotype of *Veterupristisaurus* (Rauhut 2011). The general morphology of this ilium is similar to the ilium of SHN.036. These specimens share the same relative dimensions of the pubic and ischial processes and the broad brevis fossa with sub-parallel medial and lateral margins. However, the outline of both ilia is somewhat distinct being more strongly convex in the African specimen and the cuppedicus fossa is more developed in the Portuguese specimen.

Conclusion

The new specimen, SHN.036, represents a juvenile individual presenting a set of characters that allow to interpret it as a basal allosauroid closely related with other Portuguese taxa, *Lourinhanosaurus* and *Allosaurus*. However, the specimen also presents differences in respect to both taxa, some of which may be related to ontogeny, but others are interpreted as having potential phylogenetic significance. The characters verified in SHN.036 indicate a unique combination of features not present in other taxa known in the Portuguese record or in any other

theropod dinosaur. These features include the position of the parapophysis in the ventral surface of the axis, the absence of ventral keel on the anterior dorsal vertebrae, the presence of a pair of large recesses in the neural arch of anterior dorsal vertebra, the sprl projecting from the medial surface of the prezygapophyseal process, and the almost flat ventral surface of the pubic boot with the anterior and posterior processes placed at the same level.

The discovery of other fossils that would allow a more comprehensive knowledge of *Lourinhanosaurus* and the variability among the Portuguese forms of *Allosaurus* may establish if SHN.036 could be considered as a juvenile individual of one of these taxa, or a member of a new taxon. At the moment, this specimen is considered as an indeterminate allosauroid.

Acknowledgments

We thank to S. Brusatte and O. Rauhut for the comments and suggestions to the paper, to Willi Henning Society for the available free TNT program, to J. J. Santos, M. Cachão and N. Pimentel for field assistance and comments to the paper, to E. Cuesta for photographs of specimens, and for allow accessing specimens to Bruno. C. Silva (SHN), Rui Castanhinha and Carla Tomás (ML), Vanda Santos (MUHNAC), Ronan Allain (MNHN), Luis Chiappe (NHMLAC), Kenneth Carpenter (DMNH), Rodney Scheetz and Brooks Britt (BYU), Mike Getty, Mark Loewen, and Randall Irmis (NHMU), Daniel Chure (DINO), Sandra Chapman (NHMUK), and Paul Jeffery (OUMNH).

Disclosure statement

No potential conflict of interest was reported by the authors.

Funding

This work was supported by the Fundação para a Ciência e Tecnologia (Portugal) under a PhD scholarship [grant number SFRH/BD/84746/2012]; Individual grants to E.M. visits for review collections were financed by the Jurassic Foundation, Fundação Luso-Americana para o Desenvolvimento [grant number L07-V-22/2010]; Synthesys [grant numbers GB-TAF-2160, FR-TAF-4911]; and also supported by a protocol between CMTV and SHN.

References

Allain R. 2001. Redescription of *Streptospondylus altdorfensis*, Cuvier's theropod dinosaur, from the Jurassic of Normandy. Geodiversitas. 23:349–367.

Antunes MT, Mateus O. 2003. Dinosaurs of Portugal. C R Paleovol. 2:77–95.

Antunes MT, Sigogneau D. 1992. La faune de petits dinosaures du Crétacé terminal Portugais [The faune of small dinosaurs from the late Portuguese Cretaceous]. Comunicações Serviços Geológicos Portugal. 7:49–62.

Araújo R, Castanhinha R, Martins RMS, Mateus O, Hendrickx C, Beckmann F, Schell N, Alves LC. 2013. Filling the gaps of dinosaur eggshell phylogeny: Late Jurassic theropod clutch with embryos from Portugal. Sci Rep. 3:1–8.

Benson RBJ. 2010. A description of *Megalosaurus bucklandii* (Dinosauria: Theropoda) from the Bathonian of the UK and the relationships of Middle Jurassic theropods. Zool J Linn Soc. 158:882–935.

Brochu CA. 1996. Closure of neurocentral sutures during crocodilian ontogeny: implications for maturity assessment in fossil archosaurs. J Vert Paleontol. 16:49–62.

Brusatte SL, Benson RBJ, Hutt S. 2008. The osteology of *Neovenator salerri* (Dinosauria: Theropoda) from the Wealden Group (Barremian) of the Isle of Wight. Monogr Palaeontogr Soc. 162:1–166.

Brusatte SL, Sereno PC. 2008. Phylogeny of Allosauroidea (Dinosauria: Theropoda): comparative analysis and resolution. J Syst Palaeontol. 6:155–182.

Canale JI, Novas FE, Salgado L, Coria RA. 2014. Cranial ontogenetic variation in *Mapusaurus roseae* (Dinosauria: Theropoda) and the probable role of heterochrony in carcharodontosaurid evolution. Paläont Ges. 89:983–993.

Carrano MT, Benson RBJ, Sampson SD. 2012. The phylogeny of Tetanurae (Dinosauria: Theropoda). J Syst Palaeontol. 10:211–300.

Chure DJ. 2000. A new species of *Allosaurus* from the morrison formation of Dinosaur National Monument (UT-CO) and a revision of the theropod family Allosauridae [PhD dissertation]. New York City: Columbia University.

Currie PJ, Carpenter K. 2000. A new specimen of *Acrocanthosaurus atokensis* (Theropoda, Dinosauria) from the lower cretaceous antlers formation (lower cretaceous, aptian) of Oklahoma, USA. Geodiversitas. 22:207–246.

Currie PJ, Zhao XJ. 1993. A new carnosaur (Dinosauria, Theropoda) from the Jurassic of Xinjiang, People's Republic of China. Can J Earth Sci. 30:2037–2081.

Eddy DR, Clarke JA. 2011. New information on the cranial anatomy of *Acrocanthosaurus atokensis* and its implications for the phylogeny of Allosauroidea (Dinosauria: Theropoda). *PLoS One* 6:e17932.

Evers S. 2014. The postcranial osteology of a large specimen of *Allosaurus* "*jimmadseni*" (Dinosauria: Theropoda) from the Late Jurassic of Wyoming, U.S.A. [dissertation]. Munich: Ludwig-Maximilians-University.

Fürsich FT. 1981. Salinity-controlled benthic associations from the Upper Jurassic of Portugal. Lethaia. 14:203–223.

Galton PM. 1996. Notes on Dinosauria from the Upper Cretaceous of Portugal. Neu Jb Geol Paläont, Mh. 2:83–90.

Gauthier J. 1986. Saurischian monophyly and the origin of birds. In: Padian K, editor. The origin of birds and the evolution of flight. San Francisco (CA): California Academy of Science; p. 1–55.

Gilmore CW. 1920. Osteology of the carnivorous Dinosauria in the United States National Museum, with special reference to the genera *Antrodemus* (*Allosaurus*) and *Ceratosaurus*. Bull US Natl Mus. 110:1–159.

Goloboff PA, Farris JS, Nixon KC. 2008. TNT 1.1, a free program for phylogenetic analysis. Cladistics. 24:774–786.

Hendrickx C, Mateus O. 2012. Ontogenetical changes in the quadrate of basal tetanurans. In: Royo-Torres R, Gascó F, Alcalá L, editors. Fundamental 20. 10th Annual Meeting of the European Association of Vertebrate Palaeontologists; Teruel, Spain.

Hendrickx C, Mateus O. 2014a. Abelisauridae (Dinosauria: Theropoda) from the Late Jurassic of Portugal and dentition-based phylogeny as a contribution for the identification of isolated theropod teeth. Zootaxa. 3759:1–74.

Hendrickx C, Mateus O. 2014b. *Torvosaurus gurneyi* n. sp., the largest terrestrial predator from Europe, and a proposed terminology of the maxilla anatomy in nonavian theropods. PLoS One. 9:e88905.

Hendrickx C, Mateus O, Araújo R. Forthcoming. A proposed terminology of theropod teeth (Dinosauria. Saurischia). J Vert Paleontol. doi: 10.1080/02724634.2015.982797

Hendrickx C, Mateus O, Araújo R. 2015. The dentition of megalosaurid theropods. Acta Palaeontol Pol. 60:627–642.

Hill G. 1988. The sedimentology and lithostratigraphy of the Upper Jurassic Lourinhã Formation, Lusitanian Basin Portugal [PhD dissertation]. Milton Keynes: The Open University.

Irmis RB. 2007. Axial skeleton ontogeny in the Parasuchia (Archosauria: Pseudosuchia) and its implications for ontogenetic determination in archosaurs. J Vert Paleontol. 27:350–361.

Lapparent AF, Zbyszewski G. 1957. Les dinosauriens du Portugal [The dinosaurs of Portugal]. Memórias Serviços Geológicos de Portugal. 2:1–63.

Madsen JH. 1976/1993. *Allosaurus fragilis*: a revised osteology. 2nd ed. Utah Geol Mineral Sur Bull. 109:1–163.

Madsen JH, Welles SP. 2000. *Ceratosaurus* (Dinosauria, Theropoda) a revised osteology. Utah Geol Sur Miscellaneous Publ. 2:1–80.

Makovicky P, Sues HD. 1998. Anatomy and phylogenetic relationships of the theropod dinosaur *Microvenator celer* from the Lower Cretaceous of Montana. Am Mus Novit. 3240:1–27.
Malafaia E, Ortega F, Silva B, Escaso F. 2008. Fragmento de un maxilar de terópodo de Praia da Corva (Jurásico Superior. Torres Vedras, Portugal). In: Esteve J, Meléndez G, editors. Palaeontologica Nova, SEPAZ 8 VI Encuentro de Jóvenes Investigadores en Paleontología. Alcalá de Henares.
Malafaia E, Ortega F, Escaso F. 2014. New post-cranial elements assigned to coelurosaurian theropods from the Late Jurassic of Lusitanian Basin, Portugal. Fundamental. 20:123–126.
Malafaia E, Ortega F, Escaso F, Silva B. 2014. New cranial remains assigned to Megalosauridae (Dinosauria: Theropoda) from the Late Jurassic of Lusitanian Basin (Portugal). In: Maxwell E, Miller-Camp J, editors. 74th Meeting of the Society of Vertebrate Paleontology; Berlin, Germany. 5th–8th November. Program and Abstracts. p. 175.
Malafaia E, Ortega F, Escaso F, Silva B. 2015. New evidence of *Ceratosaurus* (Dinosauria: Theropoda) from the Late Jurassic of the Lusitanian Basin, Portugal. Hist Biol. 27:938–946.
Malafaia E, Ortega F, Silva B, Escaso F, Dantas P. 2008. A new specimen of Allosauroidea (Dinosauria: Tetanurae) from the Upper Jurassic of Valmitão (Lourinhã, Portugal). In: Ruiz-Omeñaca JI, Piñuela L, García-Ramos JC, editors. XXIV Jornadas de la Sociedad Española de Paleontología; Asturias, Spain (in Spanish).
Malafaia E, Ortega F, Escaso F, Silva B, Ramalheiro G, Dantas P, Moniz C, Barriga F. 2007. A preliminary account of a new *Allosaurus* individual from the Lourinhã Group (Upper Jurassic of Torres Vedras, Portugal). In: Huerta P, Torcida Fernández-Baldor F, editors. Abstracts book of the IV International Symposium about Dinosaurs Palaeontology and their Environment, Salas de los Infantes. p. 243–251.
Malafaia E, Ortega F, Escaso F, Dantas P, Pimentel N, Gasulla JM, Ribeiro B, Barriga F, Sanz JL. 2010. Vertebrate fauna at the *Allosaurus* fossil-site of Andrés (Upper Jurassic), Pombal, Portugal. J Iber Geol. 36:193–204.
Manuppella G, Antunes MT, Pais J, Ramalho MM, Rey J. 1999. Explicative news, sheet 30-A, Lourinhã. Lisboa: Departamento de Geologia, Instituto Geológico e Mineiro. Portuguese.
Manuppella G, Rey J, Ramalho MM, Leinfelder R, Batista R. 1996. Geological map, sheet 30-A, Lourinhã 1:50 000. 2nd ed. Lisboa: Departamento de Geologia, Instituto Geológico e Mineiro.
Marsh OC. 1878. Notice of new dinosaurian reptiles. Am J Sci Arts. 15:241–244.
Marsh OC. 1881. Principal characters of American Jurassic dinosaurs. Part V. Am J Sci. 21:417–423.
Mateus O. 1998. *Lourinhanosaurus antunesi*, a new upper Jurassic allosauroid (Dinosauria: Theropoda) from Lourinhã, Portugal. Memórias da Academia de Ciências de Lisboa. 37:111–124.
Mateus O. 2005. Dinossauros do Jurássico Superior de Portugal com destaque para os saurísquios [Dinosaurus from the Upper Jurassic of Portugal highlighting the saurischians] [PhD dissertation]. Lisbon: Universidade Nova de Lisboa.
Mateus O, Antunes MT. 2000. *Torvosaurus* sp (Dinosauria: Theropoda) in the Late Jurassic of Portugal. I Congresso Ibérico de Paleontología/XVI Jornadas de la Sociedad Española de Paleontología; Évora, Portugal.
Mateus O, Antunes MT, Taquet P. 2001. Dinosaur ontogeny: the case of *Lourinhanosaurus* (Late Jurassic, Portugal). J Vert Paleontol. 21:78A.
Mateus O, Walen A, Antunes MT. 2006. The large theropod fauna of the Lourinhã Formation (Portugal) and its similarity to the Morrison Formation, with a description of a new species of *Allosaurus*. In: Foster JR, Lucas SG, editors. Paleontology and geology of the Upper Jurassic Morrison Formation. Vol. 36. New Mexico Museum of Natural History and Science, Bulletin, p. 123–129.
Naish D. 1999. Theropod dinosaur diversity and palaeobiology in the Wealden Group (Early Cretaceous) of England: evidence from a previously undescribed tibia. Geologie en Mijnbouw. 78:367–373.
Novas FE, Agnolín FL, Ezcurra MD, Porfiri J, Canale JI. 2013. Evolution of the carnivorous dinosaurs during the Cretaceous: the evidence from Patagonia. Cretaceous Res. 45:174–215.
O'Connor PM. 2006. Postcranial pneumaticity: an evaluation of soft-tissue influences on the postcranial skeleton and the reconstruction of pulmonary anatomy in archosaurs. J Morphol. 267:1199–1226.
Ortega F, Escaso F, Gasulla JM, Dantas P, Sanz JL. 2006. Dinosaurs from the Iberian Peninsula. Estudios Geológicos. 62:219–240 (in Spanish).
Ortega F, Escaso F, Sanz JL. 2010. A bizarre, humped carcharodontosauria (Theropod) from the Lower Cretaceous of Spain. Nature. 467:203–206.
Parsons WL, Parsons KM. 2015. Morphological variations within the ontogeny of *Deinonychus antirrhopus* (Theropoda, Dromaeosauridae). PLoS One. 10:e0121476.
Paul GS. 1988. Predatory Dinosaurs of the World. New York (NY): Simon and Schuster.
Pérez-Moreno BP, Chure DJ, Pires C, Silva CM, Santos V, Dantas P, Póvoas L, Cachão M, Sanz JL, Galopim de Carvalho AM. 1999. On the presence of *Allosaurus fragilis* (Theropoda: Carnosauria) in the Upper Jurassic of Portugal: first evidence of an intercontinental dinosaur species. J Geol Soc. 156:449–452.
Persons SW, Currie PJ. 2011. Dinosaur speed demon: the caudal musculature of Carnotaurus sastrei and implications for the evolution of South American abelisaurids. PLos ONE. 6:e25763.
Rauhut OWM. 2003. A tyrannosauroid dinosaur from the Upper Jurassic of Portugal. Palaeontology. 46:903–910.
Rauhut OWM. 2005. Osteology and relationships of a new theropod dinosaur from the Middle Jurassic of Patagonia. Palaeontology. 48:87–110.
Rauhut OWM. 2011. Theropod dinosaurs from the Late Jurassic of Tendaguru (Tanzania). Spec Pap Palaeontol. 86:195–239.
Rauhut OWM, Carrano MT. Forthcoming. The theropod dinosaur *Elaphrosaurus bambergi* Janensch, 1920, from the Late Jurassic of Tendaguru, Tanzania. Zool J Linn Soc.
Rauhut OWM, Fechner R. 2005. Early development of the facial region in a non-avian theropod dinosaur. Proc R Soc Lond Ser B Biol Sci. 272:1179–1183.
Sadleir R, Barrett PM, Powell HP. 2008. The anatomy and systematics of *Eustreptospondylus oxoniensis*, a theropod dinosaur from the Middle Jurassic of Oxfordshire, England. Monogr Palaeontol Soc. 160:1–82.
Schneider S, Fürsich FT, Werner W. 2009. Sr-isotope of the Upper Jurassic of central Portugal (Lusitanian Basin) based on oyster shells. Int J Earth Sci Geol Rundsch. 98:1949–1970.
Seeley HG. 1887. On the classification of the fossil animals commonly named Dinosauria. Proc R Soc Lond. 43:165–171.
Wilson JA. 1999. A nomenclature for vertebral laminae in sauropods and other saurischian dinosaurs. J Vert Paleontol. 19:639–653.
Wilson JA. 2012. New vertebral laminae and patterns of serial variation in vertebral laminae of sauropod dinosaurs. Contrib Mus Paleontol Univ Mich. 32:91–110.
Wilson JA, D'Emic MD, Ikejiri T, Moacdieh EM, Whitlock JA. 2011. A nomenclature for vertebral fossae in sauropods and other saurischian Dinosaurs. PLoS One. 6:e17114.
Xu X, Zhao Q, Norell M, Sullivan C, Hone D, Erickson G, Wang XL, Han FL, Guo Y. 2008. A new feathered maniraptoran dinosaur fossil that fills a morphological gap in avian origin. Chin Sci Bull. 54:430–435.
Zhao X-J, Benson RBJ, Brusatte SL, Currie PJ. 2010. The postcranial skeleton of *Monolophosaurus jiangi* (Dinosauria: Theropoda) from the Middle Jurassic of Xinjiang, China, and a review of Middle Jurassic Chinese theropods. Geol Mag. 147:13–27.
Zinke J. 1998. Small theropod teeth from the Upper Jurassic coal mine of Guimarota (Portugal). Palaont Z. 72:179–189.

SUPPLEMENTARY MATERIAL

Table 1. Osteological elements of theropods collected in the Valmitão fossil site

Inventory number	Element
SHN.036/18	Odontoid
SHN.036/19	Atlantal intercentrum
SHN.036/22	Articulated axis, axial intercentrum and neurapophyses
SHN.036/4, 16 and 17	Cervical neural spines
SHN.036/33 and 35	Isolated cervical prezygapophyses
SHN.036/87	Fragments of the proximal end of cervical ribs
SHN.036/20 and 21	Anterior dorsal vertebrae
SHN.036/1, 3, 6–10, and 14	Mid and posterior dorsal vertebrae
SHN.036/23, 25–28,	Dorsal neural spines
SHN.036/34	Isolated dorsal prezygapophyses
SHN.036/70 and 71	Dorsal ribs
SHN.036/85 and 86	Fragments of dorsal ribs
SHN.036/72	Proximal end of posterior dorsal rib
SHN.036/11	First sacral vertebra
SHN.036/40	Sacral vertebra
SHN.036/12	Last sacral vertebra
SHN.036/29	Sacral neural spine
SHN.036/5	Sacral neural arch
SHN.036/2	Anterior caudal neural arch
SHN.036/13, 50–52	Anterior caudal vertebrae
SHN.036/53–58	Mid caudal vertebrae
SHN.036/59 and 61	Posterior caudal vertebrae
SHN.036/15	Fragment of caudal vertebra
SHN.036/43	Caudal neural spine
SHN.036/41, 42, and 45	Fragment of vertebral centrum
SHN.036/44	Fragment of neural spine
SHN.036/60, 62–68	Chevrons
SHN.036/80	Right ilium
SHN.036/81	Fragment of the postacetabular process of the left ilium
SHN.036/89	Ischial peduncle of the left ilium
SHN.036/90	Pubic peduncle of the left ilium
SHN.036/82	Pubes
SHN.036/83	Left ischium
SHN.036/84	Right ischium
SHN.036/88	Iliac articular surface of the left ischium
SHN.036/30–32	Teeth

Table 2. Measurements of the osteological elements of SHN.036

		Measurements (mm)	
Odontoid	SHN.036/19		
Maximum length (without the facet for axial centrum)	14.16		
Maximum width	33.15		
Maximum depth	19.1		
Atlantal intercentrum	SHN.036/18		
Maximum length	15.7		
Width dorsally between the facets for neurapophyses	47.65		
Depth at the level of the facet for neurapophysis	26.41		
Axis and axial intercentrum	SHN.036/22		
Axial intercentrum, maximum width	38.43		
Axial intercentrum, maximum length	26.96		
Axial centrum, length (excluding the articular facets)	40.54*		
Posterior facet of the axial centrum , width	54.63		
Axial centrum, width	34.42		
Axial centrum, ratio length : width	0.74		
Cervical neural spines	SHN.036/16	SHN.036/17	SHN.036/4
Maximum depth	44.32*	58.82*	76.44*
Length at mid-height	22.6	23.4	27.92
Length dorsally	18.51	19.6	27.38
Width at mid-length	10.39	16.55	15.49
Anterior dorsal vertebrae	SHN.036/21	SHN.036/20	
Centrum, length (excluding the articular facets)	58.58	47.44*	
Centrum, width	33.68	36.26*	
Centrum, depth	35.83	36.7*	
Anterior articular facet, width	34.07*	45.05*	
Anterior articular facet, depth	49.14*	37.33*	
Posterior articular facet, width	51.72	51.65	
Posterior articular facet, depth	54.29	51.64	
Centrum, elongation index	1.63	1.29*	

Table 2. (Continued)

	Measurements (mm)							
Posterior dorsal vertebrae	SHN.036/14	SHN.036/7	SHN.036/1	SHN.036/10	SHN.036/6	SHN.036/8	SHN.036/9	SHN.036/3
Centrum, length	49.12	41.83	32.59	56.13	55.26	40.04	43.6	39.18
Centrum, width	22.61	15.84*	28.85	35.84	21.12*	17.85*	25.96*	26.01*
Centrum, depth	38.64	46.66	61.3	38.33	59.38	50.97	45.01*	?
Anterior articular facet, width	47.27	44.92*	72.02	68.44	50.75*	45.46*	65.27	?
Anterior articular facet, depth	44.48	52.61	70.71	56.31	64.34*	55.36	65.15	?
Posterior articular facet, width	50.02	47.51*	64.55	73.84	50.36	46*	?	?
Posterior articular facet, depth	48.75	59.42	72.72	50,.93	63.09	61.94	70.27*	?
Centrum, elongation index	1.27	0.90	0.53	1.46	0.93	0.79	0.97*	?

Dorsal neural spines	SHN.036/23	SHN.036/25	SHN.036/28	SHN.036/26	SHN.036/27
Maximum depth	95.15*	69.90*	96.85	84.76	87.88*
Length at mid-height	32.13	33.8	39	36.71	30.49
Length dorsally	30.64	31.92	36.35	33.59	27.07
Maximum transverse width at mid-length	16.24	13.49	19.94	18.85	19.15

Sacral vertebrae	SHN.036/11	SHN.036/40	SHN.036/12
Centrum, length	47.21	65,4	57
Centrum, width	38.58	42.18*	33.7
Centrum, depth	52.81	43.16*	51.34
Anterior articular facet, width	81.81	?	?
Anterior articular facet, depth	77.68	?	60.35*
Posterior articular facet, width	?	?	75.55
Posterior articular facet, depth	?	?	68.03
Centrum, elongation index	0.89	1.51*	1.11

Sacral neural spine	SHN.036/29
Maximum depth	59.01*
Length at mid-height	37.14
Maximum width at mid-length	9.12

Table 2. (Continued)

	Measurements (mm)											
Caudal vertebrae	SHN.036/13	SHN.036/50	SHN.036/51	SHN.036/52	SHN.036/53	SHN.036/54	SHN.036/55	SHN.036/56	SHN.036/57	SHN.036/58	SHN.036/61	SHN.036/59
Centrum, length	61.07	61.21	59.16	60.19	60.12	63.93	63.2	66.39	60.88	60.73	68.62	66.37
Centrum, width	23.12*	23.52	33.76	17.94*	21.87	17.03*	24.53	23.75	25.79	24.57	24.79	27.47
Centrum, depth	62.52	53.31	39.55	40.78	29.88	31.96	23.27	22.43	31.25	21.28	27.49	25.55
Anterior articular facet, width	62.86	54.37	67.61	49.32	41.16	38.46	42.13	41.75	40.61	38.45	37.52	37.4
Anterior articular facet, depth	80.16	57.06	59.7	59.68	35.32	38.71	35.52	33.28	35.04	36.21	35.57	34.11
Posterior articular facet, width	51.43*	50.51	61.42	44.59	39.57	37.32	40.41	42.15	37.85	38.66	38.32	39.11
Posterior articular facet, depth	81.33*	56.63	58.25	54.72	35.26	38.99	37.29	34.93	37.54	35.34	34.97	33.32
Centrum, elongation index	0.98	1.15	1.50	1.48	2.01	2.00	2.72	2.96	1.95	2.85	2.50	2.60

Ilium	SHN.036/80
Length	420
Iliac blade depth above the acetabulum	128
Length of the preacetabular process measured from the level of the anterior margin of the acetabulum	145*
Length of the postacetabular process measured from the level of the posterior margin of the acetabulum	175*
Iliac length : depth	3.28
Pubic peduncle, length	94.43
Pubic peduncle, transverse width	34.25
Pubic peduncle maximum depth	93.77
Pubic peduncle length : depth	2.76
Ischial peduncle, length	27.98
Ischial peduncle, transverse width	37.95
Ischial peduncle maximum depth	55.35
Pubic peduncle depth : ischial peduncle depth	1.69

Table 2. (Continued)

	Measurements (mm)	
Pubes	SHN.036/82	
Shaft length	330	
Shaft minimum diameter at mid-length	23.32	
Maximum length of the proximal end	122.81	
Transverse width of the proximal end at the level of the acetabulum	28.5	
Boot length	240	
Ratio shaft length : boot length	1.38	
Ischia	SHN.036/83	SHN.036/84
Shaft length excluding the proximal and distal ends	265	270
Maximum diameter of the shaft at mid-length	25.3	23,66
Length of the proximal end	130.69	?
Maximum transverse width of the proximal end across the pubic process	38.7	?
Maximum transverse width of the proximal end across the iliac articulation	40.36	?
Length of the acetabulum	57.38	?
Length of the proximal distal end	57.14	63.11
Maximum transverse width of the distal end	27.93	15.32

* Estimated measurements

Table 3. Measurements of the theropod teeth collected in the Valmitão fossil site

	Measurements (mm)																
	CBL	CBW	CH	AL	CBR	CHR	CDA	CMA	MA	MC	MB	DA	DC	DB	MAVG	DAVG	DSDI
SHN.036/31	10	5.2	23.7	26	0.5	2.4	91.6	65.6	19	21	0	17	17	17	13.3	17.0	1.2
SHN.036/32	5.7	3.9	12.5	13.5	0.7	2.2	88.1	67.3	?	25*	0	22	23	26	?	23.7	?
SHN.036/30	11	4.4	18.1	20.8	0.4	1.6	88.2	60.2	19	23	0	17	20	22	14	19.7	1.1

* Estimated measurements

Abbreviations.—AL, Apical Length; CBL, Crown Base Length; CBR, Crown Base Ratio (= CBW/CBL); CBW, Crown Base Width; CDA, Crown Distal Angle (= arcos (CH2+CBL2-AL2)/2×CBL×AL); CH, Crown Height; CHR, Crown Height Ratio (= CH/CBL); CMA, Crown Mesial Angle (= arcos (CBL2+AL2-CH2)/2×CBL×AL); DA, Distoapical Denticles Density; DB, Distobasal Denticles Density; DC, Distocentral Denticles Density; DAVG, Average Distal Denticle Density; DSDI, Denticle Size Density Index; MA, Mesioapical Denticle Density; MAVG, Average Mesial Denticle Density; MB, Mesiobasal Denticles Density; MC, Mesiocentral Denticles Density.

Figure 1. Mid and posterior caudal vertebrae of SHN.036. SHN.036/53 in anterior (a), left lateral (f), posterior (k), ventral (p), and dorsal (u) views; SHN.036/54 in anterior (b), left lateral (g), posterior (i), ventral (q), and dorsal (v) views; SHN.036/57 in anterior (c), left lateral (h), posterior (m), ventral (r), and dorsal (w) views; SHN.036/58 in anterior (d), left lateral (i), posterior (n), ventral (s), and dorsal (x) views; SHN.036/61 in anterior (e), left lateral (j), posterior (o), ventral (t), and dorsal (y) views . Scale bar = 50 mm.

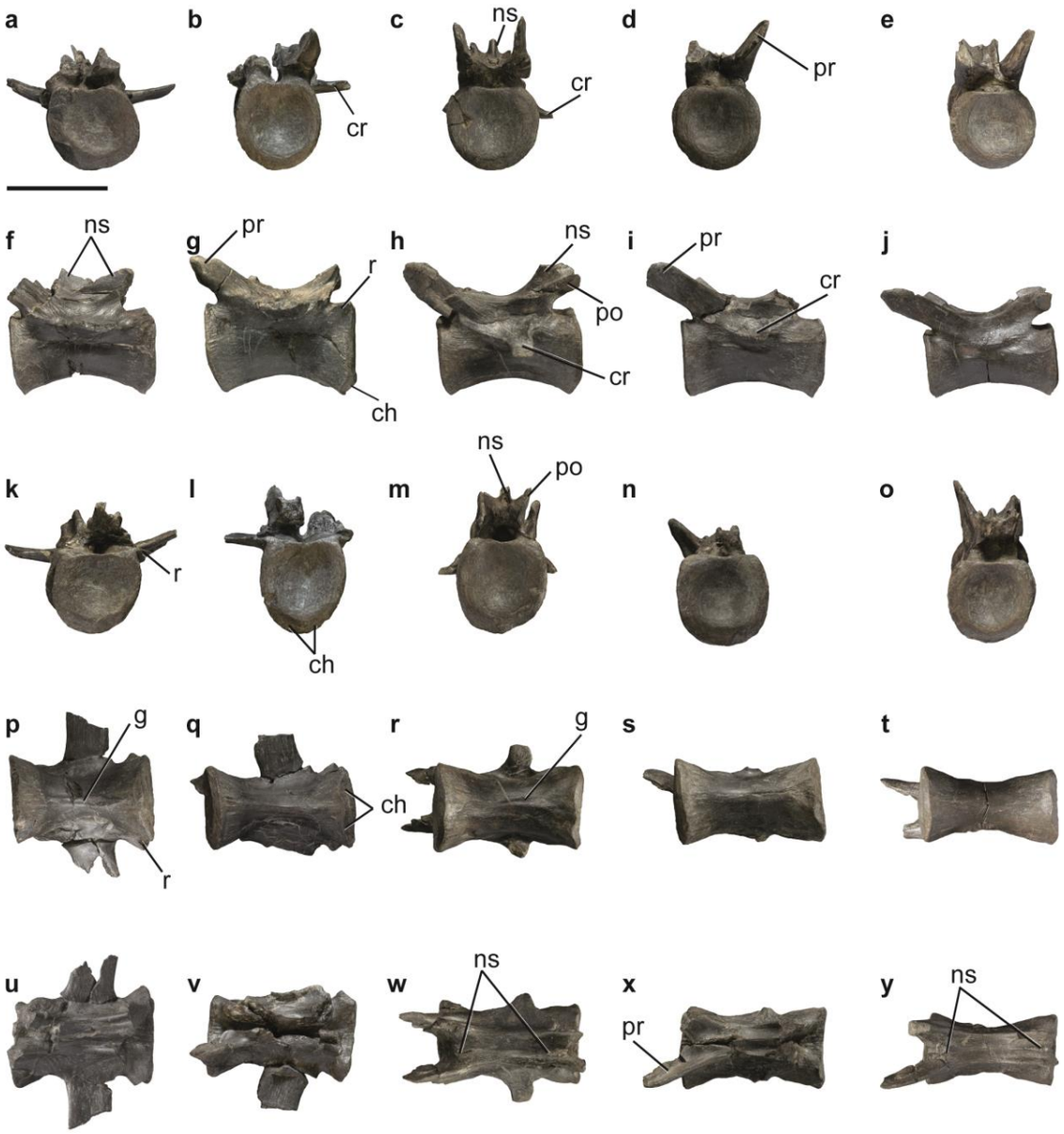

APPENDIX 6.4.1

Characters used in the phylogenetic analysis of SHN.036

(1) Premaxilla, inter-premaxillary suture in adults: open (0), fused (1). (Carrano et al. 2012: 1)

(2) Premaxilla, height/length ratio ventral to external naris: 0.5–2.0 (0), < 0.5 (1), > 2.0 (2). (Carrano et al. 2012: 2)

(3) Premaxilla, subnarial process and ventral border of naris: contacts nasals, excluding maxilla from narial margin (0), reduced and separate from nasals by maxillary contribution to narial margin (1). (Carrano et al. 2012: 3)

(4) Premaxilla, posterior extent of nasal process relative to posterior tip of subnarial process: even (0); posterior (1). (Carrano et al. 2012:4)

(5) Premaxilla, form of premaxilla-nasal suture: V-shaped (0), W-shaped (1). (Carrano et al. 2012: 5)

(6) Premaxilla, proportions and position anterior to external nares: shorter than premaxilla ventral to nares, angle between anterior and alveolar margins > 75° (0), longer than body ventral to nares, angle < 70°, external naris overlaps some of the premaxillary body (1); external naris entirely posterior to premaxillary body (2). (Carrano et al. 2012: 6)

(7) Premaxilla, diastema ('subnarial gap') adjacent to maxilla along dentigerous margin: absent (0), present (1). (Carrano et al. 2012: 7)

(8) Premaxilla, mediolateral constriction of posterior portion: absent (0), present (1). (Carrano et al. 2012: 8)

(9) Premaxilla, development of maxillary process: well–developed (0), reduced to a short triangle (1). (Carrano et al. 2012: 9)

(10) Premaxilla, morphology of subnarial foramen: distinct foramen (0), expanded channel (1). (Carrano et al. 2012: 10)

(11) Premaxilla, articulation with maxilla: planar (0), interlocking (1). (Carrano et al. 2012: 11)

(12) Maxilla, development of anterior ramus: anteroposteriorly short or absent (0), moderate (1), anteroposteriorly long (2). (Carrano et al. 2012: 12)

(13) Maxilla, orientation of anteriormost alveolus: vertical (0), angled anteriorly (1). (Carrano et al. 2012: 13)

(14) Maxilla, shape of ascending ramus: smooth curve or straight (0), abruptly changes orientation (1). (Carrano et al. 2012: 14)

(15) Maxilla, morphology of palatal process: long, ridged or fluted prong (0), long and plate-shaped (1). (Carrano et al. 2012: 15)

(16) Maxilla, position of palatal process: ventral, immediately dorsal to paradental plates (0), dorsal, immediately ventral to dorsal surface of maxillary anterior ramus (1). (Carrano et al. 2012: 16)

(17) Maxilla, anterior end of junction between medial wall and paradental plates: horizontal (0); inclined anteroventrally (1). (Carrano et al. 2012: 17)

(18) Maxilla, horizontal ridge (prominent 'lingual bar') between palatal process and antorbital fenestra: absent (0), present (1). (Carrano et al. 2012: 18)

(19) Maxilla, depth of paradental plates relative to anteroposterior width: low, < 1.8 (0); tall > 1.8 (1). (Carrano et al. 2012: 19; Novas et al. 2013: 26)

(20) Maxilla, ventral extent of paradental plates relative to lateral wall: as far ventral (0); fall short (1). (Carrano et al. 2012: 20)

(21) Maxilla, arrangement of nutrient foramina on lateral surface: single row or no distinct pattern (0), two parallel rows (1). (Carrano et al. 2012: 21)

(22) Maxilla, anteroventral border of antorbital fossa: graded or stepped (0), demarcated by raised ridge (1). (Carrano et al. 2012: 22)

(23) Maxilla, anterior margin of antorbital fossa: rounded (0); squared (1). (Carrano et al. 2012: 23)

(24) Maxilla, ventral extent of antorbital fossa: moderate (0), absent (1), dorsoventrally deep (2). (Carrano et al. 2012: 24)

(25) Maxilla, position of anterior end of antorbital fossa relative to naris: posterior (0), ventral (1). (Carrano et al. 2012: 25)

(26) Maxilla, development of maxillary 'fenestra': absent (0), fossa (1), fenestra (2). (Carrano et al. 2012: 26)

(27) Maxilla, development of promaxillary fenestra: absent (0), fenestrated open medially (1), present but shallow (2), present and extends into anterior ramus as a canal (3). (modified from Carrano et al. 2012: 27 based on Brusatte and Sereno 2008: 10)

(28) Maxilla, dimensions of promaxillary fenestra opening: small foramen (0), large fenestra (1). (Carrano et al. 2012: 28)

(29) Maxilla, development of pneumatic fossa (excavation pneumatica) in ascending process: absent (0), present (1). (Carrano et al. 2012: 29)

(30) Maxilla, pneumaticity on medial side of posterior section of ascending ramus: absent (0), present (1). (Carrano et al. 2012: 30)

(31) Maxilla, posterior end of tooth row relative to orbit: beneath (0), anterior (1). (Carrano et al. 2012: 31)

(32) Maxilla, articulation with jugal: slot or groove (0), lateral shelf (1).(Carrano et al. 2012: 32)

(33) Maxilla, anteroposterior length of jugal contact relative to total jugal length: less than 50% (0), more than 50% (1). (Carrano et al. 2012: 33)

(34) Maxilla and nasal, external surface texture: smooth (0), sculptured (1). (Carrano et al. 2012: 34)

(35) Nasal, inter-nasal contact in adults: separate (0), partly or fully fused (1). (Carrano et al. 2012: 35)

(36) Nasal, posterior narial margin: absent or weak fossa (0), large fossa (1), laterally splayed hood (2). (Carrano et al. 2012: 36)

(37) Nasal, participation in antorbital fossa: absent or at edge (0), present (1). (Carrano et al. 2012: 37)

(38) Nasal, antorbital fossa in lateral view: visible (0); occluded by ventrolaterally overhanging lamina (1). (Carrano et al. 2012: 38)

(39) Nasal, pneumatic foramina: absent (0), present (1). (Carrano et al. 2012: 39)

(40) Nasal, development of dorsolateral surfaces: none, nasals low and dorsally convex (0), pronounced dorsolateral rims, sometimes with lateral crests (1), tall, parasagittal crests (2), inflated and forming a hollow midline crest (3). (Carrano et al. 2012: 40)

(41) Nasals, ornamentation: weak or absent (0); homogenous (1); strong rugosities and knob-like projections in some portions of the bone (2); high median crest starting directly posteriorly to the external nares (3) (Novas et al. 2013: 34).

(42) Lacrimal, anterior process: dorsoventrally deep (0), dorsoventrally narrow, includes antorbital fossa and rim (0), dorsoventrally narrow, antorbital fossa only (1). (Carrano et al. 2012: 42)

(43) Lacrimal, morphology of lateral lamina of ventral process of lacrimal: anteriormost point situated around midheight of ventral process (0); anteriormost point situated dorsal to midheight of ventral process and a distinct rugose patch is present on the lateral surface (1). (Carrano et al. 2012: 43)

(44) Lacrimal, dorsal and ventral portions of antorbital fossa: separated by anterior projection of lateral lamina (0), continuous, lateral lamina does not project far anteriorly (1). (Carrano et al. 2012: 44)

(45) Lacrimal, lacrimal fenestra morphology: absent (0); present as small foramen (1); present as large oval opening with associated dorsal rugosity, swelling or 'horn' (2). (Carrano et al. 2012: 45)

(46) Lacrimal, openings in lacrimal recess: single (0), multiple (1). (Carrano et al. 2012: 46)

(47) Lacrimal, horn morphology: small rugosity (0); low, broad, rugose bar (1); triangular horn (2). (Carrano et al. 2012: 47)

(48) Lacrimal, suborbital process: absent (0), present (1). (Carrano et al. 2012: 48)

(49) Lacrimal, angle between anterior and ventral rami: ~90° (0), < 75° (1). (Carrano et al. 2012: 49)

(50) Lacrimal, length of anterior process relative to ventral process: subequal (0), ~75% (1). (Carrano et al. 2012: 50)

(51) Jugal, position of anterior end: posterior to internal antorbital fenestra, but reaching its posterior rim (0), excluded from internal antorbital fenestra (1), expressed at rim of internal antorbital fenestra, with distinct anterior process extending beneath it (2). (Carrano et al. 2012: 51)

(52) Jugal, pneumatisation: absent (0), internally hollowed and transversely inflated by foramen in posterior rim of antorbital fossa (1). (Carrano et al. 2012: 52)

(53) Jugal, antorbital fossa: absent (0), present (1). (Carrano et al. 2012: 53)

(54) Jugal, morphology of lacrimal articulation: abuts, no flange (0), overlapping, flange present (1) (Fig. 19). (Carrano et al. 2012: 54)

(55) Jugal, orientation of orbital margin: angled posterodorsally (0), vertical (1). (Carrano et al. 2012: 55)

(56) Jugal, dorsoventral size of posterior process: shallow (0), deep (1). (Carrano et al. 2012: 56)

(57) Postorbital, articulation with jugal: planar (0), grooved, ventral process with U-shaped cross-section (1). (Carrano et al. 2012: 57)

(58) Postorbital, suborbital flange: absent (0), present as small eminence (1), present as large flange (2). (Carrano et al. 2012: 58)

(59) Postorbital, ventral extent relative to ventral margin of orbit: substantially above (0), approximately same level (1). (Carrano et al. 2012: 59)

(60) Postorbital, participation in supratemporal fossa: fossa extends onto dorsal surfaces of anterior and posterior processes (0), anterior process only (1), posterior process only (2). (Carrano et al. 2012: 60)

(61) Supraorbital shelf formed mostly by 'palpebral': absent (0), present (1). (Carrano et al. 2012: 61)

(62) Postorbital, anterior prominence: absent or small (0), large (1), contacts lacrimal (2). (Carrano et al. 2012: 62)

(63) Postorbital, articulation with squamosal: tongue-in-groove (0), helical (1). (Carrano et al. 2012: 63)

(64) Laterosphenoid, articulations: frontal and postorbital (0), postorbital only (1). (Carrano et al. 2012: 64)

(65) Prefrontal, condition in adults: separate, moderate (0), separate, reduced (1), partly or completely fused to postorbital (1). (Carrano et al. 2012: 65)

(66) Prefrontal, articulation with frontal: planar (0), peg-and-socket (1). (Carrano et al. 2012: 66)

(67) Frontal, exposure along orbital rim: broad (0), narrow or absent (1). (Carrano et al. 2012: 67)

(68) Parietal, articulation with supraoccipital: abuts (0), overlaps (1). (Carrano et al. 2012: 68)

(69) Parietal, development of median skull table: flat and broad (0), narrow with sagittal crest (1), very broad, widely separating upper temporal fenestrae (2). (Carrano et al. 2012: 69)

(70) Parietal, size and elevation of nuchal wedge and alae: moderate (0), tall and expanded (1). (Carrano et al. 2012: 70)

(71) Supratemporal fossa, anteromedial corner: open dorsally (0); partially roofed over by a small shelf of the frontalparietal (1). (Carrano et al. 2012: 71)

(72) Squamosal, constriction of lower temporal fenestra: absent (0), present (1). (Carrano et al. 2012: 72)

(73) Squamosal, anterodorsal lamina: emarginated by upper temporal fenestra (0); continuous (1). (Carrano et al. 2012: 73)

(74) Squamosal, flange covering quadrate head laterally: absent (0), present (1). (Carrano et al. 2012: 74)

(75) Squamosal, articulation with quadratojugal: at tip (0), absent (1), broad (2). (Carrano et al. 2012: 75)

(76) Quadratojugal, anteriormost point of ventral process relative to lower temporal fenestra: ventral (0), anterior (1). (Carrano et al. 2012: 76)

(77) Quadrate, pneumatisation: absent (0), present (1). (Carrano et al. 2012: 77)

(78) Quadrate, height of dorsal ramus relative to orbit height: less (0), greater (1). (Carrano et al. 2012: 78)

(79) Quadrate, axis in posterior view: vertical (0), oblique (1). (Carrano et al. 2012: 79)

(80) Quadrate, height of pterygoid flange relative to complete bone: 2/3 (0) subequal (1). (Carrano et al. 2012: 80)

(81) Quadrate foramen: present (0), absent (1). (Carrano et al. 2012: 81)

(82) Quadrate, axis in lateral view: vertical (0), anterior (1), posterior (2). (Carrano et al. 2012: 82)

(83) Quadrate, head shape in dorsal view: oval (0), subrectangular (1). (Carrano et al. 2012: 83)

(84) Quadrate, medial foramina adjacent to condyles: absent (0), present (1). (Carrano et al. 2012: 84)

(85) Paroccipital process, position of ventral rim of base relative to occipital condyle: at same level (0), below (1). (Carrano et al. 2012: 85)

(86) Paroccipital process, position of ventral edge of distal end relative to occipital condyle: at or above dorsal border of condyle, process approximately horizontal or dorsolaterally inclined (0), at or below mid-height of condyle, process ventrolaterally oriented (1). (Carrano et al. 2012: 86)

(87) Supraoccipital, anteroposterior depth of median ridge relative to occipital condyle length: less (0), greater (1). (Carrano et al. 2012: 87)

(88) Supraoccipital, width of knob relative to foramen magnum diameter: equal (0), 1.5x (1). (Carrano et al. 2012: 88)

(89) Supraoccipital, participation in foramen magnum: absent, exoccipitals contact dorsally (0), narrow, separating exoccipitals on dorsal edge of foramen (1), wide, supraoccipital extends ventrolaterally around foramen magnum (2). (Carrano et al. 2012: 89)

(90) Basioccipital, ventrolateral pair of pneumatic cavities invading neck of occipital condyle and joining medially: absent (0), present (1). (Carrano et al. 2012: 90)

(91) Basioccipital, sharp dorsoventrally oriented lamina situated immediately ventral to occipital condyle: absent (0), present (1). (Carrano et al. 2012: 91)

(92) Basioccipital, fossa ventral to occipital condyle in basioccipital apron: narrow and groove-like, one-half or less the width of the occipital condyle (0), broad depression approximately two-thirds the width of occipital condyle (1). (Carrano et al. 2012: 92)

(93) Basioccipital, notch along contact with exoccipital-opisthotic: absent (0), present (1). (Carrano et al. 2012: 93)

(94) Basioccipital, width of basal tubera relative to occipital condyle width: ≥ (0), < (1). (Carrano et al. 2012: 94)

(95) Basisphenoid, location of basipterygoid processes relative to basal tubera: anterior or slightly anteroventral, basisphenoid recess opens ventrally (0), ventral, basisphenoid recess narrow and opens posteroventrally (1), anteroventrally, basisphenoid recess opens posteroventrally (2). (Carrano et al. 2012: 95)

(96) Basisphenoid, depth of basisphenoid recess: shallow (0), very deep (1). (Carrano et al. 2012: 96)

(97) Basisphenoid, shape of opening for basisphenoid recess: ovoid (0), teardrop-shaped (1). (Carrano et al. 2012: 97)

(98) Basisphenoid, depth of indentation between basal tubera and basipterygoid processes: deep notch (0), shallow embayment (1). (Carrano et al. 2012: 98)

(99) Basisphenoid, proportions of basipterygoid processes: elongate (0), broad (1). (Carrano et al. 2012: 99)

(100) Braincase, number of foramina (representing cranial nerves XII, XI and X) exiting ventrolateral to occipital condyle: two (0); three (1). (Carrano et al. 2012: 100)

(101) Braincase, ventral extension of subcondylar recess: pronounced (0); shallow/absent (1); narrow incisure (2). (Carrano et al. 2012: 101)

(102) Braincase, shape of ventral margin of paroccipital process and stapedial groove/foramen ovale: open curve (0); acute/closed curve (1). (Carrano et al. 2012: 102)

(103) Braincase, anteroposterior angle of occiput in lateral view: vertical (0), sloping anterodorsally–posteroventrally (1). (Carrano et al. 2012: 103)

(104) Braincase, morphology of trigeminal foramen: single (0), partly split (1), fully split (2). (Carrano et al. 2012: 104)

(105) Braincase, median ridge separating exits of left and right sixth cranial nerves: present (0), absent (1). (Carrano et al. 2012: 105)

(106) Braincase, number of tympanic recesses: two (0), three (1). (Carrano et al. 2012: 106)

(107) Braincase, internal carotid pneumatization: absent (0), fossa (1), opening (2). (Carrano et al. 2012: 107)

(108) Braincase, ossification of interorbital region: weak or absent (0), extensive, ossified sphenethmoid and interorbital septum (1). (Carrano et al. 2012: 108)

(109) Palatine, shape: triradiate (0), tetraradiate, well-developed jugal process (1). (Carrano et al. 2012: 109)

(110) Palatine, anteroposterior extent of maxillary flange: short (0), extended (1). (Carrano et al. 2012: 110)

(111) Palatine, morphology of jugal process: tapered process (0), expanded process (1). (Carrano et al. 2012: 111)

(112) Palatine, orientation of maxillary contact: lateral (0), ventral (1). (Carrano et al. 2012: 112)

(113) Palatine, pneumatic recess: absent (0), present (1). (Carrano et al. 2012: 113)

(114) Pterygoid, pocket on ectopterygoid flange: absent (0), present (1). (Carrano et al. 2012: 114)

(115) Ectopterygoid, dorsoventral depth: narrow (0), deep (1). (Carrano et al. 2012: 115)

(116) Ectopterygoid, ventral fossa: absent (0), present (1). (Carrano et al. 2012: 116)

(117) Ectopterygoid, lateral depth of ectopterygoid fossa: shallow (0), deep (1). (Carrano et al. 2012: 117)

(118) Mandible, size of external mandibular fenestra: small to moderate (0), large (1). (Carrano et al. 2012: 118)

(119) Mandible, position of anterior end of external mandibular fenestra relative to last dentary tooth: posterior (0), ventral (1). (Carrano et al. 2012: 119)

(120) Dentary, shape of anterior end in lateral view: blunt and unexpanded (0), dorsoventrally expanded, rounded, and slightly upturned (1), 'squared off' in lateral view via anteroventral process (2). (Carrano et al. 2012: 120)

(121) Dentary, size of mesialmost alveoli: subequal (0), third alveolus circular and enlarged (1). (Carrano et al. 2012: 121)

(122) Dentary, shape in dorsal view: straight (0), curves anteromedially (1). (Carrano et al. 2012: 122)

(123) Dentary, paradental groove: narrow along entire length (0), wide anteriorly defining a distinct gap between medial dentary wall and paradental plates (1). (Carrano et al. 2012: 123)

(124) Dentary, longitudinal groove housing dorsally situated row of neurovascular foramina on lateral surface: absent or weak (0), present and well-defined (1). (Carrano et al. 2012: 124)

(125) Dentary, number of Meckelian foramina: one (0), two (1). (Carrano et al. 2012: 125)

(126) Dentary, morphology of posterior end: notched by external mandibular fenestra (0), straight or slightly concave (1). (Carrano et al. 2012: 126)

(127) Dentary, morphology of surangular articulation just above external mandibular fenestra: small notch (0), large socket (1). (Carrano et al. 2012: 127)

(128) Splenial, contour of posterior edge: straight (0), curved (1), notched (2). (Carrano et al. 2012: 128)

(129) Splenial, size of splenial ('mylohyoid') foramen: small (0), large (1). (Carrano et al. 2012: 129)

(130) Splenial, foramen in ventral part: completely enclosed by bone (0), open anteroventrally (1). (Carrano et al. 2012: 130)

(131) Surangular, horizontal ridge on lateral surface below mandibular joint: weak or absent (0), strong (1). (Carrano et al. 2012: 131)

(132) Surangular, number of posterior surangular foramina: one (0), two (1). (Carrano et al. 2012: 132)

(133) Mandibular glenoid, morphology of medial edge: flat or rounded (0), projecting (1). (Carrano et al. 2012: 133)

(134) Mandibular glenoid, development of anterior wall: weak (0), tall (1). (Carrano et al. 2012: 134)

(135) Retroarticular process, length: long (0), blunt (1). (Carrano et al. 2012: 135)

(136) Retroarticular process, mediolateral width relative to posterior width of dentary: ≤ (0), > (1). (Carrano et al. 2012: 136)

(137) Retroarticular process, orientation of attachment surface: posterodorsal (0), posterior (1). (Carrano et al. 2012: 137)

(138) Paradental plates, continuity and replacement groove: separated, groove present (0), forming a continuous medial lamina ('fused'), groove absent (1). (Carrano et al. 2012: 138)

(139) Paradental plates, visibility in medial view: widely exposed, subpentagonal and moderate–tall (0), obscured by (1). (Carrano et al. 2012: 139)

(140) Paradental plates, surface texture: smooth (0), vertically striated or ridged (1). (Carrano et al. 2012: 140)

(141) Teeth, curvature: present, marked (0), reduced or absent (1). (Carrano et al. 2012: 141)

(142) Teeth, crown striations: absent (0), present (1). (Carrano et al. 2012: 142)

(143) Teeth, enamel wrinkles: absent (0), present, extending as bands across labial and lingual tooth surfaces (1), pronounced marginal enamel wrinkles (2). (Carrano et al. 2012: 143)

(144) Teeth, mid-crown cross-section: elliptical (0), circular (1). (Carrano et al. 2012: 144)

(145) Teeth, root shape: broad (0), tapered (1). (Carrano et al. 2012: 145)

(146) Teeth, maxillary and dentary, serrations: present (0), absent (1). (Carrano et al. 2012: 146)

(147) Teeth, maxillary and dentary, extent of anterior carina: to base of crown (0), at mid-height of crown or more dorsally (1). (Carrano et al. 2012: 147)

(148) Premaxillary teeth, arrangement of carinae: nearly symmetrical, on opposite sides (0), more asymmetrical, both on lingual side (1). (Carrano et al. 2012: 148)

(149) Premaxillary teeth, serrations: present (0), absent (1). (Carrano et al. 2012: 149)

(150) Premaxillary teeth, number: four (0), three (1), five (2), six/seven (3). (Carrano et al. 2012: 150)

(151) Premaxillary teeth, spacing: even (0), paired and spaced (1). (Carrano et al. 2012: 151)

(152) Premaxillary teeth, size of tooth 1 relative to others: subequal (0), smaller (1). (Carrano et al. 2012: 152)

(153) Maxillary teeth, number: > 17 (0), 11–17 (1), < 11. (Carrano et al. 2012: 153)

(154) Maxillary teeth, mid-tooth spacing: adjacent (0), with diastemata (1). (Carrano et al. 2012: 154)

(155) Dentary teeth, size and number relative to maxillary teeth: approximately equal (0), smaller and approximately 1.5 times as numerous (1). (Carrano et al. 2012: 155)

(156) Presacral vertebrae, anterior face of anterior elements: flat (0), convex (1). (Carrano et al. 2012: 156)

(157) Presacral vertebrae, pleurocoel posterior to parapophysis (anterior pleurocoel) in anterior elements: absent (0), present (1). (Carrano et al. 2012: 157)

(158) Presacral vertebrae, posterior pleurocoel in anterior elements: absent (0), present (1). (Carrano et al. 2012: 158)

(159) Presacral vertebrae, extent of anterior pleurocoel: to D4 (0), to sacrum (1). (Carrano et al. 2012: 159)

(160) Vertebrae, internal structure of pneumatic centra: absent, 'pleurocoels' if present, form fossae, not foramina (0), camerate (1), camellate (2). (Carrano et al. 2012: 160)

(161) Atlas, length of epipophyses: moderate (0), elongate (1). (Carrano et al. 2012: 161)

(162) Axis, spinous process shape: dorsal end expanded transversely (0), tapers mediolaterally (1). (Carrano et al. 2012: 162)

(163) Axis, orientation of intercentrum ventral surface: horizontal or slightly anteroventral (0), tilted anterodorsally (1). (Carrano et al. 2012: 163)

(164) Axis, length of epipophyses: moderate (0), long (1), short (2). (Carrano et al. 2012: 164)

(165) Axis, morphology of spinopostzygapophyseal lamina: broad, well-developed (0), invaginated (1). (Carrano et al. 2012: 165)

(166) Axis, development of parapophyses: moderate/large (0), reduced/absent (1). (Carrano et al. 2012: 166)

(167) Axis, development of diapophyses: moderate (0), reduced or absent (1). (Carrano et al. 2012: 167)

(168) Axis, pleurocoels: absent (0), present (1). (Carrano et al. 2012: 168)

(169) Axis, ventral keel: present (0); absent (1) (Novas et al. 2013: 96)

(170) Cervical vertebrae, morphology of anterior pleurocoel: single opening (0), two openings oriented anteroventralposterodorsal or very plastic morphology (1). (Carrano et al. 2012: 169)

(171) Cervical vertebrae, middle, shape of anterior pleurocoel: round (0), anteroposteriorly elongate (1). (Carrano et al. 2012: 170)

(172) Cervical vertebrae, anterior, ventral keel: present (0), absent or weak ridge (1). (Carrano et al. 2012: 171)

(173) Cervical vertebrae, anterior, demarcation of dorsal surface of neural arch from diapophyseal surface: gently sloping (0), ridge (prominent prezygapophyseal–epipophyseal lamina) (1). (Carrano et al. 2012: 172)

(174) Anterior and mid-cervical vertebrae, postzygadiapophyseal laminae: feebly developed and posteriorly concave (0); developed as a thick lamina and subvertically oriented, being the diapophyses extensive and subtriangular in lateral view (1). (Novas et al. 2013: 99)

(175) Mid-cervical vertebrae, neural spines: thin, with an homogeneous anteroposterior lenght along all its depth (0); robust, with its base strongly anteroposteriorly wider than its distal end (1). (Novas et al. 2013: 100)

(176) Cervical vertebrae, hyposphene-hypantrum accesory articulations: absent (0); present (1). (Novas et al. 2013: 102)

(177) Cervical vertebrae, prezygoepipophyseal laminae: absent (0); present as a ridge, separating the neural arch in a dorsal and lateral faces (1); present as a deep lamina (2). (Novas et al., 103)

(178) Cervical vertebrae, anterior and middle cervical vertebra centra: anterior and posterior articular surfaces at the same horizontal level (0); posterior articular surface strongly ventrally offset from the anterior one (1). (Novas et al. 2013: 282)

(179) Cervical vertebrae, anterior and middle cervical prezygapohyses: most with a pointing anterior margin (0); most with a rounded anterior margin (1). (Novas et al. 2013: 283)

(180) Cervicals, posterior articular face of mid cervical centra, width: approximately as broad as tall (0); at least 20% broader than tall (1). (Brusatte and Sereno 2008: 62)

(181) Cervical vertebrae, position of parapophysis on centrum: anterior (0), middle (1). (Carrano et al. 2012: 173)

(182) Cervical vertebrae, articular surface of prezygapophyses: planar (0), flexed (1). (Carrano et al. 2012: 174)

(183) Cervical vertebrae, perimeter of anterior articular surface: not rimmed by a flattened peripheral band (0), flat, forming a distinct rim (1). (Carrano et al. 2012: 175)

(184) Cervical vertebrae, anterior, transverse distance between prezygapophyses relative to width of neural canal: < (0), >, prezygapophyses situated lateral to neural canal (1). (Carrano et al. 2012: 176)

(185) Cervical vertebrae, anterior, morphology of epipophyses: low, blunt (0), long, thin (1), long, robust (2). (Carrano et al. 2012: 177)

(186) Cervical vertebrae, anteroposterior length of neural spines: nearly as long as centrum (0), ≤ 75% centrum length (1). (Carrano et al. 2012: 178)

(187) Cervical vertebrae, longest post-axial elements: first five (0), last five (1). (Carrano et al. 2012: 179)

(188) Cervical vertebrae, middle, length/height ratio of centra: less than 3 (0), more than 3 (1). (Carrano et al. 2012: 180)

(189) Anterior dorsals, opithocoelous: absent (0); present (1). (Novas et al. 2013: 105)

(190) Dorsal vertebrae, pneumaticity/webbing at base of neural spines: absent (0), present (1). (Carrano et al. 2012: 181)

(191) Dorsal vertebrae, accessory centrodiapophyseal lamina: absent (0), present (1). (Carrano et al. 2012: 182)

(192) Dorsal vertebrae, size of infraprezygapophyseal fossa: small (0), expanded (1). (Carrano et al. 2012: 183)

(193) Dorsal vertebrae, anterior, ventral keel: absent or developed as a weak ridge (0), pronounced, around 1/3 the height of centrum and inset from lateral surfaces (1). (Carrano et al. 2012: 184)

(194) Dorsal vertebrae, anterior, size of pneumatic foramen in centrum: small (0); enlarged (1). (Carrano et al. 2012: 185)

(195) Dorsal vertebrae, elevation of parapophyses: slightly elevated from centrum (0), project far laterally, more than half the diapophyseal length (1). (Carrano et al. 2012: 186)

(196) Dorsal vertebrae, orientation of hyposphene laminae: diverge ventrolaterally (0), parallel and sheet-like (1). (Carrano et al. 2012: 187)

(197) Dorsal vertebrae, position of parapophyses in posteriormost elements: on the same level as transverse process (0); distinctly below transverse process (1). (Carrano et al. 2012: 188)

(198) Dorsal vertebrae, distinct step-like ridge lateral to hyposphene, running posterodorsally from dorsal border of neural canal to posterior edge of postzygapophyses: absent (0); present (1); ridge present and is developed into a prominent lamina that bisects the infrapostzygapophyseal fossa in posterior dorsal vertebrae (2). (Carrano et al. 2012: 189)

(199) Dorsal vertebrae, middle and posterior, postzygapophyses with tab-like lateral extensions of articular facets: absent (0); present (1). (Carrano et al. 2012: 190)

(200) Dorsal vertebrae, morphology of neural spines: transversely compressed sheets (0), transversely broad anteriorly and posteriorly, central regions of lateral surface embayed by deep vertical troughs (1). (Carrano et al. 2012: 191)

(201) Dorsal vertebrae, posterior, inclination of neural spines: vertical or posterior (0), anterior (1). (Carrano et al. 2012: 192)

(202) Dorsal vertebrae, height of neural spines relative to centrum height: low, ≤ 1.3x (0), moderate, 1.4-1.8x (1); tall, ≥ 2.0x (2). (Carrano et al. 2012: 193)

(203) Dorsal vertebrae, posterior, centrum constriction: weak (0), strong (1). (Carrano et al. 2012: 194)

(204) Dorsal vertebrae, centrum length relative to height: more than 2 (0), less than 2 (1). (Carrano et al. 2012: 195)

(205) Sacral vertebrae, centrum pneumaticity: absent (0), pleurocoelous fossae (1); pneumatic foramina (2). (Carrano et al. 2012: 196)

(206) Sacral vertebrae, number: 2 [primordial sacrals only] (0), 5 [1 dorsosacral, 2 caudosacrals] (1), 6 [2 dorsosacrals, 2 caudosacrals] (2). (Carrano et al. 2012: 197)

(207) Sacral vertebrae, transverse dimensions of middle centra relative to other sacrals: equivalent (0), constricted (1). (Carrano et al. 2012: 198)

(208) Sacral vertebrae, orientation of ventral margin of middle centra: approximately horizontal (0), strongly arched (1). (Carrano et al. 2012: 199)

(209) Sacral vertebrae, dorsal edge of neural spines: as thin as remainder of spine (0), transversely thickened (1). (Carrano et al. 2012: 200)

(210) Sacral vertebrae, pneumaticity of neural arches: weak or absent (0), paired fossa ventral to diapophyses (1). (Carrano et al. 2012: 201)

(211) Sacrum, fenestrae between sacral neural spines: absent (0); present (1) (Benson 2010: 127)

(212) Caudal vertebrae, hyposphene-hypantrum accesory articulations: absent or poorly developed, restricted to the base of the tail (0); well-developed and extended approximately along the first third of the tail (1). (Novas et al. 2013: 111)

(213) Caudal vertebrae, anterior, morphology of ventral surface: flat (0), groove (1), ridge (2). (Carrano et al. 2012: 202)

(214) Caudal vertebrae, L-shaped neural spines: absent (0), present (1). (Carrano et al. 2012: 203)

(215) Caudal vertebrae, neural spines: simple, undivided (0); separated into anterior and posterior alae throughout much of caudal sequence (1). (Novas et al. 2013: 287)

(216) Caudal vertebrae, pleurocoels (large pneumatic foramina in centrum): absent (0), present (1). (Carrano et al. 2012: 204)

(217) Caudal vertebrae, anterior, centrodiapophyseal laminae on neural arch: weak or lacking (0), as prominent as in dorsal vertebrae, defining deep infradiapophyseal fossa that penetrates neural arch (pneumatic) (1). (Carrano et al. 2012: 205)

(218) Caudal vertebrae, anterior, proportions of neural arch base relative to centrum proportions: < (0), ≥ (1). (Carrano et al. 2012: 206)

(219) Caudal vertebrae, middle, morphology of neural spines: rod-like and posteriorly inclined (0), subrectangular and sheet-like (1), rod-like and vertical (2). (Carrano et al. 2012: 207)

(220) Distal caudal vertebrae, prezygapophyses length: reaching at least 40% or more preceding vertebral centrum (0); less than 40% (1). (Novas et al. 2013: 114)

(221) Cervical ribs, articulation with cervical vertebrae in adults: separate (0), fused (1). (Carrano et al. 2012: 208)

(222) Cervical ribs, length of anterior process: short (0), long (1). (Carrano et al. 2012: 209)

(223) Dorsal ribs: apneumatic (0); proximally pierced by foramina (1). (Novas et al. 2013: 116)

(224) Gastralia, posteriormost gastral segments: separate (0), united into single, boomerang-shaped elements (1). (Carrano et al. 2012: 210)

(225) Sacral ribs, articulations in adults: separate (0), fused together (1). (Carrano et al. 2012: 211)

(226) Sacral ribs, position of posterior attachment to ilium: ventral (0), posterodorsal (1). (Carrano et al. 2012: 212)

(227) Sacral ribs, depth relative to ilium height: < 85% (0), ≥ 90% (1). (Carrano et al. 2012: 213)

(228) Chevrons, morphology in middle caudal vertebrae: rod-like or only slightly expanded ventrally (0), L-shaped (1). (Carrano et al. 2012: 214)

(229) Chevrons, proximal articular surface: divided into anterior and posterior facets by distinct transverse ridge (0), no ridge, but low lateral mounds may be present, one on each side (1). (Carrano et al. 2012: 215)

(230) Chevrons, curvature: straight or gently curved (0), strongly curved (1). (Carrano et al. 2012: 216)

(231) Chevrons, anterior process: absent (0); present (1). (Carrano et al. 2012: 217)

(232) Chevrons, morphology of distal end in anterior and middle elements: expanded anteroposteriorly (0), unexpanded, tapers ventrally (1). (Carrano et al. 2012: 218)

(233) Scapula, angle between blade and acromion: gradual, oblique (0), abrupt, perpendicular (1). (Carrano et al. 2012: 219)

(234) Scapula, size of acromion process: moderate (0), marked (1). (Carrano et al. 2012: 220)

(235) Scapula, midshaft expansion of blade: absent (0), present (1). (Carrano et al. 2012: 221)

(236) Scapula, distal expansion of blade: marked (0), weak/absent (1). (Carrano et al. 2012: 222)

(237) Scapula, length:width ratio of blade: ≤ 7 (0), 7.5–9 (1), > 10 (2). (Carrano et al. 2012: 223)

(238) Scapulocoracoid, shape of anterior margin: indented or notched between acromial process and coracoid suture (0), smoothly curved and uninterrupted across scapula–coracoid contact (1). (Carrano et al. 2012: 224)

(239) Scapulocoracoid, glenoid lip: moderate (0), marked (1). (Carrano et al. 2012: 225)

(240) Coracoid, development of posteroventral process: low, rounded posteroventral eminence (0), pronounced, posteroventrally tapering process (1). (Carrano et al. 2012: 226)

(241) Coracoid, development of biceps tubercle (= acrocoracoid process): absent or poorly developed (0), conspicuous and well developed as tuber (1), developed as a posteroventrally oriented ridge (2). (Carrano et al. 2012: 227)

(242) Coracoid, prominent fossa on ventral surface posteroventral to glenoid (subglenoid fossa): absent (0); present (1). (Carrano et al. 2012: 228)

(243) Humerus, shape of head: elongate (0), globular (1). (Carrano et al. 2012: 229)

(244) Humerus, longitudinal torsion of shaft: absent (0), present (1). (Carrano et al. 2012: 230)

(245) Humerus, size of trochanters relative to midshaft diameter: < (0), > 150% (1) > 250% (2). (Carrano et al. 2012: 231)

(246) Humerus, development of internal tuberosity: low/rounded (0), hypertrophied (1). (Carrano et al. 2012: 232)

(247) Humerus, length of deltopectoral crest relative to total bone length: < 0.4 (0), 0.43–0.49 (1) > 0.52 (2). (Carrano et al. 2012: 233)

(248) Humerus, height of deltopectoral crest: low (0), prominent (1). (Carrano et al. 2012: 234)

(249) Humerus, orientation of deltopectoral crest apex: anteriorly (0), anterolaterally (1). (Carrano et al. 2012: 235)

(250) Humerus, relative orientation of proximal & distal condyles in anteroposterior view: parallel, humerus straight (0), distal canted (1). (Carrano et al. 2012: 236)

(251) Humerus, anterior surface of bone adjacent to ulnar condyle: smooth or gently depressed (0), bears well-defined fossa (1). (Carrano et al. 2012: 237)

(252) Humerus, shape of distal condyles: rounded (0), flattened (1). (Carrano et al. 2012: 238)

(253) Radius and ulna, development of radial external tuberosity and ulnar internal tuberosity: low, rounded (0), hypertrophied distal ends of radius and ulna broadened (1). (Carrano et al. 2012: 239)

(254) Radius, shaft: straight (0); curves laterally (1). (Carrano et al. 2012: 240)

(255) Radius, development of medial biceps tubercle: small or indistinct (0), hypertrophied (1). (Carrano et al. 2012: 241)

(256) Ulna, olecranon process: absent (0), present (1). (Carrano et al. 2012: 242)

(257) Ulna, morphology of olecranon process: transversely robust (0); transversely compressed and 'blade-like' (1). (Carrano et al. 2012: 243)

(258) Ulna, crest extending distally along posterior surface from olecranon process: absent (0), present (1). (Carrano et al. 2012: 244)

(259) Ulna, hypertrophied medial and lateral processes on proximal end: absent (0), present (1). (Carrano et al. 2012: 245)

(260) Ulna, length relative to minimum circumference: stout, < 2.3 (0); gracile > 2.6 (1). (Carrano et al. 2012: 246)

(261) Carpus, morphology and articulations of distal carpals: separate dc1 and dc2 over separate metacarpals, flattened proximodistally (0), fused dc1 and dc2, dc1 overlaps metacarpals I and II, flattened proximodistally (1), fused dc1 and dc2, dc1 overlaps metacarpals I and II, strongly arched proximodistally (2). (Carrano et al. 2012: 247)

(262) Manus, length relative to length of arm + forearm: < (0), ≥ (1). (Carrano et al. 2012: 248)

(263) Manus, composition: digit IV and V present (0), digit IV present, digit V absent (1), MC IV present, IV phalanges and digit V absent (2), digits IV and V absent (3). (Carrano et al. 2012: 249)

(264) Manual digits, lengths: III longest (0), II longest (1). (Carrano et al. 2012: 250)

(265) Metacarpals, transverse width of proximal articular ends relative to minimum transverse shaft width: < (0), ≥ 2x (1). (Carrano et al. 2012: 251)

(266) Metacarpal I, length to minimum width ratio: 1.4–1.9 (0), ≥ 2.4 (1). (Carrano et al. 2012: 252)

(267) Metacarpal I, length relative to length of metacarpal II: > 50% (0), < 50% (1). (Carrano et al. 2012: 253)

(268) Metacarpal I, extent of contact with metacarpal II relative to shaft length: < 1/3 (0), 1/2 (1). (Carrano et al. 2012: 254)

(269) Metacarpal I, angle between facet for metacarpal II and proximal articular facet: perpendicular (0), obtuse (1). (Carrano et al. 2012: 255)

(270) Metacarpal III, position of base relative to those of other metacarpals: at same level (0), on palmar surface (1). (Carrano et al. 2012: 256)

(271) Metacarpal III, shape of proximal end: rectangular (0), triangular (1). (Carrano et al. 2012: 257)

(272) Metacarpal III, width relative to width of metacarpal II: > 50% (0), < 50% (1). (Carrano et al. 2012: 258)

(273) Manual ungual I, length:height ratio: < 2.5x (0), > 2.5x (1). (Carrano et al. 2012: 259)

(274) Manual unguals, proximal height:width ratio: transversely broad, < 2.0 (0), transversely narrow, > 2.4 (1). (Carrano et al. 2012: 260)

(275) Pelvic elements, articulations in adults: separate (0), fused (1). (Carrano et al. 2012: 261)

(276) Ilium, large external pneumatic foramina and internal spaces: absent (0), present (1). (Carrano et al. 2012: 262)

(277) Ilium, vertical ridge on lateral surface of blade dorsal to acetabulum: absent (0), low swollen ridge (1), low double ridge (2). (Carrano et al. 2012: 263)

(278) Ilium, posterior width of brevis fossa: subequal to anterior width, fossa margins subparallel (0), twice anterior width, fossa widens posteriorly (1). (Carrano et al. 2012: 264)

(279) Ilium, height of lateral wall of brevis fossa relative to medial wall: taller along whole length (0), shorter anteriorly, exposing medial wall in lateral view (1). (Carrano et al. 2012: 265)

(280) Ilium, morphology between supraacetabular crest and brevis shelf on lateral surface: gap (0), continuous ridge (1). (Carrano et al. 2012: 266)

(281) Ilium, ventrolateral development of supraacetabular crest: large/pendant 'hood' (0), reduced shelf (1). (Carrano et al. 2012: 267)

(282) Ilium, orientation of pubic peduncle: mostly ventral (0), mostly anterior or 'kinked' double facet with anterior and ventral components (1). (Carrano et al. 2012: 268)

(283) Ilium, shape of acetabular margin of pubic peduncle: transversely convex or flat (0); transversely concave (1). (Carrano et al. 2012: 269)

(284) Ilium, relative sizes of pubic and ischial articulations: subequal (0), pubic articulation ≥ 130% of iliac articulation (1). (Carrano et al. 2012: 270)

(285) Ilium, morphology of ischial peduncle: rounded (0), acuminate (1). (Carrano et al. 2012: 271)

(286) Ilium, pubic peduncle length to width ratio: ≤ 1 (0), 1.3–1.75 (1), > 2 (2). (Carrano et al. 2012: 272)

(287) Ilium, ridge on medial surface adjacent to preacetabular notch: absent (0), present (1), strongly developed, forming a shelf (2). (Carrano et al. 2012: 273)

(288) Ilium, preacetabulum length relative to anterior edge of pubic peduncle: reaches anteriorly to same point as ('brachyiliac') (0), or well past ('dolichoiliac') (1). (Carrano et al. 2012: 274)

(289) Ilium, dorsal margin of blade, position relative to sacral neural spines: separated by a gap (0); lies against neural spines and opposing iliac blades may make contact above neural spines in some individuals (1). (Novas et al. 2013: 150)

(290) Ilium, ratio of anteroposterior length to dorsoventral depth above acetabulum: equal or greater than 2.8, ilium is long and low (0); less than 2.8, ilium is subovoid shape (1). (Novas et al. 2013: 153)

(291) Ilium, exposition of fossa brevis in lateral view: widely exposed and inviding the base of the ischiadic peduncle (0); mostly hidden by the brevis shelf and not inviding the base of the ischiadic peduncle (1). (Novas et al. 2013: 154)

(292) Ilium, anterior margin of preacetabular process, profile: gently convex (0); straight (1). (Brusatte and Sereno 2008: 77)

(293) Ilium, depth of preacetabular process: shallow (0), deep (1). (Carrano et al. 2012: 275)

(294) Ilium, anteroventral lobe of preacetabular process: absent (0), present (1). (Carrano et al. 2012: 276)

(295) Ilium, shape of dorsal margin: convex (0), straight (1). (Carrano et al. 2012: 277)

(296) Ilium, postacetabulum length relative to ischial peduncle length: ≤ (0), > (1), 2x (2). (Carrano et al. 2012: 278)

(297) Ilium, depth of postacetabular process: shallow (0), deep (1). (Carrano et al. 2012: 279)

(298) Ilium, shape of posterior margin of postacetabular process: convex (0), concave (1), straight (2), with prominent posterodorsal process but lacking posteroventral process (3). (Carrano et al. 2012: 280)

(299) Ilium, fossa cuppedicus: absent (0); present (1); present and bounded dorsomedially by a prominent shelf (2). (Novas et al., 2012: 148)

(300) Puboischiadic plate, morphology and foramina/notches: fully closed along midline, 3 fenestrae (0), open along midline, 1 fenestra (obturator foramen of pubis) and 1–2 notches (1), open along midline, 0 fenestrae, 1–2 notches (2). (Carrano et al. 2012: 281)

(301) Pubis, shaft in lateral view: straight (0); anteriorly convex (1); anteriorly concave (2). (Novas et al. 2013: 156)

(302) Pubis, articulation between apices in adults: unfused (0); fused (1). (Carrano et al. 2012: 283)

(303) Pubis, contact between distal portions: separate distally (0), contacting (1), contacting with slit-like opening proximal to distal expansion (interpubic fenestra) (2). (Carrano et al. 2012: 284)

(304) Pubis, angle between long axes of shaft and boot: 75– 90° (0), < 60° (1). (Carrano et al. 2012: 285)

(305) Pubis, morphology of symphysis: marginal (0), broad (1). (Carrano et al. 2012: 286)

(306) Pubis, pubic symphisis in anterior view: continuous up to the distal end of the bone (0); interrupted distally by a large median fenestra (1). (Novas et al. 2013: 159)

(307) Pubis, morphology of obturator foramen: small and subcircular (0), large and oval (1). (Carrano et al. 2012: 287)

(308) Pubis, obturator opening: foramen (0); incipient notch (1); wide and well-developed opening (2). (Novas et al. 2013: 155)

(309) Pubis, anterior expansion of distal end: absent (0), present (1). (Carrano et al. 2012: 288)

(310) Pubis, pubic boot, position of anterior process relative to posterior process: displaced dorsally, resulting in a highly convex ventral margin of the boot (0); placed at the same level, ventral margin of the boot essentially straight (1). (Novas et al. 2013: 161)

(311) Pubis, boot length relative to shaft length: < (0), > 30% (1), > 60% (2). (Carrano et al. 2012: 289)

(312) Pubis, shape of boot in ventral view: broadly triangular (0), narrow, with subparallel margins (1). (Carrano et al. 2012: 290)

(313) Pubis, articulation with ilium: planoconcave (0), peg-and-socket (1). (Carrano et al. 2012: 291)

(314) Pubis, pubic tubercle: absent (0); present as a convexity on the anterior margin of the pubis (1); present as a rugose flange that is discretely offset from the anterior margin of the pubis and is bordered posteriorly by heavy rugosities on the lateral surface on the obturator region of the pubis (2). (Novas et al. 2013: 158)

(315) Ischium, length relative to pubis length: 75–80% (0), ≤ 70% (1), > 80% (2). (Carrano et al. 2012: 292)

(316) Ischium, shaft orientation: straight (0), ventrally curved (1). (Carrano et al. 2012: 293)

(317) Ischium, articulation with ilium: planoconcave (0), peg-and-socket (1). (Carrano et al. 2012: 294)

(318) Ischium, morphology of antitrochanter: large and notched (0), reduced (1). (Carrano et al. 2012: 295)

(319) Ischium, obturator opening: absent (0); foramen (1); notch (2). (Novas et al. 2013: 163)

(320) Ischium, notch ventral to obturator process: absent (0), present (1). (Carrano et al. 2012: 296)

(321) Ischium, morphology of symphysis: unexpanded (0), expanded as apron (1). (Carrano et al. 2012: 297)

(322) Ischium, cross-sectional shape of paired midshafts: oval (0), heart-shaped, medial portions of shafts extend posteriorly as midline flange (1). (Carrano et al. 2012: 298)

(323) Ischium, morphology of distal end: rounded (0), expanded, triangular (1). (Carrano et al. 2012: 299)

(324) Ischium, posteriorly-directed flange on iliac peduncle: absent (0); present (1). (Brusatte and Sereno 2008: 82)

(325) Ischium, articulation at distal end in adults: separate (0), fused (1). (Carrano et al. 2012: 300)

(326) Femur, head orientation: 45° anteromedial (0), 10–30° anteromedial (1), medial (2). (Carrano et al. 2012: 301)

(327) Femur, head angle: ventromedial (0), horizontal (medial) (1), dorsomedial (2). (Carrano et al. 2012: 302)

(328) Femur, groove on proximal surface of head oriented oblique to long axis of head ('articular groove'): absent (0), present (1). (Carrano et al. 2012: 303)

(329) Femur, oblique ligament groove on posterior surface of head: shallow, groove bounding lip does not extend past posterior surface of head (0), deep, bound medially by well-developed posterior lip (1). (Carrano et al. 2012: 304)

(330) Femur, placement of lesser trochanter relative to femoral head: does not reach ventral margin (0), rises past ventral margin (1), rises to proximal surface (2). (Carrano et al. 2012: 305)

(331) Femur, anterior trochanter with an anterior proyection at mid-length: present (0); absent, anterior margin of the anterior trochanter straight or gently convex in lateral or medial view (1). (Novas et al. 2013: 176)

(332) Femur, morphology of anterolateral muscle attachments at proximal end: continuous trochanteric shelf (0), distinct lesser trochanter and attachment bulge (1). (Carrano et al. 2012: 306)

(333) Femur, development of fourth trochanter: prominent semioval flange (0), very weak or absent (1). (Carrano et al. 2012: 307)

(334) Femur, distinctly projecting accessory trochanter (derived from lesser trochanter): weak, forms slightly thickened margin of lesser trochanter (0), present as triangular flange (1). (Carrano et al. 2012: 308)

(335) Femur, M. femorotibialis externus origin medially on anterodistal surface: faint, small rugose patch (0), pronounced rugose depression that extends to distal femur (1). (Carrano et al. 2012: 309)

(336) Femur, development of medial epicondyle: rounded (0), ridge (1). (Carrano et al. 2012: 310)

(337) Femur, medial epicondyle (=mediodistal crest), length: poorly developed or short (0); pronounced, extending 30% or more up the length of the femoral shaft (1). (Brusatte and Sereno 2008: 85)

(338) Femur, extensor groove: absent (0); wide and shallow (1); narrow and deep (2). (Novas et al. 2013: 181)

(339) Femur, morphology and orientation of tibiofibularis crest: broad (0), narrow, longitudinal (0), lobular, oblique (2). (Carrano et al. 2012: 312)

(340) Femur, tibiofibular crest: sub-triangular or sub-rectangular (0); kidney-shaped (1). (Novas et al. 2013: 178)

(341) Femur, infrapopliteal ridge connecting medial distal condyle and crista tibiofibularis: absent (0), present (1). (Carrano et al. 2012: 313)

(342) Femur, orientation of long axis of medial condyle in distal view: anteroposterior (0), posterolateral (1). (Carrano et al. 2012: 314)

(343) Femur, projection of lateral and medial distal condyles: approximately equal (0), lateral projects distinctly further than medial, distal surface of medial is gently flattened (1). (Carrano et al. 2012: 315)

(344) Femur, morphology of distal end: central depression connected to crista tibiofibularis by a narrow groove (0), anteroposteriorly oriented shallow trough separating medial and lateral convexities (1). (Carrano et al. 2012: 316)

(345) Femur, lateral condyle, shape in distal view: circular or ovoid (0); ovoid, but with an anterior bulge that is slightly separated from the remainder of the condyle (1). (Novas et al. 2013: 177)

(346) Femur, tibiofibular fossa: wide, more than 90° between the lateral margin of tibiofibular crest and posterior margin of lateral condyle (0); narrow, less than 90° between the lateral margin of tibiofibular crest and posterior margin of lateral condyle (1). (Novas et al. 2013: 183)

(347) Tibia, lateral malleolus: backs astragalus (0), overlaps calcaneum (1). (Carrano et al. 2012: 317)

(348) Tibia, maximum length: equal to or less than 12 times the anteroposterior width at mid-length (0); more than 12 times the anteroposterior width at mid-length (1). (Novas et al. 2013: 186)

(349) Tibia, shape of edge of lateral malleolus: smoothly curved (0), tabular notch (1). (Carrano et al. 2012: 318)

(350) Tibia, morphology of distal cnemial process: rounded (0), expanded proximodistally (1). (Carrano et al. 2012: 319)

(351) Tibia, morphology of lateral (fibular) condyle: large (0), small and lobular (1). (Carrano et al. 2012: 320)

(352) Tibia, anterolateral process of lateral condyle: absent or horizontal projection (0), prominent, curves ventrally (1). (Carrano et al. 2012: 321)

(353) Tibia, lateral condyle: confluent with cnemial crest anteriorly in proximal view (0); strongly offset from cnemial crest by incisura tibialis (1). (Eddy and Clarke 2011: 166)

(354) Tibia, anteromedial buttress for astragalus: absent (0), ventral (1), marked oblique step-like ridge (2), reduced oblique ridge (3), bluntly rounded vertical ridge on medial side (4). (Carrano et al. 2012: 322)

(355) Tibia, morphology of fibular crest: narrow (0), bulbous (1). (Carrano et al. 2012: 323)

(356) Tibia, development of fibular crest: extends to proximal end of tibia as high crest (0), extends to proximal end of tibia as low ridge (1), does not extend to proximal end of tibia (2). (Carrano et al. 2012: 324)

(357) Tibia, median prominence in the anterior surface of the distal end: absent, anterior margin straight or gently concave in distal view (0); present (1). (Novas et al., 2012: 188)

(358) Tibia, lateral malleolus, distal extension relative to medial malleolus: even with or extends slightly distally (0); extent beyond the medial malleolus 7% or more of the length of the tibia (1). (Brusatte and Sereno 2008: 91)

(359) Fibula, depth of fibular fossa on medial aspect: groove (0), shallow fossa (1), deep fossa (2). (Carrano et al. 2012: 325)

(360) Fibula, position of fibular fossa on medial aspect: posterior edge (0), central (1). (Carrano et al. 2012: 326)

(361) Fibula, size of iliofibularis tubercle: faint scar (0), large (1), anterolaterally curving flange (2). (Carrano et al. 2012: 327)

(362) Fibula, ratio of anteroposterior width of distal end to minimum shaft width: 2.3 or greater (0); 1.9–2.1 (1); less than 1.7 (2). (Novas et al. 2013: 194)

(363) Fibula, size of proximal end relative to width of proximal tibia: < 75% (0), ≥ 75% (1). (Carrano et al. 2012: 328)

(364) Fibula, length compared with femoral length: subequal (0); shorter (ca. 70 %) (1). (Novas et al. 2013: 192)

(365) Astragalus, articulation between ascending process and fibula in adults: separate (0), fused (1). (Carrano et al. 2012: 329)

(366) Astragalus, orientation of distal condyles: ventral (0), 30-45° anterior (1). (Carrano et al. 2012: 330)

(367) Astragalus, ascending process morphology: absent (0), blocky (1), laminar (2). (Carrano et al. 2012: 331)

(368) Astragalus, angle of dorsal margin of ascending process: low and oblique (0), high and oblique (1). (Carrano et al. 2012: 332)

(369) Astragalus, transverse width of ascending process: not occupying total width of anterior surface of distal tibia (0); occupying total width of anterior surface of distal tibia (1). (Novas et al. 2013: 196)

(370) Astragalus, ascending process height relative to depth of astragalar body: less (0), subequal (1), > 1.6 times (2). (Carrano et al. 2012: 333)

(371) Astragalus, prominent proximolateral extension: absent (0); present (1). (Carrano et al. 2012: 334)

(372) Astragalus, round fossa at base of ascending process: absent (0), small (1), large (2). (Carrano et al. 2012: 335)

(373) Astragalus, development of articular surface for distal end of fibula: large, dorsal (0), reduced, lateral (1). (Carrano et al. 2012: 336)

(374) Astragalus, posterolateral crest: absent (0), present (1). (Carrano et al. 2012: 337)

(375) Astragalus, posteromedial crest: absent (0), present (1). (Carrano et al. 2012: 338)

(376) Astragalus, articulation with calcaneum in adults: separate (0), fused (1). (Carrano et al. 2012: 339)

(377) Metatarsal I, length relative to length of metatarsal II: ≥ 50% (0), < 50% (1). (Carrano et al. 2012: 340)

(378) Metatarsal III, shape of proximal end: rectangular (0), shallow notch (1), deep notch (2). (Carrano et al. 2012: 341)

(379) Metatarsal III, midshaft cross-sectional shape: rectangular (0), wedge-shaped, plantar surface pinched (1). (Carrano et al. 2012: 342)

(380) Metatarsal III, relative proportions of shaft: short and thick, length:transverse width ratio < 12.0 (0), long and gracile, ratio > 12.5 (1). (Carrano et al. 2012: 343)

(381) Metatarsal IV, proportions of distal end: broader than tall (0), taller than broad (1). (Carrano et al. 2012: 344)

(382) Metatarsal V, morphology of distal end: articular (0), non-articular (1). (Carrano et al. 2012: 345)

(383) Metatarsal V, length relative to length of metatarsal IV: > 50% (0), < 50% (1). (Carrano et al. 2012: 346)

(384) Antarctometatarsus: absent (0), present (1). (Carrano et al. 2012: 347)

(385) Pedal unguals, morphology of lateral and medial grooves: single (0), double (1). (Carrano et al. 2012: 348)

(386) Pedal unguals, digits III and IV, cross-sectional shape: triangular (0), elliptical (0). (Carrano et al. 2012: 349)

(387) Pedal unguals, digit II, mediolateral symmetry: symmetrical (0), asymmetrical (1). (Carrano et al. 2012: 350)

(388) Pedal digit phalanges, length of I-1 + I-2 relative to III-1: greater (0), less than or equal (1). (Carrano et al. 2012: 351)

APPENDIX 6.4.2

Data matrix

#NEXUS

begin data;

dimensions ntax=36 nchar=388;

format missing=? symbols="0~4";

matrix

Allosaurus 00101{01}0000010001010000000211111100011011000 02{01}2{01}001011000000001011111000110200000002001101100011010010010201 20?1111111120001001102011111111110000100011020010011001101110011{01}0{01}1000011000001011010010000100010111100000011 1?000000000101?1101101200120011101011000010001113100111111000011101001021101011101101021201102101000200121100 10{12}101101011 1?2000001001 0001012021021011001110102111012101110 0101

Acrocanthosaurus 020?1100?0000001111000000211111100010?0000002111012111000202120 11?21111020110?02??110121000001001101000120111 11?1100210010102001 0?11111?0001000100000100011012?001100101?000001001?00121101001000110011211110?00?021100001000101??11101101200120 01110?001011110000113110111111000????010?10??1???? 110110?0212011?21?20??20112110010220110 10111?2200111001?00101302?1?102110 ?11?10?1??012101110 01?1

Afrovenator ?????????001010110000010013001100 0?????0?000201001?011001011000?????????00?001 111001???0000000001?????10?11001?0?011000001000000?0?00110110?0001?001?000001?????????1?0000?0????1?01010??????????0111?????00?0?????0?31001111?100001?10?0110101?00? 1?011?0?012?11?0000?000101211000011101010000?2100000001?0000?20???11011?0 110????111 0 11?011100??1

Baryonyx 111?020101121011 0?0000???03???1??01????0000120201 1?0??????0??0?1111100??????0?110 11010001011?01??010210?011??????????001101010?{12}101???1??0100101100013001011100{12}?1001001?001000000??001101111110100011000101010?0??????000??000??1??1?00??0?1?01000111111000100110 10????????????10?0?11010?101 ?1??0?110110?00?2?1???0??????00121000?????11????00?210010?00????????????1 101??0????? ?????????0????????

Carcharodontosaurus ??????0??0000001111000010021011101011110 20?02?1?0??111100??21211211?211????0????????110121?0??0100??0112112 1???1???????2?10?????????????1000020000?????10?110?2????? ??0???01?0??1???1?00101?0????1????0?????????????????100??0????1???1???1??1???????? ???11???2??0????????0???112????1?22??1?10111?2???01??11?00??????????02110?????????? ???????? ?? ??

Ceratosaurus

021010001000000000000000000201000101 20?0000002020011000000010000111111000101001001000101010100000000011010000111000 0?10001000000 1??1000000100100010000010100100011021?0100010000000000?0000211000000001010000101021 1???01000002110 0?0100001101011110100100110000????0??1??1?01?00010?010?11100?000010?0?1101110111101?00000010{01}0000100101001100{01}0011?02?1000101001 00?200?02 1101001000102 1??1?0001??10???

Concavenator

?????0???????0??????001002??0?1?00?1111?20102010000?110??10??2????1??1020?0??????{01}0??100?????????0????10?100?????{12}?1?1?10?????1???0211?1?1????{01}1100?01000????1?111110?10?1??0?0??10??0?1010001?????????????0?0?0?10? 11??1000?11011010???????2????0?2011????1??22??1?100?????????????????????2????00??0?1?01?????0???0?1?00???

Dilophosaurus

01?11211000010000000{01}001000200000000?100230100??00?200100001?0001001000?11011010000
00000?000000200101000001??0??0?????201100010000?1000000{01}10000000100000101011101??000111
?0010???????00001011?000000000000101010000??10?0002?01???10000100000010010010010000001010
001?111011000100010010001100001????100110?0{01}00?1?0?0?000?1000?1?00?100110?{01}0000?00?0
000?00?1000?201 ??002?1?0000?10101101000110000?0?

Elaphrosaurus

??
??0110{12}?????????0010???????0000?011?000001?00000
00002111???00?0001?1???010???????0???11?01100100001000?????????????????000111000000?1????111
111?10?{12}?????????0??0?0?0001?100110??0011?1???000?01?0000?200????2?1??0???????111?001???1????

Eustreptospondylus

?1???2000011?01100000010130?1???0???????100200001??????10?10001?1??00000???01111000010??10
01000100?11000012?????????00110111???????????00000?0?0100000100110011???01101?0010???????001
10110?000010011000101?100????1??0000??????1????????111?0???0111210?00?????????????????????0011
010110001????1?0113?30?2?1???0?000?0010?0100??11111?10000?01?0000?01?0000?201??110?1??110?10
2111??1001??000??

Giganotosaurus

02???000??0?00?11?100001002101???10?111020002111 0????????2021211??11211??0??1?00020?110121???00100?0011211?1??????111??201010?????1?1111110?0020000??000100110 12?01?0??1011001111010101?1?010?100?11001?21?2??????02?1000010????1??0?10??0???01?0??????????????????????????????00?1101001021100 0?1101101021201 1?21020002011211001022011?101???1??0???0?10001?1302?02102110?10??????????????????????

Majungasaurus

021010001000000100000001002000001 1120?10020000?101200000020202012?111101101100001000101 00?00000010?01101?101000001010110010100110010001001010000000100001000110210011001?0011???????00012110?000001010000001021?11??11?0012?01??01000011?1011?10?01100200001 0??????0?????????????0??011100000001 1????111111?1??????0?????1???1????????0??????0????1?????0?00?0100?200??211?1?1111?1021111?0001??1101?

Mapusaurus

??????0???000001111000010021 01?10101111020002111 0??1111102?2121121????????{02}01?000?0???????????????????????????????00201010?01001?????10000200 00?0???10011012???01????1??0?1?1????0010??01001??01?00102012??????02110000 1??1???????1?11012?0????1???10?10???????0????1????????000???0?0?102?100101101101 0???????2????0??0112?1001022??1110111?1??00?1?11000??13020121021?0110???2111012101??0010?

Marshosaurus

000??000000001001000110201200 1?000010?000??????????0?1001?10000????1000000?10?0?01?0100020000001001?0?00?1?0???????????10001??0???1?011??001001000100000100110 01?0111110?0010???????00012110?0000000120011 01?1??????????????????10???????0?1????????????1?????????????????????????00?11010010101????1?0110?000201???0?000??001?1100?0??????1?????????????????????????21??????????0????????????????

Masiakasaurus

0?????0???001001000001000020 00???0?????????10???????????0??20101?10?????????0?001??00????000?0001??00???010??????????1110100001100??00?000100000000???002000110 2?0011001?0011???????000111?0?0000010100000000201 11??10?0010?11??0100001?0101111100110010000 1??????????????????????001001?100000001????1?1111?111201?0?0?001?0010?01???100110?10011?12?1000?01?0100?200??2?1?1?1111?2021111?0011??1101?

Megalosaurus

?????????0000?01101100?00120?1?000?????????????????1?111???000101?????0?01100001001O?01??00?100???01????????0???0??0??????1????1?0?1????1000201110000101?10000???0?010?????01110?00000111211O?000010000?????????????001010101101010?0?1101131310{12}??0??????00?10?0?1?000111010100002?000000010000O?21111??0???0?1?0???1????1001??00???

Neovenator

00???10000010001010100000220O1???1011011O???1?????????110000???????????1000010001?020010011012?1?????1111100001110100121101001000110101011O?0????0211000001?1??1?10?10?1011?0120?????????????????????????????01?11010010221??0?110110{12}011201??2102000000012?10101020?1010111?2000011001000011?302012102100?10???1????210111?010?

Ornitholestes

000??000?00000?????000002200?1?000010000010100012?11000001000?1??10001?020?00??0??1000?00???0????0??0?????????????00000?0??0?0?0?0100111?000000??00001001100{12}??????????010???????0101?0?0?00?000100000001010O????1??0001?0???010??11?????????00101100000000???01??11??111??1??00?000101112111????110110?02???????????0?1001?0000?021??2?11??0?00?0000?0?????????2????0???0??????????????2001??0????

Piatnitzkysaurus

??????????000?0100001002012O?1???0?????????????????????????????????1???0????????????10?0100000010?1101000?10???????????2010?1????????????0010010?01?????0000100l?0011110?00100000???000121101000100012002101110000100121?0??000?0???010?????01011?11200111110110O??100?1?????????????001?1010010101??0?1?011?0?002?1000000000000000100000l1?11010000?000000000100000121116021011?0?100???1????1001??0????

Sinraptor

000010000000000000000100022111110001101000021100001110001000100l?11000011200100020110110001001001001120100111?111110000001100200111110000000010?0?100001001100110110010011000010000001211010011000110012110l0?0??11??000??0010010???1?01011100?????????????????????2???????11?000201010010101010111011212112110120000002101210100111011010111?2000001001100000211002100100110010211101210111001O1

Torvosaurus

00???100?0010?01101101010130O0??00????00?10120000l?011111011000?{01}??????????001111?01?????????????????????????????????010?0????????????000001000100100100110110102100l?00100000??000112110100011001100010111000O?1111100000?0?010?10100111000000011121100000010O?0{12}???0011011010000010101101011001?1101131300{12}?1?000000012001001000011l0??10000?01?0000?0100000?2020111021001100102111012101110010l

Herrerasaurus

000010000000000????0?0001000?0?0?00000?0000100??00120100000000000?000001000000002O?000010?00000?10??00000000?000000?10000?0?0000?000010010000?0?0?0100000000000000100001O??000?????000000000?0000?0?1000000?000000??00?0000?0???001??00?1?011?0??000001000000100000101000100000000000100000000?0???0000000?0000?0???0?010?0000?0?000000??0?00010?00?0000?00?00000000??0??0?100000?1000000000000000000

Dubreuillosaurus

01???100?00101010000001001300O1??0??0??002?0001?0????10110000011?0000002?????????10??101110??0?11100101?0??????010?01101110?201??????????0000?0100000100110O1?????????00???????????01?00010?1??????10???????11100001?001?????0110?????0?????????????????????????????????0??1?1???0000?0?????????????????1?0?1?????????????????1??????

Lourinhanosaurus

??????????????

Condorraptor

????????????

REFERENCES

Benson RBJ. 2010. A description of *Megalosaurus bucklandii* (Dinosauria: Theropoda) from the Bathonian of the UK and the relationships of Middle Jurassic theropods. Zool J Linn Soc. 158(4):882–935.

Brusatte SL, Sereno PC. 2008. Phylogeny of Allosauroidea (Dinosauria: Theropoda): comparative analysis and resolution. J Syst Palaeontol. 6(2):155–182.

Carrano MT, Benson RBJ, Sampson SD. 2012. The phylogeny of Tetanurae (Dinosauria: Theropoda). J Syst Palaeontol. 10(2):211–300.

Eddy DR, Clarke JA. 2011. New Information on the Cranial Anatomy of *Acrocanthosaurus atokensis* and its Implications for the Phylogeny of Allosauroidea (Dinosauria: Theropoda). PLoS ONE 6(3):e17932.

Novas FE, Agnolín FL, Ezcurra MD, Porfiri J, Canale JI. 2013. Evolution of the carnivorous dinosaurs during the Cretaceous: the evidence from Patagonia. Cretaceous Res. 45:174–215.

6.5. A NEW ALLOSAUROID THEROPOD SPECIMEN FROM CAMBELAS (TITHONIAN. TORRES VEDRAS, PORTUGAL)

E. Malafaia[1,2,3]*, P. Mocho[4,5,2], F. Escaso[5,2], P. Dantas[2,6], F. Ortega[5,2]

[1] Departamento de Geologia, Faculdade de Ciências and Instituto Dom Luiz, Universidade de Lisboa. Edifício C6. Campo Grande. 1749-016 Lisboa, Portugal, emalafaia@gmail.com

[2] Laboratório de Paleontologia e Paleoecologia, Sociedade de História Natural. Polígono Industrial do Alto do Ameal, Pav. H02 e H06, Torres Vedras, Portugal

[3] Museu Nacional de História Natural e da Ciência, Universidade de Lisboa. Rua da Escola Politécnica 56/58. 1250-102 Lisboa, Portugal

[4] The Dinosaur Institute, Natural History Museum of Los Angeles County, 900 Exposition Blvd. Los Angeles, CA 90007, USA

[5] Grupo de Biología Evolutiva. Facultad de Ciencias. Universidad Nacional de Educación a Distancia. C/ Senda del Rey, 9, 28040 Madrid, Spain

[6] Museu da Comunidade Concelhia da Batalha. Largo Goa, Damão e Diu, nº 4, 2440-901 Batalha, Portugal

*Corresponding author

RESUMO

Neste trabalho é descrito um novo exemplar de um dinossáurio terópode descoberto no Jurássico Superior da Bacia Lusitânica. O exemplar corresponde a um único individuo, que está representado por uma sequência de vértebras caudais, um pé direito praticamente completo e outros fragmentos do esqueleto apendicular. Este exemplar inclui o pé mais completo de um dinossáurio terópode conhecido actualmente na Bacia Lusitânica e representa um dos mais recentes registos destes terópodes identificado no Jurássico Superior português. A análise sistemática desenvolvida sobre este conjunto de elementos permitiu identificar o exemplar como pertencendo a um terópode allossauroide. Dentro de Allosauroidea, o exemplar partilha diversas características invulgares com alguns carcharodontossáurios, sobretudo com *Neovenator* e *Concavenator* do Cretácico Inferior de Inglaterra e Espanha, respectivamente e com *Veterupristisaurus* do Jurássico Superior da Formação de Tendaguru. Com base nesta combinação de características, o exemplar é identificado como pertencendo ao clado Carcharodontosauria. Este exemplar representa a primeira evidência destes allossauroides derivados em Portugal e amplia o registo, já bem conhecido, do Cretácico Inferior da Europa até ao Jurássico Superior. Este exemplar representa também o registo mais antigo de carcharodontossáurios na Laurasia, acrescentando informação relevante para o conhecimento das primeiras fases da história evolutiva do grupo. A presença de Carcharodontosauria, um grupo de terópodes aparentemente ausente em níveis correlativos da América do Norte, contrasta com a semelhança geral que tem sido reconhecida entre estas faunas do Jurássico Superior de ambos lados do proto-Atlântico Norte e tem importantes implicações paleobiogeográficas. A composição das faunas de terópodes do Jurássico Superior da Bacia Lusitânica e da Formação de Morrison sugere um cenário paleobiogeográfico no qual a evolução destas faunas terá sido determinada por processos de vicariância incipiente e, possivelmente, por padrões diferenciais de extinção regional e/ou de preferências ambientais.

Palavras-chave: Allosauroidea; Carcharodontosauria; Jurássico Superior, Sub-bacia de Turcifal; paleobiogeografia

ABSTRACT

A new specimen of a theropod dinosaur found in the Upper Jurassic of the Lusitanian Basin is described. The specimen corresponds to a single individual and includes a sequence of articulated caudal vertebrae, an almost complete right pes, and other fragments of the appendicular skeleton. This specimen includes the most complete pes of a theropod dinosaur currently known in the Lusitanian Basin and represents one of the youngest records of these dinosaurs currently known in the Portuguese Upper Jurassic. A systematic analysis of the specimen is performed. The recovered combination of characters allows interpret this specimen as an allosauroid theropod. Within Allosauroidea, this specimen shares several unusual features with some carcharodontosaurs, especially *Neovenator* and *Concavenator* from the Lower Cretaceous of England and Spain, respectively, and *Veterupristisaurus* from the Upper Jurassic of the Tendaguru Formation. This combination of characters indicates that the specimen might be related with Carcharodontosauria representing the first evidence for the presence of this clade in Portugal extending its record already well represented in the Lower Cretaceous of Europe. Beside, this specimen represents the oldest record of carcharodontosaurian theropods in the Laurasian record providing relevant information to fill the gap on the early radiation of the group. The presence of Carcharodontosauria, a theropod group that apparently is absent in correlative North American strata contrasts with the general similarity that has been recognized among these faunas from both sides of the proto-North Atlantic during the Late Jurassic and has important paleobiogeographic implications. The faunal composition of theropods in the Late Jurassic of the Lusitanian Basin suggests a scenario in which its paleobiogeographic evolution would be determined by incipient vicariance processes and possibly by differential patterns of regional extinction and/or local environmental preferences.

Keywords: Allosauroidea; Carcharodontosauria; Late Jurassic, Turcifal Sub-basin; paleobiogeography

6.5.1. INTRODUCTION

The currently known Portuguese record of theropod dinosaurs is relatively abundant and diverse, especially in Upper Jurassic sediments of the Lusitanian Basin (e.g. Lapparent and Zbyszewski 1957; Antunes and Mateus 2003; Mateus et al. 2006; Ortega et al. 2006). Despite some classical occurrences of theropod osteological remains, corresponding mainly to isolated elements (Sauvage 1897-98; Lapparent and Zbyszewski 1957), it was not until the end of the twenty century that the understanding of this record improved. The specimens described by Sauvage (1897-98) and Lapparent and Zbyszewski (1957) were assigned to different species of *Megalosaurus*, at that time a poorly understood taxon including some material from the Middle Jurassic of Stonesfield (Oxfordshire, UK), but also several other fossils from different ages worldwide (Benson 2008, 2010; Carrano et al. 2012; Rauhut et al. 2016). Most of the classical occurrences of theropod dinosaurs from the Upper Jurassic of Portugal were referred to *Megalosaurus insignis*, or to a supposedly exclusive Portuguese form, *Megalosaurus pombali* (Sauvage 1897-98; Lapparent and Zbyszewski 1957). These specimens were later reinterpreted as belonging to indeterminate theropods or assigned to other dinosaur groups (Mateus 2005; Mocho et al. 2016).

The current Late Jurassic record of theropods from the Lusitanian Basin includes mainly medium to large-sized forms belonging to early-diverging theropod clades, such as Ceratosauria, or basal tetanurans, including Megalosauroidea and Allosauroidea (e.g. Mateus 1998; Pérez-Moreno et al. 1999; Mateus and Antunes 2000a, 2000b; Rauhut and Fechner 2005; Mateus et al. 2006; Malafaia et al. 2010, 2015; Araújo et al. 2013; Hendrickx and Mateus 2014a, 2014b). Small-sized and more derived theropods have been also identified in this record based mainly on isolated elements (Zinke 1998; Rauhut 2003a; Hendrickx and Mateus 2014b; Malafaia et al. 2014).

Most of the theropod specimens known in this Portuguese record come from sediments of the Praia da Amoreira-Porto Novo Formation (*sensu* Manuppella et al. 1999) in the coastal region of the Bombarral Sub-basin (corresponding to the Consolação Sub-basin *sensu* Taylor et al. 2014). This Formation is interpreted as late Kimmeridgian in age and crops out along most of the littoral region between Torres Vedras and Peniche. Scarce, but scientifically important fossil sites with theropod remains are known at the northern area of the Bombarral Sub-basin, such as the Guimarota mine (Leiria), or the Andrés fossil site (Pombal). Theropod material is currently unknown in the Arruda Sub-basin, located in the southeast part of the Central Sector of the Lusitanian Basin, and only few occurrences are known in the Turcifal Sub-basin (Lapparent and Zbyszewski 1957), which is located west of the Arruda Sub-basin and is bounded on the north by the Torres Vedras-Montejunto fault and on the east by the Runa fault.

Herein, a partial postcranial skeleton of a theropod dinosaur found in the coastal region in the northern end of the Turcifal Sub-basin, at the Cambelas locality (Torres Vedras municipality), is described. A systematic discussion of the specimen and a preliminary taphonomic analysis are also proposed.

6.5.2. GEOLOGICAL SETTINGS

The Cambelas fossil site (TVSPC 12 in the Geographic Information System Applied to Palaeontology of the Sociedade de História Natural- SIGAP database) is situated in the littoral area of the southern part of Torres Vedras municipality, approximately 45 km north from Lisbon. This locality is placed in the Central Sector of the Lusitanian Basin and in the northern part of the Turcifal Sub-basin (Fig. 6.5.1). The sediments in the area of Cambelas consists of thick layers of red mudstones, with abundant levels of well-developed pedogenic carbonate concretions (caliche), intercalated with cross-bedded sandstones. These sediments are interpreted as belonging to the Freixial Formation that is dated from the late Tithonian based on foraminifers and dasycladaceans (Leinfelder 1993; Kullberg et al. 2006; Schneider et al. 2009). The top boundary of the Freixial Fm. is defined by the transition of a mudstone dominated sequence to the richest sandstone levels of the Lower Cretaceous Porto da Calada Formation (Rey 1993). The Freixial Fm. in the area of Cambelas is interpreted as corresponding to deposits of coastal delta plains and distal fluvial environments (Hill 1988).

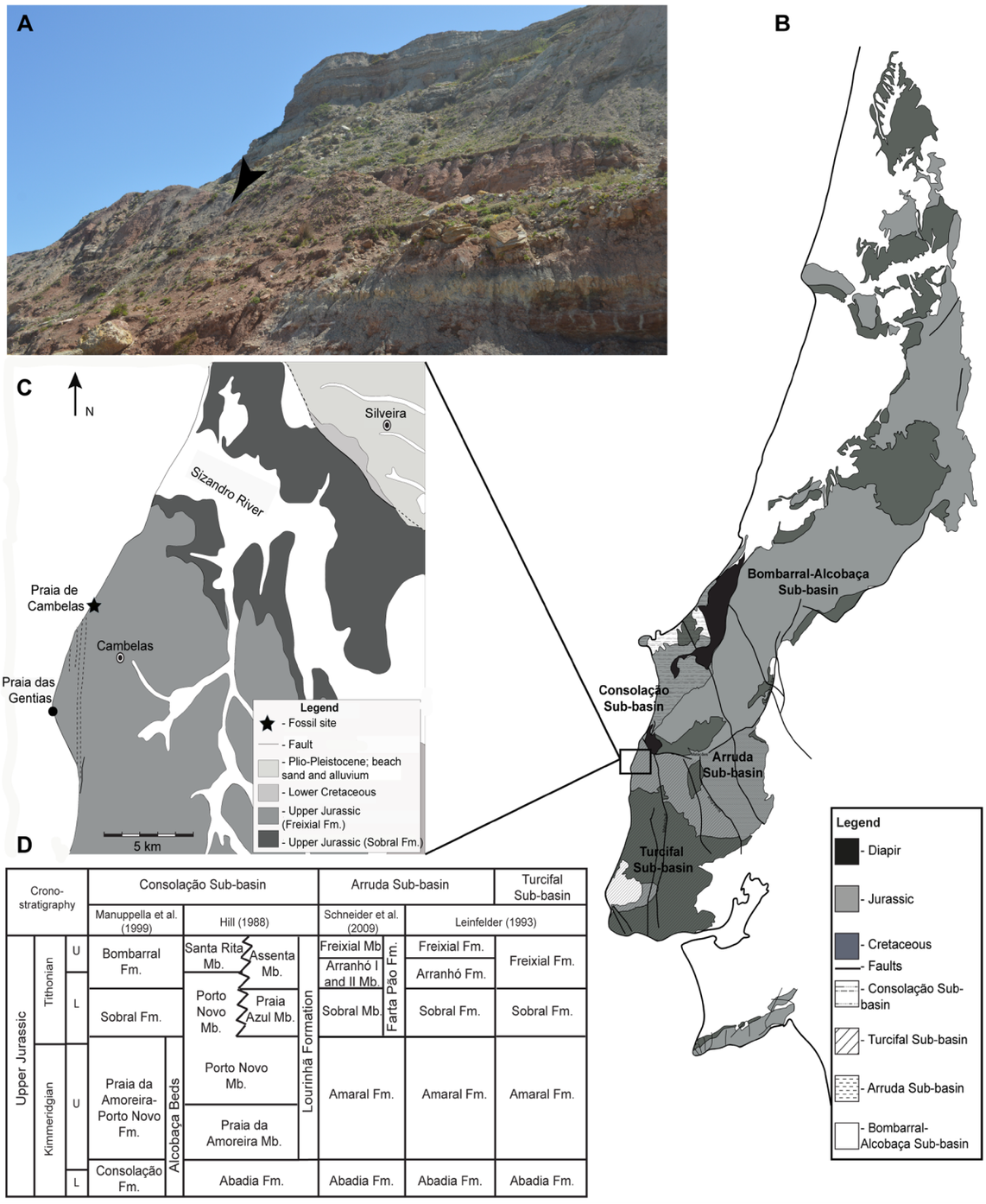

Figure 6.5.1. Geographic and geological context of the Cambelas fossil site. (A), aspect of the sedimentary levels in the area of Cambelas. The black arrow marks the position of the fossil site; (B), simplified geological map of the Lusitanian Basin in which Mesozoic deposits and location of the different Sub-basins are represented (adapted from Oliveira et al. 1992 and Taylor et al. 2014); (C), simplified geological map of the area of Cambelas (adapted from Matos 1954 and Zbyszewski et al. 1955); (D), stratigraphic correlation of the sedimentary unities in the different Sub-basins of the central sector of the Lusitanian Basin (adapted from Hill 1988; Leinfelder 1993; Manuppella et al. 1999; Schneider et al. 2009; Mocho et al. 2016).

6.5.3. TAPHONOMIC SETTING OF SHN.019

The set of osteological remains collected in Cambelas is interpreted as belonging to a single individual. The caudal vertebrae are articulated and the elements of the right pes were found associated and near its original relative position. Some elements are well-preserved and relatively complete, but others are much incomplete and distorted. In particular, the series of caudal vertebrae is partially articulated, but to

the anterior part of the tail the vertebrae become strongly distorted and more incomplete. This different preservation of the osteological elements coincides with a transition of sediments from grey siltstones with parallel lamination in the posterior part of the sequence to red and brown mudstones with evidences of incipient paleosols to the anterior section. This suggests that parts of the skeleton would have been rapidly covered by sediments, whereas other portions were exposed longer. On the other hand, several ichnofossils were identified in some elements of the Cambelas specimen, which were interpreted as marks of activity of organisms in a subaerial depositional context and that might have had an important role in the distortion of some elements (Moniz et al. 2007). Among this ichnofossils there are evidences of tooth marks and abundant marks interpreted as insect traces, which are mostly present in the articular facets of the metatarsals and phalanges, but also affected some areas with cortical bones.

Tooth marks were identified in the distal articular facet of the metatarsal I (Fig. 6.5.2A). These marks correspond to a series of shallow and subparallel traces with approximately the same orientation along the lateral margin of the lateral condyle. These linear marks have between 1.05 mm and 3.73 mm in length and cut the surface of the bone transversely forming shallow grooves with irregular margins. These marks are interpreted as traces produced by an indeterminate vertebrate as result of feeding on the carcass. In Cambelas, a small theropod tooth crown (SHN.019/1) and some isolated elements (a vertebra and a tooth) of a small crocodydiliform (SHN.019/14 and SHN.019/15) were collected. The theropod tooth corresponds to a small, strongly recurved crown measuring 14.98 mm in height (AL) and 6.73 mm in length at the base (CBL). Both the theropod and the crocodydiliform are possible tracemarkes for the bite marks identified in SHN.019.

The insect traces show different morphotypes including pits, furrows and borings. In the phalanx 1 of the digit II a single deep cavity (interpreted as corresponding to a boring *sensu* Britt et al. 2008) is visible in the proximal articular facet (Fig. 6.5.2B). This deep cavity is filled with fine, matrix-supported bone fragments and the plantar margin is collapsed probably due loss of bone. Marks with pit-shape are the most abundant ichnofossils identified in SHN.019 (see Table 6.5.1). These marks correspond to shallow concavities with irregular borders and diameter between 0.5 mm and 10 mm. They usually occur associated in massive clusters resulting in a corroded aspect of the surface probably due to loss of bone, which may vary between few millimeters to near a centimeter (Fig. 6.5.2C). Some elements show relatively long and sinuous canals (furrows *sensu* Britt et al. 2008) approximately 3 mm wide and between 14 mm and 30 mm in length (Fig. 6.5.2D–E). These furrows occur sometimes associated with clusters of pits or as multiple canals with subparallel orientation. Other marks correspond to circular rings of modified bone that may be simple, with a single contour, or concentric with a small central area of unmodified bone (rosette shape *sensu* Bader et al. 2008). These marks are much shallow and are mostly found in the surface of the diaphysis of long bones (Fig. 6.5.2F–G). Finally, some marks consisting of relatively large oval concavities with approximately 10 mm in length and between 4 and 6 mm in diameter were also identified. These marks contrary to the pits described above have smooth borders and are found near the articular facets, but in the surface of the diaphysis of the metatarsal II and III (Fig. 6.5.2H–I).

Traces attributed to arthropods, particularly insects, on osteological fossils are relatively abundant in the fossil record. Fossil bone modification by insects has been reported in some dinosaur specimens from Jurassic and Cretaceous strata mainly in North America, China, Patagonia and Madagascar (Genise et al. 2004; Roberts et al. 2007; Bader et al. 2008; Britt et al. 2008, 2009; Xing et al. 2015; Li et al. 2016). Traces attributed to insects include usually circular-to-oval pits, scratches, furrows and tunnels (borings) and the identification of the possible tracemakers is usually based on comparisons with traces on bone produced by current forms (Bader et al. 2008; Britt et al. 2008).

Currently known insect bone modifiers include termites (Isoptera), some species of ants (Hymenoptera), tineid moths (Lepidoptera), beetles of the families Dermestidae and Cleridae (Coleoptera) and mayflies (Ephemeroptera) (Watson and Abbey 1986; Deyrup et al. 2005; Freymann et al. 2007; Fernández-Jalvo and Monfort, 2008; Abdel-Maksoud et al. 2011; Backwell et al. 2012; Holden et al. 2013; Parkinson 2013; Zanetti et al. 2014, 2015; Xing et al. 2015). However, some authors suggested that most of these insects are

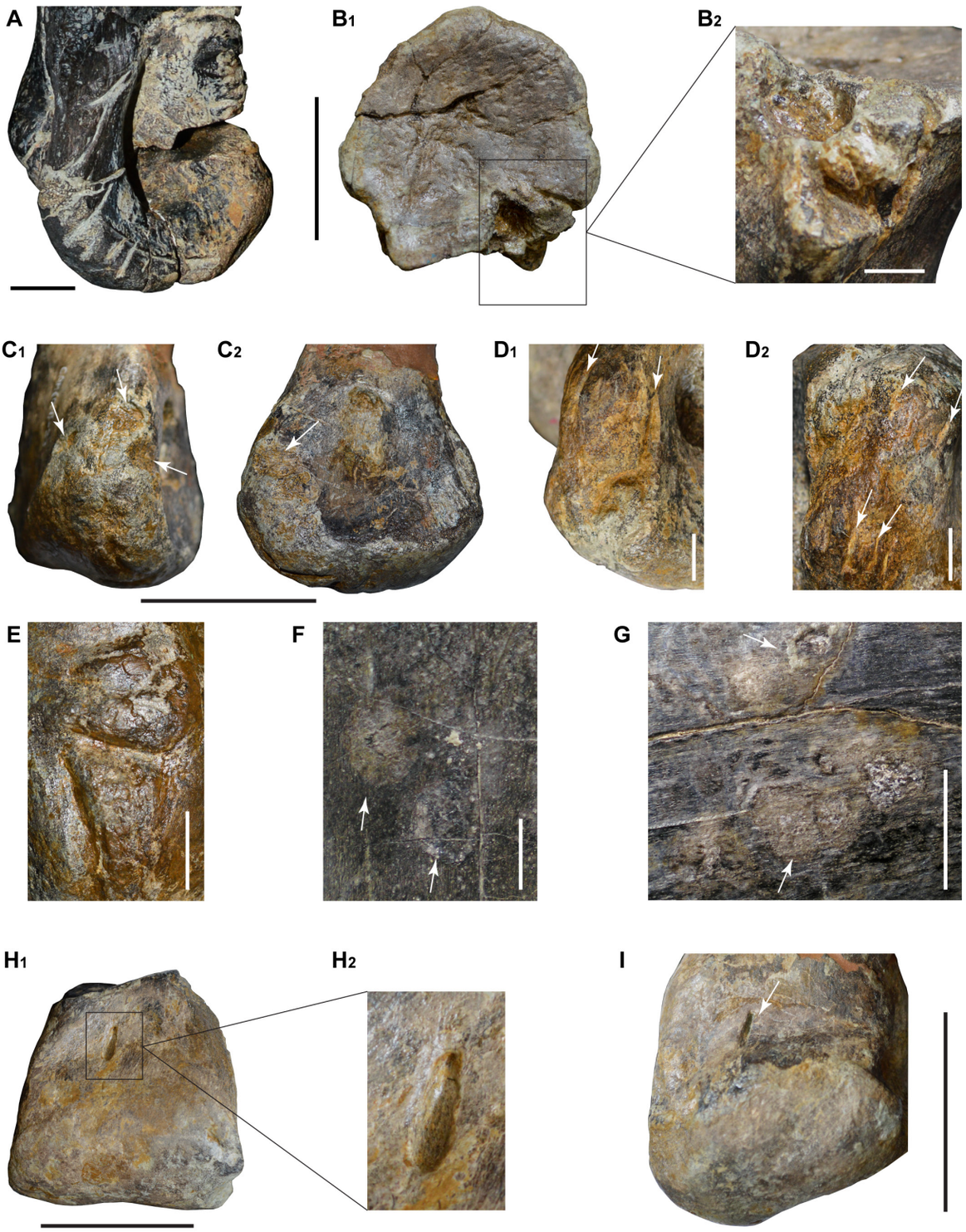

Figure 6.5.2. Ichnofossils identified in the specimen from Cambelas. (A), tooth marks in the distal articular facet of the metatarsal I; (B), deep cavity (boring *sensu* Britt et al. 2008) in the proximal articular facet of the phalanx 1 of the digit II; (C), massive clusters of pit-shaped marks in the distal articular facet of the metatarsal IV in anterior (C1) and lateral (C2) views; (D–E), sinuous canals (furrows *sensu* Britt et al. 2008) in the distal articular facet of mematarsal II (D); and in the distal articular facet of metatarsal IV (E); (F–G), circular ring marks in the diaphysis of the tibia and femur; (H–I), large oval concavities interpreted as pupation chambers of dermestid beetles in the distal articular facet of metatarsal III (H); and in the distal articular facet of metatarsal II (I).

incapable of excavating bone and restricted the possible bone damaging insects to dermestid beetles, moths and termites, which can damage small delicate bones or less well ossified bone in the absence of flesh (Britt et al. 2008). Dermestidae are the beetles most commonly proposed as tracemakers (Rogers 1992; Chin and Bishop 2006; Roberts et al. 2007; Britt et al. 2008; Bader et al. 2008).

The morphotypes of the invertebrate traces identified in SHN.019 are generally similar to some ichonfossils described in dinosaur skeletons from the Morrison Formation (Bader et al. 2008; Britt et al. 2008). Shallow pits in these specimens were interpreted as pupation chambers produced by the larvae of dermestids by some authors (Laws et al. 1996; Hasiotis et al. 1999; Hasiotis 2004; Bader et al. 2008). However, some studies suggested that this ichnofossil morphology most closely matches foraging traces (Hill 1987; Tappen 1994; Dangerfield et al. 2005; Britt et al. 2008). The pits identified in SHN.019 usually occur in clusters mostly affecting the articular facets of the elements and are associated with bone loss, sometimes to a depth of near one centimeter. This pattern suggests that the pit marks represent more probably foraging areas instead of pulpal chambers. The lack of mandible marks in the pits identified in SHN.019 may indicate a non-Coleoptera tracemaker since at least some of these beetle form pits with stellar patterns in which there are recognized mandible marks (Britt et al. 2008). The pits, boring and furrow patterns may instead be associated possibly representing foraging areas and galleries produced by termites. The borings are usually filled with fine, matrix-supported bone fragments and associated with collapse of the bone surface suggesting that the bone was consumed. Termites are social insects that construct complex nest systems (Wilson 1971; Ran 2014; Xing et al. 2015), which are apparently not developed in the Portuguese specimen. However, this apparently less developed boring system in SHN.019 may be related with the poor preservation of several parts of the skeleton. There are several other insects that may produce these borings and furrows such as polymitarcyid mayfly nymphs, tineid moth larvae and larval and adult dermestids (Britt et al. 2008; Xing et al.2015). On the other hand, the association of some furrows with patches of pits may indicate a common producer for both morphotypes.

The hemispherical pits corresponding to large, oval concavities with smooth borders are usually interpreted as pupation chambers of dermestid beetles since neither ants or termites form pupation chambers (Bader et al. 2008; Britt et al. 2008). These pits are similar, but significantly smaller than the ichnogenus *Cubiculum* described in some dinosaur specimens from the Middle Jurassic Chuanjie Formation of China (Xing et al. 2015). Finally, the rosettes (or rings *sensu* Britt et al. 2008) are also usually interpreted as pupation chambers produced by dermestid beetles (Bader et al. 2008). However, Britt et al. (2008) suggested that these marks may reflect the behavior of an extinct termite or simply a feeding pattern not yet observed in modern termites. The authors proposed that the rings are made by a single individual rotating around a fixed point and that the unusual concentric patterns may be taxonomically diagnostic.

Term	Description	Interpretation	Bone affected
Deep V-Shaped Linear Grooves	Deep linear and parallel grooves.	Bite marks of a small indeterminate vertebrate.	Articular facets. Distal articular facet of metatarsal 1-I.
Pits (*sensu* Britt et al. 2008)	Shallow depressions (depth between 0.5 mm and 10 mm), elliptical to round in outline and with irregular borders. Usually usually occur associated in massive clusters.	Foraging feeding behavior produced by holometabolous insects (likely Isoptera or Coleoptera).	Articular facets. Proximal articular facet of metatarsal IV; distal articular facet of metatarsal II; distal articular facet of phagangx 1-I; distal articular facet of phalangx 4-IV.
Borings (*sensu* Britt et al. 2008)	Deep depressions (depth > 50 mm). The depressions are usually filled with fine, matrix-supported bone fragments.	Feeding galleries produced by holometabolous insects (likely Isoptera or Coleoptera).	Articular facets. Proximal articular facet of phalangx 1-II.
Furrows (*sensu* Britt et al. 2008)	Relatively long and sinuous canals (3 mm wide and14 mm to 30 mm in length). Occur associated with clusters of pits or as multiple canals with subparallel orientation.	Feeding galleries produced by holometabolous insects (likely Isoptera or Coleoptera).	Articular facets. Distal articular facet of mematarsal II; distal articular facet of metatarsal IV.
Hemispherical pits (*sensu* Beder, 2008)	Large oval concavities (10 mm length and 4 to 6 mm in diameter) with smooth borders.	Pupation chambers likely of dermestid beetles.	Trabecular bones. Distal end of the diaphysis of metatarsal II and III.
Rosettes (*sensu* Beder, 2008)	Concentring rings of modified bone with a small central area of unmodified bone.	Pupation chambers constructed in dried flesh that were in contact with the bone (likely produced by dermestid beetles).	Trabecular bones. Diaphysis of the tibia and femur.

Table 6.5.1. Terms used for described the trace fossils identified in SHN.019.

6.5.4. MATERIAL AND METHODS

SHN.019 consists of a partial skeleton, including a sequence of articulated caudal vertebrae and an almost complete right pes. Several other isolated elements, including caudal vertebrae and fragments of the hind limb, were also collected. In the Cambelas fossil site (TVSPC 12) some isolated elements of other vertebrate groups were also found, including a vertebra and a tooth fragment of an indeterminate crocodyliform and a tooth of an indeterminate small theropod (see Supplementary Table 6.5.1 for a complete list of fossils collected in Cambelas).

The Cambelas fossil site was excavated during two fieldworks, in 2000 and 2002, performed by a team led by researchers of the Museu Nacional de História Natural (Lisbon, Portugal), the Sociedade de História Natural (Torres Vedras, Portugal), and the Universidad Autónoma de Madrid (Madrid, Spain). The specimens are housed in the collections of the Sociedade de História Natural in Torres Vedras.

The nomenclature used in the description of pneumaticity, laminae and fossae for the axial elements is that proposed by Wilson (1999) and Wilson et al. (2011). Following Persons and Currie (2011), the lateral projections of caudal vertebrae are here referred as "caudal ribs" in preference to the term "transverse processes".

6.5.5. INSTITUTIONAL ABBREVIATIONS

BYU, Brigham Young University, USA; DINO, Dinosaur National Monument, USA; ML, Museu da Lourinhã, Portugal; SHN, Sociedade de História Natural, Portugal.

6.5.6. ANATOMICAL ABBREVIATIONS

ac, anterior condyle; acdl, anterior centrodiapophyseal lamina; alr, anterior lateral ridge; apr, anterior process; as, anterior spur; ast, surface for articulation with the astragalus; cdl, centrodiapophyseal lamina; ch, chevron; cpol, centropostzygapohyseal lamina; cprl, centroprezygapophyseal lamina; cprf, centroprezygapophyseal fossa; cr, caudal rib; f, foramen; fch, facet for chevron; fg, flexor groove; fi, surface for articulation with the fibula; gt, greater trochanter; ift, iliofibularis tubercle; lc, lateral condyle; lr, lateral ridge; lt, lesser trochanter; 4t, fourth trochanter; mc, medial condyle; mclp, medial collateral ligament pit; md, medial depression; Mt I, surface for articulation with metatarsal I; Mt III, surface for articulation with metatarsal III; Mt IV, surface for articulation with metatarsal IV; Mt V, surface for articulation with metatarsal V; nc, neural canal; ns, neural spine; pcd, pleurocentral depression; plr, posterior lateral ridge; po, postzygapophysis; ppr, posterior process; pr, prezygapophysis; prdl, prezygodiapophyseal lamina; sc, scar; spol, spinopostzygapophyseal lamina; sprl, spinoprezygapophyseal lamina; t III, surface for articulation with distal tarsal III; t IV, surface for articulation with distal tarsal IV; ti, surface for articulation with the tibia; vg, ventral groove.

6.5.7. SYSTEMATIC PALAEONTOLOGY

Theropoda Marsh, 1881

Tetanurae Gauthier, 1986

Avetheropoda Paul, 1988

Allosauroidea Marsh, 1878

Carcharodontosauria Benson, Brusatte and Carrano, 2010

6.5.8. DESCRIPTION

6.5.8.1. Axial skeleton

Caudal vertebrae. A block containing seventeen articulated and well-preserved caudal vertebrae and fragments of other more anterior caudal vertebra was collected. Additionally, two other isolated more anterior caudal vertebrae were recovered. These two isolated caudal vertebrae preserve the centra and the base of the neural arches (Fig. 6.5.3). The neural arches are fused with the centra, but the neurocentral suture is still visible. The centra are moderately elongated with strongly offset articular facets and shallow pleurocentral depressions on the lateral surface. The pleurocentral depression is dorsally located near the base of the neural arch and occupies almost the entire length of the centrum. The ventral surface of the centrum has a well-developed longitudinal groove bounded by crests extending along most of its length, but that is deeper adjacent to the posterior articular facet (Fig. 6.5.3D, J). The articular facets are strongly concave with subcircular outlines (see Supplementary Table 6.5.2). Well-developed facets for chevrons are present on the ventral margin of the anterior and posterior articular facets with the posterior facet larger than the anterior one. In SHN.019/3, a small pit is visible in the posterior surface of the neural arch, below the left postzygapophysis (Fig. 6.5.3B–C).

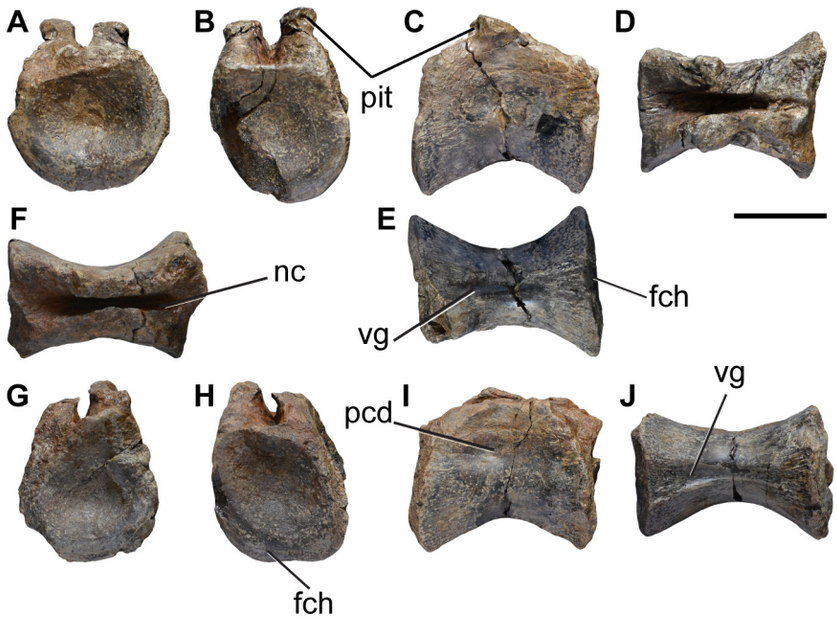

Figure 6.5.3. Isolated caudal vertebrae of SHN.019. (A–E), SHN.019/3; (F–J), SHN.019/4, in anterior (A, G); posterior (B, H); right lateral (C, I); dorsal (D, F); and ventral (E, J) views. Scale bar: 50mm.

The articulated section of the tail measures 156 cm in length and comprises eight vertebrae anterior to the so-called "transition point", which refers to the point between the last vertebra bearing transverse processes and the first with distinctly elongate prezygapophyses (*sensu* Russell 1972), and nine vertebrae posterior to this point (Fig. 6.5.4–5). Taking for comparison other allosauroids, in which the "transition point" is placed at approximately the 25th or 26th caudal vertebra (e.g. Madsen 1976; Chure 2000), the articulated caudal vertebrae from Cambelas would correspond to a section of the tail between the 17th or 18th and the 34th or 35th caudal vertebrae. These vertebrae are well-preserved, but the anteriormost elements are somewhat broken and distorted, especially the neural arches. All the vertebrae preserve more or less complete chevrons near its original position in the tail.

The centra are moderately elongated. The length:height ratio average is approximately 1.94 in the anteriormost vertebrae and the centra become slightly more elongated to the tip of the tail (see Supplementary Table 6.5.2). The centra are transversely compressed especially in the anteriormost caudal

vertebrae, and they have well-marked longitudinal grooves in the ventral surface as in the isolated caudal vertebra described above (Fig. 6.5.5). These grooves become progressively shallower along the caudal series and disappear in the centra posterior to the "transition point". In lateral view, the mid anterior centra are hourglass-shaped, deeply concave ventrally and with strongly expanded articular facets, but become straighter to the tip of the tail. The lateral surface of the anteriormost centra is somewhat concave with a shallow pleurocentral depression below the caudal ribs. However, the centra posterior to the fifth caudal vertebra in the preserved series are slightly convex (Fig. 6.5.5B$_2$–B$_3$).

The ventral surface of the centra has well-developed anterior and posterior facets for the chevrons with the posterior facets larger than the anterior ones as is typical in theropods. In the last two preserved vertebrae, the facets for the chevrons are reduced and almost indistinguishable. The neural spines are badly preserved especially in the anteriormost elements, so its interpretation is somewhat complex. However, the sixth caudal vertebra of the preserved series has an almost complete neural spine, which consists of an anterior spur-shaped process and a long, blade-shaped main spine extending posteriorly (Fig. 6.5.5B$_2$, C). The anterior spur extends dorsally from about the level of the caudal ribs, whereas the posterior process extends dorsoposteriorly between the postzygapophyses. A well-developed spinopostzygapophyseal lamina (spol) projecting from the dorsomedial surface of the postzygapophysis and connects with the posterior surface of the spine. The spol extends along most of the height of the neural spine. The neural spines are present at least till the sixth caudal vertebra posterior to the "transition-point". In this vertebra the neural spine is still well above the dorsal margin of the postzygapophyses. In the last preserved vertebra a reduced process of the spine is visible, but it does not extend beyond the dorsal margin of the postzygapophyses. This condition differs from the caudal series of *Allosaurus*, in which the neural spines become reduced at approximately the twenty-eighth caudal vertebra (Madsen 1976).

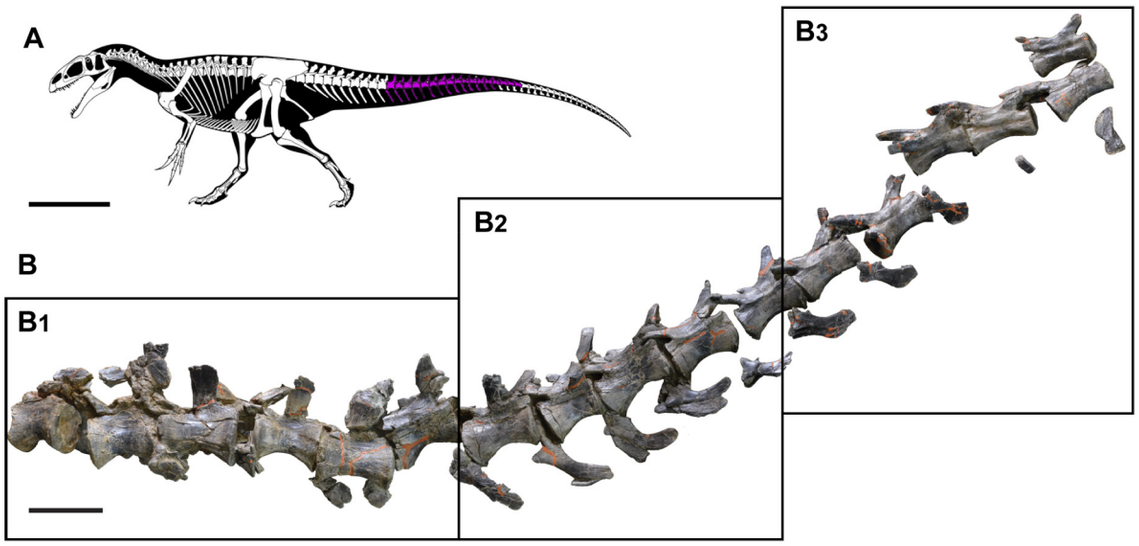

Figure 6.5.4. Sequence of caudal vertebrae of SHN.019. (A), reconstitution of the skeleton of a *Neovenator* individual in which the estimated position of the tail section collected in Cambelas is marked; (B), sequence of seventeen partially articulated caudal vertebrae of SHN.019. Copyright of the skeleton of *Neovenator* Scott Hartman (2013). Scale bar (A): 1m; (B): 100mm.

The prezygapophyses are reduced in the anteriormost preserved caudal vertebrae extending only slightly in front of the anterior articular facet of the vertebra. In the posterior part of the series the prezygapophyses become progressively longer and in the posteriormost preserved elements the length of the prezygapophyses surpasses half the length of the preceding centrum. The prezygapophyseal processes extend anterodorsally forming an angle of approximately 45º with the dorsal surface of the centrum. The lateral surface of the prezygapophysis is slightly concave in some preserved vertebrae, but become almost flat with a low longitudinal crest to the tip of the tail. The postzygapophyses of the anteriormost vertebrae are badly preserved and are not visible because the articulation of the vertebrae. In the sixth caudal vertebra

of the preserved series the postzygapophyses are relatively well-preserved corresponding to short processes projecting dorsally in an angle of approximately 60º with respect to the dorsal surface of the centra (Fig. 6.5.5B$_2$, C).

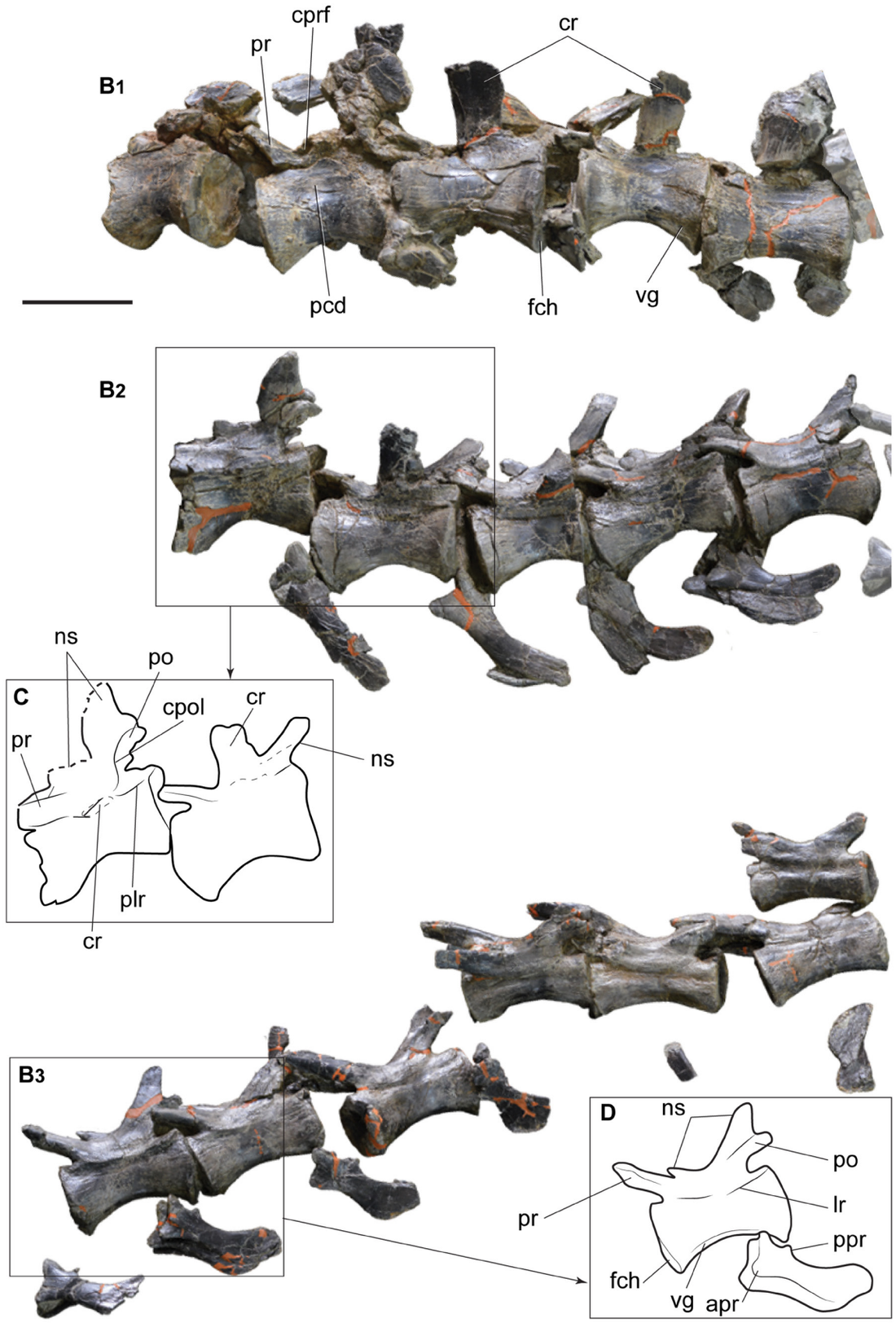

Figure 6.5.5. Details of different segments of the caudal sequence of SHN.019. (B1–B3) detail of the tail segments marked in figure 3; (C–D) line drawing interpretation of some caudal vertebrae. Scale bar: 50mm.

In the second caudal vertebra of the preserved series, a well-developed lamina extends from the lateral surface of the base of the prezygapophysis and apparently would connect with the caudal rib bounding a small, but deep fossa bellow the caudal rib (Fig. 6.5.5B$_1$). These lamina and fossa are interpreted as corresponding to the prezygodiapophyseal lamina (prdl) and centroprezygapophyseal fossa (cprf) respectively. A well-developed centroprezygapophyseal lamina (cprl) is visible in several vertebrae projecting from the anterior part of the prezygapophysis up to the level of the base of the caudal rib, on the centrum. Some vertebrae (e.g. the sixth and eight of the preserved series) show a well-developed centropostzygapophyseal lamina (cpol) extending from the posterior end of the postzygapophysis up to the dorsal surface of the centrum above the level of the caudal rib (Fig. 6.5.5B$_2$, C). In the eight preserved caudal vertebra the cpol connects with the posterior surface of the caudal rib forming a well-developed longitudinal and uninterrupted lamina.

The caudal ribs of the anteriormost vertebrae are fan-shaped, strongly expanded anteroposteriorly to the distal part. These processes extend from the dorsal surface of the centrum at approximately the mid-length. Despite somewhat fractured and distorted it seems that the caudal ribs extend laterally with an almost horizontal position. A short lamina corresponding to the anterior centrodiapophyseal lamina (acdl) is present at the base of the ventral surface of the caudal ribs and delimits a shallow centrodiapophyseal fossa (cprf) adjacent to the anterior margin of the rib. A conspicuous lateral ridge is present in the dorsal surface of the centrum in several vertebrae. This longitudinal ridge is more evident in the vertebrae posterior to the sixth caudal of the preserved series and is especially well-developed in the ninth to eleventh vertebrae, but disappears in the posteriormost preserved elements. The lateral ridge is higher adjacent to the posterior articular facet, but an anterior lower ridge is also present in these vertebrae.

Chevrons. More or less complete chevrons corresponding to the second to the sixteenth vertebrae of the preserved series were recovered near its original position in the tail. The chevrons corresponding to the seventh and eighth preserved vertebrae have almost straight shafts and slightly taper distally. To the posterior tip of the tail they become more curved and the distal end is slightly expanded anteroposteriorly. The posteriormost chevrons have a morphology commonly described as hatchet-shaped with strongly expanded anteroposteriorly distal ends. All preserved chevrons have well-developed anterior processes and additional, spur-shaped posterior processes projecting posterodorsally (Fig. 6.5.5D).

6.5.8.2. Appendicular elements

Several fragments of appendicular elements were collected, including fragments of a right femur, a diaphysis fragment of a tibia, a diaphysis fragment of a left fibula, at least two proximal tarsals, and an almost complete right pes.

Femur. The femur is represented by a fragment of the proximal part and a fragment of the diaphysis (Fig. 6.5.6). The proximal fragment has the lesser and greater trochanters partially preserved. The lesser trochanter is broken distal and to the front, but based on the preserved fragment, it is possible verify that it would be broad and robust. This trochanter has an aliform-shape and is separated from the greater trochanter by a notch in lateral view and from the diaphysis by a broad concavity in medial view. The anteromedial surface of the proximal part of the femur has a large foramen that pierces the base of the lesser trochanter (Fig. 6.5.6B). The lateral surface of the lesser trochanter is slightly convex and shows a low vertical ridge extending along the mid-length of the trochanter (Fig. 6.5.6E). The lateral surface of the lesser trochanter is also ornamented by a series of thin vertical grooves and ridges mainly adjacent to the posterior margin.

The fragment of the diaphysis preserves the fourth trochanter, which corresponds to a robust crest extending proximodistally along the posteromedial surface of the femur. This trochanter is distally higher and becomes proximally lower to gradually merge with the diaphysis. The fourth trochanter

shows a strongly striated lateral surface due to the presence of well-marked crests and grooves extending anteroposteriorly. Beside, a shallow and rugose concavity is present in the medial surface of the femur adjacent to the proximal part of the fourth trochanter, and other smaller depression adjacent to the distal margin of the trochanter (Fig. 6.5.6C). The first depression is subcircular, whereas the last one is more oval and is bounded laterally by a well-developed crest. Distally to the fourth trochanter, the femoral diaphysis is circular in cross-section.

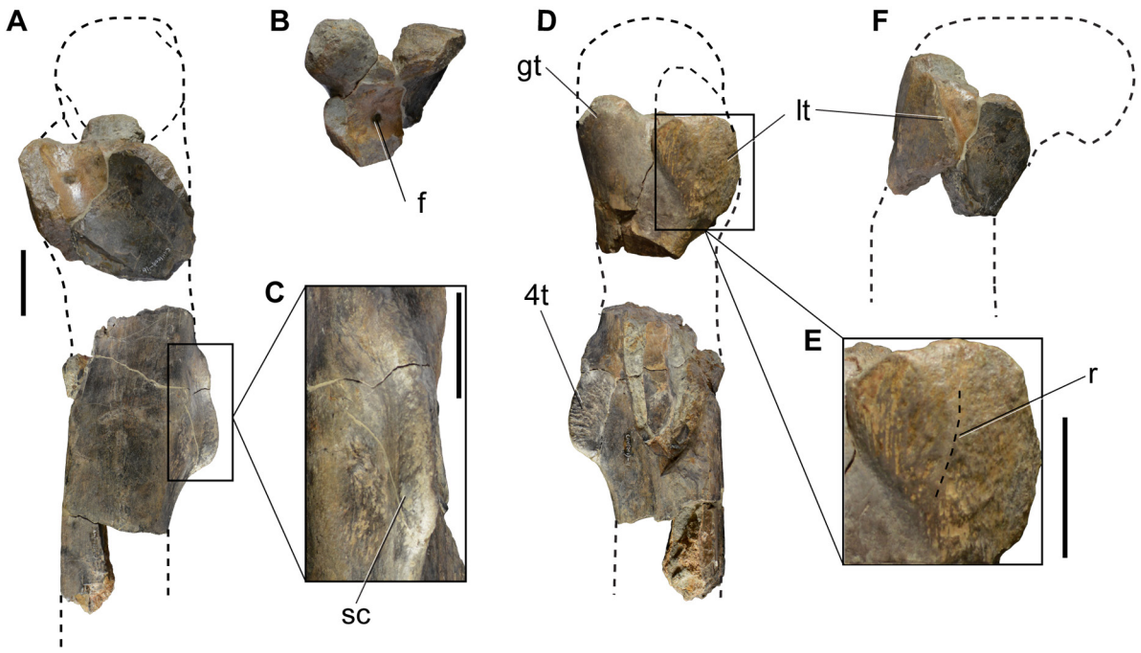

Figure 6.5.6. Fragments of a right femur of SHN.019 in medial (A) and lateral (D) views; (B, F), fragment of the proximal end in dorsal (B) and anterior (F) views; (C), detail of the fourth trochanter showing the deep and rough concavity in the posterior surface of the diaphysis adjacent to the trochanter; (E) detail of the lesser trochanter showing the vertical ridge on the lateral surface. The dashed lines correspond to interpretation for the missing parts based on other allosauroid specimens. Scale bar: 50mm.

Tibia. The tibia is represented by a fragment of the mid-section of the diaphysis (Fig. 6.5.7D–E). This fragment is too incomplete to allow a more accurate description of the element being only possible to verify that the diaphysis has a crescent shape cross-section with flat anterior surface as is typical in theropods.

Fibula. The fibula preserves a fragment of the mid-section of the diaphysis and a fragment of the distal part (Fig. 6.5.7A–C). This element is interpreted as a left fibula based on the position of the proximal tubercle corresponding to the insertion of the iliofibularis muscle. This insertion does not form a real tubercle, but is a poorly defined, slightly rough surface that extends proximodistally along the anterior margin of the fibular diaphysis. The medial surface of the fibula is strongly concave along nearly the entire preserved fragment. This concavity is broad proximally, but gradually tapers distally ending above the distal part of the fibula. The lateral surface of the fibula is strongly convex and the posterior surface is nearly flat.

The fragment of the distal part has is oval in distal view and the distal surface is approximately flat. The lateral surface has a series of deep vertical grooves extending adjacent to the distal margin. The lateral surface is somewhat concave, whereas the medial surface is slightly convex.

Tarsals. The tarsals are represented by a complete and well-preserved left calcaneum, a right tarsal IV and a fragment interpreted as a tarsal III (Fig. 6.5.8).

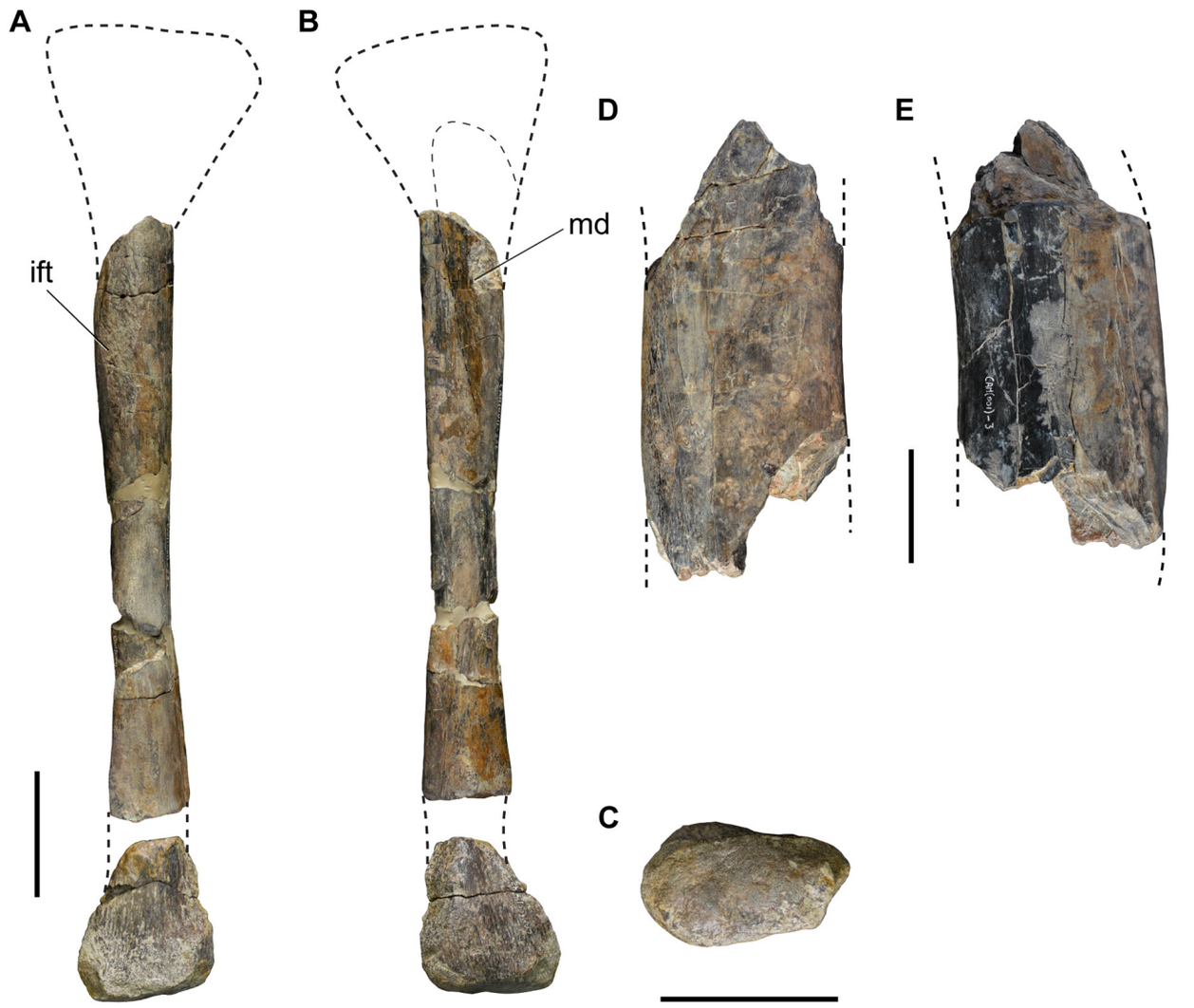

Figure 6.5.7. (A–C), Left fibula and (D–E), fragment of a tibia of SHN.019 in lateral (A); medial (B); distal (C); posterior (D); and anterior (E) views. The dashed lines correspond to interpretation for the missing parts based on other allosauroid specimens. Scale bar: 50mm.

The calcaneum has a transversely compressed and crescent-shape (Fig. 6.5.8A–F). In lateral view, the calcaneum has a shallow and somewhat roughened concavity that occupies almost the entire lateral surface. The anterior surface is transversely convex and smooth with a sigmoidal medial margin. In anterior view, the calcaneum slightly tapers dorsally. The posterior surface shows a broad, shallow concavity extending laterodorsally in the proximal margin of the calcaneum, which represents the facet for articulation with the distal end of the fibula. The medial surface of the calcaneum is concave along its entire height and has a deep pit in the distal part, which would receive the lateral tuberosity of the astragalus. Despite this element is well-preserved, it shows some collapsed areas especially in the distal part so it is not clear if the facet for insertion with the astragalus has a single pit or if this would be subdividing in two smaller pits as occur in *Allosaurus* (Madsen 1976).

The tarsal IV has is rectangular-shaped in proximal view, slightly wider to the front than to the rear (Fig. 6.5.8I–N). It has a broadly concave proximal surface and a nearly flat distal surface. The lateral surface has two deep pits, whereas the medial surface is transversely convex and does not bear evidences for the presence of a pit, contrary to the condition described in *Allosaurus* (Madsen 1976).

A fragment interpreted as belonging to a tarsal III was also recovered, but it is too incomplete to allow a detailed description (Fig. 6.5.8G–H).

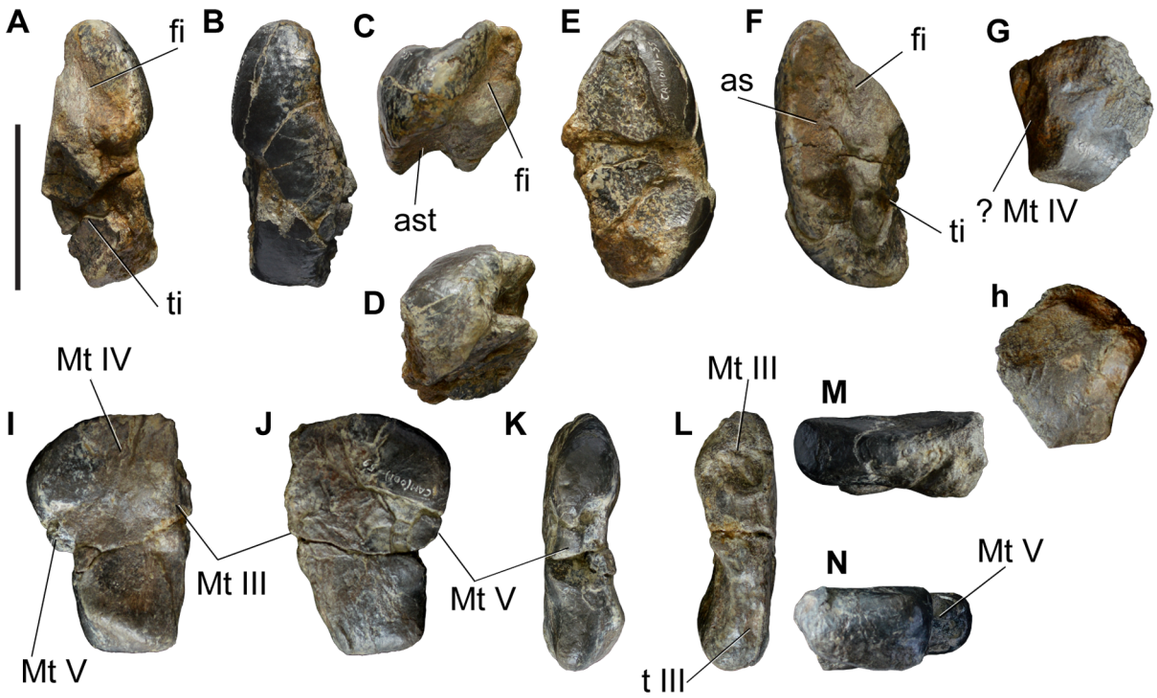

Figure 6.5.8. Proximal tarsals of SHN.019. (A–F), left calcaneum; (G–H), fragment of a ? tarsal III; (I–N), right tarsal IV in proximal (A, H, J); distal (B, G, I); anterior (C, N); posterior (D, M); lateral (E, K), medial (F, I) views. Scale bar: 50mm.

Pes. The right pes is almost complete and well-preserved (Fig. 6.5.9–11). All phalanges of the four digits are preserved and there are five partially preserved metatarsals. The metatarsals I and V are almost complete and are much shorter than the other metatarsals. The metatarsal II is broken proximally so the morphology of the proximal end is unknown. The metatarsal III preserves a fragment of the mid-section of the shaft and the distal part, but the proximal end is missing. The metatarsal IV is almost complete and well-preserved.

The metatarsal I is a dorsoventrally reduced, but relatively robust element that tapers proximally and has a triangular-shape in proximal view, with the shaft strongly compressed transversely above the distal condyles. Distally it has a large, rounded anterior condyle and two well-developed condyles separated by a deep flexor groove in posterior view. This ball-shaped articular facet would allow a wide movement and position range of the first digit (Fowler et al. 2011). The flexor groove connects with a shallow concavity in the posterior surface of the distal part of the metatarsal. The distal end projects slightly to the front, but is mostly parallel to the shaft contrasting with the J-shaped morphology typical of some abelisaurids in which the distal end projects perpendicular to the shaft (Coria et al. 2002). In distal view, the condyles have a circular-shape and are strongly convex transversely. The medial condyle has a ridge extending posteromedially well beyond the level of posterior margin of the lateral condyle (Fig. 6.5.10A–B). The lateral collateral ligament pit is shallow and poorly defined contrasting with the deep and proximodistally elongated medial pit. The shaft shows a slightly rough area extending along the medial and posterior surfaces, which is interpreted as the surface for articulation with the metatarsal II. The metatarsal I was probably tied by ligaments to the mid-shaft of metatarsal II and did not reach the tarsus as occur in most theropods (Rauhut 2003b; Galton et al. 2015).

The metatarsal II is a robust and moderately large element (see Supplementary Table 6.5.3). It is broken at approximately the mid-length of the shaft and the proximal end is missing. Distal it has two well-developed and rounded condyles projecting somewhat anteroposteriorly. The lateral condyle is oval with the long axis oriented anteroposteriorly and is slightly larger than the medial one. The distal condyles are separated by a deep flexor groove in the posterior surface and by a shallow groove extending anteroposteriorly in the distal surface. Deep and well-delimited lateral and medial collateral ligament

pits are present and the medial pit is slightly deeper than the lateral one. The shaft is rectangular-shaped in dorsal view with flat anterior surface, slightly convex posterior surface and nearly parallel lateral and medial margins. The posterior margin of the shaft shows a flattened oval surface extending proximally from about 78 mm above the distal condyles (Figure 6.5.10C). This surface is interpreted as the area for attachment with the metatarsal III. The medial surface of the shaft is somewhat concave in anterior view.

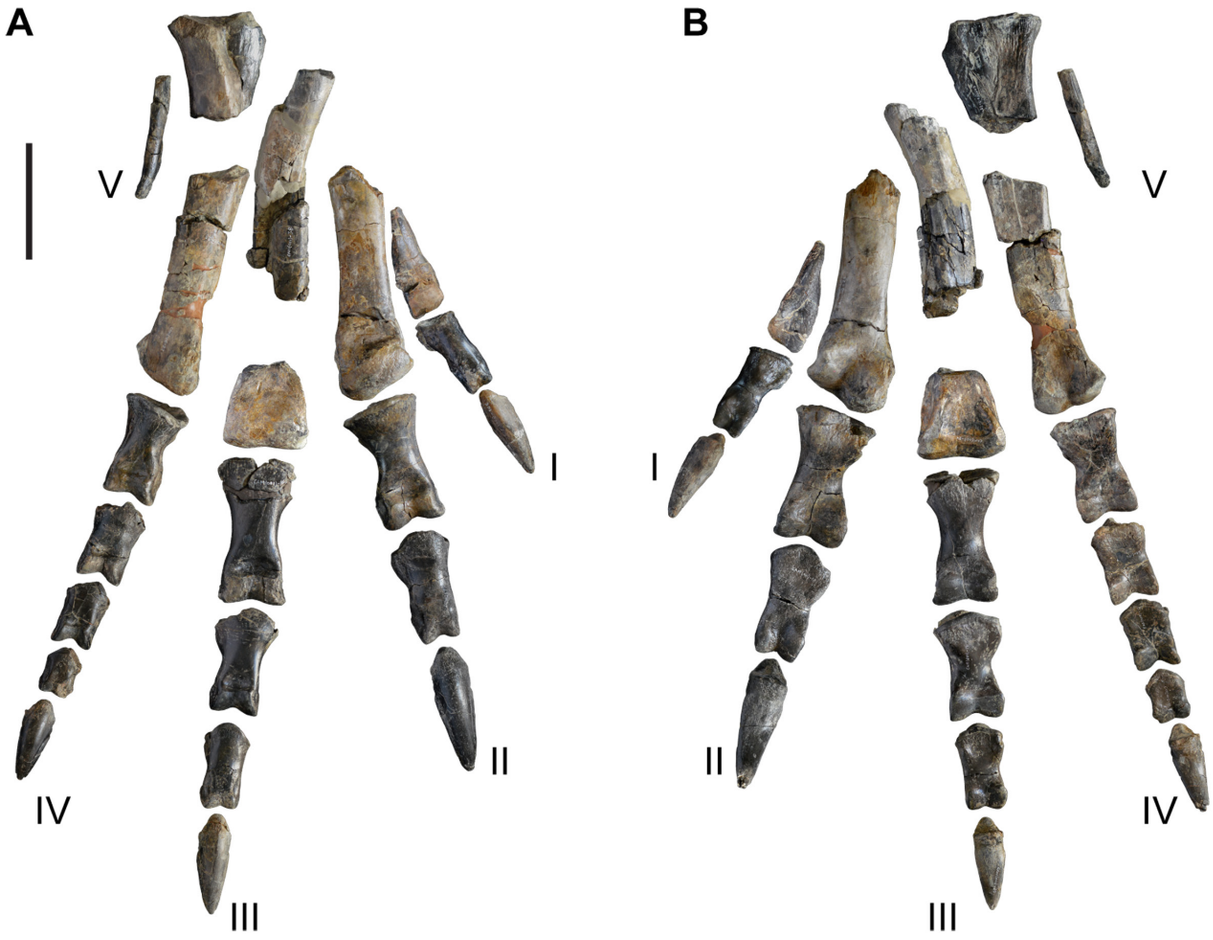

Figure 6.5.9. Right pes of SHN.019 in anterior (A) and posterior (B) views. Scale bar: 100mm.

The metatarsal III is much incomplete and distorted, but preserves a fragment of the mid-section of the shaft and the distal part. The preserved fragment of the shaft does not show evidences of a proximal constriction of this metatarsal corresponding to the arctometatarsalian condition that characterizes several coelurosaurian theropods, including ornithomimids, troodontids, caenagnathids, and tyrannosaurids (Currie 2000). In anterior view, the shaft seems to have a pronounced curvature, being concave medially and convex laterally. The medial surface is somewhat flat, especially the distal part of the preserved fragment. This flattened area probably corresponds to the area for attachment with the metatarsal IV. The distal part is robust, rectangular-shaped in distal view and transversely convex with poorly defined condyles separated by a shallow groove in the distal surface. A shallow concavity is present in the anterior surface above the proximalmost part of the distal articular surface. The distal condyles extend mostly distally not anterodistally as in the metatarsals I and II. The posterior surface has two low and parallel ridges extending from the distal condyles (Figure 6.5.9B). Deep and circular collateral ligament pits are present in the medial and lateral surfaces with the lateral pit slightly shallower than the medial one.

The metatarsal IV is almost complete and well-preserved lacking a fragment of the mid-section of the shaft. The shaft is crescent shaped in cross-section with a flat medial surface along approximately the entire length. The distal part has two well-developed condyles separated to the rear by a deep flexor groove.

The distal articular facet is triangular-shaped in distal view. The condyles are separated to the rear by a deep flexor groove extending to the distal surface of the articular surface. The medial condyle is oval and anteroposteriorly projected and is slightly larger than the medial condyle. The lateral condyle has a ridge-shape and extends posteromedially well-beyond the level of the posterior margin of the medial condyle (Figure 6.5.10I). Only the lateral collateral ligament pit is present, but is shallow and poorly preserved. The shaft strongly expands proximally and the proximal part is two times longer anteroposteriorly than transversely (see Supplementary Table 6.5.3). The proximal surface is concave and slightly tapers to the rear. The medial surface of the proximal part has a deep concavity extending distally from the proximal end of the posteromedial margin of the shaft and bounded anteriorly by a sharp longitudinal crest. This concavity represents the surface for articulation with the metatarsal III.

The metatarsal V is broken proximally and the proximal end is missing. This element is reduced and consists of a thin shaft tapering distally. The shaft has a flat medial surface probably for articulation with the metatarsal IV and a rough dorsal surface.

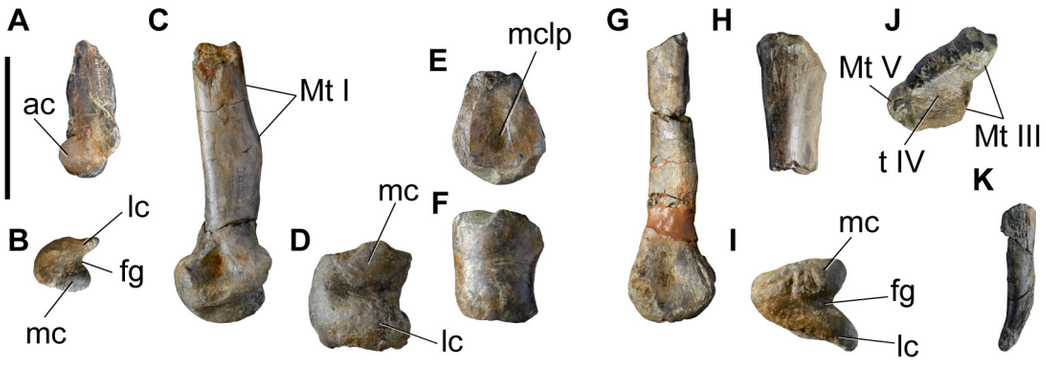

Figure 6.5.10. Metatarsals preserved of the right pes of SHN.039. (A–B) metatarsal I; (C–D) metatarsal II; (E–F) metatarsal III; (G–J) metatarsal IV; and (K) metatarsal V in anterolateral (A); distal (B, D, F, I), left lateral (C, E, G, H, K); and proximal (J) views. Scale bar: 100mm.

SHN.019 preserves all phalanges of the right pes. The third digit is the longest, with a total length of the phalanges approximately 330 mm, and the second and fourth digits have near the same length (see Supplementary Table 6.5.3). The phalanges are relatively slender and longer than wide. All non-ungual phalanges have well-developed distal condyles and nearly symmetrical distal ends except the phalanges 1-I and 2-II in which they are somewhat asymmetrical (the medial condyle is slightly more projected to the rear than the lateral one). The proximal articular facets of all phalanges are slightly concave and generally circular in outline except the ungual phalanges, which have oval proximal margins, anteroposteriorly longer than transversely wide (Figure 6.5.10). Lateral and medial collateral ligament pits are well-marked in all phalanges. The lateral pit is slightly shallower than the medial one in most phalanges of the digits I, II and III (except in the phalanx 1-III and 2-III in which the lateral and medial pits are almost equally developed), but in the phalanges of the digit IV the lateral pit is deeper than the medial one. A shallow concavity is present in the anterior surface above the distal condyles in most non-ungual phalanges except in the penultimate phalanges of each digit. This concavity is much developed and well-marked in the phalanges 1-II and 1-III in which it occupies almost the entire transverse width of the distal part.

The phalanges 1-II and 1-III are the most robust of all phalanges (see Supplementary Table 6.5.3). These elements have the proximal and distal parts strongly offset from the shaft, which gives a somewhat constricted appearance to the phalanx. This morphology is also present in the phalanges 2-III and 1-IV, whereas the other non-ungual phalanges have straighter shafts. The phalanges 2, 3, and 4 of the digit IV are rectangular in outline with subparallel medial and lateral margins. The posterior surface of the phalanges 1-I, 1-II, and 1-III has slightly concave and rough areas adjacent to the proximal margin. In the phalanx 1-II, this rough area is delimited by well-developed medial and lateral ridges. On the contrary, the phalanx 2-II has almost flat posterior surfaces.

In lateral view, the ungual phalanges are strongly arched, concave ventrally and convex dorsally (Figure 6.5.11). They have triangular cross-sections with a nearly flat ventral surface, transversely wider than the dorsal surface. The ungual phalanx of the digit II is the largest of all unguals, whereas the ungual of the digit I is slightly larger than the ungual of digit IV, but smaller than those of digits II and III (see Supplementary Table 6.5.3). A pair of longitudinal grooves extends near the mid-height of the lateral and medial surfaces in all ungual phalanges. These grooves extend from the ventral margin of the proximal margin to the distal tip of the phalanx. The lateral groove is slightly shallower than the medial one. The proximal margin of the ungual phalanges has an anteroposteriorly oriented ridge that subdivides the articular facet in two concavities for articulation with the distal condyles of the previous phalanx. The proximal articular facets of most non-ungual phalanges, except in the first phalanges of the digits I to IV, have also similar ridges. The anterior margin of the proximal end of the ungual phalanges extends more proximally than the ventral margin forming a blunted anterior process.

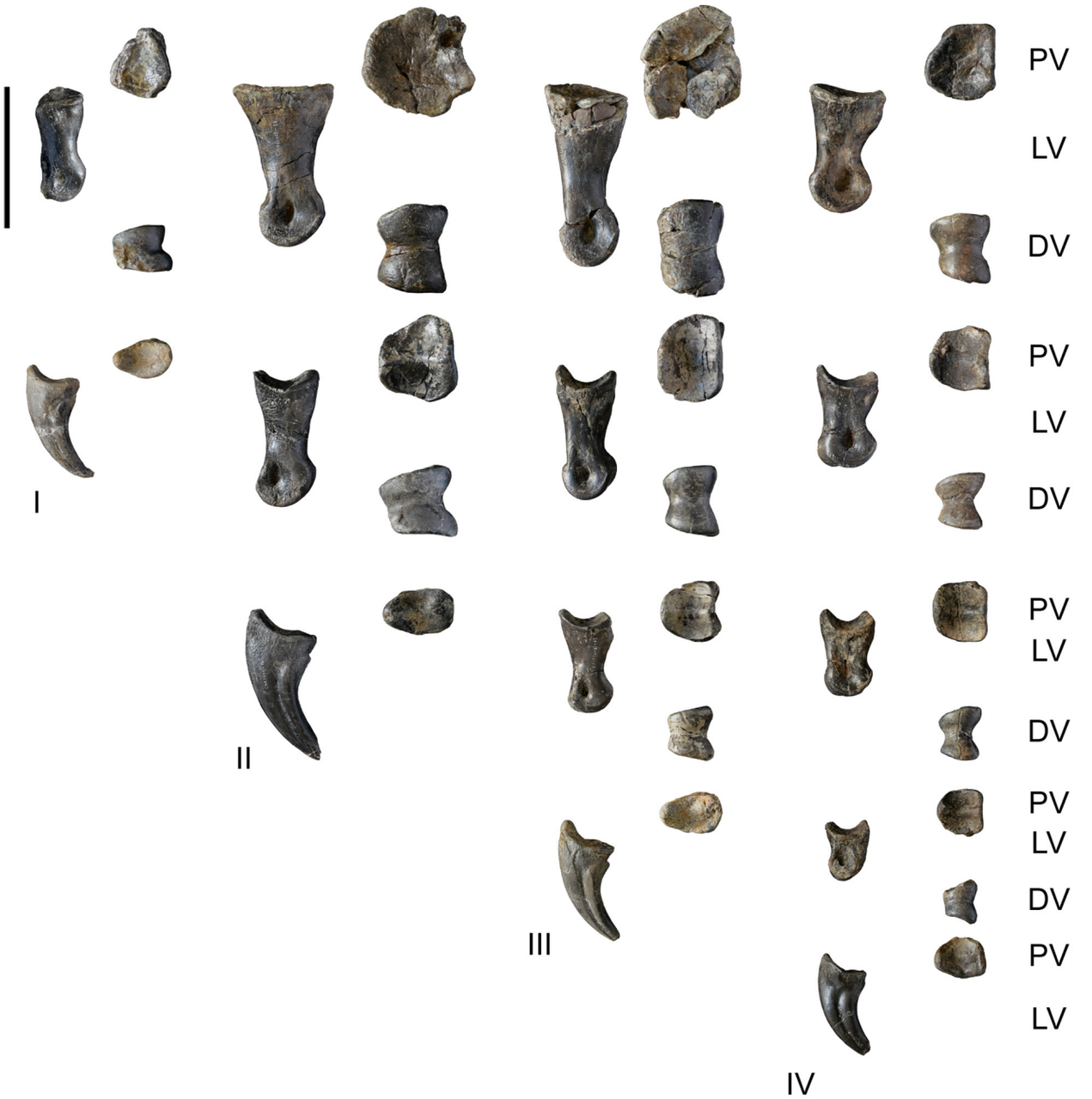

Figure 6.5.11. Phalanges of the right pes of SHN.019. Legend: PV, proximal view; LV, left lateral view; DV, distal view. Scale bar: 100mm.

6.5.9. PHYLOGENETIC DISCUSSION

The new specimen, SHN.019, shares with Orionides the following set of features: (i) anterior spur-shaped process in the neural spine of mid caudal vertebrae (Rauhut 2003b); (ii) distal caudal vertebrae with strongly elongated prezygapophyses, overhanging at least one-quarter of the length of the preceding centra (Rauhut 2003b); (iii) femoral lesser trochanter proximally located (Benson 2010); (iv) distal end of metatarsal IV deeper than broad (Carrano and Sampson 2008; Carrano et al. 2012); (v) reduced length of metatarsal I, less than 50% of metatarsal II (Carrano et al. 2012); and (vi) reduced metatarsal I, with a broadly triangular shaft, and distally placed (Rauhut 2003b). Within Orionides, SHN.019 shares with avetheropods the morphology of the metatarsal III, with the shaft wedge-shaped in cross-section. This feature has been considered as a synapomorphy for this clade (Benson 2010; Carrano et al. 2012). SHN.019 differs from coelurosaurs and some derived carcharodontosaurids (e.g. *Giganotosaurus* and *Mapusaurus*) by having a well-developed and semi-oval flange-shaped fourth trochanter of the femur (Coria and Currie 2006; Brusatte et al. 2008; Benson 2010). Also the pes does not show the strongly constriction of the third metatarsal that is typical in most coelurosaurian theropods (e.g. Currie 2000; Brochu 2003). SHN.019 shares with some ceratosaurians, *Lourinhanosaurus*, some methriacantosaurids, *Concavenator*, and some coelurosaurians the tapered distal end of anterior mid caudal chevrons (Benson 2010; Ortega et al. 2010; Carrano et al. 2012). However, the posteriorly inclined neural spines of mid caudal vertebrae contrast with the vertical or even slightly inclined to the front spines of most ceratosaurians, including *Ceratosaurus* and abelisaurids (Rauhut 2003b).

Late Jurassic tetanuran theropods currently known in the Portuguese record include the megalosaurid *Torvosaurus*, the allosauroids *Allosaurus* and *Lourinhanosaurus* and the tyrannosauroid *Aviatyrannis* (e.g. Mateus 1998; Pérez-Moreno et al. 1999; Rauhut 2003a; Mateus et al. 2006; Hendrickx and Mateus 2014). *Torvosaurus* is represented by some cranial, axial and appendicular elements that cannot be compared with the available material of SHN.019. However, as discussed above, the specimen herein described shares several features with avetheropod tetanurans and may be assigned with confidence as belonging to this clade.

Allosaurus is, at the moment, the most abundant and well represented theropod taxon in the Upper Jurassic of the Lusitanian Basin. SHN.019 shows some similarities with *Allosaurus*, but differs from this taxon in several details, including: (i) caudal neural spines that still well-developed at least up to the thirty-first caudal vertebra whereas it disappears at about the twenty-eight caudal in *Allosaurus* (Gilmore 1920; Madsen 1976); (ii) distal surface of metatarsal II nearly flat with a much shallower groove separating the condyles; and (iii) distal end of metatarsal IV with a wing-shaped lateral condyle extending farther to the rear than the medial condyle (Figure 6.5.12).

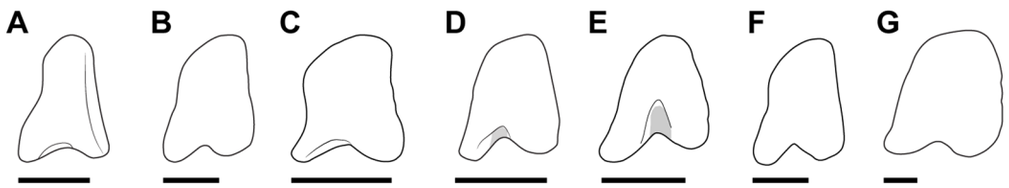

Figure 6.5.12. Line drawing of posterior articular surfaces of the metatarsal IV in (A) *Masiakasaurus* (Carrano et al. 2002); (B) *Torvosaurus* (Hanson and Makovicky 2003); (C) *Sinraptor* (Currie and Zhao 1993); (D) *Allosaurus* (Madsen 1976); (E) SHN.019; (F) *Neovenator* (Brusatte et al. 2008); and (G) *Tyrannosaurus* (Brochu 2003). Scale bars: 50mm.

Lourinhanosaurus antunesi was based on a partial skeleton (ML 370) of a single individual collected in Peralta (Lourinhã) that includes cervical, dorsal, sacral and caudal vertebrae, dorsal ribs, chevrons, an almost complete pelvic girdle, and elements of the hind limbs, including partial femora, right tibia and fibula, a fragment of a metatarsal III, and the proximal articular surface of a first phalanx of the second digit. It was originally described as an allosauroid (Mateus 1998) and latter interpreted as a more

basal tetanuran closely related with eustreptospondyline megalosaurids (Mateus 2005; Mateus et al. 2006). Subsequently, it was recovered as a member of the basal allosauroid clade Metriacanthosauridae by Benson (2010) and as a possible coelurosaur by Carrano et al. (2012). A recent phylogenetic analysis including some theropod specimens from the Upper Jurassic of Portugal supports the interpretation of *Lourinhanosaurus* as a member of Allosauroidea, but placed this taxon at the base of a more derived group comprising *Allosaurus* + Carcharodontosauria (Malafaia et al. 2016).

The overlapping available material of SHN.019 and *Lourinhanosaurus* is limited to few caudal vertebrae and a partially preserved femur. The new specimen shares with this taxon the presence of well-developed anterior centrodiapophyseal lamina and associated centroprezygapophyseal fossa in anterior mid caudal vertebrae (Figure 6.5.13) and the tapered distal end of the mid chevrons (also shared with SHN.036: Malafaia et al. 2016).

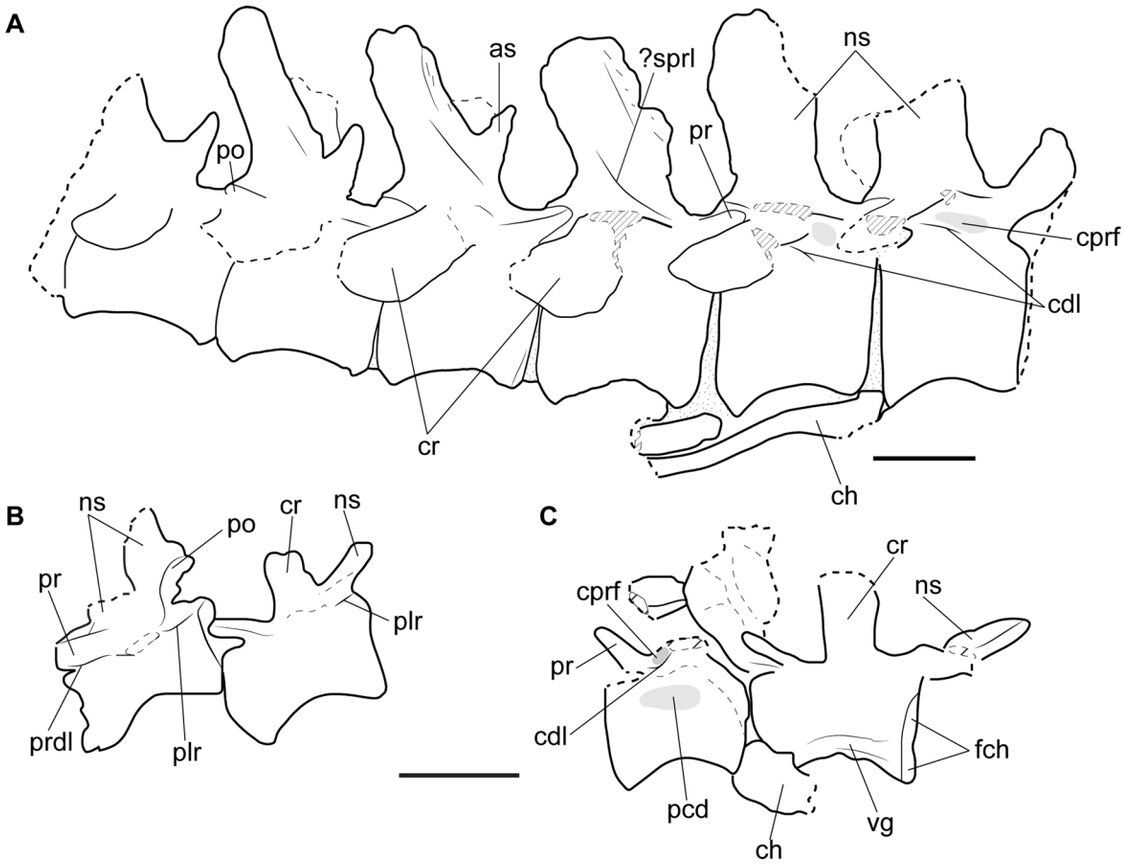

Figure 6.5.13. Interpretative line drawing of caudal vertebrae of *Lourinhanosaurus* and SHN.019 showing some of the structures discussed in the text; (A), anterior mid caudal sequence of *Lourinhanosaurus* in right lateral view; and (B–C) mid caudal vertebrae of SHN.019 in left lateral view. Scale bars: 50mm.

The femur of SHN.019 is incomplete and it is not possible to verify the presence of a nutrient foramen (the principal nutrient foramen of the femur) in the anteromedial surface at the base of the lesser trochanter as is present in *Allosaurus*, *Neovenator* and most other theropods (e.g. Madsen 1976; Brusatte et al. 2008). On the other hand, SHN.019 has a foramen between the lesser trochanter and the femoral diaphysis on the medial surface of the proximal end of the femur (Figure 6.5.6B). If this foramen corresponds to the principal nutrient foramen, its position is uncommon for theropods.

SHN.019 shows some unusual features such as a low vertical crest in the lateral surface of the lesser trochanter and a well-developed and rugose concavity in the medial surface adjacent to the proximal margin of the fourth trochanter (Figure 6.5.6). These characters were considered diagnostic for *Neovenator* (Brusatte et al. 2008). However, a similar ridge on the lateral surface of the lesser trochanter is also present

in *Acrocanthosaurus* (D'Emic et al. 2011), *Australovenator* (Hocknull et al. 2009), and *Concavenator* (E.M. pers. obs. 2016), suggesting a wider distribution of this feature among Carcharodontosauria. This combination of features suggests that SHN.019 is likely to represent a basal carcharodontosaurian theropod.

SHN.019 has strongly developed anterior spur-shaped processes in the mid caudal neural spines. The presence of these processes is shared by some megalosauroids, including *Afrovenator* (Sereno et al. 1994) and *Wiehenvenator* (Rauhut et al. 2016), *Lourinhanosaurus* (Mateus 1998), *Allosaurus* (Madsen 1976), most methriacanthosaurids (e.g. *Sinraptor*: Currie and Zhao 1993 and *Siamotyrannus*: Buffetaut et al. 1996), and most carcharodontosaurs, including *Concavenator* (Ortega et al. 2010), *Acrocanthosaurus* (Currie and Carpenter 2000), and *Mapusaurus* (Coria and Currie 2000). However, in these taxa the additional anterior process of the caudal neural spines is not so developed as in *Lourinhanosaurus* and this feature was considered one of the autapomorphies for this taxon (Mateus 1998). The preserved caudal vertebrae of *Lourinhanosaurus* consist of two sequences from the anterior and mid-section of the tail. Caudal vertebrae of corresponding position are not preserved or have broken neural spines in SHN.019, thus direct comparison between the two specimens is not possible. However, some mid posterior caudal vertebrae of SHN.019 preserve well-developed processes, larger than those of correspondent caudal vertebrae in *Allosaurus*, but much lower and more rounded than those of *Lourinhanosaurus* (see Figure 6.5.14).

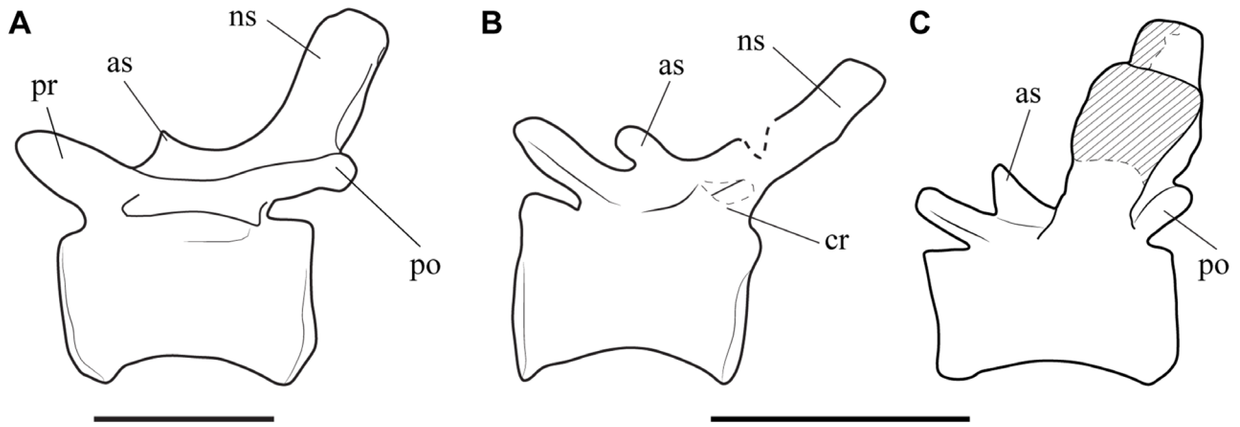

Figure 6.5.14. Line drawing of mid caudal vertebrae in left lateral view of (A), *Allosaurus* (nineteen caudal vertebrae after Madsen 1976); (B), SHN.019 (nineteen or twenty caudal vertebrae); and (C) *Lourinhanosaurus* (anterior mid-caudal vertebrae after Mateus 1988), showing the different development of the anterior spur process of the neural spine. Scale bar: 50mm.

The specimen from Cambelas shares with a juvenile allosauroid specimen collected in Valmitão, SHN.036 (Malafaia et al. 2016) the presence of a strongly developed lateral lamina projecting from the posterior articular facet to the base of the caudal rib. In some vertebrae, especially those near the "transition point", a lower lateral lamina extending from the base of the prezygapophysis along the anterior end of the centrum is also present. Similar anterior lateral lamina is interpreted as a synapomorphy for Carcharodontosauria (Brusatte et al. 2008) and is present in some anterior mid caudal vertebrae of *Concavenator* (E.M. pers. obs. 2016) and in *Veterupristisaurus* (Rauhut, 2011). However, in these taxa the anterior lateral lamina is more developed than the posterior one, whereas the Portuguese specimens show the opposite condition.

6.5.10. CONCLUSIONS

SHN.019 is one of the few theropod specimens known from the Turcifal Sub-basin and adds important information for the knowledge of the dinosaur faunas from the end of the Jurassic (upper Tithonian) in this sector of the Lusitanian Basin. The specimen consists on a partial skeleton of a large-sized theropod represented by caudal vertebrae, including an articulated sequence of the mid and posterior

part of the tail, an almost complete right pes and several isolated pelvic and appendicular elements. It shares with the poorly understood allosauroid species *Lourinhanosaurus antunesi* the presence of a well-developed spur-shaped anterior process of the neural spine on mid caudal vertebrae, which is a feature considered as an autapomorphy for this Portuguese taxon. On the other hand, the specimen from Cambelas shares two unusual characters shared with some carcharodontosaurian allosauroids, including *Neovenator*, *Acrocanthosaurus*, *Australovenator*, and *Concavenator*: i) presence of a robust suboval eminence on the lateral surface of the lesser trochanter and ii) of a well-developed, and rugose depression in the lateral surface adjacent to the proximal end of the fourth trochanter. Beside, other theropod specimens from the Upper Jurassic of the Lusitanian Basin (SHN.036) also show a combination of feautures that indicates the presence of a member of the Carcharodontosauria clade. These specimens represent the first evidence for the presence of carcharodontosaurian theropods in Portugal and the oldest record of this clade in the Laurasian record. The presence of Carcharodontosauria, a clade that is apparently absent in the Morrison Formation contrasts with the general similarity that has been recognized in these faunas from both sides of the proto-North Atlantic during the Late Jurassic. The faunal composition of theropods from the Upper Jurassic of the Lusitanian Basin suggests a scenario in which the evolution of these faunas would be determined by incipient vicariance processes and possibly by differential patterns of regional extinction and/or local environmental preferences.

An interesting taphonomic aspect of the Cambelas fossil site is the presence of distinct bioerosion patterns in several elements of the theropod specimen including bite marks identified as belonging to an indeterminate vertebrate and traces of insects. The insect traces are mostly related with feeding activity of an osteophagic insect group possible of termites. The activity of these insects is associated with bone loss mainly in the articular facets of the metatarsals and phalanges, but it is possible that the poor preservation of other strongly fractured elements could be related with the activity of these organisms.

6.3.11. ACKNOWLEDGMENTS

This work was supported by the Fundação para a Ciência e Tecnologia (Portugal) under a PhD scholarship [SFRH/BD/84746/2012] and by a protocol between CMTV and SHN. Individual grants to E.M. visits for review collections were financed by the Jurassic Foundation, Fundação Luso-Americana para o Desenvolvimento [grant number L07-V-22/2010] and Synthesys [grant number GB-TAF-2160 and FR-TAF-4911]. We thank Graça Ramalheiro for preparation of some elements of SHN.019, to Cristina Moniz and Mário Cachão for comments to the paper, and to the following for access to specimens: Bruno C. Silva (SHN), Rui Castanhinha and Carla Tomás (ML), Vanda dos Santos (MUHNAC), Ronan Allain (MNHN), Luis Chiappe (NHMLAC), Kenneth Carpenter (DMNH), Rodney Scheetz and Brooks Britt (BYU), Mike Getty, Mark Loewen, and Randall Irmis (NHMU), Daniel Chure (DINO), Sandra Chapman (NHMUK), Paul Jeffery (OUMNH), Thomas Schossleitner and Daniela Schwarz (MfN).

REFERENCES

Antunes MT, Mateus O. 2003. Dinosaurs of Portugal. Comptes Rendus Paleovol 2:77–95.

Araújo R, Castanhinha R, Martins RMS, Mateus O, Hendrickx C, Beckmann F, Schell N, Alves LC. 2013. Filling the gaps of dinosaur eggshell phylogeny: Late Jurassic theropod clutch with embryos from Portugal. Scientific Reports 3:1924.

Backwell LR, Parkinson AH, Roberts EM, d'Errico F, Huchet JB. 2012. Criteria for identifying bone modification by termites in the fossil record. Palaeogeography, Palaeoclimatology, Palaeoecology 337–338:72–87.

Bader KS, Hasiotis ST, Martin LD. 2008. Application of forensic science techniques to trace fossils on dinosaur bones from a quarry in the Upper Jurassic Morrison Formation, northeastern Wyoming. Palaios 24:140–158.

Benson RBJ. 2008. A redescription of '*Megalosaurus*' *hesperis* (Dinosauria, Theropoda) from the Inferior Oolite (Bajocian, Middle Jurassic) of Dorset, United Kingdom. Zootaxa 1931:57–67.

Benson RBJ. 2010. A description of *Megalosaurus bucklandii* (Dinosauria: Theropoda) from the Bathonian of the UK and the relationships of Middle Jurassic theropods. Zoological Journal of the Linnean Society 158:882–935.

Benson RBJ, Carrano MT, Brusatte SL. 2010. A new clade of archaic large-bodied predatory dinosaurs (Theropoda: Allosauroidea) that survived to the latest Mesozoic. Naturwissenschaften 97:71–78.

Brochu CA. 2003. Osteology of *Tyrannosaurus rex*: insights from a nearly complete skeleton and high-resolution computed tomographic analysis of the skull. Memoir Society of Vertebrate Paleontology 7:1–138.

Britt BB. 1991. Theropods of Dry Mesa Quarry (Morrison Formation, Late Jurassic), Colorado, with emphasis on the osteology of *Torvosaurus tanneri*. Brigham Young University Geology Studies 37:1–72.

Britt BB, Scheetz RD, Dangerfield A. 2008. A suite of dermestid beetle traces on Dinosaur bone from the upper Jurassic Morrison Formation, Wyoming, USA. Ichnos. 15(2):59–71.

Britt BB, Eberth DA, Scheetz RD, Greenhalgh BW, Stadtman KL. 2009. Taphonomy of debris-flow hosted dinosaur bonebeds at Dalton Wells, Utah (Lower Cretaceous, Cedar Mountain Formation, USA). Palaeogeography, Palaeoclimatology, Palaeoecology 280:1–22.

Brusatte SL, Benson RBJ, Hutt S. 2008. The osteology of *Neovenator salerri* (Dinosauria: Theropoda) from the Wealden Group (Barremian) of the Isle of Wight. Monograph of the Palaeontographical Society 162(631):1–166.

Brusatte SL, Norell MA, Carr TD, Erickson GM, Hutchinson JR, Balanoff AM, Bever GS, Choiniere JN, Makovicky PJ, Xu X. 2010. Tyrannosaur paleobiology: new research on ancient exemplar organisms. Science 329:1481–1485.

Buffetaut E, Suteethorn V, Tong H. 1996. The earliest known tyrannosaur from the Lower Cretaceous of Thailand. Nature 381:689–691.

Calvo JO, Porfiri JD, Veralli C, Novas F, Poblete F. 2004. Phylogenetic status of *Megaraptor namunhuaiquii* Novas based on a new specimen from Neuquén, Patagonia, Argentina. AMEGHINIAN 41(4):565–575.

Carrano MT, Sampson SD. 2008. The phylogeny of Ceratosauria (Dinosauria: Theropoda). Journal of Systematic Palaeontology 6 (2):183–236.

Carrano MT, Benson RBJ, Sampson SD. 2012. The phylogeny of Tetanurae (Dinosauria: Theropoda). Journal of Systematic Palaeontology 10:211–300.

Carrano MT, Sampson SD, Foster CA. 2002. The osteology of *Masiakasaurus knopfleri*, a small abelisauroid (dinosauria: theropoda) from the Late Cretaceous of Madagascar. Journal of Vertebrate Paleontology 22(3):510–534.

Chin K, Bishop JR. 2006. Exploited twice: bored bone in a theropod coprolite from the Jurassic Morrison Formation of Utah, USA. Special Publications-SEPM. 88:379.

Chure DJ. 2000. A new species of *Allosaurus* from the Morrison Formation of Dinosaur National Monument (UT-CO) and a revision of the theropod family Allosauridae. [Ph.D. dissertation], Columbia University, New York, 1021 pp.

Coria RA, Currie PJ. 2006. A new carcharodontosaurid (Dinosauria, Theropoda) from the Upper Cretaceous of Argentina. Geodiversitas 28(1):71–118.

Coria RA, Chiappe LM, Dingus L. 2002. A new close relative of *Carnotaurus sastrei* Bonaparte 1985 (Theropoda: Abelisauridae) from the Late Cretaceous of Patagonia. Journal of Vertebrate Paleontology 22(2):460–465.

Currie PJ. 2000. Theropods from the Cretaceous of Mongolia. In: Benton MJ, Shishkin MA, Unwin DM, Kurochkin EN. (Eds). The age of dinosaurs in Russia and Mongolia. Cambridge University Press, Cambridge. 434–455.

Cuesta E, Díaz-Martínez I, Ortega F, Sanz JL. 2015. Did all theropods have chicken-like feet? First evidence of a non-avian dinosaur podotheca. Cretaceous Research 56:53–59.

Currie PJ, Carpenter K. 2000. A new specimen of *Acrocanthosaurus atokensis* (Theropoda, Dinosauria) from the Lower Cretaceous Antlers Formation (Lower Cretaceous, Aptian) of Oklahoma, USA. Geodiversitas 22(2):207–246.

Currie PJ, Zhao XJ. 1993. A new carnosaur (Dinosauria, Theropoda) from the Jurassic of Xinjiang, People's Republic of China. Canadian Journal of Earth Sciences 30:2037–2081.

Dangerfield A, Britt B, Scheetz R, Pickard M. 2005. Jurassic dinosaurs and insects: The paleoecological role of termites as carrion feeders: Geological Society of America, Abstracts with Programs 37:443p.

D'Emic MD, Melstrom KM, Eddy DR. 2012. Paleobiology and geographic range of the large-bodied Cretaceous theropod dinosaur *Acrocanthosaurus atokensis*. Palaeogeography, Palaeoclimatology, Palaeoecology 333–334:13–23.

Deyrup M, Deyrup N, Eisner M, Eisner T. 2005. A caterpillar that eats tortoise shells. American Entomologist. 51(4):245–248.

Dunstan B. 1923. Mesozoic insects of Queensland. Part I. Introduction and coleoptera. Geological Survey of Queensland Publication 273:1–88.

Eddy DR, Clarke JA. 2011. New information on the cranial anatomy of *Acrocanthosaurus atokensis* and its implications for the phylogeny of Allosauroidea (Dinosauria: Theropoda). PLoS ONE 6(3):e17932. ´

Fowler DW, Freedman EA, Scannella JB, Kambic RE. 2011. The Predatory Ecology of *Deinonychus* and the Origin of Flapping in Birds. PLoS ONE 6(12):e28964.

Galton PM, Carpenter K, Dalman SG. 2015. The holotype pes of the Morrison dinosaur *Camptonotus amplus* Marsh, 1879 (Upper Jurassic, western USA) – is it *Camptosaurus*, Sauropoda or *Allosaurus*? Neues Jahrbuch für Geologie und Paläontologie Abhandlungen 275(3):317–335.

Gauthier J. 1986. Saurischian monophyly and the origin of birds. In: Padian K. (Eds). The Origin of Birds and the Evolution of Flight. California Academy of Science, San Francisco. 55pp.

Genise JF, de Valais S, Apesteguía S, Novas FE. 2004. A trace fossil association in bones from the Later Cretaceous of Patagonia, Argentina. In: Buatois LA, Magnano MG. (Eds). Abstract Book of the Ichnia First International Congress on Ichnology. Trelew: Museum Palaeotologico Egidio Feruglio. 37–38.

Gerke O, Wings O. 2016. Multivariate and cladistic analyses of isolated teeth reveal sympatry of theropod dinosaurs in the Late Jurassic of Northern Germany. PLoS ONE 11(7):e0158334.

Gilmore CW. 1920. Osteology of the carnivorous Dinosauria in the United States National Museum, with special reference to the genera *Antrodemus* (*Allosaurus*) and *Ceratosaurus*. Bulletin United States National Museum 110:1–159.

Goloboff PA, Farris JS, Nixon KC. 2008. TNT 1.1, a free program for phylogenetic analysis. Cladistics 24(5):774–786.

Han F, Clark JM, Xu X, Sullivan C, Choiniere J, Hone DWE. 2011. Theropod teeth from the Middle-Upper Jurassic Shishugou Formation of northwest Xinjiang, China. Journal of Vertebrate Paleontology 31(1):111–126.

Hanson M, Makovicky PJ. 2013. A new specimen of *Torvosaurus tanneri* originally collected by Elmer Riggs. Historical Biology 26(6):775–784.

Harris JD. 1998. A reanalysis of *Acrocanthosaurus atokensis*, its phylogenetic status, and paleobiogeographic implications, based on a new specimen from Texas. New Mexico Museum of Natural History and Science Bulletin 13:1–75.

Hasiotis ST. 2004, Reconnaissance of Upper Jurassic Morrison Formation ichnofossils, Rocky Mountain Region, USA: Paleoenvironmental, stratigraphic, and paleoclimatic significance of terrestrial and freshwater ichnocoenoses: Sedimentary Geology 167:177–268.

Hasiotis ST, Fiorillo AR, Hanna RR. 1999. Preliminary report on borings in Jurassic dinosaur bones: evidence for invetebrate-vertebrate interactions. Utah Geological Survey Miscellaneous Publications 99(1):193–200.

Hendrickx C, Mateus O. 2014a. Abelisauridae (Dinosauria: Theropoda) from the Late Jurassic of Portugal and dentition-based phylogeny as a contribution for the identification of isolated theropod teeth. Zootaxa 3759(1):1–74.

Hendrickx C, Mateus O. 2014b. *Torvosaurus gurneyi* n. sp., the largest terrestrial predator from Europe, and a proposed terminology of the maxilla anatomy in nonavian theropods. PLoS ONE 9(3):e88905.

Hill AP. 1987, Damage to some fossil bones from Laetoli. In: Leakey MD, Harris JM. (Eds). Laetoli: A Pliocene Site in Northern Tanzania: Clarendon Press, Oxford. 543–545.

Hill G. 1988. The sedimentology and lithostratigraphy of the Upper Jurassic Lourinhã Formation, Lusitanian Basin Portugal. [Ph.D. dissertation], The Open University.

Hocknull SA, White MA, Tischler TR, Cook AG, Calleja ND, Sloan T, Elliott DA. 2009. New mid-Cretaceous (Latest Albian) dinosaurs from Winton, Queensland, Australia. PLoS ONE 4:e6190.

Holden AR, Harris JM, Timm RM. 2013. Paleoecological and taphonomic implications of insect-damaged pleistocene vertebrate remains from Rancho La Brea, southern California. PLoS One. 8(7):e67119.

Kadej M, Háva J. 2011. First record of a fossil *Trinodes* larva from Baltic amber (Coleoptera: Dermestidae: Trinodinae). Genus-International Journal of Invertebrate Taxonomy 22(1):1–6.

Kiselyova T, Mchugh JV. 2006. A phylogenetic study of Dermestidae (Coleoptera) based on larval morphology. Systematic Entomology 31(3):469–507.

Kullberg JC, Rocha RB, Soares AF, Rey J, Terrinha P, Callapez P. 2006. A Bacia Lusitaniana: estratigrafia, paleogeografia e tectónica. In: Dias R, Araújo A, Terrinha P, Kullberg JC. (Eds). Geologia de Portugal no Contexto da Ibéria. Universidade de Évora, Évora. 317–368.

Lapparent AF, Zbyszewski G. 1957. Les dinosauriens du Portugal. Memórias dos Serviços Geológicos de Portugal 2:1–63,36 pls.

Laws GR, Hasiotis ST, Fiorillo A, Chure D, Breithaupt BH, Horner J. 1996. The demise of a Jurassic dinosaur after death: Three cheers for the dermestid beetle: Geological Society of America National Meeting, Denver, Colorado 28(7):299p.

Leinfelder RR. 1993. A sequence stratigraphic approach to the Upper Jurassic mixed carbonate - siliciclastic succession of the central Lusitanian Basin, Portugal. Profil 5:119–140.

Li F, Bi S, Pittman M, Brusatte SL, Xu X. 2016. A new tyrannosaurine specimen (Theropoda: Tyrannosauroidea) with insect borings from the Upper Cretaceous Honglishan Formation of Northwestern China, Cretaceous Research. doi: 10.1016/j.cretres.2016.06.002.

Madsen JHJr. 1976. *Allosaurus fragilis*: a revised osteology. Utah Geological and Mineralogical Survey 109:1–163.

Malafaia E, Ortega F, Escaso F, Dantas P, Pimentel N, Gasulla JM, Ribeiro B, Barriga F, Sanz JL. 2010. Vertebrate fauna at the *Allosaurus* fossil-site of Andrés (Upper Jurassic), Pombal, Portugal. Journal of Iberian Geology 36(2):193–204.

Malafaia E, Ortega F, Escaso F. 2014. New post-cranial elements assigned to coelurosaurian theropods from the Late Jurassic of Lusitanian Basin, Portugal. Fundamental 24:123–126.

Malafaia E, Ortega F, Escaso F, Silva B. 2015. New evidence of *Ceratosaurus* (Dinosauria: Theropoda) from the Late Jurassic of the Lusitanian Basin, Portugal. Historical Biology 27(7):938–946.

Malafaia E, Mocho P, Escaso F, Ortega F. 2016. A juvenile allosauroid theropod (Dinosauria, Saurischia) from the Upper Jurassic of Portugal. Historical Biology: doi:10.1080/08912963.2016.1231183.

Manuppella G. 1998. Geologic data about the "Camadas de Alcobaça" (Upper Jurassic) north of Lourinhã, and facies variation. Memórias da Academia de Ciências Lisboa 37:17–24.

Manuppella G, Antunes MT, Pais J, Ramalho MM, Rey J. 1999. Notícia explicativa da Folha 30-A, Lourinhã. Departamento de Geologia do Instituto Geológico e Mineiro, Lisboa.

Manuppella G, Antunes MT, Almeida C, Azerêdo AC, Barbosa B, Cardoso JL, Crispim JA, Duarte LV, Martins LT, Ramalho MM, Santos VF, Terrinha P. 2000. Notícia Explicativa da Folha 27-A, Vila Nova de Ourém. Instituto Geológico e Mineiro, Lisboa.

Marques B, Oloriz F, Caetano PS, Rocha RB, Kullberg JC. 1992. Upper Jurassic of the Alcobaça Region. Stratigraphic Contributions. Comunicações dos Serviços Geológicos de Portugal 78(1):63–69.

Marsh OC. 1878. Notice of new dinosaurian reptiles. American Journal of Science and Arts 15:241–244.

Marsh OC. 1881. Principal characters of American Jurassic dinosaurs. American Journal of Science Part V. 21:417–423.

Martin T. 2000. The dryolestids and the primitive 'peramurid' from the Guimarota mine. In: Martin T, Krebs B. (Eds). Guimarota. A Jurassic Ecosystem. Verlag Dr. Friedrich Pfeil, München. 109–120.

Mateus O. 1998. *Lourinhanosaurus antunesi*, a new upper Jurassic allosauroid (Dinosauria: Theropoda) from Lourinhã, Portugal. Memórias da Academia de Ciências de Lisboa 37:111–124.

Mateus O. 2005. Dinossauros do Jurássico Superior de Portugal com destaque para os saurísquios. [Ph.D. dissertation], Universidade Nova de Lisboa, Lisboa.

Mateus O, Antunes MT. 2000a. *Ceratosaurus* sp. (Dinosauria: Theropoda) in the Late Jurassic of Portugal. 31st International Geological Congress.

Mateus O, Antunes MT. 2000b. *Torvosaurus* sp. (Dinosauria: Theropoda) in the Late Jurassic of Portugal. I Congresso Ibérico de Paleontología/XVI Jornadas de la Sociedad Española de Paleontología: 115–117.

Mateus O, Walen A, Antunes MT. 2006. The large theropod fauna of the Lourinhã Formation (Portugal) and its similarity to the Morrison Formation, with a description of a new species of *Allosaurus*. In: Foster JR, Lucas SG. (Eds). Paleontology and Geology of the Upper Jurassic Morrison Formation. New Mexico Museum of Natural History and Science 36. 123–129.

Matos R. 1954. Carta Geológica de Portugal, na escala 1:50 000 Folha 30-C (Torres Vedras). Serviços Geológicos de Portugal.

Mocho P, Royo-Torres R, Malafaia E, Escaso F, Ortega F. 2016. Systematic review of Late Jurassic sauropods from the Museu Geológico collections (Lisboa, Portugal). Journal of Iberian Geology 42(2):227–250.

Moniz C, Carvalho C, Dantas P, Ortega F, Malafaia E, Ramalheiro G, Escaso F, Silva B, Barriga F. 2007. Aspectos tafonómicos de un terópodo del yacimiento de Cambelas (Jurásico Superior, Torres Vedras, Portugal). IV Jornadas Internacionales sobre Paleontología de Dinosaurios y su Entorno:81–83.

Oliveira JT, Pereira H, Ramalho M, Antunes MT. 1992. Carta Geológica de Portugal, na escala 1:50 0000. Serviços Geológicos de Portugal.

Ortega F, Escaso F, Gasulla JM, Dantas P, Sanz JL. 2006. Dinosaurios de la Península Ibérica. Estudios Geológicos 62(1):219–240.

Ortega F, Escaso F, Sanz JL. 2010. A bizarre, humped carcharodontosauria (Theropod) from the Lower Cretaceous of Spain. Nature 467:203–206.

Parkinson AH. 2013. *Dermestes maculatus* and *Periplaneta americana*: bone modification criteria and establishing their potential as climatic indicators. [MsD dissertation] Johannesburg: University of the Witwatersrand.

Paul GS. 1988. Predatory Dinosaurs of the World. Simon & Schuster, New York.

Pérez-Moreno BP, Chure DJ, Pires C, Silva CM, Santos V, Dantas P, Póvoas L, Cachão M, Sanz JL, Galopim de Carvalho AM. 1999. On the presence of *Allosaurus fragilis* (Theropoda: Carnosauria) in the Upper Jurassic of Portugal: first evidence of an intercontinental dinosaur species. Journal of the Geological Society 156:449–452.

Persons SW, Currie PJ. 2011. Dinosaur speed demon: the caudal musculature of Carnotaurus sastrei and implications for the evolution of South American abelisaurids. PLos ONE. 6:e25763.

Peyer K. 2006. A reconsideration of *Compsognathus* from the upper Tithonian of Canjuers, southeastern France. Journal of Vertebrate Paleontology 26(4):879–896.

Ran H. 2014. Fantastic ants: wonder of evolution. Beijing: Tsinghua University Press.

Rauhut OWM. 2001. Herbivorous dinosaurs from the Late Jurassic (Kimmeridgian) of Guimarota, Portugal. Proceedings of the Geologists' Association 112:275–283.

Rauhut OWM. 2003a. A tyrannosauroid dinosaur from the Upper Jurassic of Portugal. Palaeontology 46(5):903–910.

Rauhut OWM. 2003b. The interrelationships and evolution of basal theropod dinosaurs. Special Papers in Palaeontology 69: 1–213.

Rauhut OWM. 2005. Osteology and relationships of a new theropod dinosaur from the Middle Jurassic of Patagonia. Palaeontology 48:87–110.

Rauhut OWM. 2011. Theropod dinosaurs from the Late Jurassic of Tendaguru (Tanzania). Special Papers in Palaeontology 86:195–239.

Rauhut OWM, Fechner R. 2005. Early development of the facial region in a non-avian theropod dinosaur. Proceedings of the Royal Society B: Biological Sciences 272:1179–1183.

Rauhut OWM, Hübner TR, Lansen K-P. 2016. A new megalosaurid theropod dinosaur from the late Middle Jurassic (Callovian) of north-western Germany: Implications for theropod evolution and faunal turnover in the Jurassic. Palaeontologia Electronica 19.2.26A:1–65.

Rey J. 1993. Les unités lithostratigraphiques du Grupe de Torres Vedras (Estremadura, Portugal). Comunicações do Instituto Geológico e Mineiro 79:75–85.

Roberts EM, Rogers RR, Foreman BZ. 2007. Continental insect borings in dinosaur bone: examples from the late cretaceous of Madagascar and Utah. Journal of Paleontology 81(1):201–208.

Rogers RR. 1992. Non-marine borings in dinosaur bones from the Upper Cretaceous Two Medicine Formation, northwestern Montana: Journal of Vertebrate Paleontology 12:528–531.

Rusell D. 1972. Ostrich dinosaurs from the Late Cretaceous of Western Canada. Canadian Journal of Earth Sciences 9 (4): 376-402.

Sauvage HE. 1897-1898. Vértébrés fossiles du Portugal. Contribution à l' étude des poissons et des reptiles du Jurassique et du Crétacique. Memoires Direction des Travaux Géologiques du Portugal:1–48.

Schneider S, Fürsich FT, Werner W. 2009. Sr-isotope stratigraphy of the Upper Jurassic of central Portugal (Lusitanian Basin) based on oyster shells. International Journal of Earth Sciences 98(8):1949–1970.

Schudack ME. 2000. Geological setting and dating of the Guimarota-beds. In: Martin T, Krebs B. (Eds). Guimarota: A Jurassic Ecosystem. Verlag Dr. Friedrich Pfeil, München. 21–26.

Sereno PC, Wilson JA, Larsson HCE, Dutheil DB, Sues H-D. 1994. Early Cretaceous dinosaurs from the Sahara. Science 266:267–270.

Tappen M. 1994, Bone weathering in the tropical rain forest: Journal of Archaeological Science 21:667–673.

Taylor AM, Gowland S, Leary S, Keogh KJ, Martinius AW. 2014. Stratigraphical correlation of the Lourinhã Formation in the Consolação Sub-basin (Lusitanian Basin), Portugal. Geological Journal 49(2):143–162.

Watson JAL, Abbey HM. 1986. The effecfs of termites (Isoptera) on bone: some areheological implications. Sociobiology. 11(3):245–254.

White MA, Benson RBJ, Tischler TR, Hocknull SA, Cook AG, Barnes DG, Poropat SF, Wooldridge SJ, Sloan T, Sinapius GHK, Elliott DA. 2013. New *Australovenator* hind limb elements pertaining to the holotype reveal the most complete neovenatorid leg. PLoS ONE 8(7):e68649.

Wilson EO. 1971. The insect societies. Cambridge (NY): Cambridge University Press.

Wilson JA. 1999. A nomenclature for vertebral laminae in sauropods and other saurischian dinosaurs. Journal of Vertebrate Paleontology 19:639–653.

Wilson JA, D'Emic MD, Ikejiri T, Moacdieh EM, Whitlock JA. 2011. A Nomenclature for vertebral fossae in Sauropods and other Saurischian Dinosaurs. PlosONE 6(2):e17114.

Xing L, Parkinson AH, Ran H, Pirrone CA, Roberts EM, Zhang J, Burns ME, Wang T, Choiniere J. 2015. The earliest fossil evidence of bone boring by terrestrial invertebrates, examples from China and South Africa. Historical Biology 28(8): 1108–1117.

Zanetti NI, Visciarelli EC, Centeno ND. 2014. Taphonomic marks on pig tissue due to cadaveric coleoptera activity under controlled conditions. Journal of Forensic Sciences 59(4):997–1001.

Zbyszewski G, Moitinho de Almeida F, Torres de Assunção C. 1955. Carta geológica de Portugal na escala de 1:50 000: notícia explicativa da folha 30-C, Torres Vedras: rochas eruptivas. Serviços Geológicos de Portugal, Lisboa.

Zinke J. 1998. Small theropod teeth from the Upper Jurassic coal mine of Guimarota (Portugal). Palaontologische Zeitschrift 72:179–189.

SUPPLEMENTARY MATERIAL

Inventory number	Osteological elements
SHN.019/1	Theropod tooth
SHN.019/2	Sequence of 17th caudal vertebrae
SHN.019/3	Isolated anterior caudal vertebra
SHN.019/4	Isolated anterior caudal vertebra
SHN.019/5	Fragment of the proximal end of a right femur
SHN.019/6	Fragment of the diaphysis of a ? right femur
SHN.019/7	Fragment of the diaphysis of a tibia
SHN.019/8	Fragment of the diaphysis of a fibula
SHN.019/9	Fragment of the distal end of a fibula
SHN.019/10	Left calcaneum
SHN.019/11	Left IV tarsal
SHN.019/12	Fragment of a ? III tarsal
SHN.019/13	Right pes
SHN.019/14	Vertebra crocodylomorpha
SHN.019/15	Fragment of tooth of crocodylomorpha

Supplementary Table 6.5.1. List of osteological elements collected in the Cambelas fossil site.

	019/3	019/4	c_1	c_2	c_3	c_4	c_5	c_6	c_7	c_8	c_9	c_{10}	c_{11}	c_{12}	c_{13}	c_{14}	c_{15}	c_{16}	c_{17}
Centrum length	82.6	89.8	90	91	95.2	91.1	100.4	99.1	96.1	93.1	95.4	94.5	89.7	89.3	79.2	86.9	84.4	80.4	78.5
Centrum height	48.8	47.2	56.9	56.1	55.1	50.9	52.9	40.6	46.9	38.3	39.9	35.7	31.4	29.4	28.7	28.3	23.1	21.4	21
Centrum transverse width	38.8	34.2	31.6	26.7	27.7	29.3	30.2	26.1	28.5	18.8	26.8	23.3	19.7	22.9	19.9	19.8	18.2	17.8	?
Centrum length/transverse width	2.1	2.6	2.8	3.4	3.4	3.1	3.3	3.8	3.4	5	3.6	4.1	4.6	3.9	4	4.4	4.6	4.5	?
Centrum length/height	1.7	1.9	1.6	1.6	1.7	1.8	1.9	2.4	2	2.4	2.4	2.6	2.9	3	2.8	3.1	3.6	3.8	3.7
Anterior articular facet width	76	64.6	61	50.1	62.9	55.3	57.3	51.2	43.8	43.6*	43.5*	?	35.3*	33.8*	38.7	35.6	?	34.4	26.9
Anterior articular facet height	67.2	64.9	76.7	66.6	57.1	55	63.5	51.9	55.8	60.1	52.0	52.4	46.7	44.8	44.7	34.7	36.8	36.1	32.5
Anterior articular facet height/width	0.9	1	1.3	1.3	0.9	1	1.1	1	1.3	1.4*	1.2*	?	1.3*	1.3*	1.2	1	?	1	1.2
Posterior articular facet width	66.4	61.1	55.7	51.6	51.1	60.5	56.6	46.3*	40*	?	?	32.3*	?	32.6*	?	?	41.6	31.9	32
Posterior articular facet height	67.5	68.1	68.8	58.9	62.9	62.7	54.9	49.9	58.6	51.9	52.9	52.8	47	40.4	42.4	37.4	35.6	36.2	34.2
Posterior articular facet height/width	1	1.1	1.2	1.1	1.2	1	1	1.1*	1.5*	?	?	1.6*	?	1.2*	?	?	0.9	1.1	1.1

Supplementary Table 6.3.2. Measurements of the caudal vertebrae of SHN.019. All measurements in milimeters (* estimated measurements).

Appendicular elements							
				femur	tibia	fibula	
Transverse width of the diaphysis				66.51	53.73	23.61	
Anteroposterior width of the diaphysis				88.14	84.44	29.35	
Pes							
	Mt	Ph.1	Ph.2	Ph.3	Ph.4	Ph.5	
Maximum length							Total length excluding the Mt
Digit I	95.53	75.96	70.01				235
Digit II	326.64*	103.27	88.82	113.42			280
Digit III	374.68*	112.11	89.89	71.97	90.74		332
Digit IV	326.4*	84.8	71.88	58.33	40.67	74.92	275
Digit V	106.06*						
Proximal end, maximum transverse width							
Digit I	9.84	36.94	24.3				
Digit II	?	64.92	49.75	30.83			
Digit III	?	66.8	54.56	39.34	27.24		
Digit IV	77.22*	56.34	45.13	39.12	30.79	25.55	
Digit V	12.52						
Proximal end, maximum anteroposterior wide							
Digit I	17.25	35.7	37.98				
Digit II	?	64.53	44.12	49.19			
Digit III	?	56.02	39.72	33.96	40.38		
Digit IV	40.36	50.99	40.06	34.27	30.12	32.49	
Digit V	25.1						
Distal end, maximum transverse width							
Digit I	30.54	26.3	7.16				
Digit II	66.01	51.35	39.79	11.88			
Digit III	69.43	57.04	42.08	32.96	9.62		
Digit IV	57.91	46.49	38.91	33.9	30.22	10.74	
Digit V	8.72						
Distal end, maximum anteroposterior wide							
Digit I	35.05	27.68	7.53				
Digit II	57.57	41.3	36.78	11.37			
Digit III	59.75	37.58	31.95	27.76	8.1		
Digit IV	73.75	41.35	35.36	28.8	22.04	10.93	
Digit V	11.18						
Maximum diameter at mid-length							
Digit I	34.73	26.86	25.21				
Digit II	39.27	36.38	35.12	30.87			
Digit III	42.16	38	32.96	29.61	26.16		
Digit IV	45.83	36.22	35.96	34.67	26.56	24.5	
Digit V	19.8						

Supplementary Table 6.5.3. Measurements of the appendicular elements of SHN.019. All measurements in millimeters (* estimated measurements).

CHAPTER 7: COELUROSAURIA

7.1. COELUROSAURIAN THEROPODS FROM THE UPPER JURASSIC OF THE LUSITANIAN BASIN

The record of coelurosaurian theropods from the Upper Jurassic of the Lusitanian Basin consists mainly on isolated elements (Zinke 1998; Rauhut 2003; Hendrickx and Mateus 2014; Malafaia et al. 2014). The only coelurosaurian taxon currently known in the Portuguese record is the small tyrannosauroid *Aviatyrannis jurassica* from the Guimarota fossil site (Rauhut 2003). This species was described based on pelvic elements (ilia and a partial right ischium) and some isolated premaxillary teeth. The species was diagnosed based on the presence of a strongly developed ridge above the acetabulum of the ilium and a dorsally concave anterior margin of the acetabular blade. The type ilium of *Aviatyrannis* was originally referred to the basal tyrannosauroid *Stokesosaurus* by Rauhut (2000), but later considered distinct from this taxon based on the general shape and orientation of the ridge above the acetabulum (Rauhut 2003). A posterodorsally inclined ridge was posteriorly proposed as an autapomorphy of *Stokesosaurus* shared by *Stokesosaurus langhami* from the lower Tithonian of England and *Stokesosaurus clevelandi* from the Kimmeridgian of North America, whereas the equivalent ridge in *Aviatyrannis*, *Guanlong* and tyrannosaurids is strictly vertical (Benson 2008). A small ilium from the Morrison Formation of South Dakota referred to *Stokesosaurus clevelandi* by Foster and Chure (2000) shares with *Aviatyrannis* the vertical orientation of the ridge above the acetabulum and the same morphology of the postacetabular blade and was tentatively related to this taxon (Rauhut 2003).

Aviatyrannis and *Stokesosaurus* were originally considered the older representatives of the tyrannosauroid lineage (Madsen 1974; Rauhut 2003). However, later discoveries demonstrate the presence of a group of basal tyrannosauroids, the Proceratosauridae, which includes *Kileskus* from Russia, *Guanlong* from China and *Proceratosaurus* already at least during the Bathonian (Xu et al. 2006; Averianov et al. 2010; Brusatte et al. 2010; Rauhut et al. 2010). Jurassic tyrannosauroids have so far been reported only from the Northern Hemisphere being known in Asia (Xu et al. 2006), North America (Madsen 1974; Chure and Madsen 1998; Foster and Chure 2000), and Europe (Zinke 1998; Rauhut 2000, 2003; Benson 2008). The presence of *Stokesosaurus* and *Aviatyrannis* in Europe, and of *Stokesosaurus* and an *Aviatyrannis*-like ilium in North America support the hypothesis of a palaeobiogeographic relationship between parts of Europe and North America during the Late Jurassic (Benson 2008).

A great diversity of coelurosaurian theropods has been tentatively identified based on isolated teeth, including velociraptorine dromaeosaurids, compsognathids, troodontids and taxa with uncertain relationship, such as *Paronychodon* and *Richardoestesia* (Zinke and Rauhut 1994; Zinke 1998; Rauhut 2003; Malafaia et al. 2010; Hendrickx and Mateus 2014; Malafaia et al. in press). *Archaeopteryx* is also reported in this record based on some isolated teeth collected in Guimarota (Weigert 1995; Zinke 1998). However, some authors consider that the teeth assigned to cf. *Archaeopteryx* by Weigert (1995), and Zinke (1998) differ from this early avian taxon in several features, including the presence of a twisted and serrated carina, which is a feature unknown in archaeopterygids and in birds in general (Elzanowski 2002; Louchart and Pouech 2017). Based on this argumentation these teeth from Guimarota were interpreted as probably representing a yet undescribed non-avian theropod (Louchart and Pouech 2017).

REFERENCES

Averianov AO, Krasnolutskii SA, Ivantsov SV. 2010. A new basal coelurosaur (Dinosauria: Theropoda) from the Middle Jurassic of Siberia. Proceedings of the Zoological Institute RAS 34(1):42–57.

Benson RBJ. 2008. New information on *Stokesosaurus*, a tyrannosauroid (Dinosauria: Theropoda) from North America and the United Kingdom. Journal of Vertebrate Paleontology 28(3):732–750.

Brusatte SL, Norell MA, Carr TD, Erickson GM, Hutchinson JR, Balanoff AM, Bever GS, Choiniere JN, Makovicky PJ, Xu X. 2010. Tyrannosaur paleobiology: new research on ancient exemplar organisms. Science 329:1481–1485.

Chure DJ, Madsen JH. 1998. An unusual braincase (*Stokesosaurus clevelandi*) from the Cleveland–Lloyd Dinosaur Quarry, Utah (Morrison Formation, Late Jurassic). Journal of Vertebrate Paleontology 18:115–125.

Elzanowski A. 2002. Archaeopterygidae (Upper Jurassic of Germany). In: Chiappe LM, Witmer LM. (Eds). Mesozoic Birds: Above the Heads of Dinosaurs. University of California Press, Berkeley:129–159.

Foster JR, Chure DJ. 2000. An ilium of a juvenile *Stokesosaurus* (Dinosauria, Theropoda) from the Morrison Formation (Upper Jurassic: Kimmeridgian), Meade County, South Dakota. Brigham Young University Geology Studies 45:5–10.

Hendrickx C, Mateus O. 2014. Abelisauridae (Dinosauria: Theropoda) from the Late Jurassic of Portugal and dentition-based phylogeny as a contribution for the identification of isolated theropod teeth. Zootaxa 3759(1):1–74.

Louchart A, Pouech J. 2017. A tooth of Archaeopterygidae (Aves) from the Lower Cretaceous of France extends the spatial and temporal occurrence of the earliest birds. Cretaceous Research 73:40–46.

Madsen JH. 1974. A new theropod dinosaur from the Upper Jurassic of Utah. Journal of Paleontology 48:27–31.

Malafaia E, Ortega F, Escaso F, Dantas P, Pimentel N, Gasulla JM, Ribeiro B, Barriga F, Sanz JL. 2010. Vertebrate fauna at the *Allosaurus* fossil-site of Andrés (Upper Jurassic), Pombal, Portugal. Journal of Iberian Geology 36(2):193–204.

Malafaia E, Ortega F, Escaso F. 2014. New post-cranial elements assigned to coelurosaurian theropods from the Late Jurassic of Lusitanian Basin, Portugal. Fundamental 20:123–126.

Malafaia1 E, Escaso F, Mocho P, Serrano-Martínez A, Torices A, Cachão M, Ortega F. (in press). Analysis of diversity, stratigraphic and geographical distribution of isolated theropod teeth from the Upper Jurassic of the Lusitanian Basin, Portugal. Journal of Iberian Geology.

Rauhut OWM. 2000. The dinosaur fauna from the Guimarota mine. In: Martin T, Krebs B. (Eds). Guimarota, A Jurassic ecosystem. Verlag Dr. Friedrich Pfeil, Munich. 75–82.

Rauhut OWM. 2003. A tyrannosauroid dinosaur from the Upper Jurassic of Portugal. Palaeontology 46:903–910.

Rauhut OWM, Milner AC, Moore-Fay S. 2010. Cranial osteology and phylogenetic position of the theropod dinosaur *Proceratosaurus bradleyi* (Woodward, 1910) from the Middle Jurassic of England. Zoological Journal of the Linnean Society 158:155–195.

Weigert A. 1995. Isolierte Zähne von cf. *Archaeopteryx* sp. aus dem Oberen Jura der Kohlengrube Guimarota (Portugal). Neues Jahrbuch für Geologie und Paläontologie 9:562–576.

Xu X, Clark JM, Forster CA, Norell MA, Erickson GM, Eberth DA, Jia C, Zhao Q. 2006. A basal tyrannosauroid dinosaur from the Late Jurassic of China. Nature 439:715–718.

Zinke J. 1998. Small theropod teeth from the Upper Jurassic coal mine of Guimarota (Portugal). Palaontologische Zeitschrift 72:179–189.

Zinke J, Rauhut OWM. 1994. Small theropods (Dinosauria, Saurischia) from the Upper Jurassic and Lower Cretaceous of the Iberian Peninsula. Berliner geowiss. Abh. E13, 163–177.

THIRD PART

CHAPTER 8: GENERAL CONTEXT OF THE THEROPOD FAUNA FROM THE LATE JURASSIC OF THE LUSITANIAN BASIN

8.1. Introduction

8.2. Analysis of diversity, stratigraphic and geographical distribution of isolated theropod teeth from the Upper Jurassic of the Lusitanian Basin, Portugal

8.3. The paleobiogeographic context of the Late Jurassic Portuguese theropods

CHAPTER 9: RESULTS AND CONCLUSIONS

9.1. Results

9.2. Resultados

9.3. Conclusions

9.4. Conclusões

CHAPTER 10: ACKNOWLEDGEMENTS

10.1. Acknowledgements

10.2. Agradecimentos

CHAPTER 8: GENERAL CONTEXT OF THE THEROPOD FAUNA FROM THE LATE JURASSIC OF THE LUSITANIAN BASIN

8.1. INTRODUCTION

Most of the theropod specimens currently known in the Portuguese Upper Jurassic record come from the coastal region of the Central Sector of the Lusitanian Basin, mainly between Peniche and Torres Vedras (Fig. 8.1.1). Scarce, but scientifically important fossil sites with theropod remains are known at the northern area of the Bombarral-Alcobaça Sub-basin, such as Guimarota (Leiria) and Andrés (Pombal). Theropod material is currently unknown in the Arruda Sub-basin and only few occurrences are known in the Turcifal Sub-basin. However, this higher incidence of findings along the coastline may in part be a sampling bias due to more prospection in these areas.

Among the theropod taxa known in this record, *Ceratosaurus* is currently restricted to a single site in the coastal region of the Consolação Sub-basin. The specimens were found in sediments corresponding to deposits of a distal fluvial meander system belonging to the Praia da Amoreira-Porto Novo Formation (Mateus et al. 2006; Malafaia et al. 2015). However, some isolated teeth attributed to ceratosaurian theropods indicate a geographically and stratigraphically broader distribution of this taxa spanning from the late Kimmeridgian to the Tithonian (Malafaia et al. 2017a). *Torvosaurus* is known in the Consolação and Bombarral-Alcobaça Sub-basin from fluvial and transitional (deltaic) deposits of the Praia da Amoreira-Porto Novo and Sobral formations respectively (Mateus et al. 2006; Hendrickx and Mateus 2014b; Malafaia et al. 2017b). Stratigraphically, this taxon span from the upper Kimmeridgian to the lower Tithonian. *Lourinhanosaurus* is currently restricted to the Kimmeridgian–Tithonian Sobral Formation (Mateus 1998).

The holotype of *Allosaurus europaeus* was found in some isolated blocks in the Praia de Vale Frades and the original horizon of the type locality was interpreted as belonging to the Porto Novo Member of the Lourinhã Formation (Mateus et al. 2006). Later, Mateus et al. (2013) considered this species as part of the dinosaur fauna of the Praia Azul/Sobral Member. The sedimentary sequence in Praia de Vale Frades corresponds mainly to the Bombarral Formation (equivalent to the Santa Rita Member of the Lourinhã Formation sensu Hill 1988), which overlaps the Sobral Formation (Fig. 8.1.1). Therefore, the provenance of this specimen should be the Sobral Formation as was mentioned by Mateus et al (2013), or even the Bombarral Formation, but not the Porto Novo Member. *Allosaurus* is currently the best represented Portuguese theropod taxa and it shows a geographical and stratigraphic wide distribution spaning from the Kimmeridgian to the late Tithonian (Pérez-Moreno et al. 1999; Rauhut and Fechner 2005; Mateus et al. 2006). This taxon is known from the Praia de Vale Frades in the Consolação Sub-basin and is also well represented in the northern sector of the Bombarral-Alcobaça Sub-basin, in the Guimarota and Andrés fossil sites corresponding to the Alcobaça and Bombarral formations, respectively.

Coelurosaurian theropods are represented mostly by isolated teeth assigned to indeterminate tyrannosauroids, *Richardoestesia* and indeterminate dromaeosaurids (Hendrickx and Mateus 2014b; Malafaia et al. 2017a). Most of these specimens were collected in the coastline of the Lusitanian Basin between Lourinhã and Torres Vedras in sediments of the Praia da Amoreira-Porto Novo Formation. The only coelurosaurian taxa currently known in the Upper Jurassic of the Lusitanian Basin is the small tyrannosauroid *Aviatyrannis* found in Guimarota (Rauhut 2003). In this upper Kimmeridgian fossil site, a great diversity of small theropods was also described based on isolated teeth, including specimens tentatively assigned to *Compsognathus*, velociraptorine dromaeosaurids, *Dromaeosaurus*, *Paronychodon*, *Richardoestesia*, troodontids, and tyrannosaurids (Zinke 1998).

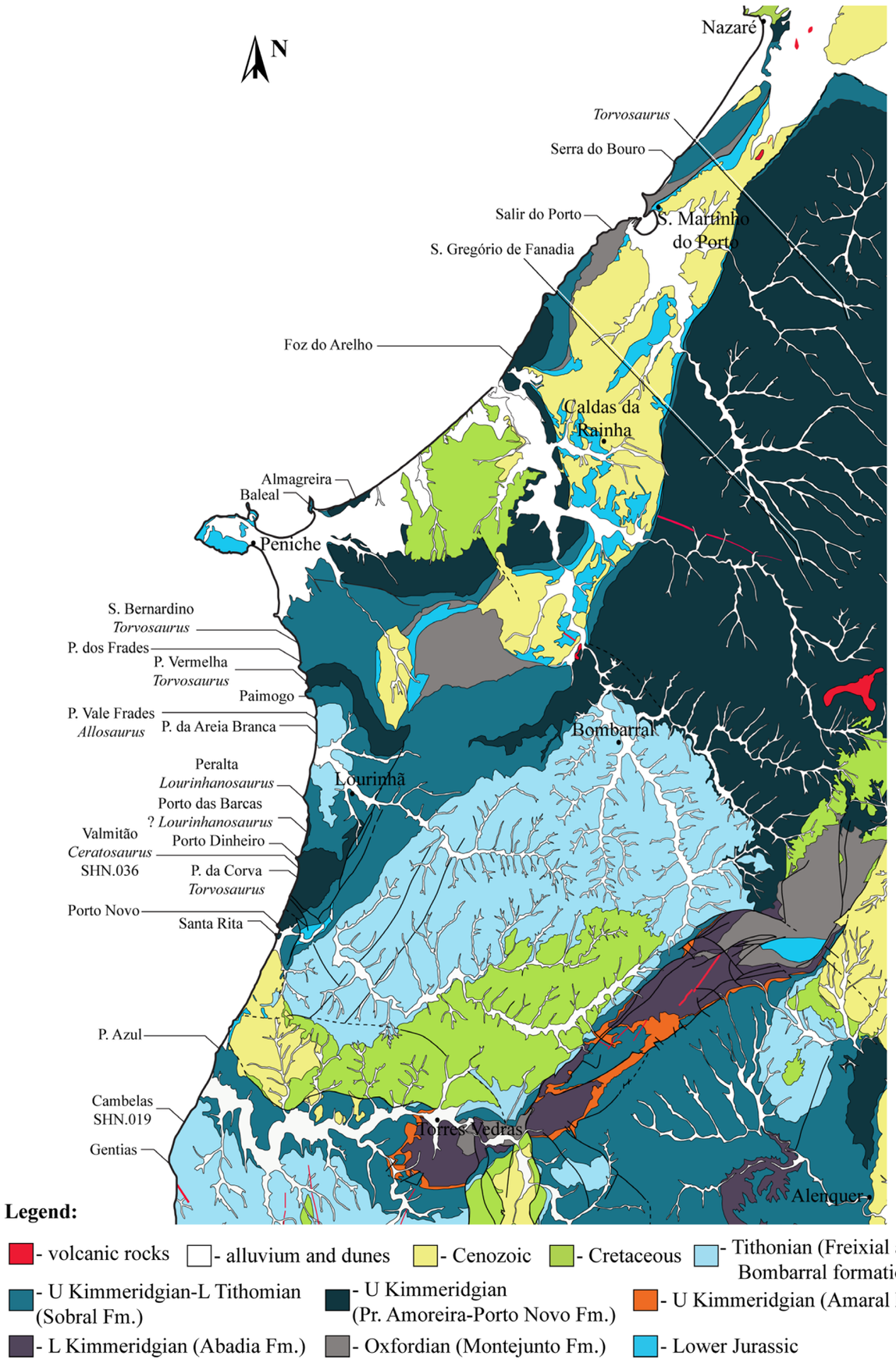

Figure 8.1.1. Geological map of the coastal sector between Nazaré and Torres Vedras showing the localities with theropod specimens (adapted from Matos 1954; Zbyszewski and Matos 1959; Oertel et al. 1960; Camarate França et al. 1962; Manuppella et al. 1996; Zbyszeweski et al. 1965). Legend: U- Upper; L, Lower; Fm, Formation.

REFERENCES

Camarate França J, Zbyszewski G, Veiga Ferreira O. 1954. Carta geológica de Portugal na escala de 1/50000. Folha 30-D, Alenquer. Serviços Geológicos de Portugal.

Hendrickx C, Mateus O. 2014a. *Torvosaurus gurneyi* n. sp., the largest terrestrial predator from Europe, and a proposed terminology of the maxilla anatomy in nonavian theropods. PLoS ONE 9(3):e88905. doi.org/10.1371/journal.pone.0088905.

Hendrickx C, Mateus O. 2014b. Abelisauridae (Dinosauria: Theropoda) from the Late Jurassic of Portugal and dentition-based phylogeny as a contribution for the identification of isolated theropod teeth. Zootaxa 3759(1):1–74.

Hill G. 1988. The sedimentology and lithostratigraphy of the Upper Jurassic Lourinhã Formation, Lusitanian Basin, Portugal. [Ph.D. dissertation] Open University, London.

Malafaia E, Ortega F, Escaso F, Silva B. 2015. New evidence of *Ceratosaurus* (Dinosauria: Theropoda) from the Late Jurassic of the Lusitanian Basin, Portugal. Historical Biology 27(7):938–946.

Malafaia E, Escaso F, Mocho P, Serrano-Martínez A, Torices A, Cachão M, Ortega F. 2017a. Analysis of diversity, stratigraphic and geographical distribution of isolated theropod teeth from the Upper Jurassic of the Lusitanian Basin, Portugal. Journal of Iberian Geology. doi:10.1007/s41513-017-0021-7

Malafaia E, Mocho P, Escaso F, Ortega F. 2017b. New data on the anatomy of *Torvosaurus* and other remains of megalosauroid (Dinosauria, Theropoda) from the Upper Jurassic of Portugal. Journal of Iberian Geology 43:33–59.

Manuppella G, Rey J, Ramalho MM, Leinfelder R, Batista R. 1996. Carta geológica de Portugal na escala de 1/50000. Folha 30-A, Lourinhã. Serviços Geológicos de Portugal.

Mateus O, Dinis J, Cunha PP. 2013. Upper Jurassic to Lowermost Cretaceous of the Lusitanian Basin, Portugal - landscapes where dinosaurs walked. Ciências da Terra, número especial VIII.

Mateus O, Walen A, Antunes MT. 2006. The large theropod fauna of the Lourinhã Formation (Portugal) and its similarity to the Morrison Formation, with a description of a new species of *Allosaurus*. In: Foster JR, Lucas SG. (Eds). Paleontology and Geology of the Upper Jurassic Morrison Formation. New Mexico Museum of Natural History and Science, Bulletin 36:123–129.

Matos R. 1954. Carta geológica de Portugal na escala de 1/50000. Folha 30-C, Torres Vedras. Serviços Geológicos de Portugal.

Oertel G, Freire de Andrade C, Zbyszewsli G, Veiga Ferreira O. 1960. Carta geológica de Portugal na escala de 1/50000. Folha 26-C, Peniche. Serviços Geológicos de Portugal.

Pérez-Moreno BP, Chure DJ, Pires C, Marques da Sila C, dos Santos V, Dantas P, Póvoas L, Cachão M, Sanz JL, Galopim de Carvalho AM. 1999. On the presence of *Allosaurus fragilis* (Theropoda: Carnosauria) in the Upper Jurassic of Portugal: first evidence of an intercontinental dinosaur species. Journal of the Geological Society, London 156:449–452.

Rauhut OWM. 2003. A tyrannosauroid dinosaur from the Upper Jurassic of Portugal. Palaeontology 46:903–910.

Rauhut OWM, Fechner R. 2005. Early development of the facial region in a non-avian theropod dinosaur. Proceedings of the Royal Society B: Biological Sciences 272:1179–1183.

Zbyszewski G, de Matos R. 1959. Carta geológica de Portugal na escala de 1/50000. Folha 26-D, Caldas da Rainha. Serviços Geológicos de Portugal.

Zbyszewski G, Camarate França J, Veiga Ferreira O, Manuppella G. 1959. Carta geológica de Portugal na escala de 1/50000. Folha 30-B, Bombarral. Serviços Geológicos de Portugal.

Zinke J. 1998. Small theropod teeth from the Upper Jurassic coal mine of Guimarota (Portugal). Palaontologische Zeitschrift 72:179–189.

8.2. ANALYSIS OF DIVERSITY, STRATIGRAPHIC AND GEOGRAPHICAL DISTRIBUTION OF ISOLATED THEROPOD TEETH FROM THE UPPER JURASSIC OF THE LUSITANIAN BASIN, PORTUGAL

Reference: Malafaia E, Escaso F, Mocho P, Serrano-Martínez A, Torices A, Cachão M, Ortega F. 2017a. Analysis of diversity, stratigraphic and geographical distribution of isolated theropod teeth from the Upper Jurassic of the Lusitanian Basin, Portugal. Journal of Iberian Geology. doi:10.1007/s41513-017-0021-7

RESUMO

Dentes isolados de terópodes são abundantes no registo fóssil do Jurássico Superior da Bacia Lusitânica e são uma fonte importante de informação para o conhecimento da diversidade destes dinossáurios, bem como da sua distribuição geográfica e estratigráfica. Contudo, a identificação de dentes isolados é complexa, sobretudo quando se trata de morfótipos relacionados com grupos escassamente representados. Neste trabalho, é descrita e analisada uma colecção de dentes isolados de terópodes, provenientes de diferentes localidades do Jurássico Superior da Bacia Lusitânica, representando um intervalo de tempo entre o Kimmeridgiano superior e o final do Tithoniano. Os exemplares foram agrupados em dezassete morfótipos, com base em dados morfológicos e em análise estatística multivariante. Esta análise indica a presença de diversos grupos de terópodes, como por exemplo *Ceratosaurus*, *Torvosaurus* e *Allosaurus*, para além de outros morfótipos atribuídos a formas indeterminadas de Megalosauroidea e de Allosauroidea e morfótipos identificados, preliminarmente, como pertencendo a Tyrannosauroidea, Dromaeosauridae e *Richardoestesia*. Esta composição faunística, sobretudo a presença de megalossauroides não-megalossaurídeos, possivelmente relacionados ao género de piatnitzkyssaurídeo *Marshosaurus*, indica uma maior diversidade de terópodes no Jurássico Superior da Bacia Lusitânica do que a conhecida anteriormente com base em exemplares mais completos. Os resultados obtidos nesta análise são parcialmente congruentes com estudos anteriores de outras colecções com dentes isolados de terópodes do Jurássico Superior português, como por exemplo as da mina da Guimarota. Contudo, a presença de dromaeossaurídeos velociraptorinos, compsognathídeos e troodontídeos, referida nesta jazida, não foi possível confirmar com base na amostra aqui analisada. Este estudo indica também uma grande semelhança entre as faunas de terópodes do Jurássico Superior da Bacia Lusitânica e de outras localidades correlativas europeias, em Espanha e Alemanha.

Palavras-chave: Análise multivariante, Ceratosauria, Megalosauroidea, Allosauroidea, Coelurosauria.

J Iber Geol
DOI 10.1007/s41513-017-0021-7

RESEARCH ARTICLE

Analysis of diversity, stratigraphic and geographical distribution of isolated theropod teeth from the Upper Jurassic of the Lusitanian Basin, Portugal

Elisabete Malafaia[1,2,3] · Fernando Escaso[2,4] · Pedro Mocho[2,4,5] · Alejandro Serrano-Martínez[4] · Angelica Torices[6] · Mário Cachão[1] · Francisco Ortega[2,4]

Received: 27 November 2016 / Accepted: 6 June 2017

Abstract
Purpose Isolated theropod teeth are abundant in the Upper Jurassic of the Lusitanian Basin and are an important source to reconstruct the diversity of this group as well as its geographic and stratigraphic distribution. However, reliably identification of isolated teeth is complex, especially for those morphotypes related to poorly represented groups. Herein a set of isolated theropod teeth collected in different sites from the Upper Jurassic of the Lusitanian Basin ranging from the late Kimmeridgian to late Tithonian in age are described and discussed.
Methods These teeth were grouped in seventeen distinct morphotypes based first on morphology and comparative anatomy. Multivariate statistical analyses were performed in order to assign each morphotype to a certain taxon.
Results The current analysis shows the presence of several groups of theropods such as *Ceratosaurus, Torvosaurus,* and *Allosaurus* beside morphotypes identified as belonging to indeterminate Megalosauroidea and Allosauroidea and morphotypes tentatively assigned to Tyrannosauroidea, Dromaeosauridae, and *Richardoestesia*. This faunal composition, namely the presence of a non-megalosaurid megalosauroid possibly related to the piatnitzkysaurid *Marshosaurus*, indicates a higher diversity of theropods in the Late Jurassic of the Lusitanian Basin than previously known, based on more complete specimens. Results obtained from this analysis partially agree with previous studies of other collections with isolated theropod teeth from the Upper Jurassic of Portugal such as those of the Guimarota coal mine. However, the presence of velociraptorine dromaeosaurids, compsognathids, and troodontids reported from this site could not be confirmed in the sample herein analyzed. This analysis also indicates a great similarity of the theropod faunas from the Late Jurassic of the Lusitanian Basin and other European chronocorrelative localities such as those from Spain and Germany.

Electronic supplementary material The online version of this article (doi:10.1007/s41513-017-0021-7) contains supplementary material, which is available to authorized users.

✉ Elisabete Malafaia
emalafaia@gmail.com

Fernando Escaso
fescaso@ccia.uned.es

Pedro Mocho
pmocho@nhm.org

Alejandro Serrano-Martínez
paleo.asm@gmail.com

Angelica Torices
angelica.torices@unirioja.es

Mário Cachão
mcachao@fc.ul.pt

Francisco Ortega
fortega@ccia.uned.es

[1] Faculdade de Ciências and Instituto Dom Luiz, Universidade de Lisboa, Campo Grande, 1749-016 Lisbon, Portugal

[2] Laboratório de Paleontologia e Paleoecologia, Sociedade de História Natural, Apartado 25, 2564-909 Torres Vedras, Portugal

[3] Museu Nacional de História Natural e da Ciência, Universidade de Lisboa, Rua da Escola Politécnica 56/58, 1250-102 Lisbon, Portugal

[4] Grupo de Biología Evolutiva, Universidad Nacional de Educación a Distancia, Madrid, Spain

[5] The Dinosaur Institute, Natural History Museum of Los Angeles County, 900 Exposition Blvd, Los Angeles, CA 90007, USA

[6] Departamento de Ciencias Humanas, Universidad de La Rioja, Luis de Ulloa s/n, 26004 Logroño, La Rioja, Spain

Published online: 14 July 2017

Keywords Multivariate analysis · Ceratosauria · Megalosauroidea · Allosauroidea · Coelurosauria

Resumen

Objetivo Los dientes aislados de dinosaurios terópodos son un registro abundante en el Jurásico Superior de la cuenca lusitánica pudiendo llegar ser una importante contribución para comprender la diversidad y la distribución geográfica y estratigráfica de estas faunas. Sin embargo, la identificación de dientes aislados y su asignación a un determinado taxón es compleja, especialmente en el caso de morfotipos relacionados con grupos poco conocidos en el mismo registro. En este estudio se presenta el resultado del análisis de un conjunto de dientes aislados de terópodos procedentes de diferentes localidades de la cuenca lusitánica datadas en el Jurásico Superior, concretamente entre el Kimmeridgiense superior y el Tithoniense superior.

Métodos Estos dientes se han agrupado en diecisiete morfotipos a partir del estudio morfológicco y de la comparación anatómica. Se realizaron análisis estadístico multivariante para comprobar la identificación de cada morfotipo.

Resultados El resultado de este análisis ha revelado una gran diversidad de grupos de terópodos que incluye *Ceratosaurus*, *Torvosaurus* y *Allosaurus* además de morfotipos identificados como pertenecientes a Megalosauroidea indet. y Allosauroidea indet. Además, se han reconocido también algunos morfotipos preliminarmente asignados a Tyrannosauroidea, Dromaeosauridae y *Richardoestesia*. Esta composición faunística, tal como la presencia de non-megalosauridos megalosauroides posiblemente relacionado al piatnitzkysaurido *Marshosaurus*, sugiere una mayor diversidad de terópodos de la que se conoce actualmente a partir de ejemplares más completos. Los resultados obtenidos soportan, en parte, algunos estudios previos de otras colecciones con dientes aislados del Jurásico Superior de Portugal, como por ejemplo los de la mina de Guimarota. No obstante, la presencia de terópodos velociraptorinos, compsognathidos y troodontidos, citados en Guimarota, no se ha podido confirmar en la muestra estudiada. Este análisis indica también una grande semejanza de las faunas de terópodos del Jurásico Superior de la cuenca lusitánica y de otras localidades sincrónicas europeas como por ejemplo de España y Alemania.

Palabras clave Análisis multivariante · Ceratosauria · Megalosauroidea · Allosauroidea · Coelurosauria

1 Introduction

The Portuguese record of theropod dinosaurs is abundant and diverse, including mainly medium- to large-sized forms belonging to primitive theropods, such as Ceratosauria or basal groups of Tetanurae (e.g. Mateus 1998; Pérez-Moreno et al. 1999; Rauhut and Fechner 2005; Mateus et al. 2006; Hendrickx and Mateus 2014a, b; Malafaia et al. 2015). Small-sized and more derived theropods are so far represented mainly by isolated teeth. These include the primitive tyrannosauroid *Aviatyrannis* from the Guimarota fossil site and several isolated elements, identified as belonging to compsognathids, dromaeosaurids, troodontids, and to taxa with uncertain relationship, such as *Paronychodon* and *Richardoestesia* (Zinke and Rauhut 1994; Zinke 1998; Rauhut 2003; Malafaia et al. 2010; Hendrickx and Mateus 2014b). *Archaeopteryx* is also reported in this record based on a single tooth (Weigert 1995).

Previous studies on Late Jurassic dinosaur faunas from the Lusitanian Basin have referred isolated theropod teeth to a particular genus and/or species (Zinke and Rauhut 1994; Zinke 1998; Hendrickx and Mateus 2014b). Yet some authors have suggested that most isolated theropod teeth are not diagnostic to specific or generic levels, especially when it is not possible to compare them with those associated with diagnostic cranial or postcranial elements collected from equivalent sedimentary levels (e.g. Williamson and Brusatte 2014). However, some recent works proposed that a combination of morphological and statistical analysis may allow assignment of isolated theropod teeth to a higher taxonomic level (Smith et al. 2005; Hendrickx and Mateus 2014b; Hendrickx et al. 2015; Gerke and Wings 2016). The specimens studied here are grouped into morphotypes, which are identified primarily based on morphological features. A multivariate statistical analysis of morphometric data is also used to help the identification of the specimens.

Institutional abbreviations: CPT, Conjunto Paleontológico de Teruel-Dinópolis, Teruel, Spain; ML, Museu da Lourinhã, Lourinhã, Portugal; SHN, Sociedade de História Natural, Torres Vedras, Portugal.

Morphometric abbreviations: AL, apical length; CBL, crown base length; CBR, crown base ratio; CBW, crown base width; CDA, crown distal angle; CH, crown height; CHR, crown height ratio; CMA, crown mesial angle; DC, distocentral denticle density; MC, mesiocentral denticle density; DSDI, denticle size density index.

2 Materials and methods

A total of 118 isolated theropod teeth are described. These specimens were found in different localities where the Upper Jurassic formations of the Lusitanian Basin crop out (see below and Supplementary Data, Table 1S). The specimens were grouped into 17 morphotypes based first

on morphology and comparative anatomy. Also a principal components analysis (PCA) using PAST3 software package (Hammer et al. 2001) was performed to test the individualization of the different morphotypes (Fig. 1). We also performed a cladistic analysis of the morphotypes herein described based on the datamatrix of Hendrickx and Mateus (2014b), but the result obtained when including our sample is a large politomy, which does not help the identification of the studied teeth.

All specimens are deposited in the publicly accessible collections of the Sociedade de História Natural (SHN) in Torres Vedras, Portugal. These specimens derive from surface collection surveys and from paleontological excavations performed by the SHN.

Measurements of the specimens were taken with standard digital calipers (see Supplementary Data, Table 2S). Pictures of the denticles and other morphological observations were taken with a Zeiss Stemi 2000-C binocular microscope. The measurement variables include CBL (crown base length), CBW (crown base width), CH (crown height), AL (apical length), and the number of mesial (MC) and distal (DC) denticles at the crown mid-height. The CBR (crown base ratio = CBW/CBL), CHR (crown height ratio = CH/CBL), CMA (crown mesial angle = ar cos $((CBL^2 + AL^2 - CH^2)/2 \times CBL \times AL)))$ and CDA (crown distal angle = ar cos $((CBL^2 + CH^2 - AL^2)/2 \times CBL \times CH))$ were also calculated, but were not included in the multivariate analysis because they are non-independent variables that would weight those variables. Descriptive terminology follows Hendrickx et al. (2016).

Multivariate statistical analyses were performed in order to assign each morphotype to a certain taxon. A stepwise discriminant function analysis (DFA) using the software IBM SPSS Statistics 17.0 program (SPSS Inc., Chicago, IL, USA) was developed using squared Mahalanobis distances and the covariance matrix for separated groups. Multivariate analyses were performed using the datasets published by Hendrickx et al. (2015) and Gerke and Wings (2016). A first analysis was performed using the complete dataset of Gerke and Wings (2016) (see Supplementary Data, Table 3S). The percentage of correct classified sample obtained was low, with only 54.6–62.6% of cases correctly identified. A reduced analysis, excluding all taxa represented by less than three specimens and that were also incorrectly classified on the first analysis (*Berberosaurus* and *Megalosaurus*) increased the reclassification rate to 80.5%. Because there are some differences in the measurement methodology used for the specimens in the datasets of Gerke and Wings (2016) and Hendrickx et al. (2015) we performed separated analyses based on the two datasets in order to verify results congruence.

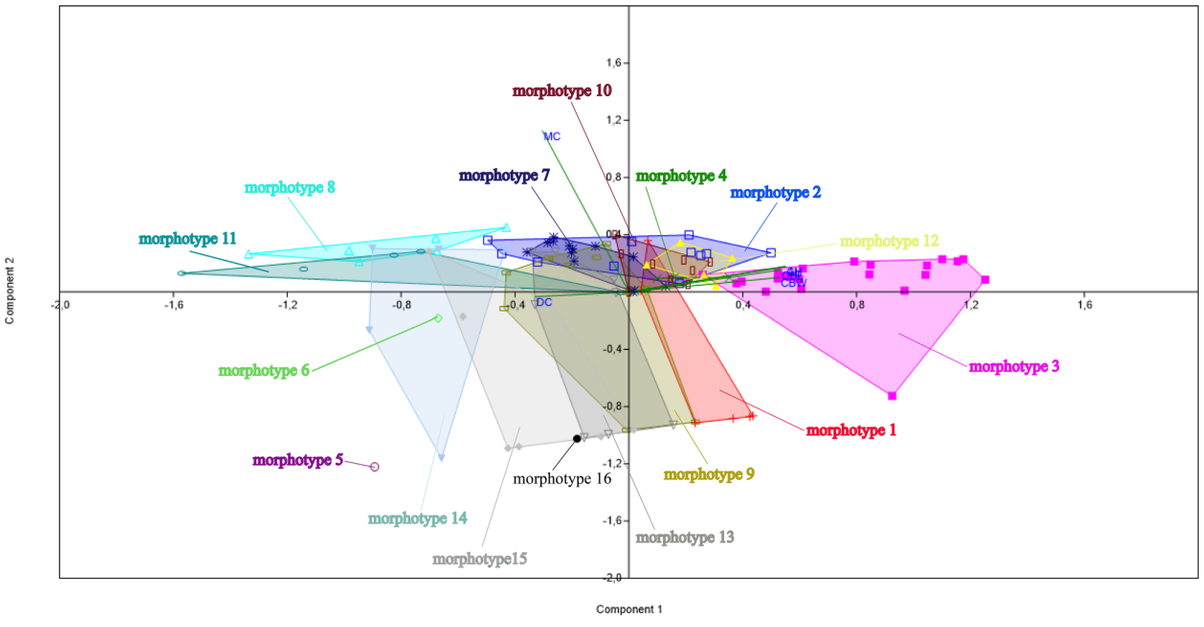

Fig. 1 Plot of loadings from the principal component analysis showing the morphospace occupied by the different morphotypes described here. The specimens are grouping along the first two canonical axes of the principal components (Eigenvalue of axis 1 = 0.294, which accounts for 58.111% of the total variation; Eigenvalue of axis 2 = 0.187, which accounts for 37.138% of the total variation). The variables log-transformed CBL, CBW, CH, AL, MC, and DC were used in the analysis

3 Geological setting

The teeth studied in this work were recovered from different outcrops in the Central Sector of the Lusitanian Basin, mainly in the coastal area of the southern end of the Bombarral Sub-basin (=Consolação Sub-basin sensu Taylor et al. 2014) and in the northern end of the Turcifal Sub-basin (Fig. 2). Most of these specimens were collected in the Praia da Amoreira-Porto Novo Formation (sensu Manuppella et al. 1999), which is interpreted as late Kimmeridgian in age and crops out along most of the littoral region between Torres Vedras and Peniche. This sedimentary sequence consists mainly of sandstone channel bodies intercalated with massive mudstone levels, representing deposits of distal fluvial meander systems (Hill 1989; Mateus et al. 2013; Taylor et al. 2014).

Other specimens come from the upper Kimmeridgian–lower Tithonian Sobral Formation (Praia Azul Member sensu Hill 1988). This unite is mainly composed of marls and mudstones with rare intercalations of sandstone channel bodies (Hill 1989) and is interpreted as representing transitional systems such as deltas, sandy bay shorelines and brackish lagoons (Fürsich 1981; Werner 1986; Mateus et al. 2013; Taylor et al. 2014).

Some teeth collected in the northern part of the Consolação Sub-basin come from sediments of the Bombarral Formation interpreted as Tithonian in age (Manuppella et al. 1999; Schneider et al. 2009). These sediments correspond mostly to micaceous sandstones deposited in meandering fluvial systems, punctuated by marine marls (Rocha et al. 1996; Kullberg et al. 2013).

Finally, in the Arruda Sub-basin, (southern part of the Lusitanian Basin), a few teeth were also collected in Tithonian levels of the Freixial Formation (chronologically equivalent to the Bombarral Formation). The Freixial Formation is composed of thick layers of red mudstones, with abundant levels of well-developed pedogenic carbonate concretions, intercalated with cross-bedded sandstones. These sediments are interpreted as deposits of coastal delta plains and distal fluvial environments (Hill 1988).

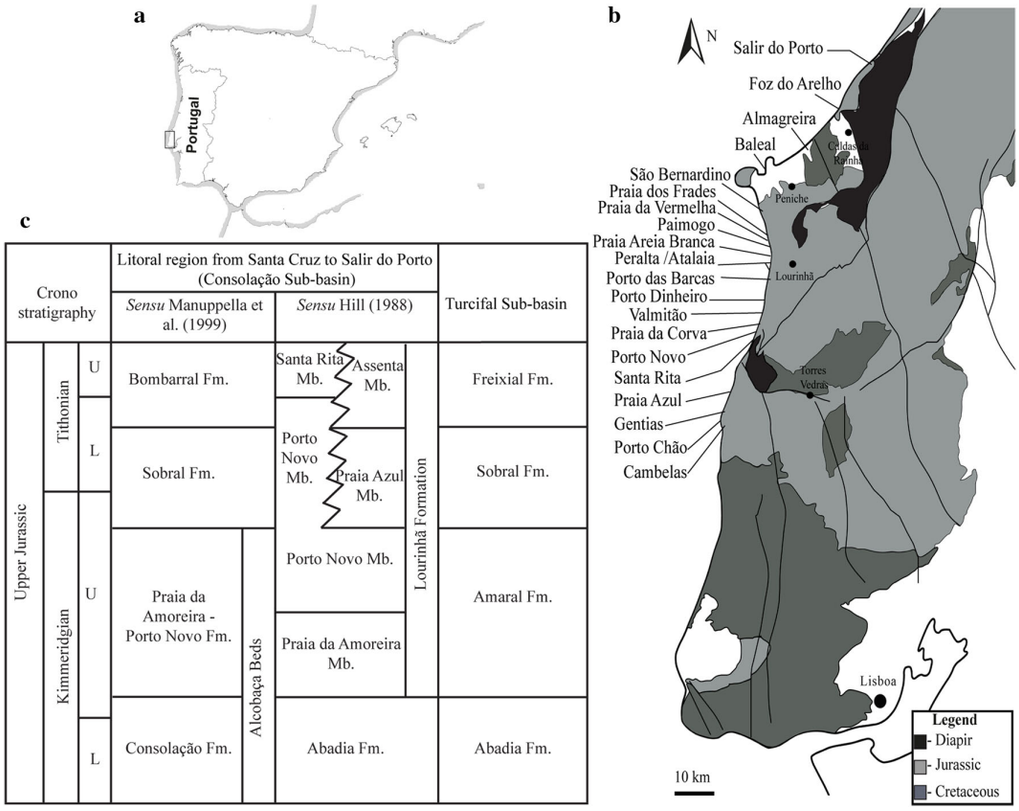

Fig. 2 Geologic and stratigraphic settings of the specimens described; **a** location of the Lusitanian Basin in the Iberian context; **b** simplified geological map of the Central Sector of the Lusitanian Basin (modified from Oliveira et al. 1992) showing the sites where the specimens were collected; **c** chronostratigraphic table for the Upper Jurassic of the Lusitanian Basin showing the correlation between the nomenclatures proposed by different authors (Hill 1988; Manuppella et al. 1999) for the Consolação Sub-basin and the chronostratigraphy for the Turcifal Sub-basin. *L* lower, *U* upper

4 Description, results and discussion of the morphotypes

4.1 Ceratosauria

4.1.1 Morphotype 1

Ceratosauridae
Ceratosaurus sp.

Material: SHN.205, 236, 254, 457, 461, 462 (Fig. 3).

Geographical provenance: Praia da Corva (Torres Vedras), Porto Dinheiro (Lourinhã), and Praia da Vermelha (Peniche).

Stratigraphical distribution: Praia da Amoreira-Porto Novo Formation (upper Kimmeridgian).

Description: This morphotype is represented by six fairly complete tooth crowns, which correspond to moderately large teeth with AL of 31.27–37.58 mm (average 34.79 mm) (see Supplementary Data, Table 2S). The crowns are moderately elongated (CHR: 2.41–3.56; average 2.97) and subcircular in cross-section (CBR: 0.92–1.43; average 1.26). The mesial margins are slightly convex and the distal margins are nearly straight; thus the crowns are subtriangular in lateral view and the apex is centrally positioned.

Transverse undulations are generally absent or slight. Most of these specimens do not have interdenticular sulci except SHN.461 (Fig. 3e), which has very short sulci, perpendicular to the carina, between the distal denticles. The enamel texture is made of a series of thin and irregular crenulations (braided enamel texture) and the crown lingual surface shows well-marked vertical ridges (flutes sensu Hendrickx et al. 2016). Most crowns have 5–6 flutes extending almost the whole crown height. The flutes are restricted to the mid-section of the lingual surface in SHN.205 (Fig. 3a) and only two well-marked flutes are visible in SHN.254 (Fig. 3b). Most of these teeth have rounded mesial margins devoid of a mesial carina except in SHN.205 and 254, which both have a serrated mesial carina extending from the apex down to the crown mid-height or restricted to the apex, respectively. When present, the mesial carina slightly curves toward the lingual surface basally. The distal carina is centrally positioned or slightly displaced labially. Slightly concave vertical surfaces are present on the lingual surface adjacent to the distal carina and a small concave surface is also visible on the labial surface of SHN.205.

Mesial denticles are much smaller than the distal ones, with 19 and 11.5 denticles per 5 mm at the central part of the mesial and distal carinae respectively (DSDI >1.2). The mesial denticles are rounded (Fig. 3a_{VIII}) and the distal denticles are subquadrangular to slightly higher mesiodistally than apicobasally, with symmetrically rounded external margins (e.g. Fig. 3d_{VI}, e_{III}). The distal denticles are closely packed with narrow interdenticular space.

Results and discussion: The DFA analysis assigned two specimens (SHN.236 and SHN.457) to *Torvosaurus* and one specimen (SHN.205) to *Raptorex* and *Erectopus* (see Supplementary Data, Table 4S). However, the general morphology of these specimens, subcircular in cross-section, presence of a large number of small denticles in the distal carinae, absence of mesial carina or restricted to the apical end, and the presence of well-marked vertical flutes in the lingual surface, is also compatible with mesial teeth of *Ceratosaurus* (Gilmore 1920; Madsen and Welles 2000). In particular, the presence of flutes is an unusual character for theropod teeth only known in some juvenile specimens of *Coelophysis* (Buckley 2009), some ceratosaurs (Madsen and Welles 2000; Carrano et al. 2002), *Sinosaurus* (Hendrickx, pers. commun.), spinosaurids (Charig and Milner 1997; Canudo et al. 2008; Serrano-Martínez et al.2015, 2016), *Paronychodon* (Larson 2008; Larson and Currie 2013), some compsognathids, including *Scipionyx* (Dal Sasso and Maganuco 2011), some dromaeosaurids such as *Austroraptor* (Novas et al. 2008a; Williamson and Brusatte 2014; Hendrickx et al. 2015), *Richardoestesia*, and *Zapsalis* (Larson and Currie 2013; Hendrickx, pers. commun.).

Some specimens assigned to *Paronychodon* have well-developed flutes in the lingual surface, but teeth identified to this taxon typically lack denticles, are much smaller and more labiolingually compressed (Larson and Currie 2013) than those of morphotype 1. *Paronychodon*-like teeth from the Cretaceous of Spain (Rauhut 2002) and from the Upper Jurassic and Upper Cretaceous of Portugal (Zinke and Rauhut 1994; Zinke 1998) have serrated distal carinae and in some of them both carinae are serrated, but in these specimens there are well-developed flutes in both lingual and labial surfaces. On the other hand, in some dromaeosaurids such as *Velociraptor*, the flutes are rather rounded ridges on the labial surface (Hendrickx and Mateus 2014b; Hendrickx et al. 2015). Finally, morphotype 1 can be distinguished from the teeth of coelophysoids and compsognathids based in the larger size of the crowns as these taxa possess small crowns (CH <15 mm) and in the much higher number of distal denticles (>30 denticles per 5 mm) (Hendrickx and Mateus 2014a; Hendrickx et al. 2015).

Vertical grooves and ridges on the lingual side of the crowns are present in premaxillary and mesial dentary teeth of *Ceratosaurus* (Madsen and Welles 2000) and in some other ceratosaurs such as *Masiakasaurus* (Carrano et al. 2002). This feature has been traditionally considered

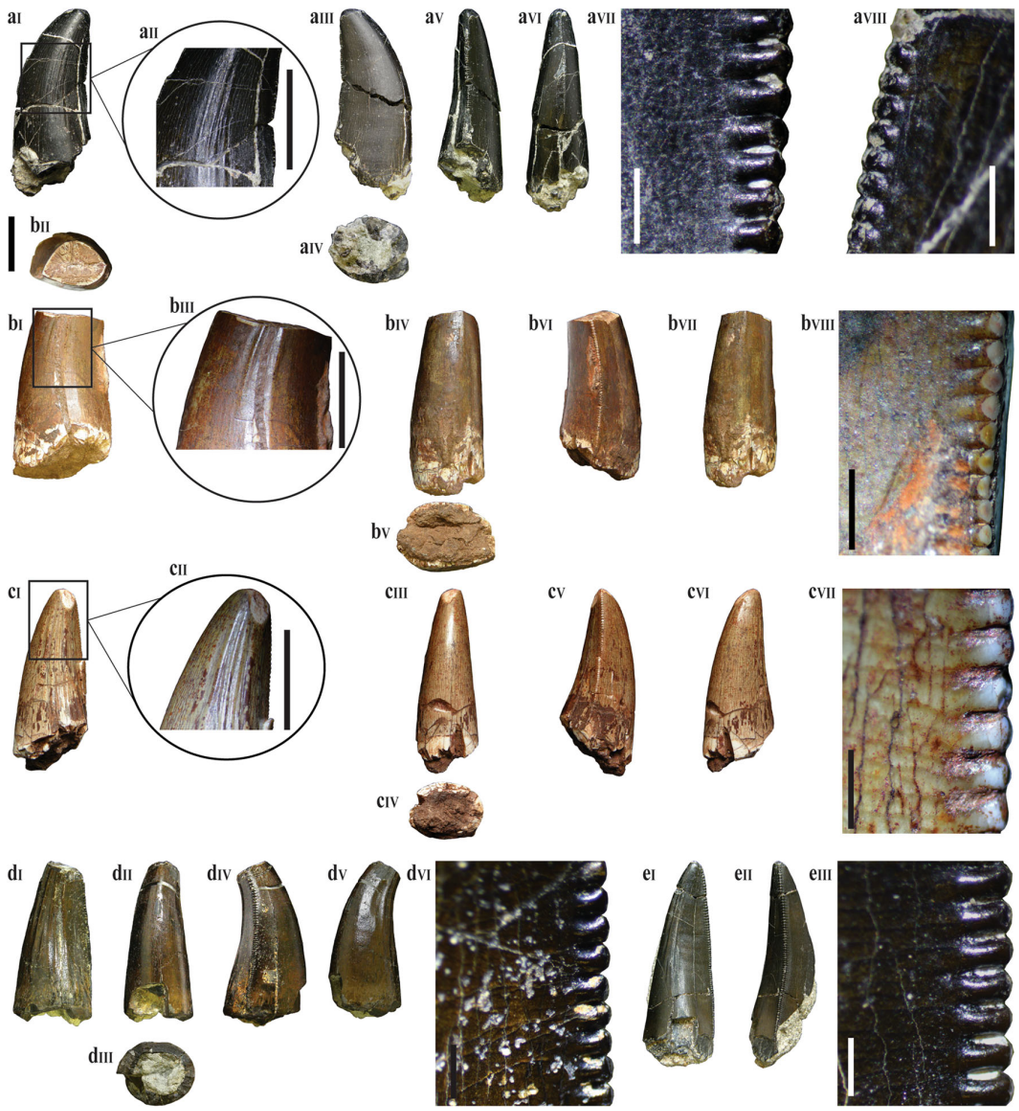

Fig. 3 Morphotype 1: **a** SHN.205; **b** SHN.254; **c** SHN.236; **d** SHN.457; **e** SHN.461 in lingual ($\mathbf{a_I}$, $\mathbf{b_I}$, $\mathbf{c_I}$, $\mathbf{d_I}$, $\mathbf{e_I}$), labial ($\mathbf{a_{III}}$, $\mathbf{b_{IV}}$, $\mathbf{c_{III}}$, $\mathbf{d_{II}}$), distal ($\mathbf{a_{IV}}$, $\mathbf{b_{VI}}$, $\mathbf{c_V}$, $\mathbf{d_{IV}}$, $\mathbf{e_{II}}$), and mesial ($\mathbf{a_{VI}}$, $\mathbf{b_{VII}}$, $\mathbf{c_{VI}}$, $\mathbf{d_V}$) views; detail of the flutes ($\mathbf{a_{II}}$, $\mathbf{b_{III}}$, $\mathbf{c_{II}}$); cross-section at the apical end ($\mathbf{b_{II}}$) and at the crown base ($\mathbf{a_{IV}}$, $\mathbf{b_V}$, $\mathbf{c_{IV}}$, $\mathbf{d_{III}}$); detail of the distal ($\mathbf{a_{VII}}$, $\mathbf{b_{VIII}}$, $\mathbf{c_{VII}}$, $\mathbf{d_{VI}}$, $\mathbf{e_{III}}$) and mesial ($\mathbf{a_{VIII}}$) denticles. *Scale bars* for the crowns: 10 mm; for the denticles: 1 mm

diagnostic for mesial teeth of *Ceratosaurus* and been used for the identification of isolated teeth of this taxon (Meyer and Thuring 2003). Some teeth from Upper Jurassic levels of the Tendaguru Formation, first assigned as *Labrosaurus* (?) *stechowi* by Janensch (1920), were interpreted afterwards as *Ceratosaurus* sp. based on the presence of flutes in the lingual surface (Madsen and Welles 2000; Rauhut 2011). Likewise, a tooth from the Upper Jurassic Virgula beds, near Moutier in Switzerland, first assigned as *Labrosaurus meriani* by Janensch (1920) and as *Megalosaurus meriani* by Huene (1926), was assigned to *Ceratosaurus* sp. by Madsen and Welles (2000) based on this character. This feature is also reported in other ceratosaurs such as *Masiakasaurus* or a specimen from the Late Jurassic–Early Cretaceous of Uruguay (Carrano et al. 2002; Soto and Perea 2008). However, the presence of vertical grooves on the lingual surface of the crown may be a diagnostic feature at least among Upper Jurassic theropods from the Morrison Formation and from the Lusitanian Basin (Hendrickx, pers. commun.).

Flutes are present also, with various degrees of development, in the baryonychines *Baryonyx* (Charig and Milner 1997; Fowler 2007; Buffetaut 2007, 2011; Canudo et al. 2008; Mateus et al. 2011), *Suchomimus* (Sereno et al. 1998), in other spinosaurids such as *Irritator* (Sues et al. 2002) and some specimens of *Spinosaurus* (Bouaziz et al. 1988). The fluted mesial teeth of *Ceratosaurus* show remarkable similarity with baryonychine teeth and based on this similarity it was recently proposed that some teeth originally identified as belonging to *Ceratosaurus* from the Late Jurassic of Tendaguru could not be assigned with confidence to this taxon (Fowler 2007). Later, Buffetaut (2011) reinterpreted two teeth from this African record as belonging to a new species of spinosaurid *Ostafrikasaurus crassiserratus*. However, these teeth show some differences with spinosaurid teeth, such as the number of denticles, suggesting that their identification remains uncertain (Rauhut 2011).

In general, teeth of baryonychines (e.g. *Baryonyx* and *Suchomimus*) differ from those of morphotype 1 in the greater number of denticles (25 denticles per 5 mm) on both mesial and distal carinae (Charig and Milner 1986; Sereno et al. 1998; Mateus et al. 2011). More derived spinosaurids, including *Spinosaurus* (Sereno et al. 1998; Dal Sasso et al. 2005) and *Irritator* (Sues et al. 2002), have teeth with non-serrated carinae. The teeth of spinosaurids have, in general, a larger number of flutes (between 2 to 20; Hendrickx, pers. commun.) and usually in both lingual and labial surfaces (Charig and Milner 1997; Sues et al. 2002; Canudo et al. 2008; Mateus et al. 2011).

Summarizing, morphotype 1 shares with *Ceratosaurus* several features, including: (1) larger size of the denticles (also shared with the putative spinosaurid *Ostafrikasaurus*), (2) lower number of flutes, which are only on the lingual surface, (3) irregular crenulated enamel, which is more similar to ceratosaurs ornamentation than to the veined surface structure (sensu Hendrickx et al. 2016) of most spinosaurids (Sues et al. 2002; Buffetaut 2007; Sereno et al. 1998; Mateus et al. 2011; Serrano-Martínez et al. 2016), and (4) restriction of the mesial carina to the apical part of the crown (also shared with some *Baryonyx* teeth from Spain), whereas in spinosaurids the mesial carina extends to the root (Canudo et al. 2008).

SHN.205 is somewhat distinct from the other specimens included here in morphotype 1 because it has a well-developed and serrated mesial carina, a more oval cross-section of the crown base, and the flutes are restricted to the mid-section of the lingual surface. This tooth has a morphology similar to some teeth from the Tendaguru Formation identified as possibly belonging to *Ceratosaurus* (Madsen and Welles 2000; Rauhut 2011) and may correspond to a more distal position in the tooth row.

Based on the shared morphological characters and on the presence of other *Ceratosaurus* specimens represented by non-dental material in the Upper Jurassic of the Lusitanian Basin (Mateus et al. 2006; Malafaia et al. 2015), morphotype 1 is here identified as mesial teeth of *Ceratosaurus*.

4.1.2 Morphotype 2

Ceratosauridae
cf. Ceratosaurus

Specimens: SHN.212, 218, 263, 269, 305a, 307, 321a–c, 359c, 459 (Fig. 4).

Geographical provenance: Cambelas, Santa Rita, Porto Novo and Praia da Corva (Torres Vedras), Peralta (Lourinhã), Praia da Vermelha and Baleal (Peniche).

Stratigraphical distribution: Praia da Amoreira-Porto Novo Formation (upper Kimmeridgian), ?Sobral Formation (upper Kimmeridgian-lower Tithonian), and Freixial Formation (upper Tithonian).

Description: Large ziphodont teeth with AL between 21.48 and 74.42 mm (average 43.93 mm), CBL between 6.9 and 29.02 mm (average 17.9 mm), and CBW between 5.05 and 13.46 mm (average 8.31 mm). The crowns are quite elongated (CHR between 1.54 and 2.86; average 2.34), blade-shaped and strongly labiolingually-compressed (CBR between 0.32 and 0.5; average 0.41).

These teeth have slight transverse undulations. The interdenticular sulci are absent in most specimens. The enamel is generally smooth, but in some specimens it may show a series of thin irregular crenulations. The crowns have well-developed and serrated mesial and distal carinae that extends to the cervix. They are usually parallel and centrally positioned. However, in some specimens the distal carina slightly twists labially at the base of the crown. The crowns are slightly recurved apically with the mesial margin convex and the distal margin almost straight to slightly concave in lateral view. The basal cross-section is lenticular and in some specimens there is a shallow depression on the lingual surface. The lingual and labial surfaces of most crowns are almost flat or slightly convex.

There is an average of 14 denticles per 5 mm in the central section of both carinae (see Supplementary Data, Table 2S). The mesial denticles are short mesiodistally with rounded to almost flat apices. The distal denticles are subquadrangular in the mid-section of the carina (Fig. 4a_{IX}, b_{VII}, c_{VII}), but become horizontally subrectangular toward the base of the crown (Fig. 4a_{VIII}).

Results and discussion: The DFA based on the reduced dataset of Gerke and Wings (2016) and on the dataset of Hendrickx et al. (2015) recovered three specimens (SHN.263, 269, 305a) as belonging to *Piatnitzkysaurus* and *Erectopus* respectively, one specimen (SHN. 459) as

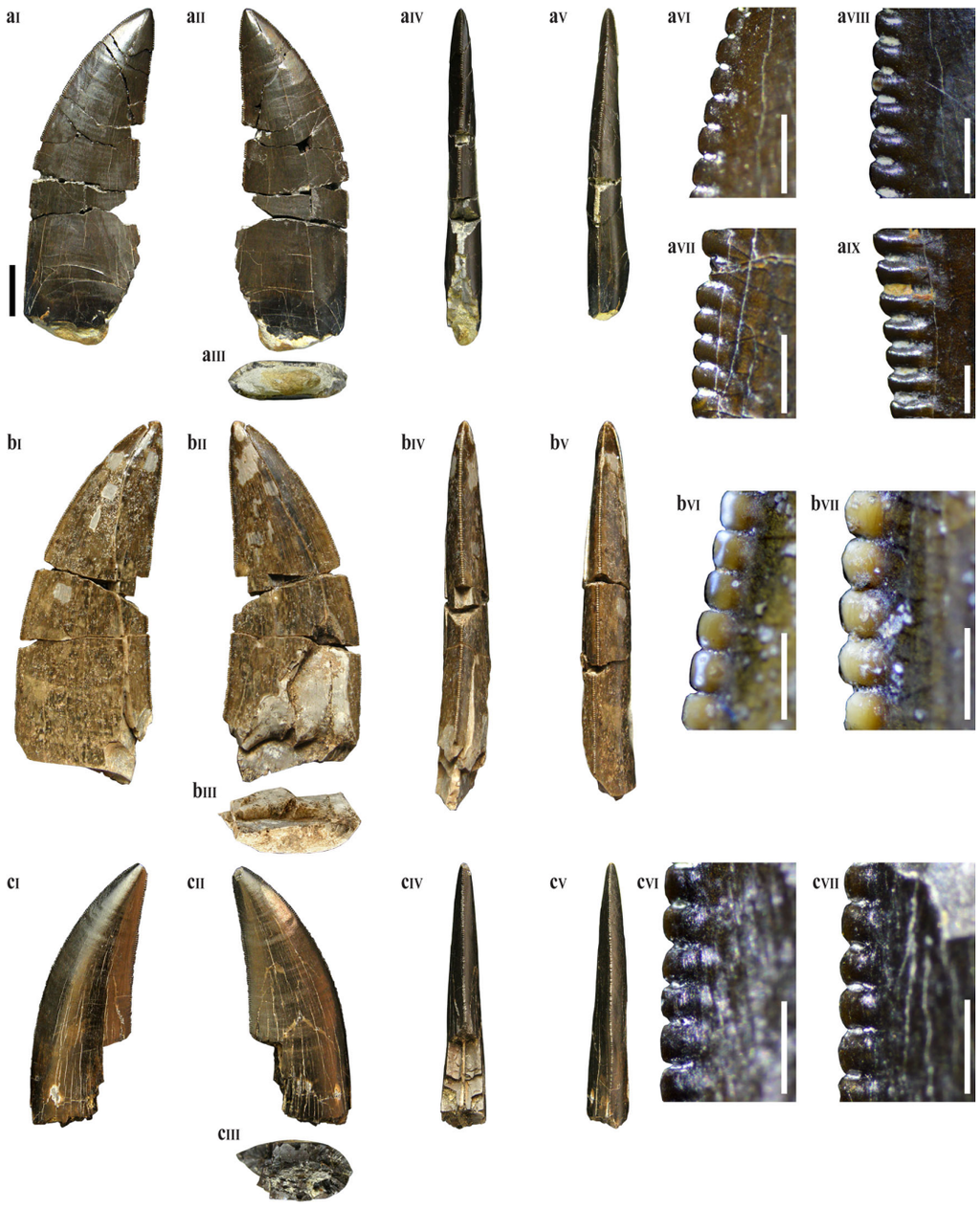

Fig. 4 Morphotype 2: **a** SHN.305a; **b** SHN.263; **c** SHN.269 in lingual ($\mathbf{a_I}$, $\mathbf{b_I}$, $\mathbf{c_I}$), labial ($\mathbf{a_{II}}$, $\mathbf{b_{II}}$, $\mathbf{c_{II}}$), distal ($\mathbf{a_{IV}}$, $\mathbf{b_{IV}}$, $\mathbf{c_{IV}}$), and mesial ($\mathbf{a_V}$, $\mathbf{b_V}$, $\mathbf{c_V}$) views; cross-section at the crown base ($\mathbf{a_{III}}$, $\mathbf{b_{III}}$, $\mathbf{c_{III}}$), detail of the mesial denticles at the apical end ($\mathbf{a_{VI}}$) and at the mid-section ($\mathbf{a_{VII}}$, $\mathbf{b_{VI}}$, $\mathbf{c_{VI}}$) of the crown; detail of the distal denticles at the apical end ($\mathbf{a_{VIII}}$) and at the mid-section ($\mathbf{a_{IX}}$, $\mathbf{b_{VII}}$, $\mathbf{c_{VII}}$) of the crown. *Scale bars* for the crowns: 10 mm; for the denticles: 1 mm

Alioramus and one specimen (SHN.321b) as *Raptorex* and *Neovenator* (see Supplementary Data, Table 4S).

This morphotype shows some unusual features, such as the strongly labiolingually-compressed crowns (in most specimens CBR <0.5), with almost flat lingual and labial surfaces and the presence of mesial carina extending to the cervix. The strongly compressed crowns are similar to those of *Ceratosaurus* (Madsen and Welles 2000; Hendrickx et al. 2015), *Genyodectes* (Rauhut 2004), *Erectopus* (Allain 2005), and some isolated teeth from the Upper

Jurassic of Germany (morphotypes C and D of Gerke and Wings 2016). However, morphotype 2 differs from the lateral teeth of most *Ceratosaurus* and *Genyodectes* in the absence of a concave or flat, vertical surface adjacent to the distal and/or mesial carinae, a character that has been interpreted as a ceratosaurian synapomorphy (Rauhut 2004; Hendrickx et al. 2015). The strongly compressed blade-shaped morphology of morphotype 2 is also shared with two different morphotypes of isolated theropod teeth from the Upper Jurassic of Germany identified as belonging to a possible megalosaurid and as Ceratosauria *incerta sedis* (morphotypes C and D of Gerke and Wings 2016) and with some teeth from the Upper Jurassic of the African Tendaguru Formation identified as possibly belonging to a carcharodontosaurid (Rauhut 2011). The specimens from Germany are interpreted as belonging to a possible ceratosaurian theropod based on the strongly compressed crowns and the mesial carina extending to the cervix (Gerke and Wings 2016). However, these specimens, similarly to morphotype 2, do not have the characteristic concave surface along the mesial and/or distal carinae that is generally present in ceratosaurian teeth (Rauhut 2004).

The numbers of mesial and distal denticles is slightly higher in the teeth of morphotype 2 than in *Ceratosaurus* and other ceratosaurs such as *Majungasaurus*, as well as in *Carcharodontosaurus* (Smith et al. 2005; Hendrickx et al. 2015). The morphology of these specimens from the Lusitanian Basin is similar to the possible metriacanthosaurid *Erectopus* from the Lower Cretaceous of France. They share compressed crowns, both mesial and distal carinae extending to the cervix and the number and shape of denticles (Allain 2005). The general morphology of morphotype 2 is similar to those of lateral teeth of *Ceratosaurus*, sharing with this taxon the following features: (1) strongly labiolingually compressed crowns, (2) mesial carina reaching the cervix, (3) sigmoid mesial carina and centrally positioned distal one, and (4) presence of numerous, closely-packed traverse undulations (Hendrickx et al. 2015). Based on this similarity and despite the absence of a concave surface along the mesial and/or distal carinae, morphotype 2 is here tentatively interpreted as lateral teeth of *Ceratosaurus*.

4.2 Megalosauroidea

4.2.1 Morphotype 3

Megalosauridae
Megalosaurinae
Torvosaurus gurneyi
Specimens: SHN.067, 202, 215, 221, 247, 257, 266, 268, 294, 303–304, 319–320, 362, 364, 374, 381, 401, 440–442, 470 (Fig. 5).

Geographical provenance: Gentias, Santa Rita, and Praia da Corva (Torres Vedras), Valmitão, Porto Dinheiro, and Peralta (Lourinhã), Praia dos Frades, Baleal, and Almagreira (Peniche), Salir do Porto (Caldas da Rainha).

Stratigraphical distribution: Praia da Amoreira-Porto Novo Formation (upper Kimmeridgian), ?Sobral Formation (upper Kimmeridgian-lower Tithonian), and Freixial Formation (upper Tithonian).

Description: Very large ziphodont teeth, with AL between 37.98 and 152.84 mm (average 87.17 mm), CBL between 21.54 and 48.38 mm (average 32.25 mm), and CBW between 12.02 and 23.49 mm (average 16.78 mm). The crowns are very elongated (CHR between 1.45 and 3.01; average 2.46), blade-shaped and moderately labiolingually compressed (CBR between 0.35 and 0.72; average 0.54). The crowns are slightly recurved distally with the distal margin somewhat concave. The mesial margin is convex and the apex is positioned near the level of the base of the distal carina.

Most crowns have well-marked transverse undulations extending across the entire mesiodistal length of both labial and lingual surface, and some of them show additional marginal undulations next to the distal carinae. Interdenticular sulci delimited by well-developed caudae extending obliquely to the carina are also present in most specimens, typically adjacent to the distal carinae (Fig. 5d_I). The enamel has a rough ornamentation due to the presence of thin, sinuous and apicobasally-oriented grooves and ridges (braided texture). The mesial and distal carinae are serrated and centrally positioned at their margins. However, in some specimens the mesial carina is slightly twisted lingually. The mesial carina extends along half or three-quarters of the crown height but in some teeth (SHN.257, 401, 440) it is restricted on the apical part of the crown. On the other hand, the distal carina extends always well below the cervix. Most crowns are lanceolate in cross section (Fig. 5a_V, b_{III}), but some specimens have a reniform section (Fig. 5c_{III}) due the presence of a well-marked concavity at the base of the lingual surface (lingual depression sensu Hendrickx et al. 2015). The lingual and labial surfaces are slightly convex.

There is an average of 7.5 denticles per 5 mm in the central section of the mesial and distal carinae. The mesial denticles are short, with rounded or almost flat apices (Fig. 5b_{VII}, c_{VIII}, d_{VII}) and the distal denticles are subquadrangular, with symmetrically rounded apices (Fig. 5b_{VI}, c_{VII}, d_{VI}) and positioned perpendicularly to the carinae. The denticles are separated by broad interdenticular spaces especially in the mid-section of the distal carina (Fig. 5a_{VIII}), but they are usually more closely packed toward the apex (Fig. 5a_{IX}) and near the base of the crown.

Fig. 5 Morphotype 3: **a** SHN.067; **b** SHN.401; **c** SHN.441; **d** SHN.266; in labial ($\mathbf{a_{IV}}$, $\mathbf{b_{I}}$, $\mathbf{c_{I}}$, $\mathbf{d_{II}}$), lingual ($\mathbf{a_{II}}$, $\mathbf{b_{II}}$, $\mathbf{c_{III}}$, $\mathbf{d_{III}}$), distal ($\mathbf{a_{VI}}$, $\mathbf{b_{IV}}$, $\mathbf{c_{IV}}$, $\mathbf{d_{IV}}$), and mesial ($\mathbf{a_{VII}}$, $\mathbf{b_{V}}$, $\mathbf{c_{V}}$, $\mathbf{d_{V}}$) views; cross-section at the crown base ($\mathbf{a_{V}}$, $\mathbf{b_{III}}$, $\mathbf{c_{III}}$), detail of the distal denticles at the mid-section ($\mathbf{a_{VIII}}$, $\mathbf{b_{V}}$, $\mathbf{c_{VII}}$, $\mathbf{d_{VI}}$) and at the apical part ($\mathbf{c_{VI}}$) of the crown; detail of the mesial denticles ($\mathbf{a_{IX}}$, $\mathbf{b_{VII}}$, $\mathbf{c_{VIII}}$, $\mathbf{d_{VII}}$); detail of the marginal undulations ($\mathbf{a_{I}}$) and of the enamel ornamentation ($\mathbf{a_{III}}$); detail of the interdenticular sulci and caudae ($\mathbf{d_{I}}$). *ce* cervix. *Scale bars* for the crowns: 50 mm; for the denticles: 1 mm; ($\mathbf{a_{I}}$, $\mathbf{a_{III}}$, and $\mathbf{d_{I}}$): 10 mm

Results and discussion: The DFA based on the dataset of Hendrickx et al. (2015) assigns fourteen specimens of morphotype 3 to *Torvosaurus*, one (SHN.362) to *Megalosaurus*, one (SHN.294) to *Ceratosaurus*, and one (SHN.470) to *Erectopus*. The results based on the reduced dataset of Gerke and Wings (2016) is more ambiguous, assigning five specimens to *Torvosaurus* and the other teeth to different taxa including *Carcharodontosaurus*, *Acrocanthosaurus*, and *Tyrannosaurus* (see Supplementary Data, Table 4S). This result probably reflects the similarity in the tooth to the general morphology among most large-sized theropod taxa based on morphometric features (Hendrickx and Mateus 2014b; Hendrickx et al. 2015).

The most distinctive feature of this morphotype is the large size of some crowns, which is comparable with *Torvosaurus* (Britt 1991; Hendrickx et al. 2015), *Tyrannosaurus* (Smith 2005; Brochu 2003) and some carcharodontosaurids such as *Acrocanthosaurus* (Harris 1998; Currie and Carpenter 2000). These teeth are comparable to other specimens previously described in the Upper Jurassic of the Lusitanian Basin and assigned to *Torvosaurus* (Hendrickx and Mateus 2014a, 2014b; Hendrickx et al. 2015). Similarities between the morphotype 3 and lateral teeth of *Torvosaurus* include: (1) moderately labiolingually compressed crowns, (2) centrally-positioned mesial carina that ends at approximately crown mid-height whereas the distal carina terminates well beneath the cervix, and (3) shallow concavity present on the basolingual central part of the crown (Hendrickx and Mateus 2014a, b; Hendrickx et al. 2015). The unusually low denticle density, the presence of well-marked interdenticular sulci and caudae, sometimes in both carinae, and the braided texture of the enamel are other features shared with some megalosaurids, including *Torvosaurus* and *Megalosaurus* (Hendrickx et al. 2015; Hendrickx and Mateus 2014a).

Morphotype 3 also shares some characteristics with some specimens described in the Upper Jurassic of Spain (Suñer et al. 2005; Canudo et al. 2006; Royo-Torres et al. 2009; Cobos et al. 2014; Gascó et al. 2012) and Germany (Gerke and Wings 2016). These similarities may indicate that they probably belong to the same taxon or a closely related form, as was previously suggested.

4.2.2 Morphotype 4

Megalosauridae
Megalosaurinae
cf. Torvosaurus gurneyi
Specimens: SHN.305b, 359a, 456 (Fig. 6).
Geographical provenance: Cambelas and Porto Novo (Torres Vedras), Porto Dinheiro (Lourinhã).

Stratigraphical distribution: Praia da Amoreira-Porto Novo Formation (upper Kimmeridgian) and Freixial Formation (upper Tithonian).

Description: Moderately large, mostly slender and relatively elongated crowns (CHR: 2.4 and CBL: 16.57 mm in average). The general morphology of these specimens is similar to morphotype 3, but the crowns are narrower mesiodistally and the mesial carina extends almost to the cervix and twists lingually at the base. Also the distal carina is displaced labially in morphotype 4 whereas in morphotype 3 this carina is somewhat parabolic in distal view, but is centrally positions on the distal margin.

SHN.359a (Fig. 6b) has several deep transverse and marginal undulations in both labial and lingual surfaces, but these structures are absent in the other specimens. The crowns have braided ornamented enamel (Fig. 6a_{VI}, c_{VIII}), which is more clearly visible in SHN.459a and SHN.456.

The denticles are large, with about 10 denticles per 5 mm in the central section of the mesial and distal carinae. The distal denticles have symmetrical hemicircular apices (Fig. 6b_{VI}, c_{VI}) and are subquadrangular in lateral view in the mid-section of the carina, but are slightly wider mesiodistally than apicobasally close to the base of the crown. The mesial denticles are rectangular, wider apicobasally than mesiodistally and the apices are almost flat (Fig. 6b_{VII}, c_{VII}). The denticles are smaller toward the apex and toward the base in both carinae. The mesial and distal denticles are perpendicular to the carinae along the entire height of the crowns and are separated by narrow interdenticular spaces. Interdenticular sulci and caudae are absent in all specimens.

Results and discussion: The DFA result assigns the specimens of morphotype 4 to *Carcharodontosaurus*, *Majungasaurus*, and *Allosaurus* (see Supplementary Data, Table 4S). However, these specimens are similar to morphotype 3 in several features, such as (1) distal carina that extends well below the cervix, (2) similar density of large denticles on the mesial and distal carinae, (3) well-developed transverse and marginal undulations, and (4) ornamentation of the enamel. Morphotype 4 differs from morphotype 3 in the lingually-displaced mesial carina extending to the cervix.

These specimens are also similar to some isolated teeth from the Upper Jurassic of Germany, interpreted as belonging to an indeterminate megalosaurid (morphotype A of Gerke and Wings 2016) and to some specimens from the Tendaguru Formation of Tanzania tentatively assigned to Carcharodontosauria (Rauhut 2011). Morphotype 4 shares with these German and Tanzanian specimens a mesial carina that reaches the cervix, similar denticles density, quadrangular mesial denticles and the well-developed marginal undulations (Rauhut 2011; Gerke and Wings 2016).

In *Torvosaurus*, it seems that the mesial carinae always ends well above the cervix (Hendrickx and Mateus 2014a; Hendrickx et al. 2015). However, in one isolated tooth from Portugal (ML857: Hendrickx and Mateus 2014b), as well as in some specimens of morphotype 3 described above, the mesial denticles extend for about one fifth of the crown height, suggesting that this feature is somewhat variable for this taxon. The general similarity between morphotype 3 and 4 may suggest that they belong to the same taxon and that these differences could be related with intraspecific variation or with different positions in the tooth row.

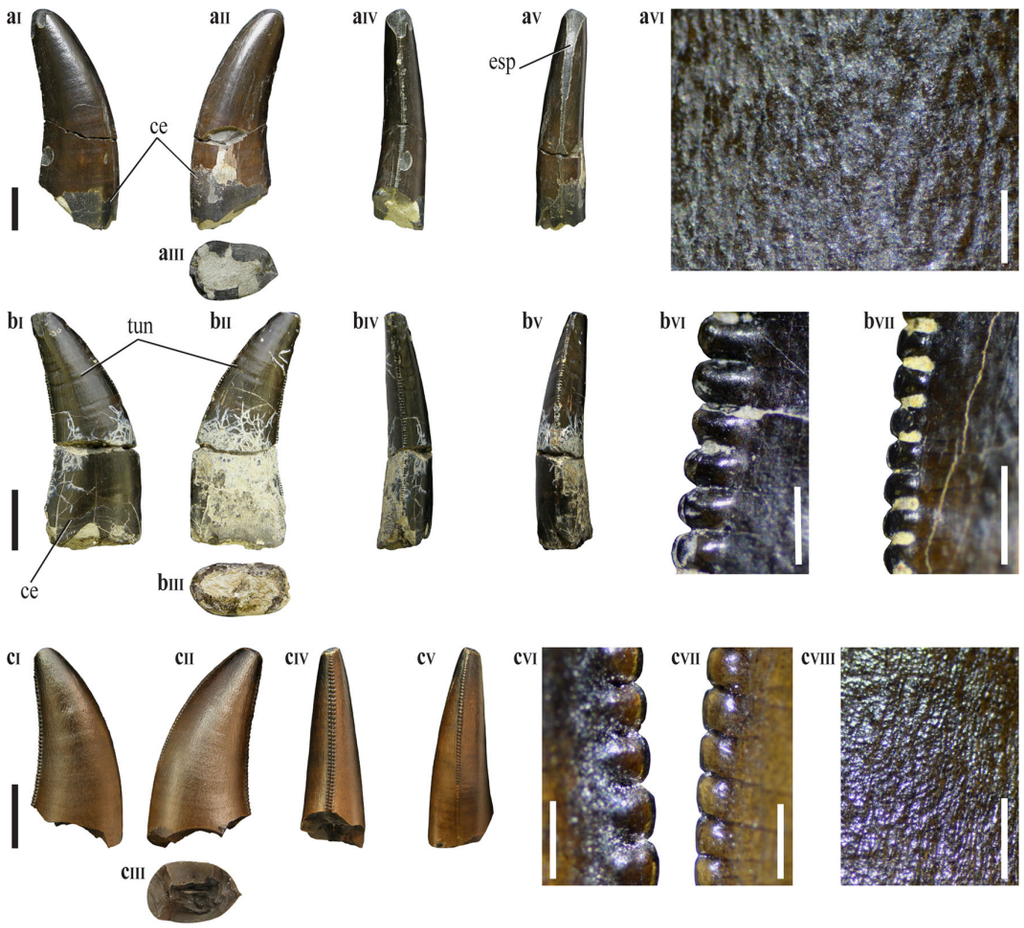

Fig. 6 Morphotype 4: **a** SHN.305b; **b** SHN.359a; **c** SHN.456 in labial ($\mathbf{a_I}$, $\mathbf{b_I}$, $\mathbf{c_I}$), lingual ($\mathbf{a_{II}}$, $\mathbf{b_{II}}$, $\mathbf{c_{II}}$), distal ($\mathbf{a_{IV}}$, $\mathbf{b_{IV}}$, $\mathbf{c_{IV}}$), and mesial ($\mathbf{a_V}$, $\mathbf{b_V}$, $\mathbf{c_V}$) views; cross-section at the crown base ($\mathbf{a_{III}}$, $\mathbf{b_{III}}$, $\mathbf{c_{III}}$); detail of the enamel ornamentation ($\mathbf{a_{VI}}$, $\mathbf{c_{VIII}}$); detail of the distal ($\mathbf{b_{VI}}$, $\mathbf{c_{VI}}$) and mesial ($\mathbf{b_{VII}}$, $\mathbf{c_{VII}}$) denticles. *ce* cervix, *esp* enamel spalling, *tun* transverse undulations. *Scale b*ars for the crowns: 10 mm; for the denticles: 1 mm; ($\mathbf{a_{VI}}$ and $\mathbf{c_{VIII}}$): 10 mm

4.2.3 Morphotype 5

Megalosauridae
Megalosaurinae
cf. Torvosaurus gurneyi
Specimens: SHN.264 (Fig. 7).

Geographical provenance: Valmitão (Torres Vedras).

Stratigraphical distribution: Praia da Amoreira-Porto Novo Formation (upper Kimmeridgian).

Description: This morphotype includes a single specimen corresponding to a complete and well-preserved crown. This specimen is very small, with AL of 7.62 mm, CBL of 4.35 mm, and CBW of 2.26 mm. The crown is very short (CHR: 1.56), slightly compressed labiolingually with an oval cross-section at the base (CBR: 0.52). The crown is strongly recurved apically with the mesial margin strongly convex apically, but almost straight in the basal three-quarters. The distal margin is almost straight. The crown shows a tenuous braided enamel texture and well-developed interdenticular sulci between the distal denticles. Both carinae are serrated with the distal carina extending to the cervix whereas the mesial carina is only restricted to the apical end. The crown is symmetrical, with the mesial and distal carina positioned in the mesial and distal margins, respectively.

There is an average of 5 and 5.5 denticles per mm in the central and centroapical section of the distal and mesial carinae, respectively (DSDI near 1), but denticles are absent in the central section of the mesial carina (see Supplementary Data, Table 2S). The distal denticles are rectangular, slightly higher mesiodistally than apicobasally and with symmetrically circular apices (Fig. 7f). The

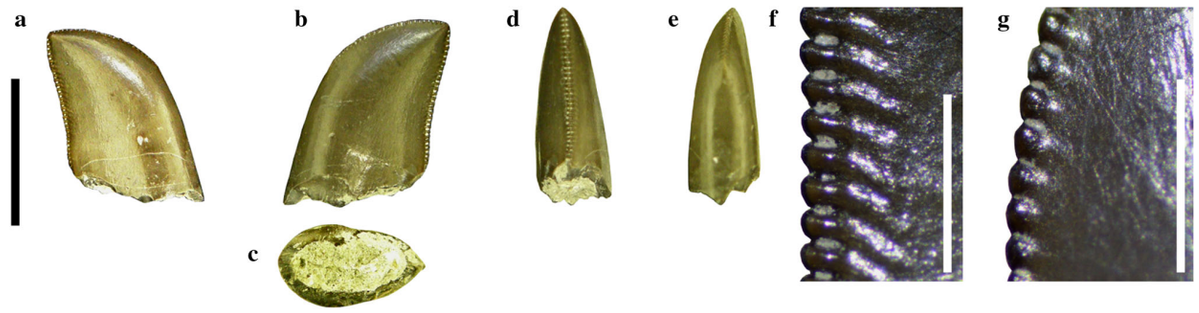

Fig. 7 Morphotype 5: SHN.264 in labial (**a**), lingual (**b**), distal (**d**), and mesial (**e**) views; cross-section at the crown base (**c**); detail of the distal (**f**) and mesial (**g**) denticles. *Scale bars* for the crown: 5 mm; for the denticles: 1 mm

mesial denticles are very low and subquadrangular (Fig. 7g). The distal denticles are smaller near the base and gradually increase in size to the apex. In the mid-section of the distal carina, the denticles are separated by broad interdenticular spaces, which are more than one third of the apicobasal width of the denticle (Fig. 7f).

Results and discussion: The DFA based on the reduced dataset of Gerke and Wings (2016) classifies the specimen SHN.264 to *Torvosaurus* whereas the result based on the dataset of Hendrickx et al. (2015) assigned this tooth as *Neovenator* (see Supplementary Data, Table 4S). This specimen shares with some dromaeosaurids such as *Velociraptor* and *Bambiraptor* a subequal number of denticles in the mesial (apically) and distal (at mid-crown) carinae and the broad interdenticular space between mid-crown denticles on the distal carina (Godefroit et al. 2008; Hendrickx et al. 2014b). The general morphology of the crown is similar to some lateral teeth of *Compsognathus* in the relatively straightness of the base and the strongly backward curvature of the tip (Peyer 2006). Other isolated theropod teeth tentatively assigned to *Compsognathus* were described in the Upper Jurassic of the Lusitanian Basin (Zinke 1998). The specimen described here shares morphology with some of these isolated teeth from the Guimarota fossil site, especially with a morphotype interpreted as belonging to the anterior part of the tooth row, the strongly recurved apical end of the crown. However, these specimens from Guimarota differ from SHN.264 in several aspects, including the absence of denticles on the mesial carina or on both mesial and distal carinae in some teeth and the presence of a small constriction between the crown and the root (Zinke 1998). In some *Compsognathus* specimens, the teeth are confluent between the crown and the root and not constricted as occur in morphotype 5, but mesial denticles are not present in mesial or lateral teeth (Zinke 1998; Peyer 2006). However, compsognathid teeth like those of *Compsognathus* (Peyer 2006), *Scipionyx* (Dal Sasso and Maganuco 2011), *Juravenator* (Göhlich and Chiappe 2006), and *Sinosauropteryx* (Currie and Chen 2001) are typically very elongated, with few relatively large denticles. Beside, most compsognathid teeth, with the exception of *Juravenator*, have an unserrated mesial carina and interdenticular sulci are generally absent. The low crown of SHN.264 suggests that this tooth probably comes from the distalmost part of the jaw. The denticle size and shape, the presence of interdenticular sulci and the braided enamel texture are similar to those of *Torvosaurus*. Based on these shared features and the results of the DFA analysis, morphotype 5 is here tentatively identified as belonging to a juvenile *Torvosaurus*.

4.2.4 Morphotype 6

Megalosauroidea
Specimens: SHN.446, 450 (Fig. 8).
Geographical provenance: Santa Rita (TorresVedras) and Peralta (Lourinhã).

Stratigraphical distribution: Praia da Amoreira-Porto Novo Formation (upper Kimmeridgian), ?Sobral Formation (upper Kimmeridgian-lower Tithonian).

Description: This morphotype includes two specimens, but SHN.450 is incomplete lacking the apical part. SHN.446 is a complete, moderately large-sized crown with AL of 14.63 mm, CBL 6.2 mm, and CBW 3.57 mm (see Supplementary Data, Table 2S). This specimen has a slender, elongated (CHR: 2.26) crown in lateral view. The crown is slightly recurved distally with the distal margin concave, the mesial margin is convex, and the apex is positioned distally to the base of the distal carina. The crown cross-section is oval, slightly labiolingually compressed (CBR: 0.57), with the labial surface convex and the lingual surface flat. The mesial and distal carinae are serrated with the distal carina extending slightly below the cervix and the mesial carina ending approximately at mid-height. The mesial carina is placed in the mesial margin, but the distal carina is displaced labially and is strongly sigmoidal in distal view. The enamel is smooth without transverse

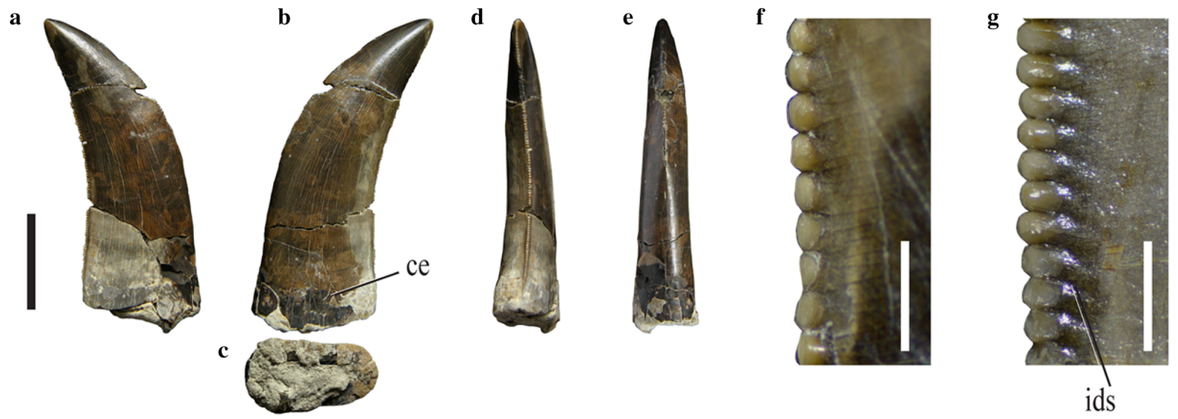

Fig. 8 Morphotype 6: SHN.446 in lingual (**a**), labial (**b**), distal (**d**), and mesial (**e**) views, cross-section at the crown base (**c**), detail of the mesial (**f**) and distal (**g**) denticles. *ce* cervix, *ids* interdenticular sulci. *Scale bars* for the crowns: 10 mm; for the denticles: 1 mm

undulations. However, short interdenticular sulci are present between the denticles, but only at mid-section of the distal carina (Fig. 8g). The distal carina has 20 denticles per 5 mm in the central section; the mesial denticles are poorly preserved so it is not possible quantify their density.

Results and discussion: The DFA excluding the variable MC, since the poor preservation of the mesial carina does not allow the determination of the number of denticles, assigns SHN.446 and SHN.450 as *Deinonychus*, *Majungasaurus*, and *Dromaeosaurus* (see Supplementary Data, Table 4S). This morphotype has a general morphology similar to morphotype 4, namely in the slender and elongated shape of the crown, in lateral view. However, SHN.446 differs from morphotype 4 in several aspects, including the higher number of denticles, the presence of interdenticular sulci, and absence of ornamentation of the enamel. This specimen has a general morphology similar to lateral teeth of *Megalosaurus* (Benson 2010) and some isolated teeth from the Upper Jurassic of Germany tentatively assigned to the piatnitzkysaurid *Marshosaurus* (morphotype J of Gerke and Wings 2016). These specimens share the slender, elongation of the crown and similar serration density in the distal carinae (Hendrickx et al. 2015; Gerke and Wings 2016). However, SHN.446 differs from the German morphotype in being slightly larger and less labiolingually compressed. A PCA performed upon the set of teeth belonging to *Megalosaurus*, *Torvosaurus*, some isolated teeth from the Upper Jurassic of Spain and Germany and the specimens of morphotypes 3, 4, 5, and 6 described here show that the specimens of morphotype 4 fall outside the morphospace occupied by morphotype 3, herein interpreted as belonging to *Torvosaurus* and within the morphospace occupied by *Megalosaurus* (Fig. 9). There is an almost complete overlap of the morphospaces of morphotype 3, *Torvosaurus*, the morphotype A from Germany and some isolated megalosauroid teeth from Spain. The specimen SHN.450 is placed within the morphospace of *Megalosaurus*, but SHN.446 falls outside the morphospace of all represented taxa. Based on these results and on the general similarity with *Megalosaurus* and especially with some isolated teeth from Germany, morphotype 6 is here assigned to an indeterminate megalosauroid.

4.2.5 Morphotype 7

Megalosauroidea

Specimens: SHN.226a–b, 239, 318, 321d, 330, 444–445, 448, 451–453, 464 (Fig. 10).

Geographical provenance: Praia da Corva and Porto Novo (Torres Vedras), Valmitão, Atalaia, Peralta, and Paimogo (Lourinhã), Almagreira (Peniche).

Stratigraphical distribution: Praia da Amoreira-Porto Novo Formation (upper Kimmeridgian), Sobral Formation (upper Kimmeridgian-lower Tithonian).

Description: Teeth of medium to small sizes (AL average: 31.35 mm; CBL average: 12.86 mm and CBW average: 6.55 mm). The crowns are relatively elongated (CHR average: 2.18) and strongly compressed labiolingually (CBR average: 0.51). These specimens have slightly recurved crowns in which the distal margin is slightly concave, the mesial margin is strongly convex and the apex is positioned slightly distal to the base of the distal carina.

Slight transverse undulations on the crown are present in several specimens. Well-marked, diagonal interdenticular sulci are present in most teeth (Fig. 10c_{VI}, d_{VI}). They are more developed between distal denticles, but in some specimens also present in the mesial carina. The enamel is mostly smooth or shows ornamentation consisting on a

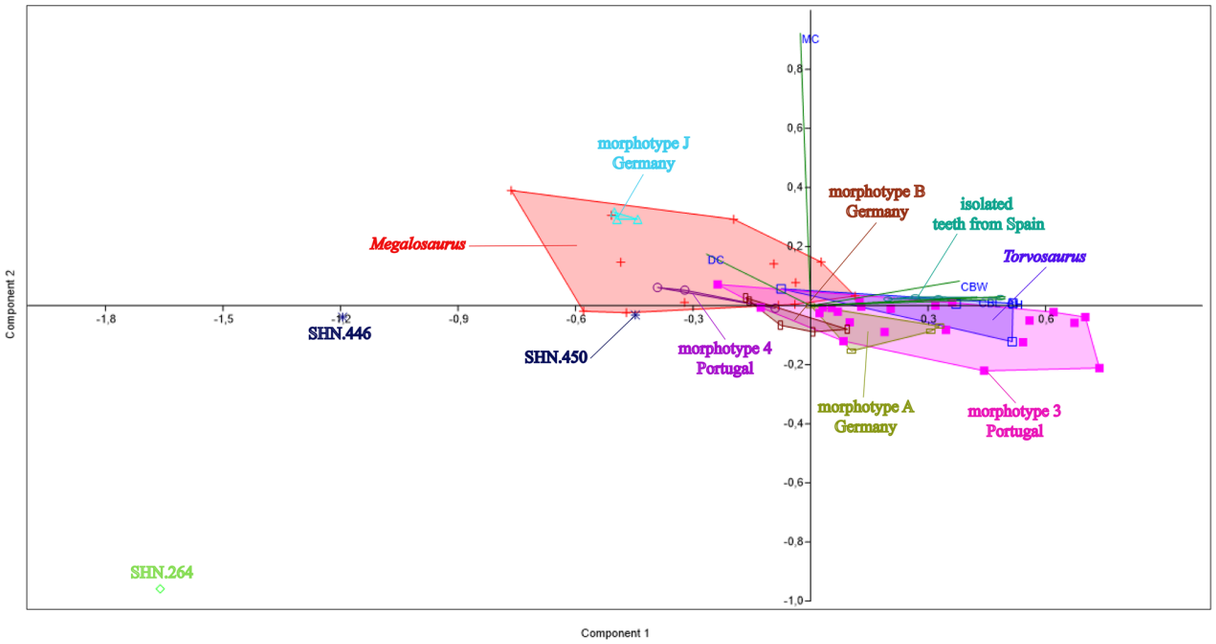

Fig. 9 Plot of loadings from the principal component analysis of a set of teeth belonging to *Megalosaurus*, *Torvosaurus*, the morphotypes 3, 4, 5, and 6 described here, and some isolated teeth from the Upper Jurassic of Spain and Germany (morphotype *A, B* and *J*). The specimens are grouping along the first two canonical axes of the principal components (Eigenvalue of axis 1 = 0.196, which accounts for 82.69% of the total variation; Eigenvalue of axis 2 = 0.030, which accounts for 12.858% of the total variation). The variables CBL, CBW, CH, AL, MC, and DC log-transformed were used in the analysis

series of very thin and irregular crenulations only visible with binocular microscope. The mesial and distal carinae are serrated, with the mesial carina usually extending approximately until the crown mid-height or being restricted to the apical end. The mesial carina is centrally positioned, but the distal carina shows a marked labial displacement. The lingual surface is usually flat or slightly convex and the labial surface is convex. In distal view, the distal margin slightly curves lingually forming a slight concavity at the base of the lingual surface. The cross-section of the crown base is elliptical or lenticular.

The number of denticles is much higher in the mesial than in the distal carina (DSDI equal or higher than 1.2). There is an average of 19.5 and 15.7 denticles per 5 mm in the mid-section of the mesial and distal carinae respectively. The interdenticular space is narrow in both carinae. The mesial denticles are usually vertical rectangular and with rounded or flat apices whereas the distal denticles are horizontal rectangular and have slightly asymmetrical rounded apices.

Results and discussion: The results of DFA for morphotype 7 is ambiguous with the specimens assigned to different theropod taxa including *Allosaurus*, *Raptorex*, *Piatnitzkysaurus*, *Megalosaurus*, *Erectopus*, and *Alioramus* (see Supplementary Data, Table 4S).

The specimens grouped here in morphotype 7 are similar to those of morphotype 6 except in the more slender and elongated crown in morphotype 6. The general morphology of morphotype 7 is similar to those of some anteriormost lateral teeth of *Allosaurus*, but differs from this taxon in the more labiolingually compressed crowns (CBR average = 0.51), the mesial carina restricted to the apical part of the crown, whereas in *Allosaurus* the mesial carinae usually extend close to the cervix, and a higher number of mesial than distal denticles (DSDI equal or higher than 1.2) (Hendrickx et al. 2015). The combination of features of morphotype 7 is compatible with megalosauroid lateral teeth. In particular, the mesial denticles that are slightly smaller than the distal ones and the slender, elongated crown are shared with *Marshosaurus* (Madsen 1976; Hendrickx et al. 2015; Gerke and Wings 2016). Based on this combination of features and the similarity with some isolated teeth from the Upper Jurassic of Germany (morphotype J of Gerke and Wings, 2016), morphotype 7 is here assigned as belonging to an indeterminate megalosauroid taxa tentatively related to *Marshosaurus*.

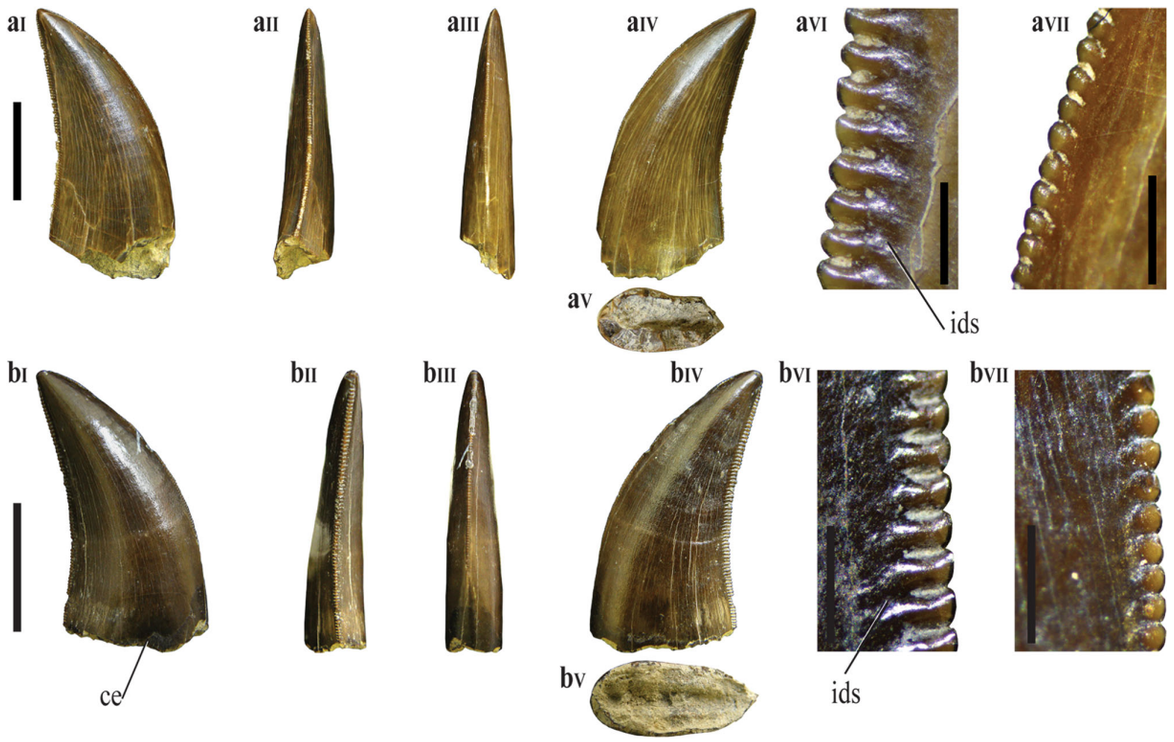

Fig. 10 Morphotype 7: **a** SHN.452; **b** SHN.444 in labial ($\mathbf{a_I}$, $\mathbf{b_I}$), distal ($\mathbf{a_{II}}$, $\mathbf{b_{II}}$), mesial ($\mathbf{a_{III}}$, $\mathbf{b_{III}}$), and lingual ($\mathbf{a_{IV}}$, $\mathbf{b_{IV}}$) views; cross-section at the crown base ($\mathbf{a_V}$, $\mathbf{b_V}$); detail of the distal ($\mathbf{a_{VI}}$, $\mathbf{b_{VI}}$) and mesial ($\mathbf{a_{VII}}$, $\mathbf{b_{VII}}$) denticles at the mid-crown. *ce* cervix, *ids* interdenticular sulci. *Scale bars* for the crowns: 10 mm; for the denticles: 1 mm

4.2.6 Morphotype 8

Megalosauroidea

Specimens: SHN.289, 290,323, 346, 359b, 455 (Fig. 11).

Geographical provenance: Praia da Corva and Porto Novo (Torres Vedras), Valmitão, Porto das Barcas, and Peralta (Lourinhã), ?Salir do Porto (Caldas da Rainha).

Stratigraphical distribution: Praia da Amoreira-Porto Novo Formaton (upper Kimmeridgian) and ?Sobral Formation (upper Kimmeridgian-lower Tithonian).

Description: Small crowns with AL between 8.85 and 19.37 mm (average 13.61 mm), CBL between 3.66 and 8.35 mm (average 6.29 mm), and CBW between 1.73 and 4.21 mm (average 3.29 mm). The crowns are relatively elongated (CHR between 1.72 and 2.38; average 2.08), triangular in lateral view and incrassate to slightly labiolingually compressed (CBR between 0.45 and 0.65; average 0.52).

These teeth show an irregular enamel texture and subtle transverse undulations. Both carinae are serrated with the distal reaching the cervix whereas the mesial carina is restricted to the apical part of the crown. The mesial carina is centrally positioned, but the distal carina twists strongly labially to the base of the crown. The crowns are slightly curved apically with the mesial margin convex and the distal margin slightly concave in lateral view. The crowns are lenticular (Fig. 11b_{III}, c_{III}) to subcircular (Fig. 11a_{III}) in cross-section. The lingual and labial surfaces are slightly convex.

An average of 5.8 and 4.6 denticles per mm is found in the central section of the mesial and distal carinae respectively and the DSDI is higher than 1.2 in most specimens (see Supplementary Data, Table 2S). The mesial denticles are mesiodistally short with rounded apices. The distal denticles are subquadrangular in outline with slightly asymmetrical rounded apices and they have a slight apical orientation in the apical end of the crown.

Results and discussion: The result of DFA for morphotype 8 assigns the specimens to different taxa, including *Masiakasaurus*, *Proceratosaurus*, and *Deinonychus* (see Supplementary Data, Table 4S).

The general morphology of morphotype 8 is similar to morphotype 9 described below, but they differ in some details, including (1) the mesial carina is restricted to the apical part of the crown, whereas it extends near the cervix in morphotype 9 and (2) DSDI >1.2 in morphotype 8 and

Fig. 11 Morphotype 8: **a** SHN.323; **b** SHN.289; **c** SHN.290 in labial ($\mathbf{a_I}$, $\mathbf{b_I}$, $\mathbf{c_I}$), lingual ($\mathbf{a_{II}}$, $\mathbf{b_{II}}$, $\mathbf{c_{II}}$), distal ($\mathbf{a_{Iv}}$, $\mathbf{b_{Iv}}$, $\mathbf{c_{IV}}$), mesial ($\mathbf{a_V}$, $\mathbf{b_V}$, $\mathbf{c_V}$) views; cross-section at the crown base ($\mathbf{a_{III}}$, $\mathbf{b_{III}}$, $\mathbf{c_{III}}$); detail of the distal denticles at mid-crown ($\mathbf{a_{VI}}$, $\mathbf{b_{VI}}$, $\mathbf{c_{VI}}$) and apically ($\mathbf{b_{VII}}$); detail of the mesial denticles ($\mathbf{a_{VII}}$). *Scale bars* for the crowns: 10 mm; for the denticles: 1 mm

near 1 in morphotype 9. This combination of features is more compatible with megalosauroid theropods and particularly the higher number of mesial than distal denticles is a feature shared with *Marshosaurus* (Hendrickx et al. 2015; Gerke and Wings 2016). Morphotype 8 is here identified as belonging to a juvenile megalosauroid tentatively related to the piatnitzkysaurid *Marshosaurus*.

4.3 Allosauroidea

4.3.1 Morphotype 9

Allosauridae
Allosaurus sp.
Specimens: SHN.255, 285, 316, 321e, 354, 363b, 373, 375, 384,449 (Fig. 12).

Geographical provenance: Porto Novo (Torres Vedras), Porto Dinheiro, Atalaia, Porto das Barcas, Peralta, and Praia da Areia Branca, (Lourinhã), Praia dos Frades and Almagreira (Peniche).

Stratigraphical distribution: Praia da Amoreira-Porto Novo Formation (upper Kimmeridgian), ?Sobral Formation (upper Kimmeridgian-lower Tithonian), and Freixial Formation (upper Tithonian).

Description: Teeth of medium to small sizes (AL average: 28.98 mm; CBL average: 11.9 mm and CBW average: 6.26 mm). The crowns are relatively elongated (CHR average: 2.23) and strongly compressed labiolingually (CBR average: 0.53). These specimens have slightly recurved crowns in which the distal margin is slightly concave, the mesial margin is strongly convex and the apex

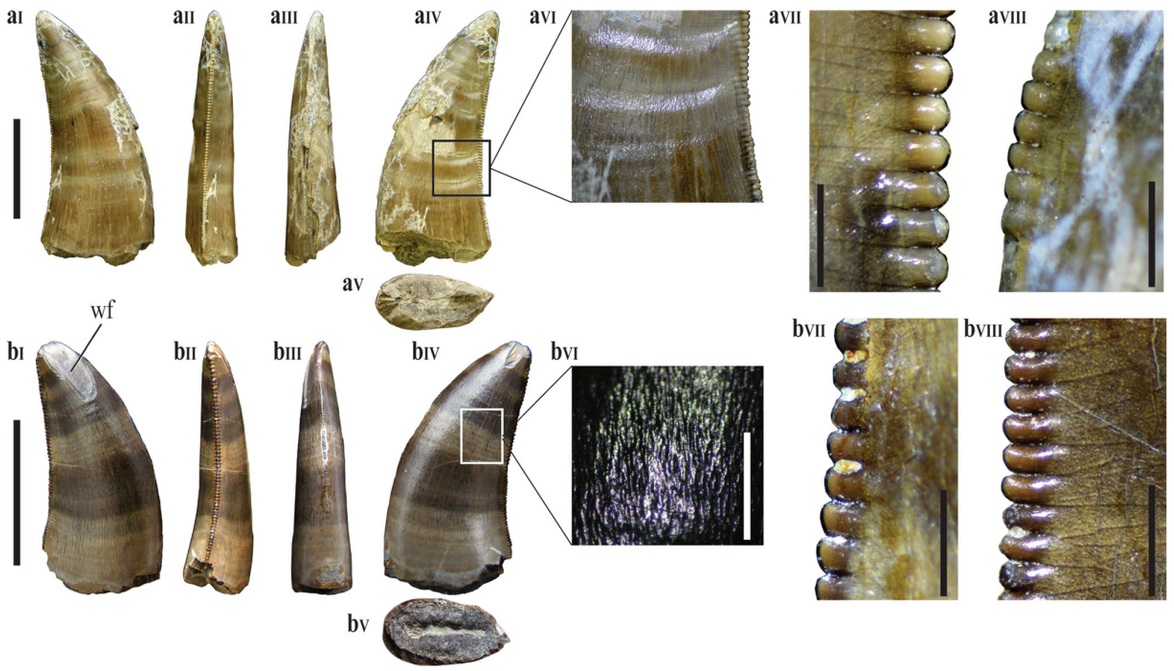

Fig. 12 Morphotype 9: **a** SHN.285; **b** SHN.375 in labial ($\mathbf{a_I}$, $\mathbf{b_{IV}}$), distal ($\mathbf{a_{II}}$, $\mathbf{b_{II}}$), mesial ($\mathbf{a_{III}}$, $\mathbf{b_{III}}$), and lingual ($\mathbf{a_{IV}}$, $\mathbf{b_I}$) views; cross-section at the crown base ($\mathbf{a_V}$, $\mathbf{b_V}$); detail of the transverse undulations ($\mathbf{a_{VI}}$) and of the enamel ornamentation ($\mathbf{b_{VI}}$); detail of the distal denticles at the mid-section ($\mathbf{a_{VII}}$, $\mathbf{b_{VIII}}$) and at the base ($\mathbf{b_{VII}}$) of the crown; detail of the mesial denticles ($\mathbf{a_{VIII}}$) denticles. *wf* wear facet. *Scale bars* for the crowns: 10 mm; for the denticles: 1 mm; ($\mathbf{b_{VI}}$): 1 mm

is positioned at the level of the distalmost point of the crown base.

Transverse undulations on the crown are present in several specimens. In some crowns (SHN.285: Fig. 12a) they are very deeply-marked extending across the lingual and labial surfaces. The deep undulations in this specimen might be related with some kind of biological or taphonomic process. Well-marked, diagonal interdenticular sulci are present in most teeth. They are more developed between distal denticles, but in some specimens are also present in the mesial carina. The enamel usually shows an ornamentation consisting on a series of very thin and irregular crenulations only visible with binocular microscope (Fig. 12b_{VI}). The mesial and distal carinae are serrated with the mesial carina extending more than two thirds of the crown height. The mesial carina is centrally positioned, but the distal carina shows a marked labial displacement. The lingual surface is flat or slightly convex and the labial surface is convex. In distal view, the distal margin slightly curves lingually forming a slight concavity at the base of the lingual surface. The cross-section of the crown base is elliptical. Some specimens show a flat or slightly concave vertical surface adjacent to the distal carina on the lingual surface (Fig. 12b_I).

The number of denticles in the mesial carina is slightly lower than in the distal carina, with an average of 11.9 and 16.8 denticles per 5 mm in the mid-section of the respective carinae, but the DSDI is near 1 in all specimens. The interdenticular space is narrow in both carinae. The mesial denticles are vertical rectangular and bear rounded or flat apices, whereas the distal denticles are horizontal rectangular and have slightly asymmetrical, rounded apices.

Results and discussion: The results of DFA for morphotype 9 identify these teeth to distinct taxa, including *Allosaurus*, *Erectopus*, *Megalosaurus Raptorex*, and *Alioramus* (see Supplementary Data, Table 4S). Morphotype 9 shares with allosauroid lateral teeth the moderate labiolingually-compressed crowns, the distal denticles slightly inclined toward the tip of the crown, especially in the apical end of the crown, and the presence of a concave surface adjacent to the mesial carina on the lingual side (Han et al. 2011; Hendrickx et al. 2015; Gerke and Wings 2016).

The combination of morphological characters of the teeth grouped in the morphotype 9 herein described is compatible with lateral teeth of *Allosaurus*. Based on this combination of features and since the presence of *Allosaurus* in the Upper Jurassic of the Lusitanian Basin is well documented (Pérez-Moreno et al. 1999; Rauhut and

Fechner 2005; Mateus et al. 2006; Malafaia et al. 2010), morphotype 9 is tentatively assigned as lateral teeth of *Allosaurus*.

4.3.2 Morphotype 10

Allosauridae
Allosaurus sp.
Specimens: SHN.204, 232, 250, 274–275, 363a, 367, 454, 460 (Fig. 13).
Geographical provenance: Gentias, Amoeiras, Santa Rita, and Praia da Corva (Torres Vedras), Valmitão and Peralta (Lourinhã), Almagreira (Peniche).

Stratigraphical distribution: Praia da Amoreira-Porto Novo Formation (upper Kimmeridgian), ?Sobral Formation (upper Kimmeridgian-lower Tithonian), and Freixial Formation (upper Tithonian).

Description: Moderately large teeth, with AL between 31.47 and 41.27 mm (average 35 mm), CBL between 13.87 and 19.55 mm (average 16.39 mm), and CBW between 9.88 and 15.01 mm (average 13.28 mm). The crowns are moderately elongated (CHR between 1.74 and 2.33; average 2.07) and subcircular in cross-section with low labiolingually compression ratios (CBR between 0.51 and 1; average 0.78). The crowns are triangular in lateral view with the distal carina slightly concave and the mesial carina strongly convex. The apex is centrally positioned and does not surpass the level of the distal carina.

Most of these specimens show well-marked transverse undulations and interdenticular sulci between distal denticles. In SHN.454 (Fig. 13d), the crown shows unusual deep transverse undulations, especially in the mid-section of both lingual and labial surfaces. In the remaining part of the crown transverse undulations are much shallower and widely spaced. These deep undulations similar to those of SHN.285 (morphotype 9) may be related to some kind of abnormal biological or taphonomic process.

The enamel is usually smooth or shows thin and irregular crenulations (Fig. 13a_{IV}, b_{IV}). Serrated mesial and distal carinae are present and both extend to the cervix (except in SHN.204 in which the mesial ends slightly above the cervix). Both carinae are positioned in the lingual surface. In SHN.460 (Fig. 13e), the mesial carina is positioned mostly in the mesial margin, but strongly twists lingually to the base. This specimen is also more labiolingually compressed relative to the other elements of morphotype 10. These features suggest that SHN.460 corresponds to a more distal position in the tooth row and is compatible with lateral teeth of *Allosaurus* (Hendrickx et al. 2015).

In lateral view, the mesial margin is slightly convex and the distal margin is almost straight. Crown cross-sections are subcircular and in some specimens they are salinon-shaped (sensu Hendrickx et al. 2016) with the mesial and distal carinae facing linguomesially and linguodistally, respectively, and vertical concavities on the lingual surface adjacent to both carinae (Fig. 13a_{III}).

An average of 13 and 12 denticles per 5 mm is found in the mid-section of the mesial and distal carinae, respectively (see Supplementary Data, Table 2S). The mesial denticles are round and very short mesiodistally whereas the distal denticlea are subquadrangular with rounded apices. The denticles are separated by narrow interdenticular spaces and project perpendicularly to the carina.

Results and discussion: The results of the DFA based on the dataset of Hendrickx et al. (2015) assign three teeth (SHN.204, 232, and 275) to *Allosaurus* and the remaining elements to different taxa including *Genyodectes* (SHN.460), *Torvosaurus* (SHN.274), the tyrannosaurids *Gorgosaurus* and *Daspletosaurus* (SHN.454 and 363a), and *Suchomimus* (SHN.367) (see Supplementary Data, Table 4S). The classification of some specimens to spinosaurids and basal tyrannosauroids is not surprising due to the similar morphometric data, especially the CBR and CHR.

The teeth herein grouped in morphotype 10 share with mesial teeth of *Allosaurus* the incrassate crowns (CBR >0.6), a character also typical in teeth of some spinosaurids (e.g. *Baryonyx*, *Suchomimus*, *Spinosaurus*) and tyrannosauroids (Charig and Milner 1997; Dal Sasso et al. 2005; Smith 2005; Sereno et al. 1998; Hendrickx et al. 2015). These teeth also share with mesial teeth of *Allosaurus* the strongly twisted mesial carina that extends to the cervix and the presence of shallow concave surfaces adjacent to the distal and in some crowns additionally on the mesial carina in the lingual surface, giving them a salinon-shaped cross-section (Hendrickx et al. 2016). The general morphology of these crowns is similar to the mesial teeth of *Allosaurus* and other allosauroids such as *Sinraptor* (Currie and Zhao 1993; Hendrickx et al. 2015), but may be distinguished from those of more derived allosauroids including *Acrocanthosaurus* (Currie and Carpenter 2000) because in these taxa the mesial carina ends well above the cervix. Spinosaurid teeth usually have fluted teeth and with either non-serrated carinae or higher number of denticles (Charig and Milner 1986; Sues et al. 2002; Sereno et al. 1998; Mateus et al. 2011). Tyrannosauroids have incrassate crowns, but the lingual and labial surfaces are convex and the mesial carina ends well above the cervix (Smith 2005; Hendrickx et al. 2015; Gerke and Wings 2016).

Based on the combination of features discussed above the specimens of morphotype 10 are assigned with confidence to *Allosaurus*, most of them corresponding to mesial teeth, except SHN.460, which is a lateral tooth.

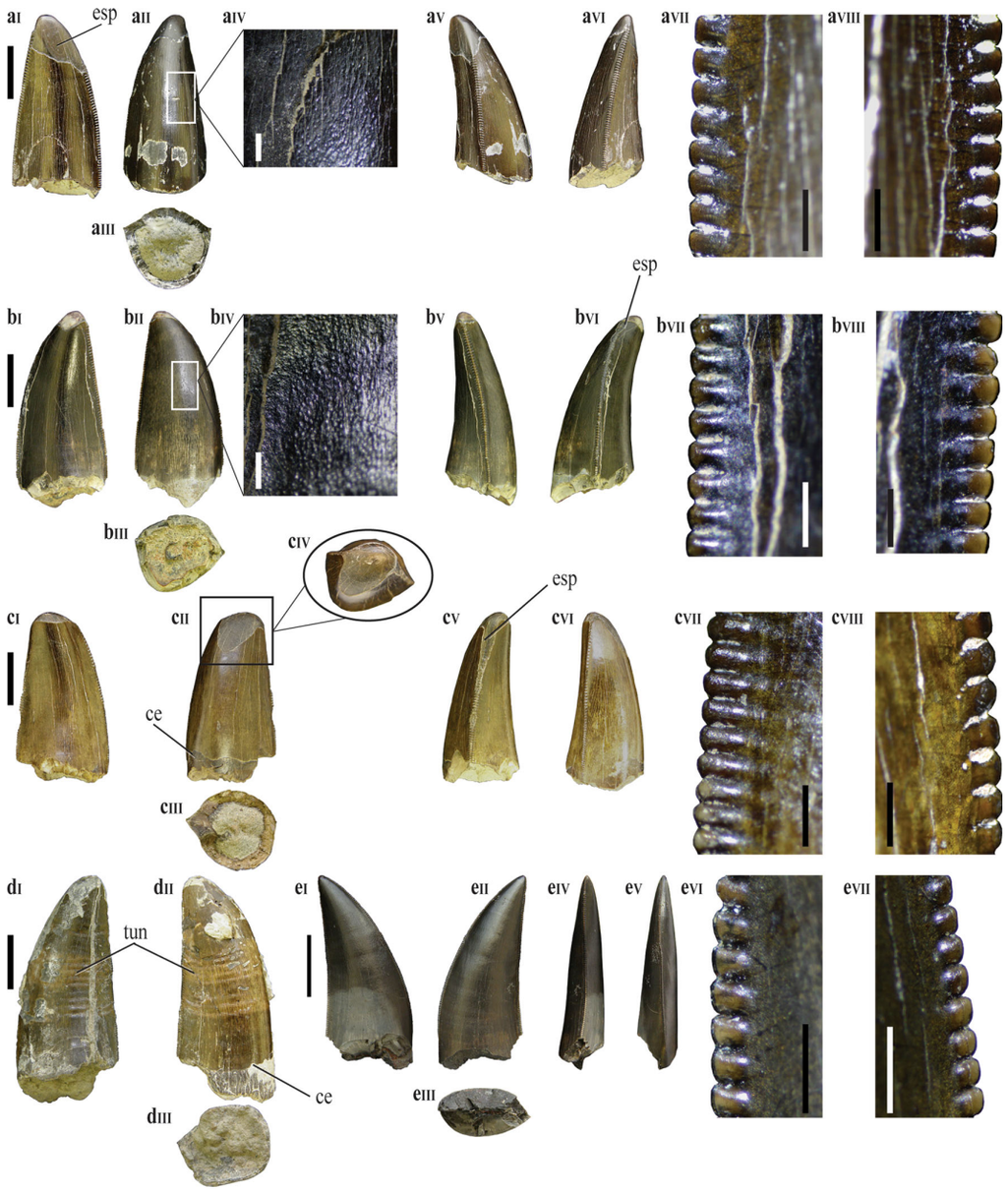

Fig. 13 Morphotype 10: **a** SHN.232; **b** SHN.275; **c** SHN.274; **d** SHN.454; **e** SHN.460 in lingual ($\mathbf{a_I}$, $\mathbf{b_I}$, $\mathbf{c_I}$, $\mathbf{d_I}$, $\mathbf{e_{II}}$), labial ($\mathbf{a_{II}}$, $\mathbf{b_{II}}$, $\mathbf{c_{II}}$, $\mathbf{d_{II}}$, $\mathbf{e_I}$), distal ($\mathbf{a_{VI}}$, $\mathbf{b_V}$, $\mathbf{c_V}$, $\mathbf{e_{IV}}$), and mesial ($\mathbf{a_V}$, $\mathbf{b_{VI}}$, $\mathbf{c_{VI}}$, $\mathbf{e_V}$) views; cross-section at the crown base ($\mathbf{a_{III}}$, $\mathbf{b_{III}}$, $\mathbf{c_{III}}$, $\mathbf{d_{III}}$, $\mathbf{e_{III}}$); detail of the enamel ornamentation ($\mathbf{a_{IV}}$, $\mathbf{b_{IV}}$); detail of the distal ($\mathbf{a_{VII}}$, $\mathbf{b_{VIII}}$, $\mathbf{c_{VII}}$, $\mathbf{e_{VI}}$) and mesial ($\mathbf{a_{VIII}}$, $\mathbf{b_{VII}}$, $\mathbf{c_{VIII}}$, $\mathbf{e_{VII}}$) denticles; detail of the wear facet ($\mathbf{c_{IV}}$). *ce* línea cervical, *eps* enamel spalling, *tun* transverse undulations. *Scale bars* for the crowns: 10 mm; for the denticles: 1 mm; ($\mathbf{a_{IV}}$ and $\mathbf{b_{IV}}$): 1 mm

4.3.3 Morphotype 11

Allosauridae
Allosaurus sp.
Specimens: SHN.227, 283,345, 368, 434 (Fig. 14).

Geographical provenance: ?Santa Rita (Torres Vedras), Valmitão and Porto Dinheiro (Lourinhã), Praia da Vermelha (Peniche), Salir do Porto (Caldas da Rainha).

Stratigraphical distribution: Praia da Amoreira-Porto Novo Formation (upper Kimmeridgian).

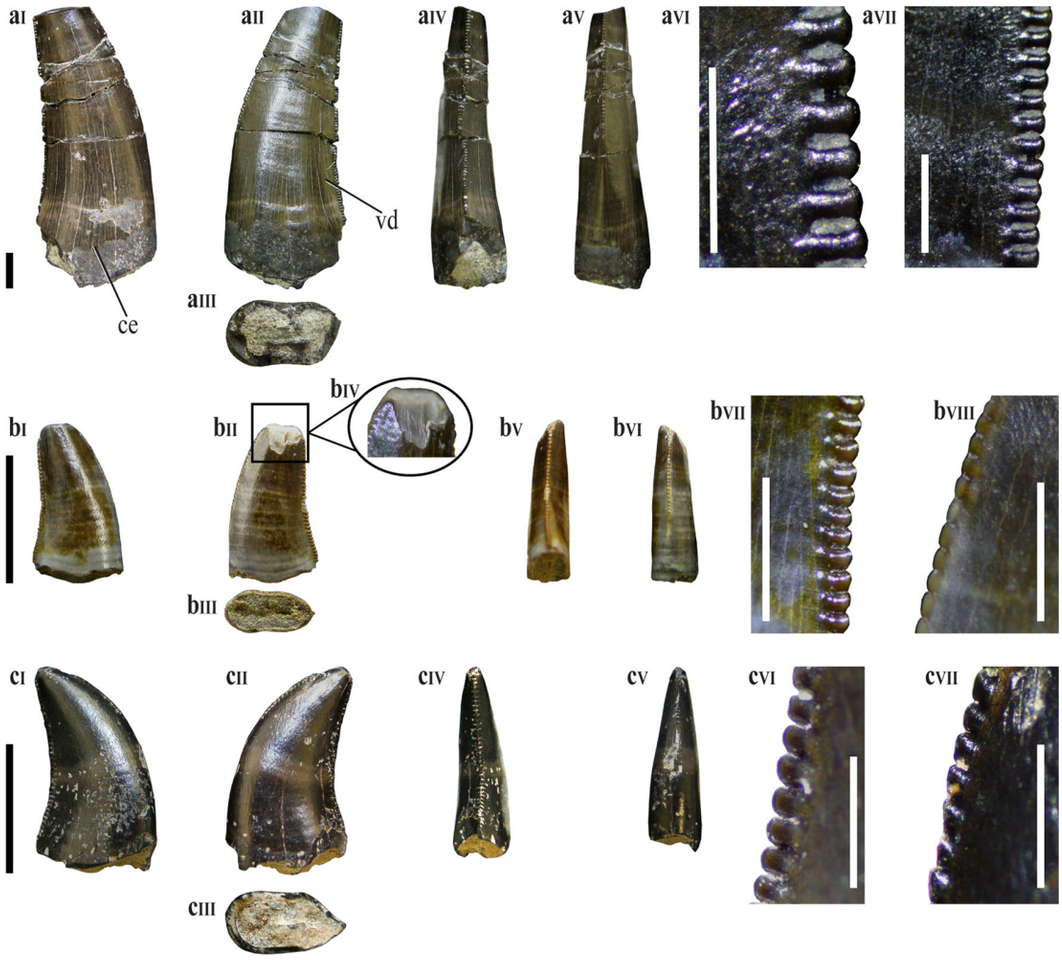

Fig. 14 Morphotype 11: **a** SHN.345; **b** SHN.283; **c** SHN.434 in labial ($\mathbf{a_I}$, $\mathbf{b_I}$, $\mathbf{c_I}$), lingual ($\mathbf{a_{II}}$, $\mathbf{b_{II}}$, $\mathbf{c_{II}}$); distal ($\mathbf{a_{IV}}$, $\mathbf{b_V}$, $\mathbf{c_{IV}}$); and mesial ($\mathbf{a_V}$, $\mathbf{b_{VI}}$, $\mathbf{c_V}$) views; cross-section at the crown base ($\mathbf{a_{III}}$, $\mathbf{b_{III}}$, $\mathbf{c_{IIII}}$); detail of the distal denticles at the mid-section ($\mathbf{a_{VI}}$, $\mathbf{b_{VIII}}$, $\mathbf{c_{VI}}$) and at the base ($\mathbf{a_{VII}}$) of the crown; detail of the mesial denticles ($\mathbf{b_{VIII}}$, $\mathbf{c_{VII}}$); detail of the wear facet ($\mathbf{b_{IV}}$). *Scale bars* for the crowns: 5 mm; for the denticles: 1 mm

Description: Small crowns with AL between 6.09 and 17.14 mm (average 12.16 mm), CBL between 3.08 and 6.56 mm (average 5.01 mm), and CBW between 1.23 and 3.35 mm (average 2.50 mm). The crowns are relatively elongated (CHR between 1.76 and 2.83; average 2.30), blade-shaped and slightly labiolingually compressed (CBR between 0.40 and 0.52; average 0.49).

These teeth show an irregular enamel texture and subtle transverse undulations. Both carinae are serrated with the distal reaching the cervix whereas the mesial carina extends for approximately two-thirds of the crown height. The mesial carina is always centrally positioned and not twisted, whereas the distal carina in some specimens is strongly displaced labially and somewhat sigmoidal in distal view. The crowns are slightly curved apically, with the mesial margin convex and the distal margin slightly concave in lateral view. The crowns are lenticular (Fig. 14b_{III}, c_{III}) in cross-section and some specimens have shallow basal concavities more marked in the lingual surface (Fig. 14a_{III}). Some specimens have a flat vertical surface adjacent to the distal carina in the lingual surface (Fig. 14a_{II}). The lingual surface of most crowns is flat and the labial surface is convex.

An average of 5.25 and 5 denticles per mm is present in the central section of the mesial and distal carinae respectively (see Supplementary Data, Table 2S). The mesial denticles are mesiodistally short with rounded apices. The distal denticles are subquadrangular in outline with slightly asymmetrical rounded apices and they have a slight apical orientation in the apical end of the crown.

Results and discussion: Except for the small size of the specimens, the general morphology of morphotype 11 is similar to morphotype 9. Morphotype 11 shares with

morphotype 9 the distal carina strongly displaced labially and DSDI close to one. The denticles are slightly inclined apically. These features are also present in most lateral teeth of *Allosaurus* as was discussed above (Han et al. 2011; Hendrickx et al. 2014a; Gerke and Wings 2016). Some of these small specimens (e.g. SHN.345: Fig. 14a) share with some isolated teeth, assigned to a possible juvenile allosaurid collected in the Guimarota coal mine (Zinke 1998), the presence of well-developed median ridges on the lingual surface, which gives the appearance of two longitudinal grooves between the carinae and the median ridge (Fig. 14a_{II}).

The result of DFA for morphotype 11 based on the reduced dataset of Gerke and Wings (2016) assigns three specimens (SHN.345, 368, and 434) to *Masiakasaurus* and one tooth (SHN.283) to *Velociraptor*. Based on the dataset of Hendrickx et al. (2015) most of the specimens (SHN.283, 345, 368) are identified to *Eoraptor* and one tooth (SHN.434) to *Masiakasaurus* (see Supplementary Data, Table 4S). This result may be explained because the specimens in the database for *Allosaurus* and other non-coelurosaurian tetanurans are large and possible adult or sub-adult individuals. However, based on the similarity with morphotype 9, including the shared presence of a slightly concave surface adjacent to the distal carina, the mesial carina ending slightly above the cervix, and DSDI close to 1, morphotype 11 is interpreted as belonging to a juvenile *Allosaurus*.

4.3.4 Morphotype 12

Allosauroidea
Specimens: SHN.213, 248, 344, 365, 430 (Fig. 15).
Geographical provenance: Gentias and Porto Chão (Torres Vedras), Praia dos Frades (Peniche).

Stratigraphical distribution: Praia da Amoreira-Porto Novo Formation (upper Kimmeridgian) and Freixial Formation (upper Tithonian).

Description: Moderately large crowns, relatively short (AL average: 42.12 mm; CHR average: 1.83), but robust (CBL average: 20.55 mm; CBW average: 11.56 mm). The crowns are slightly labiolingually compressed (CBR average: 0.56) and oval in cross-sections.

Transverse undulations and interdenticular sulci are usually absent or very slight. However, in SHN.365, short caudae are present especially between distal denticles (Fig. 15b_{VI}). The enamel usually shows a series of thin irregular non-oriented texture. These teeth have well-developed and serrated mesial and distal carinae. The mesial carina ends approximately at mid-length, except in SHN.213 in which the mesial carina reaches the cervix, and the distal carina extends to the cervix. The mesial carina strongly twists lingually at the base of the crown whereas the distal carina is centrally positioned or slightly displaced labially. There are about 12 denticles per 5 mm in the mid-section of the mesial and distal carinae (see Supplementary Data, Table 2S). The crowns are slightly recurved apically with a convex mesial and an almost flat distal margin, in lateral view. The lingual surface is nearly flat to slightly convex whereas the labial surface is more convex.

Results and discussion: The outcome of the DFA is very indistinct with the specimens assigned to different taxa, including *Acrocanthosaurus*, *Carcharodontosaurus*, *Mapusaurus*, *Neovenator*, *Allosaurus*, *Megalosaurus*, *Duriavenator*, and *Genyodectes* (see Supplementary Data, Table 4S).

Morphotype 12 shows a great similarity with some teeth (ML327 and ML966) described by Hendrickx and Mateus (2014b) from the Upper Jurassic of Portugal and interpreted as Abelisauridae. The specimens herein described lack the longitudinal ridge and the apically hooked denticles described in ML327, but these features are not present in ML966. Morphotype 12 is also similar to some isolated teeth described in the Upper Jurassic of Germany (morphotype K of Gerke and Wings 2016). These Portuguese specimens may be distinguished from the German elements based on the presence of mesial denticles that are smaller apically than at the mid-section of the crown, while in the German specimens, they become progressively coarser toward the apex (Gerke and Wings 2016). Despite of the similarity of the German specimens with abelisaurid teeth, Gerke and Wings (2016) opted for consider these teeth as *Allosaurus* sp. because the presence of Abelisauridae in the Upper Jurassic of Laurasia needs to be confirmed based on more complete material (Rauhut 2012; Gerke and Wings 2016). Based on the combination of features described above, morphotype 12 is here interpreted as possible belonging to an indeterminate Allosauroidea.

4.4 Coelurosauria

4.4.1 Morphotype 13

Tyrannosauroidea
Specimens: SHN.222, 230, 249, 253, 337, 355, 429, 435 (Fig. 16).

Geographical provenance: Santa Rita and Praia da Corva (Torres Vedras), Valmitão, Porto Dinheiro, and Peralta (Lourinhã).

Stratigraphical distribution: Praia da Amoreira-Porto Novo Formation (upper Kimmeridgian) and ?Sobral Formation (upper Kimmeridgian-lower Tithonian).

Fig. 15 Morphotype 12: **a** SHN.213; **b** SHN.365; **c** SHN.248 in lingual ($\mathbf{a_I}$, $\mathbf{b_{II}}$, $\mathbf{c_I}$), labial ($\mathbf{a_{II}}$, $\mathbf{b_I}$, $\mathbf{c_{II}}$), distal ($\mathbf{a_{IV}}$, $\mathbf{b_{IV}}$, $\mathbf{c_{IV}}$), and mesial ($\mathbf{a_V}$, $\mathbf{b_V}$, $\mathbf{c_V}$) views; cross-section at the crown base ($\mathbf{a_{III}}$, $\mathbf{b_{III}}$, $\mathbf{c_{III}}$); detail of the distal denticles at the mid-section ($\mathbf{a_{VI}}$, $\mathbf{b_{VI}}$, $\mathbf{c_{VI}}$) at the base ($\mathbf{c_{VII}}$) of the crown; detail of the mesial denticles ($\mathbf{a_{VII}}$, $\mathbf{b_{VII}}$, $\mathbf{c_{VIII}}$). *Scale bars* for the crowns: 10 mm; for the denticles: 1 mm

Description: The specimens of morphotype 13 are similar to those of morphotype 9. The crowns are slightly smaller (AL average: 25.96 mm; CBL average: 11.28 mm; CBW average: 6.20 mm; and CHR average: 2.12), but the compression rate is similar (CBR average: 0.55) as well as the number of denticles in both carinae. The most distinctive character of morphotype 13 relative to morphotype 9 is the presence of a slight concavity centrally positioned at the base of the lingual surface (Fig. 16c_{IV}). In some crowns, well-marked concavity is present on the labial and lingual sides (Fig. 16a_I), giving them a reniform or eight-shaped cross-sections. Most specimens have some slight vertical ridges inside the basal concavity (Fig. 16a_I, c_{IV}). Another difference between morphotype 13 and morphotype 9 is the strongly twisted mesial carina in the specimens of morphotype 13 while in morphotype 9 the mesial carina is straight and centrally positioned.

Results and discussion: The result of the DFA for morphotype 13 is ambiguous. The specimens are assigned to different taxa, including *Raptorex*, *Torvosaurus*, *Ceratosaurus*, *Majungasaurus*, *Masiakasaurus*, and dromaeosaurids (see Supplementary Data, Table 4S).

The presence of a concave surface centrally positioned in the lingual surface at the crown base is reported in some allosauroid teeth (Hendrickx et al. 2015). Morphotype 13 is also similar to *Allosaurus* teeth in having asymmetrical crowns with the distal carina placed in the labial surface (Hendrickx et al. 2015). However, several features in some specimens (SHN.222), including: (1) mesial carina restricted to the apical part of the crown and curving lingually, (2) eight-shaped cross-section of the crown base, (3) relative incrassate crowns (CBR near 0.60 in most specimens), (4) presence of slight transversal undulations, (5) DSDI >1.2 are more compatible with coelurosaur

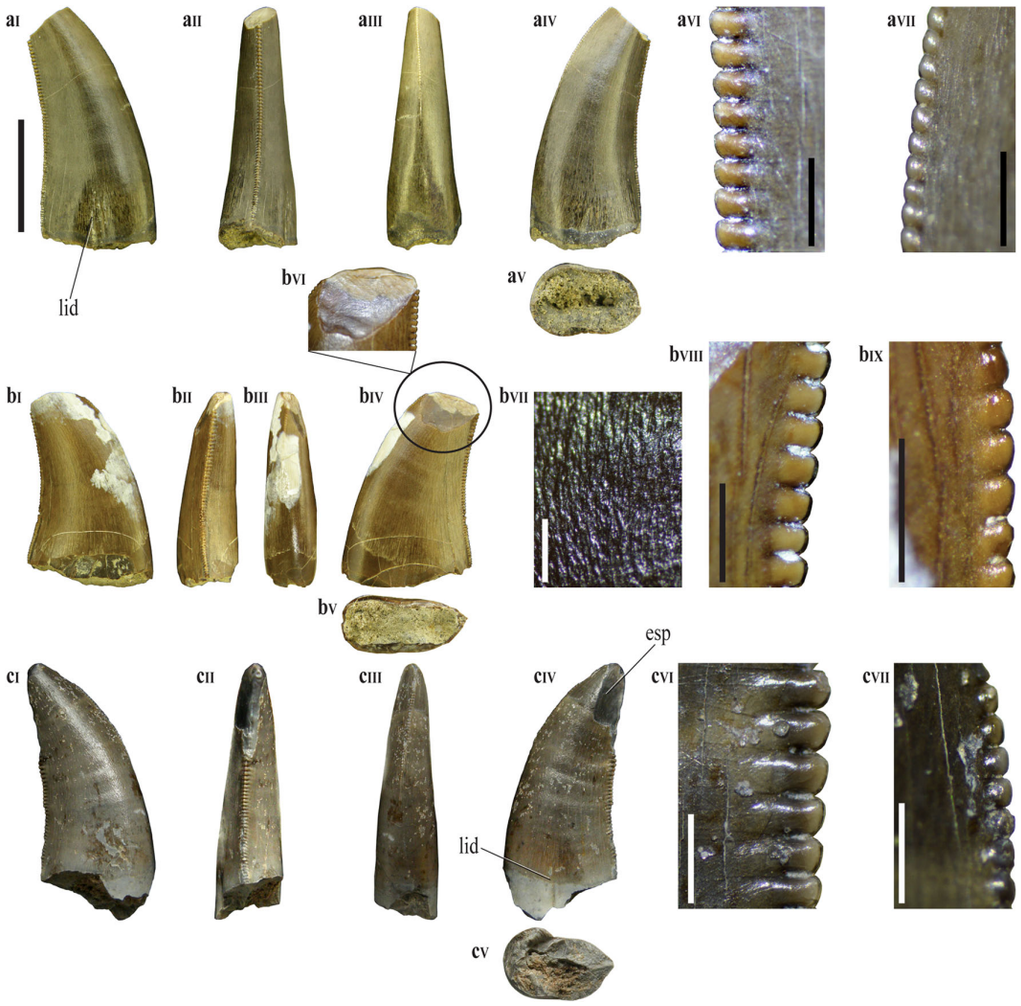

Fig. 16 Morphotype 13: **a** SHN.222; **b** SHN.429; **c** SHN.355 in lingual ($\mathbf{a_I}$, $\mathbf{b_I}$, $\mathbf{c_{IV}}$), distal ($\mathbf{a_{II}}$, $\mathbf{b_{II}}$, $\mathbf{c_{II}}$), mesial ($\mathbf{a_{III}}$, $\mathbf{b_{III}}$, $\mathbf{c_{III}}$), and labial ($\mathbf{a_{IV}}$, $\mathbf{b_{IV}}$, $\mathbf{c_I}$) views; cross-section at the crown base ($\mathbf{a_V}$, $\mathbf{b_V}$, $\mathbf{c_V}$); detail of the distal ($\mathbf{a_{VI}}$, $\mathbf{b_{VIII}}$, $\mathbf{c_{VI}}$) and mesial ($\mathbf{a_{VII}}$, $\mathbf{b_{IX}}$, $\mathbf{c_{VII}}$) denticles; detail of the wear facet ($\mathbf{b_{VI}}$) and of the enamel ornamentation ($\mathbf{b_{VII}}$). *eps* enamel spalling, *id* lingual depression. *Scale bars* for the crowns: 10 mm; for the denticles: 1 mm

tetanurans (Hendrickx et al. 2015). Based on this combination of features morphotype 13 is here tentatively assigned to a basal tyrannosauroid possibly related with *Aviatyrannis*, which is the only tyrannosauroid taxon currently known in the Portuguese record.

4.4.2 Morphotype 14

Tyrannosauroidea
Specimens: SHN.209, 219, 260, 265, 431 (Fig. 17).

Geographical provenance: Valmitão (Lourinhã), Foz do Arelho (Caldas da Rainha).

Stratigraphical distribution: Praia da Amoreira-Porto Novo Formation (upper Kimmeridgian), Bombarral Formation (Tithonian).

Description: Very small crowns with AL between 8.53 and 23.49 mm (average 14.53 mm), CBL between 4.35 and 7.68 mm (average 5.63 mm), and CBW between 3.26 and 5.36 mm (average 4.03 mm). The crowns are elongated (CHR between 2.01 and 2.88; average 2.44), and have a rounded cross-section at the base (CBR between 0.63 and 0.81; average 0.73). The crowns are slightly recurved with the mesial margin slightly convex and the distal margin almost flat to slightly concave. In some specimens, well-marked transverse undulations are present and the enamel

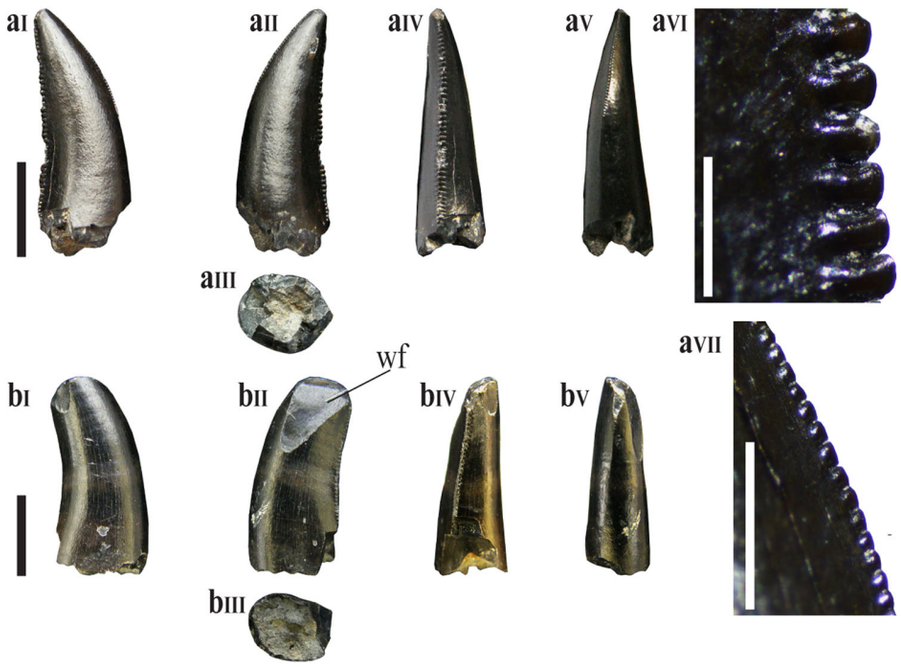

Fig. 17 Morphotype 14: **a** SHN.209; **b** SHN.431 in labial ($\mathbf{a_I}$, $\mathbf{b_I}$), lingual ($\mathbf{a_{II}}$, $\mathbf{b_{II}}$), distal ($\mathbf{a_{IV}}$, $\mathbf{b_{IV}}$), and mesial ($\mathbf{a_V}$, $\mathbf{b_V}$) views; cross-section at the crown base ($\mathbf{a_{III}}$, $\mathbf{b_{III}}$); detail of the distal ($\mathbf{a_{VI}}$) and mesial ($\mathbf{a_{VII}}$) denticles. *wf* wear facet. *Scale bars* for the crowns: 5 mm; for the denticles: 1 mm

shows irregular texture crenulations. Both carinae are serrated, with the distal carina extending to the cervix whereas the mesial carina ends approximately at mid-height of the crown. The distal carina is strongly displaced labially and the mesial carina is mostly centrally positioned or slightly twisted toward the base (Fig. 17b_{IV}). Both lingual and labial surfaces are strongly convex.

An average of 5 and 3.35 denticles per mm is found in the central section of the mesial and distal carinae respectively and the DSDI is greater than 1.2. The mesial denticles are very short mesiodistally with almost flat apices and the distal denticles are subquadrangular in outline with symmetrical rounded apices and positioned perpendicularly to the carinae.

Results and discussion: The DFA result based in the dataset of Hendrickx et al. (2015) identifies the specimens of morphotype 14 as belonging to *Masiakasaurus* (SHN.209), *Nuthetes* (SHN.260), *Megalosaurus* (SHN.265), and *Torvosaurus* (SHN.431) (see Supplementary Data, Table 4S). These teeth have a relatively high DSDI (>1.2), which is a feature shared by some basal tyrannosauroids such as *Proceratosaurus* and *Alioramus* and most dromaeosaurids including *Deinonychus*, *Dromaeosaurus*, and *Velociraptor* (Rauhut and Werner 1995; Rauhut et al. 2010; Gerke and Wings 2016). Morphotype 14 shares with some isolated teeth interpreted as possibly belonging to basal tyrannosauroids from the Upper Jurassic of Portugal (Zinke 1998) and Germany (Gerke and Wings 2016) the presence of a rounded cross-section of the crown base, the distal carina placed in the lingual surface and the presence of a concave vertical surface adjacent to the distal carinae. In addition, some specimens (SHN.209) show a braided enamel texture similar to that of basal tyrannosauroids. Based on this features the specimens of morphotype 14 are here interpret as belonging to a basal tyrannosauroid.

4.4.3 Morphotype 15

cf. Richardoestesia

Specimens: SHN.240, 272, 278, 308–309, 433, 436 (Fig. 18).

Geographical provenance: Praia Azul and Praia da Corva (Torres Vedras), Valmitão, Porto Dinheiro, and Porto das Barcas (Lourinhã).

Stratigraphical distribution: Praia da Amoreira-Porto Novo Formation (upper Kimmeridgian) and Sobral Formation (upper Kimmeridgian-lower Tithonian).

Description: Small crowns with AL between 13.06 and 19.21 mm (average 15.43 mm), CBL between 8.89 and 9.82 mm (average 7.60 mm), and CBW between 3.73 and 5.54 mm (average 4.38 mm). The crowns are low (CHR between 1.77 and 2.01; average 1.87), and slightly compressed labiolingually (CBR between 0.54 and 0.67; average 0.58). The crowns have a triangular shape in lateral view and are strongly curved distally. The distal carina is nearly straight or slightly concave and the mesial one is convex apically, but nearly straight in the basal half of the crown. The apex does not surpass the level of the distal carina.

These teeth have smooth enamel, without any undulations or interdenticular sulci. Both carinae are serrated with

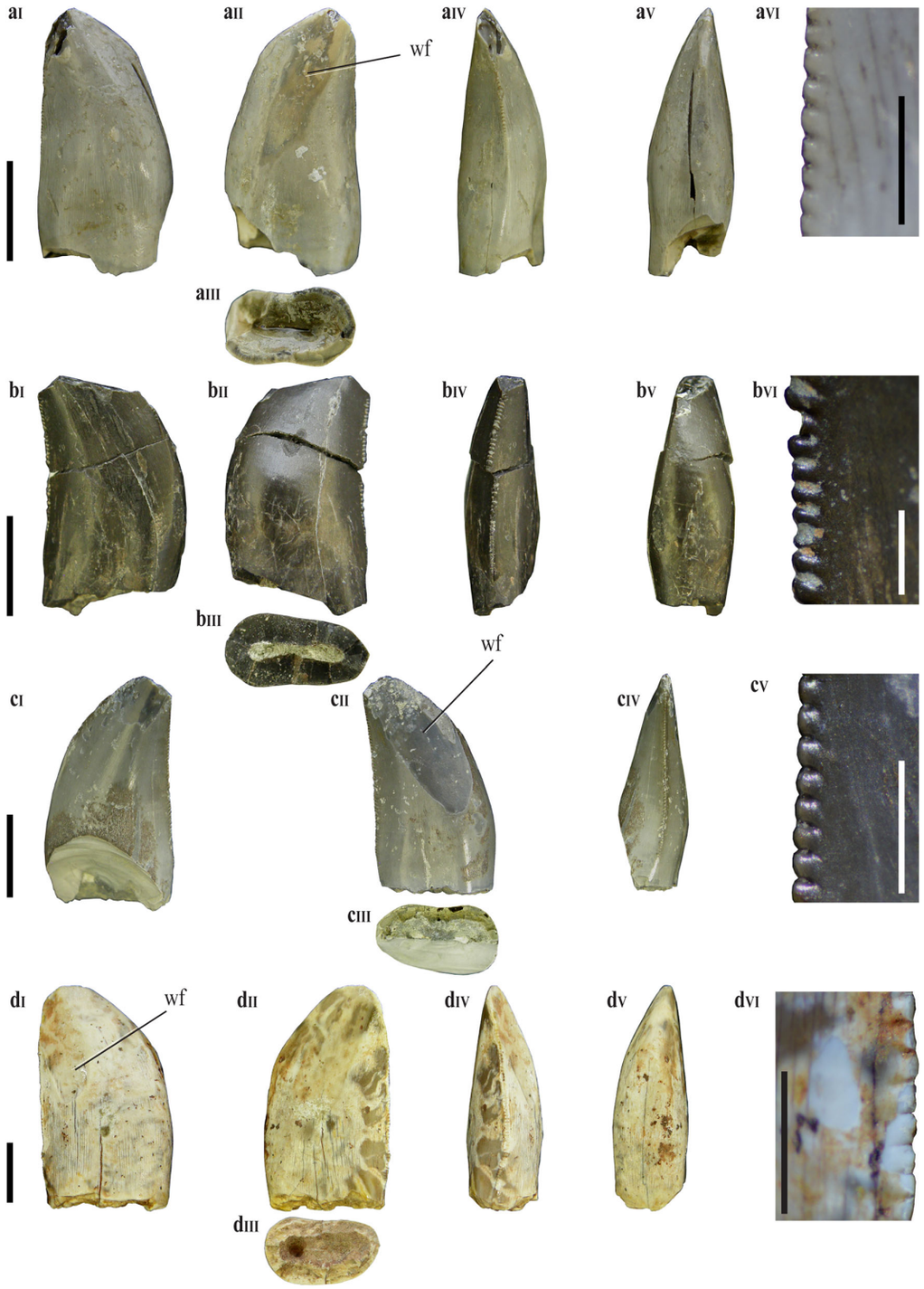

Fig. 18 Morphotype 15: **a** SHN.278; **b** SHN.436; **c** SHN.272; **d** SHN.433 in labial ($\mathbf{a_I}$, $\mathbf{b_{II}}$, $\mathbf{c_{II}}$, $\mathbf{d_I}$), lingual ($\mathbf{a_{II}}$, $\mathbf{b_I}$, $\mathbf{c_I}$, $\mathbf{d_{II}}$), distal ($\mathbf{a_{IV}}$, $\mathbf{b_{IV}}$, $\mathbf{c_{IV}}$, $\mathbf{d_{IV}}$), and mesial ($\mathbf{a_V}$, $\mathbf{b_V}$, $\mathbf{d_V}$) views; cross-section at the crown base ($\mathbf{a_{III}}$, $\mathbf{b_{III}}$, $\mathbf{c_{III}}$, $\mathbf{d_{III}}$); detail of the distal denticles ($\mathbf{a_{VI}}$, $\mathbf{b_{VI}}$, $\mathbf{c_V}$, $\mathbf{d_{VI}}$). *wf* wear facet. *Scale bars* for the crowns: 10 mm; for the denticles: 1 mm

the distal carina extending to the cervix and the mesial carina is restricted to the apical part of the crown. In most teeth, the mesial carina is strongly displaced lingually and curves lingually to the crown base and the distal carina is straight or slightly twists lingually to the base of the crown and placed mainly in the lingual surface. There are well-developed transverse concavities in the lingual and labial surfaces at the base of the crown (except in SHN.433: Fig. 18d) and therefore these specimens are eight-shaped in cross-section (Fig. 18a_{III}). A well-marked labiolingual and slight mesiodistal constrictions at the crown base are also present in all specimens, but is less marked in SHN.433. The lingual surface is almost flat to slightly concave and the labial surface is strongly convex.

An average of 5 and 4 denticles per mm can be found in the central section of the mesial and distal carinae, respectively (see Supplementary Data, Table 2S). The mesial denticles are short mesiodistally with rounded apices. The distal denticles are subquadrangular with rounded apices and positioned perpendicularly to the carinae.

Results and discussion: The result of DFA is not consistent. Based on the dataset of Hendrickx et al. (2015) these specimens are assigned to *Nuthetes* (SHN.272), *Megalosaurus* (SHN.308), and *Torvosaurus* (SHN.436) (see Supplementary Data, Table 4S).

These teeth have morphology distinct from all other morphotypes here described. Also, this morphology is not so common in theropod teeth from the Upper Jurassic. They show a well-marked labiolingual constriction between the crown and root. The crowns are strongly labiolingually inflated near the base and slightly recurved apically, with almost straight to slightly concave distal margin in lateral view. The mesial carina strongly twists lingually and is restricted to the apical part of the crown, and the cross-section of the crown base is eight-shaped due to the presence of well-marked concavities in both lingual and labial surfaces. The presence of a basal mesiodistal constriction between the crown and root is a character shared by many coelurosaurs, including some isolated teeth assigned to *Compsognathus* from the Guimarota fossil site (Zinke 1998), troodontids (Norell et al. 2000; Currie and Zhiming 2001), the dromaeosaurid *Microraptor* (Xu et al. 2000; Hendrickx et al. 2015), some carcharodontosaurins such as *Carcharodontosaurus* and *Giganotosaurus* (Hendrickx, pers. commun.), the ornithomimosaur *Pelecanimimus* (Pérez-Moreno et al. 1994; Hendrickx and Mateus 2014b), the alvarezsaurids *Shuvuuia* and *Mononykus* (Perle et al. 1993; Hendrickx and Mateus 2014b), basal oviraptorosaurs (Osmólska et al. 2004; Hendrickx and Mateus 2014b), therizinosaurs (Kirkland et al. 2005; Hendrickx and Mateus 2014b), and *Archaeopteryx* (Louchart and Pouech, 2017). A slight constriction is also present in at least some premaxillary teeth of *Proceratosaurus*, but not in the lateral teeth (Rauhut et al. 2010; Hendrickx et al. 2015).

An eight-shape cross-section of the crown base is a feature shared by some deinonychosaur coelurosaurians, including *Saurornitholestes* (Sullivan 2006; Hendrickx et al. 2015), *Pyroraptor* (Allain and Taquet 2000), and *Buitreraptor* (Gianechini et al. 2011), the enigmatic theropod *Richardoestesia gilmorei* (Currie et al. 1990; Larson 2008; Hendrickx et al. 2015), the tyrannosaurids *Proceratosaurus* (Rauhut et al. 2010) and *Alioramus* (Brusatte et al. 2009) and the neovenatorid *Orkoraptor* (Novas et al. 2008b).

This combination of features: (1) presence of mesiodistal and labiolingual constrictions, (2) eight-shaped cross-section at the crown base, (3) slight distal curvature, and (4) mesial carina restricted to the apical part of the crowns and twisting lingually is compatible with the morphotype generally assigned to *Richardoestesia* (Hendrickx and Mateus 2014b). Morphotype 15 also has morphology similar to some isolated teeth from the Guimarota coal mine identified as cf. *Compsognathus* (Zinke, 1998). However, Guimarota specimens lack basal concavities and they have a higher number of denticles (Zinke 1998). Recently, Hendrickx and Mateus (2014b) described an isolated tooth (ML 939) from the Upper Jurassic of the Lusitanian Basin with morphology similar to morphotype 15 and interpreted them as *Richardoestesia* aff. *R. gilmorei*. ML 939 differs from the morphotype 15 by the presence of: (1) slightly more labiolingually-compressed crowns (the crowns of morphotype 15 have an inflated appearance labiolingually at the crown base), and (2) a much higher number of denticles in the distal carina (Hendrickx and Mateus 2014b). Morphotype 15 and ML 939 differ from *Richardoestesia gilmorei* in a mesial restricted to the apical part of the crown (Hendrickx and Mateus 2014b).

Richardoestesia gilmorei was described by Currie et al. (1990) on the basis of a pair of lower jaws with a replacement tooth collected in the Upper Cretaceous of the Dinosaur Park Formation in Canada (Larson 2008; Torices et al. 2015). *Richardoestesia*-like teeth have been recovered from several sites and different ages including the Upper Jurassic of Portugal (Zinke 1998; Hendrickx and Mateus 2014b), the Lower and Upper Cretaceous of Spain (Rauhut 2002; Torices et al. 2015), and the Upper Cretaceous of Romania (Codrea et al. 2002; Weishampel et al. 2010). However, as proposed by some authors, isolated teeth from different stratigraphic intervals do most likely not belong to the same species although they may be similar in form to those of the type specimen from the Dinosaur Park Formation (Larson 2008). Based on this argumentation morphotype 15 is here assigned as cf. *Richardoestesia*.

4.4.4 Morphotype 16

Dromaeosauridae
Specimens: SHN.359d (Fig. 19).

Geographical provenance: Porto Novo (Torres Vedras).

Stratigraphical distribution: Praia da Amoreira-Porto Novo Formation (upper Kimmeridgian).

Description: This morphotype consists of a single specimen represented by a complete and well-preserved crown. This specimen is relatively small-sized with AL of 19.06 mm, CBL of 8.88 mm, and CBW of 4.76 mm (see Supplementary Data, Table 2S). The crown is relatively elongated (CHR: 1.97), slightly compressed labiolingually with oval cross-section at the base (CBR: 0.54). The crown is strongly recurved with a convex mesial margin and strongly concave distal margin. The apex is positioned quite distally to the level of the base of the distal carina. The enamel is smooth and neither transverse undulations nor interdenticular sulci are visible. Both carinae are serrated, with the distal carina extending to the cervix whereas the mesial carina is restricted to the apical end. The distal carina is strongly displaced lingually and the mesial carina is also twisted toward the base, but is mostly positioned on the mesial surface. The lingual and labial surfaces are convex and shallow concavities are visible at the base of the crown in both lingual and labial surfaces. The lingual concavity is associated with two small vertical ridges (Fig. 19d).

There is an average of 3.5 denticles per mm on the central section of the distal carina. The mesial denticles are poorly preserved and it is not possible verify their density on this carina. The distal denticles are rectangular, higher mesiodistally than apicobasally and are separated by narrow interdenticular sulci. In the basal part of the distal carina, the denticles are parabolic with symmetrically circular apices (Fig. 19g), but in the apical part of the distal carina, the denticles are slightly apically hooked (Fig. 18h).

Results and discussion: The DFA based on the dataset of Gerke and Wings (2016) classifies SHN.359d as *Majungasaurus*, whereas the result based on the dataset of Hendrickx et al. (2015) assigns this specimen to *Australovenator* (see Supplementary Data, Table 4S). This specimen shares with the lateral teeth of most dromaeosaurids the presence of a wide concavity on the basal end of both labial and lingual surfaces of the crown, the presence of two longitudinal ridges restricted to the crown base, the slightly apically hooked distal denticles, a DSDI >1.2, a lingually twisted mesial carina at the base of the crown, and the moderately labiolingual compression of the crown (Hendrickx and Mateus 2014b; Hendrickx et al. 2015). Based on these features, SHN.359d is here tentatively assigned to an indeterminate eudromaeosaurid. This clade has been tentatively identified in the Upper Jurassic of the Lusitanian Basin based on isolated specimens (Zinke 1998; Malafaia et al. 2014). However, this identification is only tentative, pending the discovery of more complete specimens.

4.5 Tetanurae indet

4.5.1 Morphotype 17

Specimens: SHN.277 (Fig. 20).
Geographical provenance: Peralta (Lourinhã).

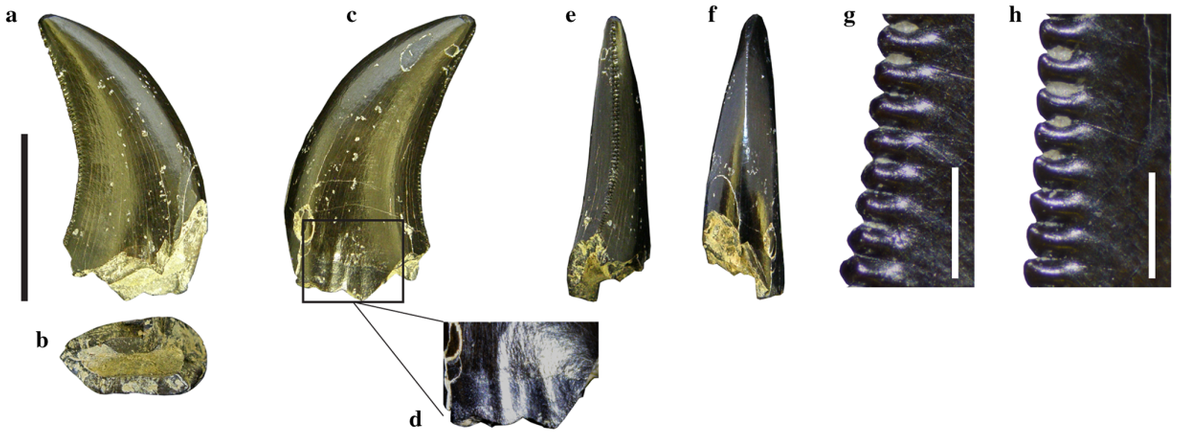

Fig. 19 Morphotype 16: SHN.359d in labial (**a**), lingual (**c**), distal (**e**), and mesial (**f**) views; cross-section at the crown base (**b**); detail of the crests at the base of the lingual surface (**d**); detail of the distal denticles at the base (**g**) and at the mid-section (**h**) of the crown. *Scale bars* for the crown: 10 mm; for the denticles: 1 mm

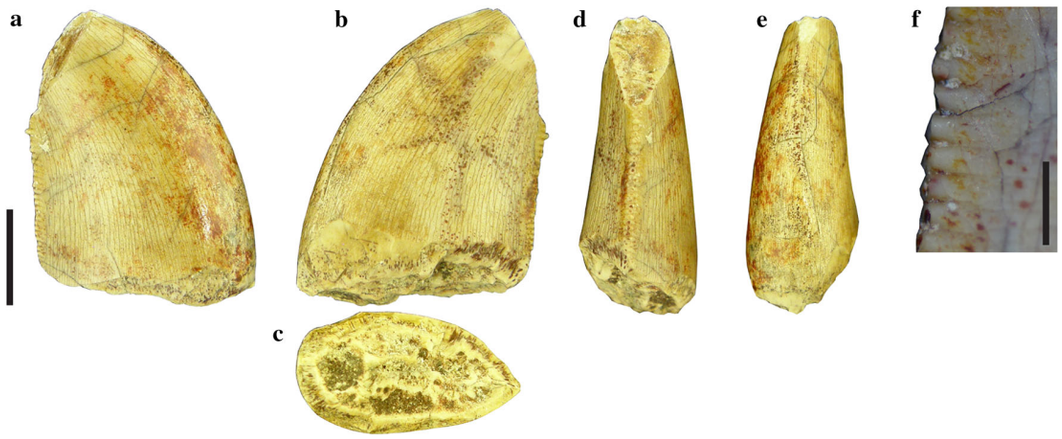

Fig. 20 Morphotype 17: SHN.277 in labial (**a**), lingual (**b**), distal (**d**), and mesial (**e**) views; cross-section at the crown base (**c**); detail of the distal denticles (**f**). *Scale bars* for the crown: 10 mm; for the denticles: 1 mm

Stratigraphical distribution: ?Sobral Formation (upper Kimmeridgian-lower Tithonian).

Description: This morphotype includes a single, partially preserved crown that preserves a small part of the cervical line delimiting the crown from the root adjacent to the distal margin. This specimen is relatively small, with AL of 19.64 mm, CBL of 12.26 mm, and CBW of 6.62 mm. The crown is short (CHR: 1.39), slightly compressed-labiolingually with oval cross-section at the base (CBR: 0.54). The crown is strongly recurved apically with the mesial margin strongly convex, but the distal margin is almost straight. The enamel is smooth and interdenticular sulci are absent. Both carinae are serrated with the distal carina extending to the cervix whereas the mesial carina ends above it and strongly twists lingually toward the base.

There is an average of 3 denticles per mm in the central section of the distal carina (see Supplementary Data, Table 2S). The mesial denticles are much eroded and it is not possible verifying the denticle density in this carina. The distal denticles are subquadrangular, separated by narrow interdenticular spaces (Fig. 20f).

Results and discussion: The DFA results excluding the MC variable classifies the specimen SHN.277 to *Neovenator* (see Supplementary Data, Table 4S). The general morphology of this specimen is similar to some isolated teeth from the Guimarota fossil site interpreted as putative premaxillary teeth of *Dromaeosaurus* (Zinke 1998). However, based on the CBR value, SHN.277 is here interpreted as a lateral crown and it shares with the specimens from Guimarota the strongly twisted mesial carina extending near to the cervix and the similar number of denticles in the central section of the distal carina. Nevertheless, the presence of strongly twisted mesial carina is also shared with several other tetanuran theropods, including *Allosaurus* (which also have similar number of denticles in the distal carina). The poor preservation of morphotype 17 does not allow an accurate identification and is here assigned as belonging to an indeterminate tetanuran.

4.6 Incomplete and poorly preserved teeth not assigned to a morphotype

Specimens: SHN.223, 313, 432 (Fig. 21).

SHN.223 is an incomplete, distorted, and very small tooth crown (AL ~10.35 mm) collected in the upper Kimmeridgian of Santa Rita (Torres Vedras). The crown is strongly compressed labiolingually and recurved distally. Thin but well-marked transverse undulations are visible in both lingual and labial surfaces. There is an average of 6 denticles per millimeter in the mesial carina, but the distal carina is not preserved. The mesial carina is incomplete to the base, so it is not possible verify the extension of the denticles. Nevertheless, they are present at least in ¾ of the crown height. The denticles are subquadrangular in outline with almost flat to slightly rounded apices.

SHN.313 (Fig. 21a) was collected in the upper Kimmeridgian of Valmitão (Torres Vedras) and corresponds to an almost complete crown, but it is somewhat worn, especially the distal carina. The crown is very slender, relatively tall, but narrow mesiodistally (AL: 12.7 mm; CBL: 4.6 mm). The cross-section of the base is oval in outline (CBR: 0.64) and both lingual and labial surfaces are slightly convex. The crown is recurved distally with the mesial margin convex and the distal margin concave. The distal carina is broken and the mesial carina is also poorly preserved with the denticles almost entirely abraded, but the mesial carina is mostly centrally positioned and slightly twisted toward the base.

SHN.432 (Fig. 21b) is an incomplete and poorly-preserved crown collected in Porto das Barcas (Lourinhã). The

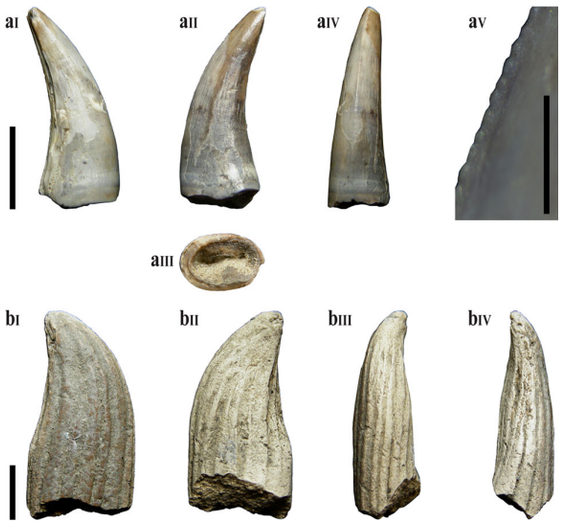

Fig. 21 Poorly preserved teeth not assigned to any morphotype: **a** SHN.313; **b** SHN.432 in labial ($\mathbf{a_I}$, $\mathbf{b_I}$), lingual ($\mathbf{a_{II}}$, $\mathbf{b_{II}}$), mesial ($\mathbf{a_{IV}}$, $\mathbf{b_{III}}$), and distal ($\mathbf{b_{IV}}$) views; cross-section at the crown base ($\mathbf{a_{III}}$); detail of the mesial denticles ($\mathbf{a_V}$). *Scale bars* for the crowns: 10 mm; for the denticles: 1 mm

most striking feature of this specimen is the presence of a series of vertical ridges and grooves that extend along the entire labial and lingual surfaces. Carinae seems to be absent in both mesial and distal surfaces, but this may be due to wear of the crown surface. The crown is wide and columnar in the basal part with almost straight mesial and distal margins, but strongly tapers to the apical end, becoming strongly convex mesially and concave distally.

The DFA based on the dataset of Gerke and Wings (2016) excluding the MC and DC variables classifies SHN.223 and SHN.313 as *Masiakasaurus* and SHN.432 as *Majungasaurus*. Based on the dataset of Hendrickx et al. (2015), SHN.223 is assigned to *Liliensternus*, SHN.313 to *Nuthetes*, and SHN.432 as *Dubreuillosaurus* (see Supplementary Data, Table 4S). SHN.223 has a general shape similar to those of lateral teeth of *Allosaurus* and shares with this taxon the mesial carina extending to near the cervix and the presence of numerous thin transverse undulations in the lingual and labial surfaces. SHN.313 has a conical shape of the crown, similar to those of baryonychines. The mesial carina does not reach the cervix contrary to most barionychines, with the exception of some isolated teeth from Spain (Canudo et al. 2008). However, the enamel texture seems to be smooth not veined as is the case in baryonychines. The vertical ridges in SHN.432 are similar to some isolated teeth described in the Upper Jurassic of Guimarota and in the Lower Cretaceous of Galve in Spain interpreted as a form closely related to *Paronychodon* (Zinke and Rauhut 1994). However, SHN.432 differs from the teeth of *Paronychodon* in the higher number of longitudinal ridges thatextend along the entire crown and are strongly twisted. This specimen could correspond to a mesial tooth of this taxon or a closely related taxon. Because the incompleteness and poor preservation of these specimens, they are here assigned as Theropoda indet.

5 General discussion of the diversity and stratigraphic distribution of the sample of isolated teeth herein described

The multivariate analysis of the sample of isolated teeth described here provide relatively robust results for the large morphotypes, but the classification of the smaller teeth based on this methodology proved to be more difficult. Similar results have been obtained by different authors (e.g. Gerke and Wings 2016). This may be caused in part because the small teeth could represent either smaller taxa or juvenile forms. Since ontogenetic changes in theropod teeth are rather poorly understood, the results of the multivariate analyses should be carefully considered (Gerke and Wings 2016).

Most of the isolated teeth herein analyzed may be related with well-known taxa in the Portuguese Upper Jurassic such as *Ceratosaurus*, *Torvosaurus*, and *Allosaurus* (Table 1). However, there are also some morphotypes that are not clearly related to a particular recognized taxon, including a morphotype assigned to a-non megalosaurid megalosauroid tentatively related to the piatnitzkysaurid *Marshosaurus* and an indeterminate allosauroid distinct from *Allosaurus*. This last morphotype could correspond either to a taxon whose teeth are still unknown (*Lourinhanosaurus*) or may represent a form not yet identified in the Portuguese record.

The most abundant specimens are those assigned to *Torvosaurus*, with a frequency of 22%, followed by those specimens assigned to *Allosaurus* with 20% (Fig. 22a). Small theropod teeth, despite being scarcer than those of large morphotypes, are also relatively abundant and diverse in the Upper Jurassic of the Lusitanian Basin. These teeth show morphologies traditionally related to derived coelurosaurian theropods more typical of Cretaceous strata (e.g. Larson 2008). The taxonomic identification of these morphotypes is complex; however the sample is particularly valuable for documenting these poorly represented clades in the Portuguese fossil record. Two morphotypes compatible with Tyrannosauroidea, a morphotype assigned to Dromaeosauridae, and a morphotype with morphology traditionally assigned to *Richardoestesia* were identified (Table 1).

Stratigraphically, most of the isolated teeth herein analyzed (70%) were collected in the Praia da Amoreira-Porto

Table 1 Taxonomic identification of the different tooth morphotypes described in this work

Morphotypes	Taxonomic identification
Morphotype 1	*Ceratosaurus* sp.
Morphotype 2	cf. *Cetatosaurus*
Morphotype 3	*Torvosaurus gurneyi*
Morphotype 4	cf. *Torvosaurus gurneyi*
Morphotype 5	cf. *Torvosaurus gurneyi*
Morphotype 6	Megalosauroidea
Morphotype 7	Megalosauroidea
Morphotype 8	Megalosauroidea
Morphotype 9	*Allosaurus* sp.
Morphotype 10	*Allosaurus* sp.
Morphotype 11	*Allosaurus* sp.
Morphotype 12	Allosauroidea
Morphotype 13	Tyrannosauroidea
Morphotype 14	Tyrannosauroidea
Morphotype 15	cf. *Richardoestesia*
Morphotype 16	Dromaeosauridae
Morphotype 17	Tetanurae indet.

Novo Formation, which is the most extensive sedimentary unit in the coastal region of the Central Sector of the Lusitanian Basin (Fig. 22b). The greatest diversity of theropod groups is also verified in the Praia da Amoreira-Porto Novo Formation with all morphotypes represented in this unit (Fig. 23). This distribution is coincidental with the abundance of theropods and other dinosaurs known in the Portuguese record based on non-dental remains. However, this higher incidence of finds along the coastline and in particular in the Praia da Amoreira-Porto Novo Formation may in part be an artifact due to more prospection in these areas.

6 Conclusion

The sample of isolated theropod teeth studied here represents a relatively diverse theropod fauna that includes *Ceratosaurus*, *Torvosaurus*, Megalosauroidea indet., *Allosaurus*, Allosauroidea indet., Tyrannosauroidea, cf. *Richardoestesia*, and Dromaeosauridae. This faunal composition indicates a higher diversity of theropods than currently known based on most complete specimens, especially among the small and more derived forms. The results of this analysis partially agree with previous studies of other collections with isolated theropod teeth from the Upper Jurassic of Portugal such as the analysis of the Guimarota coal mine collection. However, the presence of velociraptorine dromaeosaurids, compsognathids, and troodontids, which was reported in Guimarota is not confirmed in the sample analyzed here.

The composition of the theropod fauna resulting from the present study on isolated teeth supports previous hypotheses of a close relationship with the theropod faunas recorded from the North American Morrison Formation. Some similarity with isolated theropod teeth groups described in other Upper Jurassic sites of Europe, especially in Spain and Germany, is also recognized. Some morphotypes identified in this work show some similarity with isolated theropod teeth described in the Tendaguru Formation in Tanzania, which may have some paleobiogeographic implications. However, most of these African specimens are still poorly known and a more

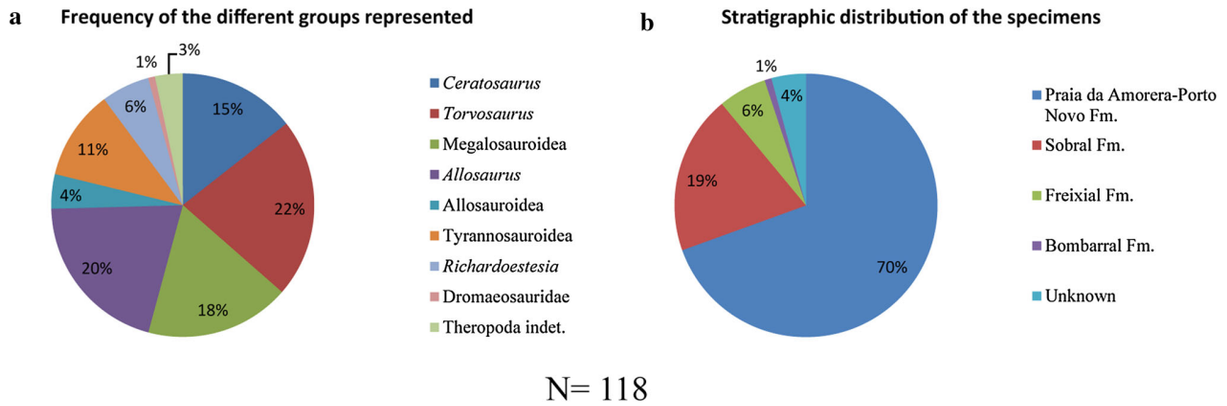

Fig. 22 Diversity and stratigraphic distribution of the isolated theropod teeth in the sample. **a** Frequency of the morphotypes; **b** distribution of the relative abundance of the specimens in the different stratigraphic units cropping out in the Central Sector of the Lusitanian Basin

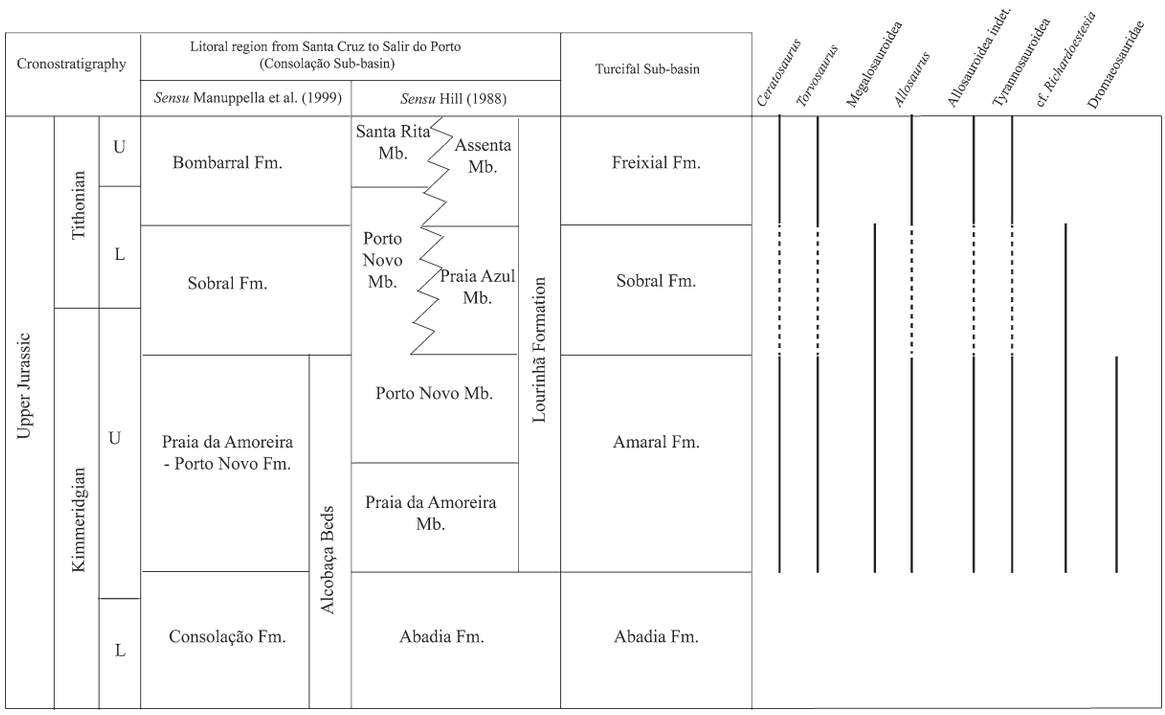

Fig. 23 Stratigraphic distribution of the different morphotypes of teeth identified in the sample

comprehensive comparison of these records is not possible at the moment.

Acknowledgements This work was supported by SFRH/BD/84746/2012 PhD scholarship, financed by the "Fundação para a Ciência e Tecnologia" (Portugal). Individual Grants to E.M. visits for review collections were financed by the Jurassic Foundation, Fundação Luso-Americana para o Desenvolvimento [Grant Number L07-V-22/2010] and Synthesys [Grant Number GB-TAF-2160 and FR-TAF-4911]. The study was also supported by a protocol between CMTV and SHN. We thank to the reviewers D. Weishampel, C. Hendrickx and O. Gerke for the comments and suggestions to the paper. We also thank S. Pereira for photographs of some elements, J. J. Santos and N. Pimentel for field assistance, and for allow accessing specimens to B. C. Silva (SHN, Portugal), R. Castanhinha and C. Tomás (ML, Portugal), V. Santos (MUHNAC, Portugal), E. Espilez and R. Royo-Torres (Fundación Conjunto Paleontológico de Teruel-Dinópolis, Spain), E. D. Berenguer and J. I. Canudo (Museo Paleontológico de Zaragoza, Spain), R. Allain (MNHN, France), L. Chiappe (NHMLAC, USA), L. Ivy and K. Carpenter (DMNH, USA), R. Scheetz and B. Britt (BYU, USA), M. Getty, M. Loewen, and R. Irmis (NHMU, USA), D. Chure (DINO, USA), S. Chapman (NHMUK, UK), P. Jeffery (OUMNH, UK), and T. Schossleitner and D. Schwarz (MfN).

References

Allain, R. (2005). The enigmatic theropod dinosaur *Erectopus superbus* (Sauvage 1882) from the Lower Albian of Louppy-le-Château (Meuse, France). In K. Carpenter (Ed.), *The Carnivorous Dinosaurs* (pp. 72–86). Bloomington: University of Indiana Press.

Allain, R., & Taquet, P. (2000). A new genus of Dromaeosauridae (Dinosauria, Theropoda) from the Upper Cretaceous of France. *Journal of Vertebrate Paleontology, 20,* 404–407. doi:10.1671/0272-4634(2000)020[0404:ANGODD]2.0.CO;2.

Benson, R. B. J. (2010). A description of *Megalosaurus bucklandii* (Dinosauria: Theropoda) from the Bathonian of the UK and the relationships of Middle Jurassic theropods. *Zoological Journal of the Linnean Society, 158*(4), 882–935. doi:10.1111/j.1096-3642.2009.00569.x.

Bouaziz, S., Buffetaut, E., Ghanmi, M., Jaeger, J.-J., Martin, M., Mazin, J.-M., et al. (1988). Nouvelles découvertes de vertébrés fossils dans l'Albien du Sud tunisien. *Bulletin de la Société Géologique de France, 8*(4), 335–339.

Britt, B. (1991). Theropods of Dry Mesa Quarry (Morrison Formation, Late Jurassic), Colorado, with emphasis on the osteology of *Torvosaurus tanneri*. In B. J. Kowallis & K. Seeley (Eds.), *Young University Geology Studies* (Vol. 37, pp. 1–72).

Brochu, C. A. (2003). Osteology of *Tyrannosaurus rex*: Insights from a nearly complete skeleton and high-resolution computed tomographic analysis of the skull. *Journal of Vertebrate Paleontology, Memoir, 7,* 1–138.

Brusatte, S. L., Carr, T. D., Erickson, G. M., Bever, G. S., & Norell, M. A. (2009). A long-snouted, multihorned tyrannosaurid from the Late Cretaceous of Mongolia. *Proceedings of the National academy of Sciences of the United States of America, 41,* 17261–17266. doi:10.1073/pnas.0906911106.

Buckley, L. (2009). Determining ontogenetic and individual variation in Coelophysis bauri (Theropoda: Coelophysoidea) using

multivariate analyses and implications for identifying isolated theropod teeth. *Journal of Vertebrate Paleontology, 29*(Supplement to Number 3), 72A.

Buffetaut, E. (2007). The spinosaurid dinosaur *Baryonyx* (Saurischia, Theropoda) in the Early Cretaceous of Portugal. *Geological Magazine, 144*(6), 1021–1025. doi:10.1017/S0016756807003883.

Buffetaut, E. (2011). An early spinosaurid dinosaur from the Late Jurassic of Tendaguru (Tanzania) and the evolution of the spinosaurid dentition. *Oryctos, 10,* 1–8.

Canudo, J. I., Gasulla, J. M., Gómez-Fernández, D., Ortega, F., Sanz, J. L., & Yagüe, P. (2008). First evidence of isolated teeth referred to Spinosauridae (Theropoda) from the lower Aptian (Lower Cretaceous) from Europe: Arcillas de Morella Formation (Spain). [In Spanish, with English abstract]. *Ameghiniana, Revista de la Asociación Paleontogica Argentina. Buenos Aires, 45*(4), 649–662.

Canudo, J. I., Ruiz-Omeñaca, J. I., Aurell, M., Barco, J. L., & Cuenca-Bescós, G. (2006). A megatheropod tooth from the late Tithonian-middle Berriasian (Jurassic-Cretaceous transition). *Neues Jahrbuch für Geologie und Paläontologie, 239,* 77–99.

Carrano, M. T., Sampson, S. D., & Forster, C. A. (2002). The osteology of *Masiakasaurus knopfleri*, a small abelisauroid (Dinosauria: Theropoda) from the Late Cretaceous of Madagascar. *Journal of Vertebrate Paleontology, 22*(3), 510–534. doi:10.1671/0272-4634(2002)022[0510:TOOMKA]2.0.CO;2.

Charig, A. J., & Milner, A. C. (1997). *Baryonyx walkeri*, a fish-eating dinosaur from the Wealden of Surrey. *Bulletin of the Natural History Museum of London, 53,* 11–70.

Cobos, A., Lockley, M. G., Gascó, F., Royo-Torres, R., & Alcalá, L. (2014). Megatheropods as apex predators in the typically Jurassic ecosystems of the Villar del Arzobispo Formation (Iberian Range, Spain). *Palaeogeography, Palaeoclimatology, Palaeoecology, 399,* 31–41. doi:10.1016/j.palaeo.2014.02.008.

Codrea, V., Smith, T., Dica, P., Folie, A., Garcia, G., Godefroit, P., et al. (2002). Dinosaur egg nests, mammals and other vertebrates from a new Maastrichtian site of the Hateg Basin (Romania). *Comptes Rendus Palevol, 1,* 173–180.

Currie, P. J., & Carpenter, K. (2000). A new specimen of *Acrocanthosaurus atokensis* (Theropoda, Dinosauria) from the Lower Cretaceous Antlers Formation (Lower Cretaceous, Aptian) of Oklahoma, USA. *Geodiversitas, 22*(2), 207–246.

Currie, P. J., & Chen, P.-J. (2001). Anatomy of *Sinosauropteryx prima* from Liaoning, northeastern China. *Canadian Journal of Earth Sciences, 38*(1), 705–727. doi:10.1139/cjes-38-12-1705.

Currie, P. J., Rigby, J. K. Jr., & Sloan, R. E. (1990). Theropod teeth from the Judith River Formation of southern Alberta, Canada. In K. Carpenter & P. J. Currie (Eds.), *Dinosaur Systematics: Approaches and Perspectives* (pp. 107–125) Cambridge: Cambridge University Press. doi:10.1017/cbo9780511608377.011.

Currie, P. J., & Zhao, X.-J. (1993). A new carnosaur (Dinosauria, Theropoda) from the Jurassic of Xinjiang, People's Republic of China. *Canadian Journal of Earth Sciences, 30*(10–11), 2037–2081.

Currie, P. J., & Zhiming, D. (2001). New information on Cretaceous troodontids (Dinosauria, Theropoda) from the People's Republic of China. *Canadian Journal of Earth Sciences, 38,* 1753–1766.

Dal Sasso, C., & Maganuco, S. (2011). *Scipionyx samniticus* (Theropoda: Compsognathidae) from the Lower Cretaceous of Italy. *Osteology, ontogenetic assessment, phylogeny, soft tissue anatomy, taphonomy and palaeobiology*. Memoire della Società Italiana di Scienze Naturali e del Museo Civico do Storia Naturale di Milano. Volume XXXVII (Fascilolo I).

Dal Sasso, C., Maganuco, S., Buffetaut, E., & Mendez, M. A. (2005). New information on the skull of the enigmatic theropod *Spinosaurus*, with remarks on its size and affinities. *Journal of Vertebrate Paleontology, 25*(4), 888–896. doi:10.1671/0272-4634(2005)025[0888:NIOTSO]2.0.CO;2.

Fowler, D. W. (2007). Recently rediscovered baryonychine teeth (Dinosauria: Theropoda): New morphologic data, range extension & similarity to *Ceratosaurus*. *Journal of Vertebrate Paleontology, 27*(3), 76A.

Fürsich, F. T. (1981). Salinity-controlled benthic associations from the Upper Jurassic of Portugal. *Lethaia, 14,* 203–223. doi:10.1111/j.1502-3931.1981.tb01690.x.

Gascó, F., Cobos, A., Royo-Torres, R., Alcalá, L., & Mampel, L. (2012). Theropod teeth diversity from Villar del Arzobispo Formation (Tithonian–Berriasian) at Riodeva (Teruel, Spain). *Palaeobiodiversity and Palaeoenvironments, 92*(2), 273–286.

Gerke, O., & Wings, O. (2016). Multivariate and cladistic analyses of isolated teeth reveal sympatry of theropod dinosaurs in the Late Jurassic of northern Germany. *PLoS One, 11*(7), e0158334. doi:10.1371/journal.pone.0158334.

Gianechini, F. A., Makovicky, P. J., & Apesteguía, S. (2011). The teeth of the unenlagiine theropod *Buitreraptor* from the Cretaceous of Patagonia, Argentina, and the unusual dentition of the Gondwanan dromaeosaurids. *Acta Palaeontologica Polonica, 56*(2), 279–290. doi:10.4202/app.2009.0127.

Gilmore, C. W. (1920). Osteology of the carnivorous Dinosauria in the United States National Museum, with special reference to the genera *Antrodemus* (*Allosaurus*) and *Ceratosaurus*. *Bulletin United States National Museum, 110,* 1–159.

Godefroit, P., Currie, P. J., Hong, L., Yong, S. C., & Zhi-Ming, D. (2008). A new species of *Velociraptor* (Dinosauria: Dromaeosauridae) from the Upper Cretaceous of Northern China. *Journal of Vertebrate Paleontology, 28*(2), 432–438. doi:10.1671/0272-4634(2008)28[432:ANSOVD]2.0.CO;2.

Göhlich, U. B., & Chiappe, L. M. (2006). A new carnivorous dinosaur from the Late Jurassic Solnhofen archipelago. *Nature, 440,* 329–332. doi:10.1038/nature04579.

Hammer, Ø., Harper, D. A. T., Ryan, P. D. (2001). PAST: Paleontological statistics software package for education and data analysis. *Palaeontologia Electronica, 4*(1), 9.

Han, F., Clark, J. M., Xu, X., Sullivan, C., Choiniere, J., & Hone, D. W. E. (2011). Theropod teeth from the Middle-Upper Jurassic Shishugou Formation of northwest Xinjiang, China. *Journal of Vertebrate Paleontology, 31*(1), 111–126. doi:10.1080/02724634.2011.546291.

Harris, J. D. (1998). *A reanalysis of Acrocanthosaurus atokensis, its phylogenetic status, and paleobiogeographic implications, based on a new specimen from Texas*. New Mexico Museum of Natural History and Science, Bulletin (Vol. 13).

Hendrickx, C., & Mateus, O. (2014a). *Torvosaurus gurneyi* n. sp., the largest terrestrial predator from Europe, and a proposed terminology of the maxilla anatomy in nonavian theropods. *PLoS One, 9*(3), e88905. doi:10.1371/journal.pone.0088905.

Hendrickx, C., & Mateus, O. (2014b). Abelisauridae (Dinosauria: Theropoda) from the Late Jurassic of Portugal and dentition-based phylogeny as a contribution for the identification of isolated theropod teeth. *Zootaxa, 3759*(1), 1–74. doi:10.11646/zootaxa.3759.1.1.

Hendrickx, C., Mateus, O., & Araújo, R. (2015). The dentition of megalosaurid theropods. *Acta Palaeontologica Polonica, 60*(3), 627–642. doi:10.4202/app.00056.2013.

Hendrickx, C., Mateus, O., & Araújo, R. (2016). A proposed terminology of theropod Teeth (Dinosauria, Saurischia). *Journal of Vertebrate Paleontology*. doi:10.1080/02724634.2015.982797.

Hill, G. (1988). The sedimentology and lithostratigraphy of the Upper Jurassic Lourinhã Formation, Lusitanian Basin, Portugal. *Unpublished PhD Thesis*, Open University.

Hill, G. (1989). Distal alluvial fan sediments from the Upper Jurassic of Portugal: Controls on their cyclicity and channel formation. *Journal of the Geological Society of London, 146,* 539–555. doi:10.1144/gsjgs.146.3.0539.

Huene, F. (1926). The carnivorous Saurischia in the Jura and Cretaceous Formations, principally in Europe. Revista del Museo de La Plata *29*, 35–167.

Janensch, W. (1920). Ueber Elaphrosaurus bambergi und die Megalosaurier aus den Tendaguru-Schichten Deutsch-Ostafrikas. In: Sitzungsberichte der Gesellschaft naturforschender Freunde zu Berlin (pp. 225–235).

Kirkland, J. I., Zanno, L. E., Sampson, S. D., Clark, J. M., & DeBlieux, D. D. (2005). A primitive therizinosauroid dinosaur from the Early Cretaceous of Utah. *Nature, 7038,* 84–87. doi:10.1038/nature03468.

Kullberg, J. C., Rocha, R. B., Soares, A. F., Rey, J., Terrinha, P., Azerêdo, A. C., Callapez, P., Duarte, L. V., Kullberg, M. C., Martins, L., Miranda, R., Alves, C., Mata, J., Madeira, J., Mateus, O., Moreira, M., & Nogueira. C. R. (2013). A Bacia Lusitaniana: Estratigrafia, Paleogeografia e Tectónica. In R. Dias, A. Araújo, P. Terrinha & J. C. Kullberg (Eds.), *Geologia de Portugal, Volume II—Geologia Meso-cenozóica de Portugal* (pp. 195–347).

Larson, D. W. (2008). Diversity and variation of theropod dinosaur teeth from the uppermost Santonian Milk River Formation (Upper Cretaceous), Alberta: A quantitative method supporting identification of the oldest dinosaur tooth assemblage in Canada. *Canadian Journal of Earth Sciences, 45,* 1455–1468.

Larson, D. W., & Currie, P. J. (2013). Multivariate analyses of small theropod dinosaur teeth and implications for paleoecological turnover through time. *PLoS One, 8*(1), e54329. doi:10.1371/journal.pone.0054329.

Louchart, A. & Pouech, J. (2017). A tooth of Archaeopterygidae (Aves) from the Lower Cretaceous of France extends the spatial and temporal occurrence of the earliest birds. *Cretaceous Research, 73*, 40–46. doi:10.1016/j.cretres.2017.01.004.

Madsen, J. H., Jr. (1976). A second new theropod dinosaur from the Late Jurassic of east central Utah. *Utah Geology, 3*(1), 51–60.

Malafaia, E., Ortega, F., & Escaso, F. (2014). New post-cranial elements assigned to coelurosaurian theropods from the Late Jurassic of Lusitanian Basin, Portugal. Fundamental, 20, 123–126.

Malafaia, E., Ortega, F., Escaso, F., Dantas, P., Pimentel, N., Gasulla, J. M., et al. (2010). Vertebrate fauna at the *Allosaurus* fossil-site of Andrés (Upper Jurassic), Pombal, Portugal. *Journal of Iberian Geology, 36*(2), 193–204. doi:10.5209/rev_JIGE.2010.v36.n2.7.

Malafaia, E., Ortega, F., Escaso, F., & Silva, B. (2015). New evidence of *Ceratosaurus* (Dinosauria: Theropoda) from the Late Jurassic of the Lusitanian Basin, Portugal. *Historical Biology, 27*(7), 938–946. doi:10.1080/08912963.2014.915820.

Manuppella, G., Antunes, M. T., Pais, J., Ramalho, M. M., & Rey, J. (1999). *Notícia explicativa da Folha 30-A, Lourinhã*. Lisboa: Departamento de Geologia do Instituto Geológico e Mineiro.

Mateus, O. (1998). *Lourinhanosaurus antunesi*, a new upper Jurassic allosauroid (Dinosauria: Theropoda) from Lourinhã, Portugal. *Memórias da Academia de Ciências de Lisboa, 37,* 111–124.

Mateus, O., Araújo, R., Natário, C., & Castanhinha, R. (2011). A new specimen of the theropod dinosaur *Baryonyx* from the early Cretaceous of Portugal and taxonomic validity of *Suchosaurus*. *Zootaxa, 2827,* 54–68.

Mateus, O., Dinis, J, & Cunha, P.P. (2013). Upper Jurassic to Lowermost Cretaceous of the Lusitanian Basin, Portugal—Landscapes where dinosaurs walked. Ciências da Terra, número especial VIII.

Mateus, O., Walen, A., & Antunes, M. T. (2006). The large theropod fauna of the Lourinhã Formation (Portugal) and its similarity to the Morrison Formation, with a description of a new species of *Allosaurus*. In J. R. Foster & S. G. Lucas (Eds.), *Paleontology and Geology of the Upper Jurassic Morrison Formation* (Vol. 36, pp. 123–129). New Mexico Museum of Natural History and Science, Bulletin.

Meyer, C. A., & Thuring, B. (2003). Dinosaurs of Switzerland. *Comptes Rendus Palevol, 2,* 103–117. doi:10.1016/S1631-0683(03)00005-8.

Norell, M. A., Makovicky, O. P., & Clark, J. M. (2000). A new troodontid theropod from Ukhaa Tolgod, Mongolia. *Journal of Vertebrate Paleontology, 20*(1), 7–11.

Novas, F. E., Ezcurra, M. D., & Lecuona, A. (2008a). *Orkoraptor burkei* nov. gen. et sp., a large theropod from the Maastrichtian Pari Aike Formation, Southern Patagonia,Argentina. *Cretaceous Research, 29,* 468–480. doi:10.1016/j.cretres.2008.01.001.

Novas, F. E., Pol, D., Canale, J. I., Porfiri, J. D., & Calvo, J. O. (2008b). A bizarre Cretaceous theropod dinosaur from Patagonia and the evolution of Gondwanan dromaeosaurids. *Proceedings of the Royal Society B, 276,* 1101–1107. doi:10.1098/rspb.2008.1554.

Oliveira, J. T., Pereira, H., Ramalho, M., & Antunes, M. T. (1992). Carta Geológica de Portugal, na escala 1:50 0000. Serviços Geológicos de Portugal.

Osmólska, H., Currie, P. J., & Barsbold, R. (2004). Oviraptorosauria. In D.B. Weishampel, P. Dodson & H. Osmólska (Eds.), *The Dinosauria*, Second edition (pp. 517–606). Berkeley, Los Angeles, and London: University of California Press. doi:10.1017/s001675680624305x.

Pérez-Moreno, B. P., Chure, D. J., Pires, C., da Silva, C. M., Santos, V., Dantas, P., et al. (1999). On the presence of *Allosaurus fragilis* (Theropoda: Carnosauria) in the Upper Jurassic of Portugal: First evidence of an intercontinental dinosaur species. *Journal of the Geological Society, 156,* 449–452.

Pérez-Moreno, B. P., Sanz, J. L., Buscalioni, A. D., Moratalla, J. J., Ortega, F., & Rasskin-Gutman, D. (1994). A unique multitoothed ornithomimosaur dinosaur from the Lower Cretaceous of Spain. *Nature, 370,* 363–367. doi:10.1038/370363a0.

Perle, A., Norell, M. A., Chiappe, L. M., & Clark, J. M. (1993). Flightless bird from the Cretaceous of Mongolia. *Nature, 362,* 623–626. doi:10.1038/362623a0.

Peyer, K. (2006). A reconsideration of *Compsognathus* from the upper Tithonian of Canjuers, southeastern France. *Journal of Vertebrate Paleontology, 26*(4), 879–896. doi:10.1671/0272-4634(2006)26[879:AROCFT]2.0.CO;2.

Rauhut, O. W. M. (2002). Dinosaur teeth from the Barremian of Uña, Province of Cuenca, Spain. *Cretaceous Research, 23,* 255–263. doi:10.1006/cres.2002.1003.

Rauhut, O. W. M. (2003). The interrelationships and evolution of basal theropod dinosaurs. *Special Papers in Palaeontology, 69,* 1–213.

Rauhut, O. W. M. (2004). Provenance and anatomy of *Genyodectes serus*, a large-toothed ceratosaur (Dinosauria: Theropoda) from Patagonia. *Journal of Vertebrate Paleontology, 24*(4), 894–902. doi:10.1671/0272-4634(2004)024[0894:PAAOGS]2.0.CO;2.

Rauhut, O. W. M. (2011). Theropod dinosaurs from the Late Jurassic of Tendaguru (Tanzania). *Special Papers in Palaeontology, 86,* 195–239.

Rauhut, O. W. M. (2012). A reappraisal of a putative record of abelisauroid theropod dinosaur from the Middle Jurassic of England. *Proceedings of the Geologists' Association, 123,* 779–786. doi:10.1016/j.pgeola.2012.05.008.

Rauhut, O. W. M., & Fechner, R. (2005). Early development of the facial region in a non-avian theropod dinosaur. *Proceedings of the Royal Society B: Biological Sciences, 272,* 1179–1183. doi:10.1098/rspb.2005.3071.

Rauhut, O. W. M., Milner, A. C., & Moore-Fay, S. (2010). Cranial osteology and phylogenetic position of the theropod dinosaur

Proceratosaurus bradleyi (Woodward, 1910) from the Middle Jurassic of England. *Zoological Journal of the Linnean Society, 158,* 155–195. doi:10.1111/j.1096-3642.2009.00591.x.

Rauhut, O. W. M., & Werner, C. H. (1995). First record of the family Dromaeosauridae (Dinosauria: Theropoda) in the Cretaceous of Gondwana (Wadi Milk Formation, northern Sudan). *Paläontologische Zeitschrift, 69*(3/4), 475–489. doi:10.1007/BF02987808.

Rocha, R. B, Marques, B. L., Kullberg, J. C., Caetano, P. C., Lopes, C., Soares, A. F., Duarte, L.V., Marques, J. F., & Gomes, C. R. (1996). *The 1st and 2nd rifting phases of the Lusitanian Basin: Stratigraphy, sequence analysis and sedimentary evolution*. Final Report C.E.C. Proj. MILUPOBAS 4 vol. Lisboa.

Royo-Torres, R., Cobos, A., & Alcalá, L. (2009). Tooth of a large-sized theropod dinosaur (Allosauroidea) from the Villar del Arzobispo Formation (Tithonian–Berresian) of Riodeva (Spain). [In Spanish, with English abstract]. *Estudios Geológicos, 65*(1), 91–99.

Schneider, S., Fürsich, F. T., & Werner, W. (2009). Sr-isotope of the Upper Jurassic of central Portugal (Lusitanian Basin) based on oyster shells. *International Journal of Earth Sciences, Geologische Rundschau, 98,* 1949–1970. doi:10.1007/s00531-008-0359-3.

Sereno, P. C., Beck, A. L., Dutheil, D. B., Gado, B., Larsson, H. C. E., Lyon, G. H., et al. (1998). A long-snouted predatory dinosaur from Africa and the evolution of spinosaurids. *Science, 282,* 1298–1302.

Serrano-Martínez, A., Ortega, F., Sciscio, L., Tent-Manclús, J. E., Bandera, I. F., & Knoll, F. (2015). New theropod remains from the Tiourarén Formation (?Middle Jurassic, Niger) and their bearing on the dental evolution in basal tetanurans. *Proceedings of the Geologists' Association, 126*(1), 107–118. doi:10.1016/j.pgeola.2014.10.005.

Serrano-Martínez, A., Vidal, D., Sciscio, L., Ortega, F., & Knoll, F. (2016). Isolated theropod teeth from the Middle Jurassic of Niger and the early dental evolution of Spinosauridae. *Acta Palaeontologica Polonica, 61*(2), 403–415. doi:10.4202/app.00101.2014.

Smith, J. B. (2005). Heterodonty in *Tyrannosaurus rex*: Implications for the taxonomic and systematic utility of theropod dentitions. *Journal of Vertebrate Paleontology, 25*(4), 865–887. doi:10.1671/0272-4634(2005)025[0865:HITRIF]2.0.CO;2.

Smith, J. B., Vann, D. R., & Dodson, P. (2005). Dental morphology and variation in theropod dinosaurs: Implications for the taxonomic identification of isolated teeth. *The Anatomical Record Part A, 285,* 699–736. doi:10.1002/ar.a.20206.

Soto, M., & Perea, D. (2008). A ceratosaurid (Dinosauria, Theropoda) from the Late Jurassic-Early Cretaceous of Uruguay. *Journal of Vertebrate Paleontology, 28*(2), 439–444. doi:10.1671/0272-4634(2008)28[439:ACDTFT]2.0.CO;2.

Sues, H.-D., Frey, E., Martill, D. M., & Scott, D. M. (2002). *Irritator challengeri*, a spinosaurid (Dinosauria: Theropoda) from the Lower Cretaceous of Brazil. *Journal of Vertebrate Paleontology, 22*(3), 535–547. doi:10.1671/0272-4634(2002)022[0535:ICASDT]2.0.CO;2.

Sullivan, R. M. (2006). *Saurornitholestes robustus*, n. sp. (Theropoda: Dromaeosauridae) from the Upper Cretaceous Kirtland Formation (De-Na-Zin Member), San Juan Basin, New Mexico. In S. G. Lucas, & R. M. Sullivan (Eds*.), Late Cretaceous vertebrates from the Western Interior* (Vol. 35, pp. 253–256). New Mexico Museum of Natural History and Science Bulletin.

Suñer, M., de Santisteban, C., & Galobart, A. (2005). New Upper Jurassic—Lower Cretaceous Theropoda remains from 'Los Serranos' region (Valencia). [In Spanish, with English abstract] *Revista Española de Paleontología, N.E. X, 10*, 93–99.

Taylor, A. M., Gowland, S., Leary, S., Keogh, K. J., & Martinius, A. W. (2014). Stratigraphical correlation of the Late Jurassic Lourinhã Formation in the Consolação Sub-basin (Lusitanian Basin), Portugal. *Geological Journal, 49*(2), 143–162. doi:10.1002/gj.2505.

Torices, A., Currie, P. J., Canudo, J. I., & Pereda-Suberbiola, X. (2015). Theropod dinosaurs from the Upper Cretaceous of the South Pyrenees Basin of Spain. *Acta Palaeontologica Polonica, 60*(3), 611–626. doi:10.4202/app.2012.0121.

Weigert, A. (1995). Isolierte Zähne von cf. *Archaeopteryx* sp. aus dem Oberen Jura der Kohlengrube Guimarota (Portugal). *Neues Jahrbuch für Geologie und Paläontologie, 9,* 562–576.

Weishampel, D. A., Csiki, Z., Benton, M. J., Grigorescu, D., & Codrea, V. (2010). Palaeobiogeographic relationships of the Hateg biota—Between isolation and innovation. *Palaeogeography, Palaeoclimatology, Palaeoecology, 293,* 419–437.

Madsen, J. H. Jr., & Welles, S. P. (2000). *Ceratosaurus (Dinosauria, Theropoda) a revised osteology*. Utah Geological Survey. Miscellaneous Publication (Vol. 00-2, pp. 1–80).

Werner, W. (1986). Palökologische und biofazielle Analyse des Kimmeridge (Oberjura) von Consolacao, Mittelportugal [Paleoecological and biofacies analysis of the Kimmeridgian (Upper Jurassic) of Consolação, central Portugal]. *Zitteliana, 13,* 3–109.

Williamson, T. E., & Brusatte, S. L. (2014). Small theropod teeth from the Late Cretaceous of the San Juan Basin, northwestern New Mexico and their implications for understanding latest Cretaceous dinosaur evolution. *PLoS One, 9*(4), e93190.

Xu, X., Zhou, Z.-H., & Wang, X.-L. (2000). The smallest known non-avian theropod dinosaur. *Nature, 408,* 705–708.

Zinke, J. (1998). Small theropod teeth from the Upper Jurassic coal mine of Guimarota (Portugal). *Palaontologische Zeitschrift, 72,* 179–189.

Zinke, J., & Rauhut, O. W. M. (1994). Small theropods (Dinosauria, Saurischia) from the Upper Jurassic and Lower Cretaceous of the Iberian Peninsula. *Berliner geowiss. Abh., E13,* 163–177.

SUPPLEMENTARY MATERIAL

Morphotype	Specimen	Geographic provenance	Stratigraphic formation
Morphotype 1	SHN.205	Praia da Corva, Torres Vedras	Praia da Amoreira-Porto Novo
	SHN.236	Porto Dinheiro, Lourinhã	Praia da Amoreira-Porto Novo
	SHN.254	Praia da Corva, Torres Vedras	Praia da Amoreira-Porto Novo
	SHN.457	Porto Dinheiro, Lourinhã	Praia da Amoreira-Porto Novo
	SHN.461	Porto Dinheiro, Lourinhã	Praia da Amoreira-Porto Novo
	SHN.462	Praia da Vermelha, Peniche	Praia da Amoreira-Porto Novo
Morphotype 2	SHN.212	Baleal, Peniche	Praia da Amoreira-Porto Novo
	SHN.218	Praia da Vermelha, Peniche	Praia da Amoreira-Porto Novo
	SHN.263	Praia da Corva, Torres Vedras	Praia da Amoreira-Porto Novo
	SHN.269	Peralta, Lourinhã	? Sobral
	SHN.305a	Cambelas, Torres Vedras	Freixial
	SHN.307	Peralta, Lourinhã	? Sobral
	SHN.321a	Porto Novo, Torres Vedras	Praia da Amoreira-Porto Novo
	SHN.321b	Porto Novo, Torres Vedras	Praia da Amoreira-Porto Novo
	SHN.321c	Porto Novo, Torres Vedras	Praia da Amoreira-Porto Novo
	SHN.359c	Porto Novo, Torres Vedras	Praia da Amoreira-Porto Novo
	SHN.459	Santa Rita, Torres Vedras	Praia da Amoreira-Porto Novo
Morphotype 3	SHN.067	Almagreira, Peniche	Praia da Amoreira-Porto Novo
	SHN.202	Gentias, Torres Vedras	Freixial
	SHN.215	Santa Rita, Torres Vedras	Praia da Amoreira-Porto Novo
	SHN.221	Peralta, Lourinhã	? Sobral
	SHN.247	Valmitão, Lourinhã	Praia da Amoreira-Porto Novo
	SHN.257	Baleal, Peniche	Praia da Amoreira-Porto Novo
	SHN.266	Praia da Corva, Torres Vedras	Praia da Amoreira-Porto Novo
	SHN.268	Porto Dinheiro, Lourinhã	Praia da Amoreira-Porto Novo
	SHN.294	Valmitão, Lourinhã	Praia da Amoreira-Porto Novo
	SHN.303	Salir do Porto, Caldas da Rainha	Praia da Amoreira-Porto Novo
	SHN.304	Valmitão, Lourinhã	Praia da Amoreira-Porto Novo
	SHN.319	Valmitão, Lourinhã	Praia da Amoreira-Porto Novo
	SHN.320	Valmitão, Lourinhã	Praia da Amoreira-Porto Novo
Morphotype 3	SHN.362	Salir do Porto, Caldas da Rainha	Praia da Amoreira-Porto Novo
	SHN.364	Praia da Corva, Torres Vedras	Praia da Amoreira-Porto Novo
	SHN.374	Praia da Corva, Torres Vedras	Praia da Amoreira-Porto Novo
	SHN.381	Valmitão, Lourinhã	Praia da Amoreira-Porto Novo
	SHN.401	Porto Dinheiro, Lourinhã	Praia da Amoreira-Porto Novo
	SHN.440	Valmitão, Lourinhã	Praia da Amoreira-Porto Novo
	SHN.441	Praia dos Frades, Peniche	Praia da Amoreira-Porto Novo
	SHN.442	Valmitão, Lourinhã	Praia da Amoreira-Porto Novo
	SHN.470	Porto Dinheiro, Lourinhã	Praia da Amoreira-Porto Novo
Morphotype 4	SHN.305b	Cambelas, Torres Vedras	Freixial
	SHN.359a	Porto Novo, Torres Vedras	Praia da Amoreira-Porto Novo
	SHN.456	Porto Dinheiro, Lourinhã	Praia da Amoreira-Porto Novo
Morphotype 5	SHN.264	Valmitão, Lourinhã	Praia da Amoreira-Porto Novo
Morphotype 6	SHN.446	Santa Rita, Torres Vedras	Praia da Amoreira-Porto Novo
	SHN.450	Peralta, Lourinhã	? Sobral
Morphotype 7	SHN.226a	Unknown	Unknown
	SHN.226b	Unknown	Unknown
	SHN.239	Between Praia da Corva and Valmitão	Praia da Amoreira-Porto Novo
	SHN.318	Paimogo, Lourinhã	Sobral
	SHN.321d	Porto Novo, Torres Vedras	Praia da Amoreira-Porto Novo
	SHN.330	Peralta, Lourinhã	? Sobral
	SHN.444	Peralta or Atalaia, Lourinhã	? Sobral
	SHN.445	Almagreira, Peniche	Praia da Amoreira-Porto Novo
	SHN.448	Valmitão, Lourinhã	Praia da Amoreira-Porto Novo
	SHN.451	Peralta, Lourinhã	? Sobral
	SHN.452	Peralta, Lourinhã	? Sobral
	SHN.453	Praia da Corva, Torres Vedras	Praia da Amoreira-Porto Novo
	SHN.464	Atalaia, Lourinhã	? Sobral

Table 1S. Geographic and stratigraphic distribution of the specimens studied in this work.

Morphotype 8	SHN.289	Praia da Corva, Torres Vedras	Praia da Amoreira-Porto Novo
	SHN.290	Porto das Barcas, Lourinhã	? Sobral
	SHN.323	Valmitão, Lourinhã	Praia da Amoreira-Porto Novo
	SHN.346	Peralta, Lourinhã	? Sobral
	SHN.359b	Porto Novo, Torres Vedras	Praia da Amoreira-Porto Novo
	SHN.455	Peralta, Lourinhã	? Sobral
Morphotype 9	SHN.255	Porto Dinheiro, Lourinhã	Praia da Amoreira-Porto Novo
	SHN.285	Atalaia, Lourinhã	? Sobral
	SHN.316	Porto das Barcas, Lourinhã	? Sobral
	SHN.321e	Porto Novo, Torres Vedras	Praia da Amoreira-Porto Novo
	SHN.354	Peralta, Lourinhã	? Sobral
	SHN.363b	Almagreira, Peniche	Praia da Amoreira-Porto Novo
	SHN.373	Unknown	Unknown
	SHN.375	Praia dos Frades, Peniche	Praia da Amoreira-Porto Novo
	SHN.384	Praia da Areia Branca, Lourinhã	Praia da Amoreira-Porto Novo
	SHN.449	Porto Dinheiro, Lourinhã	Praia da Amoreira-Porto Novo
Morphotype 10	SHN.204	Santa Rita, Torres Vedras	Praia da Amoreira-Porto Novo
	SHN.232	Valmitão, Lourinhã	Praia da Amoreira-Porto Novo
	SHN.250	Gentias, Torres Vedras	Freixial
	SHN.274	Valmitão, Lourinhã	Praia da Amoreira-Porto Novo
	SHN.275	Unknown	Unknown
	SHN.363a	Almagreira, Peniche	Praia da Amoreira-Porto Novo
	SHN.367	Peralta, Lourinhã	? Sobral
	SHN.454	Amoreiras, Torres Vedras	? Praia da Amoreira-Porto Novo
	SHN.460	Praia da Corva, Torres Vedras	Praia da Amoreira-Porto Novo
Morphotype 11	SHN.227	? Santa Rita, Torres Vedras	? Praia da Amoreira-Porto Novo
	SHN.283	Porto Dinheiro, Lourinhã	Praia da Amoreira-Porto Novo
	SHN.345	Praia da Vermelha, Peniche	Praia da Amoreira-Porto Novo
	SHN.368	Salir do Porto, Caldas da Rainha	Praia da Amoreira-Porto Novo
	SHN.434	Valmitão, Lourinhã	Praia da Amoreira-Porto Novo
Morphotype 12	SHN.213	Gentias, Torres Vedras	Freixial
	SHN.248	Unknown	Unknown
	SHN.344	Praia dos Frades, Peniche	Praia da Amoreira-Porto Novo
	SHN.365	Porto Chão, Torres Vedras	Freixial
	SHN.430	Gentias, Torres Vedras	Freixial
Morphotype 13	SHN.222	Santa Rita, Torres Vedras	Praia da Amoreira-Porto Novo
	SHN.230	Praia da Corva, Torres Vedras	Praia da Amoreira-Porto Novo
	SHN.249	Peralta, Lourinhã	? Sobral
	SHN.253	Valmitão, Lourinhã	Praia da Amoreira-Porto Novo
	SHN.337	Peralta, Lourinhã	? Sobral
	SHN.355	Praia da Corva, Torres Vedras	Praia da Amoreira-Porto Novo
	SHN.429	Porto Dinheiro, Lourinhã	Praia da Amoreira-Porto Novo
	SHN.435	Santa Rita, Torres Vedras	Praia da Amoreira-Porto Novo
Morphotype 14	SHN.209	? Valmitão, Lourinhã	? Praia da Amoreira-Porto Novo
	SHN.219	Valmitão, Lourinhã	Praia da Amoreira-Porto Novo
	SHN.260	? Salir do Porto, Caldas da Rainha	? Praia da Amoreira-Porto Novo
	SHN.265	Foz do Arelho, Caldas da Rainha	Bombarral
	SHN.431	Valmitão, Lourinhã	Praia da Amoreira-Porto Novo
Morphotype 15	SHN.240	Valmitão, Lourinhã	Praia da Amoreira-Porto Novo
	SHN.272	Praia da Corva, Torres Vedras	Praia da Amoreira-Porto Novo
	SHN.278	Praia da Corva, Torres Vedras	Praia da Amoreira-Porto Novo
	SHN.308	Porto Dinheiro, Lourinhã	Praia da Amoreira-Porto Novo
	SHN.309	Valmitão, Lourinhã	Praia da Amoreira-Porto Novo
	SHN.433	Porto das Barcas, Lourinhã	? Sobral
	SHN.436	Praia Azul, Torres Vedras	Sobral
Morphotype 16	SHN.359d	Porto Novo, Torres Vedras	Praia da Amoreira-Porto Novo
Morphotype 17	SHN.277	Peralta, Lourinhã	? Sobral
Incomplete specimens	SHN.223	Santa Rita, Torres Vedras	Praia da Amoreira-Porto Novo
	SHN.432	Porto das Barcas, Lourinhã	? Sobral
	SHN.313	Valmitão, Lourinhã	Praia da Amoreira-Porto Novo

Table 1S (cont.). Geographic and stratigraphic distribution of the specimens studied in this work.

Morphotype	Specimen	CBL	CBW	CH	AL	CBR	CHR	CDA	CMA	MC	DC	DSDI
Morphotype 1	SHN.205	14,3	11,2	35,27	36,04	0,7832	2,46643	81,6558	75,4241	19	12	1,58333
	SHN.236	12,4	13,52	32,56	34,26	1,0903	2,62581	87,2904	71,6594	0	11	0
	SHN.254	17,97	12,6	?	?	0,7012	?	?	?	0	11	0
	SHN.457	14,95	12,36	34,41	37,58	0,8268	2,30167	90,24	66,2964	0	11,5	0
	SHN.461	?	?	34,71	?	?	?	?	?	?	12	?
	SHN.462	12,34	8,33	29,66	31,27	0,675	2,40357	85,9744	71,0693	0	?	?
Morphotype 2	SHN.212	?	?	?	?	?	?	?	?	13,5	14	0,96429
	SHN.218	18,43	7,78	43,02	43,61	0,4221	2,33424	79,6589	75,9304	?	16	?
	SHN.263	27,86	8,89	72,13	74,42	0,3191	2,58902	83,9009	74,448	11,5	12,5	0,92
	SHN.269	19,62	8,49	49,25	52,29	0,4327	2,51019	87,87	70,242	13	13	1
	SHN.305a	20,69	6,48	59,21	59,23	0,3132	2,86177	79,9975	79,885	13	13	1
	SHN.307	6,9	3,05	?	?	0,442	?	?	?	20	19	1,05263
	SHN.321a	29,02	12,92	?	?	0,4452	?	?	?	14,5	11,5	1,26087
	SHN.321b	20,6	9,71	45,75	46,89	0,4714	2,22087	80,503	74,0779	18,5	13	1,42308
	SHN.321c	21,43	8,35	?	?	0,3896	?	?	?	19	15	1,26667
	SHN.359c	6,87	3,41	?	?	0,4964	?	?	?	25	27.5	0,90909
	SHN.459	13,36	5,51	20,56	21,48	0,4124	1,53892	75,9009	67,767	17	15,5	1,09677
Morphotype 3	SHN.067	47,99	22,89	141,52	145,07	0,477	2,94895	84,7021	76,2037	5	5	1
	SHN.202	22,09	12,5	32,05	37,98	0,5659	1,45088	87,5171	57,4319	10	10	1
	SHN.215	25,35	12,62	62,29	63,64	0,4978	2,4572	81,5771	75,4126	7,5	7,5	1
	SHN.221	30,65	17,55	79,79	84,91	0,5726	2,60326	88,9414	69,971	7	6	1,16667
	SHN.247	22,05	12,24	46,22	46,16	0,5551	2,09615	76,021	76,3423	8	11,5	0,69565
	SHN.257	22,68	15,15	57,21	60,15	0,668	2,52249	86,4415	71,6398	8	8	1
	SHN.266	26,31	12,02	57,2	66,55	0,4569	2,17408	97,6281	58,1239	8	10	0,8
	SHN.268	36,27	16,93	91,72	98,86	0,4668	2,52881	90,3614	68,0876	5	6	0,83333
	SHN.294	23,23	13,75	52,25	56,71	0,5919	2,24925	88,8328	67,0917	8	8	1
	SHN.303	34,04	18,48	?	?	0,5429	?	?	?	7	6	1,16667
	SHN.304	25,11	14,17	65,5	65,99	0,5643	2,60852	80,1648	77,8954	?	8	?
	SHN.319	33,69	20,4	93,87	97,05	0,6055	2,78629	85,3697	74,549	8	8,5	0,94118
	SHN.320	39,71	21,6	109,51	116,79	0,5439	2,75774	90,436	69,6581	7	7	1

Table 2S. Morphometric variabless of the isolated teeth studied in this work. All measurements are in millimeters. * estimated measurement

Morphotype 3	SHN.362	26,39	14,58	52,77	57,95	0,5525	1,99962	87,6971	65,4675	6,5	7	0,92857
	SHN.364	21,54	15,58	54,46	54,81	0,7233	2,52832	79,6128	77,7197	?	8	?
	SHN.374	47,09	16,75	104,99	117,91	0,3557	2,22956	93,4197	62,676	6	7	0,85714
	SHN.381	31,28	17,44	?	?	0,5575	?	?	?	8,5	8	1,0625
	SHN.401	48,35	20,64	145,55	152,84	0,4269	3,01034	89,3702	72,2207	7	6	1,16667
	SHN.440	25,75	14,04	70,29	78,49	0,5452	2,72971	97,9193	62,235	0	7	0
	SHN.441	42,44	23,49	123,67	129,76	0,5535	2,914	88,659	72,3223	7,5	6,5	1,15385
	SHN.442	29,1	16,41	84,13	86,24	0,5639	2,89107	84,4282	76,0936	?	7	?
	SHN.470	48,38	19,94	145,54	152,44	0,4122	3,00827	88,8946	72,6578	7	7,5	0,93333
Morphotype 4	SHN.305b	19,32	11,65	49,7	52,38	0,603	2,57246	87,1768	71,3619	?	?	?
	SHN.359a	16,26	7,87	38,76	40,25	0,484	2,38376	83,5666	73,0266	10	10	1
	SHN.456	14,14	9,85	31,76	31,60	0,6966	2,24611	76,4038	77,7375	10,5	8,5	1,24
Morphotype 5	SHN.264	4,35	2,26	6,8	7,62	0,5195	1,56322	83,8536	62,3677	0	25	0
Morphotype 6	SHN.446	6,2	3,57	14,02	14,63	0,5758	2,26129	83,3642	72,0474	?	20	?
	SHN.450	14,76	8,37	30,27	30,49	0,5671	2,05081	76,868	75,1139	?	10	?
Morphotype 7	SHN.226a	10,57	5,4	?	?	0,5109	?	?	?	18	14	1,28571
	SHN.226b	14,87	8,77	29,68	29,53	0,5898	1,99597	74,8177	76,0152	?	14,5	?
	SHN.239	11,53	5,81	25,91	28,9	0,5039	2,24718	92,6611	63,5517	22	19	1,15789
	SHN.318	15,64	8,38	38,34	40,6	0,5358	2,45141	87,0117	70,5435	?	15	?
	SHN.321d	15,61	8,11	32,7	34,03	0,5195	2,09481	81,6153	71,7663	15	12,5	1,2
	SHN.330	10,41	5,35	?	?	0,5139	?	?	?	22	19	1,15789
	SHN.444	11,7	4,97	21,44	24,77	0,4248	1,83248	91,6796	59,8903	20	17	1,17647
	SHN.445	13,8	7,26	34,28	35,9	0,5261	2,48406	85,5575	72,1249	?	16	?
	SHN.448	12,75	5,67	26,99	33,01	0,4447	2,11686	103,649	51,5211	19	16	1,1875
	SHN.451	12,12	5,92	26,54	27,21	0,4884	2,18977	80,3219	73,9001	24	15,5	1,54839
	SHN.452	13,02	5,78	28,11	30,54	0,4439	2,15899	88,0543	66,8977	20	17	1,17647
	SHN.453	13,64	6,65	30,39	33,49	0,4875	2,22801	90,7512	65,1404	19	15	1,26667
	SHN.464	11,49	7,08	24,88	26,89	0,6162	2,16536	87,4064	67,5396	16	13,5	1,18519

Table 2S (cont.). Morphometric variabless of the isolated teeth studied in this work. All measurements are in millimeters. * estimated measurement

Morphotype 8	SHN.289	8,35	4,21	14,42	15,9	0,5042	1,72695	84,6303	64,4324	25	20	1,25
	SHN.290	6,07	2,74	10,57	11,7	0,4514	1,74135	85,2832	64,1146	25	20	1,25
	SHN.323	4,88	3,15	11,61	12,24	0,6455	2,3791	85,7809	71,027	30	25	1,2
	SHN.346	7,42	4,01	?	?	0,5404	?	?	?	30	20	1,5
	SHN.359b	7,33	3,87	16,96	19,37	0,528	2,31378	96,8414	60,1625	30	22,5	1,33333
	SHN.455	3,66	1,73	8,14	8,85	0,4727	2,22404	88,8212	66,8595	35	30	1,16667
Morphotype 9	SHN.255	14,65	7,25	34,16	36,72	0,4949	2,33174	88,2333	68,3993	19	20	0,95
	SHN.285	11,39	5,31	25,21	26,55	0,4662	2,21335	84,271	70,781	17,5	16	1,09375
	SHN.316	9,75	5,46	17,99	18,92	0,56	1,84513	80,5246	69,4696	15,5	16	0,96875
	SHN.321e	11,43	6,07	26,55	28,27	0,5311	2,32283	86,7752	69,6312	15	15,5	0,96774
	SHN.354	7,76	4,37	?	?	0,5631	?	?	?	0	18	0
	SHN.363b	13,03	8,14	31,2	31,79	0,6247	2,39447	80,7885	75,5344	?	18	?
	SHN.373	14,16	7,32	?	?	0,5169	?	?	?	0	15	0
	SHN.375	8,9	4,36	18,51	19,46	0,4899	2,07978	82,8459	70,5606	?	19	?
	SHN.384	13,28	6,66	29,21	31,83	0,5015	2,19955	88,8862	66,5607	16	14	1,14286
	SHN.449	14,64	7,65	35,36	38,28	0,5225	2,4153	90,0357	67,4761	?	16	?
Morphotype 10	SHN.204	15,19	9,88	33,86	34,17	0,6504	2,2291	78,3487	75,9607	13	11,5	1,13043
	SHN.232	13,87	13,91	31,42	31,47	1,0029	2,26532	77,4808	77,0576	10	10	1
	SHN.250	?	?	?	?	?	?	?	?	?	?	?
	SHN.274	17	15,01	29,57	32,42	0,8829	1,73941	84,1511	65,0099	9	10	0,9
	SHN.275	16,3	14,67	34,09	36,17	0,9	2,09141	84,181	69,5577	11	10	1,1
	SHN.363a	19,55	12,7	33,65	37,17	0,6496	1,72123	84,7527	64,2461	13	12	1,08333
	SHN.367	13,87	13,03	29,14	32,32	0,9394	2,10094	90,1959	64,3695	22	20	1,1
	SHN.454	18,96	13,8	38,96	41,27	0,7278	2,05485	83,6108	69,6269	12	10	1,2
	SHN.460	14,44	7,38	33,7	35,14	0,5111	2,3338	83,8124	72,3535	16	14	1,14286
Morphotype 11	SHN.227	?	?	?	?	?	?	?	?	?	17,5	?
	SHN.283	3,08	1,23	5,64	6,09	0,3994	1,83117	83,5597	66,8226	30	30	1
	SHN.345	6,56	3,35	18,24	17,14	0,5107	2,78049	68,6276	88,9513	25	25	1
	SHN.368	5,61	2,92	15,89	16,47	0,5205	2,83244	86,0582	74,2241	25	25	1
	SHN.434	4,8	2,48	8,43	8,93	0,5167	1,75625	80,3571	68,2839	25	25	1

Table 2S (cont.). Morphometric variabless of the isolated teeth studied in this work. All measurements are in millimeters. * estimated measurement

Morphotype 12	SHN.213	24,06	13,46	42,82	49,84	0,5594	1,77972	91,7105	59,1632	12	12	1
	SHN.248	16,99	9,09	29,23	36,44	0,535	1,72042	98,5841	52,0112	13	12,5	1,04
	SHN.344	20,36	12,37	35,79	38,81	0,6076	1,75786	83,1226	66,1175	10	10,5	0,95238
	SHN.365	18,76	11,27	40,83	41,84	0,6007	2,17644	80,1541	73,8964	17	13,5	1,25926
	SHN.430	22,57	11,63	38,86	43,68	0,5153	1,72175	86,7564	62,6044	8	?	?
Morphotype 13	SHN.222	10,36	5,96	21,73	24,51	0,5753	2,09749	92,3945	62,3245	20	16	1,25
	SHN.230	9,45	5,7	20,48	21,14	0,6032	2,1672	81,0972	73,0066	?	18	?
	SHN.249	11,11	6,6	25,22	26,95	0,5941	2,27003	86,8239	69,0937	19	17	1,11765
	SHN.253	12,27	6,93	27,78	30,47	0,5648	2,26406	90,4705	65,7385	0	16	0
	SHN.337	14,3	7,52	26,74	28,61	0,5259	1,86993	82,9106	67,8886	11	12	0,91667
	SHN.355	9,23	5,39	21,31	21,8	0,584	2,30878	80,8392	74,6813	0	16	0
	SHN.429	11,24	5	15,24	19,14	0,4448	1,35587	91,0313	52,7531	0	18	0
	SHN.435	12,28	6,54	32,64	35,06	0,5326	2,65798	90,8674	68,5681	?	17	?
Morphotype 14	SHN.209	4,63	3,49	12,75	12,86	0,7538	2,75378	81,0044	78,2482	30	17,5	1,71429
	SHN.219	4,4	3,26	8,86	8,53	0,7409	2,01364	70,4661	79,545	?	?	?
	SHN.260	7,12	4,52	17,17	17,64	0,6348	2,41152	82,1441	74,5174	25	26	0,9615
	SHN.265	7,68	5,36	22,1	23,49	0,6979	2,8776	90,6968	70,1774	22	16	1,375
	SHN.431	4,35	3,53	9,23	10,11	0,8115	2,12184	88,7601	65,8813	0	20	0
Morphotype 15	SHN.240	6,89	4,62	?	?	0,6705	?	?	?	?	20	?
	SHN.272	7,11	3,86	13,59	14,83	0,5429	1,91139	85,8363	65,9943	0	20	0
	SHN.278	7	4,5	13,04	13,59	0,6429	1,86286	79,5976	70,4564	?	?	?
	SHN.308	7,34	4,23	14,77	16,47	0,5763	2,01226	89,8181	63,7375	25	22,5	1,11111
	SHN.309	7,73	4,18	?	?	0,5408	?	?	?	0	?	?
	SHN.433	9,82	5,54	17,61	19,21	0,5642	1,79328	84,2926	65,6856	0	?	?
	SHN.436	7,29	3,73	12,91	13,06	0,5117	1,77092	75,0107	72,5692	0	20	0
Morphotype 16	SHN.359d	8,88	4,76	17,5	19,06	0,536	1,97072	86,304	66,3321	0	17,5	0
Morphotype 17	SHN.277	12,26	6,62	17,02	19,64	0,54	1,38825	83,5308	59,2317	?	15	?
Incomplete specimens	SHN.223	5,08	2,63	10,04	10,35	0,5177	1,97638	79,3213	72,2105	30	?	?
	SHN.313	4,6	2,96	12,5	12,7	0,6435	2,71739	82,0698	77,0419	?	?	?
	SHN.432	10,03	5,76	19,57	19,81	0,5743	1,95115	76,7399	73,9224	0	0	0

Table 2S (cont.). Morphometric variabless of the isolated teeth studied in this work. All measurements are in millimeters. * estimated measurement

	Specimen	Classification DFA	Prob	2nd Class	Prob	Res
Morphotype 1	SHN.205	*Raptorex*	0,965	*Berberosaurus*	0,035	
	SHN.236	*Megalosaurus*	0,822	*Torvosaurus*	0,178	
	SHN.457	*Torvosaurus*	0,518	*Megalosaurus*	0,482	
Morphotype 2	SHN.263	*Megalosaurus*	0,519	*Berberosaurus*	0,416	
	SHN.269	*Erectopus*	0,408	*Piatnitzkysaurus*	0,377	
	SHN.305a	*Piatnitzkysaurus*	0,719	*Berberosaurus*	0,254	
	SHN.321b	*Berberosaurus*	0,628	*Raptorex*	0,371	
	SHN.459	*Alioramus*	0,886	*Berberosaurus*	0,109	
Morphotype 3	SHN.067	*Megalosaurus*	0,746	*Giganotosaurus*	0,249	61,1%
	SHN.202	*Giganotosaurus*	0,494	*Megalosaurus*	0,424	
	SHN.215	*Megalosaurus*	0,615	*Torvosaurus*	0,285	
	SHN.221	*Torvosaurus*	0,688	*Megalosaurus*	0,283	
	SHN.247	*Giganotosaurus*	0,452	*Torvosaurus*	0,370	
	SHN.257	*Torvosaurus*	0,482	*Giganotosaurus*	0,310	
	SHN.266	*Torvosaurus*	0,755	*Giganotosaurus*	0,127	
	SHN.268	*Torvosaurus*	0,666	*Megalosaurus*	0,334	
	SHN.294	*Torvosaurus*	0,835	*Megalosaurus*	0,110	
	SHN.319	*Giganotosaurus*	0,478	*Megalosaurus*	0,280	
	SHN.320	*Torvosaurus*	0,460	*Giganotosaurus*	0,478	
	SHN.362	*Torvosaurus*	0,954	*Megalosaurus*	0,045	
	SHN.374	*Torvosaurus*	0,908	*Megalosaurus*	0,092	
	SHN.401	*Giganotosaurus*	0,727	*Megalosaurus*	0,272	
	SHN.440	*Megalosaurus*	1,000			
	SHN.441	*Giganotosaurus*	0,601	*Megalosaurus*	0,264	
	SHN.470	*Giganotosaurus*	0,602	*Megalosaurus*	0,394	
Morphotype 4	SHN.359a	*Giganotosaurus*	0,670	*Megalosaurus*	0,281	
	SHN.456	*Giganotosaurus*	0,502	*Majungasaurus*	0,190	
Morphotype 5	SHN.264	*Giganotosaurus*	0,536	*Megalosaurus*	0,232	
Morphotype 6	SHN.446	*Deinonychus*	0,775	*Masiakasaurus*	0,222	54,6%
	SHN.450	*Majungasaurus*	0,740	*Giganotosaurus*	0,129	
Morphotype 7	SHN.239	*Allosaurus*	0,779	*Berberosaurus*	0,200	
	SHN.321d	*Piatnitzkysaurus*	0,560	*Berberosaurus*	0,198	
	SHN.444	*Raptorex*	0,990	*Berberosaurus*	0,007	
	SHN.448	*Raptorex*	0,984	*Berberosaurus*	0,013	
	SHN.451	*Berberosaurus*	0,980	*Raptorex*	0,018	
	SHN.452	*Raptorex*	0,976	*Berberosaurus*	0,015	
	SHN.453	*Raptorex*	0,983	*Berberosaurus*	0,016	
	SHN.464	*Alioramus*	0,528	*Berberosaurus*	0,285	
Morphotype 8	SHN.289	*Masiakasaurus*	0,998	*Deinonychus*	0,002	61,1%
	SHN.290	*Masiakasaurus*	0,822	*Deinonychus*	0,178	
	SHN.323	*Proceratosaurus*	0,543	*Masiakasaurus*	0,457	
	SHN.455	*Coelophysis*	0,981	*Velociraptor*	0,012	
Morphotype 9	SHN.255	*Raptorex*	0,987	*Berberosaurus*	0,012	
	SHN.285	*Raptorex*	0,956	*Berberosaurus*	0,036	
	SHN.316	*Alioramus*	0,524	*Berberosaurus*	0,337	
	SHN.321e	*Berberosaurus*	0,451	*Raptorex*	0,451	
	SHN.384	*Berberosaurus*	0,559	*Allosaurus*	0,181	

Table 3S. Results of the DFA analysis based on the complete dataset of Gerke and Wings (2016). Prob, probability; Res, resolution.

Morphotype 10	SHN.204	*Genyodectes*	0,751	*Allosaurus*	0,105	61,1%
	SHN.232	*Allosaurus*	0,311	*Giganotosaurus*	0,295	
	SHN.274	*Giganotosaurus*	0,678	*Megalosaurus*	0,284	
	SHN.275	*Megalosaurus*	0,454	*Giganotosaurus*	0,244	
	SHN.363a	*Duriavenator*	0,969	*Megalosaurus*	0,020	
	SHN.367	*Acrocanthosaurus*	0,731	*Berberosaurus*	0,190	
	SHN.454	*Megalosaurus*	0,392	*Daspletosaurus*	0,367	
	SHN.460	*Berberosaurus*	0,497	*Raptorex*	0,377	
Morphotype 11	SHN.283	*Velociraptor*	0,997	*Masiakasaurus*	0,003	
	SHN.345	*Masiakasaurus*	0,799	*Allosaurus*	0,200	
	SHN.368	*Masiakasaurus*	1,000			
	SHN.434	*Masiakasaurus*	0,959	*Velociraptor*	0,041	
Morphotype 12	SHN.213	*Megalosaurus*	0,759	*Giganotosaurus*	0,117	
	SHN.248	*Megalosaurus*	0,583	*Berberosaurus*	0,230	
	SHN.344	*Giganotosaurus*	0,688	*Megalosaurus*	0,249	
	SHN.365	*Berberosaurus*	0,985	*Acrocanthosaurus*	0,007	
Morphotype 13	SHN.222	*Raptorex*	0,979	*Berberosaurus*	0,018	61,1%
	SHN.249	*Raptorex*	0,983	*Berberosaurus*	0,013	
	SHN.253	*Megalosaurus*	0,797	*Torvosaurus*	0,203	
	SHN.337	*Majungasaurus*	0,464	*Megalosaurus*	0,214	
	SHN.355	*Megalosaurus*	0,992	*Torvosaurus*	0,008	
	SHN.429	*Torvosaurus*	0,933	*Megalosaurus*	0,067	
Morphotype 14	SHN.209	*Masiakasaurus*	1,000			
	SHN.260	*Masiakasaurus*	1,000			
	SHN.265	*Berberosaurus*	0,999			
	SHN.431	*Megalosaurus*	0,692	*Giganotosaurus*	0,235	
Morphotype 15	SHN.272	*Megalosaurus*	0,515	*Torvosaurus*	0,388	
	SHN.308	*Masiakasaurus*	1,000			
	SHN.436	*Torvosaurus*	0,507	*Megalosaurus*	0,432	
Morphotype 16	SHN.359d	*Majungasaurus*	0,286	*Deinonychus*	0,283	62,6%
Morph 17	SHN.277	*Neovenator*	0,548	*Berberosaurus*	0,162	
Incomplete specimens	SHN.223	*Masiakasaurus*	0,798	*Liliensternus*	0,146	
	SHN.313	*Masiakasaurus*	0,991	*Baryonyx*	0,009	
	SHN.432	*Majungasaurus*	0,363	*Alioramus*	0,233	

Table 3S (cont.). Results of the DFA analysis based on the complete dataset of Gerke and Wings (2016). Prob, probability; Res, resolution.

	Spec.	Classification DFA	Prob	2nd Class	Prob	Res	Classification DFA	Prob	2nd Class	Prob	Res
Morph 1	SHN.205	*Raptorex*	1,000				*Erectopus*	0,480	*Neovenator*	0,390	
	SHN.236	*Torvosaurus*	1,000				*Torvosaurus*	1,000			
	SHN.457	*Torvosaurus*	0,996	*Acrocanthosaurus*	0,004		*Torvosaurus*	1,000			
Morph 2	SHN.263	*Piatnitzkysaurus*	0,954	*Erectopus*	0,042		*Erectopus*	0,795	*Neovenator*	0,205	
	SHN.269	*Piatnitzkysaurus*	0,613	*Erectopus*	0,386		*Erectopus*	0,947	*Neovenator*	0,048	
	SHN.305a	*Piatnitzkysaurus*	0,999	*Raptorex*	0,001		*Erectopus*	0,995	*Neovenator*	0,005	
	SHN.321b	*Raptorex*	1,000				*Neovenator*	0,997	*Acrocanthosaurus*	0,003	
	SHN.459	*Alioramus*	0,995	*Allosaurus*	0,003		*Alioramus*	0,897	*Neovenator*	0,088	
Morph 3	SHN.067	*Carcharodontosaurus*	1,000				*Torvosaurus*	1,000			
	SHN.202	*Tyrannosaurus*	0,840	*Daspletosaurus*	0,081		*Torvosaurus*	0,653	*Gorgosaurus*	0,109	
	SHN.215	*Torvosaurus*	1,000				*Torvosaurus*	0,593	*Majungasaurus*	0,364	
	SHN.221	*Torvosaurus*	1,000				*Torvosaurus*	0,995	*Tyrannosaurus*	0,005	
	SHN.247	*Carcharodontosaurus*	0,841	*Torvosaurus*	0,147		*Torvosaurus*	0,538	*Megalosaurus*	0,433	
	SHN.257	*Torvosaurus*	0,989	*Ceratosaurus* pm	0,010		*Torvosaurus*	0,508	*Daspletosaurus*	0,453	
	SHN.266	*Torvosaurus*	0,969	*Carcharodontosaurus*	0,030	80,5%	*Torvosaurus*	0,994	*Tyrannosaurus*	0,006	85,2%
	SHN.268	*Torvosaurus*	1,000				*Torvosaurus*	0,947	*Tyrannosaurus*	0,063	
	SHN.294	*Ceratosaurus* pm	0,371	*Ceratosaurus*	0,324		*Ceratosaurus*	0,500	*Megalosaurus*	0,234	
	SHN.319	*Carcharodontosaurus*	0,991	*Torvosaurus*	0,009		*Torvosaurus*	0,972	*Erectopus*	0,017	
	SHN.320	*Carcharodontosaurus*	0,888	*Torvosaurus*	0,112		*Torvosaurus*	1,000			
	SHN.362	*Tyrannosaurus*	0,897	*Acrocanthosaurus*	0,103		*Megalosaurus*	0,999	*Tyrannosaurus*	0,001	
	SHN.374	*Acrocanthosaurus*	0,748	*Carcharodontosaurus*	0,252		*Torvosaurus*	0,949	*Carcharodontosaurus*	0,050	
	SHN.401	*Carcharodontosaurus*	0,815	*Raptorex*	0,112		*Torvosaurus*	1,000			
	SHN.440	*Acrocanthosaurus*	0,989	*Majungasaurus*	0,007		*Torvosaurus*	0,993	*Acrocanthosaurus*	0,007	
	SHN.441	*Carcharodontosaurus*	1,000				*Torvosaurus*	0,998	*Erectopus*	0,002	
	SHN.470	*Piatnitzkysaurus*	0,895	*Genyodectes*	0,097		*Erectopus*	0,812	*Torvosaurus*	0,188	
Morph 4	SHN.359a	*Carcharodontosaurus*	0,973	*Allosaurus*	0,021		*Allosaurus*	0,578	*Majungasaurus*	0,418	
	SHN.456	*Majungasaurus*	0,675	*Allosaurus*	0,306		*Majungasaurus*	0,930	*Allosaurus*	0,065	
Morph 5	SHN.264	*Torvosaurus*	0,980	*Carcharodontosaurus*	0,020		*Neovenator*	1,000			
Morph 6	SHN.446	*Deinonychus*	0,771	*Masiakasaurus*	0,221	82,1%	*Dromaeosaurus*	0,883	*Raptorex*	0,059	76,9%
	SHN.450	*Majungasaurus*	0,902	*Allosaurus*	0,046		*Majungasaurus*	0,900	*Indosuchus*	0,053	

Table 4S. MResults of the DFA analysis based on the reduced dataset of Gerke and Wings (2016) and on the dataset of Hendrickx et al. (2015). The green lines mark the specimens identified to the same taxon on both analyses. Inc spec, incomplete specimens; Morph, morphotype; Prob, probability; Res, resolution; Spec, specimen.

Morph 7	SHN.239	*Allosaurus*	0,606	*Raptorex*	0,250		*Megalosaurus*	1,000			
	SHN.321d	*Piatnitzkysaurus*	0,663	*Erectopus*	0,238		*Erectopus*	0,735	*Alioramus*	0,080	
	SHN.444	*Raptorex*	0,994	*Allosaurus*	0,004		Dromaeosaurid	0,996	*Megalosaurus*	0,004	
	SHN.448	*Raptorex*	0,994	*Allosaurus*	0,006		*Megalosaurus*	0,932	*Allosaurus*	0,046	
	SHN.451	*Raptorex*	0,984	*Allosaurus*	0,016		*Acrocanthosaurus*	1,000			
	SHN.452	*Raptorex*	0,986	*Allosaurus*	0,014		*Megalosaurus*	0,691	Dromaeosaurid	0,307	
	SHN.453	*Raptorex*	0,998	*Allosaurus*	0,002		Dromaeosaurid	0,501	*Megalosaurus*	0,479	
	SHN.464	*Alioramus*	0,601	*Piatnitzkysaurus*	0,198		*Erectopus*	0,886	*Alioramus*	0,039	
Morph 8	SHN.289	*Masiakasaurus*	0,998	*Deinonychus*	0,002		*Deinonychus*	0,979	*Megalosaurus*	0,014	
	SHN.290	*Masiakasaurus*	0,822	*Deinonychus*	0,178		*Deinonychus*	0,858	*Masiakasaurus*	0,142	
	SHN.323	*Proceratosaurus*	0,543	*Masiakasaurus*	0,457		*Masiakasaurus*	0,662	*Eoraptor*	0,268	
	SHN.455	*Masiakasaurus*	1,000				*Masiakasaurus*	0,733	*Velociraptor*	0,242	
Morph 9	SHN.255	*Raptorex*	0,999	*Allosaurus*	0,001		*Megalosaurus*	1,000			
	SHN.285	*Raptorex*	0,990	*Allosaurus*	0,010		*Megalosaurus*	0,546	*Raptorex*	0,357	
	SHN.316	*Alioramus*	0,834	*Raptorex*	0,090		*Alioramus*	0,981	*Megalosaurus*	0,016	
	SHN.321e	*Raptorex*	0,736	*Erectopus*	0,110		*Allosaurus*	0,417	*Erectopus*	0,282	
	SHN.384	*Raptorex*	0,540	*Allosaurus*	0,373	80,5%	*Erectopus*	0,643	*Allosaurus*	0,211	85,2%
Morph 10	SHN.204	*Genyodectes*	0,630	*Allosaurus*	0,322		*Allosaurus*	0,634	*Megalosaurus*	0,198	
	SHN.232	*Torvosaurus*	0,637	*Allosaurus*	0,341		*Allosaurus*	0,953	*Indosuchus*	0,026	
	SHN.274	*Allosaurus*	0,716	*Tyrannosaurus*	0,254		*Torvosaurus*	0,646	*Allosaurus*	0,305	
	SHN.275	*Carcharodontosaurus*	0,915	*Allosaurus*	0,072		*Allosaurus*	0,636	*Gorgosaurus*	0,345	
	SHN.363a	*Daspletosaurus*	0,487	*Acrocanthosaurus*	0,388		*Daspletosaurus*	0,835	*Mapusaurus*	0,132	
	SHN.367	*Acrocanthosaurus*	1,000				*Spinosaurus*	0,995	*Acrocanthosaurus*	0,004	
	SHN.454	*Torvosaurus*	0,698	*Daspletosaurus*	0,243		*Gorgosaurus*	0,718	*Daspletosaurus*	0,199	
	SHN.460	*Raptorex*	0,828	*Allosaurus*	0,161		*Genyodectes*	0,491	*Megalosaurus*	0,243	
Morph 11	SHN.283	*Velociraptor*	0,997	*Masiakasaurus*	0,003		*Eoraptor*	0,959	*Masiakasaurus*	0,036	
	SHN.345	*Masiakasaurus*	0,798	*Allosaurus*	0,200		*Eoraptor*	0,701	*Nuthetes*	0,297	
	SHN.368	*Masiakasaurus*	1,000				*Eoraptor*	0,999	*Megalosaurus*	0,001	
	SHN.434	*Masiakasaurus*	0,959	*Velociraptor*	0,041		*Masiakasaurus*	0,834	*Nuthetes*	0,165	
Morph 12	SHN.213	*Acrocanthosaurus*	0,909	*Tyrannosaurus*	0,090		*Mapusaurus*	0,949	*Megalosaurus*	0,043	
	SHN.248	*Genyodectes*	0,772	*Erectopus*	0,192		*Megalosaurus*	0,317	*Erectopus*	0,236	
	SHN.344	*Carcharodontosaurus*	0,916	*Tyrannosaurus*	0,047		*Duriavenator*	0,482	*Ceratosaurus*	0,215	
	SHN.365	*Allosaurus*	0,427	*Acrocanthosaurus*	0,353		*Neovenator*	0,980	*Acrocanthosaurus*	0,041	

Table 4S (cont.). MResults of the DFA analysis based on the reduced dataset of Gerke and Wings (2016) and on the dataset of Hendrickx et al. (2015). The green lines mark the specimens identified to the same taxon on both analyses. Inc spec, incomplete specimens; Morph, morphotype; Prob, probability; Res, resolution; Spec, specimen.

Morph 13	SHN.222	*Raptorex*	0,999	*Allosaurus*	0,001	80,5%	Dromaeosaurid	0,875	*Megalosaurus*	0,125	85,2%
	SHN.249	*Raptorex*	0,998	*Allosaurus*	0,002		Dromaeosaurid	0,785	*Megalosaurus*	0,215	
	SHN.253	*Torvosaurus*	1,000				*Torvosaurus*	1,000			
	SHN.337	*Majungasaurus*	0,780	*Allosaurus*	0,179		*Ceratosaurus*	0,438	*Majungasaurus*	0,397	
	SHN.355	*Torvosaurus*	1,000				*Torvosaurus*	0,998	*Nuthetes*	0,002	
	SHN.429	*Masiakasaurus*	1,000				*Torvosaurus*	0,991	*Genyodectes*	0,004	
Morph 14	SHN.209	*Masiakasaurus*	1,000				*Masiakasaurus*	0,997	*Eoraptor*	0,003	
	SHN.260	*Masiakasaurus*	1,000				*Nuthetes*	0,999	*Eoraptor*	0,001	
	SHN.265	*Raptorex*	0,821	*Allosaurus*	0,179		*Megalosaurus*	0,998	*Raptorex*	0,002	
	SHN.431	*Torvosaurus*	1,000				*Torvosaurus*	0,667	*Neovenator*	0,333	
Morph 15	SHN.272	Megaraptor juvenile	0,982	*Torvosaurus*	0,018		*Nuthetes*	0,551	*Torvosaurus*	0,396	
	SHN.308	*Masiakasaurus*	1,000				*Megalosaurus*	0,981	*Nuthetes*	0,015	
	SHN.436	Megaraptor juvenile	0,999	*Torvosaurus*	0,001		*Torvosaurus*	0,924	*Erectopus*	0,067	
Morph 16	SHN.359d	*Majungasaurus*	0,269	*Deinonychus*	0,266	67,5%	*Australovenator*	0,770	Raptorex	0,172	58,3%
Morph 17	SHN.277	*Neovenator*	0,589	*Majungasaurus*	0,201		*Neovenator*	0,379	*Abelisaurus*	0,344	
Inc spec	SHN.223	*Masiakasaurus*	0,798	*Liliensternus*	0,146		*Liliensternus*	0,355	*Masiakasaurus*	0,328	
	SHN.313	*Masiakasaurus*	0,991	*Baryonyx*	0,009		*Nuthetes*	0,644	*Masiakasaurus*	0,328	
	SHN.432	*Majungasaurus*	0,397	*Alioramus*	0,255		*Dubreuillosaurus*	0,297	*Alioramus*	0,328	

Table 4S (cont.). MResults of the DFA analysis based on the reduced dataset of Gerke and Wings (2016) and on the dataset of Hendrickx et al. (2015). The green lines mark the specimens identified to the same taxon on both analyses. Inc spec, incomplete specimens; Morph, morphotype; Prob, probability; Res, resolution; Spec, specimen.

8.3. THE PALEOBIOGEOGRAPHIC CONTEXT OF THE LATE JURASSIC PORTUGUESE THEROPODS

Traditionally, the continental vertebrate faunas from the Late Jurassic of the Lusitanian Basin were interpreted as closely related with those of correlative units from the Tendaguru and Morrison formations. Among the dinosaur record of the more than sixteen taxa known from Kimmeridgian-Tithonian sediments of the Lusitanian Basin several were first interpreted as belonging to forms shared with the North American record, including the ornithischians *Stegosaurus* (Escaso et al. 2007a) and *Uteodon* (Escaso et al. 2010, McDonald 2011), the sauropods *Apatosaurus* (Lapparent and Zbyszewski 1957; currently *Lourinhasaurus sensu* Dantas et al. 1998; Antunes and Mateus 2003; Mocho et al. 2014) and *Brachiosaurus* (Lapparent and Zbyszewski 1957; currently *Lusotitan sensu* Antunes and Mateus 2003) and the theropods *Ceratosaurus* (Mateus and Antunes 2000a; Malafaia et al. 2015), *Torvosaurus* (Mateus and Antunes 2000b; Hendrickx and Mateus 2014), *Allosaurus* (Pérez-Moreno et al. 1999; Rauhut and Fechner 2005; Mateus et al. 2006), and *Aviatyrannis* (Rauhut 2003). This faunal composition was explained by faunal exchanges between the landmasses of the East North America and Iberia during the Late Jurassic (e.g. Pérez-Moreno et al. 1999; Escaso et al. 2007a; Brikiatis 2016).

Current paleogeographical reconstructions indicate that since the Late Jurassic, the landmasses of North America and West Eurasia have been separated by shallow and/or deeper marine basins and channels, which development was associated with the North Atlantic rift system (Ziegler 1988; Scotese 2002; Dercourt et al. 2000). For this time interval, several marine seaways have been reconstructed on the basis of distribution patterns of marine invertebrates (Cecca 2002). One of these marine passages is the "Viking Corridor" (Westermann 1993), which was an epicontinental seaway nearly superimposed to the North Atlantic rift, that acted (intermittently) as a marine dispersal way since the late Early Jurassic (Bardet et al. 2014; Brikiatis 2016). This paleogeographical context should have limited the possibility of direct dispersal of terrestrial faunas between North America and Europa. During much of the Jurassic and Cretaceous, Europe was composed by several major islands (e.g. Britain, Iberia and Eastern Europe), some of which had intermittent contact with North America or Asia (Upchurch et al. 2002) and some authors (e.g. Escaso et al. 2007a; Brikiatis 2016) suggest the existence of ephemeral land bridges between East North America and Iberia during the late Kimmeridgian to the earliest Tithonian (Fig. 8.3.1).

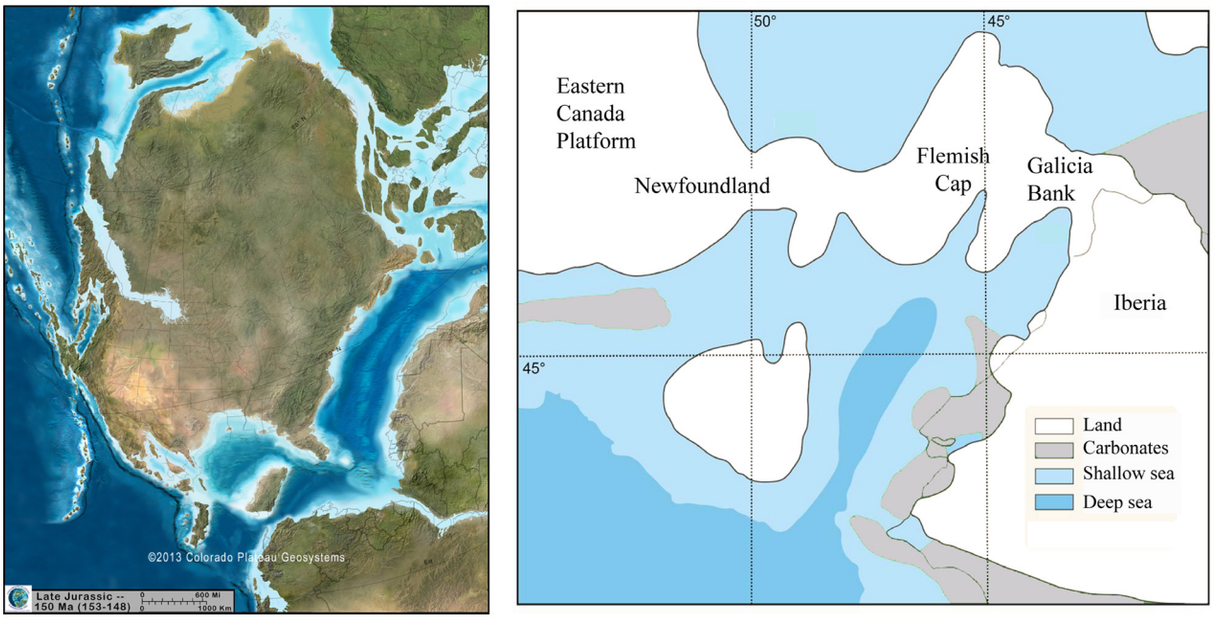

Figure 8.3.1. Paleogeographical reconstruction of the central Atlantic during the Late Jurassic based on Ron Blakey (2013) and interpretation of a land bridge between North America and Europe at chron M23 (latest Kimmeridgian, 153 Ma) proposed by some authors (modified from Brikiatis 2016).

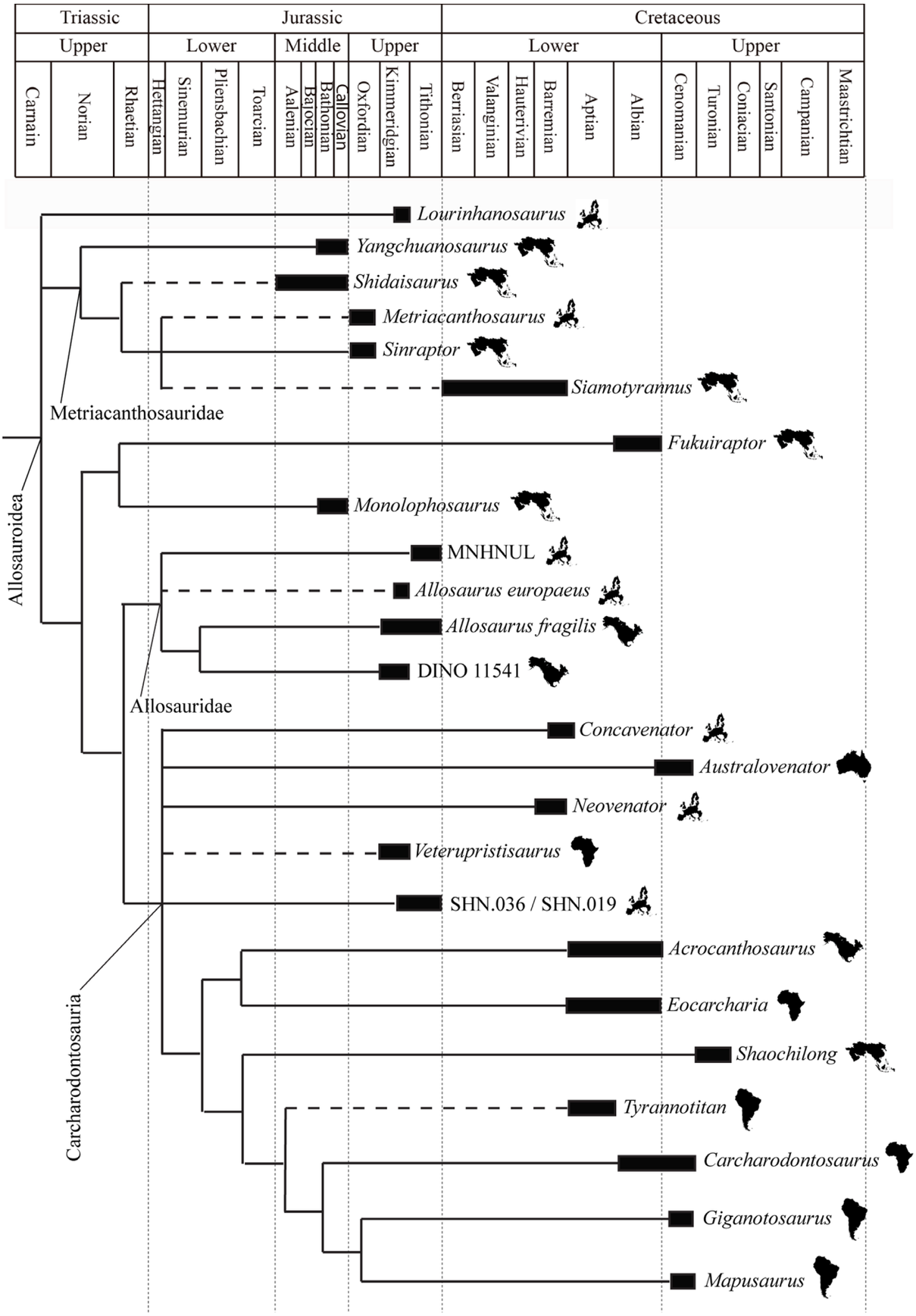

Figure 8.3.2. Time-calibrated strict consensus cladogram from 1027 most parsimonious trees [Tree length = 369 steps; CI = 0.510 and RI = 0.594] including the allosauroid taxa from the Late Jurassic of the Lusitanian Basin. The dashed lines represent interpretation of the phylogenetic position of taxa pruned from the analysis.

The composition of the theropod fauna from the African Tendaguru Formation apparently contrasts with that of both the North American Morrison Formation and the Lusitanian Basin because in the latter the theropod faunas were dominated by tetanurans and also abundant coelurosaurs whereas in the former ceratosaur taxa are the more abundant and diverse and coelurosaurs are unknown. These differences in the faunal composition between the Tendaguru Formation and those of the Morrison Formation and Lusitanian Basin are compatible with the traditional interpretation of the initial phase of Pangaean fragmentation with separation into Laurasian and Gondwanan during the Callovian (Upchurch et al. 2002). However, some studies (e.g. Sereno 1997, 1999) have noted that dinosaurian distributions do not support this north-south paleogeographical separation. The paleogeography indicates that the initial phase of Pangaean fragmentation involved the isolation of Asia, followed by a later separation of North America from Gondwana (Upchurch et al. 2002).

The faunal composition of theropods from the Morrison Formation and the Lusitanian Basin is much similar with most of the genera currently known in the Portuguese record having a closely related taxon at the North American record. Allosauroidea is at the moment the clade that more information has added for the paleobiogeographic discussion. This clade is well-represented and relatively diverse in the

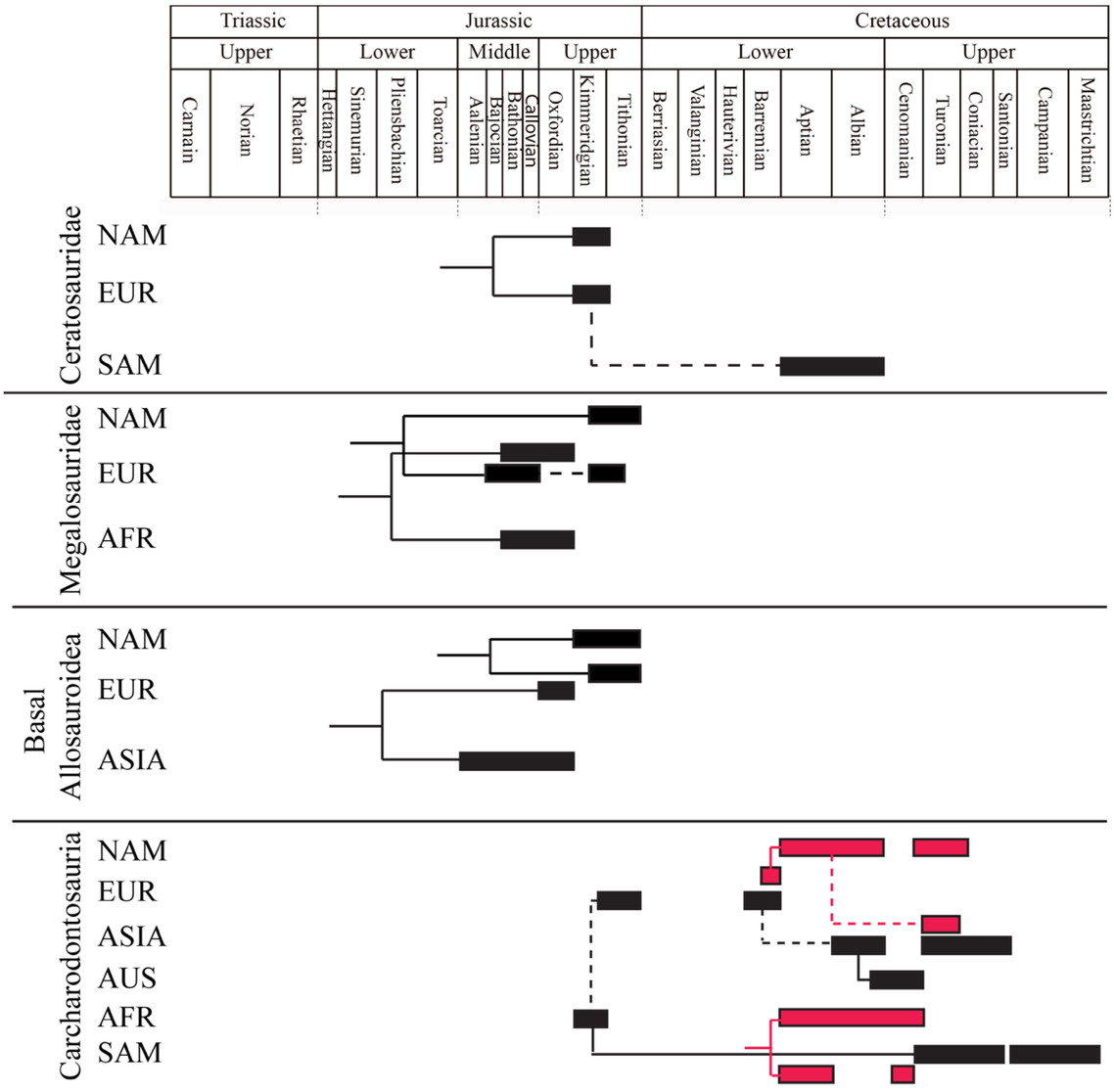

Figure 8.3.3. Dinosaur relationships and paleogeographic distributions through time. The pink rectangles represent Carcharodontosauridae and the dashed lines represent possible relationships among clades. Legend: NAM, North America; EUR, Europe; SAM, South America; AFR, Africa; ASIA, Asia; AUS, Australia.

Portuguese record, including *Allosaurus*, *Lourinhanosaurus* and some specimens that have affinities with more derived allosauroids possibly related with Carcharodontosauria (Fig. 8.3.2). Among these theropods, *Allosaurus* is shared with the North American record and despite more recently it has been considered that the Portuguese specimens may belong to a separate species exclusive for the Lusitanian Basin, *Allosaurus europaeus*, the similarity with the forms known in the Morrison Formation is remarkable. This is also the case of other genera (*Torvosaurus*, *Ceratosaurus*, and possibly *Aviatyrannis*), which based on the available material, are scarcely distinguishable from the species described in the North American record (Rauhut 2003; Mateus et al. 2006; Hendrickx & Mateus 2014; Malafaia et al. 2015, 2017). On the other hand, *Lourinhanosaurus* is so far the only theropod genus interpreted as exclusive for the Portuguese record.

This faunal composition seems to indicate an incipient vicariant evolution of the dinosaur faunas from the Late Jurassic of the Lusitanian Basin, suggesting that the seaway(s) between North America and Iberia represented barriers to the dispersion of these faunas. However, these barriers may have had different effects on different species (Ronquist 1997), which would explain the stronger affinities of the fauna of theropods between the Lusitanian Basin and Morrison Formation than those of other dinosaur faunas such as the sauropods.

Despite the similarity of the dinosaur faunas from the Late Jurassic of the Lusitanian Basin and the Morrison Formation, it has been identified in the Portuguese record some groups that apparently are absent in correlative North American strata (e.g. the theropods Carcharodontosauria, the sauropods Turiasauria: Royo-Torres et al. 2006, and the stegosaurs Dacentrurinae: Lapparent and Zbyszewski 1951; Escaso et al. 2007b). Some of these clades are instead more closely related with some Gondwanan faunas, especially those known from the North African record (Fig. 8.3.3). These differences in the composition of the dinosaur faunas between the Lusitanian Basin and the Morrison Formation may indicate differential patterns of regional extinction and ecological constraints such as environmental preferences (Benson et al. 2012).

The relationships of the Late Jurassic theropod faunas from the Lusitanian Basin and other European landmasses are difficult to ascertain due to the scarce fossil record. However, few specimens, mainly isolated teeth, known in Spain, Germany and France show some similarities in the general faunal composition among these territories (Cobos et al. 2013; Vullo et al. 2014; Gerke and Wings 2016). However, as during the Jurassic most of Europe was composed of several major islands separated by shallow seas it is possible that the Upper Jurassic European faunas of theropod dinosaurs have some regional endemism as is recorded for those of the Middle Jurassic (Benson 2010; Rauhut et al. 2016).

REFERENCES

Antunes MT, Mateus O. 2003. Dinosaurs of Portugal. Comptes Rendus Paleovol 2:77–95.

Bardet N, Falconnet J, Fischer V, Houssaye A, Jouve S, Pereda Suberbiola X, Pérez-García A, Rage J-C, Vincent P. 2014. Mesozoic marine reptile palaeobiogeography in response to drifting plates. Gondwana Research. http://dx.doi.org/10.1016/j.gr.2014.05.005

Benson RBJ. 2010. A description of *Megalosaurus bucklandii* (Dinosauria: Theropoda) from the Bathonian of the United Kingdom and the relationships of Middle Jurassic theropods. Zoological Journal of the Linnean Society 158:882–935.

Benson RBJ, Rich TH, Vickers-Rich P, Hall M. 2012. Theropod Fauna from Southern Australia Indicates High Polar Diversity and Climate-Driven Dinosaur Provinciality. PLoS ONE 7(5):e37122. doi:10.1371/journal.pone.0037122

Brikiatis L. 2016. Late Mesozoic North Atlantic land bridges. Earth Science Reviews. doi: 10.1016/j.earscirev.2016.05.002

Cecca F. 2002. Palaeobiogeography of Marine Fossil Invertebrates - Concepts and Methods. Taylor & Francis, London.

Cobos A, Lockley MG, Gascó F, Royo-Torres R, Alcalá L. 2014. Megatheropods as apex predators in the typically Jurassic ecosystems of the Villar del Arzobispo Formation (Iberian Range, Spain). Palaeogeography, Palaeoclimatology, Palaeoecology 399:31–41.

Dantas P, Sanz JL, Silva CM, Ortega F, Santos VF, Cachão M. 1998. *Lourinhasaurus* n. gen. Novo dinossáurio saurópode do Jurássico superior (Kimeridgiano superior-Titoniano inferior) de Portugal. V Congresso Nacional Geologia 84(1): A91–A94.

Dercourt J, Gaetani M, Vrielynck B, Barrier E, Biju-Duval B, Brunet MF, Cadet JP, Crasquin S, Sandulescu M, 2000. Atlas Peri-Tethys of Palaeoenvironmental Maps. Commission for the Geologic Map of the World, Paris.

Escaso F, Ortega F, Dantas P, Malafaia E, Pimentel NL, Pereda-Suberbiola X, Sanz JL, Kullberg JC, Kullberg MC, Barriga F. 2007a. New evidence of shared dinosaur across Upper Jurassic proto-North Atlantic: *Stegosaurus* from Portugal. Naturwissenschaften 94:367–374.

Escaso F, Ortega F, Dantas P, Malafaia E, Silva B, Sanz JL. 2007b. Elementos postcraneales de *Dacentrurus* (Dinosauria: Stegosauria) del Jurásico Superior de Moçanfaneira (Torres Vedras, Portugal). Cantera Paleontológica:157–172.

Escaso F, Silva B, Ortega F, Malafaia E, Sanz JL. 2010. A Portuguese specimen of *Camptosaurus aphanoecetes* (Ornithopoda: Camptosauridae) increases the dinosaurian similarity among the Upper Jurassic Alcobaça and Morrison Formation. Abstracts of the 70th Annual Meeting of the Society of Vertebrate Paleontology, Pittsburgh, USA. 86A pp.

Gerke O, Wings O. 2016. Multivariate and cladistic analyses of isolated teeth reveal sympatry of theropod dinosaurs in the Late Jurassic of northern Germany. PLoS ONE 11(7): e0158334. doi:10.1371/journal.pone.0158334.

Hendrickx C, Mateus O. 2014. *Torvosaurus gurneyi* n. sp., the largest terrestrial predator from Europe, and a proposed terminology of the maxilla anatomy in nonavian theropods. PLoS One. 9:e88905.

Lapparent AF, Zbyszewski G. 1951. Découverte d'une riche faune de Reptiles Dinosauriens dans le Jurassique supérieur du Portugal. Comptes Rendus de l'Académie des Sciences à Paris 233:1125–1127.

Lapparent AF, Zbyszewski G. 1957. Les dinosauriens du Portugal [The dinosaurs of Portugal]. Memórias Serviços Geológicos de Portugal. 2:1–63.

Malafaia E, Mocho P, Escaso F, Ortega F. 2017. New data on the anatomy of *Torvosaurus* and other remains of megalosauroid (Dinosauria, Theropoda) from the Upper Jurassic of Portugal. Journal of Iberian Geology 43:33–59.

Malafaia E, Ortega F, Escaso F, Silva B. 2015. New evidence of *Ceratosaurus* (Dinosauria: Theropoda) from the Late Jurassic of the Lusitanian Basin, Portugal. Historical Biology 27:938–946.

Mateus O, Antunes MT. 2000a. *Ceratosaurus* sp. (Dinosauria: Theropoda) in the Late Jurassic of Portugal. Proceedings of the 31st International Geological Congress, Rio de Janeiro, Brazil.

Mateus O, Antunes MT. 2000b. *Torvosaurus* sp. (Dinosauria: Theropoda) in the Late Jurassic of Portugal. I Congresso Ibérico de Paleontología/XVI Jornadas de la Sociedad Española de Paleontología; Évora, Portugal.

Mateus O, Walen A, Antunes MT. 2006. The large theropod fauna of the Lourinhã Formation (Portugal) and its similarity to the Morrison Formation, with a description of a new species of *Allosaurus*. In: Foster JR, Lucas SG. (Eds). Paleontology and geology of the Upper Jurassic Morrison Formation. Vol. 36. New Mexico Museum of Natural History and Science, Bulletin:123–129.

McDonald AT. 2011. The taxonomy of species assigned to *Camptosaurus* (Dinosauria: Ornithopoda). Zootaxa 2783:52–68.

Mocho P, Royo-Torres R, Ortega F. 2014. Phylogenetic reassessment of *Lourinhasaurus alenquerensis*, a basal Macronaria (Sauropoda) from the Upper Jurassic of Portugal. Zoological Journal of the Linnean Society, 170:875–916.

Pérez-Moreno BP, Chure DJ, Pires C, Silva CM, Santos V, Dantas P, Póvoas L, Cachão M, Sanz JL, Galopim de Carvalho AM. 1999. On the presence of *Allosaurus fragilis* (Theropoda: Carnosauria) in the Upper Jurassic of Portugal: first evidence of an intercontinental dinosaur species. Journal of the Geological Society 156:449–452.

Rauhut OWM. 2003. A tyrannosauroid dinosaur from the Upper Jurassic of Portugal. Palaeontology 46:903–910.

Rauhut OWM, Fechner R. 2005. Early development of the facial region in a non-avian theropod dinosaur. Proceedings of the Royal Society of London Series B, Biological Sciences 272:1179–1183.

Rauhut OWM, Hübner TR, Lanser K-P. 2016. A new megalosaurid theropod dinosaur from the late Middle Jurassic (Callovian) of north-western Germany: Implications for theropod evolution and faunal turnover in the Jurassic. Palaeontologia Electronica 19.2.26A:1–65.

Ron Blakey. 2013. Colorado Plateau Geosystems, Inc. http://deeptimemaps.com

Ronquist F. 1997. Dispersal-vicariance analysis: a new approach to the quantification of historical biogeography. Systematic Biology 46(1):195–203.

Royo-Torres R, Cobos A, Alcalá L. 2006. A giant european dinosaur and a new sauropod clade. Science 314(5807):1925–1927.

Scotese CR, 2002. Paleomap Website. http://www.scotese.com

Sereno PC. 1997. The origin and evolution of dinosaurs. Annual Review of Earth and Planetary Sciences 25:435–489.

Sereno PC. 1999. Dinosaurian biogeography: vicariance, dispersal and regional extinction. In: Tomida Y, Rich TH, Vickers-Rich P. (Eds), Proceedings of the Second Gondwanan Dinosaur Symposium. Tokyo, National Science Museum:249–257.

Upchurch P, Hunn CA, Norman DB. 2002. An analysis of dinosaurian biogeography: evidence for the existence of vicariance and dispersal patterns caused by geological events. Proc R Soc London B 269:613–621.

Vullo R, Abit D, Ballévre M, Billon-Bruyat J-P, Bourgeais R, Buffetaut É, Daviero-Gomez V, Garcia G, Gomez B, Mazin J-M, Morel S, Néraudeau D, Pouech J, Rage J-C, Schnyder J, Tong H. 2014. Palaeontology of the Purbeck-type (Tithonian, Late Jurassic) bonebeds of Chassiron (Oléron Island, western France). Comptes Rendus Palevol 13:421–441.

Westermann GEG. 1993. Global bio-events in Mid-Jurassic ammonites controlled by seaways. In: House MR. (Eds), Ammonoidea: Environment, Ecology, and Evolutionnary Change. Oxford University Press, Oxford:187–226.

Ziegler PA. 1988. Evolution of the Arctic - North Atlantic and the Western Tethys – A visual presentation of a series of paleogeographic-paleotectonic maps. American Association of Petroleum Geologists Memoir 43:164–196.

CHAPTER 9: RESULTS AND CONCLUSIONS

9.1. RESULTS

This study provides an updated phylogenetic approach of the Late Jurassic theropods from the Lusitanian Basin. A systematic analysis of the record of this group of dinosaurs was performed based on published and unpublished material in order to evaluate the relationships among the Portuguese faunas and the correlative faunas of North America and Africa as well as with the evidences from other European sites (Spain, France, England and Germany). The main objective of this study is to test the hypothesis about the Upper Jurassic record of theropod dinosaurs of the Lusitanian Basin that this record is composed by forms closely related with taxa described in correlative sedimentary levels from the Morrison Formation (USA), indicating the existence of dispersal events among these landmasses during the Late Jurassic.

This hypothesis was tested based on the phylogenetic analysis of all theropod taxa currently known in the Portuguese Upper Jurassic, including *Ceratosaurus*, *Torvosaurus*, *Lourinhanosaurus*, and *Allosaurus*. Furthermore, two unpublished specimens found in sediments of the Praia de Amoreira-Porto Novo (late Kimmeridgian –basal Tithonian) and Freixial (Tithonian) formations were described and its phylogenetic analysis was performed. For these analyses several more specific hypotheses and objectives were defined and the results related with each hypothesis are discussed below.

Result from testing the hypothesis 1.1. The presence of *Ceratosaurus* in the Upper Jurassic of the Lusitanian Basin is confirmed based on description of previously unpublished elements and review of described specimens. These specimens share an exclusive combination of features with *Ceratosaurus*, including: (i) low lesser trochanter of the femur relative to the dorsal margin of the femoral head; (ii) crista tibiofibularis obliquely oriented with respect to the axis of the femoral diaphysis; (iii) presence of an infrapopliteal ridge in the posterior surface of the distal femur; (iv) large cnemial crest; and (v) medial condyle of the tibia continuous with the proximal surface. This taxon is represented by some appendicular elements of a single individual collected in Valmitão and some isolated teeth. The available material is, at the moment, indistinguishable from the species Ceratosaurus nasicornis described in the Morrison Formation.

Some minor differences relative to *C. nasicornis* were noted in the original description of part of the specimen from Valmitão (ML352), including: (i) more developed fibular crest; (ii) more developed notch in the distal femoral head; (iii) relative position of the epiphyseal expansions; (iv) presence of a posterior intercondylar bridge on the femur. Based on these differences, ML352 was interpreted as *Ceratosaurus* sp. closer to *Ceratosaurus dentisulcatus* than to *C. nasicornis* or *Ceratosaurus magnicornis*. However, the species *C. dentisulcatus* and *C. magnicornis* are currently interpreted as junior synonyms of *C. nasicornis*. Besides, some of these differences may be compatible with individual variation such as ontogeny and thus the specimens from Valmitão are assigned to *Ceratosaurus* cf. *nasicornis*.

Result from testing the hypothesis 1.2. The specimens previously assigned to *Torvosaurus tanneri* from the Upper Jurassic of the Lusitanian Basin are currently interpreted as belonging to a new species exclusive of the Lusitanian Basin: *Torvosaurus gurneyi*. Some cranial and postcranial specimens herein described from different sites, mainly in the coastline between Peniche and Torres Vedras, are assigned to *T. gurneyi*.

Result from testing the hypothesis 1.3. T. gurneyi is here considered a valid species. Some previously unpublished axial elements show several differences relative to *T. tanneri*, but we cannot verify, at the moment, if these differences may be features of *T. gurneyi* or if they represent another megalosauroid taxon not yet identified in the record of the Lusitanian Basin. Beside, some isolated teeth have a combination

of feature compatible with non-megalosaurid megalosauroids and are tentatively related with the piatnitzkysaurid *Marshosaurus*. This set of specimens indicates a higher diversity of megalosauroid theropods in the Late Jurassic of the Lusitanian Basin than previously known based on more complete specimens.

Result from testing the hypothesis 1.4. The specimens originally assigned to *Allosaurus fragilis* from the Andrés fossil site together with unpublished cranial and postcranial material found in the same site are hardly distinguished from North American members of the species. Some differences observed in these specimens relative to *A. fragilis* include: (i) jugal ramus of the squamosal extending posteriorly back to the level of the pterygoid process; (ii) well-developed concavities in the posterolateral surface of the supraoccipital, adjacent to the contact with the paroccipital processes; (iii) two separated foramina for the branches of the hypoglossal nerve within the paracondylar pocket for the cranial nerve XII; (iv) presence of a naso-maxillary process in the nasal lateral surface; and (v) length of the anterior ramus of the lacrimal greater than 65% of the height of the ventral ramus. The phylogenetic analysis of the set of material attributed to *Allosaurus* from Andrés places these specimens as the sister group of the North American forms *A. fragilis* and *A.* "*jimmadseni*", recovering two autapomorphies for these Portuguese specimens: (i) presence of a naso-maxillary process in the nasal lateral surface and (ii) length of the anterior ramus of the lacrimal greater than 65% the height of the ventral ramus.

Result from testing the hypothesis 1.5. Allosaurus europaeus is considered a valid species, but a revised diagnosis is here proposed, based on review of the holotype. The revised diagnosis of this species includes the following autapomorphies: (i) no lacrimal-maxillary contact; (ii) ventral tip of the postorbital reaches the lower rim of the orbit; and (iii) dorsoventrally deep and forked posterior margin of the maxilla. The specimens from Andrés show some differences relative to the holotype of *A. europaeus* namely in two features interpreted as autapomorphies for this species: (i) lacrimal contacts the maxilla and (ii) posterior margin of the maxilla strongly tapered. However, based on the paleobiogeographic context it is here proposed the assignation of the specimens from Andrés as *Allosaurus* cf. *europaeus* pending the discovery of more complete material that would allow a better understand of this Portuguese species.

Result from testing the hypothesis 1.6. A previously unpublished specimen (SHN.036) collected in sediments of the Praia da Amoreira-Porto Novo Formation in Valmitão was described. This small juvenile individual shows a combination of characters shared by other allosauroids already known in the Upper Jurassic of the Lusitanian Basin, *Allosaurus* and *Lourinhanosaurus*, but also some differences relative to both taxa. Some of these differences may be related to the juvenile condition of the specimen, but other unusual features cannot be properly explained by ontogeny, and are here interpreted as having taxonomic significance.

An integrated phylogenetic analysis including SHN.036 together with all allosauroid taxa from the Upper Jurassic of the Lusitanian Basin recovered the specimen from Valmitão as an allosauroid more derived than *Lourinhanosaurus* and *Allosaurus*. This specimen is placed in a polytomy at the base of a more derived allosauroid group closely related with Carcharodontosauria. The follow combination of features indicate a relationship of SHN.036 with carcharodontosaurian allosauroids: (i) absence of ventral keel on anterior dorsal vertebrae; (ii) presence of well-developed lateral lamina at the base of the neural arch of mid and posterior caudal centra; (iii) presence of spinoprezygapophyseal laminae in the mid caudal vertebrae extending from the medial surface of the base of the prezygapophysis and being flanked laterally by an additional lateral lamina; (iv) presence of low, but well-defined anterior centrodiapophyseal lamina with associated shallow centroprezygapophyseal fossa in anterior mid caudal vertebrae; (v) presence of well-developed ventral ridge in the anterior caudal centra; (vi) anteroposterior length of pubic distal expansion more than 60% of pubic shaft length; (vii) iliac articular surface of the ischium deeply concave; and (viii) ventrally rather than anteroventrally oriented pubic peduncle of the ischium.

Result from testing the hypothesis 1.7. An unpublished specimen (SHN.019) collected in sediments of the Freixial Formation in Cambelas was described. This specimen is interpreted as an avetheropod based on the follow combination of features: (i) anterior spur-shaped process in the neural spine of mid caudal vertebrae; (ii) distal caudal vertebrae with strongly elongated prezygapophyses, overhanging at least onequarter of the length of the preceding centra; (iii) femoral lesser trochanter proximally located; (iv) distal end of metatarsal IV deeper than broad; (v) reduced length of metatarsal I, less than 50% of metatarsal II; (vi) metatarsal I with a broadly triangular shaft, and distally placed; and (vii) metatarsal III with a wedge shaped cross-section of the shaft.

SHN.019 shares with SHN.036 the presence of a strongly developed lateral lamina in some caudal vertebrae projecting from the posterior articular facet to the base of the caudal rib. Based on this shared feature SHN.019 and SHN.036 are interpreted as belonging to the same taxon. Besides, SHN.019 also shows some unusual features shared with carcharodontosaurian theropods such as a low vertical crest on the lateral surface of the lesser trochanter of the femur and a well-developed and rugose concavity in the medial surface adjacent to the proximal end of the fourth trochanter. This combination of features indicates a phylogenetic affinity with carcharodontosaurian allosauroids.

Result from testing the hypothesis 1.8. Lourinhanosaurus antunesi is considered a valid species characterized by two autapomorphies based on the phylogenetic analysis herein presented: (i) length of vertebral bodies of mid cervicals approximately twice the diameter of the anterior articular facet and (ii) completely enclosed obturator foramen of the pubis. This taxon is, at the moment, considered exclusive for the record of the Lusitanian Basin. Our phylogenetic analysis recovered *Lourinhanosaurus* as an allosauroid, but with an unstable position being sometimes placed within a group together with *Allosaurus* and Carcharodontosauridae representing the sister clade to Metriacanthosauridae. Other times, it is placed at the base of allosauroidea in a polytomy with metriacanthosaurids.

Result from testing the hypothesis 2. The Late Jurassic theropod fauna of the Lusitanian Basin is much similar to those of correlative levels of the Morrison Formation and is mostly composed by taxa shared with the North American record. Despite this similarity, the theropods from the Lusitanian Basin and Morrison Formation represent distinct forms indicating a pattern of incipient vicariant evolution possibly due to the existence of seaway(s) between North America and Iberia during the Late Jurassic that would have constituted barriers to terrestrial faunal dispersion. However, this vicariance processes may have had different effects on different species, which would explain the stronger affinities of the fauna of theropods among the Lusitanian Basin and Morrison Formation than those of other dinosaur faunas, such as the sauropods, and other vertebrates. On the other hand, the presence in the Portuguese record of some dinosaur groups that apparently are absent in the Morrison Formation may indicate differential patterns of regional extinction and ecological constraints such as environmental preferences.

Result from testing the hypothesis 3. The theropod paleobiodiversity for the Late Jurassic of the Lusitanian Basin includes Ceratosauridae, Megalosauridae, Allosauridae, and Coelurosauria. Besides, the study of previously unpublished specimens allowed identifying a possible non-megalosaurid megalosauroid and an allosauroid closely related with Carcharodontosauria. These previously unidentified clades indicate a higher diversity among these theropod faunas than previously known.

Result from testing the hypothesis 4. Geographically, ceratosaurian theropods are currently restricted to the Consolação Sub-basin record. Specimens assigned to these basal theropods were collected in sedimentary deposits of distal fluvial meander systems of the upper Kimmeridgian Praia da Amoreira-Porto Novo Formation. However, some isolated teeth attributed to Ceratosaurus indicate a geographically and stratigraphically broader distribution of this taxon spanning from the late Kimmeridgian to the Tithonian. Megalosauroids are represented in the Consolação and Bombarral-Alcobaça Sub-basins. The specimens assigned to Torvosaurus were mostly collected in fluvial deposits of the Praia da Amoreira-Porto Novo Formation, but scarce isolated teeth come also from sedimentary levels deposited in a

shallow carbonated platform of the Alcobaça Formation, Kimmeridgian-lowermost Tithonian in age. Allosauroids are the theropods with a broader geographical and stratigraphical distribution in the Lusitanian Basin. This clade is represented in the Consolação, Bombarral and Turcifal Sub-basins. Specimens attributed to this clade have been found in the Alcobaça, Praia da Amoreira-Porto Novo, Sobral, Freixial and Bombarral formations spanning from the Kimmeridgian to the end of the Tithonian. Fossil sites with elements assigned to allosauroids correspond to sediments deposited in fluvial meander to shallow marine and brackish paleoenvironments. Finally, the single taxon currently known of small coelurosaurian theropods is restricted to the Bombarral-Alcobaça Sub-basin and stratigraphically to Kimmeridgian-lowermost Tithonian levels of the Alcobaça Formation. However, some isolated teeth attributed to this clade indicate a greater diversity as well as a broader geographical and stratigraphic distribution of these theropods spanning from the late Kimmeridgian to the Tithonian.

Result from testing the hypothesis 5. The Upper Jurassic theropod record from the Lusitanian Basin shows similarities in the general faunal composition with other European fossil sites mainly in Spain, Germany and France. However, an enough large sample is not yet known in these records as to obtain robust conclusions on the phylogenetic relationships of the theropod faunas among these territories.

9.2. RESULTADOS

O estudo aqui apresentado resultou numa actualização da interpretação filogenética dos dinossáurios terópodes do Jurássico Superior da Bacia Lusitânica. O estudo foi desenvolvido com base na análise sistemática do registo deste grupo de dinossáurios, incluindo a revisão de exemplares publicados previamente e a descrição de material inédito. Esta análise tem como objectivo avaliar as relações de parentesco dos taxa de terópodes representados no registo português com as faunas correlativas da América do Norte e África, bem como com as escassas evidências de outros locais da Europa (Espanha, França, Inglaterra e Alemanha). O objectivo central deste estudo é testar a seguinte hipótese sobre o registo fóssil de dinossáurios terópodes do Jurássico Superior da Bacia Lusitânica: este registo está composto por formas estreitamente relacionadas com taxa descritos em níveis sedimentares correlativos da Formação de Morrison, indicando a existência de eventos de dispersão entre estas massas terrestres durante o Jurássico Superior.

Esta hipótese foi testada com base na análise filogenética de todos os taxa de terópodes conhecidos no Jurássico Superior português, incluindo *Ceratosaurus*, *Torvosaurus*, *Lourinhanosaurus* e *Allosaurus*. Para além destes taxa, foram descritos e analisados dois exemplares inéditos encontrados em sedimentos das formações de Praia da Amoreira-Porto Novo (Kimmeridgiano superior–Tithoniano inferior) e Freixial (Tithoniano). Para esta análise, diversas hipóteses e objectivos mais específicos foram definidos e os resultados relacionados com cada uma dessas hipóteses são discutidos em seguida.

Resultados obtidos relativamente à hipótese 1.1. A presença de *Ceratosaurus* no Jurássico Superior da Bacia Lusitânica é confirmada com base na descrição de elementos inéditos e revisão de exemplares previamente publicados. Estes exemplares partilham com *Ceratosaurus* uma combinação única de características que inclui: (i) trocânter menor do fémur baixo, relativamente à margem dorsal da cabeça femoral; (ii) crista tibiofibularis orientada obliquamente em relação ao áxis da diáfise femoral; (iii) presença de uma crista infrapopliteal na superfície posterior da parte distal do fémur; (iv) crista cnemial da tíbia bem desenvolvida; e (v) côndilo medial da tíbia contínuo com a superfície proximal. Este táxon está representado por alguns elementos apendiculares, relacionados a um único individuo, recolhidos em Valmitão e por um conjunto de dentes isolados. Este conjunto de material é, neste momento, indistinguível da espécie *Ceratosaurus nasicornis* descrita na Formação de Morrison.

Na descrição original de parte do exemplar recolhido em Valmitão (ML352) foram notadas algumas diferenças menores relativamente a *C. nasicornis*, incluindo: (i) crista fibular mais desenvolvida; (ii) entalhe mais desenvolvido na superfície distal da cabeça femoral; (iii) posição relativa da expansão

epífiseal; (iv) presença de uma ponte intercondilar na superfície posterior do fémur. Com base nestas diferenças, ML352 foi identificado como pertencendo a *Ceratosaurus* sp. mais estreitamente relacionado com *Ceratosaurus dentisulcatus* do que com *C. nasicornis* ou com *Ceratosaurus magnicornis*. Contudo, as espécies *C. dentisulcatus* e *C. magnicornis* são actualmente interpretadas como sinónimas de *C. nasicornis*. Além disso, algumas destas diferenças são compatíveis com variações individuais relacionadas, por exemplo, com ontogenia. Com base nestes argumentos, os exemplares de Valmitão são identificados como pertencendo a *Ceratosaurus* cf. *nasicornis*.

Resultados obtidos relativamente à hipótese 1.2. Os exemplares do Jurássico Superior da Bacia Lusitânica previamente relacionados a *Torvosaurus tanneri* são actualmente atribuídos a uma nova espécie exclusiva da Bacia Lusitânica: *Torvosaurus gurneyi*. Alguns elementos do esqueleto craniano e pós-craniano, descritos neste trabalho, provenientes de diferentes localidades, sobretudo na região litoral entre Peniche e Torres Vedras, são identificados como pertencendo a *T. gurneyi*.

Resultados obtidos relativamente à hipótese 1.3. T. gurneyi é aqui considerada uma espécie válida. Alguns elementos inéditos do esqueleto axial mostram diversas diferenças relativamente a *T. tanneri* mas não é possível verificar, actualmente, se essas diferenças correspondem a características de *T. gurneyi* ou se representam um táxon distinto de megalossauroides ainda não identificado no registo da Bacia Lusitânica. Por outro lado, alguns dentes isolados apresentam uma combinação de características compatível com megalossauroides não-megalossaurídeos sendo interpretados, de forma preliminar, como pertencendo a um piatnitzkyssaurídeo estreitamente relacionado com *Marshosaurus*. Este conjunto de materiais inéditos indica uma maior diversidade de terópodes megalossauroides no Jurássico Superior da Bacia Lusitânica do que aquela que se conhece com base em exemplares mais completos.

Resultados obtidos relativamente à hipótese 1.4. Os exemplares originalmente atribuídos a *Allosaurus fragilis* recolhidos na jazida de Andrés, juntamente com outros materiais inéditos do esqueleto craniano e pós-craniano, descobertos no mesmo local são dificilmente distinguíveis desta espécie típica do registo Norte-americano. Algumas diferenças observadas nestes exemplares relativamente a *A. fragilis* incluem: (i) ramo jugal do escamoso estende-se para a parte posterior, ultrapassando o nível do processo pterigóide; (ii) concavidade bem desenvolvida na superfície posterolateral do supraoccipital, adjacente ao contacto com os processos paroccipitais; (iii) presença de dois forâmenes distintos para os ramos do nervo hipoglosso no interior da cavidade paracondilar para o XII nervo craniano; (iv) presença de processo naso-maxilar na superfície lateral do nasal; e (v) comprimento do ramo anterior do lacrimal maior do que 65% da altura do ramo ventral. A análise filogenética do conjunto de restos identificados como pertencendo a *Allosaurus*, recolhidos em Andrés, posiciona estes exemplares como o grupo irmão das formas norte-americanas, *A. fragilis* e *A.* "*jimmadseni*". Duas autapomorfias são indicadas nesta análise para os exemplares portugueses: (i) presença de processo naso-maxilar na superfície lateral do nasal e (ii) comprimento do ramo anterior do lacrimal maior do que 65% da altura do ramo ventral.

Resultados obtidos relativamente à hipótese 1.5. Allosaurus europaeus é considerada uma espécie válida mas uma revisão da diagnose é aqui proposta com base no estudo do holótipo. A nova diagnose inclui as seguintes autapomorfias: (i) ausência de contacto entre o lacrimal e a maxila; (ii) extremidade ventral do postorbital estende-se até à margem inferior da órbita; e (iii) margem posterior da maxila alta dorsoventralmente e bifurcada. Os exemplares de Andrés apresentam algumas diferenças relativamente ao holótipo de *A. europaeus*, nomeadamente em duas características interpretadas como autapomorfias para esta espécie: (i) lacrimal contacta a maxila e (ii) margem posterior da maxila afilada para a parte posterior. Contudo, com base no contexto paleobiogeográfico, optamos por identificar os exemplares de Andrés como pertencendo a *Allosaurus* cf. *europaeus*, aguardando a descoberta de material mais completo que permita o melhor conhecimento desta espécie portuguesa.

Resultados obtidos relativamente à hipótese 1.6. Foi descrito um novo exemplar (SHN.036) recolhido em sedimentos da Formação de Praia da Amoreira-Porto Novo, em Valmitão. Este

exemplar corresponde a um pequeno individuo juvenil e apresenta uma combinação de características partilhadas com outros allossauroides conhecidos no Jurássico Superior da Bacia Lusitânica, *Allosaurus* e *Lourinhanosaurus*, mas também diferenças relativamente a ambos taxa. Algumas destas diferenças podem estar relacionadas com o estádio ontogenético do exemplar mas outras características parecem ter significado taxonómico.

A análise filogenética integrada, incluindo SHN.036 juntamente com todos os taxa de allossauroides do Jurássico Superior da Bacia Lusitânica identifica o exemplar de Valmitão como um allossauroide mais derivado do que *Lourinhanosaurus* e *Allosaurus*. Este exemplar é posicionado numa politomia na base de um grupo de allossauroides mais derivados, estreitamente relacionados com o clado Carcharodontosauria. A seguinte combinação de características indica uma relação de parentesco de SHN.036 com Carcharodontosauria: (i) ausência de quilha ventral nas vértebras dorsais anteriores; (ii) presença de lâmina lateral bem desenvolvida na base do arco neural das vértebras da secção media e posterior da cauda; (iii) presença de lâmina espinoprezigapofiseal nas vértebras caudais médias que se estende desde a superfície medial da base da pré-zigapófise; (iv) presença de uma lâmina centrodiapofiseal baixa mas bem definida, associada a uma fossa centroprezigapofiseal superficial nas vértebras caudais médias; (v) presença de uma crista ventral bem desenvolvida nos centros caudais anteriores; (vi) comprimento anteroposterior da expansão distal do púbis maior do que 60% do comprimento da diáfise; (vii) superfície articular ilíaca do ísquio côncava; e (viii) pedúnculo para o púbis orientado ventralmente.

Resultados obtidos relativamente à hipótese 1.7. Foi também descrito um exemplar (SHN.019) recolhido em sedimentos da Formação de Freixial, em Cambelas. Este exemplar é interpretado como um avetherópode com base na seguinte combinação de características: (i) processo anterior em forma de espigão na espinha neural das vértebras da secção média da cauda; (ii) vértebras caudais distais com pré-zigapófises alongadas, sobrepondo pelo menos um-quarto do comprimento de centro precedente; (iii) trocânter menor localizado na parte proximal do fémur; (iv) extremidade distal do metatarsal IV mais comprido anteroposteriormente do que largo mediolateralmente; (v) metatarsal I reduzido, com comprimento menor do que 50% do metatarsal II; (vi) metatarsal I com diáfise triangular e localizado distalmente; e (vii) secção da diáfise do metatarsal III em forma de cunha.

SHN.019 partilha com SHN.036 a presença, em algumas vértebras caudais, de lâminas laterais bem desenvolvidas e que se projectam desde a faceta articular anterior até à base da costela caudal. Com base nesta característica partilhada, SHN.019 e SHN.036 são interpretados como pertencendo ao mesmo táxon. Além disso, SHN.019 apresenta também algumas características pouco comuns partilhadas com Carcharodontosauria, como por exemplo uma suave crista na superfície lateral do trocânter menor do fémur e uma concavidade rugosa na superfície medial do fémur adjacente à extremidade proximal do quarto trocânter. Esta combinação de características indica uma afinidade filogenética com allossauroides carcharodontossaurínos.

Resultados obtidos relativamente à hipótese 1.8. Lourinhanosaurus antunesi é uma espécie válida caracterizada por duas autapomorfias, com base na análise filogenética aqui apresentada: (i) comprimento dos centros das vértebras cervicais médias aproximadamente o dobro do diâmetro da faceta articular anterior e (ii) presença de forâmen obturador do púbis completamente fechado. Este táxon é, até ao momento, considerado exclusivo do registo da Bacia Lusitânica. A análise desenvolvida no presente trabalho identifica *Lourinhanosaurus* como um allossauroide mas com uma posição instável. Este táxon é algumas vezes posicionado num grupo juntamente com *Allosaurus* e Carcharodontosauridae, que representa o grupo irmão do clado Metriacanthosauridae, e outras vezes na base de Allosauroidea, numa politomia com os metriacanthossaurídeos.

Resultados obtidos relativamente à hipótese 2. O registo de terópodes do Jurássico Superior da Bacia Lusitânica é semelhante às faunas conhecidas em níveis correlativos da Formação de Morrison e é

maioritariamente composto por taxa partilhados com o registo norte-americano. Contudo, apesar desta semelhança, os terópodes da Bacia Lusitânica e da Formação de Morrison representam formas distintas, o que indica evolução vicariante, possivelmente devido à existência de corredores marítimos entre a América do Norte e a Ibéria, que terão constituído barreiras à dispersão destas faunas. Todavia, estes processos de vicariância poderão ter-se manifestado de diferentes formas nas distintas espécies, o que explicaria a maior afinidade das faunas de terópodes nestes territórios, relativamente a outros grupos de dinossáurios, como por exemplo os saurópodes, e de outros vertebrados. Por outro lado, a presença no registo português de alguns grupos de dinossáurios que aparentemente estão ausentes na Formação de Morrison pode indicar padrões de extinções regionais e de restrições ambientais, tais como preferências ambientais.

Resultados obtidos relativamente à hipótese 3. A paleobiodiversidade de terópodes do Jurássico Superior da Bacia Lusitânica inclui representantes dos clados Ceratosauridae, Megalosauridae, Allosauridae e Coelurosauria. O estudo de diversos exemplares inéditos permitiu identificar ainda representantes de megalossauroides não-megalossaurídeos e de allossauroides estreitamente relacionados com Carcharodontosauria. A presença destes clados indica uma maior diversidade na fauna de terópodes do Jurássico Superior da Bacia Lusitânica do que aquela que se conhecia anteriormente.

Resultados obtidos relativamente à hipótese 4. Geograficamente, o registo de terópodes ceratossaurianos está actualmente restrito à Sub-bacia da Consolação. Exemplares identificados a estes terópodes primitivos foram recolhidos em depósitos sedimentares formados em sistemas meândricos distais da Formação de Praia da Amoreira-Porto Novo (Kimmeridgiano superior). Contudo, alguns dentes isolados atribuídos a *Ceratosaurus* indicam uma distribuição geográfica e estratigráfica mais ampla deste táxon, desde o Kimmeridgiano superior até ao Tithoniano. Megalossauroides estão representados nas sub-bacias de Consolação e de Bombarral-Alcobaça. Exemplares atribuídos a Torvosaurus são provenientes maioritariamente de depósitos fluviais da Formação de Praia da Amoreira-Porto Novo mas escassos dentes isolados foram também encontrados em níveis sedimentares depositados em plataforma carbonatada de baixa profundidade, pertencentes à Formação de Alcobaça (Kimmeridgiano–Tithoniano inferior). Allossauroides são os terópodes com uma distribuição geográfica e estratigráfica mais ampla na Bacia Lusitânica. Este clado está representado nas sub-bacias de Consolação, Bombarral-Alcobaça e Turcifal. Exemplares atribuídos a este clado são provenientes das formações de Alcobaça, Praia da Amoreira-Porto Novo, Sobral, Freixial e Bombarral, representando um intervalo de tempo entre o Kimmeridgiano e o final do Tithoniano. As jazidas com elementos identificados como pertencendo a estes terópodes correspondem a sedimentos depositados em paleoambientes fluviais meândricos, marinhos superficiais e salobros. Finalmente, o único táxon conhecido actualmente de terópodes coelurossáurios está restrito à Sub-bacia de Bombarral-Alcobaça e estratigraficamente a níveis do Kimmeridgiano-Tithoniano inferior da Formação de Alcobaça. Contudo, dentes isolados atribuídos a este clado indicam uma maior diversidade, bem como uma mais ampla distribuição geográfica e estratigráfica destes terópodes, estendendo-se desde o Kimmeridgian superior até ao Tithonian.

Resultados obtidos relativamente à hipótese 5. O registo de terópodes do Jurássico Superior da Bacia Lusitânica mostra algumas semelhanças, na composição geral das faunas, com outros locais da Europa (Espanha. Alemanha e França). Contudo, devido ao escasso registo de terópodes do Jurássico Superior nestes locais uma análise mais ampla das relações filogenéticas destas faunas não é possível actualmente.

9.3. CONCLUSIONS

A systematic study of the theropod fossil record of the Upper Jurassic of the Lusitanian Basin is presented. This study updates the phylogenetic approach of the theropod taxa represented in this record, which allows a better knowledge of the evolutionary history and paleobiogeographic context of these theropod dinosaur faunas from the Late Jurassic.

Theropod dinosaurs are well-represented in the Upper Jurassic of the Lusitanian Basin. This record includes mainly medium to large-sized forms belonging to primitive theropod clades, such as Ceratosauria and tetanurans, including Megalosauridae and Allosauroidea. Small-sized and more derived theropods have also been identified based mainly on isolated elements. Several unpublished specimens collected in different sites of the Consolação, Turcifal and Bombarral-Alcobaça sub-basins indicate the presence of previously unidentified clades, including non-megalosaurid megalosauroids and a form of derived allosauroid closely related with Carcharodontosauria. These new specimens suggest a greater diversity among the Late Jurassic theropod faunas from the Lusitanian Basin than previously known.

The major theropod clades represented in the Upper Jurassic record of the Lusitanian Basin does not show any particular geographic or stratigraphic pattern of distribution. They are present from the Kimmeridgian to the end of the Tithonian, mostly in the Consolação and Bombarral-Alcobaça sub-basins. Fossil sites with theropod materials are especially abundant in the Praia da Amoreira-Porto Novo and Sobral formations cropping out in the littoral area between Peniche and Torres Vedras. However, this higher incidence of findings along the coastline may in part be an artifact due to more prospection in these areas.

The Late Jurassic Portuguese theropod fauna is composed by four valid and exclusive taxa: *Torvosaurus gurneyi*, *Lourinhanosaurus antunesi*, *Allosaurus europaeus*, and *Aviatyrannis jurassica* plus a possible new allosauroid taxon closely related to Carcharodontosauria. Some specimens have more uncertain phylogenetic relationships, including the specimens identified to *Ceratosaurus*, which are at the moment indistinguishable from the species *Ceratosaurus nasicornis* described in the Morrison Formation, but that have an unstable position, due to its fragmentary nature, being assigned as *Ceratosaurus* cf. *nasicornis*. This is also the case of the material attributed to *Allosaurus* from the Andrés fossil site, which shows differences relative to the forms of *Allosaurus* known in correlative levels of the Morrison Formation, but also with the holotype of the Portuguese species *Allosaurus europaeus*. The *Allosaurus* specimens from Andrés are assigned as *Allosaurus* cf. *europaeus* pending the discovery of more complete material that would allow a better understand of this Portuguese species. *Lourinhanosaurus antunesi* is considered a valid species exclusive for the Portuguese record. The phylogenetic analysis developed in the present work recovered this taxon as an allosauroid, but with an unstable position being sometimes placed within a group together with *Allosaurus* and Carcharodontosauridae representing the sister clade to Metriacanthosauridae. Other times, it is placed at the base of Allosauroidea in a polytomy with metriacanthosaurids.

The Late Jurassic theropod fauna of the Lusitanian Basin is much similar to those of correlative levels of the Morrison Formation and is mostly composed by taxa shared with the North American record. Despite this similarity, the theropods from the Lusitanian Basin and Morrison Formation represent distinct forms indicating a pattern of incipient vicariant evolution possibly due to the existence of seaway(s) between North America and Iberia during the Late Jurassic that would have constituted barriers to terrestrial faunal dispersion. However, this vicariance processes may have had different effects on different species, which would explain the stronger affinities of the fauna of theropods among the Lusitanian Basin and Morrison Formation than those of other dinosaur faunas, such as the sauropods, and other vertebrates. On the other hand, the presence in the Portuguese record of some dinosaur groups that apparently are absent in the Morrison Formation may indicate differential patterns of regional extinction and ecological constraints such as environmental preferences.

The Upper Jurassic theropod record from the Lusitanian Basin shows similarities in the general faunal composition with other European fossil sites mainly in Spain, Germany and France. However, the scarce record does not allow a more accurate analysis of the phylogenetic relationships of the theropod faunas among these territories.

9.4. CONCLUSÕES

O estudo sistemático do registo fóssil de terópodes do Jurássico Superior da Bacia Lusitânica é aqui apresentado. Este estudo actualiza a abordagem filogenética dos taxa de terópodes representados neste registo, permitindo uma melhor compreensão da história evolutiva e contexto paleobiogeográfico destas faunas de dinossáurios terópodes do Jurássico Superior.

Os dinossáurios terópodes estão bem representados no Jurássico Superior da Bacia Lusitânica. Este registo inclui sobretudo formas de médio ou grande porte que pertencem a clados de terópodes primitivos, como por exemplo Ceratosauria ou Tetanurae (incluindo Megalosauridae e Allosauroidea). Pequenos terópodes mais derivados são também conhecidos neste registo mas estão, até ao momento, representados sobretudo por elementos isolados. Diversos exemplares inéditos recolhidos em diferentes locais nas sub-bacias de Consolação, Turcifal e Bombarral-Alcobaça indicam a presença de clados anteriormente não identificados no registo português, incluindo megalossauroides não-megalossaurídeos e uma forma de allossauroides derivados estreitamente relacionados com Carcharodontosauria. Estes novos exemplares sugerem uma maior diversidade na composição das faunas de terópodes do Jurássico Superior do que aquela que se conhecia anteriormente.

Os clados maiores de terópodes representados no registo do Jurássico Superior da Bacia Lusitânica não mostram nenhum padrão específico de distribuição geográfica e estratigráfica. Estão representados entre o Kimmeridgiano e o final do Tithoniano, sobretudo nas sub-bacias de Consolação e de Bombarral-Alcobaça. Jazidas com materiais atribuídos a terópodes são especialmente abundantes em níveis das formações de Praia da Amoreira-Porto Novo e Sobral, sobretudo ao longo da faixa costeira entre Peniche e Torres Vedras. Contudo, esta maior incidência de descobertas no litoral pode estar relacionada, em parte, com mais intensa actividade de prospecção nestas áreas.

A fauna de terópodes do Jurássico Superior português está composta por quatro espécies exclusivas para este registo: *Torvosaurus gurneyi*, *Lourinhanosaurus antunesi*, *Allosaurus europaeus* e *Aviatyrannis jurassica* para além de um possível novo táxon de allossauroides estreitamente relacionado ao clado Carcharodontosauria. Alguns exemplares apresentam relações filogenéticas mais incertas, como por exemplo os materiais atribuídos a *Ceratosaurus*. Estes exemplares incompletos são, até ao momento, indistinguíveis da espécie *Ceratosaurus nasicornis*, descrita na Formação de Morrison Formation mas apresentam uma posição instável, sendo identificados como pertencendo a *Ceratosaurus* cf. *nasicornis*. Este é também o caso de um conjunto de material atribuído a *Allosaurus* proveniente da jazida de Andrés, o qual apresenta diferenças relativamente às formas de *Allosaurus* conhecidas em níveis correlativos da Formação de Morrison mas também relativamente ao holótipo da espécie portuguesa *Allosaurus europaeus*. Os exemplares de Andrés são identificados como pertencendo a *Allosaurus* cf. *europaeus* aguardando a descoberta de material mais completo que permita uma melhor compreensão desta espécie portuguesa. *Lourinhanosaurus antunesi* é considerada uma espécie válida e exclusiva do registo português. A análise filogenética aqui desenvolvida identifica este táxon como um membro do clado Allosauroidea mas apresentando uma posição instável. Este táxon é, algumas vezes, incluído num grupo, juntamente com *Allosaurus* e Carcharodontosauridae, que representa o clado irmão de Metriacanthosauridae. Outras vezes, é posicionado na base de Allosauroidea em politomia com metriacanthossaurídeos.

A fauna de terópodes do Jurássico Superior da Bacia Lusitânica é similar à conhecida em níveis correlativos da Formação de Morrison e está composta, sobretudo, por taxa partilhados com o registo norte-americano. Apesar desta semelhança, os terópodes da Bacia Lusitânica e da Formação de Morrison representam formas distintas, o que indica evolução vicariante, possivelmente devido à existência de corredores marítimos entre a América do Norte e a Ibéria que terão constituído barreiras à dispersão destas faunas. Todavia, estes processos de vicariância poderão ter-se manifestado de diferentes formas nas distintas espécies, o que explicaria a maior afinidade das faunas de terópodes nestes territórios,

relativamente a outros grupos de dinossáurios, como por exemplo os saurópodes e de outros vertebrados. Por outro lado, a presença no registo português de alguns grupos de dinossáurios que aparentemente estão ausentes na Formação de Morrison pode indicar padrões de extinções regionais e de restrições ambientais, tais como preferências ambientais.

O registo de terópodes do Jurássico Superior da Bacia Lusitânica mostra algumas semelhanças, na composição geral das faunas, com outros locais da Europa (Espanha. Alemanha e França). Contudo, devido ao escasso registo de terópodes do Jurássico Superior nestes locais uma análise mais ampla das relações filogenéticas destas faunas não é possível actualmente.

CHAPTER 10: ACKNOWLEDGEMENTS

10.1. ACKNOWLEDGEMENTS

This research was supported by SFRH/BD/84746/2012 PhD scholarship, financed by the "Fundação para a Ciência e Tecnologia" (Portugal). Also grants to for review collections were financed by the Jurassic Foundation, Fundação Luso-Americana para o Desenvolvimento [grant number L07-V-22/2010] and Synthesys [grant number GB-TAF-2160 and FR-TAF-4911]. The study of some specimens was also supported by a protocol between CMTV and SHN.

There are many people that, in one way or another, collaborated and supported this PhD thesis. For this reason, I am extremely grateful to many people who have been determinant for getting this work out ahead. It is not possible to enumerate all the people involved, whether in the professional or personal scope. We thank for allowing access to specimens to Bruno C. Silva (SHN, Portugal), Vanda Santos, João P. Lopes, Liliana Póvoas, and Judite Alves (MUHNAC, Portugal), Rui Castanhinha, Carla Tomás, and Octávio Mateus (ML, Portugal), Miguel Ramalho and Rita Silva (MG, LNEG, Portugal), Luísa Machado (MMPM, Portugal), Cláudia Manso (MMB, Portugal), Eduardo Espilez and Rafael Royo-Torres (FCPT-Dinópolis, Spain), Ester D. Berenguer and José I. Canudo (MPZ, Spain), Ronan Allain (MNHN, France), Sandra Chapman (NHMUK, UK), Paul Jeffery (OUMNH, UK), Daniela Schwarz and Thomas Schossleitner (HNM, Germany), Luis Chiappe and Maureen Walsh (NHMLAC, USA), Logan Ivy and Kenneth Carpenter (DMNH, USA), Rood Scheetz and Brooks Britt (BYU, USA), Mike Getty, Mark Loewen, and Randy Irmis (NHMU, USA), and Daniel Chure (DINO, USA).

We thank to Graça Ramalheiro, Hugo Campos, Marina Fiães, João Reis and Fátima Marcos for preparation of specimens, to José J. Santos, Carlos Anunciação, José Amorim, Guilherme Gameiro, Fernando J. Francisco and Joel Silva for field assistance and to André Mano, Ivan Gromicho, João Barrinha, and Cristina Moniz for collaboration in different phases of this research.

A special thank to my PhD directors, Mário Cachão (FCUL) and Francisco Ortega (UNED), and to my academic tutor, José L. Sanz (UAM) for the permanent support and encouragement. I also want to thank to Pedro Dantas, with whom I began to work in paleontology and that was decisive for this project. Also a special thank to the colleagues and friends of the Grupo de Biología Evolutiva (UNED), to Fernando Escaso for the help and incentive since ever, to Pedro Mocho for his friendship (especially for introducing me to the wonderful world of craft beer) and dedication in all works we have developed together, to Iván Narváez for his good humor in all situations and for his constant availability for everything I needed (including to make the layout of this thesis), to Adán Pérez-García for teaching me all about turtles and for welcoming me so many times, to Fátima Marcos for teaching me so many things about preparing fossils and for the friendship, to José M. Gasulla for being an inspiration as professional and personal, to the doctoral colleagues Adrián Parámo, Alejandro Serrano, Carlos de Miguel Chaves, Elena Cuesta, Daniel Vidal, Francesc Gascó and Marcos Martín for the mutual help and constant availability. Thanks also to Sofia Pereira for hear me so many times complaining and for the availability for everything I needed, to Cristina Rebelo, Nuno Inês, Pedro Santos, and Bruno Pereira for being present and for the constant incentive, to Wilamy Rita, Ana Moderno, and Patricia Monteiro for the joy at work.

Thanks also to Nuno Pimentel, Carlos Marques da Silva, Ana Cristina Azerêdo, Cristina Cabral, Francisco Fatela, Luis Vitor Duarte, Pedro Callapez, Maria Helena Henriques, José Brandão, Vanda F. Santos, José C. Kullberg, Liliana Póvoas, António M. Galopim de Carvalho and César Lopes for information and comments on different aspects of the geology and paleontology of the Lusitanian Basin.

During this research I had the opportunity to meet and the honor to work with several paleontologists whose comments and discussions help and inspired me in several ways. In this perspective, I thank to Francisco Ortega (UNED, Spain), José L. Sanz (UAM, Spain), Pedro Mocho (NHMLAC, USA), Fernando Escaso (UNED, Spain), Adán Perez-García (UNED, Spain), Rafael Royo-Torres (FCPT-Dinópolis, Spain), Xabier Pereda-Suberbiola (UVP, Spain), Oliver Rauhut (SNSB, Germany), Ronan Allain (MNHN, France), Stephen Brusatte (UE, UK), Luis Chiappe (NHMLAC, USA), Brooks Britt (BYU, USA), Mark Loewen and Randy Irmis (NHMU, USA), Daniel Chure (DINO, USA), Rui Castanhinha (ML, Portugal), and Cristophe Hendrickx (UW, South Africa).

The works developed in this thesis would not be possible without the support of different institutions to which I also want to express my thanks: Sociedade de História Natural (Portugal), Museu Nacional de História Natural e da Ciência (Portugal), Departamento de Geologia da Faculdade de Ciências da Universidade de Lisboa (Portugal), Instituto Dom Luiz (Portugal), Universidad Nacional de Educación a Distáncia (Spain), Universidad Autónoma de Madrid (Spain), and Dinosaur Institute, Natural History Museum of Los Angeles County (USA).

Finally, special thanks to Ana André, Bruno André, and Bruno Florindo for the friendship, incentive and understanding of my absence during this time. To my family, which is my foundation where I find the strength to go forward, my parents, brother, sisters, niece, grandparents (especially to my grandfather Américo), uncles and cousins my deepest thanks.

10.2. AGRADECIMENTOS

Este trabalho de investigação pela bolsa de doutoramento SFRH/BD/84746/2012 financiada pela "Fundação para a Ciência e Tecnologia" (Portugal). Financiamento para estudo de colecções foi também disponibilizado pela Jurassic Foundation, Fundação Luso-Americana para o Desenvolvimento [projecto L07-V-22/2010] e Synthesys [projectos GB-TAF-2160 e FR-TAF-4911]. O estudo de parte dos exemplares foi também apoiado por um protocolo entre a CMTV e a SHN.

Muitas pessoas colaboraram e apoiaram, de uma forma ou outra, esta tese de doutoramento e que foram determinantes para a concretização deste trabalho. Não é possível enumerar todas as pessoas envolvidas, tanto a nível profissional como pessoal. Queremos agradecer pelo acesso às colecções a Bruno C. Silva (SHN, Portugal), Vanda Santos, João P. Lopes, Liliana Póvoas e Judite Alves (MUHNAC, Portugal), Rui Castanhinha, Carla Tomás e Octávio Mateus (ML, Portugal), Miguel Ramalho e Rita Silva (MG, LNEG, Portugal), Luísa Machado (MMPM, Portugal), Cláudia Manso (MMB, Portugal), Eduardo Espilez e Rafael Royo-Torres (FCPT-Dinópolis, Espanha), Ester D. Berenguer e José I. Canudo (MPZ, Espanha), Ronan Allain (MNHN, França), Sandra Chapman (NHMUK, Reino Unido), Paul Jeffery (OUMNH, Reino Unido), Daniela Schwarz e Thomas Schossleitner (HNM, Alemanha), Luis Chiappe e Maureen Walsh (NHMLAC, EUA), Logan Ivy e Kenneth Carpenter (DMNH, EUA), Rood Scheetz e Brooks Britt (BYU, EUA), Mike Getty, Mark Loewen, e Randy Irmis (NHMU, EUA) e Daniel Chure (DINO, EUA).

Agradecemos também a Graça Ramalheiro, Hugo Campos, Marina Fiães, João Reis e Fátima Marcos pela preparação de parte dos fósseis, a José J. Santos, Carlos Anunciação, José Amorim, Guilherme Gameiro, Fernando J. Francisco e Joel Silva pelo apoio nos trabalhos de campo e a André Mano, Ivan Gromicho, João Barrinha e Cristina Moniz pela colaboração em diferentes etapas desta investigação.

Um agradecimento especial aos meus orientadores, Mário Cachão (FCUL) e Francisco Ortega (UNED), e ao meu tutor académico José L. Sanz (UAM) pela permanente disponibilidade e incentivo. Quero também agradecer a Pedro Dantas, com quem comecei a trabalhar em paleontologia e cujo empenho e dedicação foram essenciais neste projecto. Um agradecimento especial também aos colegas e amigos do Grupo de Biología Evolutiva (UNED), Fernando Escaso pela ajuda e incentivo desde sempre, Pedro Mocho pela amizade (especialmente por me mostrar o mundo maravilhoso da cerveja artesanal) e dedicação em todos os trabalhos que desenvolvemos em conjunto, Iván Narváez pelo bom humor em todas as situações e pela constante disponibilidade para tudo o que necessitasse (incluindo para fazer a maquete desta tese), Adán Pérez-García por me ensinar tudo sobre tartarugas e por me acolher tantas vezes, Fátima Marcos por me ensinar tantas coisas sobre preparação de fósseis e pela amizade, José M. Gasulla por ser uma inspiração tanto a nível profissional como pessoal, aos colegar de doutoramento Adrián Parámo, Alejandro Serrano, Carlos de Miguel Chaves, Elena Cuesta, Daniel Vidal, Francesc Gascó e Marcos Martín pelo espírito de entreajuda. Obrigada também a Sofia Pereira por me ouvir tantas vezes reclamar e pela disponibilidade para tudo o que precisei, a Cristina Rebelo, Nuno Inês, Pedro Santos, Bruno Pereira por estarem presentes e pelo incentivo constante, a Wilamy Rita, Ana Moderno e Patrícia Monteiro pela alegria no trabalho.

Obrigada também a Nuno Pimentel, Carlos Marques da Silva, Ana Cristina Azerêdo, Cristina Cabral, Francisco Fatela, Luis Vitor Duarte, Pedro Callapez, Maria Helena Henriques, José Brandão, Vanda F. Santos, José C. Kullberg, Liliana Póvoas, António M. Galopim de Carvalho e César Lopes pela informação e comentários relativos a diferentes aspectos da geologia e paleontologia da Bacia Lusitânica.

Ao longo deste projecto tive oportunidade de conhecer e a honra de trabalhar com diversos paleontólogos cujos comentários e discussões me ajudaram e inspiraram de diversas formas. Neste sentido, quero agradecer a Francisco Ortega (UNED, Espanha), José L. Sanz (UAM, Espanha), Pedro Mocho (NHMLAC, EUA), Fernando Escaso (UNED, Espanha), Adán Perez-García (UNED, Espanha),

Rafael Royo-Torres (FCPT-Dinópolis, Espanha), Xabier Pereda-Suberbiola (UVP, Espanha), Oliver Rauhut (SNSB, Alemanha), Ronan Allain (MNHN, França), Stephen Brusatte (UE, UK), Luis Chiappe (NHMLAC, EUA), Brooks Britt (BYU, EUA), Mark Loewen e Randy Irmis (NHMU, EUA), Daniel Chure (DINO, EUA), Rui Castanhinha (ML, Portugal) e Cristophe Hendrickx (UW, África do Sul).

Os trabalhos desenvolvidos nesta tese não teriam sido possíveis sem o apoio de diferentes instituições, às quais quero também manifestar o meu agradecimento: Sociedade de História Natural (Portugal), Museu Nacional de História Natural e da Ciência (Portugal), Departamento de Geologia da Faculdade de Ciências da Universidade de Lisboa (Portugal), Instituto Dom Luiz (Portugal), Universidad Nacional de Educación a Distáncia (Espanha), Universidad Autónoma de Madrid (Espanha) e Dinosaur Institute, Natural History Museum of Los Angeles County (EUA).

Por último, um agradecimento especial a Ana André, Bruno André e Bruno Florindo pela amizade, incentivo e compreensão pelas minhas ausências durante tanto tempo. À minha família, que é a minha base onde encontro a força necessária para seguir em frente, aos meus pais, irmão, irmãs, sobrinha, avós (especialmente ao meu avô Américo), tios e primos o meu mais profundo agradecimento.